TECHNISCHE UNIVERSITÄT MÜNCHEN

Ingenieurfakultät Bau Geo Umwelt

Lehrstuhl für Verkehrswegebau

Analysis and Evaluation of Railway Track Systems on Soft Soil: Trackbed Thickness Design and Dynamic Track-Soil Interaction

Puguh B. Prakoso

Vollständiger Abdruck der von der Ingenieurfakultät Bau Geo Umwelt
der Technischen Universität München zur Erlangung des akademischen Grades eines
Doktor-Ingenieurs
genehmigten Dissertation.

Vorsitzender:		Prof. Dr.-Ing. Gebhard Wulfhorst
Prüfer der Dissertation:		
	1.	Prof. Dr.-Ing. Stephan Freudenstein
	2.	Prof. Indrasurya B. Mochtar, Ph.D.

Die Dissertation wurde am 04.08.2016 bei der Technischen Universität München
eingereicht und durch die Ingenieurfakultät Bau Geo Umwelt
am 23.02.2017 angenommen

Abstract

**Analysis and Evaluation of Railway Track Systems on Soft Soil:
Trackbed Thickness Design and Dynamic Track-Soil Interaction**

The study is focused on the development of trackbed thickness design, investigation of static and dynamic track-soil interaction (TSI) and improvements of slab track and ballasted track systems concerning soft soil. The analysis comprises combination of theoretical, empirical and FEA. Analytical method and design charts are developed to estimate the required thickness of trackbed and to design a track supported with a simple pile foundation on soft soil. The design criteria are based on the limits of soil's fatigue strength, shear failure and plastic deformation due to cyclic loadings. The core of the method is the use of simple parameters of *structural number (SN)* to represent the overall strength of trackbed and *coefficient of relative strength (a)* to describe the strength of individual layer of trackbed. The main feature of the method is the ability to design multilayered trackbed with different combinations of stiffness and thickness of trackbed materials. It demonstrates a good initial estimation of the required thickness of a trackbed and has been compared with other approaches available from literature. TSI static analysis reveals that to assess the performance of a slab track, soil fatigue criterion becomes more dominant than the criterion of flexural strength of concrete slab when the soil is soft. This also means that the traditional assumption of only increasing slab thickness is not always the most effective solution when the soil is far below the limit of ideal bearing capacity. Optimum solution of trackbed is achieved by gradually decrease the stiffness from the top to the bottom layers of trackbed. Advanced track model is presented, which is able to deal with simulations of nonlinear soil, uneven support, hanging sleepers, existence of gaps, cyclic loadings, loadings of running train with different speeds as well as dynamic loadings with various excitation frequencies. FEA of dynamic track-soil interaction exhibits that soil stabilization mainly influences the track response in low excitation frequencies. Optimizations of ballasted and slab track regarding soft soil include the enhancement of track performance based on the dynamic characteristics of track elements, the use of multilayer trackbed and jointed concrete slab. It is also shown that JRCP and JPCP can be an option as replacement of CRCP in the traditional slab track system. Design proposal of piled foundation of track on soft soil in an example case study is also presented.

Keywords: *trackbed*, *track-soil interaction (TSI), FEA, soft soil, pile foundation, ballasted and slab tracks*

Acknowledgement

I would like to thank to the Indonesian government through DIKTI and the German government represented by DAAD for providing me a scholarship under the Indonesian-German Scholarship Program (IGSP) and for supporting my studies and living in Germany from the beginning until finishing my PhD research project.

I would like to express my sincere gratitude, thank and deepest appreciation to Prof. Dr.-Ing. Stephan Freudenstein, for his greatest helps for supervising my dissertation and for giving me a chance to gain valuable experience during my PhD research at the Chair and Institute of Road, Railway and Airfield Construction (Prüfamt Verkehrswegebau) TU München. From the beginning I proposed this topic; he has encouraged and supported me, and also opened more and more my interest about railway engineering studies.

Greatest appreciation and gratefulness to Prof. PhD, Indrasurya B. Mochtar from the Technical University (ITS) Surabaya for his kindness and willingness to be a reviewer of my dissertation as well as worthfully comments and suggestions in the geotechnical parts.

Special thanks and greatest acknowledgement as well to Dr.-Ing. Bernhard Lechner as my mentor. While I was writing my dissertation he always warmly gave his time regularly to open discussions, guide me in my research project and gave me many valuable comments and feedbacks.

I would like also to warmly say many thanks to Dr.-Ing. Walter Stahl and Dr.-Ing. Christop Simon for helping me to find some data and literatures related to my studies, and all other senior researchers, engineers and workers at the Prüfamt Verkehrwegebau TU München for the precious and pleasant time while working together with them.

My thanks are also for my previous co-worker Natalia Papathanasiou, M.Sc. for the nice time working together during her internship, supervision of her thesis as well as for her assistances in my research projects. Thanks to the previous students of MSc Transportation Systems who ever worked and sat in the same room with me (Nima, Feranmi, Ali, Pranay, and Mahesh) for the assistances as well as spending nice and chilling times together.

Many thanks also for my colleagues, engineers and lecturers in Transportation Laboratory and Soil Mechanic Laboratory at the Universitas Lambung Mangkurat Indonesia as well as Yussae Sugara, MT from CV. Geo Inti Perkasa Geotest Consulting for sending me some examples of project, field and laboratory data regarding soft soil in Kalimantan.

My most special thank also for my lovely parents, brother, sister for always supporting me anytime and for their great-fully praying for my living and studies in Germany. This dissertation is dedicated to my parents. Last but not least many thanks to all friends, related organizations and persons who cannot be mentioned one by one.

Yours sincerely,

Puguh Prakoso

Table of Content

List of Notation and Abbreviation

Notation

Δt	Temperature difference
Δt_L	Average loading time of a wheel load
μ	Poisson's ratio
μ_z	Zimmermann's moment influence factors
A	Area
a, b, m	Soil cyclic parameters dependent on soil type after Li & Selig
a, ai	Coefficient of relative strength (of layer i) for trackbed thickness design
a_o	Dimensionless factor to describe soil or pile-soil subjected with dynamic loading
a_s	Elastic-pad or sleeper spacing
b, B	Width
C, C_{dyn}	Viscous damping coefficient/constant. Dynamic damping coefficient
C_s	Soil constant parameter for trackbed thickness design
d_p	Diameter of pile
E	Modulus of elasticity
E_{dyn}	Dynamic modulus of elasticity
E_s	Elastic or Resilient modulus of soil
E_v *or* E_{def}	Deformation modulus
$E_{v,2}$	Deformation modulus of second loading
Ev_d	Dynamic deformation modulus
$f_{c,d}, f_{c,d,ref}$	Design and reference factors due to wheel load distribution of rails in a curve
$f_{c,i}$ *and* $f_{c,j}$	Wheel load distribution factors of inner (i) and outer (j) rails in a curve
$f_{c,ratio}$	Ratio of $f_{c,i}$ and $f_{c,j}$ for wheel load distribution factor in a curve
f_d	Dynamic amplification factor (DAF)
$f_{d,ref}$	Reference dynamic amplification factor
f_{Lr}	Design factor due to different characteristic length of rail
$f_{Lr,\ ratio}$	Ratio of characteristic length design and reference value of characteristic length
f_p	Preloading clamping force of rail fastening system
f_Q	Design factor of wheel load
f_s	Unit skin friction/resistance of pile skin surface
G_s, G'	Dynamic shear modulus of soil. Effective dynamic shear modulus of soil
h	Thickness
h_{eq}	Equivalent thickness of layer(s) in a half space media
I	Moment of inertia
$K, K_{dyn}, k, k_{sys}, k_{tot}$	Spring stiffness. Dynamic spring stiffness. Spring stiffness of system or total stiffness of a set of springs
k_{FEA}	Dummy elastic foundation stiffness of subgrade in FEA
K_p	Rankine passive soil pressure coefficient
k_{rp}	Elastic-pad stiffness/resilient stiffness
k_s, k_{sub}	Modulus of subgrade reaction of soil
L, l	Length
L_{Crit}	Critical length of pile
L_m	Characteristic length, utilized as length of moment for design of critical length of floating pile
$L_{m,BOEF}$	Length of moment derived from characteristic length of a beam model
$L_{m,slab}$	Length of moment derived from characteristic length of a slab model
L_p	Length of pile
L_r, L_p, L_{pb}	Radius of relative stiffness or characteristic length of rail, and pavement idealized as slab and beam respectively
$L_{r,ref}$	Reference characteristic length of rail
M_p	Rotation moment capacity of piles or moment reaction of passive soil pressure of piles
M_r	Resilient modulus
N	Number of cyclic (repeated) loading/stress
P	Pressure
P_p	Soil's passive lateral pressure

Pz	Vertical pressure on soil
Q, Q_0, Q_d	Wheel load, wheel load in the middle of longitudinal direction of rails, designed wheel load
Q_b	Bearing capacity at pile base/tip
q_b	Unit resistance of pile base/tip
Q_{ref}	Reference wheel load = 125 kN
Q_s	Total shaft/skin friction resistance of pile
q_u	(1) unconfined compressive strength (test data), (2) ultimate bearing capacity of soil in terms of compressive strength limit (analytical or empirical approaches)
Q_u	Ultimate pile capacity
q_u'	Ultimate dynamic compression strength of soil
r	Equivalent radius of elastic-pad contact area
r_o	Radius of pile
s	Distance between rails centerlines
S_i, S_j	Rail-seat loads (forces) of inner (i) and outer (j) rails
SN	Structural Number of trackbed thickness design
SN_{des}, SN_{design}, SN_d	Design value of structural number of trackbed
SN_f	Structural number of foundation slab
SN_{ref}	Reference structural number of trackbed thickness design
S_u	Undrained shear strength of soil
Sx, Sy, Sz	Longitudinal, transverse bending tensile stress, and axial pressure respectively
t	Coefficient of variation, a statistical parameter
T	Subgrade layer depth until a rigid base
V_s	Shear wave velocity of soil
W_x	Section modulus (static/first moment area)
y_{max}	Maximum vertical displacement
β_d	Damping ratio
$\gamma_{d,i}$, $\gamma_{d,j}$	Westergaard's deflection influence factors of inner (i) and outer (j) rails
γ_s	Volumetric density
δ	Track quality factor
ε_p, ε_a	Actual and allowable cumulative soil plastic strain
η	Train speed factor
λ_{long}, λ_{lat}	Total longitudinal and lateral moment influence factors
λ_w, λ_r, λ_t	Westergaard's moment influence factors, radial and tangential directions respectively
ρ, ρ_a	Actual and allowable cumulative soil plastic deformation
σ_d	Deviator stress
σ_s	Soil compressive strength
ω	Angular excitation frequency

Abbreviation

1D, 2D and 3D	One, two and three dimensional FEA models
ACC	Active Crack Control
AF	Adjustment Factor
APDL	Ansys Parametric Design Language
BNWF	Beam on Nonlinear Winkler's Foundation model
BOEF	Beam On Elastic Foundation model
CBR	California Bearing Ratio
CH	Soils with inorganic clays of high plasticity (USCS classification)
CL	Soils with inorganic clays of low to medium plasticity (USCS classification)
CPT	Cone Penetration Test
CRCP	Continuously Reinforced Concrete Pavement
CTB	Concrete Treated Base
CZW	Combination of Zimmermann and Westergaard
CZZ	Combination of Zimmermann and Zimmermann
DAF/DMF	Dynamic Amplification (Multiplication) Factor

DF	Design Factor
EFS	Elastic foundation stiffness
FEA/FEM	Finite Element Analysis/-Method
GW	Gravel well graded soil rocks (USCS classification)
H&K	Heukelom & Klomp fatigue criterion
HST	High Speed Train
ICE-1	One example type of German high speed passenger train
JPCP	Jointed Plain Concrete Pavement
JRCP	Jointed Reinforced Concrete Pavement
L&S	Li & Selig fatigue criterion
LIN-FAST	Linear model of fastening system
MET	Method of Equivalent Thickness (Odemark)
MF	Multiplication Factor
MH	Soils with inorganic clayey silts, plastic silts (USCS classification)
ML	Soils with inorganic silts & clayey silts (USCS classification)
NL-FAST	Nonlinear model of fastening system
N-SPT	Designed number of blows of Standard Penetration Test
OH	Organic clays and silty clays (USCS classification)
OL	Organic silts and silt-clays, low plasticity (USCS classification)
PBT	Plate Bearing Test
PC	Power cars or traction cars of a set of train locomotives
SC	Sand clay soils (USCS classification)
SF	Safety Factor
SM	Sand silty soils (USCS classification)
SPT	Standard Penetration Test
TC	Trailer cars or passenger cars of a set of train locomotives
TSI	Track-Soil Interaction
UCL	Upper Confident Limit, a statistical parameter
UDS	Undisturbed Soil Sample (Test)
USCS	Unified Soil Classification System

1. Introduction

1.1. Background of the Research

Generally, analytical methods of railway track can be distinguished by the types of track model, applied loading and structural analysis. Two major groups of those methods are static and dynamic analyses, which are correlated to static and dynamic loadings respectively. In comparison to a dynamic analysis, a static analysis of a railway track by taking into account dynamic amplification factor -in some situations- is simpler and frequently used in practice. However, it has some limitations especially due to the fact that a track structure is sensitive to vibration. Actually, the motion of the train along the track generates dynamic forces as well as vibration. This affects significantly to the long-term stability and performance of a track, which is a result of dynamic interaction between track components and substructure. This is the major reason why the dynamic behaviors and interactions of railway track needs further study and become more and more important to be considered in a railway track design and analysis.

The task is even more challenging if a track is designated to fulfill the requirements of running a medium to high speed train (HST) on a track constructed on soft ground. In a case of soft soil, the impacts resulted from dynamic loading and vibration of running train can be more obvious. A typical indication regarding this is firstly settlements on soil. A settlement caused by dynamic loading is a repetitive process and different from the one caused by a steady-state static loading. Deformation on soil due to dynamic loading in a long-time period may consist of a complex combination, not only elastic but also plastic deformations. This strongly depends on the dynamic loading itself and the characteristics of soil. In addition, the problem of settlement on soil mostly occurs as differential settlements, which may lead a severe problem to the overall performance of a railway track.

Up today, there is a large number of studies and developments of conventional railway track. However, only few of them are mainly focused on tackling the problems of soft soil. It reveals a new task to understand what are the characteristics and behaviours of track on soft soil, and which approach and solution are suitable for this specific case? This problem has not been completely compensated in the conventional track design methods. Accordingly, there is a need to develop an innovative method, which incorporates advanced approaches regarding soft soil problems in the railway track design method.

Therefore, going from the overview above, this research is conducted to analyze and evaluate the behaviors of railway track systems constructed on soft soil, to understand track-soil dynamic interactions and to present advanced analysis of railway track systems by using Finite Element Method/Analysis (FEM/FEA).

1.2. Problem Definition and Research Question

Firstly, soft soil has unique characteristics, which should be carefully taken into account in railway track design. Engineers often have to face different options of which major treatment should be done: soil exchange, soil stabilization/reinforcement or increase the strength of the superstructure or combination of them. However, there is no clear definition to give a recommendation to engineers which solution is more appropriate. What is more, the current design methods of ballastless/ballasted track systems are more devoted to an ideal soil condition. These methods are though frequently based on classical static analysis of beam or slab on a continuous elastic foundation. Hence, from the point of view of static analysis, total stiffness of the track system plays very important role. A traditional assumption is still believed that only the stiffness of superstructure should be increased when the soil is soft. This is seen more as classical "static analysis viewpoint". It is indicated that among the three solutions: soil exchange, soil stabilization and/or stiffening superstructure, there must be boundary conditions to define:

1) a minimum soil bearing capacity, which majorly depends on the characteristics of soil and its safe limit against excessive deformation due to dynamic loading
2) a cost-effective superstructure design, which still guarantees certain level of stability, durability and safety to the running train.

The reason is that when bearing capacity of soil is very low, only increasing the total stiffness of superstructure is not always the best solution. This is not only regarding the cost of superstructure, but there is also a certain limit of soil bearing capacity, which should be fulfilled to give adequate level of stability to the superstructure. Nevertheless, soil exchange or stabilization has restraints as well. Therefore, a better understanding of track and soil behaviours carries more appropriate answer for this issue in railway engineering. Conventional track design methods are not sufficient to clarify this problem. For this reason, there is still a challenge to improve the traditional track design methods.

Secondly, some developments of track pavement/trackbed are fundamentally adopted from a long-time experience in the highway pavement technologies. For instance, the use of

multilayered systems, which can be applied for both ballastless and ballasted track systems and implementation of jointed slabs for ballastless track systems. An optimum design result of these types of construction considers some criteria of required strength as well as effective cost. Nevertheless, it remains a big challenge to improve those systems. On the one side, ballastless track systems are often correlated to a relatively higher initial construction cost than that of ballasted track. On the other side, conventional ballasted track system still requires further developments to deal with soft soil. In a standard application, ballasted track system gives many advantages, but which improvements should be done if this system has to deal with soft soil is still a big question.

Thirdly, to achieve an optimum performance of a track system, the behaviours and interactions among superstructure, substructure and soil demand further analysis. Track-soil interaction (TSI) is investigation of the important parameters, which play major role in the railway track design. TSI analysis allows to evaluate this problem broader, not only from the viewpoint of static analysis but also from dynamic one. Dynamic analysis describes closer to the real problem as a railway track is subjected to deal with dynamic forces generated from a running train. Furthermore, wide spectrum of dynamic analysis gives more options to enhance the performance of a track, which includes studies regarding natural frequency of track system, track response due to excitation frequencies, vibration modes and overall track structure stability. Dynamic finite element analysis (FEA) is a powerful tool for these goals.

Last but not least, there are many advanced technologies and long-year-experience, which have been developed in the fields of geotechnical engineering. However, there are only few of them which have been applied so far in the field of railway track engineering. A big challenge is still remaining: how to combine the knowledge in both fields and how to bring long time experience in geotechnical fields in the railway track engineering.

Therefore, some specific questions arise as a starting point of the research based on the problem definition above that:

1. How to develop advanced FEA models of railway infrastructure to investigate track-soil interactions (TSI)?
2. What are the important parameters and behaviours of soft soil and the essential characteristics of superstructure elements, which influence to the behaviours of a railway track, and vice versa?

3. What are the boundaries to give a recommendation of choosing or combining the three major solutions of soil exchange, soil treatments and strengthening superstructure?
4. How to include important parameters coming from TSI investigations in order to improve the current design approaches of railway track systems?
5. Which type of track infrastructure and improvements provide more effective solution regarding the condition of soft soil?

1.3. Specific Aims of the Research

The main objectives of this study are:

1. to summarize the conventional design codes, standards, and guidelines, and then to find the potential improvements related to soft soil,
2. to propose advanced analytical design method for track pavement (trackbed),
3. to present advanced FEA models, which are able to handle different ranges of analysis and simulation,
4. to investigate the behaviors of railway track on soft soil and track-soil interactions (TSI), especially due to dynamic loading and vibration,
5. to come up with proper and better practical solutions regarding foundation systems of railway track on soft soil.

1.4. Structure of the Dissertation

Chapter I begins with the introduction of the research. It discusses some points as the background of the research. Then it presents the description of the problems and research questions which are related to the PhD research topic. Then step by step it is proceeded with a clear definition of the specific goals of the research.

Chapter II describes the research design and methodology. It starts with definitions of the principal terms used in this research. Then it gives an overview about the scope of the study. Later, it briefly discusses about applied approaches and methodology of the research.

Chapter III comprises of a short literature review of railway track design procedures based on the analytical and empirical methods, which are mainly based on combination of static analysis and fatigue approaches. Then, these analytical methods are summarized into a flowchart. It also shows design procedure proposed by another researcher, which emphasizes different limit criteria of soil.

Chapter IV presents the idea of the author regarding development of analytical-empirical methods for railway track design. First part of this chapter presents a proposed computational program to analyze the static behaviours of superstructure. Then, a sensitivity analysis of the essential parameters of superstructure and soil is shown. This identifies the boundary conditions between strength of superstructure and soil bearing capacity, which is seen from static point of view.

Chapter V introduces a proposed design method of trackbed layer of a track system. This presents three criteria of trackbed design, namely using criteria of soil's cyclic fatigue limit, shear failure and plastic deformation. The method is also presented as design charts for broader applications in the practice. Evaluation regarding the influence of trackbed width and comparison of the proposed method with other methods are also demonstrated.

Chapter VI gives information about track-soil interaction. It discusses FEA of dynamic track-soil interaction and reviews the dynamic behaviours of and interactions between track and soil. Boundary conditions of soil are identified in the viewpoint of dynamic and vibration. Problems of hanging sleepers, white-spots and mud-holes, which are caused by uneven support and differential settlements of a ballasted track is evaluated in this chapter.

Chapter VII talks more in detail about the design of railway track on soft soil. Advanced FEA for analysis and evaluation of *Cakar Ayam* foundation system and conventional pile system on soft soil is performed. A static design method of *Cakar Ayam* foundation for railway application is also introduced here by the author. The optimizations based on the functions of each track element to enhance the performance of track on soft soil seeing from dynamic point of view are presented.

Chapter VIII gives evaluation of the implementation of jointed slab track resting on piled-foundation slab concerning construction on soft soil. The investigation is related to bonding condition, thermal impact, joint spacing and the use of different concrete pavement types.

Chapter IX presents an example of a case study. The location where the example data is taken is in Central Kalimantan Indonesia. Different alternative solutions are discussed and proposed.

Chapter X summarizes the important points, which are figured out in this research and then to come up with the final conclusion. Finally, it ends up this paper with the recommendations for the future works related with this topic.

2. Research Design & Methodology

2.1. Terms and Definitions

The definitions and limitations of some principal terms which are used in this dissertation are summarized as follows:

- *Track systems* are categorized into two main groups, 1) ballasted track system which employs ballast (crushed) stones and 2) ballastless track system, which is in this research limited only to a concrete slab track system (see Figure 1).
- *Superstructure* of a track system consists of fundamental elements of rail, fastening systems (elastic-pad and clamps), sleepers and ballast (ballasted), concrete slab and base layer (ballastless), and protection layer (optional).
- *Substructure* of a track system is principally composed of subgrade and subsoil.
- *Subgrade* is a construction material which is not naturally formed, but it is constructed and treated. The material might not originally come from the construction place, can be from other locations or can be a filling material or a material which needs further treatments. For instance, soil embankment, which needs some geotechnical treatments such compaction or stabilization.
- *Subsoil* is a natural soil formatted by the nature.
- *Soft soil* is here defined as the natural subsoil which has low bearing capacity levels under the ideal requirements set by the standards.
- *Stiffness* of a material or structure is an expression to describe a strength of a material. Stiffness is basically combination of elastic modulus and moment inertia of a structure. Thus, it expresses the total strength which consists elastic strength and dimension and/or shapes of structure. In some general expressions of a strength of material in this dissertation, stiffness also indirectly refers to elastic modulus when the dimension or the shape of the material is not detailed or explained.
- *Bearing capacity of soil* is here explained more as pressure load capacity of soil. The levels of bearing capacity of soil are termed as or linked to different parameters in different analyses, disciplines, standards and countries. In this research, it is frequently expressed as or correlated to the strength levels of elastic modulus, resilient modulus, deformation modulus, reaction modulus, shear strength and compressive strength of soils.

- *Low bearing capacity of soil* is pressure load capacity of soil under the ideal perquisites set by track design standard. Low bearing capacity of soil means that it needs advanced treatments and actions to have sufficient safe level for railway superstructure. The suggested margin of low bearing capacity of soil for railway application will be evaluated and defined in this research.
- The term of *trackbed* (pavement layer) is defined as the pavement layers between sleeper and subsoil in a ballasted track system, respectively as the layers between elastic-pad and subsoil in a ballastless (slab) track system (see Figure 1).
- *Foundation system* is limited to pile foundation system for strengthening low bearing capacity of soil. Hence, it is categorized as a part of substructure.
- *Cakar Ayam* is a light-weight shallow pile foundation system, which was developed in Indonesia. This foundation can be categorized as floating pile foundation or shallow piled-raft foundation, of which the concept of major bearing capacity is delivered from the passive soil resistances and not from the end-bearing capacity of the pile.
- *Dynamic loading* is the load generated from a running train on a railway track, which is majorly influenced by train speed, axle configuration, and static wheel load of a train. Dynamic impact coming from track and wheel irregularities are considered as a factor but is not specifically analyzed or modelled.
- *Vibration* is termed as vibration modes of a track structure as a response to dynamic loading. It is not vibration emission and its impact to the environment.
- *Vertical pressure on soil* is the vertical stress, which is experienced by soil in its top surface.
- *Design factor (DF)* of a trackbed thickness design is defined as a constant to be multiplied by a reference or critical number from design chart to obtain a design value.
- *Safety factor (SF)* is explained as a multiplication constant to a margin of security against risks of failure or damage within a design period.
- *Multiplication factor* (*MF*) of trackbed assessment is the total of different factors (including *DF* and *SF*) applied to a critical or reference value.
- *Adjustment factor (AF)* is a constant, which is multiplied to the results of analytical methods to be equal or closer to a reference results of FEA. This is used to do comparative analysis between analytical methods and numerical method (FEA).

- *Degradation factor* is a reduction factor of stiffness applied to soil in an initial static loading analysis. This is done to estimate the impact of cyclic loading on soil's deformation after some numbers of repeated loadings. This simplifies the analysis, which is instead of doing multiple calculations with huge number of repeated loadings applied on the soil model, the analysis can be done only in one step of static loading analysis.
- *Low frequency* range is in this study defined as excitation frequencies under 20 Hz.
- *Mid/moderate frequency* range is explained as excitation frequencies from 30 to 90 Hz.
- *High frequency range* is attributed to excitation frequencies more than 100 Hz.

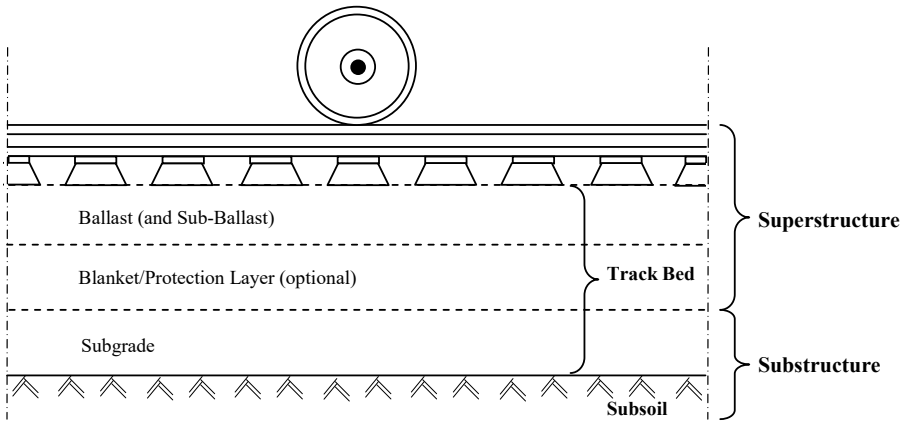

(a) Ballasted track system

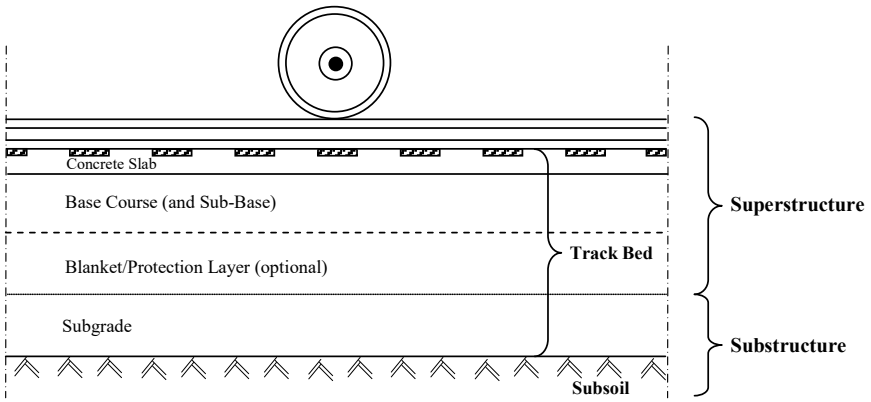

(b) Ballastless track system (slab track)

Figure 1. Ballasted and ballastless (slab) track systems

2.2. Scope of the Study

The research can be considered as a combination of theoretical, numerical and analytic-parametric studies. The core of the study is primarily focused on the Finite Element Analysis (FEA) of track-soil (-and foundation) interaction (TSI), in particular case of track systems

on soft soil dealing with dynamic loading and vibration inducing from a running train. The numerical computer modelling and simulations involve different types of structural analysis, namely: static, cyclic, harmonic, modal, implicit transient dynamic and vibration analyses using ANSYS software. The secondary part of the studies is data collection from literature, examples of laboratory tests and of measurements data.

FEA comprises two- and three-dimensional modellings, which are varied from simple to complex idealizations of superstructure, substructure, foundation system and soils. These modellings are supported by theoretical approaches as well as real and empirical data inputs. And then the results will be evaluated with current practical solutions, example data from laboratory tests and field measurements. Laboratory and field data is obtained from literature as well as from the available database in the *Chair and Institute of Road, Railway and Airfield Construction TU München*. For the example case study, the data is obtained from *CV. Geo Inti Perkasa Geotest Consulting, Banjarbaru* and *Soil Mechanics Laboratory of Civil Engineering Department, Faculty of Engineering, Lambung Mangkurat University Banjarmasin, South Kalimantan, Indonesia*.

The track line is mainly focused on a straight line. Detailed track geometry in a curve is not within the scope of this study. However, load distribution of inner and outer rails in a curve is considered as a factor in the analysis. Transition zone, switches and bridge are not discussed in this research. Nevertheless, uneven supports and differential settlements due to hanging sleepers of a ballasted track, gaps underneath of a slab track as well as gaps of a pile foundation are analyzed. Ballastless track system is more focused on the assessment of building railway on soft soil. It is only limited to slab track and is more emphasized on German Rheda-2000 system. The implementation of jointed slabs is also generally analyzed and evaluated regarding soft soils. Ballasted track system will be also investigated for an option of superstructure systems supported by piles for proposed design on the final chapters of the dissertation.

An analytical model, which is combination of classical theories is developed for trackbed design. An iteration tool is developed using computer programming to estimate the critical thickness of trackbed layer and then some combinations are presented in design charts for practical purpose.

For very soft soil, two advanced foundation types based on piles will be analyzed. One is the conventional pile foundation system. The other one is *Cakar Ayam* foundation system.

Improvements of the current analytical static design method of *Cakar Ayam* foundation system, which are based on static moment equilibrium theory will be proposed to fit the requirement for railway track applications.

In accordance with that, various soil models and pile-soil models will be then employed, with different applications for static analysis as well as transient dynamic analysis. The dynamic soil models utilize soil's impedance functions of stiffness and damping as frequency-dependent parameters as well as in time domain as frequency-independent parameters.

Standard designs with ideal design parameters, such as good level of bearing capacity of soil and cost-effective superstructure design are used as reference. And then they will be compared to the changes according to the specific cases of soft soil. The analysis is mainly focused on sensitivity, parametric and comparative analyses to identify the critical parameters delivered from track elements characteristics and behaviours.

The major variations of input data are different soil characteristics and bearing capacities, superstructure construction types, foundation types, trackbed thickness and layer combinations, loading cases, excitation frequencies and train speeds. Output parameters of the analysis are focused on the indicators of displacements and stress levels. Margins of the assessment of these indicators are fatigue strengths, ultimate stress limits and allowable displacements of rail, trackbed layers and deformation on soil, which are based on criteria of safety, economical and certain level of serviceability aspects.

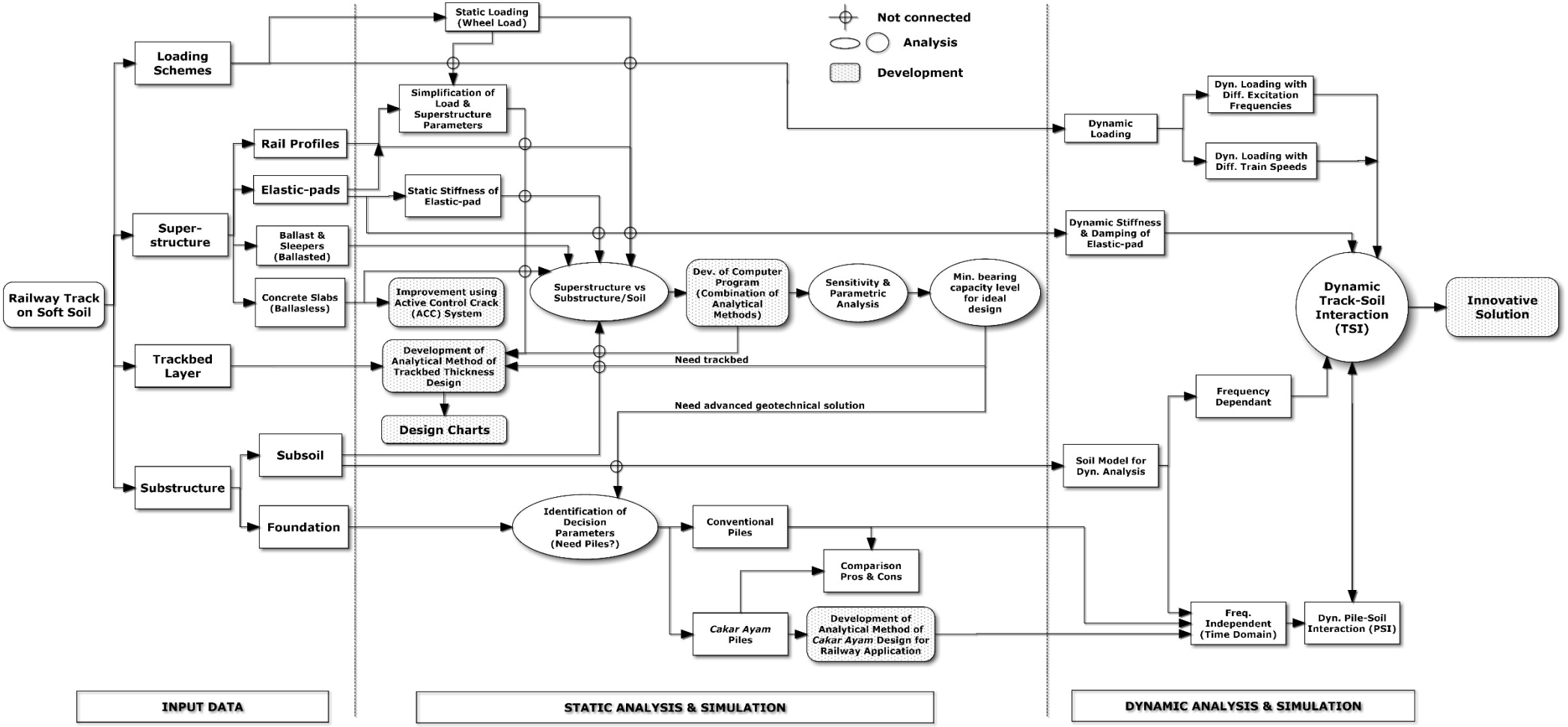

Figure 2. Description of the Scope of the Research

2.3. Methodology

The types of investigation, hypothesis of the causes and interactions, predicted impacts, indicators, types of analysis and relationships among the parameters are generally summarized in the Table 1 below. The workflow of analysis is illustrated in the Figure 3.

2.3.1. Theoretical Approach and Analysis

The theoretical railway track design methods are combination of:

- classical beam/slab on elastic foundation of rail/trackbed models (e.g. Winkler, Zimmermann, Westergaard),
- soil stress distribution methods (e.g. Boussinesq, Westergaard, Odemark),
- ultimate state limit methods (e.g. Wöhler, Smith, Heukelom & Klomp fatigue approaches, Li & Selig soil fatigue model),
- classical soil bearing capacity methods (e.g. Terzaghi, Rankine, Meyerhof, Skempton),
- conventional pile and *Cakar Ayam* bearing capacity design methods.

These methods are discussed to give an overview of different classical approaches. The combination of these methods is summarized into a flowchart to briefly explain the design procedures of a railway track. The analytical methods are associated and a computer program is built to identify the important parameters from different variations of superstructure and soil bearing capacity. It is then proceeded by giving recommendation of possible improvements of the classical design methods.

Table 1. Types of Investigation, Indicator, Simulation and Analysis

No	Point of Investigation	Major Cause / Interaction	Impact	Indicator	Analyzed/ Modelled		Variation of Simulation	Method & Analysis
					Yes	No		
1	On Subsoil (Ideal &Soft)	Induced from dynamic loading and vibration	× Non-uniform settlements × Loss of substructure support (soil failures) × Reduction of overall structure stability	Displacements	✓		× Different loading cases (static & dynamic): static wheel load, load with excitation frequencies, train speeds and load cycles × Different soil bearing capacity levels and soil models × Different material properties of superstructure elements × Different types of construction of superstructure × Different foundation systems (conventional, piles, *Cakar Ayam*) × Different foundation configurations (width, pile length, pile spacing)	× Combination of theoretical-classical static analysis × Computer programming × FEA-static analysis – critical track components' displacements and stresses – superstructure stiffness versus soil improvement (static) – cyclic analysis of soil due to repeated loading – thermal impact analysis of concrete slab × FEA-modal and harmonic analyses: – critical frequencies of the rail, fastening, concrete slab, and soil in frequency domain – natural frequencies of the rail, fastening, concrete slab, foundation (piles) – vibration modes & damping characteristics of the system × FEA-transient dynamic analysis – superstructure stiffness versus soil improvement (dynamic) – critical displacements on the rail, concrete slab, foundation and soil due to loading with different excitation frequencies – critical displacements on the rail, concrete slab, foundation and soil due to different train speeds – vibration & damping characteristics of the system
				Excessive plastic deformations	✓			
		Low bearing capacity of soil		Shear failures	✓			
				Gaps	✓			
				Critical vibration modes	✓			
2	On the Rail	Induced from dynamic loading and vibration	× Risk of crack × Rail fatigue × Rail corrugation × Track irregularities × Misalignments	Critical displacements	✓			
				Critical stresses level	✓			
		Settlements on soft soil		Risk of crack	✓			
		Dynamic characteristics and interactions of track elements		Irregularities, misalignments and corrugation		✓		
				Critical vibration modes	✓			
3	On the Ballast/ Sleeper (Ballasted)	Induced from dynamic loading and vibration	× Ballast settlements × Ballast attrition × Hanging sleepers	Displacements and deformations	✓			
		Settlements on soft soil		Ballast attrition		✓		
				Gaps and hanging sleepers	✓			
4	On the Concrete Slab (Ballastless)	Settlement on soft soil	× Risk of crack × Concrete fatigue × Pumping effect	Displacements	✓			
				Critical stresses level	✓			
				Risk of crack	✓			
		Dynamic characteristics and interactions of track elements		Concrete fatigue		✓		
				Pumping effect		✓		
				Critical vibration modes	✓			
5	On the Foundation	Settlement on soft soil (low bearing capacity of soil)	× Settlement of foundation × Loss of support	Displacements	✓			
				Critical vibration modes	✓			
				Pile & foundation-soil gaps	✓			
		Dynamic characteristics & interactions between soil and foundation		Pile group interaction		✓		
				Fatigue		✓		

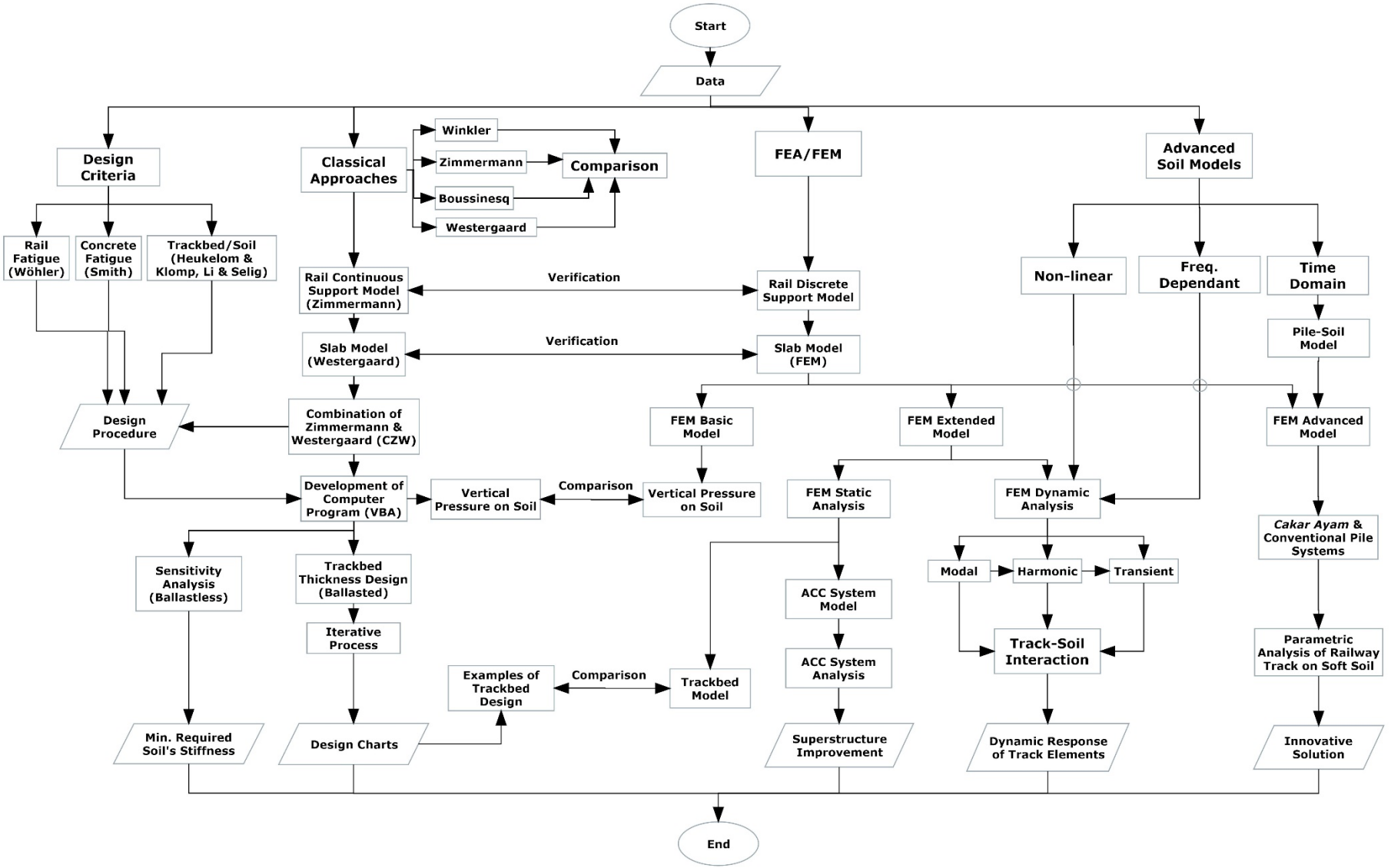

Figure 3. Flowchart of analysis

2.3.2. Modelling Tools

a. Finite Element Software

The FEA software which is chosen for modelling and simulation is ANSYS version 14. The models are built and simulations are run using *ANSYS Parametric Design Language* (APDL) programming language.

b. Types of Analysis in FEA

To investigate the track-soil interaction (TSI), there are five different types of structural analysis conducted in ANSYS, namely:

- *Static Analysis (steady-state and conservative analysis)*, which has characteristics of:
  - simulation of steady loading conditions (do not change within a time)
  - to investigate track structure responses of a static loading case (static design and analysis) and to improve the standard design procedures
  - to be used as reference and comparison to the analytical methods
  - to verify the results from the FEA models built for the simulations
- *Cyclic Nonlinear Analysis (non-conservative static analysis)*, which has characteristics of:
  - to predict cyclic behaviour of a structure after some times or some numbers of repeated loadings
  - useful in fatigue analysis of a structure
  - to estimate degradation factor of a structure after cyclic loading
  - to predict the total amount of cumulative plastic deformation of a structure after certain numbers of cyclic loading
- *Modal Analysis*, which has characteristics of:
  - to analyze natural frequencies and mode shapes of a track structure
  - to understand dynamic response of a track
  - to optimize the dynamic mass-spring systems of TSI
  - to do sensitivity analysis of different parameters of TSI
- *Harmonic Analysis*, which has characteristics of:
  - simulation of the sinusoidal load behaviour (repetitive loading)
  - to understand dynamic response of a track
  - to identify natural frequencies of a track system

- to study the vibration modes of a track

- *Transient Dynamic Analysis (time-history analysis)*, which has characteristics of:
  - simulation of the response of a structure subjected to time dependent loads (time periods/frequencies)
  - to analyze a track dynamic and vibration response which is subjected with different excitation frequencies
  - to perform dynamic response of a track due to different loading induced by a train running with different speeds
  - to investigate the impacts of damping and mass (inertia) characteristics of a material to the dynamic response of a track.

2.3.3. Proposed Design Method and Solution

Two methods are proposed of railway track analysis and design, namely computational method and graphical method of using design charts. Computational method employs mathematical formulations, iterative as well as forward- and back- (reversed) calculations as well as computational algorithm. Hence, this algorithm can be programmed in computer to perform fast computation of huge amount of calculations, iterations and different variations of track design parameters. The computer programs are built using *Visual Basic Application* (*VBA*) for *Microsoft Excel* as well as *MATHCAD* software.

A graphical design method of trackbed layer is developed based on this iteration tool. The design charts are built for design practice and are used to estimate the required thickness of trackbed. Furthermore, a static design method of *Cakar Ayam* foundation, which is specified for railway application is also developed by extending this tool.

3. Design Procedure of Railway Track

3.1. Zimmermann, Westergaard and Ultimate Limit State Methods

Examples of well-known classical theoretical approaches of railway track analysis are Zimmermann and Westergaard methods. Development of these methods, for instance the one proposed by Freudenstein, et. al (2015)[43] for a slab track analysis. This can be done in two steps to analyze the major part of railway track components. The first step is the calculation of the stresses on the rail and rail-seat reaction forces (or rail-seat loads) by using Zimmermann method. The results of the rail-seat forces in each position of the elastic-pad from the first step are then used in the second step as the discrete loads of the ballast or concrete slab. The second step is calculation of the stresses on the trackbed/pavement structure (ballast or concrete slab). This can be done either by using Zimmermann or Westergaard or by comparing both results. The major difference is that Zimmermann method idealizes ballast or concrete slab as a beam, meanwhile Westergaard method assumes ballast or concrete slab as a plane/slab, and both are laid on continuous soil support. And then the stresses on the trackbed layer until the soil surface can be estimated by using the Boussinesq or Westergaard method in combination with Odemark's half-space theory. The summary of these methods can be seen in the Appendix 1, Section A.1.1, pp. 216.

This method considers a static analysis. Therefore, in a design, to contemplate the quasi-static and dynamic impacts of the running train, a dynamic -amplification (or -multiplication) factor (*DAF/DMF*) is employed. *DAF* is obtained based on the empirical and statistical data from measurements, by considering track quality level, train speed and safety factor. One example of widely used *DAF* formulation is the approach proposed by Eisenmann (1972)[36][105], as follows:

[17] [36]

$$\varphi = 1 + \delta.\eta.t \qquad \textit{Eq. 1}$$

where: δ is the track quality factor, η is the train speed factor, and t is coefficient of variation based on upper confident limit. Train speed factor can be empirically estimated as follows:

[17] [36] [43]

$$\eta = 1 + \frac{V - 60}{V_t} \qquad \textit{Eq. 2}$$

in which V_t = 140 for general trains with speed from 60 up to 200 km/hour, 380 for passenger trains and 160 for freight trains [17] [36] [43].

For a moderate track quality with track quality factor $\delta = 0.25$ and statistical parameter $t = 1.96$ and upper confident limit of 95%, the increase of *DAF* levels is shown in the Figure 4 below and see Appendix 4, pp. 227 for an example of calculation in more detail.

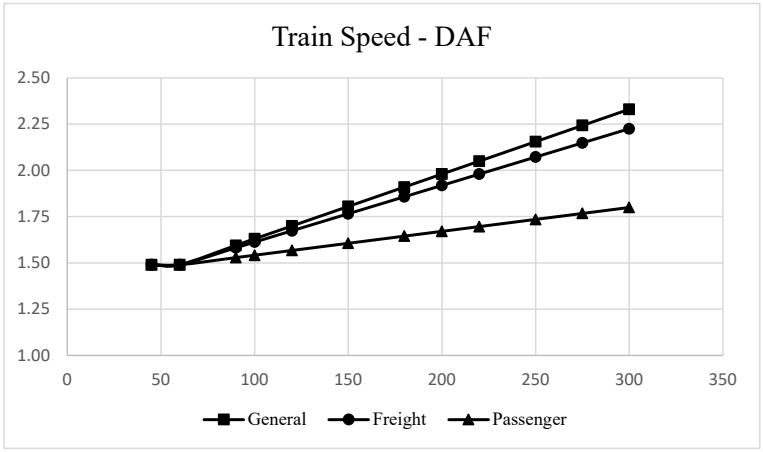

Figure 4. Dynamic amplification factor of a moderate track quality

The illustration of the design procedure of railway track system by combining analytical methods and ultimate limit criteria (see Appendix 1, Section A.1.2, pp. 221) can be seen in the Figure 5. These approaches are still extensively used in the conventional design and analysis of railway track. Yet, because of the steps are separated in order to do analysis in each main track component, the first calculation using Zimmerman takes into account only the stiffness of elastic-pads for a ballastless track and the total stiffness of elastic-pads, ballast and soil for a ballasted track system. The resulted rail-seat forces are estimated in this way.

In an analysis of ballastless track system, then it is assumed in the first step that the bottom surface of the elastic-pads is initially fixed and there is no deflection at that location. This assumption indicates that a good condition (ideal) of bearing capacity of soil is required. Meanwhile, in an analysis of ballasted track system, the bottom of substructure layer is initially assumed to be rigid. This does not reflect perfectly to the real situation, in which rail, elastic-pad, sleeper, trackbed/pavement layer and soil are associated. In addition, possibility of settlements of substructure is not taken into account. In the case of a slab track, the deflection within the concrete slab might be considered relatively small in a standard design, non-floating slab and good bearing capacity of base layer and soil. Hence, this approximation within this assumption is quite acceptable. However, if the design has to compromise with a weak soil condition or a floating slab system, in which the deflection of the concrete slab might be somehow higher, this is the major limitation of this static approach.

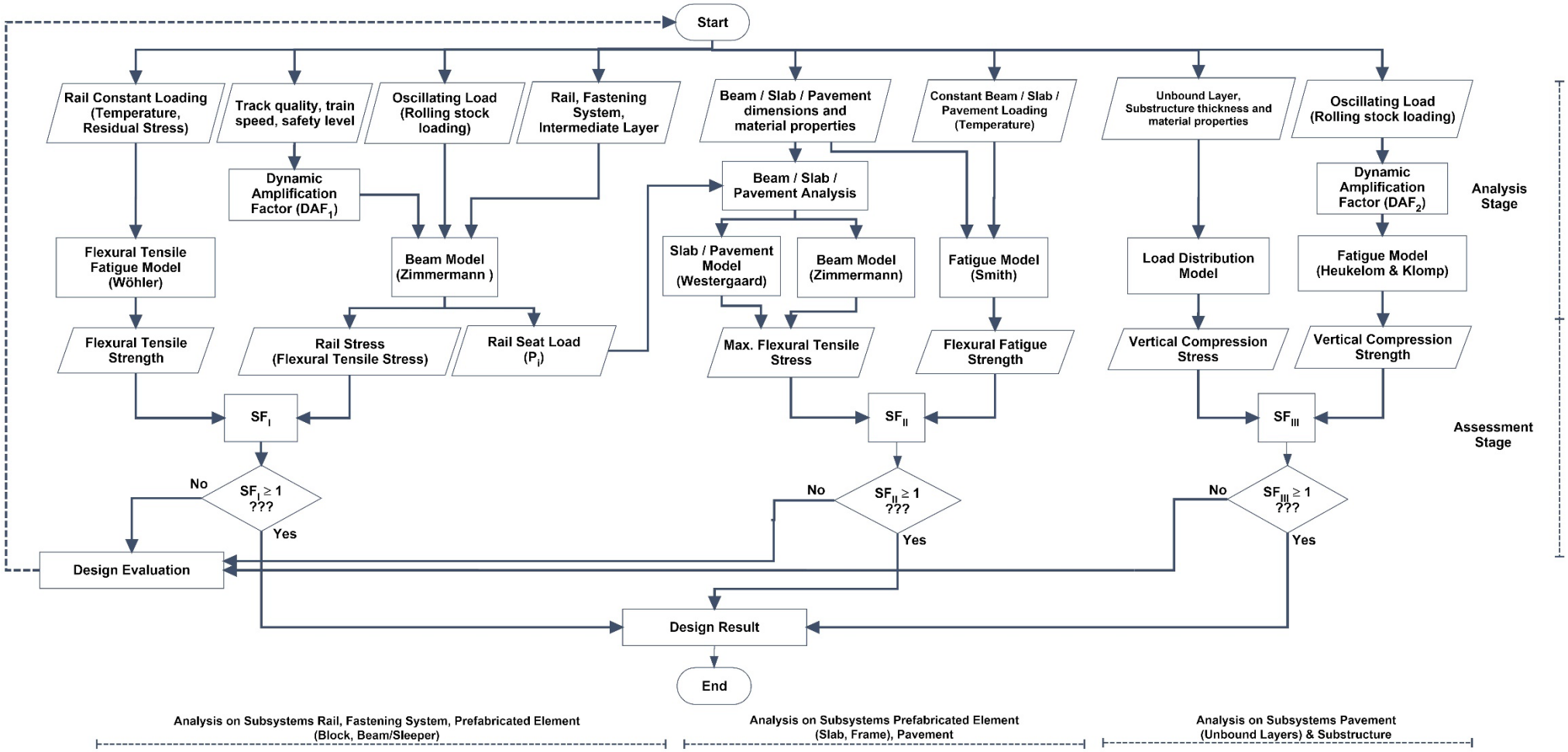

Figure 5. Schematic view of the analytical design procedure

3.2. Li and Selig Method

Li and Selig (1998)[74][75] developed an analytical method to estimate a minimum required thickness of granular layer (ballast) of a ballasted track system. The major criteria of the assessment are based on the limits of progressive shear stress failure and excessive plastic deformation of subsoil due to the deviator stress induced by a running train. This leads to a limitation, so that the deviator stress level which is subjected to subsoil should be below the critical limit against shear failure and plastic deformation of subsoil. Therefore, sufficient thickness of ballast should be designed to fulfill these limit criteria. The design procedures using this approach are described in the Figure 6, which is based on prevention of subgrade's shear failure and in the Figure 7, which is based on avoidance of disproportionate subgrade's plastic deformation[74][75].

Li and Selig (1998) method incorporates the dynamic impact through train speed factor as well as number of load repetition to model the train traffic. Soil characteristics are also taken into account in the approach, which are conveyed from fatigue strength of soil due to cyclic loading. The estimation of fatigue is based on some numbers of tests of fine-grained soils under repeated stress applications done by them. The superstructure analysis is conveyed from *GEOTRACK* software, which was simulated with some variations of multiple design loads, properties of rails and sleepers and a single homogenous deformable granular layer with different thicknesses and resilient moduli. Li, 1994[76], Li and Selig, 1996[73] did analysis of these variations to get different deviator stress levels on the subsoil for the assessment of the required thickness of the granular layer (ballast). The results then presented into design charts[74][75].

Subsoil's cumulative plastic strain (ε_p) and plastic deformation (ρ) are formulated as these following functions (according to Li, 1994[76]; Li and Selig, 1996[73]):

[74][75] $$\varepsilon_p(\%) = a\left(\frac{\sigma_d}{\sigma_s}\right)^m N^b \text{ , with criteria of } \varepsilon_p \leq \varepsilon_{pa} \qquad \textit{Eq. 3}$$

[74][75] $$\rho = \int_0^T \varepsilon_p . dt = \frac{a.N^b}{100.(\sigma_s)^m} \int_0^T (\sigma_d)^m . dt \text{ , with criteria of } \rho \leq \rho_a \qquad \textit{Eq. 4}$$

where: ε_p is cumulative soil plastic strain; ρ is cumulative soil plastic deformation; N is the number of repeated stress; $\sigma_d = \sigma_1 - \sigma_3$ (soil deviator caused by train load); σ_s is soil compressive strength, which can be obtained from unconfined compressive strength (q_u); T is subgrade layer depth until a rigid base; *a, m, b* are parameters dependent on soil type (see

Table 2); ε_{pa} is allowable plastic strain and ρ_a is allowable plastic deformation at the subsoil for the design period.

Table 2. Typical values of soil parameters a, b, and m for various type of soil after Li and Selig (1998)

Soil Type	**a**	**b**	**m**
CH (fat clay)	1.20	0.18	2.4
CL (lean clay)	1.10	0.16	2.0
MH (elastic silt)	0.84	0.13	2.0
ML (silt)	0.64	0.10	1.7
Note: Values are cited from Li and Selig (1996)[73] and [74][75]			

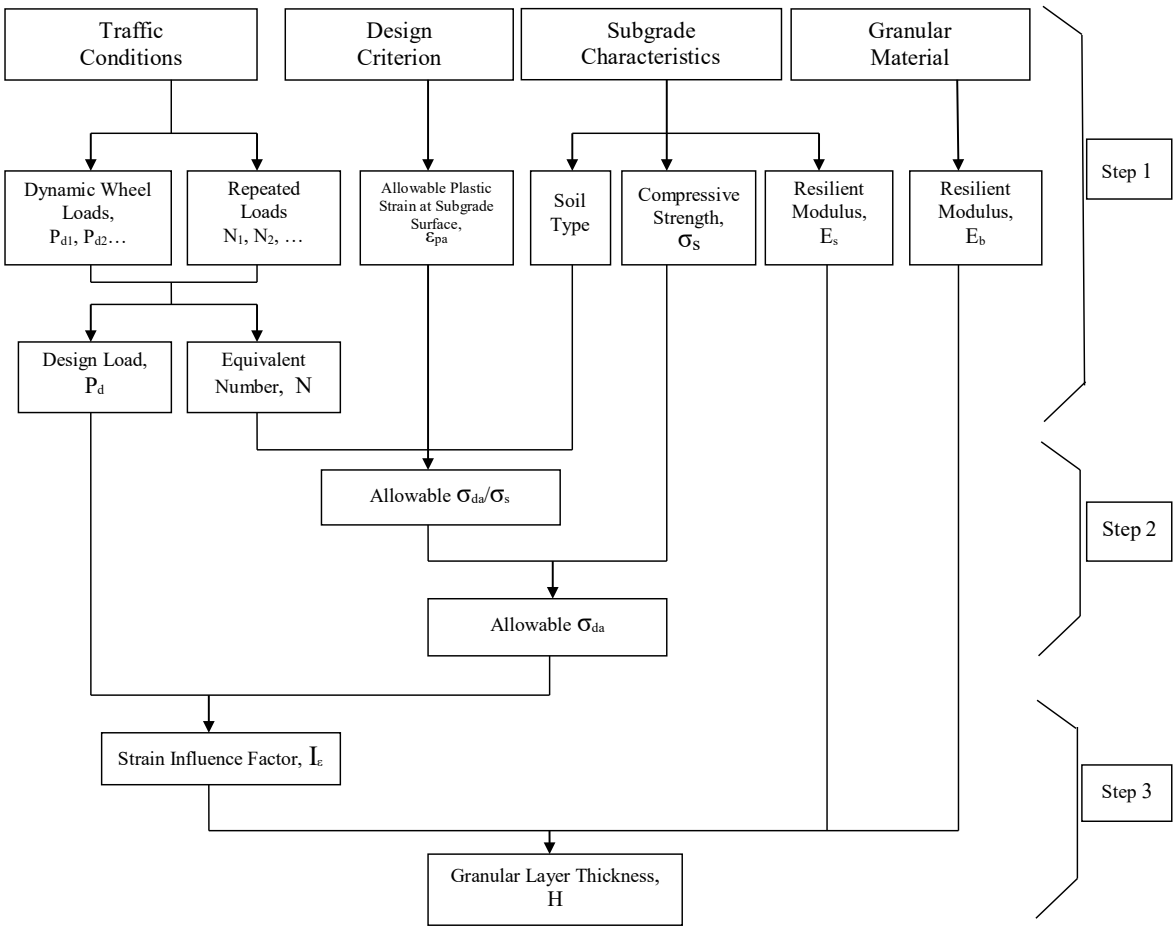

Note: The diagram is reproduced and cited from Li & Selig (1998) [75]

Figure 6. Design Procedure 1 (limiting subgrade shear failure) of trackbed thickness design after Li and Selig (1998)

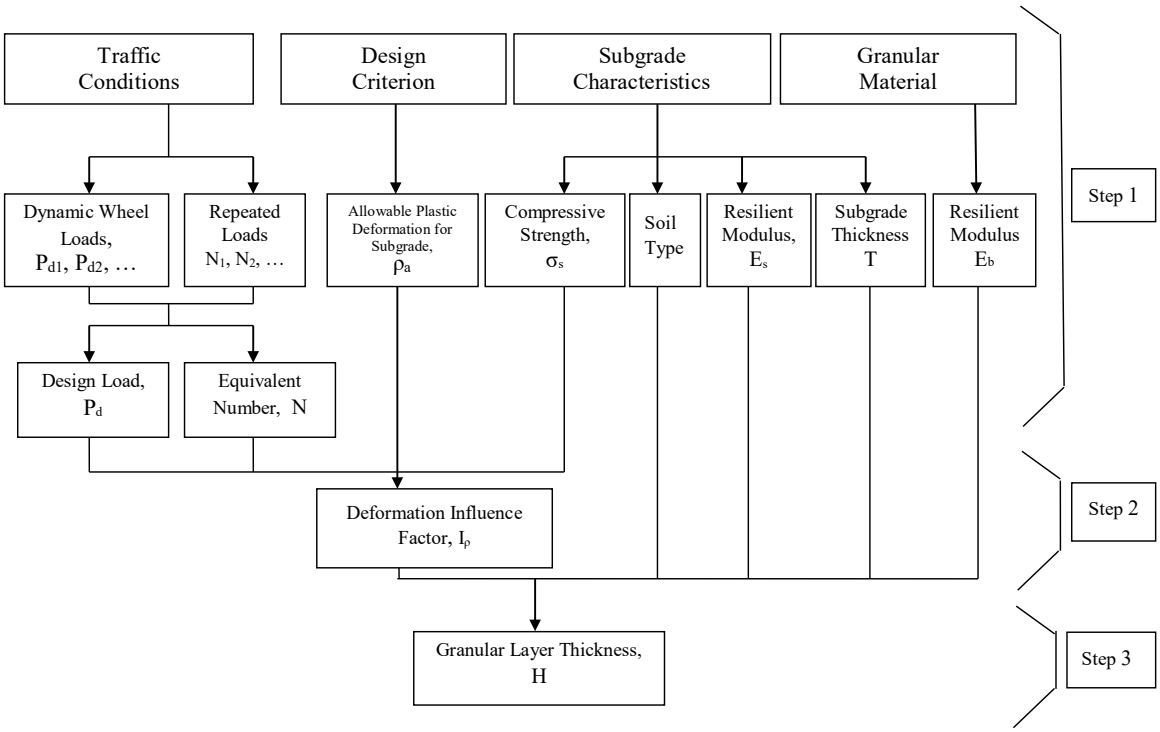

Note: The diagram is reproduced and cited from Li & Selig (1998) [75]

Figure 7. Design Procedure 2 (limiting subgrade plastic deformation) of trackbed thickness design after Li and Selig (1998)

4. Computational Method of Railway Superstructure Analysis

4.1. Mathematical Model for Superstructure Analysis of Slab Track

One extension of using the classical approaches is to develop a mathematical model from their equations. Hence the model can be easily solved by doing computational procedures such as back-calculations and/or iterations.

4.1.1. Analysis of Rail and Elastic-pad Stiffness

A mathematical model can be developed for instance to calculate the number of rail-seat loads, which should be considered in the next analysis of the ballast or concrete slab.

The rail's deflection line of one-axle-load analysis is symmetrical and there are two parts of the curve: the rail's downward deflections and uplifts. The rail's line influence of deflection produced by Zimmermann method is symmetrical, therefore, the calculation is necessary to be done only in half part of the line.

Combining the Zimmermann's formulations of single point load shown in the Eq. 108 and Eq. 109 (Appendix 1, pp. 216), to solve this equation, the function for calculating the number of considered rail-seat loads for a ballastless track can be also expressed as *f(n)*:

[17] $$f(n) = \frac{sin(X) + cos(X)}{e^{(X)}}$$ *Eq. 5*

where $$X = \frac{a_s.n}{L_r} and \;\; L_r = \sqrt[4]{\frac{4.E_r.I_r.a_s}{k_{rp}}}$$ *Eq. 6*

and a_s is elastic-pad spacing [mm]; n is the number of considered rail-seat loads; L_r is characteristic length/radius of relative stiffness [mm] of-, E_r is the modulus elasticity [N/mm^2] of-, and I_r is the area moments of inertia [mm^4] of-the rail beam; and k_{rp} is the stiffness of elastic-pad [N/mm].

Due to symmetrical line shape and by considering only half part of the rail's influence line from the position of single load on the top of the rail ($n=0$), then there are two intervals of the line, where:

- $f(n) > 0$, which is the half of the downward deflection area, and
- $f(n) < 0$, which is the one of the two uplift areas

This equation can be solved using Newton-Raphson iteration [147] in computer to get the n half number of supports after a single point load, which is expressed by:

[147]

$$n_{i+1} \approx n_i - \frac{f(n_i)}{f'(n_i)} \qquad \textit{Eq. 7}$$

where: *f'(n)* is the derivative function of *f(n)*:

$$f'(n) = \frac{-2.a_s.e^{-X}}{L_r}.sin(X) \qquad \textit{Eq. 8}$$

and valid for $n \geq 1$.

After getting the *n* number of rail-seat loads, then the rail deflections y_0 to y_n and rail-seat loads S_0 to S_n at the positions of elastic-pad can be calculated using this equation:

[17]

$$y_i = \frac{Q.a_s}{2.k_{rp}.L_r}.\frac{sin\left[\frac{n.a_s}{L_r}\right] + cos\left[\frac{n.a_s}{L_r}\right]}{e^{\left[\frac{n.a_s}{L_r}\right]}}, 0 \leq i \leq n \qquad \textit{Eq. 9}$$

$$S_i = k_{rp}.y_i, 0 \leq i \leq n \qquad \textit{Eq. 10}$$

where: Q is wheel load [N].

S_0 to S_n are then used as discrete loads for doing analysis on the ballast or concrete slab and trackbed layers.

Example A

An example of calculation for ballastless track system using that formulation can be seen in Table 3. The input parameters are: static wheel load of 125 kN, rail profile 60E2 (formerly given code as UIC60) with elastic modulus of 2.1×10^5 MPa and moment of inertia of 30.55×10^6 mm^4. Minimum elastic-pad is estimated by considering the desired maximum deflection of rail (see Eq. 118 in the Appendix 1, Section A.1.1, pp. 218).

Table 3. Example of calculation of required elastic-pad stiffness and the number of rail-seat support based on Zimmermann method for ballastless track system

y_{max} [mm]	$k_{rp,min}$ [kN/mm]	Considered *n* supports (half side)	
		calculated	rounded
1.0	54.7	2.7	3
1.5	31.8	3.1	3
2.0	21.7	3.4	3
2.5	16.1	3.7	4
3.0	12.6	3.9	4
4.0	8.6	4.3	4

4.1.2. Analysis of Bending Tensile Stress of Concrete Slab

a) Approach I. Beam-Slab Model (Combination of Zimmermann, 1888 & Westergaard, 1926 / CZW Method)

The idea of back-calculation for a ballastless track system is to combine Zimmermann (beam model) and Westergaard (slab model) methods. Therefore, all of the parameters from the rail, elastic-pad, and trackbed (e.g. concrete slab) are mixed together in closed formulations. This can be described in this following figure:

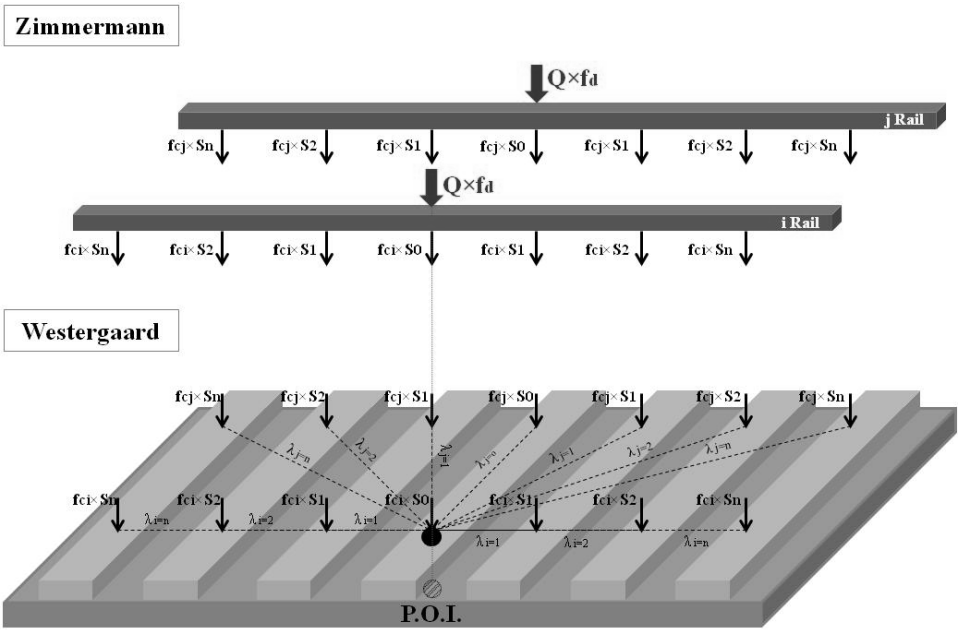

Figure 8. Sketch of Combination Method of Zimmermann and Westergaard

As it is shown in the Figure 8, Q is a wheel load, which is multiplied by dynamic amplification factor f_d (see Eq. 1). The loads in the inner rail (i position) and in the outer rail (j position) can be different, especially considering a case in a curve. Empirically, load distribution factors $f_{c,i}$ of 1.2 for inner rail and $f_{c,j}$ of 0.8 respectively for outer rail are taken into account [36][43].

Zimmermann (1888) method is applied for calculation of deflection, bending moment, rail-seat reaction force and bending stress of the rail. Meanwhile Westergaard (1926) method can be used to analyze bending stress and deflection of the concrete slab. This utilizes the radius of relative stiffness (L_r of rail and L_p of concrete slab) and moment influence factors (μ_z and λ_w) from both methods (see Appendix 1, Section A.1.1, pp. 216-219 for more detail).

The combination formula for longitudinal bending moment on the concrete slab at the center is shown below:

Eq. 11 (a)

$$M_{long} = \overbrace{\frac{Q_0.a_s.f_d}{2.L_r}}^{\text{factor of } Q_0} \left\{ \begin{array}{l} \overbrace{f_{c,i}\frac{0.275(1-\mu_p)}{6}\left[log\left(\frac{E_p.{h_p}^3}{k_s.{b_r}^4}\right)-0.436\right]}^{\text{factor of } S_0} \\ +2.f_{c,i}\sum_{i=1}^{n}\left(\frac{sin\left(\frac{i.a_s}{L_r}\right)+cos\left(\frac{i.a_s}{L_r}\right)}{e^{\left(\frac{i.a_s}{L_r}\right)}}\right)\lambda_{long,i} \\ +f_{c,j}\left[\underbrace{\lambda_{long,j=0}}_{\text{factor of } S_{j=0}} + \underbrace{2.\sum_{j=1}^{n}\left(\frac{sin\left(\frac{j.a_s}{L_r}\right)+cos\left(\frac{j.a_s}{L_r}\right)}{e^{\left(\frac{j.a_s}{L_r}\right)}}\right)\lambda_{long,j}}_{\text{factor of } S_{j,\,1\geq j\geq n}}\right] \end{array} \right\} \text{factor of } S_{i,\,1\geq i\geq n}$$

$$L_r = \sqrt[4]{\frac{4.E_r.I_r.a_s}{k_{rp}}} \quad \text{rail \& rail pad stiffness contribution} \qquad \textit{(b)}$$

where: *i* is the notation for the inner rail and *j* for the outer rail respectively; Q_0 is wheel load [N]; f_d is dynamic amplification factor [-], L_r is the Zimmermann's radius of relative stiffness of rail [mm], a_s is the discrete support spacing or elastic-pad spacing [mm] (see again Eq. 6, pp. 23); μ_p is Poisson's ratio of-, E_p is modulus of elasticity [MPa] of- and h_p is the thickness of-concrete slab; b_r is the radius of load distribution in the bottom of the concrete slab [mm] (see Eq. 122 in the Appendix 1, pp. 219); $f_{c,i}$ and $f_{c,j}$ are load distribution factors of inner (*i*) and outer (*j*) rails respectively [-]; and k_s is modulus of subgrade reaction [N/mm^3].

The bending tensile stress of the concrete slab at the center can be derived using the formula:

[17]

$$\sigma_{max} = \frac{M_{max}}{W_x}, \ and \ W_x = \frac{1}{6}b_p{h_p}^2 \qquad \textit{Eq. 12.(a)}$$

$$and\ for\ (semi)infinite\ slab\ analysis\ b_p = 1,$$
$$then\ \sigma_{max} = \frac{6M_{max}}{{h_p}^2} \qquad \textit{(b)}$$

where: σ_{max} is the maximum bending tensile stress [MPa] of-, b_p is the considered concrete slab width [1 mm], h_p is thickness [mm] of- and W_x is the section modulus (static/first moment area) [mm^3] of-concrete slab.

From the Eq. 11, it can be seen that factor of Q_0 comes from single wheel load applied on the top of the rail and based on the combination of Zimmermann and Westergaard. Factor of S_0 is brought from Westergaard stress calculation of a single load at the center. Factor of $S_{j=0}$ represents a single wheel load acting on the outer rail. Factors of S_i $(1 \geq i \geq n)$ and S_j $(1 \geq j \geq n)$ deliver the rail-seat loads calculation using Zimmermann method from both rails outside of the wheel load location (left and right sides), therefore they are multiplied by 2. Finally, $\lambda_{long,i}$ contributes the influence factor of rail-seat load S_i of the inner rail from 1 to *n*, and

$\lambda_{long,j}$ gives the influence factor of rail-seat load S_j of the outer rail from 1 to n. The same way can be applied for transverse bending moment by using transverse influence factors respectively.

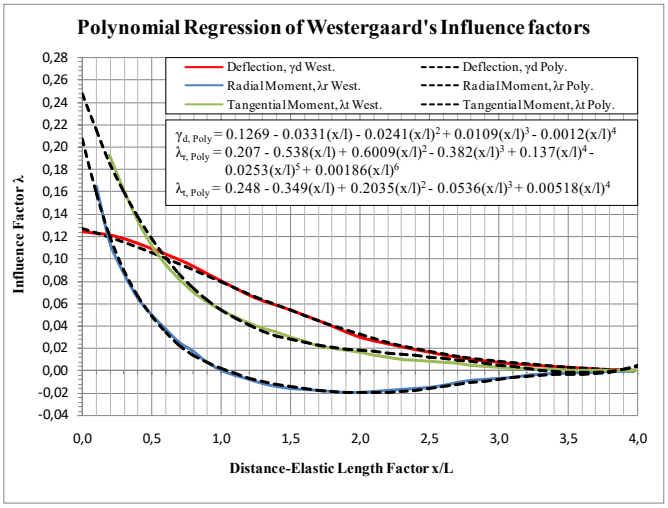

Figure 9. Polynomial regression of Westergaard influence factors

Based on the original Westergaard's moment influence line chart (see Figure 143 in the Appendix 2, pp. 225), 4- and 6-degree of polynomial regression functions of radial and respectively tangential λ moment influence lines are defined as drawn in the Figure 9. The regression functions are expressed in these following equations:

- Westergaard's moment influence factor of neighboring longitudinal rail-seat loads of the inner rail and outside of the wheel load location, for $1 \leq i \leq n$:

$$x_i = i.a_s \qquad \textit{Eq. 13.(a)}$$

$$\textbf{if } 0 < \frac{x_i}{L_p} < 4 \textit{ then}:$$

$$\lambda_{long,i} = \lambda_{r,i} \quad \textit{where } \lambda_{r,i} = \lambda_{r,k=i} \qquad \textit{(b)}$$

$$\lambda_{lat,i} = \lambda_{t,i} \quad \textit{where } \lambda_{t,i} = \lambda_{t,k=i} \qquad \textit{(c)}$$

$$\textbf{else if } \frac{x_i}{L_p} \geq 4 \textbf{ then}:$$

$$\lambda_{long,i} = \lambda_{lat,i} = 0 \qquad \textit{(d)}$$

- Westergaard's moment influence factor of neighboring transverse rail-seat loads of the outer rail and outside of the wheel load location, for $1 \leq j \leq n$:

$$\beta_j = tan^{-1}\left(\frac{s}{j.a_s}\right) \qquad \textit{Eq. 14.(a)}$$

$$x_j = \frac{j.a_s}{cos\beta_j} \qquad \textit{(b)}$$

$$\textbf{if } 0 < \frac{x_j}{L_p} < 4 \textit{ then}:$$

$$\lambda_{long,j} = \lambda_{r,j} + 0.5(\lambda_{t,j} - \lambda_{r,j}).[1 - cos(2\beta_j)] \quad \textit{where } \lambda_{r,j} = \lambda_{r,k=j} \qquad \textit{(c)}$$

$$\lambda_{lat,j} = \lambda_{r,j} + 0.5(\lambda_{t,j} - \lambda_{r,j}).[1 + cos(2\beta_j)] \quad where\ \lambda_{r,j} = \lambda_{r,k=j} \qquad (d)$$

else if $\frac{x_j}{L_p} \geq 4$ ***then***:

$$\lambda_{long,j} = \lambda_{lat,j} = 0 \qquad (e)$$

- Westergaard's moment influence factor of neighboring transverse rail-seat load of the outer rail on the single point of wheel load location, for *j=0*:

$x_j = s$, *where s is the distance between center lines of inner and outer rail* *Eq. 15.(a)*

if $0 < \frac{x_j}{L_p} < 4$ *then*:

$$\lambda_{long,j} = \lambda_{t,j} \quad where\ \lambda_{t,j} = \lambda_{t,k=j} \qquad (b)$$

$$\lambda_{lat,j} = \lambda_{r,j} \quad where\ \lambda_{r,j} = \lambda_{r,k=j} \qquad (c)$$

else if $\frac{x_j}{L_p} \geq 4$ ***then***:

$$\lambda_{long,j} = \lambda_{lat,j} = 0 \qquad (d)$$

$$and:\ L_p = \sqrt[4]{\frac{E_p.{h_p}^3}{12.k_s(1-{\mu_p}^2)}} \qquad Eq.\ 16$$

where: L_p is the Westergaard's radius of relative stiffness of concrete slab [mm]. E_p is modulus of elasticity [MPa] of-, h_p is the thickness [mm] of-, and μ_p is Poisson's ratio [-] of-concrete slab. Notations of λ_t, λ_r, λ_{long}, λ_{lat} [-] are Westergaard's moment influence factors in tangential, radial, longitudinal and lateral directions respectively. And k_s is modulus of subgrade reaction [N/mm^3].

Then for each x_k, where $k = \{i\ ,\ j\}$, the respective radial and tangential moment influence factors of inner and outer rails can be calculated using the same formulas as follow:

$$\lambda_{r,k} = 0.207 - 0.538\left(\frac{x_k}{L_p}\right) + 0.6009\left(\frac{x_k}{L_p}\right)^2 - 0.382\left(\frac{x_k}{L_p}\right)^3 + 0.137\left(\frac{x_k}{L_p}\right)^4 - 0.0253\left(\frac{x_k}{L_p}\right)^5 + 0.00186\left(\frac{x_k}{L_p}\right)^6 \qquad Eq.\ 17.(a)$$

$$\lambda_{t,k} = 0.248 - 0.349\left(\frac{x_k}{L_p}\right) + 0.2035\left(\frac{x_k}{L_p}\right)^2 - 0.0536\left(\frac{x_k}{L_p}\right)^3 + 0.00518\left(\frac{x_k}{L_p}\right)^4 \qquad (b)$$

Seeing from the original chart developed by Westergaard (1926) (see Figure 143 in the Appendix 2, pp. 225) and polynomial regression function shown in the Figure 9, if the distance of the load (x) is farther away from the point of interest of stress calculation, the influence line of moment (λ) is reduced. Furthermore, when $x/L \geq 4$, the λ values are gradually reduced close to zero. This limit can be also used to estimate the number of rail-seats should be considered in the calculation. Therefore, all of the neighboring loads which have $x/L \geq 4$ can be neglected, since they have a very small contribution to the stress magnitude at the point of interest.

b) Approach II. Beam-Beam Model (Combination of Zimmermann, 1888 & Zimmermann, 1888 / CZZ Method)

In this approach, both rail and underlying concrete slab are modelled as beams. The first calculation follows the rail and elastic-pad analysis in the sub chapter 4.1.1 above. And then similar to the analysis of the rail, the concrete slab is also idealized as a beam, which is located on a continuous support of soil and has to bear discrete rail-seat loads. Because the idealization of the whole track is as two-overlaying-beam model, thus, the analysis only considers the half part of the track (single rail analysis). Only the greatest value of load distribution factors in a curve can be considered (only $f_{c,i} = 1.2$). The closed form equation of CZZ method for longitudinal bending moment can be seen below:

$$M_{max} = \overbrace{\frac{Q_0.a_s.L_{pb}.f_d}{8.L_r}}^{\text{factor of } Q_0}\left[\underbrace{f_{c,i}}_{\text{factor of } S_0} + \overbrace{2.}^{\text{to consider both sides of a rail}}\underbrace{\sum_{i=1}^{n}\left(\frac{sin\left(\frac{i.a_s}{L_r}\right)+cos\left(\frac{i.a_s}{L_r}\right)}{e^{\left(\frac{i.a_s}{L_r}\right)}}\right)}_{\text{factor of } S_{i,\,1\geq i\geq n} \text{ and } \eta_z}.\underbrace{\left(\frac{-sin\left(\frac{i.a_s}{L_{pb}}\right)+cos\left(\frac{i.a_s}{L_{pb}}\right)}{e^{\left(\frac{i.a_s}{L_{pb}}\right)}}\right)}_{\text{factor of bending moment } \mu_z}\right] \quad \textit{Eq. 18}$$

The L_r equation is the same as shown in the Eq. 11 (a). Radius of relative stiffness of concrete slab, which is idealized as a beam on continuous support (L_{pb}) follows this expression:

[17]
$$L_{pb} = \sqrt[4]{\frac{4.E_p.I_{pb}}{b_b.k_s}} \qquad \textit{Eq. 19.(a)}$$

$$I_{pb} = \frac{1}{12}b_b.{h_p}^3, thus\ L_{pb} = \sqrt[4]{\frac{{E_p.h_p}^3}{3.k_s}} \qquad \textit{(b)}$$

where: L_{pb} is characteristic length [mm] of-, E_p is elastic modulus [MPa] of-, h_p is thickness [mm] of-concrete slab, b_b is slab width considered in the beam model [mm], k_s is modulus of subgrade reaction [N/mm^3].

In the beam model of a concrete slab, the width of the beam (b_b) is frequently assumed as a half of the actual width of the concrete slab. The bending tensile stress can be calculated using similar way as CZW method showed in the Eq. 12.(a) above by also considering a half of the actual width of the concrete slab (b_b).

4.1.3. Analysis of Deflection of Concrete Slab and Vertical Stress (Pressure) on Subgrade

a) Approach I. Beam-Slab Model (Zimmermann, 1888 & Westergaard, 1926)

Based on the Westergaard (1926) deflection formulation (see Eq. 121 in the Appendix 1, pp.219), the same way can be applied for calculation of maximum deflection of the concrete slab [mm] as described in this following formula:

$$y_{max} = \frac{Q_0.a_s.f_d}{2.L_r.k_s.{L_p}^2} \times \left\{ \begin{array}{l} \frac{f_{c,i}}{8}\left[1 + \left(0.366\log\left(\frac{r}{L_p}\right) - 0.225\right)\left(\frac{r}{L_p}\right)^2\right] \\ \quad + \left[2.f_{c,i}\sum_{i=1}^{n}\left(\frac{\sin\left(\frac{i.a_s}{L_r}\right) + \cos\left(\frac{i.a_s}{L_r}\right)}{e^{\left(\frac{i.a_s}{L_r}\right)}}\right)\gamma_{d,i}\right] \\ +f_{c,j}\left[\lambda_{y,j=0} + 2.\sum_{j=1}^{n}\left(\frac{\sin\left(\frac{j.a_s}{L_r}\right) + \cos\left(\frac{j.a_s}{L_r}\right)}{e^{\left(\frac{j.a_s}{L_r}\right)}}\right)\gamma_{d,j}\right] \end{array} \right\} \quad \textit{Eq. 20}$$

where: *r* is radius of circular load [mm]. For slab track analysis, *r* can be roughly assumed as the equivalent radius derived from the elastic-pad contact area. Meanwhile for a ballasted track system, *r* can be approximated as the equivalent radius of the area with support under a sleeper (see illustration in the Figure 141, in the Appendix 1, Section A.1.1, pp. 216).

According to the Westergaard's deflection influence line chart (Figure 144 in the Appendix 2, pp.225), 4-degree regression functions of γ_d are defined (see also Figure 9) as follows[17]:

- Westergaard's deflection influence factor of neighboring longitudinal rail-seat loads of the inner rail and outside of the wheel load location, for $1 \leq i \leq n$:

  $x_i = i.a_s$ *Eq. 21*

- Westergaard's deflection influence factor of neighboring transverse rail-seat loads of the outer rail and outside of the wheel load location, for $1 \leq j \leq n$:

  $\beta_j = tan^{-1}\left(\frac{s}{j.a_s}\right)$ *Eq. 22.(a)*

  $x_j = \frac{j.a_s}{cos\beta_j}$ *(b)*

- Westergaard's deflection influence factor of neighboring transverse rail-seat load of the outer rail on the single point of wheel load location, for $j=0$:

  $x_j = s$, *where s is the distance between center lines of inner and outer rail* *Eq. 23*

Then for each x_k, where $k = \{i , j\}$, the respective deflection influence factors of the inner and outer rails can be calculated using the same formulas as follow:

$$\textit{if } \mathbf{0} < \frac{x_k}{L_p} < 4 \textit{ then}: \qquad \textit{Eq. 24.(a)}$$

[17]
$$\gamma_{d,k} = 0.1269 - 0.0331\left(\frac{x_k}{L_p}\right) - 0.0241\left(\frac{x_k}{L_p}\right)^2 + 0.0109\left(\frac{x_k}{L_p}\right)^3 - 0.0012\left(\frac{x_k}{L_p}\right)^4 \qquad (b)$$

$$\textit{else if } \frac{x_k}{L_p} \geq 4 \textit{ then}:$$

$$\gamma_{d,k} = 0 \qquad (c)$$

Then the vertical pressure P_{max} [MPa] on the top of soil can be defined using this linear relationship:

$$P_{max,I} = k_s . y_{max} \qquad \textit{Eq. 25}$$

where: k_s is modulus of subgrade reaction [N/mm^3].

b) Approach II. Beam-Beam Model on a Continuous Support (Zimmermann, 1888 & Zimmermann, 1888)

Conforming to the Zimmermann's moment and deflection equations (see from Eq. 111 to Eq. 115 in Appendix 1, pp.217), the maximum deflection of the concrete slab can also be approximated by using beam-beam model of track laid on a continuous elastic foundation support. The mixed formula is shown in this following equation:

$$y_{max} = \frac{Q_0 . a_s . f_d}{4 . b_b . k_{sb} . L_r . L_{pb}} \left[f_{c,i} + 2 . \sum_{i=1}^{n} \left(\frac{sin\left(\frac{i.a_s}{L_r}\right) + cos\left(\frac{i.a_s}{L_r}\right)}{e^{\left(\frac{i.a_s}{L_r}\right)}} \right) . \left(\frac{sin\left(\frac{i.a_s}{L_{pb}}\right) + cos\left(\frac{i.a_s}{L_{pb}}\right)}{e^{\left(\frac{i.a_s}{L_{pb}}\right)}} \right) \right] \qquad \textit{Eq. 26}$$

Similar to the *Approach I* of beam-slab model, the vertical pressure on subgrade can be estimated using linear correlation between maximum deflection of concrete slab and modulus of subgrade reaction as shown in the Eq. 25 above.

4.2. Theoretical and Empirical Correlations of Different Soil Stiffness Parameters

The main obstacle of combining the analytical methods and different criteria mentioned above is to correlate the different parameters employed in the different formulations and models, especially soil parameters. *Combination of Zimmermann & Westergaard* (CZW) and *Combination of Zimmermann & Zimmermann* (CZZ) methods utilize a simple single stiffness parameter of soil as modulus of subgrade reaction/reaction modulus (k_s).

Heukelom & Klomp (H&K) fatigue criterion employs dynamic modulus of deformation, meanwhile Li & Selig (L&S) failure criteria consider more parameters based on soil types, soil cyclic parameters and static compression strength of soil (σ_s or q_u). The best way to

obtain these parameters is by geotechnical investigations and doing several tests in laboratory or field measurements. Yet, full-scale laboratory and complete field tests frequently demand a high cost and time for some reasons of practical purpose. Another way, several works have been done by some researchers to correlate these parameters based on theoretical and empirical approaches.

Theoretical approach assumes that the media is homogenous, isotropic and linear elastic. This follows stress-strain correlation of Young's theory of modulus of elasticity *E* and Hooke's law [146] of a spring coefficient *k*:

[146] $$k = \frac{E.A}{h}\left[\frac{N}{mm}\right]$$ *Eq. 27*

or for reaction modulus in an infinite media can be assumed as:

$$k = \frac{E}{h}\left[\frac{N}{mm^3}\right]$$ *Eq. 28*

where: *A* is the cross-section area of spring [mm^2] and *h* is the length of the spring [mm].

In a multilayer system, which consists trackbed layers resting on the top of subsoil, this approach assumes the system as a set of springs in series. When the system is assumed as a homogenous equivalent half-space media, which follows Odemark's formulation, then the *k* on the top of soil might be assumed following Eq. 28. Combining Eq. 28 and Odemark's *Method of Equivalent Stiffness* (MET) formulation (see Eq. 125 in the Appendix 1, pp.220):

$$k_s = \frac{X_s}{X_m}$$ *Eq. 29 (a)*

where:

$$X_s = \sqrt[3]{\frac{{E_s}^4}{(1-{\mu_s}^2)}} \quad and \quad X_m = \sum_{i=1}^{n} h_i . \sqrt[3]{\frac{E_i}{(1-{\mu_i}^2)}}$$ *(b)*

finally:

$$E_s = \sqrt[4]{{k_s}^3(1-{\mu_s}^2){X_m}^3}$$ *(c)*

where: k_s, E_s and μ_s are reaction modulus [N/mm^3] of-, elastic modulus [MPa] of- and Poisson's ratio [-] of- soil respectively; and E_i, h_i and μ_i are elastic modulus [MPa] of-, actual thickness [mm] of- and Poisson's ratio [-] of- layer *i* of multilayer trackbed system located on the top of soil.

The assumption of this correlation is strongly theoretical, which does not depict the actual multilayer system of concrete slab and/or trackbed and soil, especially for flexural stress analysis of a concrete slab. For that matter, concrete slab is more correct to be idealized by

utilizing plate theory than half-space theory. Nevertheless, this analytical approach can still be considered in an estimation of vertical pressure distribution in a half-space media. Furthermore, by using correction factors, those limitations can be minimized in a simple investigation of stress distribution in trackbed and soil. This is taken to gain more effective and realistic result, which is still in a safe and economical range of a design.

Based on Boussinesq theory, Timoshenko and Goodier (1951) made correlation between modulus of subgrade reaction (k_s) and deformation modulus (E_v or E_{def})[136]. This correlation is showed in the equation Eq. 30, which implies a correlation to *Plate Bearing Test* (PBT) method. Thus, this formulation looks correlating modulus of subgrade reaction closer to deformation modulus (E_v) than to elastic modulus (E_s). In practice, many engineers frequently assume deformation modulus (E_v) or resilient modulus (M_r) as elastic modulus (E_s) in a design calculation. The fact is that modulus of elasticity is actually bigger than deformation modulus. Thus, taking above assumption, the design is placed in a safer side. M_r has stronger correlation than deformation modulus (E_v) to modulus of elasticity (E_s), since it only takes into account the elastic strains due to cyclic loading in its determination. PBT method and E_v value are widely used in many design standards in many countries, especially in Europe as stiffness parameter of pavement design.

[136] $$k_s = \frac{2E_v}{\pi . r(1-\mu^2)}$$ *Eq. 30*

AASHTO (1993)[1] defined empirical correlation of M_r and k_s as follows:

[1] $$k_s = 2.029x10^{-3}M_r$$ *Eq. 31*

where k_s = modulus of subgrade reaction [N/mm^3], E_s= elastic modulus [MPa], r = radius of plate bearing test [mm], M_r = resilient modulus [MPa].

Transportation Research Board (TRD), 2008[139], summarized various correlations of subgrade stiffness parameters from several authors. They showed Thompson and Robnett (1979)[135]formulation to relate M_r and unconfined compressive strength (q_u) as follows:

[135] $$M_r[MPa] = 0.31q_u[kPa] + 5.93$$ *Eq. 32*

Tompai (2008)[138] made an investigation to get relations among static modulus of deformation of second loading (Ev_2), dynamic modulus of deformation (Ev_d) and dynamic modulus (E_{dyn}) as shown in this following table:

Table 4. Conversion formulas of static and dynamic deformation modulus, and dynamic modulus of elasticity after Tompai (2008)

Type of subsoil or subgrade layer	Ev_2 and Ev_d	Ev_2 and E_{dyn}
Coarse and fine grained soils	$Ev_2 = 1.58\ Ev_d$	$Ev_2 = 0.90\ E_{dyn}$
Silty soils	$Ev_2 = 1.30\ Ev_d$	$Ev_2 = 0.80\ E_{dyn}$
Crushed stone subgrade layers, mechanically stabilized base course	$Ev_2 = 1.69\ Ev_d$	$Ev_2 = 0.93\ E_{dyn}$

NAVFAC Design Manual (1986)[90] recommended a correlation between modulus of subgrade reaction (k_s) and unconfined compressive strength (q_u) and published this chart:

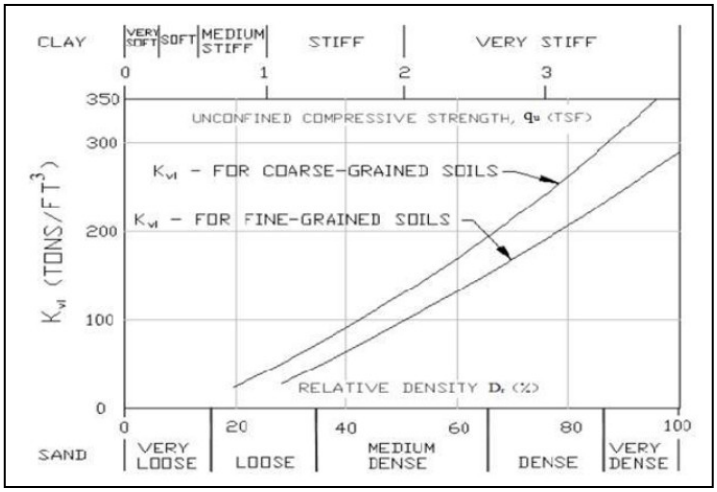

Figure 10. Correlation between modulus subgrade reaction and unconfined compressive strength after NAVFAC (1986)

NAVFAC's chart can be represented by regression equations along these formulations:

- for coarse-grained soils:

$$q_u = 7503.9k_s{}^3 - 12384.6k_s{}^2 + 4068.4k_s + 45.3 \qquad \textit{Eq. 33.(a)}$$

or $$k_s = 2x10^{-9}q_u{}^3 - 6.18x10^{-7}q_u{}^2 + 4x10^{-4}q_u - 1.9x10^{-2} \qquad \textit{(b)}$$

A proximally valid for $0.005 \leq k_s \leq 0.2$ *N/mm³and* $65 \leq q_u \leq 425$ *kPa*

- for fine-grained soils:

$$q_u = 145523.05k_s{}^3 - 34738.91k_s{}^2 + 5427.95k_s + 53.28 \qquad \textit{Eq. 34.(a)}$$

or $$k_s = -3.312x10^{-10}q_u{}^3 + 6.258x10^{-7}q_u{}^2 + 7.094x10^{-5}q_u - 3.491x10^{-3} \qquad \textit{(b)}$$

A proximally valid for $0.005 \leq k_s \leq 0.1$ *N/mm³ and* $80 \leq q_u \leq 395$ *kPa*

where: q_u is unconfined compressive strength [kPa] and k_s is modulus of subgrade reaction [N/mm^3].

Terzaghi and Peck (1948 & 1967)[133] suggested a correlation among soil consistency, N-SPT values and unconfined strength of cohesive soils as shown in the Table 5.

Table 5. Correlations among soil consistency, N-SPT values and unconfined strength of cohesive soil after Terzaghi & Peck (1948 & 1967)

Consistency	N-SPT Value	Unconfined compressive strength, q_u (kPa)
Very soft	0 - 2	< 24
Soft	2 - 4	24 - 48
Medium stiff	4 - 8	48 - 96
Stiff	8 - 15	96 - 192
Very Stiff	15 - 30	192 - 383
Hard	> 30	> 383

NAVFAC Design Manual (1986)[90] also classified the characteristics of soil groups based on the *Unified Soil Classification System* (USCS). Fine-grained soils characteristics and the typical design values for roads and airfields are summarized below in the Table 6.

Table 6. Characteristics of fine-grained soil groups pertaining to roads and airfields after NAVFAC (1986)

Type	Description	Not Subjected to Frost Action			Potential Frost Action	Typical Design Values	
		As Subgrade	As Subbase	As Base		*CBR* [%]	k_s [N/mm^3]
ML	Inorganic silts & clayey silts	poor to fair	not suitable	not suitable	medium to very high	≤ 15	0.027-0.054
CL	Inorganic clays of low to medium plasticity	poor to fair	not suitable	not suitable	medium to high	≤ 15	0.014-0.041
OL	Organic silts and silt-clays, low plasticity	Poor	not suitable	not suitable	medium to high	≤ 5	0.014-0.027
MH	Inorganic clayey silts, plastic silts	Poor	not suitable	not suitable	medium to very high	≤ 10	0.014-0.027
CH	Inorganic clays of high plasticity	poor to fair	not suitable	not suitable	medium	≤ 15	0.014-0.041
OH	Organic clays and silty clays	Poor to very poor	not suitable	not suitable	medium	≤ 5	0.007-0.027

4.3. Development of Computer Program based on Combination of Analytical-Empirical Methods of Superstructure Analysis

Based on the combinations of analytical and empirical methods described in subchapter 4.1, a programmed spreadsheet is built in *Microsoft Excel* using *Visual Basic Application* (VBA) programming language. Newton-Raphson iteration [147] is employed to calculate the required stiffness of elastic-pad and direct loop iteration is used to calculate bending tensile stress, deflection and vertical pressure. Four analytical models based on combination of Zimmermann and Westergaard methods are given codes as follows:

- ***CZW-1*** is analytical *beam-slab model* employing Combination of Zimmermann (1888) & Westergaards (1926) for *moment and bending tensile stress calculations*.

- ***CZW-2*** is analytical *beam-slab model* utilizing Combination of Zimmermann (1888) & Westergaards (1926) for *deflection and vertical pressure calculations*.
- ***CZZ-1*** is analytical *beam-beam model* utilizing Combination of Zimmermann (1888) & Zimmermann (1888) for *moment and bending tensile stress calculations*.
- ***CZZ-2*** is analytical *beam-beam model* employing Combination of Zimmermann (1888) & Zimmermann (1888) for *deflection and vertical pressure calculations*.

Example B

For the example of calculation, the input parameters are given as follows:

a) Static wheel load of 125 kN,
b) Dynamic factor DAF f_d = 1.6 (see example calculation in the Appendix 4, pp.227) and load distribution factor on a curve $f_{c,i}$ = 1.2 for inner rail and $f_{c,j}$ = 0.8 for outer rail.
c) Rail profile 60E2, with $E = 2.1 \times 10^5$ and $I = 30.55 \times 10^6$ mm^4
d) Desired rail deflection $y \leq 2.0$ mm
e) Concrete slab with thickness h_c = 300 mm, E_c = 34,000 MPa, and μ_c = 0.15.
f) Modulus of subgrade reaction k_{sub} is varied from 0.01 to 0.3 N/mm^3.

The spreadsheet program gives results: the initial estimation of the stiffness of elastic-pad for the desired rail deflection 2 mm is 22.5 kN/mm. The bending tensile stress on concrete slab (*Sx*) and vertical pressure on soil (*Pz*) for different values of soil's subgrade reaction are shown in this following figure:

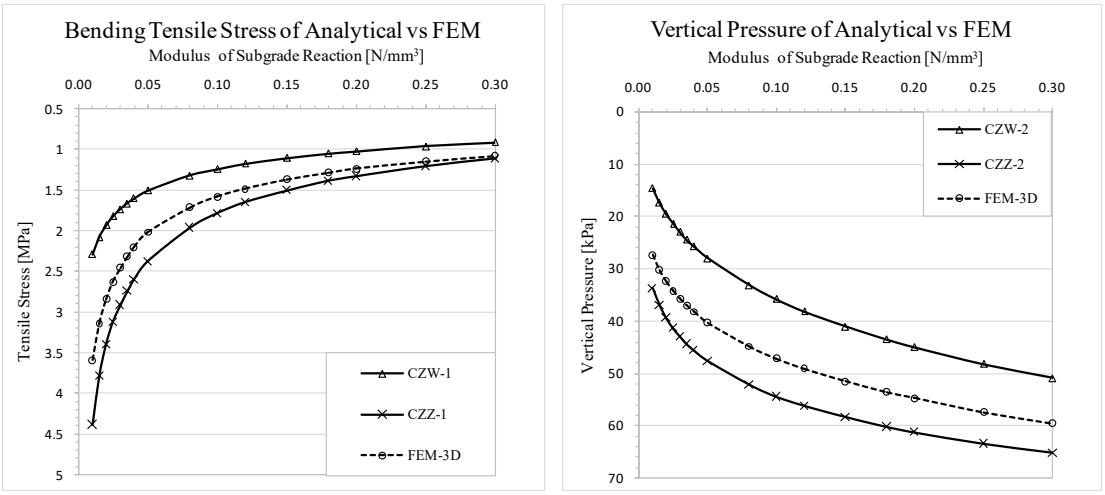

Figure 11. Comparison of bending tensile stress on concrete slab and vertical pressure on soil between Analytical Methods and FEM

It can be observed rom Figure 11 that the results of static FEM are in between the results of CZW and CZZ models. The FEM-3D can be used as reference, because in FEM, a track can

be modelled closer to the reality in particular regarding track geometry and dimension. Thus, it can be considered to deliver more reliable results.

Modelling the track as beam-beam model (CZZ model) gives higher values of bending tensile stress on concrete slab and vertical pressure on soil than FEM and beam-slab model (CZW). After some trial of calculations, it is found that the result of beam-beam model is strongly influenced by the given width of the beam. The wider the width of the beam considered in the beam analysis, the lower the resulted bending tensile stress and vertical pressure. This also indicates that the wider the given width in beam-beam model makes the idealization closer to beam-slab model. The result of CZZ model takes into account the width of the beam of 1.3 m, which is half of the actual minimum width of the concrete slab (2.6 m).

It can be also seen that the two first analytical beam-slab models (CZW-1 and -2) are underestimated in comparison with FEM. After some calculation tests, adding adjustment factor of 1.2 - 1.35 on CZW-1 and CZW-2 makes the estimation of both CZW models closer to FEM. It demonstrates that CZW-1 and CZW-2 analytical models are fairly acceptable to compute bending tensile stress and vertical pressure with a certain adjustment factor. In addition, in comparison to CZZ method, CZW model has more advantages of 1) the ability to involve the loads from both rails, 2) the capability to take into account different load distributions between inner and outer rails, e.g. in a curve, 3) beam-slab model depicts better idealization of quasi 3D of rails and concrete slab of a ballastless track, and 4) with correct adjustment factor, the result can be closer to FEM.

4.4. Critical Thickness of a Single Layer Concrete Slab on Different Subgrade Strengths

An example of applications of the CZW mathematical model is for instance to define the minimum required thickness of a concrete slab placed on subsoil. This can be estimated if reaction modulus of subsoil is given. The stress analysis is then synchronized with the limit criteria to get critical thickness of the concrete slab, which can be based on two major criteria:

- safety limit of the concrete against flexural fatigue failure, which is assessed using maximum allowable bending tensile stress of the concrete slab (e.g. using Smith approach, see Eq. 129 in the Appendix 1, pp.222)
- safety limit of the subgrade or subsoil, by taking into account:

- × maximum allowable pressure of the subgrade or subsoil (e.g. using Heukelom & Klomp formulation, see Eq. 136 in the Appendix 1, pp. 224), and/or
- × maximum allowable deviator stress due to limitation of soil shear failure and excessive plastic deformation (e.g. using Li and Selig method, see again Eq. 3 and Eq. 4, pp. 20).

Implementation of Newton-Raphson's iteration [147] to solve this complex mathematical model is very hard and the calculation process is time-consuming. The reason is that the derivation of this equation is also very complex and very long. Direct loop iteration therefore fits better to solve the equations.

The spreadsheet program is extended and two analytical models of CZW-1 and CZW-2 are utilized to compute critical thickness of single layer concrete slab laid on soil. The basic input data are the same as the Example B in the subchapter 4.3 before. Concrete slab is C35/45, which has elastic modulus of 34 GPa and mean static flexural strength (f'_t) of 3.2 MPa in accordance with EN1992-1-1[38]. The permissible levels bending tensile stress of concrete are estimated by considering central Europe condition: traffic loading 5% of the total number of load cycles of 2.10^6 and critical temperature gradient in summer and winter dependent on the thicknesses of concrete slab (according to Eid (2012) [31]). The example calculation can be seen in the Example H in Appendix 4, pp. 228.

Two analytical models in combination with two limit state criteria are used for critical thickness analysis and are given codes as follows:

- ***CZW-1+S*** is model employing Combination of Zimmermann (1888) & Westergaards (1926) for *moment and bending tensile stress calculations* and *criteria of flexural fatigue strength limit using Smith approach*.
- ***CZW-2+H&K*** is model utilizing Combination of Zimmermann (1888) & Westergaards (1926) for *deflection and pressure calculations* and *criteria of maximum pressure on the subgrade or subsoil based on Heukelom & Klomp method*.

The algorithm of direct loop iteration employing those models is illustrated in the Figure 12.

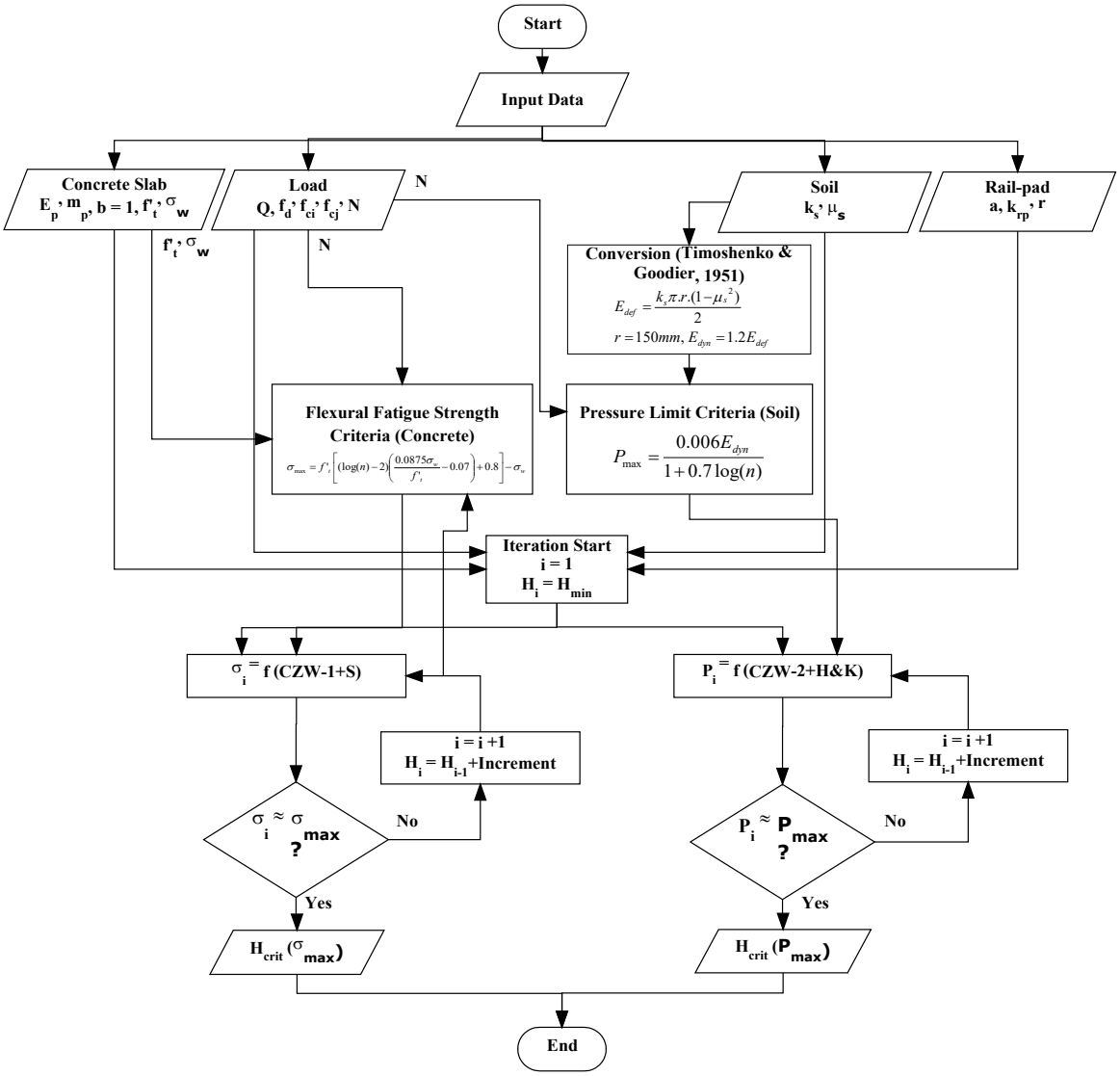

Figure 12. Flowchart of algorithm of direct loop iteration

As it is shown in the Figure 12, Heukelom & Klomp criterion needs parameter of dynamic modulus (E_{dyn}) of soil to define maximum allowable pressure on soil due to cyclic loading. However, the soil input data is variations of static modulus of reaction (k). The E_{dyn} value can be estimated using linear correlation $E_{dyn} = 1.2\ E_{def}$ and $E_{def} = k*h_{eq}$ (see Eq. 28) or Timoshenko & Goodier (1951) approach (see Eq. 30). Both conversions show contrasting results as it is depicted in the Figure 13. Using linear conversion (Eq. 28) to estimate maximum allowable pressure on soil demonstrates unrealistic result because it does not present significant change of the critical thickness of concrete slab, even when soil is very soft. Comparing both approaches, Timoshenko & Goodier (1951) estimation is more realistic to be correlated to the Heukelom & Klomp approach. The explanation of that occurrence is that Heukelom & Klomp approach was based on laboratory test of fatigue limit defined by cyclic loading test using circular plate. Thus, modulus deformation (Timoshenko & Goodier

conversion) has stronger correlation to this approach. Therefore, for conversion of k to E_{def} and E_{dyn} to estimate the allowable pressure on soil, it is suggested to use Timoshenko & Goodier (1951) approach.

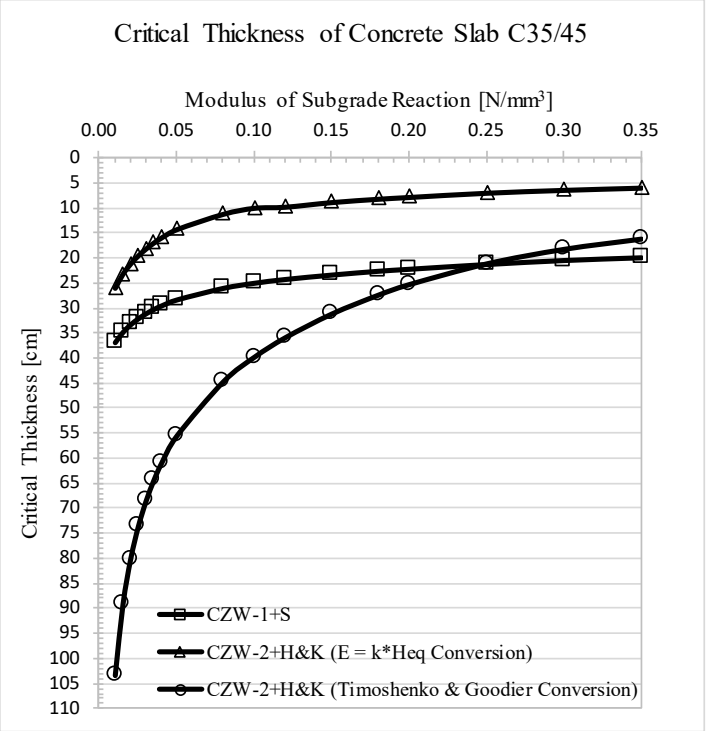

Figure 13. Comparison critical thickness estimated using different limit criteria

Comparison of the two models to estimate the minimum thickness of single layer concrete slab C35/45 located on subgrade/subsoil is depicted in the Figure 14. For the given data and defined criteria, some points can be derived from these charts on Figure 14 are:

- Both criteria of CZW-1+S and CZW-2+H&K are intersecting in a critical soil reaction modulus of 0.25 N/mm^3, which results critical thickness of concrete slab about 22 cm (Figure 14.a). The thickness value is in critical limit of pressure on soil (Figure 14.b), of flexural stress (Figure 14.c) as well as of deflection (Figure 14.d).
- Comparing the critical thicknesses between CZW-1+S and CZW-2+H&K from the Figure 14.(a): limit criterion of flexural tensile stress on concrete slab (Smith's criteria) is more decisive than criterion of limit of pressure on subgrade (Heukelom & Klomp/H&K's criterion) when the subgrade reaction moduli are more than 0.25 N/mm^3 (good to very stiff subgrade). H&K's criterion exceeds the Smith's one when the reaction moduli of subgrade are lower than 0.25 N/mm^3.
- Figure 14.(b) exhibits similar behaviour that from all thickness variations and in the subgrade reaction modulus values below 0.25 N/mm^3 (moderate to low), H&K's pressure limit criterion is more decisive than Smith's flexural limit criterion.

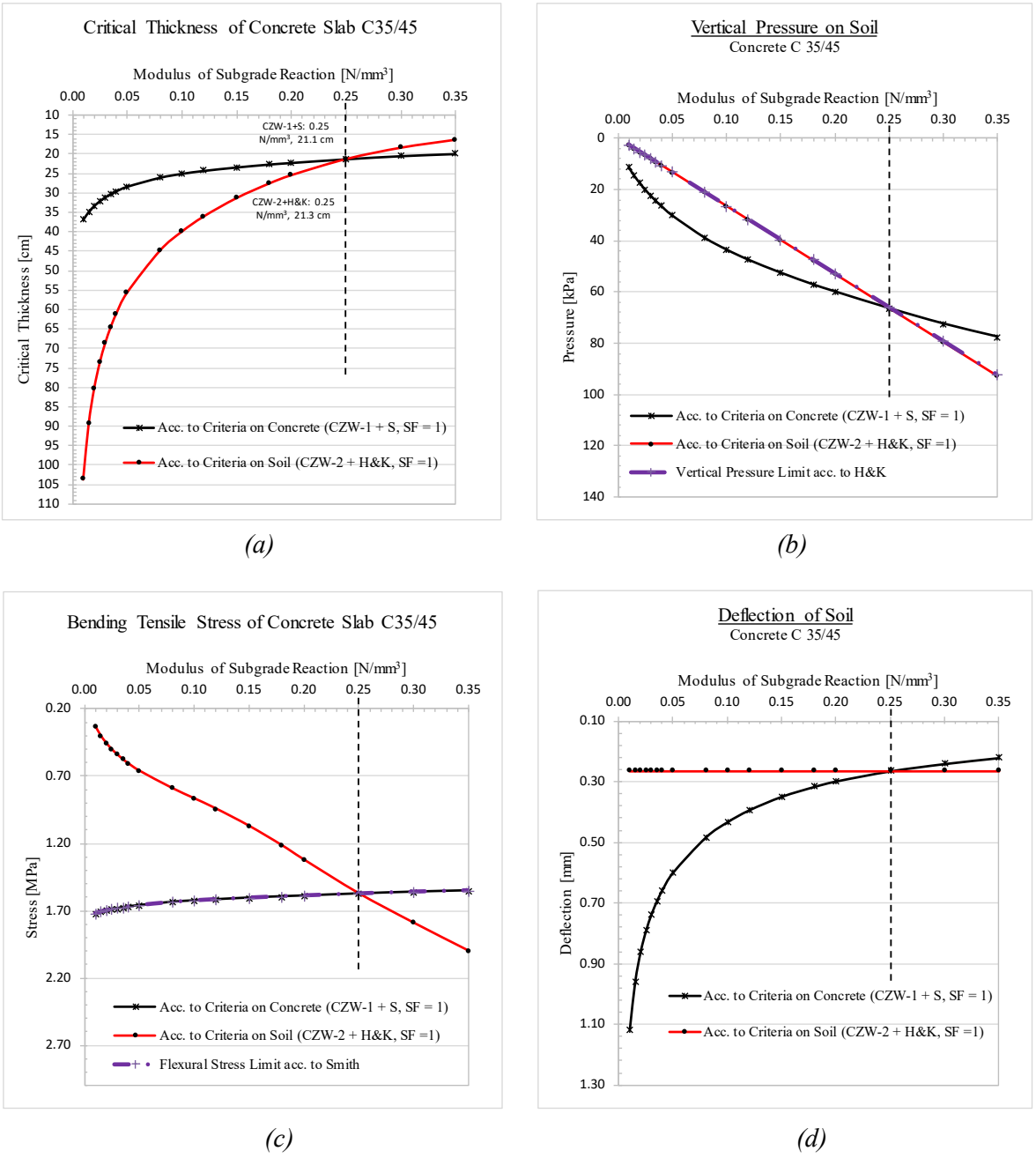

Figure 14. Critical thickness and flexural stress of concrete and deflection of and vertical pressure on soil of a slab track constructed as single layer concrete slab

For the given data above, it is shown on the Figure 14 that the values of modulus subgrade reaction of more than 0.25 N/mm^3 do not give significant influence to the change of the critical thickness of concrete slab. Thus, the reaction modulus value of 0.25 N/mm^3 can be considered as the threshold of minimum strength capacity on the top of a base layer of a slab track regarding safe limit of flexural strength of a thin concrete slab track.

The German guideline of road works *ZTV E-StB 09/2012* which regulates about the earthwork mentions that the modulus of deformation of second loading Ev_2 value of the

subgrade should not be less than 45 MPa in the design state of a low speed train, but 60 MPa is more recommended in the application state as well as for a high speed train [70][68]. However, it should be noted that for railway application, this value also needs to take into account train dynamic factor and different design life between roadway and railway.

Mattner (1986)[82] classified the condition of the subgrade or subsoil for a ballasted track system and showed that subgrade reaction modulus more than 0.14 N/mm^3 is already categorized as good strength of soil as shown in this table:

Table 7. Recommended ballast stiffness regarding different conditions of substructure/subgrade after Mattner (1986)

Ballast Stiffness (*k*)	**Conditions of Substructure/Sub-grade**
0.056 N/mm^3	Low bearing capacity of soil, e.g. uniform sands, silt
0.137 N/mm^3	Good bearing capacity of soil, e.g. compacted gravel (new construction)
0.235 N/mm^3	Very stiff sub-grade (rocky sub-grade)
0.435 N/mm^3	Rigid substructure, e.g. concrete slab, bridge deck

Theoretically, an ideal subgrade/subsoil with reaction modulus above 0.25 N/mm^3 does not need further improvement and a single layer of concrete slab might be placed on the top of it. However, in practice, providing base layer with reaction modulus in the range of 0.25 - 0.35 N/mm^3 in between concrete slab and subsoil provides more stable and a continuous rigid support to the superstructure. This is more recommended. It is also done to achieve an equilibrium structure, to be in a safe side and to cover unexpected nonlinearities behaviours which may occur in the reality. Moreover, in some cases in the practice, adding intermediate layer (trackbed) is more aimed to protect top layer and underneath layer (subsoil) against pumping effect, frost action or water penetration.

Furthermore, since the top layer is normally the most expensive one, the thickness of concrete slab should be designed at the minimum level, in which still fulfills the requirements of concrete slab regarding flexural strength and reducing the risk of excessive major cracks. From the charts above, the ideal thickness of thin slab concrete is averagely 22 cm, when the reaction modulus of the base layer is around 0.3 N/mm^3. As comparison, in a standard construction of Rheda-2000, CRCP slab with thickness of 24 cm is located on the top of concrete treated base (CTB) to achieve this purpose.

As shown in the Figure 14, theoretically by calculation, by using a very thick concrete slab more than 55 cm located on an extremely low bearing capacity of subsoil with reaction modulus below 0.05 N/mm^3, safety factor concerning limit criteria of pressure on soil can be fulfilled. However, soil stiffness in this range is not practically realistic for conventional single layer of concrete slab application without doing advanced geotechnical treatments, for instance soil reinforcements or installing piles. In addition, NAVFAC (1986)[90] (see Table 6 above) also noted that soil subgrade reaction modulus below 0.05 N/mm^3 is not suitable as a base layer. Moreover, Esveld (2001)[39] gave summary of the global values of reaction modulus and mentioned that soil with reaction modulus smaller than 0.02 N/mm^3 is categorized in poor condition and 0.2 N/mm^3 is in good condition for railway application.

Therefore, the soils with reaction modulus values greater than 0.2 N/mm^3 have a good bearing capacity. Meanwhile the ones with reaction modulus between 0.05 and 0.18 N/mm^3 can be said in between the range of soft and moderate stiff. Soil stiffness within this range may still need geotechnical treatments like soil stabilization or adding multilayer trackbed as pavement layer. Implementing trackbed layer will be discussed in the next Chapter 5.

5. Development of Analytical Design Method of Trackbed

5.1. Definition of Trackbed

There are different terminologies to describe trackbed layers in use by different countries, design standards, literature or researchers. In some literature, it is called "*Track Pavement*" layers, and in some other it is named as "*Subsystem of Superstructure "*. AFTES (2013) mentioned trackbed as reinforced concrete, plain concrete or asphalt foundations components in a ballastless track [3].

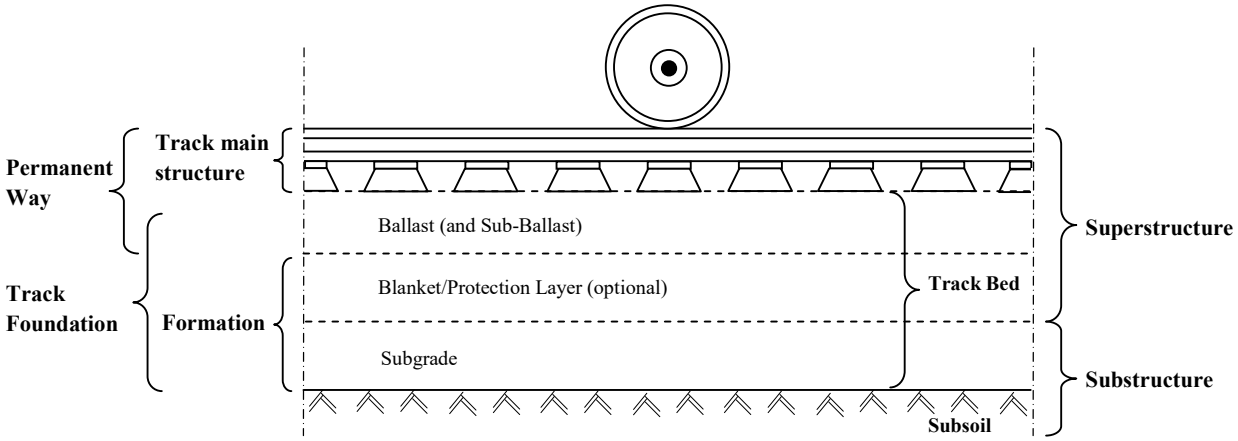

Figure 15. Illustration of different terminologies of track elements from literature

Two main different arguments of the use trackbed terminology are:

1. whether to consider trackbed only on the superstructure part (ballast, concrete or asphalt layer) and consider the sub and protection layers as a part of substructure or
2. to consider all the layers below sleepers until the top of subsoil as a trackbed layer.

In this research, the second definition is used. Therefore, in a ballasted track system, trackbed may consist of ballast, sub ballast, protection layers and subgrade. Meanwhile in a ballastless track system, trackbed may contains concrete slab, foundation and/or formation layers such concrete treated base, asphalt layer, unbound granular material, protection layer and subgrade. Composition of trackbed layers depends on the requirements of design, such major factors of geological and subsoil conditions, permanent way design, traffic and train loading, geographical and climate conditions (topography, temperature changes, frost action, rain intensity), water table level, drainage system, and some other minor factors.

Many research works concerning trackbed have been done so far, which are related to the use of different material types, variations of stiffness and thickness of the trackbed layers.

All of them depends on the design parameters and the function of the layers. However, trackbed in railway track system mostly utilizes a multilayered system.

5.2. Function and Design Parameter of Trackbed

Two main functions of trackbed are (1) to distribute and decrease gradually the load induced from the train traffic to a specified level, which can be safely supported by the subsoil and (2) to provide certain level of stability required by the upper layer (track main structure).

As mentioned by Huang et. al (1984)[55], the use of single layer (full depth) of construction for railway trackbed is inefficient. Huang et. al showed in his research that thinner asphalt layer resting on thicker base layer is more economical construction for a track supported by asphalt and base layer [55]. Especially for a track constructed on soft soil, the stress exerted from train traffic should be gradually decreased until a safe level to subsoil. In this case, when a single layer of trackbed is employed, theoretically, it requires either very high stiffness material or very high thickness of trackbed layer or combination of both. Nevertheless, due to economical aspect and practical purpose, total high of a construction is frequently limited. Furthermore, very high stiffness and thickness of single layer material placed on soft soil gives a great self-weight, which leads additional settlement on soft soil and is relatively more difficult in the construction stage.

Trackbed's static design parameters mainly consist of stiffness and thickness due to static loading of a train. The main criteria of the use multilayer system in a trackbed is to provide an equilibrium structure, which optimizes the track performance contributed from the characteristics of each layer.

5.3. Analytical Thickness Design Method of Trackbed

The end goal of developing a computer program by utilizing combination of classical theories is to build design charts of tracked thickness design for wide applications in practice. Conventional methods of Zimmermann, Westergaard, and Odemark can be applied to analyze stress distribution in a trackbed layer. And then the Heukelom & Klomp or Li & Selig methods can be used to define the permissible stress levels on subsoil as design criteria. CZW-1+S and CZW-2+H&K have demonstrated the ability to estimate the required thickness of single layer concrete slab track. Li & Selig method will also be discussed here by considering criteria of allowable deviator stress on subsoil against shear and plastic deformation failures. This model is given code as CZW-2+L&S.

It has been also figured out that a design using criteria of vertical pressure of soil is more decisive than criteria of flexural strength of concrete slab when the reaction modulus of soil is lower than 0.25 N/mm^3 (see Figure 14). This range of reaction modulus demands trackbed layer in a slab track system. Meanwhile, in a ballasted track system, flexural strength does not exist in an unbound granular trackbed material. Therefore, only vertical pressure on soil is utilized for the development of the analytical method of trackbed thickness design for ballastless and ballasted track systems.

The idea is to use an equivalent thickness of trackbed as the result of computations by combining those methods. Equivalent thickness of trackbed is the total thickness of trackbed layer, which has stiffness value equal to the stiffness of subsoil. And then this equivalent thickness is transformed back into multilayer system by applying Odemark method in reversed way. This follows linear spring stiffness correlation of homogeneous half space according to Hooke theory. Odemark formulation of multilayer elastic system can be expressed as:

$$h_{eq} = h_{eq,1} + h_{eq,2} + \cdots + h_{eq,n} \qquad \textit{Eq. 35.(a)}$$

$$h_{eq} = C_s . \sum_{i=1}^{n} h_i . \sqrt[3]{\frac{E_i}{(1-\mu_i{}^2)}} \qquad \textit{(b)}$$

$$C_s = \sqrt[3]{\frac{(1-\mu_s{}^2)}{E_s}} \qquad \textit{(c)}$$

where: $h_{eq,i}$ and $h_{eq,n}$ are the equivalent thicknesses of each layer from i to n, which depend on its modulus of elasticity and Poisson's ratio; h_i is the actual layer thickness and C_s is termed here as soil constant which depends on subsoil parameters of soil modulus of elasticity and Poisson's ratio.

Similar to the concept of multilayer thickness design for highway pavement and by introducing the terms of structural number (*SN*) and coefficient of relative strength of material (*a*), the equation above can be simplified by using scale factor of 10:

$$SN = a_1 h_1 + a_2 h_2 + \cdots + a_n h_n \qquad \textit{Eq. 36 (a)}$$

where $$SN = \frac{h_{eq}}{10.C_s} \;\; and \;\; a_i = 0.1\, x \sqrt[3]{\frac{E_i}{(1-\mu_i{}^2)}} \qquad \textit{(b)}$$

In this simplification, all of the superstructure and soil parameters is represented by ***SN*** value and the strength properties of trackbed material are characterized by constant value of ***a***. The factor of ***SN*** can be explained as a trackbed structural constant, which represents the total

required structural strength of a trackbed. The factor of a_i can be defined as coefficient of relative strength of a trackbed material ***i***, which is derived from static modulus of elasticity and Poisson's ratio of a material and represents the material strength of each layer. An approximation of coefficient of relative strength (a) of different materials can be defined using Eq. 36 (b) or taken from the general values in this table:

Table 8. Coefficient of relative strength

Material	Modulus of Elasticity [MPa]	Poisson's Ratio (μ)	Coefficient of Relative Strength (a)
Cement Concrete C50/60	38000	0.15	3.39
Cement Concrete C40/50	36000	0.15	3.34
Cement Concrete C35/45	34000	0.15	3.26
Concrete Treated Base (CTB)	15000	0.15	2.48
	10000	0.15	2.17
	5000	0.15	1.72
Asphalt Concrete	7000	0.30	1.97
	5000	0.30	1.76
	3000	0.35	1.51
	1000	0.35	1.04
	500	0.35	0.83
Crushed Stones Ballast or Base Layer	300	0.30	0.69
	250	0.30	0.65
	200	0.30	0.60
	150	0.30	0.55
	120	0.30	0.51
	100	0.30	0.47
Crushed Stones or Fine Grained Subbase Layer	80	0.33	0.45
	60	0.33	0.41
	45	0.33	0.37
	30	0.33	0.32
	25	0.35	0.31
	15	0.35	0.26

In the calculation of minimum *SN*, a multilayer system can be initially idealized as a single layer of a linear elastic homogenous half space, which has stiffness of soil and equivalent thickness of multilayer system. By using this approach, only soil stiffness parameter is needed in the analytical computation to obtain *SN*. Then afterwards, *SN* value is converted back into multilayer system, which has variation of stiffness and thickness of trackbed materials.

Thus, the actual stiffness of trackbed material, which is idealized using *SN* indirectly follows Hooke's law of series springs as well, which can be explained as follows:

$$\frac{1}{k_{sys}} = \frac{1}{k_1} + \frac{1}{k_2} + \cdots + \frac{1}{k_n} \qquad \textit{Eq. 37.(a)}$$

and Hooke's law (Eq. 28) in a homogenous half space media:

$$k_{sys} = \frac{E_s}{h_{eq}} = \frac{E_s}{h_{eq,1} + h_{eq,2} + \cdots + h_{eq,n}} \qquad \textit{(b)}$$

Therefore, Eq. 37.(a) is already directly applied in the *SN* formulation. Furthermore, *SN* also represents the two important parameters of material strength of trackbed namely stiffness and thickness. Another important factor is stiffness ratio between two adjacent layers. When there is a sharp different in thickness and stiffness, then the softer or thinner layer (normally subsoil) is more dominant for contributing the total stiffness of the trackbed system. In this approach, this correlation is compensated in the *SN* formulation of the equivalent thickness of each layer through equation Eq. 37, which represents a correlation among series of springs. The Eq. 37 gives total stiffness value which is always slightly lower than the lowest stiffness among the layers.

When subsoil is too soft, although the trackbed and track main structure layers are very stiff, but then the overall system is majorly influenced by the softest layer. Therefore, there must be an optimum stiffness ratio between layers. This case occurs in the reality, that if subsoil is very soft, hence the initial track problem comes from excessive settlement of the trackbed systems, which is majorly contributed from subsoil failures due to its low bearing capacity.

This idealization of transformation trackbed layers into a single layer half-space to initially estimate the required thickness of trackbed generally looks more appropriate for ballasted track system. The reason is that in a ballasted trackbed, the difference of the stiffness values of the layers from the top to bottom is not so sharp in comparison to the one of between a concrete slab and soft soil. This is the basic concept of two-layer system such as Westergaard method of concrete slab analysis. Fortunately, by utilizing Odemark's method of equivalent thickness, the level of the pressure on the top of soil can be approximated almost equal between single layer half-space and two-layer systems. However, it should be noted that this condition is only valid to estimate the pressure distribution in the trackbed layers within the scope of theoretical approach. It is not correct to use this idealization for analyzing the flexural stresses on concrete as the most application of Westergaard method for concrete slab analysis.

The existence of a stiff layer (concrete layer) on the top layer changes the distribution of the pressure on the underlying layer as explained by Molenaar (2009)[86] and illustrated in the following figure:

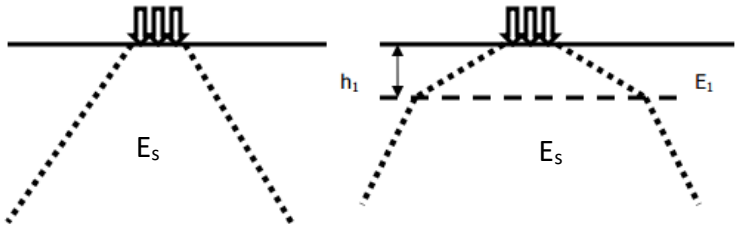

(a) half-space *(b) actual condition*

Note: picture is cited from and courtesy of Molenaar (2009) [86]

Figure 16. Effect of applying a stiff top layer on the vertical stress distribution

Molenaar (2009)[86] explained the principle of Odemark theory that stress distribution due to transformation of the stiff layer into half-space with stiffness equal to soil and equivalent thickness has the same magnitude at the bottom of the stiff layer as the one in a two-layer system as described in this figure:

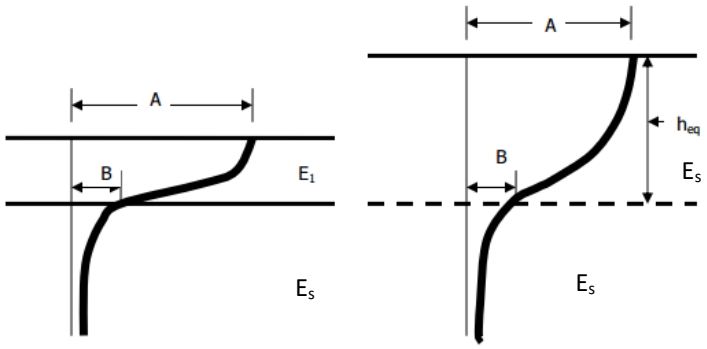

(a) two-layer system *(b) single layer half space*

Note: picture is cited from and courtesy of Molenaar (2009) [86]

Figure 17. Principle of Odemarks's Method of Equivalent Thickness

Verification of the proposed method applied for ballastless track is then performed. To validate the CZW-2 method and to observe the impact of providing stiff to very stiff top layers, the stiffness parameters (elastic modulus and thickness) of concrete slab are differentiated, namely: elastic moduli of 34 GPa and 40 GPa and thickness variations of 24, 30, 35, 40, 45 and 60 cm. Two calculations are compared using CZW-2 model, namely based on the two-layer system and conversion to a single layer half-space. All the parameters of rail, elastic-pad, and wheel load is the same as the given data before in the Example B of subchapter 4.3, pp. 36. The levels of pressure on soil due to the given variations and different reaction modulus values are shown in the Figure 18 below.

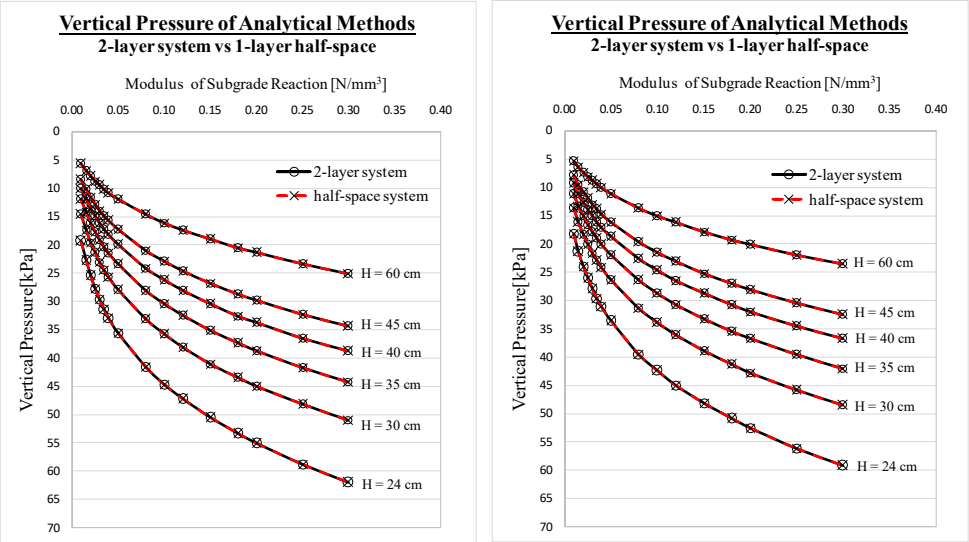

(a) Concrete slab E = 34 GPa *(b) Concrete slab E = 40 GPa*

Figure 18. Verification of transformation from 2-layer system into single layer half-space of CZW-2 model to estimate vertical pressure on soil

It is found from Figure 18 that in all variations, the levels of vertical stress on soil of both approaches are identical. Therefore, the proposed analytical method can be also applied for trackbed design of slab track based on soil pressure limit criteria.

In a three-layer trackbed system, there are three combinations of thickness, which two of the thicknesses are predefined and one of them are calculated. The two upper layers mostly have better quality and strength. Consequently, they are also normally more expensive than the lower layer. Thus, an optimum design is frequently obtained by defining h_1 and h_2 as minimum as possible according to design standard or requirements and then h_3 is calculated. Nevertheless, the other two combinations, which h_1 and h_3, and h_2 and h_3 are set as minimum can be also calculated as comparison to obtain the most optimum thickness combination.

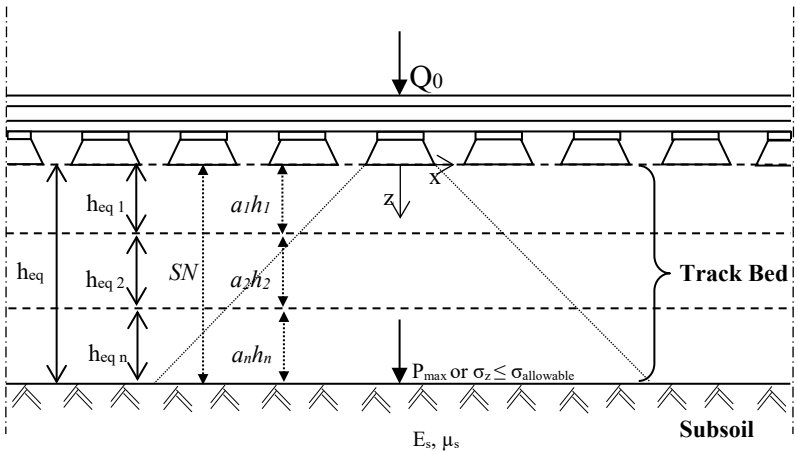

Figure 19. Sketch of trackbed thickness calculation

5.4. The Impact of Trackbed Width and Comparison between Analytical Thickness Design Method of Trackbed and FEM

Comparison of CZW-1 and CZW-2 methods with FEM of a single layer concrete slab has been performed (see Figure 11). Now the level of pressure on soil, in which trackbed is designed using the proposed method will be compared with FEM for verification of a multilayer system.

In a design of multilayer pavement system, there are four important factors: (1) stiffness of, and (2) thickness of -each layer (3) stiffness ratio- and (4) bond condition -between layers. Factors of (1), (2) and (3) are accommodated in the formulations of the proposed analytical method. Nevertheless, factor (4) considers only full bond condition between two adjacent layers. In the reality, bond condition is neither full bond nor no bond, but it is in between them. Bond condition actually affects vertical and shear forces transfer between two layers, which is neglected in this approach.

In addition, the analytical beam-slab model of CZW does not consider the actual width of the trackbed (because $B = 1$). In this approach, a trackbed is assumed as a semi-infinite plate. Widening the trackbed has actually advantages of reduction of the pressure on subgrade as well as greater areas for better distribution of the pressure subjected to subgrade.

Furtheremore, a previous study regarding different sleeper types with various dimensions and geometries (contact areas to subgrade) of ballasted track for high speed train done by Freudenstein (2004)[42] also demonstated that there are actually different levels of stress on subgrade due to different contact areas of sleepers to ballast. In this study, only the contact area of a standard sleeper B70 is considered in a ballasted track system. Greater contact areas of sleeper to the underlaying layer will reduce the level of stress on subgrade.

The investigation of the influence of different trackbed widths of a track is performed to the CZW-2 model and then static FEA result is used as reference. Two systems of slab track and ballasted track are analyzed in FEM. To compare both approaches, the trackbed layers are initally modelled in FEM with the same width as it is of the assumption of half-space in CZW-2 model. The minimum width of the trackbed layers is 2.8 m (considering the width of sleeper of 2.6 m in a ballasted track as well as 2.8 m minimum width of concrete slab track). Then the widths of the trackbed layers are varied up to 4.5 m to evaluate the CZW-2 model. The tracks are named as ST-1 (slab track) and BT-1 (ballasted).

FEM models are built in 3D as it is shown in the Figure 20. All track elements are modelled as solid elements and they are connected by rigid contact elements (full bond). Soil is modelled as solid element in the height of 1 m but the bottom parts of this element is meshed with surf element with property of modulus subgrade reaction. This is done to idealize the infinite depth of soil. The results of FEM simulations are depicted in the Figure 21 and Figure 22 below.

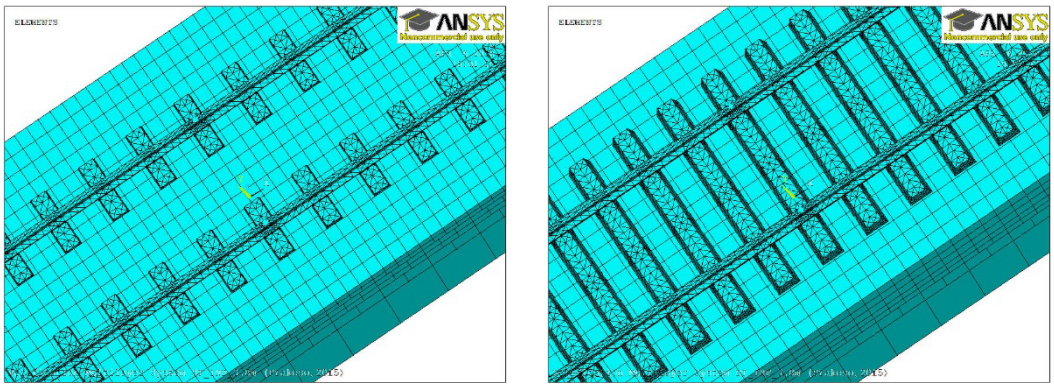

Figure 20. Mesh of 3D models of slab track and ballasted track with uniform widths of the trackbed layers

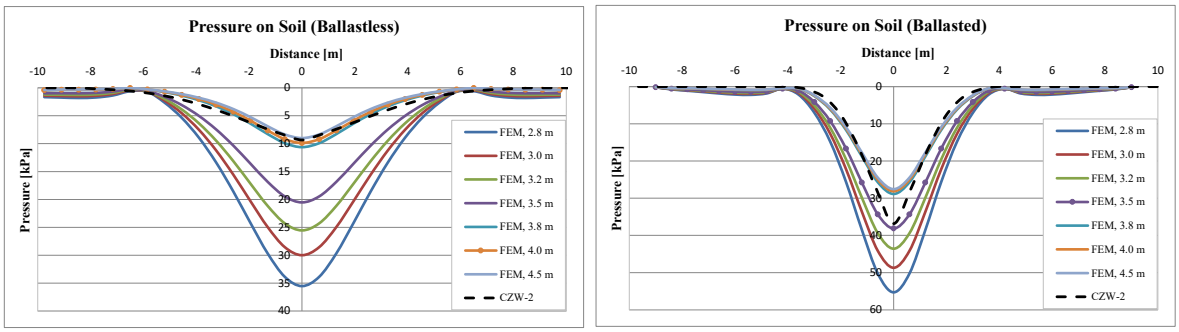

Figure 21. Comparison of the soil pressure levels between analytical approach and FEM by considering different widths of trackbed

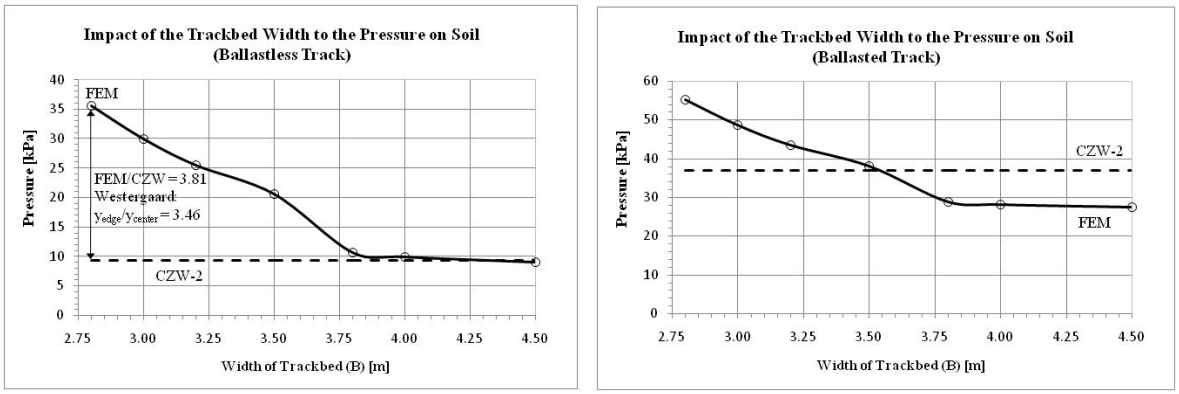

Figure 22. Impact of trackbed width to the level of pressure on soil

From the results of FEM simulations presented in the Figure 21 and Figure 22, the level of pressure on soil of both track systems almost remains constant when the widths of the trackbed are greater than 3.8 m. In this range, the levels of soil pressure of slab track estimated using CZW-2 model is similar with the ones of FEM. But the pressures on soil resulted from FEM becomes higher than CZW-2 estimations when a narrow trackbed smaller than 3.8 m is used.

The CZW-2 model is built based on Westergaard deflection formulation of slab center. When the slab is very narrow, in a slab track, the estimation of the pressure on soil is close to the original Westergaard formulation of slab edge. The rails are located close to the edge of a very narrow slab, thus the pressure on soil is also higher. According to Westergaard formulations, the deflection on slab edge is 3.46 times bigger than slab corner[17]. FEM result demonstrates that the smallest width of trackbed (2.8 m) gives 3.81 times of higher pressure on soil than CZW-2 model. If the slab is much wider, then the location of the rail (and wheel load) is close to the slab center. Therefore, the width of a slab greater than 3.8 m delivers closer estimation to CZW-2 model.

Of ballasted track system, the approximated levels of soil pressure of CZW-2 model are still higher than the one of FEM in the range of trackbed widths bigger than 3.8 m. Thus a ballasted track designed using CZW-2 model will deliver more conservative and safer design. If FEM is used as reference, adjustment factors are needed in CZW-2 model when the width of the lowest layer of trackbed is designed lower than 3.8 m in a slab track and lower than 3.5 m in ballasted track respectively.

Second investigations is to take into account the actual cross sections of tracks, as shown in the Table 9. The previous models of ST-1 and BT-1 are built in FEM according to the actual cross sections as can be seen in the Figure 23. Seven additional multilayer trackbed systems, which consist five slab track and two ballasted track systems are also given to verify the analytical method of CZW-2 model. And then FEM results are taken as reference. Superstructure parameters follow the given data in the previous subchapter 4.3 and trackbed data for these variations are shown in the Table 9.

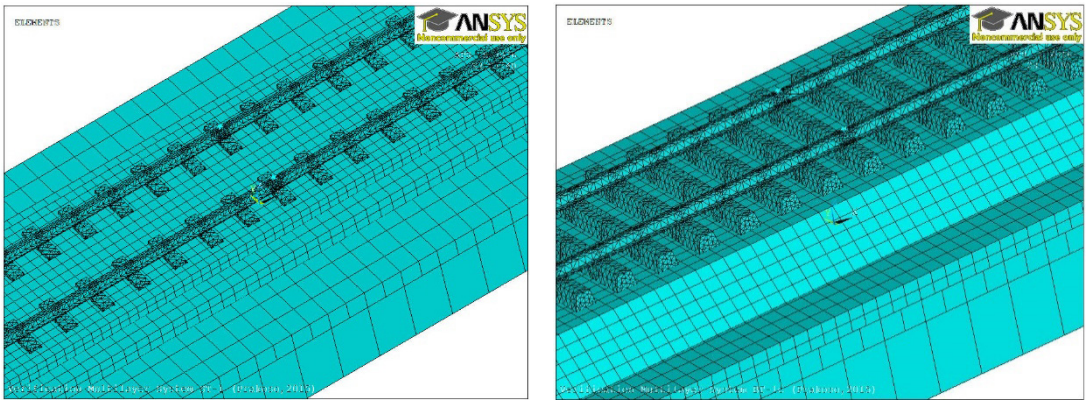

Figure 23. Mesh of ST-1 and BT-1 FEM models with the actual cross sections

Example C

Table 9. Example data of multilayer system of trackbed design

Code	Top Layer	Base Layer	Sub Base Layer	Subsoil
ST-1 (ballastless)	- Material: Concrete - H = 24 cm - E = 34 GPa, μ = 0.2 - B = 2.8 m	- Material: CTB - H = 30 cm - E = 10 GPa, μ = 0.2 - B = 3.6 m	- Material: Coarse Agg. - H = 30 cm - E = 120 MPa, μ = 0.35 - B = 6 m	- E = 60 MPa - μ = 0.4
ST-2 (ballastless)	- Material: Concrete - H = 30 cm - E = 34 GPa, μ = 0.2 - B = 3.0 m	- Material: Coarse Agg. - H = 30 cm - E = 250 MPa, μ = 0.3 - B = 4 m	- Material: Coarse Agg. - H = 40 cm - E = 120 MPa, μ = 0.33 - B = 6 m	- E = 60 MPa - μ = 0.4
ST-3 (ballastless)	- Material: Concrete - H = 35 cm - E = 36 GPa, μ = 0.2 - B = 3.2 m	- Material: Coarse Agg. - H = 60 cm - E = 250 MPa, μ = 0.3 - B = 6 m	-	- E = 80 MPa - μ = 0.4
ST-4 (ballastless)	- Material: Concrete - H = 30 cm - E = 34 GPa, μ = 0.2 - B = 2.8 m	- Material: Coarse Agg. - H = 45 cm - E = 250 GPa, μ = 0.3 - B = 3.6 m	- Material: Coarse Agg. - H = 60 cm - E = 80 MPa, μ = 0.3 - B = 6 m	- E = 45 MPa - μ = 0.4
ST-5 (ballastless)	- Material: Concrete - H = 24 cm - E = 34 GPa, μ = 0.2 - B = 3.0 m	- Material: CTB - H = 30 cm - E = 5 GPa, μ = 0.2 - B = 4 m	- Material: Coarse Agg. - H = 60 cm - E = 120 MPa, μ = 0.3 - B = 6 m	- E = 45 MPa - μ = 0.4
ST-6 (ballastless)	- Material: Concrete - H = 30 cm - E = 34 GPa, μ = 0.2 - B = 3.2 m	- Material: Coarse Agg. - H = 45 cm - E = 180 MPa, μ = 0.3 - B = 6 m	- Material: Coarse Agg. - H = 60 cm - E = 90 MPa, μ = 0.35 - B = 6 m	- E = 30 MPa - μ = 0.4
BT-1 (ballasted)	- L Sleeper = 2.6 m - Material: Ballast - H = 60 cm - E = 250 MPa, μ = 0.3 - B_{top} = 3.2 m - B_{bot} = 4.4 m (45° slope)	- Material: Coarse Agg. - H = 30 cm - E = 120 MPa, μ = 0.33 - B = 6 m	- Material: Fine Granular - H = 30 cm - E = 80 MPa, μ = 0.35 - B = 6 m	- E = 60 MPa - μ = 0.4
BT-2 (ballasted)	- L Sleeper = 2.6 m - Material: Ballast - H = 45 cm - E = 250 MPa, μ = 0.3 - B_{top} = 3.2 m - B_{bot} = 4.1 m (45° slope)	- Material: Coarse Agg. - H = 40 cm - E = 150 MPa, μ = 0.33 - B = 6 m	- Material: Fine Granular - H = 30 cm - E = 60 MPa, μ = 0.35 - B = 6 m	- E = 45 MPa - μ = 0.4
BT-3 (ballasted)	- L Sleeper = 2.6 m - Material: Ballast - H = 60 cm - E = 250 MPa, μ = 0.3 - B_{top} = 3.2 m - B_{bot} = 5.2 m (≈30° slope)	- Material: Coarse Agg. - H = 60 cm - E = 120 MPa, μ = 0.33 - B = 6 m	-	- E = 80 MPa - μ = 0.4

Table 10. Comparison of vertical stress on soil of different multilayer systems computed using Analytical Method and FEM

Code	Vertical Pressure on Soil [kPa]		Deflection on Soil [mm]	
	CZW-2	FEM-3D	CZW-2	FEM-3D
ST-1	9.33	11.92	0.59	0.76
ST-2	12.04	18.93	0.67	1.05
ST-3	13.09	19.84	0.56	0.73
ST-4	7.31	14.23	0.67	1.29
ST-5	6.75	9.39	0.64	0.89
ST-6	4.80	9.16	0.74	1.42
BT-1	36.85	28.97	1.00	0.97
BT-2	32.05	27.85	1.20	1.04
BT-3	44.10	31.23	0.84	0.60

The vertical pressures on soil, which are obtained from CZW-2 model are relatively close (note: the pressure is in kPa) to the ones of FEM in a slab track system. This shows an agreement with the results depicted in the Figure 22. The reason is that the lowest layers of trackbed of the slab tracks have widths greater than 3.8 m, then the levels of soil pressure are closer to the CZW-2 approximations. However, the results of FEM are fairly greater than CZW-2 because the top layers have widths lower than 3.8 m.

Meanwhile, in a ballasted track system the results of CZW-2 model are higher than FEM. This also affirms the previous analysis presented in the Figure 22 that although the lowest layers of trackbed have widths greater than 3.5 m, in a ballasted track system, CZW-2 model always gives higher estimations of pressure on soil within this range of width.

Based on those comparisons and considering FEM as reference, to use CZW-2 model in a safe side, trackbed layer design of a slab track requires an average adjustment factor (*AF*) about 1.6 in the estimation of vertical pressure on soil. Seeing the comparison of CZW-2 and FEM for slab track shown in the Figure 22, the impact of the width is almost in a linear correlation. If the actual width of a track model is considered in FEM, the adjustment factor can be roughly approximated from the equivalent width of the actual cross section of a track model. The equivalent width of an actual track model to the CZW-2 half space model is:

$$B_{eq} = \frac{A_{tot}}{3.8} \qquad \textit{Eq. 38.(a)}$$

$$f_B = c_f * B_{eq} \qquad \textit{(b)}$$

where: B_{eq} is equivalent width of a track model [m], A_{tot} is the actual cross section area of a track model [m^2], f_B is adjustment factor of pressure level on soil of CZW-2 model due to actual cross section area and c_f is a constant [-]. The value of c_f is 1.33 or 1.45 for a more conservative design.

Table 11. The impact of the actual cross section of a slab track to the level of pressure on soil

Slab Track System	Top Layer		Base		Sub Base		A_{tot}	B_{eq}	f_B	Pressure on Soil		
	B [m]	H [cm]	B [m]	H [cm]	B [m]	H [cm]	[m^2]	[m]		CZW-2	FEM	Ratio
ST-1	2.8	24	3.6	30	6.0	30	3.55	0.93	**1.24**	9.33	11.92	**1.28**
ST-2	3.0	30	4.0	30	6.0	40	4.5	1.18	**1.57**	12.04	18.93	**1.57**
ST-3	3.2	35	6.0	60	0.0	0	4.72	1.24	**1.65**	13.09	19.84	**1.52**
ST-4	3.0	30	3.6	45	6.0	60	6.12	1.61	**2.14**	7.31	14.23	**1.95**
ST-5	2.8	24	3.4	30	4.5	60	4.39	1.16	**1.53**	6.75	9.39	**1.39**
ST-6	3.0	30	3.6	45	5.0	60	5.52	1.45	**1.93**	4.80	9.16	**1.91**

A ballasted track design theoretically does not require adjustment factor. However, adjustment factor is still needed because CZW-2 model considers linear homogenous single layer media. In the reality there are many nonlinearities, especially delivered from loading and soil. In addition, there are various types of cross section design with different widths of each layer of trackbed. Therefore, a safety factor (SF) 2.0-2.5 for a slab track and 1.5-2.0 for ballasted can be implemented to this analytical model in a general estimation of vertical pressure level on subsoil for a trackbed design.

5.5. Design Charts of Trackbed Thickness Design

Development of design charts is aimed to ease design of trackbed in the practice. Instead of making computer programming with all complex formulas presented before, the design charts represent only the practical range of variations for trackbed design. Design charts should be built as simple as possible, but without eliminating the essential parameters. Therefore, sensitivity analysis of all of the trackbed design factors should be initially performed to identify the role of the parameters. Variations of dynamic amplification factor, axle/wheel loads, load distribution factors, rail profile and other parameters except trackbed and soil parameters should be taken out from the charts and are defined as *design factors* (*DF*). This generalizes design charts for broader applications as well as to reduce the amount of the charts. The CZW-2 model is chosen to estimate the required thickness of trackbed, which will be correlated to criteria of limitation of deflection, cumulative deformation and pressure level on the subsoil.

5.4.1. Sensitivity Analysis and Simplification of Trackbed Thickness Design Parameters

a) Simplification using load distribution factor of inner and outer rails (in a curve)

Dynamic factor (f_d) and load distribution factor of inner and outer rails ($f_{c,i}$ and $f_{c,j}$) can be taken out from Eq. 20 as a design factor to simplify the CZW-2 model. This can be done by taking initial values of f_d, $f_{c,i}$ and $f_{c,j}$ are equal to 1 as reference. Factor of f_d is linear and can be taken out directly from the formula. Factors of $f_{c,i}$ and $f_{c,j}$ can be simplified as ratio between them ($f_{c,r}$) and then the changes of $f_{c,r}$ ratio to deflection can be simply defined as design factor of load distribution of rail ($f_{c,d}$).

Vertical load distribution on the rails from a running train is derived from static forces (axle/wheel load), centrifugal forces, cross wind forces and dynamic forces. Centrifugal forces depend on train speed, curve radius and cant deficiency[39]. Criteria of limiting cant deficiency are riding comfort, tilting, safety against derailment, *Prud'homme* limit and maintenance. According to *Deutsche Bahn DB Regulation 800.0110*, the maximum design value of cant deficiency is 150 mm and maximum lateral acceleration of 0.85 m/s^2[17]. Higher load distribution factor of inner rail greater than 1.2 and up to 1.25 ($f_{c,r}$ = 1.6) demands high quality of track, a guaranteed good quality of track alignment, careful consideration of train speed and curve radius as well as the use of new train tilting technology. Therefore, it is suggested to consider the maximum load distribution factor of inner rail of 1.2 ($f_{c,r}$ = 1.5) for a general track design.

Some calculation tests are done utilizing Eq. 20 (Westergaard, 1926) with variations of subsoil's modulus of elasticity from 10 to 120 MPa and modulus of subgrade reaction k_s from 0.05 to 0.3 N/mm^3 as well as their respective equivalent thickness of trackbed. It is found that ratio $f_{c,r}$ has nonlinear correlation with $f_{c,d}$. But $f_{c,d}$ values remain almost the same in all variations of modulus elasticity when k values are greater than 0.1 N/mm^3. Factor of $f_{c,d}$ is reduced when there is unbalance combination of thickness and stiffness, which means inappropriate for practical purpose. Therefore, $f_{c,d}$ can be assumed as a simple design factor of load distribution of rails, which is defined by considering k_s greater than 0.1 N/mm^3. When this correlation is applied for soils with reaction modulus lower than 0.1 N/mm^3, then it will give safer side of a design. Furthermore, the range of trackbed design is more cost-effective in the range of k_s greater than 0.1 N/mm^3. Design factor of deflection due to load distribution is shown in the Figure 24.

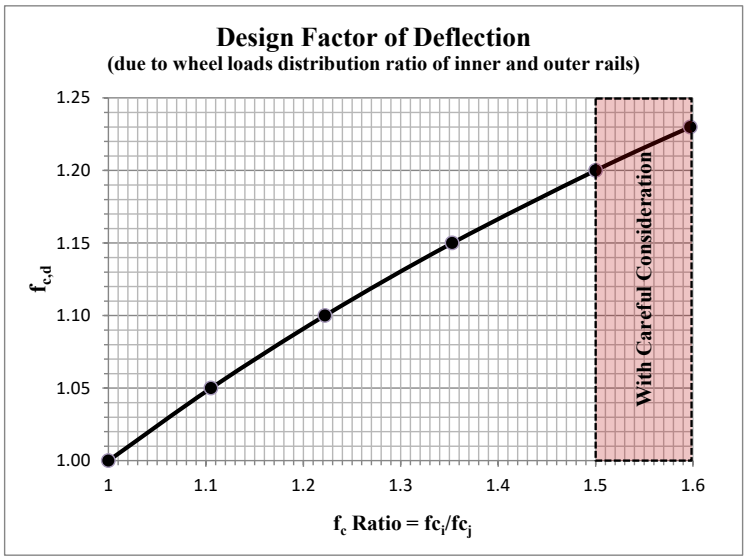

Figure 24. Design factor of deflection due to wheel loads distribution ratio

b) Simplification using design factors of rail, elastic-pad, and wheel load

Changes in the magnitude of wheel load are assumed linear to the changes of vertical pressure. Then wheel load design factor (f_Q) is a simple ratio between the design wheel load (Q_d) and reference wheel load (Q_{ref}). Rail and elastic-pad parameters are presented in the Eq. 20 of CZW-2 model in the equation of elastic length. Reference parameters are 60E2 rail profile, 22.5 kN/mm elastic-pad stiffness and sleeper spacing of 60 cm (ballasted) and 65 cm (ballastless). Those values give elastic length of around 910 mm (ballasted) and 928 mm (ballastless). Based on some examples of commercial rail profiles from light rail to heavy rail commonly used in US, UK, Germany and some other European countries as well as elastic-pad stiffness from 22.5 to 65 kN/mm, several test calculations exhibit a range of elastic length from 470 to 990 mm. This range of elastic length has a ratio from 0.52 to 1.09 to the reference value of 910 mm (ballasted) and from 0.4 to 1.2 to the reference value of 928 mm (ballastless).

Design factor due to different elastic lengths is shown in the Figure 25 below. From the Figure 25, it is shown that there is no significant different in design factor with sleeper spacing of 60 and 65 cm. But it can be obviously seen that selecting light rail profiles or stiffer elastic-pad will significantly increase the deflection and vertical pressure on subsoil. The impact of changing rail profile is less significant to the deflection and vertical pressure on subsoil when heavy rail profiles are chosen in combination with softer elastic-pad. This will reduce the deflection and vertical pressure on subsoil.

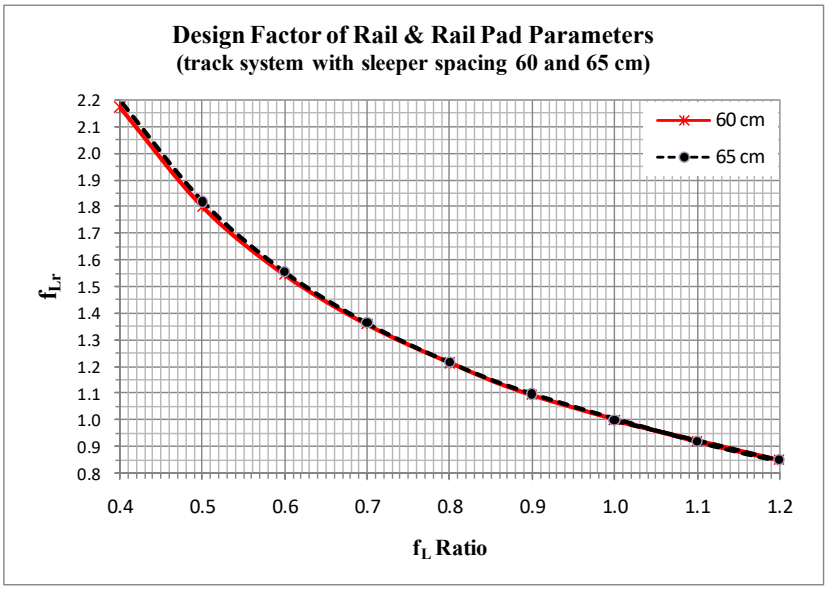

Figure 25. Design factor of rail and elastic-pad parameters

Therefore, the maximum vertical pressure on subsoil can be calculated from Eq. 20, with $f_{d,}$ $f_{c,i}$ and $f_{c,j}$ initially equal to 1, Q_{ref} and Lr_{ref} using reference values of wheel load and rail profile parameters. Then it is multiplied by real design values of f_Q, $f_{Lr,}$ f_d and $f_{c,d}$ as follows:

$$P_{design\ limit} = f_{P,ref}(Q_{ref}, L_{r,ref}, f_{d,ref}, f_{c,d,ref}) * f_Q * f_{Lr} * f_d * f_{c,d} \qquad Eq.\ 39\ (a)$$

$$f_Q = \frac{Q[kN]}{125};\ f_c\ Ratio = \frac{Q_{inner}\ [\%]}{Q_{outer}[\%]} \qquad (b)$$

$$f_{Lr}Ratio = \frac{L_r}{L_{r,ref}}, \qquad L_{r,ref} = 910\ (ballasted)\ or\ 928\ (balastless) \qquad (c)$$

where: $P_{design\ limit}$ is the vertical pressure limit design value, $f_{P,ref}$ is mathematical model to estimate soil pressure level (CZW-2) based on reference parameters, f_Q is design factor of wheel load, f_{Lr} is design factor of elastic length due to changes in rail and elastic-pad parameters, f_d is dynamic amplification factor (DAF), and $f_{c,d}$ is design factor of deflection due to wheel load distribution ratio.

By utilizing this simplification, then all the design charts can be built based on critical limit state criteria and reference parameters. Hence, additions of safety factor and correction factor and other design factors are simply multiplied with this critical limit. Reference parameters are: wheel load of 125 kN (25 tons of train axle load); elastic length of 910 mm (ballasted) and 928 mm (ballastless); dynamic amplification factor of 1 and equal distribution of axle load in inner and outer rails (straight line). Thus, all the trackbed design charts will be developed using these reference values.

Design charts are presented as correlation between soil's resilient modulus [MPa] and/or deviator stress limit [kPa] and reference structural number (SN_{ref}) [cm]. These are estimated using CZW-2 analytical model and reference parameters. SN_{ref} values are calculated using computer programming, which is based on direct loop iteration methods. SN_{ref} is obtained from critical equivalent thickness due to limitation of vertical pressure on subsoil. Critical pressure limits can be defined based on three different criteria: limit of fatigue stress of-, limit of shear failure of- or limit of plastic deformation of- subsoil.

Because soil pressure is proportional to the resulted structural number, then structural number design (SN_{design}) can be derived from reference structural number multiplied by design factors. Therefore, it allows variations in a design with various possibilities of changing rail profiles, elastic-pad stiffness, wheel loads, dynamic amplification factor (considers train speed, track quality and statistic data) and wheel load distribution factors (straight line or in a curve). At the end, safety factor (SF) can be added to obtain the designed value of SN_{design}. Selection of SF gives more flexibility in a final design, which depends on the personal judgment of the engineers. In addition, for further development in the future, empirical correction factors can be included, when experimental data from laboratory tests and/or measurements is available. Therefore, from the design charts, SN_{design} can be defined as follow:

$$SN_{design} = SF * SN_{ref(chart)} * DF \qquad Eq.\ 40$$

where

$$DF = f_Q * f_{Lr} * f_d * f_{c,d} \qquad Eq.\ 41$$

Another advantage of this method is that it avoids over multiplications of unidentified factors and safety factors included, which may lead to an overestimation of a final design. The reason is that all of these factors is set after all of the principal formulations.

CZW-2+H&K model sufficiently fits to assess the critical thickness of a slab track in the range of subsoil's reaction modulus between 0.05 and 0.25 N/mm^3. Nevertheless, it should be bear in mind that this assumption is valid if the base material has reaction modulus more than 0.25 N/mm^3 in an application of a thin concrete slab. Moreover, design value of 0.25-0.3 N/mm^3 (stiff to very rigid base) is more recommended to avoid excessive cracks, gaps, bridging and pumping effect below the concrete slab track during service time. Therefore, the selection of base material should firstly follow this requirement.

5.4.2. Trackbed Thickness Design using Fatigue Criterion

The allowable limit fatigue stress on subsoil can be considered as a criterion to define the reference *structural number (SN)*. By doing iteration of CZW-2 model, different *SN* values can be obtained from different soil bearing capacity levels. Fatigue criterion, which is defined from Heukelom & Klomp approach can be used to estimate the critical *SN*. This fatigue model considers dynamic modulus of subsoil and the number of cyclic loading. Therefore, the design chart can be built from different variations of elastic modulus of subsoil and the number or cyclic loading. Dynamic elastic modulus of subsoil is assumed as linear constant of 1.2 times than its static modulus of elasticity. The cyclic loading variations represent the number of traffic designed during the service life of track. The result of calculation of reference *SN* can be seen in the Figure 26. The magnification of this chart as well as with higher numbers of cyclic loading can be seen in the Appendix 5, pp. 230.

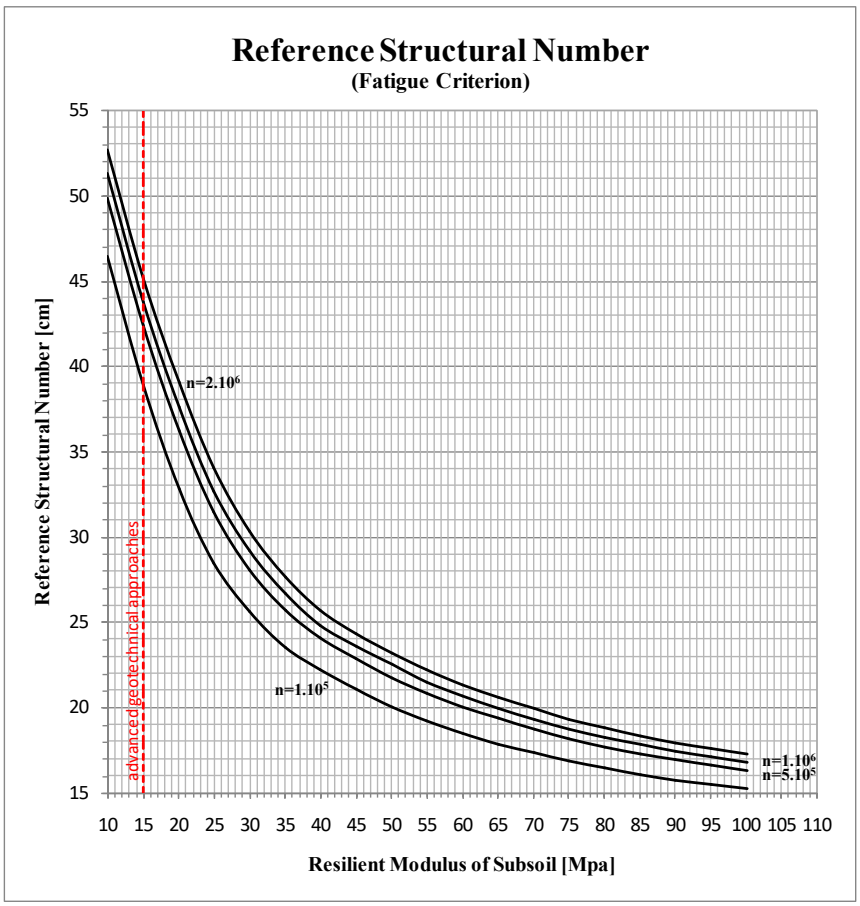

Figure 26. Reference structural number of trackbed thickness design using CZW + H&K models

The design procedure of trackbed thickness design based on fatigue limit on soil using Heukelom & Klomp criterion are described in the Figure 27.

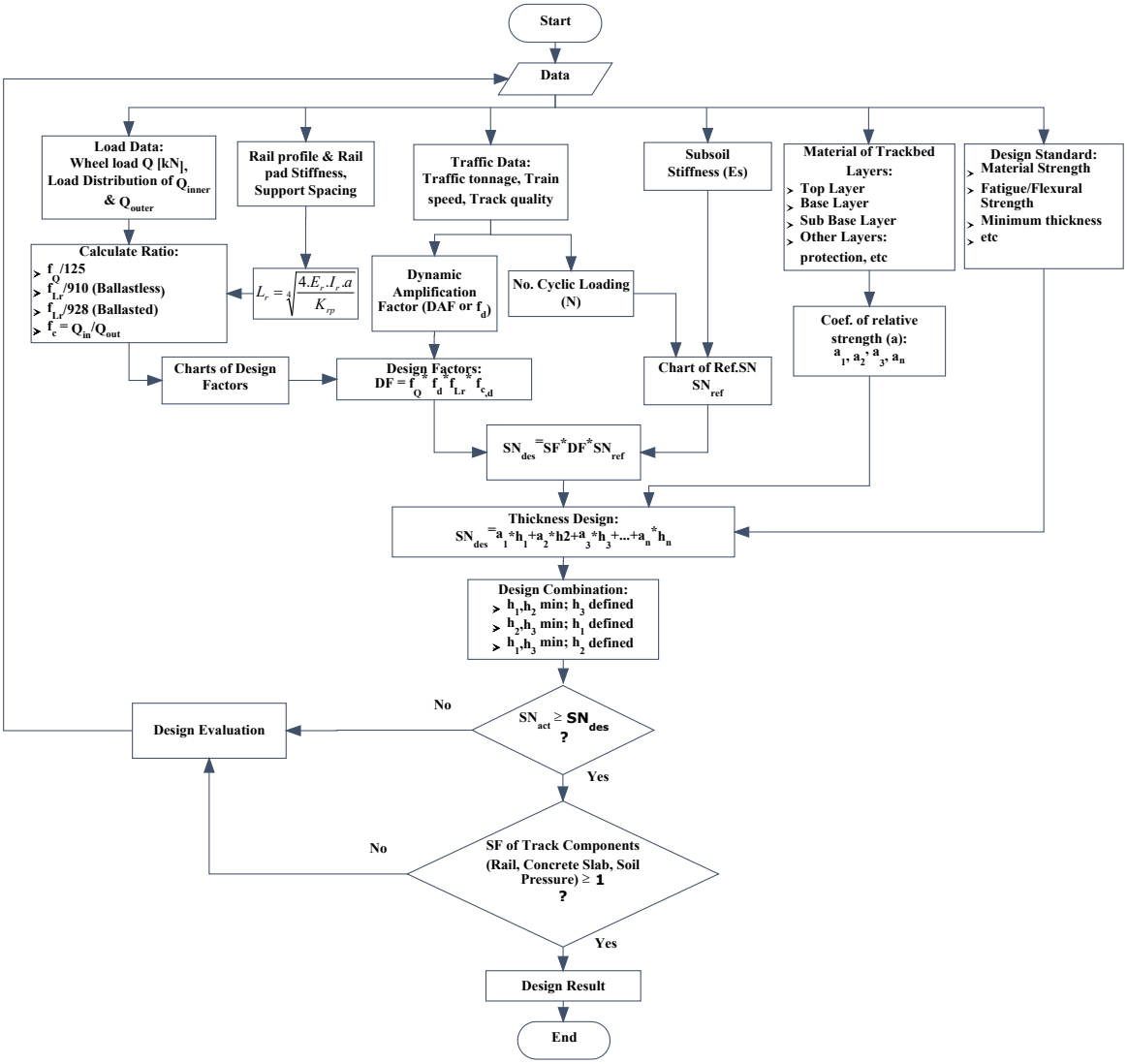

Figure 27. Design procedure of trackbed thickness based on fatigue limit on soil

Example D

Example of layered trackbed calculated by employing this model, for instance:

- Considering dynamic amplification factor from the previous subchapter 4.3 with train speed 250 km/hour: f_d = 1.6 (see again Example G in Appendix 4, pp. 227).
- Wheel load distribution factors of inner and outer rail: $f_{c,i}$= 1.2 and $f_{c,j}$= 0.8 give ratio of $f_{c,i}/f_{c,j}$ = *1.5* and then from Figure 24 it gives $f_{c,d}$= 1.2.
- Wheel load 125kN gives f_Q = 1.
- Rail profile 60E2 and elastic-pad stiffness of 40 kN/mm and: (1) elastic-pad spacing of 65 cm (ballastless) gives f_{Lr}*ratio* = 803.6/928= 0.87 and from Figure 25, f_{Lr} = 1.12 is obtained and respectively for (2) elastic-pad stiffness of 22.5 kN/mm and elastic-pad spacing of 60 cm (ballasted) gives f_{Lr} *ratio* = 910/910 = 1 and f_{Lr} = 1.
- Then the total design factors (*DF*) are:

$$DF_{(ballatless)} = f_Q * f_d * f_{c,d} * f_{Lr} = 1 * 1.6 * 1.2 * 1.12 = 2.15 \quad \textit{Eq. 42}$$
$$DF_{(ballasted)} = f_Q * f_d * f_{c,d} * f_{Lr} = 1 * 1.6 * 1.2 * 1.0 \quad = 1.92$$

Therefore, *SN* design for both systems with safety factor *SF* = 2:

$$SN_{des\ (ballatless)} = 2 * SN_{ref(chart)} * DF = 4.3 * SN_{ref(chart)} \quad \textit{Eq. 43}$$
$$SN_{des\ (ballasted)} = 2 * SN_{ref(chart)} * DF = 3.8 * SN_{ref(chart)}$$

Design traffic is for 2 million load cycles (heavy traffic line) with wheel load 125 kN (a proximally 25 tons' axle load). When a train is assumed having 2 cars and 4 axles in a car then the traffic tonnage is a proximally 400 MGT during the service time. Design examples of trackbed for ballastless and ballasted track systems using three-layer trackbed is shown in the Table 12.

Table 12. Example of trackbed thickness design using soil fatigue limit criterion

Layer	**Example I (Slab Track)**				**Example II (Ballasted)**			
	Material	***a***	***h* [cm]**	***SN***	**Material**	***a***	***h* [cm]**	***SN***
Soil	*$E_s \approx 45$ MPa, $SN_{ref} \approx 24.3$ cm,* ***$SN_{des} \approx 105$ cm***				*$E_s \approx 60$ MPa, $SN_{ref} \approx 21.4$ cm,* ***$SN_{des} \approx 81$ cm***			
Top Course	Concrete C35/45	3.26	**24**	78.2	Ballast E = 250 MPa	0.65	**30**	19.5
Base Course	Coarse Grained 120 MPa	0.51	**28**	14.3	Coarse Grained 150 MPa	0.55	**60**	33.0
Subbase Course	Fine Grained 80 MPa	0.45	**28**	12.6	Coarse Grained 80 MPa	0.45	**65**	29.3
	Total Thickness/*SN*		**80**	**105.1**	**Total Thickness/*SN***		**155**	**81.8**

For a thin slab track system, it requires a base layer with minimum stiffness of 0.25 N/mm^3. In the examples above, a base layer with elastic modulus of 120 MPa are selected. Instead of using coarse granular base, concrete treated base or asphalt pavement can be also used.

5.4.3. Trackbed Thickness Design using Shear Failure and Plastic Deformation Criteria

a) Shear Failure Criterion

Trackbed design charts using reference structural number can be also presented in a correlation to allowable deviator stress level on subsoil. These deviator stress levels can be described as a ratio between the deviator stress (σ_d, kPa) and resilient modulus of subsoil (E_v, or Es, MPa) to normalize the chart. The ratio values are ranged from 0.5 to10 kPa/MPa for medium to soft soils and from 1 to 4 kPa/MPa for moderate to stiff soils. This gives design range of soil's elastic modulus from 10 to 100 MPa and critical deviator stresses from around 5 to 500 kPa. The structural number is calculated using CZW-2 model as the given

data above, the result is shown in the Figure 28. Greater scale of these charts can be seen in the Appendix 5, pp. 232.

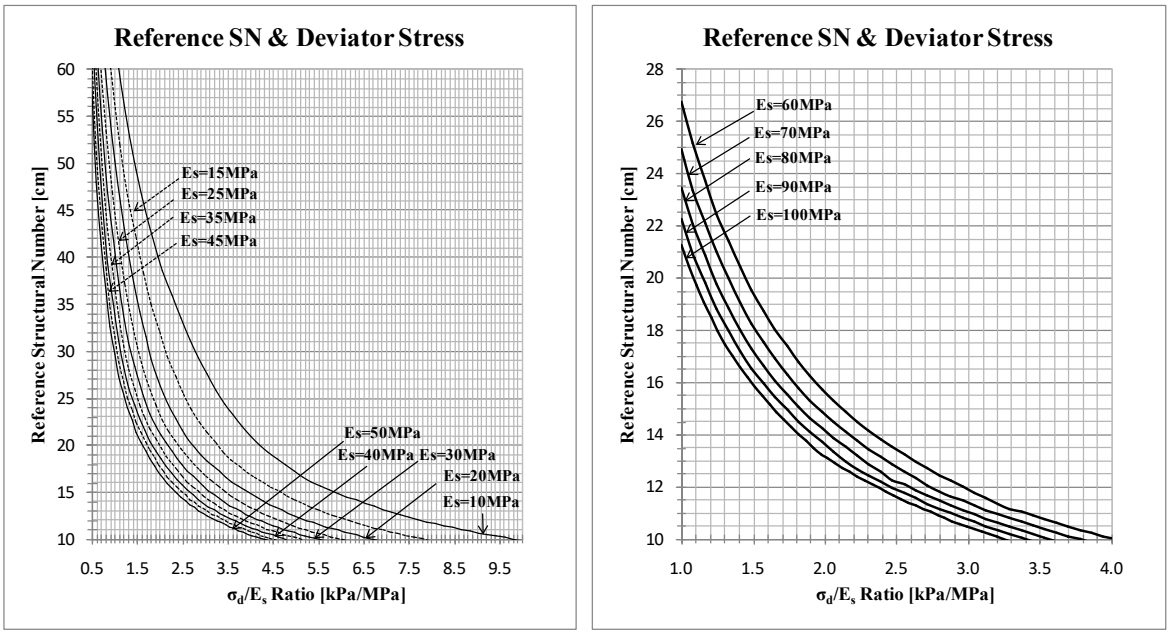

Figure 28. Reference structural number and deviator stress

Figure 28 can be used to design trackbed layer in combination with the criterion of shear failure (%) after Li & Selig (1998)[74]. This can be done by limiting the level of deviator stress on subsoil. Li & Selig's limit criterion of shear failure (see also Eq. 3) can be drawn as charts for different types of soil as well as reversed to define deviator stress as shown in the Eq. 44 and Figure 30.

[74]

$$\sigma_d = \sigma_s . \sqrt[m]{\frac{\varepsilon_p}{a.N^b}} \qquad \textit{Eq. 44}$$

where: ε_p is cumulative soil plastic strain [%], σ_s is soil compressive strength [kPa], *a, b, m* are the soil parameters defined by Li & Selig (see Table 2), *N* is the number of repeated loading.

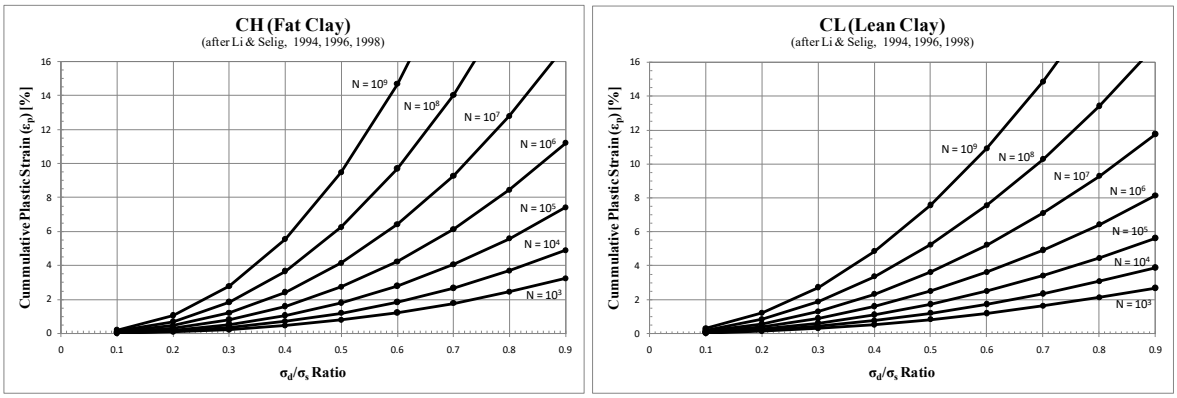

Figure 29. Deviator stress limit due to shear failure criterion for soil types CH and CL (after Li & Selig, 1998)

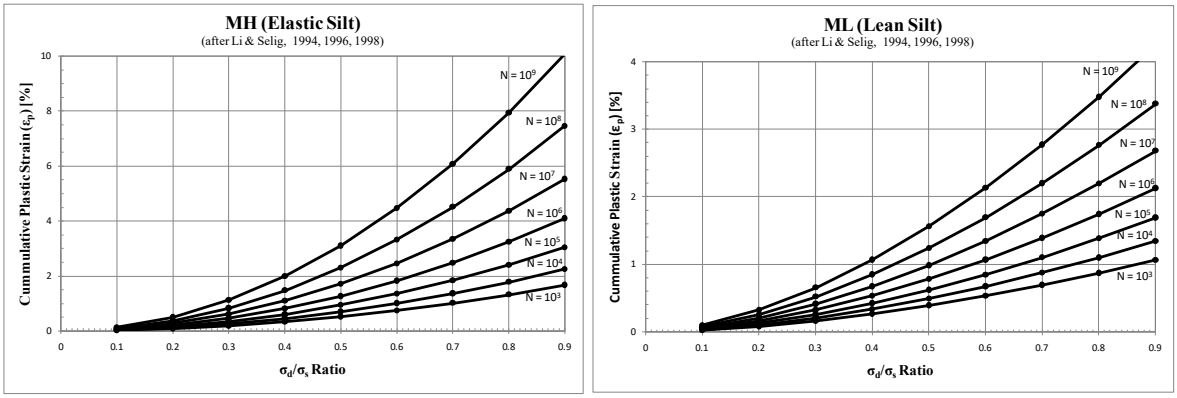

Figure 30. Deviator stress limit due to shear failure criterion for soil types MH and ML (after Li & Selig, 1998)

b) Plastic Deformation Criterion

The reference structural numbers estimated using CZW-2 model can be also combined with criterion of limiting excessive plastic deformation failure on subsoil due to cyclic loading induced by train passing. Li & Selig (1998)[74] formulation of cumulative plastic deformation can be reversed to obtain deviator limit stress (σ_d). Then *SN reference* can be defined from Figure 28 based on σ_d.

[74]

$$\sigma_d = \sigma_s . \sqrt[m]{\frac{100.\rho}{a.N^b.H}} \qquad \textit{Eq. 45}$$

where: ρ is the cumulative plastic deformation [cm], σ_s is soil compressive strength [kPa], *a, b, m* are the soil parameters defined by Li & Selig (see Table 2, pp. 21), *N* is the number of repeated loading and *H* is depth of soil until rigid base [cm].

Design procedure of trackbed thickness design using shear and plastic deformation criteria is summarized in the Figure 31 below:

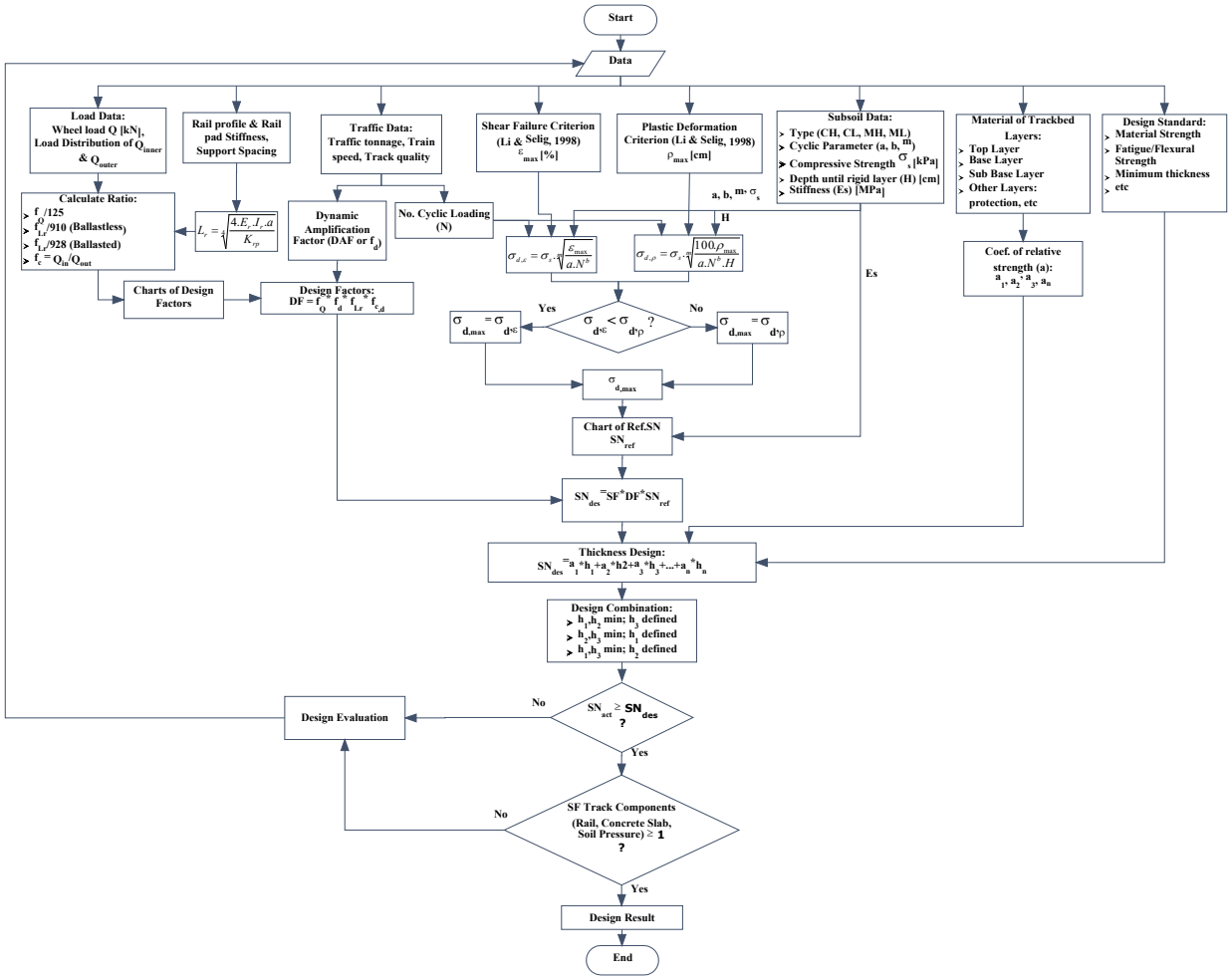

Figure 31. Design procedure of trackbed thickness based on limit of shear failure and plastic deformation criteria

Example E

An example of trackbed design based on shear failure and plastic deformation criteria is shown below when the superstructure design parameters are the same from the previous subchapter 4.3. The soil parameters and design criteria are:

- ***Limit of shear failure***: 2%. Soil type is MH, with *Es* ≈ 50 MPa, σ_s = 150 kPa. Li & Selig soil's parameters are: a = 0.84, b = 0.13 and m = 2. From Eq. 44 with N = 2 million load cycles then σ_d is 90 kPa. σ_d/E_s ratio is 1.8. From Figure 28, with σ_d/E_s= 1.8 and *Es* = 50 MPa then SN_{ref} is 18 cm. The same design factors are used from the previous Example I & II of Example D, then SN_{des} = 4.3*18 ≈ **77 cm** (ballastless) and SN_{des} = 3.8*18 ≈ **68 cm** (ballasted).
- ***Limit of plastic deformation***: 2 cm. This value is taken because this is the common height of elastic-pads or steel plates under elastic-pads, which can be inserted for track vertical re-alignment. Depth of soil until rigid support (rock layer), e.g. 2 m.

Then from Eq. 45 with N = 2 million load cycles, σ_d is 52 kPa. σ_d/E_s= 1.04 and Es = 50 MPa then from Figure 28 give $SN_{ref} \approx$ 28.5 cm. Finally, it is obtained SN_{des} = 4.3*28.5 ≈ **126 cm** (ballastless) and SN_{des} = 3.8*28.5 ≈ **108 cm** (ballasted).

Comparing both design criteria, limiting of plastic deformation is more decisive than limiting of shear failure in this example case.

Table 13. Example of trackbed thickness design using plastic deformation criterion

Layer	**Example III (Slab Track)**				**Example IV (Ballasted)**			
	Material	***a***	***h* [cm]**	***SN***	**Material**	***a***	***h* [cm]**	***SN***
Soil	$E_s \approx 50$ *MPa,* $SN_{ref} \approx 28.5$ *cm,* $\boldsymbol{SN_{des} \approx 126}$ ***cm***				$E_s \approx 50$ *MPa,* $SN_{ref} \approx 28.5$*cm,* $\boldsymbol{SN_{des} \approx 108}$ ***cm***			
Top Course	Concrete C35/45	3.26	**24**	78.2	Ballast E = 300 MPa	0.69	**60**	41.4
Base Course	Asphalt Concrete 3 GPa	1.51	**20**	30.2	Coarse Grained 120 MPa	0.51	**60**	30.6
Subbase Course	Fine Grained 80 MPa	0.45	**40**	18.0	Coarse Grained 80 MPa	0.45	**80**	36.0
	Total Thickness/*SN*		**84**	**126.4**	**Total Thickness/*SN***		**200**	**108.0**

A report by Nelder (2008)[92] mentioned that British Rail Design (Heath & Shenton, 1972)[52] sets a threshold of stress value and defined thickness design chart for several levels of static axle loads. Their design chart demonstrates that the minimum depth of construction is 30 cm and the minimum value of subgrade deformation modulus (E_v or E_d) is 5 MPa. E_v below this value is considered as too soft and needs advanced geotechnical advice. Li & Selig (1998)[74] in their paper gave example of soft soil with resilient modulus of 14 MPa. In addition, Bowless (1996)[12] made an empirical classification of different soil types and their elastic moduli (E_s) and suggested design values, that for clay, E_s of 2 - 15 MPa is categorized as very soft clay and E_s of 5 - 25 MPa is classified as soft clay.

In this dissertation, soil's resilient modulus of 15 MPa is considered to be the critical threshold for trackbed thickness design applications. A track designed under this threshold value should be carefully evaluated by comparing with different options such as soil stabilization or advanced geotechnical approaches. Therefore, the soil's resilient modulus more than 18 MPa is more recommended for trackbed design to achieve a cost-effective design.

For a ballasted track, the minimum design value of *SN* is recommended 20 cm, which gives a critical thickness of about 30 cm when a single layer trackbed (full depth) design of using granular material with elastic modulus of 250 MPa is considered. Meanwhile, for a slab track, the minimum design value of *SN* is suggested 60 cm, which results a critical thickness

of about 18 cm when a concrete type C40/50 is used. These ranges and recommended values are sufficient to provide a broader flexibility for trackbed layer design applications.

5.6. Evaluation of the Proposed Method

Several examples and their detail calculations of trackbed thickness design using the proposed method and three limit criteria are shown in the Appendix 6 Section A.6.1, A.6.2 and A.6.3, pp. 235. These examples are given to evaluate the proposed method by doing comparative analysis with FEA. These examples are calculated using the proposed analytical method and then some of them are built in FEA and following that static FEA simulations are performed. Variations of these examples for the evaluation are:

1) seven different soil bearing capacity levels, in which the soil resilient moduli are ranged from 15 to 80 MPa.
2) two main different limit criteria: Heukelom & Klomp fatigue limit (H&K), Li & Selig plastic deformation limit (L&S-Plastic).
3) two types of track: slab track and ballasted track systems
4) four different adjustment factors (*AF*), which are applied to structural number design to compare the FEA results of soil's vertical pressure with allowable criteria set in the analytical method, namely: 2.0; 1.5; 1.2 and 1.0.
5) various combinations of material types and thicknesses used in one-, two- and three-layer- trackbed.

The result of this comparative analysis is depicted in the Table 14 and Figure 32.

First of all, it can be seen that almost all of the vertical pressure obtained from FEA are below of the allowable limit set in the analytical calculation. However, some combinations of trackbed have bigger vertical pressure levels when adjustment factor (*AF*) is 1.0 and soil bearing capacity levels are low (E_S = 15 and 20 MPa). Taking FEA result as reference, this occurrence implies that for practical application *SF* more than 1.0 is required to achieve safer solution. In addition, it is shown that the lower the soil bearing capacity levels are, the bigger *SF* values are required.

Table 14. Vertical pressure on soil obtained from FEA of trackbed layers designed with analytical method

Subsoil		FEA Model			Design Criteria		FEA, AF = 1.0		FEA, AF = 1.2		FEA, AF = 1.5		FEA, AF = 2.0	
							A		B		C		D	
Es [MPa]	**Condition**	**Type**	**Model Code**	**Group No.**	**Limit Criteria**	**Allowable [kPa]**	**Pressure [kPa]**	**Ratio**	**Pressure [kPa]**	**Ratio**	**Pressure [kPa]**	**Ratio**	**Pressure [kPa]**	**Ratio**
15	Very Soft	Slab Track	E15-ST-LSP	EX-5	L&S (Plastic)	23.4	**11.67**	0.50	**11.62**	0.50	20.49	0.88	25.55	1.09
15	Very Soft	Ballasted	E15-BT-LSP	EX-6	L&S (Plastic)	23.4	6.63	0.28	9.32	0.40	12.79	0.55	16.18	0.69
20	Soft	Slab Track	E20-ST-LSP	EX-11	L&S (Plastic)	29.9	21.93	0.73	16.38	0.55	22.88	0.77	37.30	1.25
20	Soft	Ballasted	E20-BT-LSP	EX-12	L&S (Plastic)	29.9	8.77	0.29	12.85	0.43	17.40	0.58	21.47	0.72
35	Soft	Slab Track	E35-ST-HK	EX-13	H&K	46.6	18.38	0.39	27.29	0.59	43.38	0.93	-	-
35	Soft	Ballasted	E35-BT-HK	EX-14	H&K	46.6	15.13	0.32	22.14	0.48	28.91	0.62	34.95	0.75
45	Moderate	Slab Track	E45-ST-LSP	EX-19	L&S (Plastic)	63.7	26.91	0.42	39.88	0.63	58.26	0.91	-	-
45	Moderate	Ballasted	E45-BT-LSP	EX-20	L&S (Plastic)	63.7	20.76	0.33	28.15	0.44	36.55	0.57	44.24	0.69
60	Moderate	Slab Track	E60-ST-HK	EX-23	H&K	79.8	31.50	0.39	58.39	0.73	-	-	-	-
60	Moderate	Ballasted	E60-BT-HK	EX-24	H&K	79.8	25.01	0.31	36.32	0.45	45.64	0.57	52.54	0.66
80	Moderate	Slab Track	E80-ST-HK	EX-29	H&K	106.5	40.53	0.38	57.05	0.54	-	-	-	-
80	Moderate	Ballasted	E80-BT-HK	EX-30	H&K	106.5	35.43	0.33	47.09	0.44	54.89	0.52	69.33	0.65

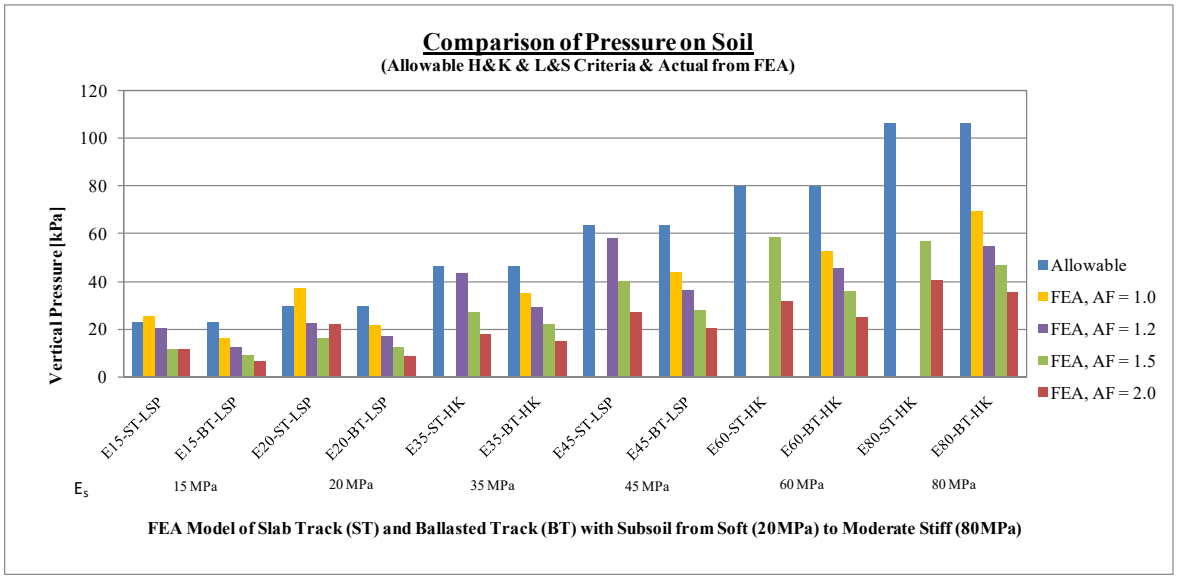

Figure 32. Comparison of pressures on soil from FEA

Secondly, with the same level of structural number, ballasted track system has lower pressure level on soil than slab track. Nevertheless, this has a consequence that the total thickness of trackbed of a ballasted track system is higher than the one of a slab track (see Appendix 6 Section A.6.3, pp. 239 for more detail). The total thickness of trackbed of a ballasted track system located on soft soil can be twice higher than a slab track. One important thing should be also bear in mind that to avoid ballast attrition and excessive settlements to the overall structure, a multilayer trackbed of a ballasted track system should be designed with gradual increase of the stiffness from bottom to top layer. This is the reason that for a soft soil condition, ballasted track requires greater thickness of trackbed. This indicates the advantage of slab track in comparison with ballasted track constructed on soft soil. In the Figure 32, it is demonstrated that ballasted track system with trackbed is more effective constructed in a moderate soil bearing capacity with resilient modulus more than 45 MPa. This results also shows an agreement with the German specification of road works *ZTV E-StB 09/2012*[70][68] that the modulus of deformation of second loading of the subgrade should be not less than 45 MPa in the design state of a low speed train, but 60 MPa is more recommended in the application state as well as for a high speed train and slab track.

Thirdly, only seeing from the criteria of required static strength of a track, it is found that for a critical design (*AF* or *SF* equal to 1.0), a slab track located on soil with resilient modulus higher than 35 MPa theoretically does not need a base layer. This is shown from the structural number which is lower than 60 cm, as it is shown as empty column bars in the Figure 32 and blank cells in the Table 14. This confirm the previous analysis which is shown

in the Subchapter 4.4 about critical thickness of slab track laid on soil. Yet, considering other criteria, for instance to avoid excessive cracks on concrete slab, pumping effect, gap; to provide protection layer and to give more stability to the overall track, a slab concrete demands a base layer. Therefore, using the analytical method for practical purpose, a safety factor 2.0-2.5 is required for a design of trackbed of a slab track on soft soil. For a moderate and ideal bearing capacity of soil more than 45 MPa, this safety factor can be reduced to 1.5 to 2.0. This confirms again the previous results shown in the Subchapter 5.4.

Fourthly, looking in more detail in the Appendix 6 Section A.6.3, pp. 239 of **Example 5-A** (AF = 2.0, base layer of CTB 10 GPa) and **Example 5-B** (AF = 1.5, base layer of crushed stones 150 MPa) of the same 24-cm slab track on soil with E_s = 15 MPa; the vertical pressures on soil of both examples are almost equal (see Table 14). This happens although the structural number design values are reduced (from AF = 2.0 to 1.5). In the one side, this again supports the previous analytical result in the Subchapter 4.4 that adding higher base layer's stiffness with reaction modulus more than 0.25 N/mm^3 does not give significant influence to the change of the critical thickness of concrete slab (or indirectly to the limit criteria of soil's pressure). Nevertheless, CTB (with reaction modulus of 0.2 - 0.3 N/mm^3) can be installed as base layer (like in Rheda-2000), which is done to provide more bearing capacity and also a protection to the thin concrete slab against excessive cracks. In the other side, this indicates that beside concrete treated base, other pavement materials such crushed stones or asphalt can be also implemented as base layer for a slab track as it has been reported in another study, e.g.[70][68].

Last but not least, the static analysis results affirm the previous analysis and other arguments from literature that the effective range of trackbed application is for soil resilient modulus greater than 18 MPa and by considering some other design aspects.

Burrow, et.al. (2011)[15] did a comparative study of different approaches to estimate the minimum required trackbed thickness of a ballasted track system. Their study compared the methods proposed by Li & Selig (1998)[74][75], British Rail (based on Heat & Shenton, 1972)[52], UIC 719R (1994)[140], Network Rail (2005)[93]. The results of their comparative study and the method proposed by the author are compared and shown in this following figure:

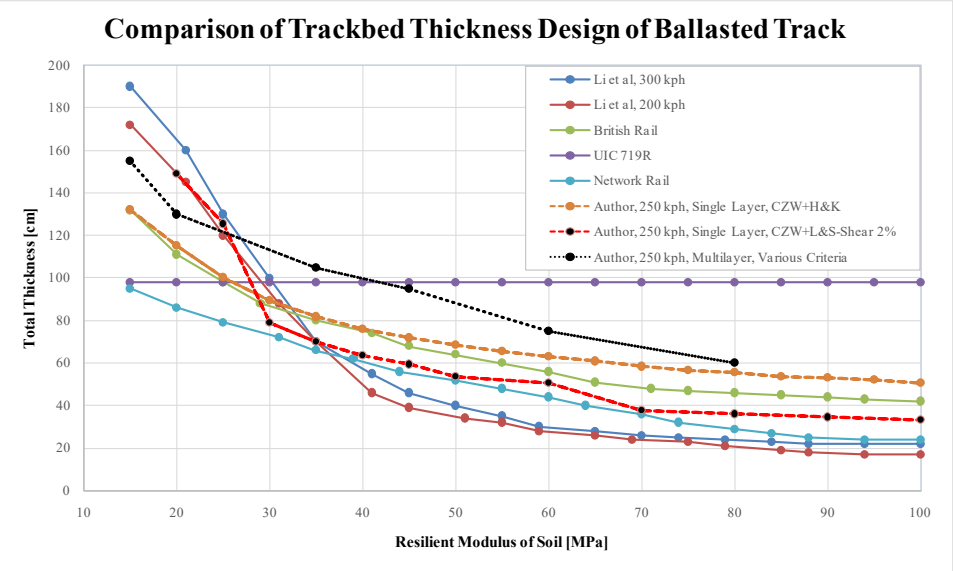

Note: the thickness values of other methods are only reproduced and cited from Burrow, et. al. (2011)[15]

Figure 33. Comparison of different approaches of trackbed thickness design

From the Figure 33, the thicknesses of single layer ballast, which are estimated using the proposed method and Heukelom & Klomp fatigue criterion, are closer to the ones by British Rail method. Meanwhile, for a multilayer design, the proposed method approximates higher thickness requirements of ballasted track in the range of soil's resilient modulus more than 30 MPa. This occurs because the proposed method for a multilayer design considers different criteria, various combinations of thickness and stiffness of material as well as different design factors. Besides dynamic factor of 1.6, load distribution factor in a curve of 1.2 is also taken into account in this example. Meanwhile other methods only estimate the total thickness of a single layer trackbed.

One thing should be noted is that this comparison is only presented to summarize some particular examples. It cannot be used as direct comparison if it is only based on a simple correlation between soil's resilient modulus and total thickness. The main reason is that besides soil's resilient modulus, there are many other parameters and assumptions, which are considered in different ways in each method.

5.7. Design Consideration

The static analytical methods of trackbed thickness design with three different criteria have been presented. Two possible solutions are offered, namely (1) closed form solution using complex combination of formulations as well as (2) simplified method utilizing design charts. Closed form solution needs computer programming and iteration process. The core of the analytical formulations is based on classical theories and can be combined with

empirical parameters. Required thickness of trackbed is estimated majorly based on criteria limiting pressure on subsoil.

According to Eisenmann (2004)[33], Giannakos (2004)[46] and Eisenmann & Rump (1997)[32], the AASHTO equation of correlation between maintenance costs and pavement quality based on tests of road constructions is also relevant for railway track. Track geometry quality (Q_g) and stress on the trackbed (P_z) can be expressed in a relation of power function: $Q_g = (P_z)^m$. In which m can be of 3 to 4 power degree[33][46] [32]. Both types of design charts of cyclic fatigue limit, shear and plastic failures depicted in the Figure 26 and Figure 28 exhibit curve shapes similar to a power function. In those charts, the thickness increments representing by SN due to various cyclic limits of soil pressure and bearing capacity are close to a nonlinear power function.

Main advantage of this graphical method firstly lays on the simplification, therefore, it is easier for design applications in the practice. The use of design charts gives flexibility to engineers to have initial design overview of trackbed. Secondly, multilayer trackbed design, which is more effective than single layer (full depth) design, is included in this method. In comparison to other method, for instance Li & Selig method takes into account only estimation of thickness of single layer ballast trackbed.

However, this method has some major limitations. Firstly, it takes into account only single axle load of a train. Secondly, it considers linear behaviours of railway track components and soil, which are not completely realistic. Thirdly, for slab track application, this method should be very carefully implemented. The reason is that between concrete material and granular material or soil, there is a sharp difference of stiffness. In addition, conversion concrete slab to a homogenous half space relative to soil is only fairly acceptable to estimate pressure distribution on soil. It is not realistic to assess flexural capacity of concrete. Analytical method which fits better for this case is plate theory. Fourthly, all trackbed layers are assumed homogenous and isotropic. Last but not least, this method strongly depends on the failure criteria and set boundaries. Therefore, correct and clear definitions of these criteria are very essential.

These limitations can be minimized if correction factors are properly estimated to achieve an optimal and equilibrium design. The design factors, which should be considered are:

1. ***Soil bearing capacity level***. Subsoil bearing capacity plays very important role to define trackbed thickness. It should be decided; which solution is more economical: with or without soil stabilization. Both options have consequences. The final output of the analytical method is thickness of trackbed layers. However, it is not always true that providing thick layers then the problem is appropriately solved. There is a limit boundary where soil stabilization is a must to have certain level of bearing capacity. In addition, there is also limitation where although with stabilization, soil bearing capacity is not sufficient and needs advanced geotechnical approach. Therefore, a minimum cost-effective soil bearing capacity limit should be defined. It should be also noted that this method is recommended to be applied in a soil from medium low to ideal soil bearing capacity (resilient modulus more than 18 MPa). A trackbed design in a very soft soil below the critical limit of resilient modulus of 15 MPa should be carefully taken into account deeper geotechnical aspects and cost-effective design consideration.

2. ***Selection of trackbed stiffness and thickness***. Consideration of thickness and stiffness combinations is very important. Firstly, in most cases the total height of construction is limited. Secondly, excessive plastic deformation of a soft soil can cause a high level of permanent deformation. Although the strength of trackbed layer is sufficient, but due to plastic deformation on subsoil, the trackbed system is also induced by soil deformation. High level of absolute deflection and flexural stress will occur on the rail as well as concrete slab (for ballastless). This will cause a severe problem in superstructure, although superstructure and trackbed system are designed well. Another important consideration is the minimum thickness of material set by design standards and/or laboratory tests.

3. ***Material characteristics and behaviours***. This is related to the mechanic behaviours of trackbed material. Bonded material (concrete or asphalt) has certain limit of flexural strength. Granular material does not have flexural strength but they are sensitive to vertical and shear stresses. Since ballast material are non-bonded, there is certain requirement of stiffness of underlying layer below ballast to avoid ballast attrition. Concrete slab has an advantage of bridging effect in certain limit of discontinuities support/settlements under this layer. However, settlements will increase the flexural stress on slab which may cause excessive cracks. Another problem is if underlying layers have insufficient bearing capacity, gaps below the

slab due to settlements of the underlying layers will cause pumping effect, which in a long term will induce other problems in the superstructure.

4. ***Special function of layer***. Selection of material and thickness of a layer of trackbed is not only consider the bearing capacity. Some layers are installed not only to distribute stresses or to increase the bearing capacity, but also they have other functions, such as protection of frost action, avoid of ballast attrition, reduction of ground-borne vibrations, or reduce the risk of excessive cracks on concrete slab.

5. ***Stiffness ratio between layers***. If the height of a construction is limited, it does not always mean that then stiffer trackbed material should be used. If there is unbalance and sharp difference of stiffness ratio between layers, then the softer layer will be more dominant. In the reality, ballast attrition problem can occur when the base layer is too soft. In a slab track system, although concrete slab has advantage of bridging effect on certain level discontinuities of support due to settlement, another problem may come as mentioned before, namely pumping effect.

6. ***Geographic and climate conditions***. This correlates to factors of topography, frost action, rain intensity, water table level, drainage system conditions. In a hilly topography, the height of embankment should be also adjusted regarding to vertical alignment of the track as well as horizontal alignment in a curve. In Western countries, the high of trackbed can be higher than the one only based on bearing capacity requirement. This is taken to avoid frost action during winter time. In tropical countries, for instance Indonesia, when the rain intensity is higher during the wet season, the high of trackbed embankment should be higher than the flood water level. This is also taken to secure the superstructure elements from water. The flood water table is frequently found higher above the subsoil surface, especially in a swamp area. Thus the total height of trackbed can be up to 4 and 5 m.

7. ***Self-weight of trackbed and soil condition***. On soft soils, the design of track requires higher total thickness of trackbed. Nevertheless, this will cause a higher self-weight of the trackbed. Then besides bearing capacity, a relatively large consolidation settlement on the top of a soft and compressible subsoil should be taken into account and anticipated in the design. The nature of consolidation settlement on soft soil is that differential settlement will be fairly large, along the transversal cross section of the embankment, even when the embankment load is assumed to be distributed quite

evenly. It follows the simple elastic half-space phenomena, that uniform load will cause non-uniform settlement on soft cohesive soils.

8. ***Avoid over and under estimated design***. Simplification of this methods takes into account safety and correction factors. Although some factors are subjectively based on the judgment of the engineers, it should be avoided to have overestimated and unnecessary factors, which can lead to overdesign result and ineffective costs of the infrastructure. In the proposed analytical method, a reference design chart is used and then at the end multiple factors are applied. This makes the range of safety and correction factors easier to be identified and analyzed.

9. ***Construction procedure***. The proposed design does not take into account the settlements due to primary consolidation of soil. Certain levels of initial settlement within the construction process and due to the natural behaviours of soils should be carefully considered. Stage per stage evaluation is highly recommended in the field applications.

6. Track Soil Interaction

In the conventional methods, linear models are widely used although there are always nonlinearities in track-soil behaviours. Concerning soft soils, questions arise how important is to include nonlinearity behaviours of track-soil in the analysis, in which condition a linear model is sufficient and in which case some major nonlinearities should be considered, and what is the impact of nonlinearities of track-soil behaviour to the overall track system.

Furthermore, there are two main treatments of building railway track on soft soil, doing soil rehabilitations or increase the strength of superstructure. However, it is still questioned: (1) what is the major priority from both treatments, (2) sensitivity analysis delivered from the parameters of both solutions, (3) what are the ranges of bearing capacity of soil which give an approximation whether it needs soil stabilization, installation of thicker trackbed layer, or advanced geotechnical approaches. Some analytical solutions have been discussed in the previous Chapters 3, 4, and 5. However, they are limited in the point of view of a static analysis problem. Hence, dynamic track-soil interaction (TSI) will be conducted as well in this study. Numerical solutions of FEA are proposed to investigate TSI and to gain more realistic solutions.

6.1. Static & Dynamic Soil Reaction Model

A fundamental requirement to investigate track-soil interaction is soil modelling. Correct idealization of soil is very essential. There are many soil models available in the literature, which have various ranges from simple to very complex models. A simple one, for instance, the approach based on several classical works from Barkan (1962)[10], Richart et.al. (1970)[118] and Novak & Beredugo (1972)[98] are still frequently referred by many researchers to estimate viscous spring-damper coefficients to idealize soil reactions. These works had been compared from literature by Dobry & Gazetas (1986)[30] from different sources. They introduced a dimensionless frequency factor a_o and presented the correlations in some charts. Initially, a_o was defined for a circular shape foundation then for a square foundation as follows (from Bowles, 1996)[12]:

Circular foundation[12]:

$$a_o = \frac{\omega . r_o}{V_s} = \omega . r_o . \sqrt{\frac{\rho_s}{G'}} \qquad \text{Eq. 46}$$

Square foundation[12]:

$$a_o = \frac{\omega . B}{V_s}, \quad V_s = \sqrt{\frac{G'}{\rho_s}} \qquad \text{Eq. 47}$$

where: ω is angular excitation frequency, r_o is radius of circular foundation, ρ_s is soil density, G' dynamic shear modulus of soil, V_s is shear wave (S-wave or secondary wave) velocity of soil and B here is the half of the width of square foundation.

Because B is derived from r_o from a circular foundation, therefore, the total width of square foundation is expressed as $2B$. It is more convenient to derive B for a square foundation from r_o and then to use an equivalent area of a square foundation proportional to a circular foundation. Dobry & Gazetas (1986)[30] had done this conversion and introduced a dimensionless constant J_a for this conversion.

The method suggested by Dobry & Gazetas (1986)[30] is able to estimate the static and dynamic spring constants (stiffness and damping) of soil resistances for vertical, horizontal, rocking and torsion motions. Formulations and correlation charts of this soil model are briefly described by Bowles (1996)[12]. The formulations to estimate static stiffness and damping of soil supporting a square foundation are expressed as follows:

Vertical[12]:
$$K_z = S_z.\frac{2L.G'}{1-\mu} \qquad \textit{Eq. 48}$$

Horizontal[12]:
$$K_y = S_y.\frac{2L.G'}{2-\mu} \qquad \textit{Eq. 49}$$

$$K_x = K_y - \frac{0.21L.G'}{0.75-\mu}\,(1-\frac{B}{L}) \qquad \textit{Eq. 50}$$

Rocking[12]:
$$K_{\theta x} = S_{\theta x}.\frac{G'}{1-\mu}(I_{\theta x})^{0.75}\left(\frac{B}{L}\right)^{-0.25} \qquad \textit{Eq. 51}$$

$$K_{\theta y} = S_{\theta y}.\frac{G'}{1-\mu}\left(I_{\theta y}\right)^{0.75} \qquad \textit{Eq. 52}$$

Torsion[12]:
$$K_t = S_i.G'(J)^{0.75}$$

S_z, S_y, $S_{\theta x}$, $S_{\theta y}$, $S_{\theta y}$ factors can be defined from the tables after Dobry & Gazetas (1986).

Dobry & Gazetas (1986)[30] introduced η_i for stiffness and λ_i for damping parameters to estimate dynamic stiffness K'_i and damping C'_i from static stiffness and damping coefficients. Lysmer, as quoted by Dobry & Gazetas (1986)[30], noted that from experimental data results, soil has a hysteresis damping, even though in a small strain level. Hence, a damping ratio parameter β_d needs to be included in the parameter of dynamic stiffness and damping[12]:

[12]
$$K_{dyn,i} = K'_i - \omega C'_i\beta_d \qquad \textit{Eq. 53}$$

[12]
$$C_{dyn,i} = C'_i + \frac{2K'_i\beta_d}{\omega} \qquad \textit{Eq. 54}$$

Barkan (1962)[10] suggested β_d values from 0.02 to 0.05. Whitman & Richart (1967)[145] had summarized β_d from various references including Barkan and suggested to take a value from 0.01 to 0.1 (from Bowles, 1996)[12].

6.2. Modelling Track-Soil Interaction

Investigation of track-soil interaction (TSI) is conducted to analyze the influence of soil bearing capacity to the stability of different track systems. The point of the analysis is focused on the dynamic behaviours of a track subjected with dynamic loading with different excitation frequencies as well as the one induced from a running train with different speeds.

6.2.1. Data for Dynamic Track-Soil Interaction

a) Soil Static and Dynamic Stiffness and Damping

There are seven example variations of soil, which have strengths ranged from soft to medium and hard soil. The types of soil are clay, silt, silt-clay, sand and gravel. Soil example data and its assumption of standard properties are shown in this following table:

Table 15. Soil data for TSI simulation

Sample	USCS Soil Class	Short Description	Soil's Parameter				
			E_s	μ	G'_s	Υ_s	V_s
			[MPa]	-	[MPa]	[kN/m^3]	[m/s]
I	CH	Fat Clay	10	0.40	3.57	17	45.4
II	CL	Lean Clay	20	0.40	7.14	17	64.2
III	MH	Elastic Silt	40	0.45	13.79	18	86.7
IV	ML	Lean Silt	50	0.45	17.24	18	96.9
V	SC	Sand Clay	60	0.30	23.08	18	112.1
VI	SM	Sand Silty	80	0.30	30.77	20	122.8
VII	GW	Gravel well graded	100	0.30	38.46	22	130.9

The estimation of stiffness and damping of soil is followed the approach from Dobry & Gazetas (1986)[30]. To estimate viscous spring-damper element of soil model for finite element analysis, soil damping ratio $\beta_d = 0.01$ is taken. A mathematical computer program in MATHCAD is developed to calculate these soil resistance parameters (see Appendix 7, pp. 251 about this program).

Stiffness and damping of soil in vertical, longitudinal and transverse directions are originally formulated by Dobry & Gazetas (1986)[30] for a simple dynamic foundation, for instance for a machine foundation. It has a finite dimension and the dynamic load is normally located in the middle of the foundation for the most of analyses.

In railway application, a track has greater areas. A single line track has a width a proximally 3 m. In FEA, the length of the track model has to be set finitely concerning limitation of model size and efficiency of the calculation time. The basic models have length of 26 m, which are used for simulations of different excitation frequencies and of 86.5 m for simulations of different train speeds. The 3D track model has two rails and both rails are assumed to be subjected with equal loads. Thus, for calculating stiffness and damping per unit area, a half of the track width (1.5 m) is considered. Then, the stiffness and damping are assumed to be distributed uniformly along the length of the track. Therefore, in the analytical calculations for modelling soil, the estimations of stiffness and damping parameters are defined per square meter of track area.

Table 16 shows the approximations of equivalent soil's static stiffness and damping following this approach and above assumptions. Static stiffness and damping in longitudinal and transverse directions are initially equal per square meters of foundation. Then in the FEA models, they are distributed to each respective direction, which means that the total stiffness in each direction will not be equal depending on the width and length of the model.

Table 16. Static stiffness & damping of soil model

Sample	Soil Class	Static Stiffness (per 1m^2)			Damping (per 1m^2)		
		Vertical	Longitudinal	Transverse	Vertical	Longitudinal	Transverse
		[kN/mm]	[kN/mm]	[kN/mm]	[kN.s/mm]	[kN.s/mm]	[kN.s/mm]
I	CH	13.51	10.05	10.05	0.14	0.08	0.08
II	CL	27.02	20.09	20.09	0.20	0.11	0.11
III	MH	56.93	40.04	40.04	0.31	0.16	0.16
IV	ML	71.16	50.06	50.06	0.35	0.18	0.18
V	SC	74.84	61.09	61.09	0.32	0.21	0.21
VI	SM	99.78	81.45	81.45	0.39	0.25	0.25
VII	GW	124.73	101.81	101.81	0.45	0.29	0.29

Frequency-dependent dynamic stiffness and damping per square meter of foundation area are calculated using the program and are depicted in the following figures:

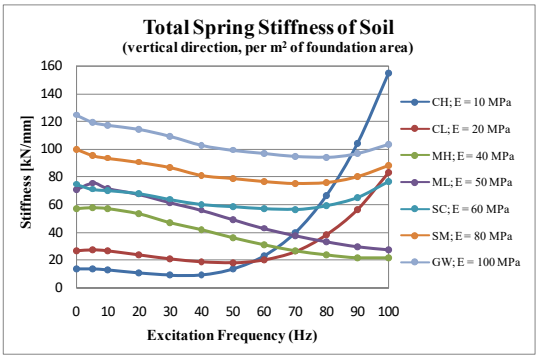

Figure 34. Dynamic stiffness of soil in vertical direction

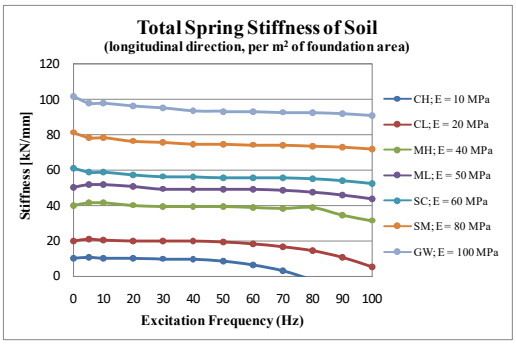

Figure 35. Dynamic stiffness of soil in longitudinal direction

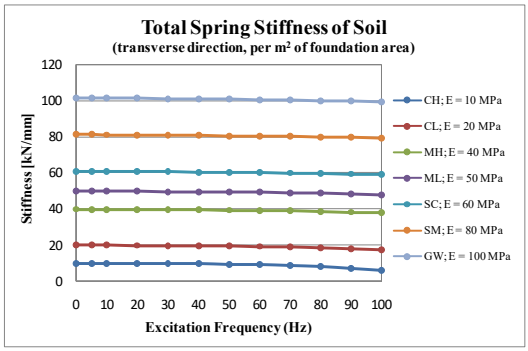

Figure 36. Dynamic stiffness of soil in transverse direction

The complete data of frequency-dependent stiffness and damping constants calculated utilizing the computer program are shown in the Table 74 in Appendix 7, pp. 257.

It can be seen that the analytical method suggested by Dobry & Gazetas (1986)[30] has a boundary of the dimensionless factor a_o, which is limited only up to 1.5. A value of a_o greater than 1.5 means a high excitation frequency and/or very soft soil, which is not in the range of this approach. Therefore, in the FEA model, stiffness and damping values for excitation frequencies above 120 Hz are assumed to remain constant.

b) Elastic-pad Stiffness and Damping Model

The basic parameters of elastic-pad stiffness and damping are obtained from some examples of the laboratory tests conducted by the *Institute of Road, Railway and Airfield Construction, TU München*. Some tests were done for the specimens which have static stiffness of 22.5 kN/mm, 40 kN/mm and 60 kN/mm. Dynamic stiffness was measured from laboratory test in the frequencies of 5 and 10 Hz and room temperature condition. Indeed, the stiffness of elastic-pad is actually dependent on the material, geometry, frequency and number of loading (dynamic and cyclic stiffness), temperature, preloading force (fastening system) and the age of the elastic-pad material (aging effect).

Some other examples of elastic-pad stiffness based on measurements from low to high frequencies available from literature [64] from [134] and [63] in [104] are shown in the Figure 37 and Figure 38.

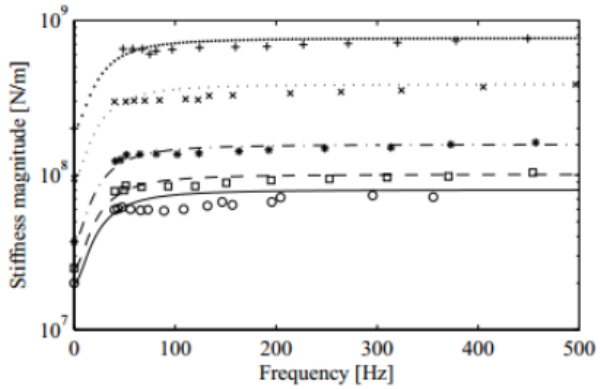

Preload: ○ 20 kN, □ 30 kN, * 40 kN, x 60 kN and + 80 kN. *Kstat* = 60.33 kN/mm

Note: picture courtesy of Koroma et al, (2013)[64] from Thompson, et.al. (1998)[134]

Figure 37. Aproximation of elastic-pad dynamic stiffness under different preload levels

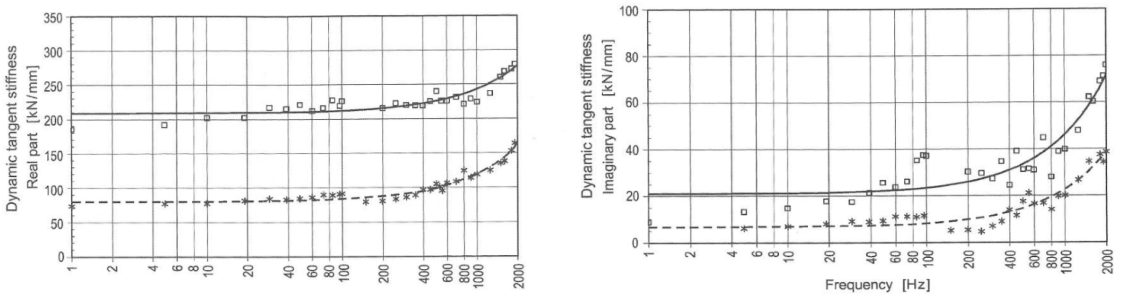

Preload: * 25 kN and □ 43 kN.

Note: picture courtesy of Knothe et al, (2003)[63]in [104]

Figure 38. Dynamic tangent stiffness of elastic-pad ZW 700 A60 SGW 95

There are two models of dynamic stiffness and damping of elastic-pad, which are used in the FEA simulations. First model utilizes input data of constant dynamic stiffness and damping (frequency-independent). The damping constants are assumed by the author as a linear damping proportional to the deformation rate of elastic-pad. They are chosen within the range of the common values used in a dynamic study of track as shown in this table:

Table 17. Data of frequency-independent dynamic stiffness and damping of elastic-pad

Static Stiffness	Dynamic Stiffness Constant	Dynamic Damping Constant
22.5 kN/mm	27.2 kN/mm	213 kN.s/m
40 kN/mm	48.5 kN/mm	132 kN.s/m
60 kN/mm	72.5 kN/mm	86 kN.s/m

Second model uses frequency-dependent dynamic stiffness and damping. It is shown in the Figure 39 and based on author's assumption by using curve fitting and referencing the data from [64][134] for static stiffness of 60 kN/mm and preload of 20 kN. Dynamic damping coefficients are estimated as simple fraction frequency-dependent damping as follows:

$$C = \frac{2\xi K}{\omega_{exc}} = \frac{\xi K}{\pi f_{exc}} \qquad [20] \qquad Eq.\ 55$$

where: K is the initial stiffness [N/mm], ξ is material damping ratio, ω_{exc} is angular excitation frequency [rad/s] or as f_{exc} [Hz]. The material damping ratio is assumed 0.02.

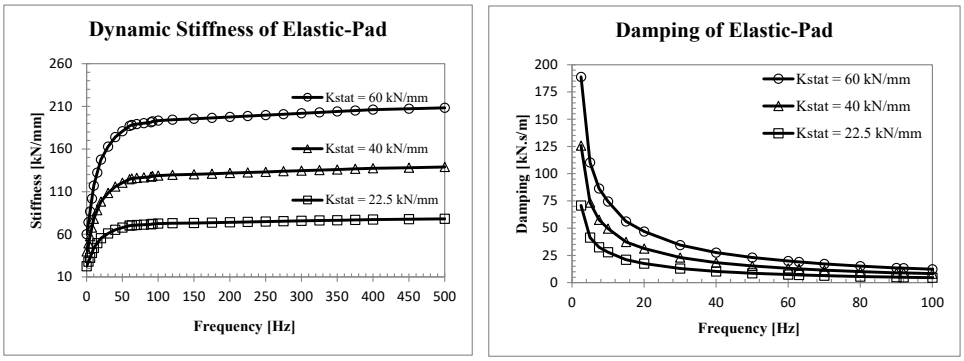

Figure 39. Frequency-dependent stiffness and damping model of elastic-pad

6.2.2. Finite Element Model for Dynamic Track-Soil Interaction

a) Slab Track Model

The sketch of track model for doing track-soil interaction analysis is presented in the Figure 40. The full model is built as 3D model in ANSYS. The discretization of the model is shown in the Figure 41. The model presents a concrete slab track system.

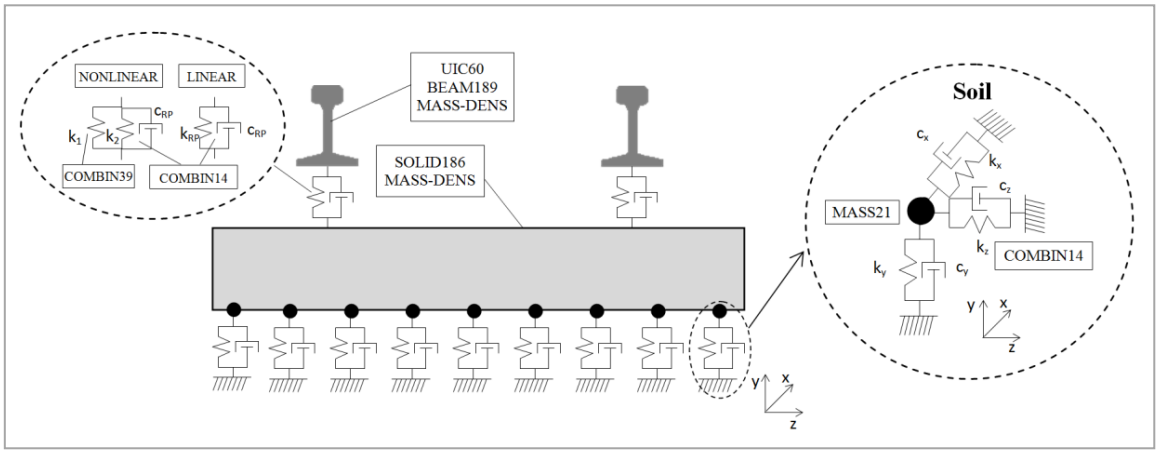

Figure 40. Sketch of slab track model

The model consists of two rails of 60E2 profile, which are modelled as beam using BEAM189 element. Elastic-pad and fastening clamps (fastening system) are idealized in two

variations, namely as linear (given code of LIN-FAST, using COMBIN14 element) and as nonlinear (given code of NL-FAST, using COMBIN14+COMBIN39 elements) viscous spring-damper elements. Linear elastic model of fastening system means that elastic-pad stiffness constant in tension and fastening clamping resistance in compression are identical. Nonlinear elastic model of fastening system takes into account three parameters: (a) compression stiffness (k_2 in COMBIN14 element), which is contributed from the elastic-pad elastomeric material; (b) tension stiffness (k_1 in COMBIN39 element), which comes from the fastening's clamping resistance (actual values around 15 - 20 kN/mm) and (c) preloading clamping force from 18 to 20 kN (f_p in COMBIN14 element).

Concrete slab is modelled as solid element using SOLID186 element. Soil is idealized as linear viscous spring-damper elements using COMBIN14 in three directions: one vertical direction and two horizontal directions (longitudinal and transverse).

Masses of rail, concrete slab and soil are considered in the analysis through their density parameters. Mass of elastic-pad is neglected. Soil mass is modelled as lumped mass using MASS21 element. Lumped mass is a mass model, which is attached to a rigid body. In the FEA models, it is coupled in the shared nodes, which connect between solid elements of the bottom surface of slab and spring-damper elements of soil. Approximation of the lumped mass is by using some trials in the calibration of the model.

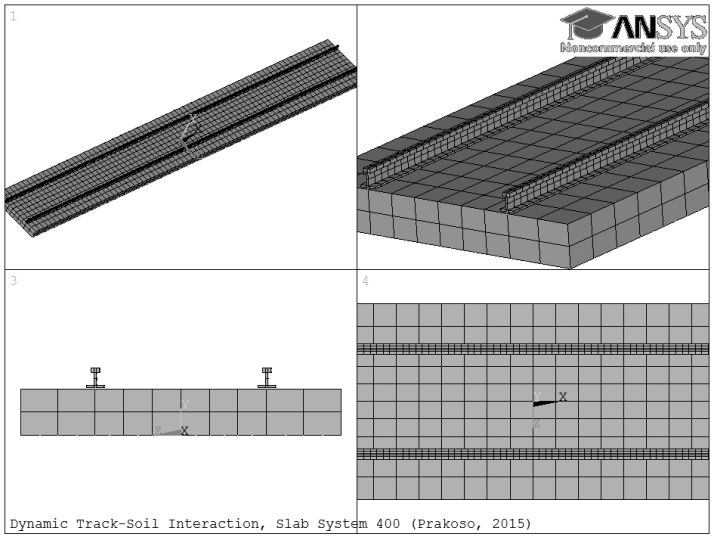

Figure 41. Discretization of FE-model for TSI Analysis.

Three major types of dynamic analysis are performed, namely transient harmonic analysis, modal analysis and transient dynamic analysis.

b) Loading Schemes

Harmonic sinusoidal load is automatically generated in ANSYS for a harmonic analysis. Each rail of the track model is subjected with single point wheel load of 125 kN. Meanwhile, for transient dynamic analysis two loading schemes are used as follows:

1. *Consistent loading with a specific excitation frequency*

   In this loading scheme, four load steps with the same period (specific excitation frequency) are modelled. Each load has magnitude of 125 kN and is automatically ramped in each load's sub-step. Track model is subjected with this load in the range of excitation frequencies of 0 Hz (static), and from 2 up to 700 Hz (dynamic).

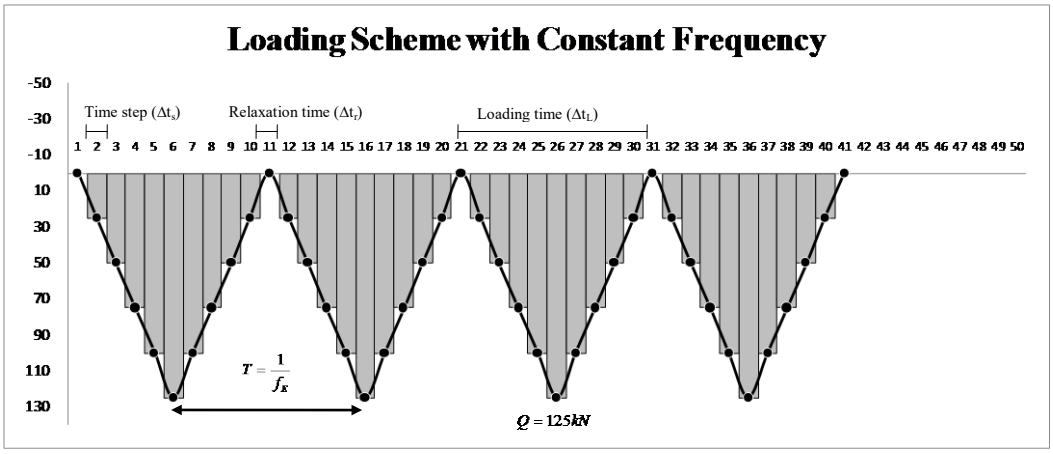

Figure 42. Loading scheme with a specific excitation frequency

2. *Train loading with different speeds*

   This loading scheme presents a train loading with different speeds. The axle configuration of German train ICE-1 is taken for this loading scheme. ICE-1 train is basically configured with two power cars (PC) and twelve passenger/trailer cars (TC) with 56 axles. Each axle of power cars generates static axle load of 196 kN and each axle of trailer cars produces 160 kN of static axle load to the rails. The load model in this loading scheme is described in the Figure 44.

   As comparison, an example of field data measurement, which was conducted by *Institute of Road, Railway and Airfield Construction TU München* is shown in the Figure 43. The data is presented as deflection line of rail induced from a running test train with ten axles. From this data measurement, train speed was approximated 115 km/hour. The data was obtained from the transducer recorders. It shows that the average loading time (Δt_L) is about 0.14 seconds. The average loading time is calculated from load cycles of ten axles. A load cycle is defined as a cycle from zero

to maximum loading and then to minimum loading. This average loading time is used as reference value of above artificial loading scheme, which is simulated in ANSYS. The train speeds for simulations are varied as follows: 45, 60, 90, 100, 120, 150, 180, 200, 220, 250, 275 and 300 km/hour. These give average loading times of 0.358s, 0.268s, 0.179s, 0.161s, 0.134s, 0.107s, 0.089s, 0.081s, 0.073s, 0.064s, 0.059s and 0.054s respectively for the set speed variations.

Due to huge increase of the size of the FEA models and calculation time, the load model is reduced and the simulations only take into account 8 axles (1 power car and 1 trailer car). This is quite reasonable because a simulation of the whole train with 56 axles is not necessary. The reason is that the most important dynamic impacts are normally generated from first, second and the axles between two cars. Furthermore, a simulation of two cars is more efficient for saving computing time in ANSYS.

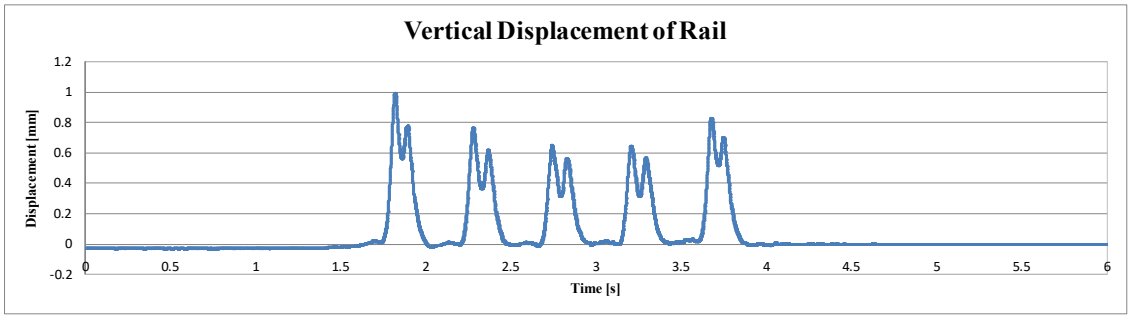

Figure 43. Example of rail's vertical deflection gained from field measurement

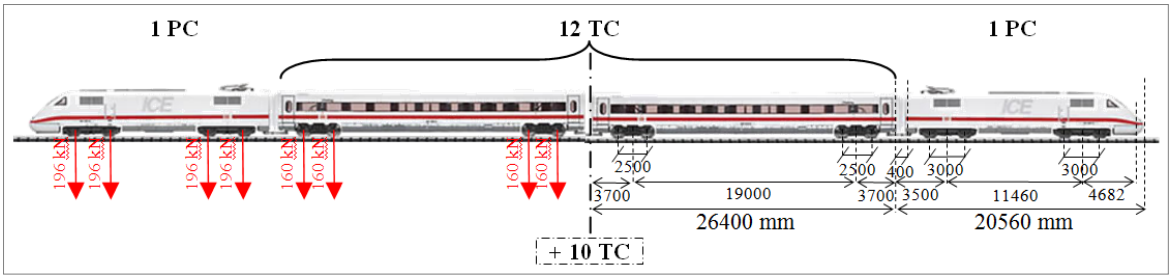

Figure 44. ICE-1 train loading scheme

In the FEA simulations, the artificial loading scheme of train ICE-1 is assumed to generate different excitation frequencies resulted from axle to axle distances (2.5 and 3 m), bogie to bogie distances (7.2, 11.5 and 19 m) and sleeper to sleeper distances (60 cm for ballasted and 65 cm for ballastless) as summarized in the following table:

Table 18. Estimation of major excitation frequencies generated from 8 axles of ICE-1 train artificial loading scheme with different speeds

Speed [kph]	DAF	Excitation Frequency [Hz]						
		Axle to Axle		Bogie to Bogie			Sleeper to Sleeper	
		2.5 m	3.0 m	7.2 m	11.5 m	19.0 m	0.6 m	0.65 m
45	1.49	5.0	4.2	1.7	1.1	0.7	20.8	19.2
60	1.49	6.7	5.6	2.3	1.4	0.9	27.8	25.6
90	1.60	10.0	8.3	3.5	2.2	1.3	41.7	38.5
100	1.63	11.1	9.3	3.9	2.4	1.5	46.3	42.7
120	1.70	13.3	11.1	4.6	2.9	1.8	55.6	51.3
150	1.81	16.7	13.9	5.8	3.6	2.2	69.4	64.1
180	1.91	20.0	16.7	6.9	4.3	2.6	83.3	76.9
200	1.98	22.2	18.5	7.7	4.8	2.9	92.6	85.5
220	2.05	24.4	20.4	8.5	5.3	3.2	101.9	94.0
250	2.16	27.8	23.1	9.6	6.0	3.7	115.7	106.8
275	2.24	30.6	25.5	10.6	6.6	4.0	127.3	117.5
300	2.33	33.3	27.8	11.6	7.2	4.4	138.9	128.2

DAF is estimated concerning a track line for general trains and moderate track quality. The higher the excitation frequency of a dynamic loading naturally decreases the vibration amplitude (displacement) of a structure. Because the loading time is also decreased. Meanwhile, a higher the speed of a train generates also a higher excitation frequency subjected to a track. Nevertheless, the dynamic amplification of a higher speed train is increased. Thus, the interaction of those factors to the displacement in a theoretical idealization can be generally illustrated as follows:

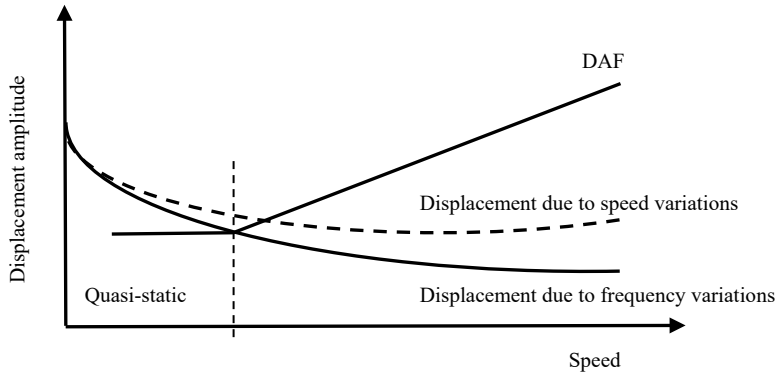

Figure 45. Illustration of theoretical relation of speed, dynamic amplification factor, and displacement due to speed and frequency variations

6.3. FEA of Dynamic Track Soil Interaction

6.3.1. Harmonic and Modal Analysis

Transient harmonic analysis is performed to understand the behaviour of a track model and to identify the dominant natural frequencies of a track system within the range of excitation frequencies. This analysis calculates steady states (forced vibration) of a structure. This linear dynamic analysis is also useful to estimate dynamic behaviours of track model, which enables to identify track's response over resonance and impacts of forced vibration induced from a running train.

The results are presented as frequency and relative displacement correlation. Instead of absolute displacement, relative displacement values are used to avoid misinterpretation of the results. The reason is that in the harmonic analysis, a track is subjected to a sinusoidal loading, which does not present the real traffic loading (then also not to the magnitude of displacement). Instead of the absolute value of displacement, the major interests in harmonic analysis are the dynamic response (natural frequency), dynamic behaviour of a track and the tendency of changes in some parameters to the vibration response of a track.

Elastic-pad is idealized as linear (LIN-FAST model). Constant stiffness of 40 kN/mm and 60 kN/mm and assumption of small constant damping coefficient of 2 kN.s/mm and 20 kN.s/mm are taken. Lumped mass of soil is not included. These variations are done to concentrate investigation of the harmonic behaviours of the viscous-elastic elements in the track model, which are elastic-pad and soil. This is also taken to understand the impact of adjustment of stiffness and damping of elastic-pad to the dynamic behavior of a track. The slab track basic model for this investigation is built using a concrete slab C35/45 with thickness of 30 cm, which is located on soil with elastic modulus of 60 MPa.

The changes of harmonic response of the track model due to the difference of stiffness and damping of elastic-pad is firstly observed. This is done to identify in which range of natural frequency is mostly influenced by elastic-pad (fastening) elements. The comparison is shown in the Figure 46 and all of the charts are built in the same scale of relative-displacements.

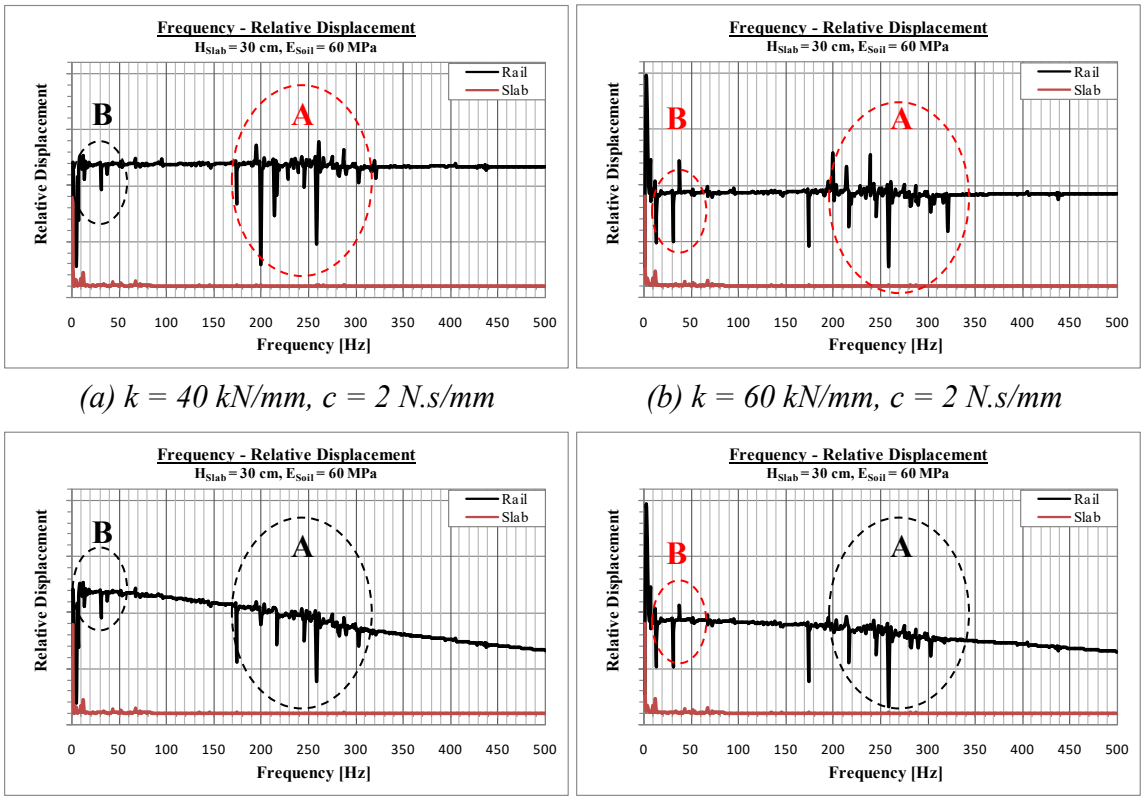

(a) k = 40 kN/mm, c = 2 N.s/mm *(b) k = 60 kN/mm, c = 2 N.s/mm*

(c) k = 40 kN/mm, c = 20 N.s/mm *(d) k = 60 kN/mm, c = 20 N.s/mm*

Figure 46. Harmonic response of track models with different stiffness and damping parameters of elastic-pads

Firstly, two important points are figured out from sensitivity analysis of elastic-pad stiffness and damping parameters, namely:

- It can be identified that contrast variations of damping coefficient of elastic-pad affect more obvious to rail's dynamic response in the high excitation frequency range between 200 and 300 Hz (marked as A, the difference between red and black ellipses).
- Adjustments of stiffness of elastic-pads influence harmonic response of rail in the range of middle frequency in between 13 and 31 Hz. (marked as B, the difference between red and black ellipses). This occurrence in the frequency about 31 Hz is the first natural frequency, which is also contributed from fastening system.

Secondly, seeing in more detail from the above figures, there are six major critical natural frequencies about 2 Hz, 13 Hz, 31 Hz, 175 Hz, 220 Hz and 260 Hz in all model variations. These can be observed from the six highest peaks (amplitudes) of the displacements. At the frequencies of 13 and 31, and especially 220 and 260 Hz it has been recognized that they are affected by the changes in stiffness and damping parameters of elastic-pad. The lowest natural frequency is 2 Hz, which obviously occurs in both rail and concrete slab. Hence, this

natural frequency comes from the stiffness and damping of soil. Other natural frequencies are resulted from interactions among stiffness, mass and damping of different track components. The impact of changes of track element's properties to the natural frequencies will be investigated further in the next subchapters.

Modal analysis is also conducted to observe the response of the track system in more detail at the critical natural frequency. Track's dynamic response is investigated from its vibration characteristics, namely natural frequency and mode shapes. The same model, which is used for harmonic analysis is simulated for modal analysis. An example of mode shapes resulted from modal analysis are shown in the following Figure 47 and Figure 48.

The natural frequencies of around 2 Hz and 175 Hz obviously affect the vibration of concrete slab in low and high frequencies. The mode shape of 2 Hz exhibits low frequency vibrations resulted from the soil dynamic properties. Meanwhile, the mode shape of 175 Hz demonstrates high frequency vibrations coming from concrete slab.

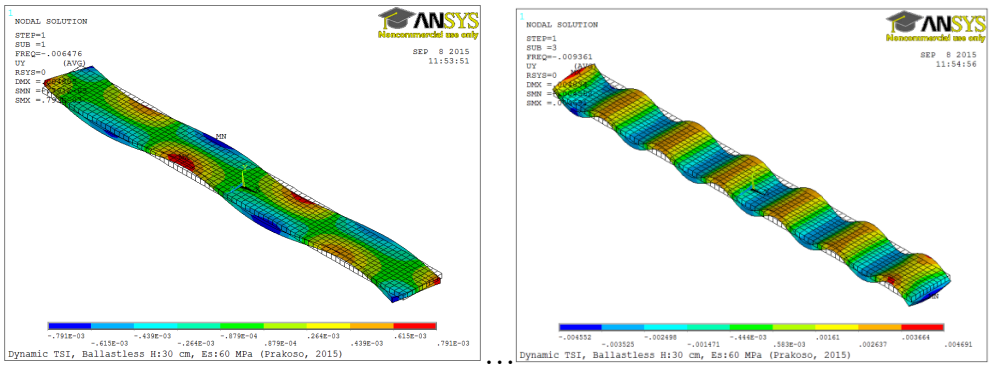

Figure 47. Mode shapes of slab track in frequencies of 2.06 and 2.16 Hz

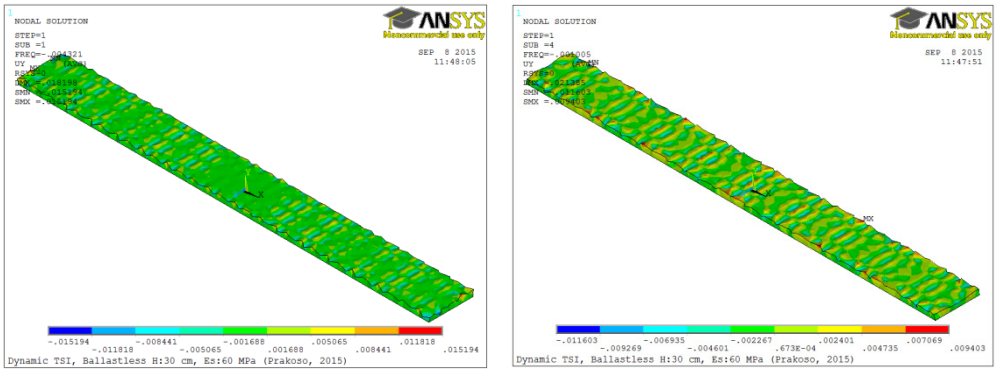

Figure 48. Mode shapes of slab track in frequencies of 175.01 and 175.08 Hz

6.3.2. Calibration of the Models

The linear FEA models are extended and calibrated. The calibrations include consideration of the impacts of nonlinear fastening system and soil mass effects (mass scaling). The detail about the calibration is discussed in the Appendix 9, pp. 263. Two important findings, which are revealed during calibration are: 1) nonlinearity which is considered in fastening system model affects the vibration characteristic of a slab track in high excitation frequencies (200 and 300 Hz). This exhibits an agreement with the harmonic analysis, 2) soil mass should be included to obtain more realistic solution in the dynamic analysis.

Final calibration is to validate all of model input parameters defined before, which are now assigned to the final FEA models for investigation of track-soil interaction. The frequency-dependent stiffness and damping model depicted in the Figure 39, nonlinear fastening idealization and calibrated soil model with lumped mass are assigned to the final models. Examples of the FEA simulation in the frequency domain using the final model are presented in these following figures. The load is according to four-constant loading in the Figure 42.

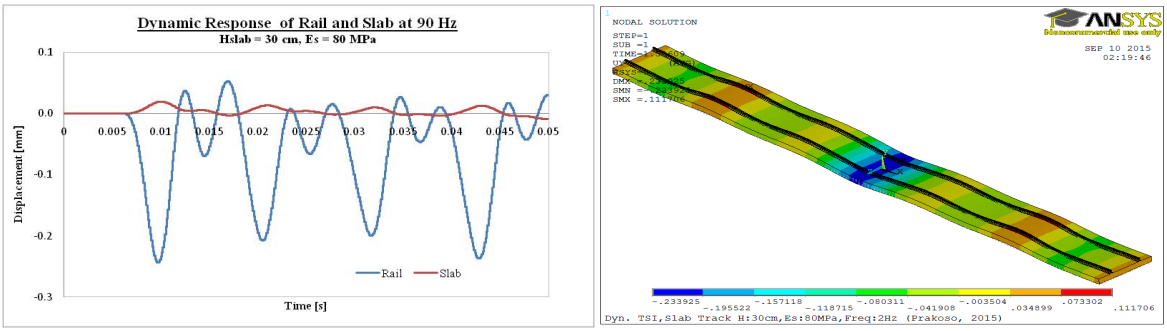

(a) *(b)*

Figure 49. (a) Dynamic response of slab track subjected with excitation frequency of 90 Hz and (b) Contour plot of vertical vibration of slab track at excitation frequency of 2 Hz

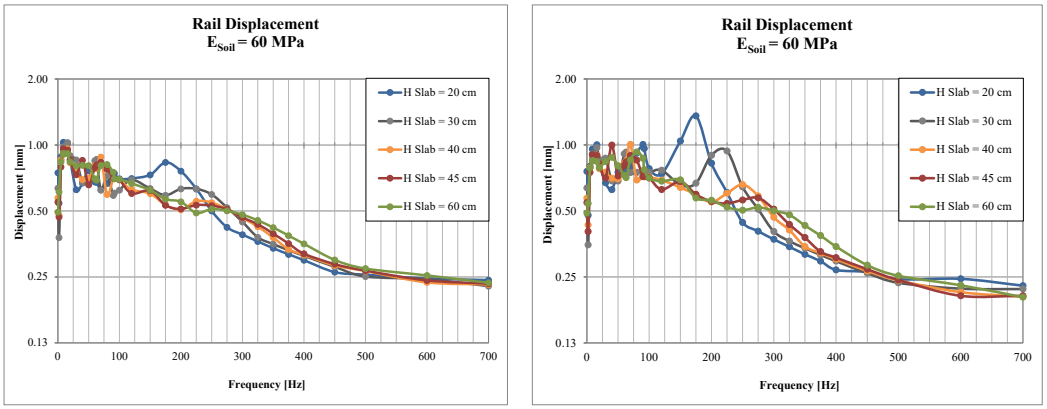

(a) Elastic-pad 22.5 kN/mm *(b) Elastic-pad 60 kN/mm*

Figure 50. Comparison of the dynamic response of rail displacements of single-layer slab tracks with elastic-pad resilient stiffness values of 22 kN/mm and 60 kN/mm

As comparison, Figure 51 illustrates the results of a measurement of vertical vibration velocity using "ballast stone accelerometer" detector developed by *Chair and Institute of Road, Railway and Airfield Construction, TU München* (Leykauf, et.al., 2006)[72]. The measurement was done by installing this detector in the ballast stones, which were constructed with different types of sleepers and resilient values of fastening system.

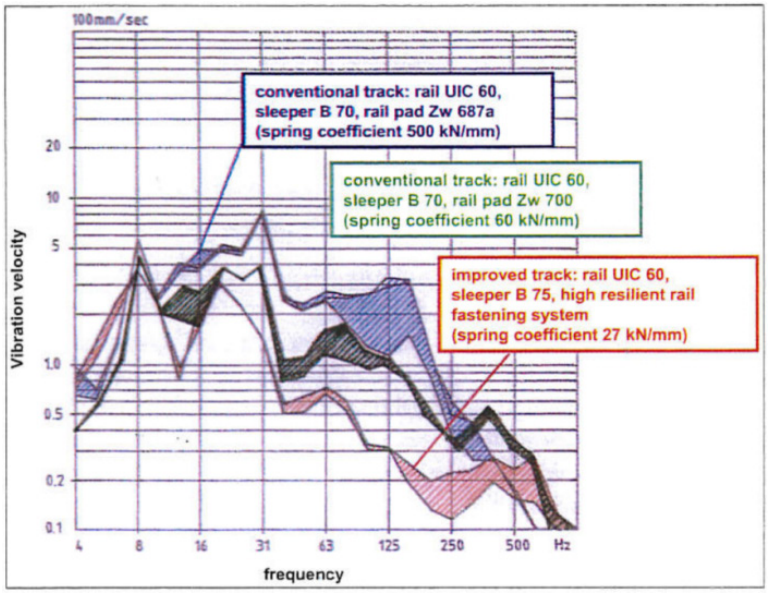

Note: picture courtesy of Leykauf et al, (2006)[72]

Figure 51. Vibration velocity of different ballasted track system under different excitation frequencies (from Leykauf, et.al. 2006)

From the measurement, it reveals a reduction of amplitude in the high frequency range as it is demonstrated as well in the final FEA models. Although measured in different way than displacement of the rail, vibration velocity also represents the dynamic behaviours of a track. One of the major differences between the slab track model and ballasted track system is that ballast also provides certain higher level of damping and elasticity.

Observing in more detail the measurement data, it can be seen that there is also peak in the frequency of 31 Hz of using stiffer fastening systems. This peak is shifted to around 18 Hz and is reduced when softer elastic-pad of 27 kN/mm is installed. The same behaviour is demonstrated from the final FEA model in the Figure 50. In addition, the harmonic and dynamic analysis conducted before also reveals a first natural frequency of 31 Hz, which is influenced by fastening systems with a stiff elastic-pad of 60 kN/mm. It confirms the identification of natural frequency from harmonic and dynamic finite element analysis that the natural frequency of 31 Hz is also influenced by fastening system. This comparison exhibits a good agreement of the dynamic behaviours between field measurement and FEA

Therefore, in the final simulations, a complex model which considers nonlinearity of fastening as well as soil's mass will be assigned to investigate slab track dynamic responses in frequency domain as well as with different train speeds.

6.3.3. Transient Dynamic Analysis in Frequency Domain

Various simulations by employing the final model are performed with soil modulus of elasticity ranged from 10 to 100 MPa, and five thickness variations of C35/45 concrete slab: 20, 30, 40, 45 and 60 cm. Consistent frequency loading scheme (see Figure 42, pp. 86) is applied with excitation frequencies ranged from 0 to 700 Hz. Fastening system is idealized as nonlinear with elastic-pad's static stiffness of 60 kN/mm and frequency-dependent dynamic stiffness and damping.

The results of FEA dynamic analysis of a single slab track model with 20-cm concrete thickness located on soil with stiffness variations are presented in the Figure 52. The right charts in the Figure 52 are the magnification of the left charts to observe clearer the changes in low and middle excitation frequency ranges. Figure 53 describes dynamic responses of a slab track with different thicknesses constructed on soil with low (10 MPa), moderate (60 MPa) and moderate stiff (100 MPa) bearing capacity levels. The complete results of the simulations with variations in concrete slab thickness and elastic-pad with static resilient of 22.5 kN/mm can be seen in the Appendix 10, pp. 269.

First of all, it can be observed from the Figure 52 that there are four critical peaks at the dynamic frequencies of 5 Hz, 16 Hz, 80-90 Hz and 150-175 Hz. The peak at the frequencies of around 175 Hz confirms the results of the harmonic analysis. An interesting behaviour, which can be observed from the bottom charts of Figure 52 is that at the low frequency range from 2 to 20 Hz, changes in soil stiffness affect significantly to both rail and slab displacements. Because the impacts take a place in the rail and slab, this is clear that it is majorly caused by soil's stiffness factor. At frequency lower than 5 Hz (quasi-static state), the impact of soil stiffness changes is more obvious to the superstructure's response.

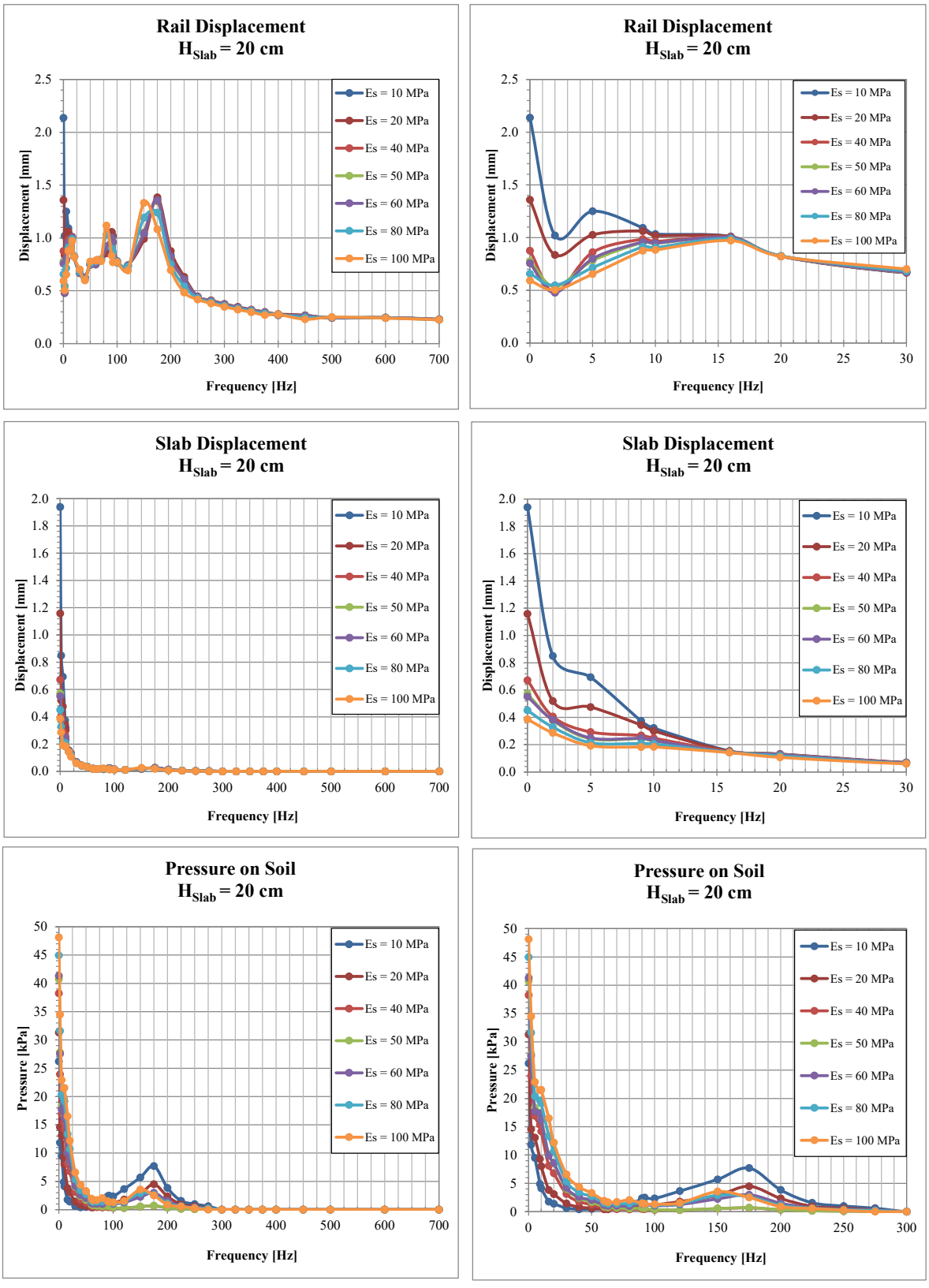

Figure 52. Dynamic response of rail, concrete slab and soil of a single-layer slab with thickness of 20 cm in different soil strengths and excitation frequencies

Only seeing from short-time condition of a railway track subjected by train loading, it implies that static and quasi-static states represent better initial estimation for preliminary

assessment of a railway track. This is the reason why static and quasi-static states are more concerned in an initial static design of a railway track. Meanwhile, transient analysis is more focused for long-term impact assessment and prediction of railway track performance within the design life.

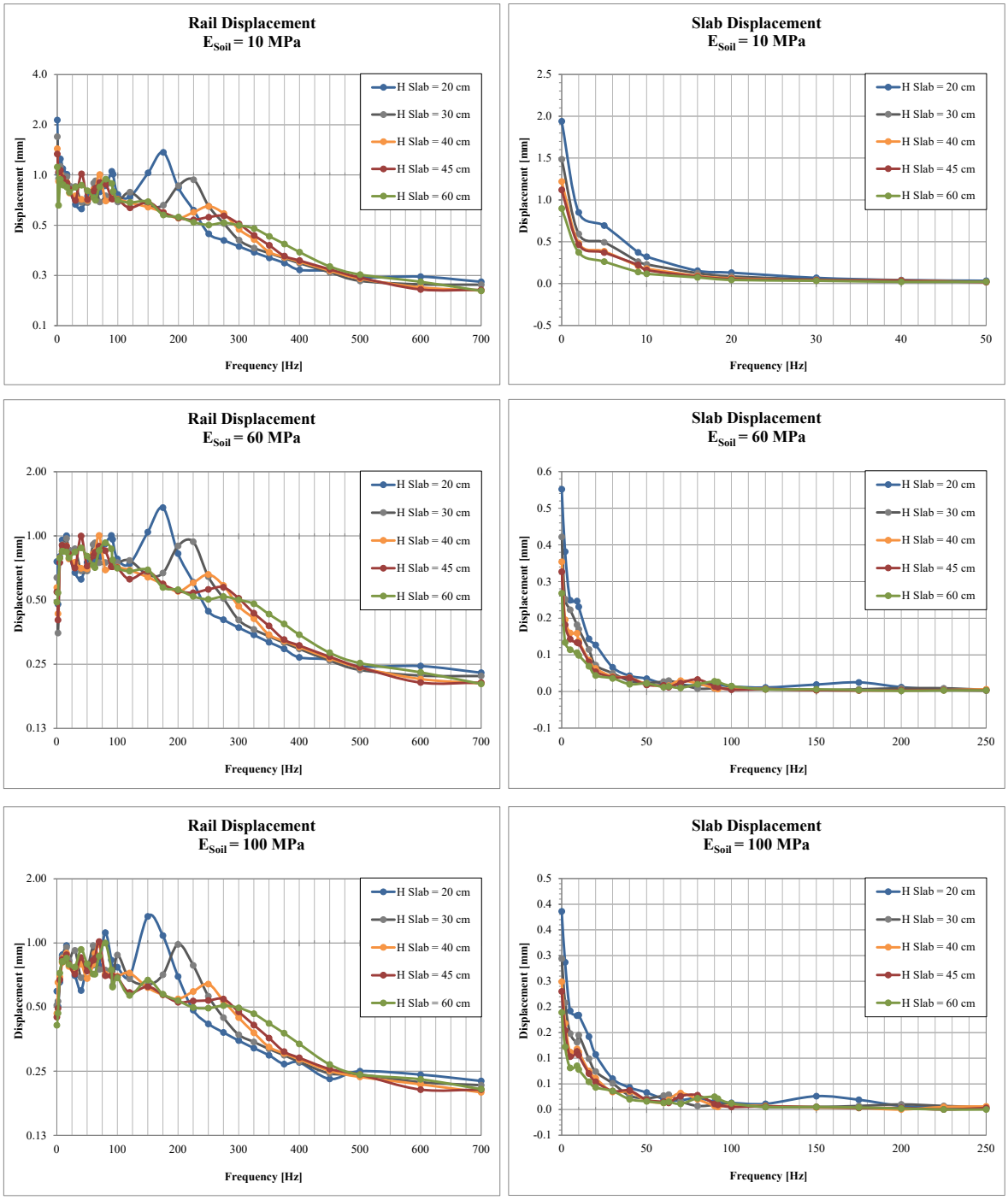

Figure 53. Dynamic response of rail and single-layer concrete slab track with different thicknesses, soil's stiffness of 10, 60 and 100 MPa and in different excitation frequencies

Secondly, from Figure 53, it can be seen that increasing the thickness of the concrete slab influences the magnitude of rail displacement in high frequency. These can be obviously

seen from the peaks at around 150 Hz and 350 Hz. The frequency range of 150 to 175 Hz is also influenced by the fastening systems. The impact of reduction of displacements on the rail within high frequency range is more significant if a thicker slab is used. The thicker the concrete slab is, the smaller is the displacement peak of the rail. In addition, the modifications of slab thickness and soil's mass effect shift the natural frequency to the higher level. This indicates that increasing thickness of concrete slab has two advantages: to reduce the rail and slab displacements in high frequency as well as to shift the natural frequency of the system. If a critical high excitation frequency induced from a running train can be identified and should be avoided to increase the overall stability of the track, therefore, slab thickness modification plays very important role for this purpose.

Thirdly, as it is shown in the Figure 53, if a thin concrete slab of 20 cm is used, two high peaks occur in all of soil bearing capacity levels, including in a moderate stiff soil of 100 MPa. This implies that a sufficient thickness of concrete slab is required. However, increasing the slab thickness has different impacts as well. It can be seen in the range of 50-90 Hz where second critical peaks occur. It is shown that increasing thickness does not improve the reduction of the peak on the rail. Even the slab with thickness of 60 cm results a peak on the rail higher than the other ones with thickness of 40 and 45 cm placed on the soil with elastic modulus of 10 MPa. Although concrete slab is very thick, but if the bearing capacity of soil is very low, it does not mitigate the level of dynamic vibration of a track.

Finally, Figure 54 presents the comparison of actual and allowable bending tensile stress of the rail, slab and pressure on soil. The permissible limit of flexural strength of rail is according to Wöhler fatigue approach (see Example I in Appendix 4, pp. 228). The allowable limit of bending tensile stress of C35/45 concrete is estimated using Smith's approach (see in Table 80 in the Appendix 8, pp. 261), meanwhile allowable limit of pressure on soil is approximated using Heukelom & Klomp formulation (see Eq. 136, pp. 224).

It is shown that to fulfill the criteria of flexural strength limit of concrete, a sufficient bearing capacity of soil and thickness of slab are demanded. Only concrete slab with thickness greater than 45 cm, which is placed on soil with elastic modulus greater than 60 MPa sufficiently fulfills both criteria. On soft soil (Es = 10 MPa), it theoretically requires a slab with thickness of 60 cm. However, placing a very thick concrete slab directly on soil (single layer system) is inefficient. This indicates the need of trackbed and multilayer design.

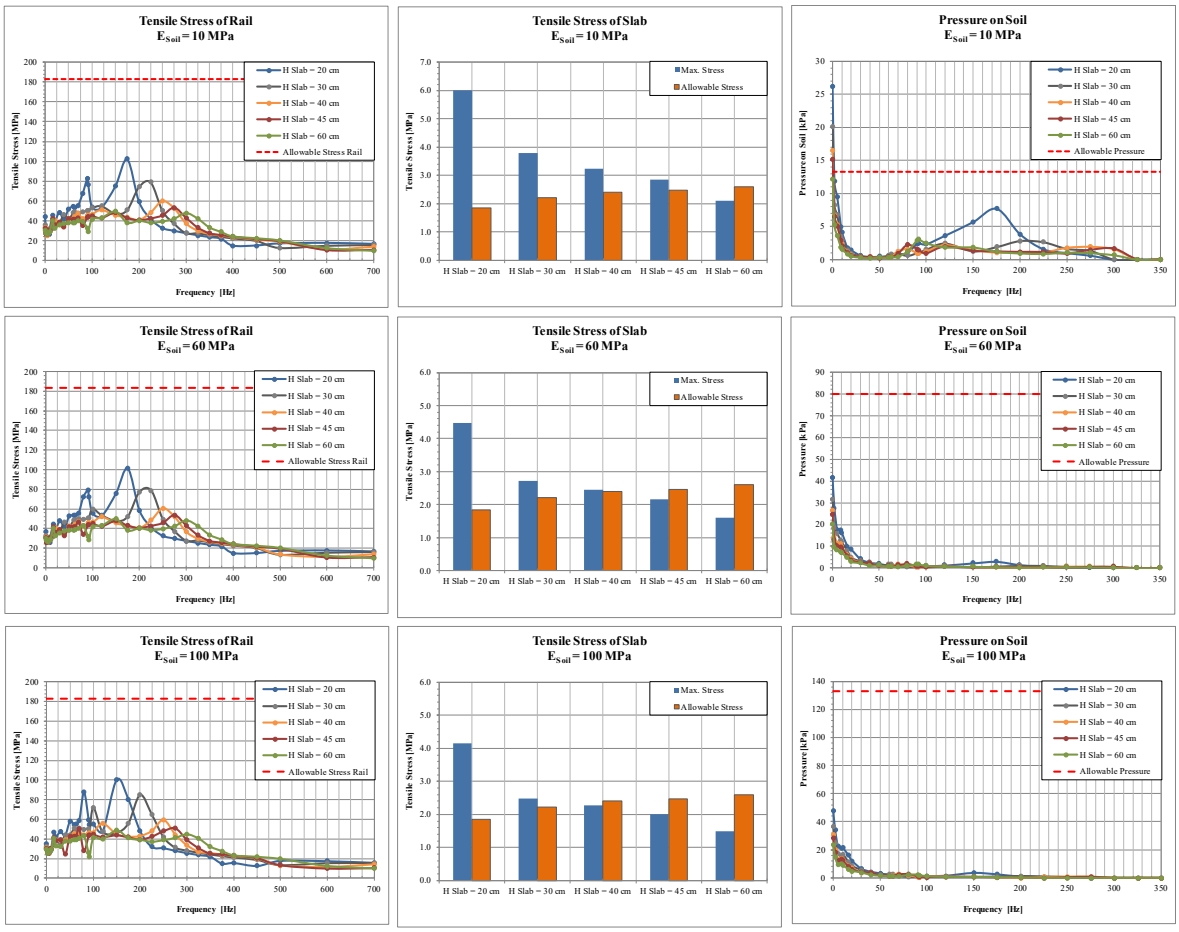

Figure 54. Actual and allowable tensile stresses of rail and single-layer slab as well as pressure on soil

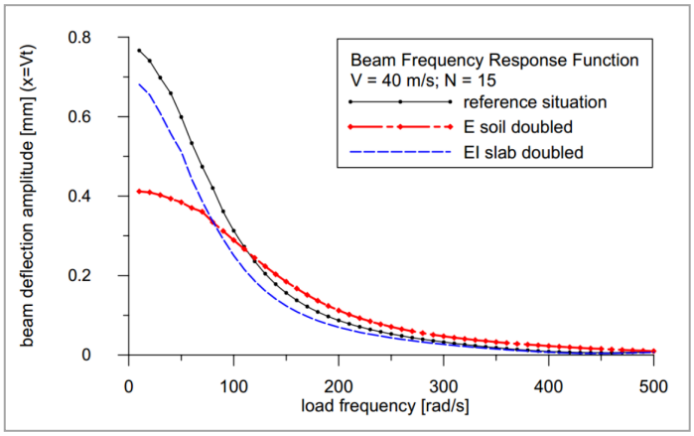

Note: picture courtesy of Steenbergen, et.al. (2006) [126][127]

Figure 55. Effects of an increase of the beam bending stiffness and a soil improvement on the slab frequency response (at subcritical load velocities), after Steenbergen, et.al. (2006)

The study about influence of stiffness of concrete slab and soil has been also shown in the work of Steenbergen et. al. (2006)[126][127]. They utilized analytical track model of a beam on 1D elastic foundation half-space under constant harmonic loading. The aim of their study is to analyze the stiffness requirements contributed from slab track and soil in a dynamic

point of view as it is shown in the Figure 55. Steenbergen et. al. (2006) generally concluded that soil improvement is more appropriate solution in low frequency and increasing slab stiffness is more effective in high frequency[126][127].

However, as conclusion from static analysis, trackbed design, and dynamic analysis performed in this research, the categorization into two sides of low and high frequency ranges as well as soil stabilizations and superstructure strengthening efforts cannot be separated as simple as those two classifications. The reason is that in the real situation there are a broader range of excitation frequencies generated from a running train, and these depend on many dynamic factors as interactions of different track elements, train speed and vehicle-track interactions. In the design phase, it is very difficult to identify the exact values of excitation frequencies and then to make a single generalization of all cases. Secondly, not only stiffness plays important role in the dynamic analysis, but also damping. It is hard to predict the particular damping ratio of track elements. The available way is only to obtain the total damping of track system from a measurement.

The author prefers to answer this issue by combining all of the advantages of soil stabilization, improvement of superstructure strength as well as optimization of other track elements by understanding the characteristics of each element. All of those efforts cannot be seen separately, but it should be integrated to optimize all of the benefits conveyed from track components. Therefore, three important characteristics of a slab track elements, which influence the performance of the track in dynamic track-soil interaction are:

- *Soil bearing capacity improvement* and *elastic-pad stiffness adjustment* are majorly done for mitigation dynamic and vibration impacts in low frequency range.
- *Concrete thickness and stiffness modification* is mainly taken into account to improve performance of slab track against dynamic impact induced from high frequency vibration of a running train.
- *Fastening's stiffness and damping alteration* is taken into action to reduce the vibration impact in high frequency range.

6.3.4. Transient Dynamic Analysis with Different Train Speeds

Dynamic simulation using artificial loading of train is performed to obtain more realistic solution of dynamic track-soil interaction. Different combinations of slab track model are subjected with artificial loading of ICE-1 train with 8 axles (1 power car and 1 passenger car) and different speeds.

Eight different speeds are selected from Table 18, which have range from 60 to 250 km/hour. The speed variation begins from 60 km/hour because a significant dynamic impact normally starts from train speed of 60 km/hour. Five variations of slab thickness: 20, 30, 40, 45 and 60 cm and six variations of soil bearing capacities with elastic modulus of 20, 60, 100, 150, 200 and 250 MPa are built as several combinations of single layer slab track models in ANSYS. Soil elastic modulus values of 20, 60 and 100 MPa are assigned to model soft, moderate and moderate stiff soils. Additional soil elastic modulus variations of 150, 200 and 250 MPa are simulated to idealize a slab track supported with a stiff base layer. Two additional combinations are slab track and ballasted track, which are constructed using multilayer trackbed system. This trackbed layers are designed using the proposed analytical methods of trackbed design. Fastening systems is idealized using nonlinear NL-FAST model. Values of dynamic stiffness of 72.5 kN/mm and constant damping coefficient of 86 N.s/mm (see Table 17) is assigned in FEA to model the fastening systems with static stiffness of 60 kN/mm and considering preloading of 20 kN. Soil is modelled as linear viscous elements the same as the previous simulations. One example of this simulation in ANSYS is depicted in this following figure:

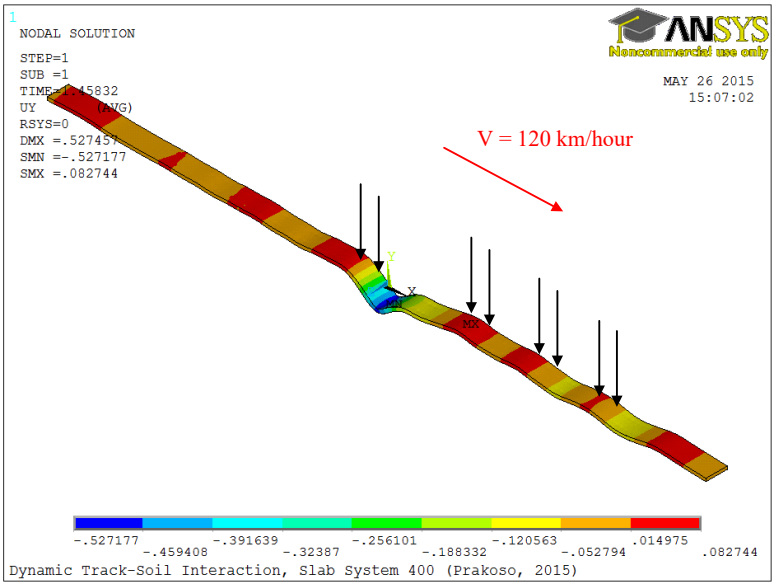

Figure 56. Example of dynamic analysis of running train with speed of 120 kph on a single-layer slab track with thickness of 40 cm and soil bearing capacity of 60 MPa

The summary of FEA simulations of running train for single layer concrete slab track is presented in the Figure 58. As comparison of the actual behaviours resulted from running train test, the result from measurement of ballasted track system in Zagreb, Croatia, which was done by *Chair and Institute of Road, Rail and Airfield Construction TU München* is shown in the Figure 57.

Figure 57: Example of running train test on a ballasted track in Zagreb, Croatia

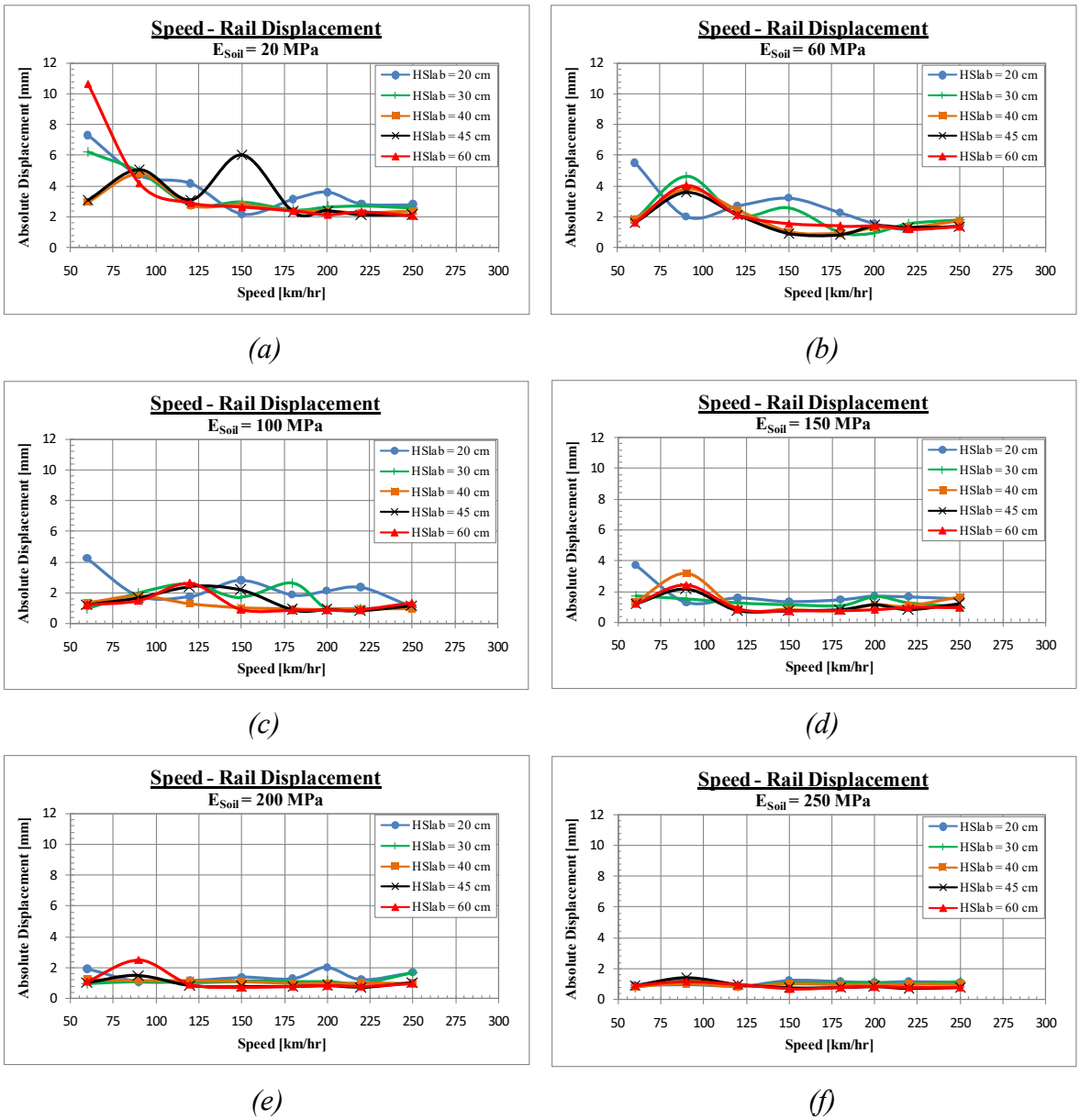

Figure 58. Correlations of train speed and rail absolute displacement of single layer slab track on different soil strengths

From the Figure 58 (a), it can be seen that in a low bearing capacity of soil, high level of absolute deflection on the rail occurs in the low speed running train. Low speed running train majorly generates excitation frequencies in a low range as it can be seen in the Table 18. This supports the previous results and arguments that soil bearing capacity influences more to the dynamic behaviours of a slab track in the low frequency range. One remarkable thing, which can be seen from this figure is that a single layer thick slab of 60 cm located on soil with elastic modulus of 20 MPa delivers the highest displacement of the rail at the low speed or low excitation frequency range. It occurs due to the single concrete slab layer with high mass lays on elastic soil support. This again support the previous arguments that increasing thickness of a single layer concrete slab when the soil is soft has a limitation and is not always a proper solution. When the soil has higher stiffness (60, 100 and 150 MPa) and a thicker slab more than 20 cm is constructed, the peaks are shifted to the higher speeds. This also indicates a shift to higher excitation frequency and the peaks occurs as a result of interaction of track elements.

Secondly, Figure 58 (a), (b), (c) and (d) exhibit that a thin concrete slab (20 cm) tends to generate the highest deflection in low speed of running train when the soil elastic modulus is lower than 150 MPa. But it starts to be more stable in the soil elastic modulus of 200 MPa. This indicates that a thin concrete slab can be installed if bearing capacity of the supporting layer is sufficient as a base layer. This also means that thin layer of concrete slab is more cost-effective if it is combined with a base layer (trackbed).

Thirdly, from Figure 58 (e) and (f), it can be concluded that track response is almost in a steady state within different train speed levels and it fulfills the desired rail deflection of 2 mm. In this bearing capacity levels with elastic modulus more than 200 MPa are normally contributed from a stiff material, such crushed stones, asphalt, or concrete treated base. This also demonstrates the requirement of base layer and trackbed layers. A cost-effective design can be achieved by combining a thin slab (20 cm) and trackbed layers.

Finally, FEA analysis of the impacts of installing multilayered trackbed is shown in the Figure 59. In this example, it can be obviously seen that 20-cm concrete slab provided with multilayered trackbed leads to a stable performance of a slab track system. The stability is shown both in the top and bottom of a track, as it can be seen from almost continuous displacements of the rail as well as reduction of the pressure on the soil. This reveals again that an equilibrium structure is achieved by designing track layers using gradual increase of

the stiffness from the bottom to the top layers and by optimizing all of the benefits contributed from the characteristics of all track components.

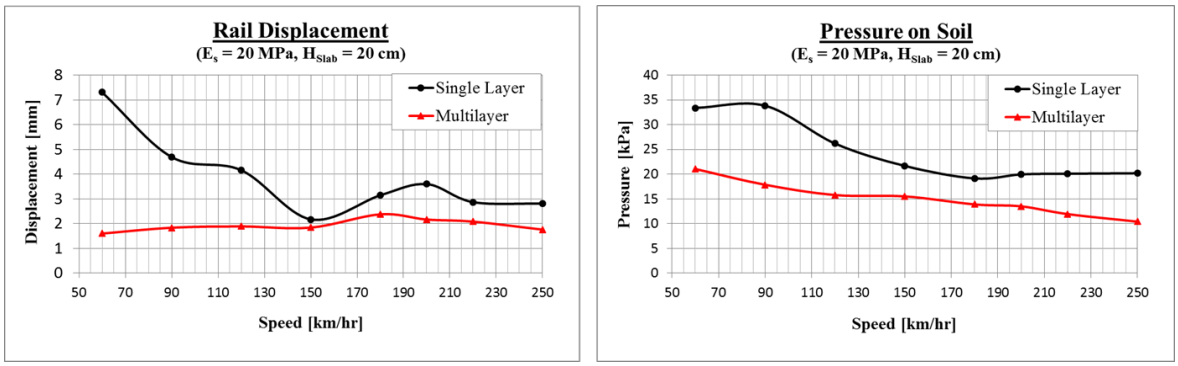

Figure 59. Correlations of train speed and rail displacement of a slab track designed using multilayer trackbed

6.4. Differential Settlements on a Ballasted Track System

The major problem of constructing railway track on soft soil is differential settlements on soil. When the soil is soft, although the trackbed is designed according to a sufficient level of bearing capacity, but the settlements on soft soil will induce the absolute settlements on the trackbed layers. On a ballasted track system, abrupt and uneven settlements may indicate the existence of gaps between the bottom of the sleepers and top surface of ballast. This problem causes hanging sleepers with uneven support along the track. Figure 61 and Figure 60 show an example measurement of hanging sleeper (Rump, 1997[120], as cited by Lechner (2011) [69]) and Puzavac, 2012[106] in the high-speed line between Hannover and Würzburg.

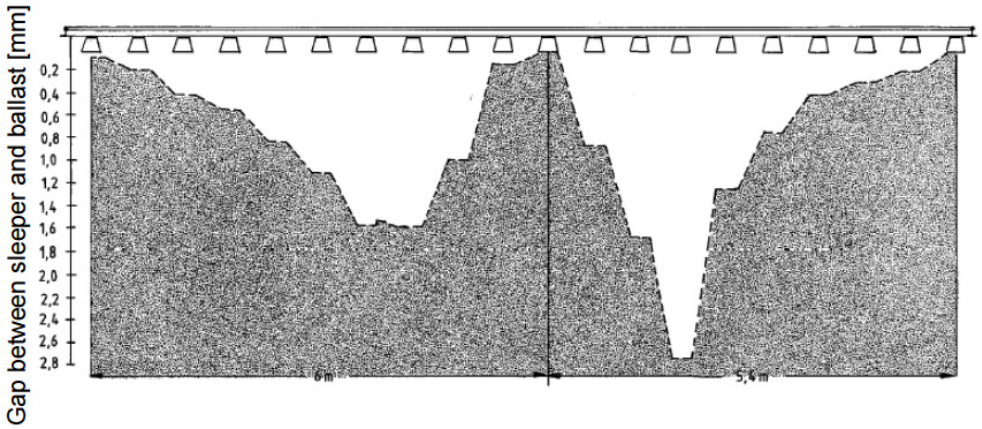

Note: picture courtesy of Rump, (1997)[120], as cited by Lechner (2011)[69]

Figure 60. Uneven support of sleepers (hanging sleepers) measured in the high-speed line Hannover – Würzburg, Germany in in 1995 of a longer track section

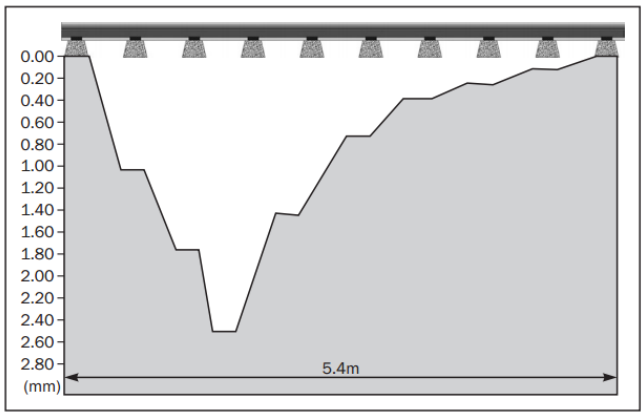

Note: picture courtesy of Rump, (1997)[120] as cited by Puzavac, et. al (2012)[106]

Figure 61. Uneven support of sleepers (hanging sleepers) measured in the high-speed line Hannover – Würzburg, Germany in 1995 in 5.4 m track section

Actually, differential gaps take a place due to nonlinearity and non-homogenous soils. However, as it is depicted in the Figure 61 and Figure 60, the length of differential settlement basin area is theoretically relevant to the initial characteristic length of a beam on continuous support. The greater the nonlinearities and variations of stiffness on each support of track makes the differential settlements far from continuous support assumption.

Investigation of uneven support of a ballasted track is conducted in FEA. The track model is illustrated in the Figure 62 and the scenarios are described in the Table 19 below.

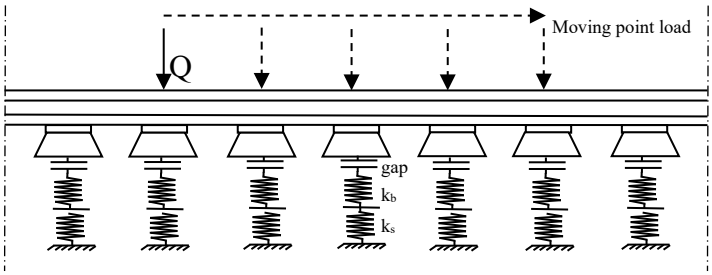

Figure 62. Ballasted track model with hanging sleepers

Sleeper profile B70 with length of 2.6 m and width of 26 cm is idealized in FEA and it considers the areas with support at the edges of sleeper and area without support in the middle of sleeper. The length of the middle part of sleeper without support is assumed 50 cm. Static load is moved within the areas of uneven support.

Ballast with uneven gaps is modelled using COMBIN40 elements. The discretization of the FEA model is shown in this following figure:

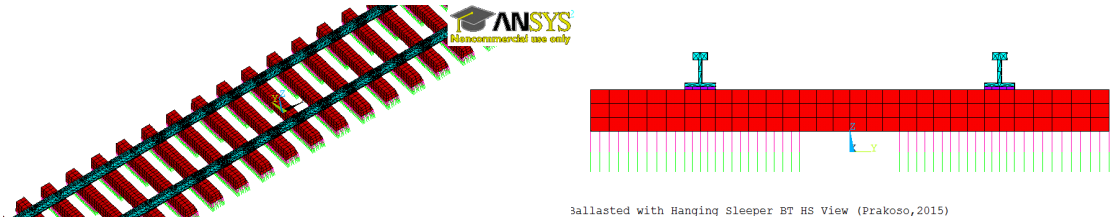

Figure 63. Discretization of ballasted track model with hanging sleepers in ANSYS

The measurement data shown in the Figure 61 is used as reference, with assumption that the track of the reference data is initially designed according to standard requirements for high speed train. As quoted by Puzavac, et. al (2012)[106] from literature, the optimum total track stiffness ranges are: 80-130 kN/mm[108], 70-80 kN/mm for a high speed lines[78] as well as freight traffic lines[131].

In the model, properties of rail profile 60E2, wheel load of 125 kN and ballast with stiffness of 180 kN/mm are considered. To define the assumed gaps on the hanging sleepers of scenarios S.3 and S.4, these steps of iteration are taken:

1) The characteristic length (L_{char}) of the track in initial condition laying on continuous support (S.1) is estimated from the actual track length of 5.4 m (reference data) as $L_{char} = L_{act}/8$ = 5.4m/8 = 675 mm (based on Zimmermann influence line theory).
2) The initial trackbed stiffness (k_{tot}) and then the maximum deflection (y_{max}) of a track on continuous support are predicted using reversed method of Zimmermann (see Eq. 107 and Eq. 111 in the Appendix 1, pp. 216-217) and L_{char} = 675 mm. This gives k_{tot} = 74.2 kN/mm and y_{max} = 0.75 mm.
3) The subgrade stiffness is approximated from trackbed k_{tot} = 74.2 kN/mm and ballast k_b = 180 kN/mm. It is obtained $k_s = 1/(1/k_{tot} - 1/k_b)$ = 126 kN/mm.
4) The the subgrade stiffness of S.1, S.2, S.3 and S.4 are assumed:
    a. Scenario S.1. k_s = 126 kN/mm of a new line with a good condition.
    b. Scenario S.2. k_s = 90 kN/mm of a line under service with uneven support.
    c. Scenario S.3. k_s = 60 kN/mm of of a poor track condition.
    d. Scenario S.4. k_s = 35 kN/mm of of a very poor track condition on soft soil.
5) Trackbed stiffness k_{tot} of S.2, S.3 and S.4 are calculated based on their k_s and k_b. It is obtained that $k_{tot} = 1/(1/k_s + 1/k_b)$ = 60 kN/mm, 45 kN/mm and 29 kN/mm are obtained for S.2, S.3 and S.4 respectively.
6) Characteristic lengths (L_{char}) and the maximum deflection (y_{max}) of a track on continuous support of S.2, S.3 and S.4 are computed using Zimmermann method.
7) Actual lengths of all scenarios are computed as $L_{ac} = 8L_{char}$.

8) The number of hanging sleeper is simply $L_{act}/60cm$ (sleeper spacing).
9) The gap distances of S.3 and S.4 are assumed proportional to the ratio of their y_{max} to y_{max} of S.2 and the reference gaps in the Figure 61.

The parameters of the scenarios are shown in the Table 19. The estimated gaps on hanging sleepers are presented in the Figure 64.

Table 19. Scenario of FEA simulation with hanging sleepers of a ballasted track

Scenario	Track Quality/ Condition	Sub-grade	Theoretical of continuous support			L_{act} [m]	No. Hanging Sleeper
		k_s [kN/mm]	k_{tot} [kN/mm]	L_{char} [mm]	y_{max} [mm]		
S.1 (no gap)	new	126	74.2	675.0	0.75	5.4	9
S.2 (ref. gap)	moderate	90	60	711.7	0.88	5.7	9
S.3 (wi. gap)	poor	60	45	764.8	1.09	6.1	10
S.4 (wi. gap)	bad	35	29.3	851.4	1.50	6.8	11

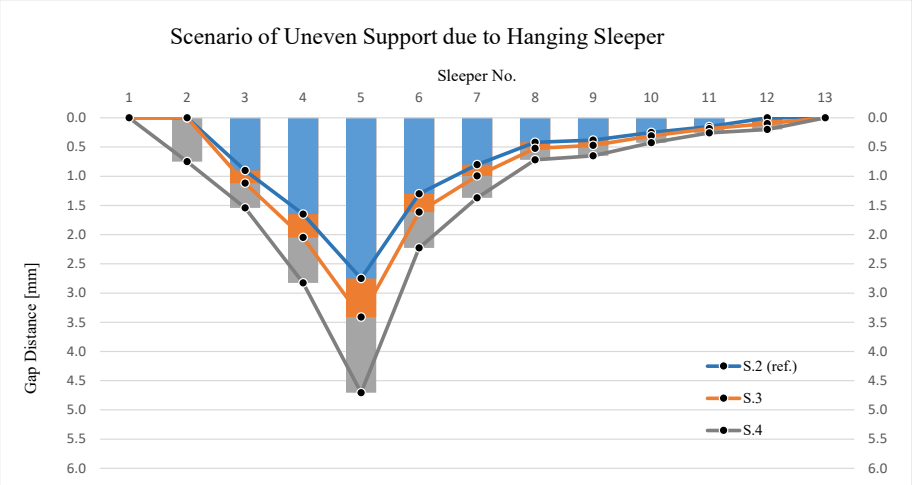

Figure 64. Distribution of the gaps on the hanging sleepers

To assess the performance of the ballasted track, permissible flexural strength of rail is estimated using Wöhler approach by taking into account 40°K of different temperature to the neutral welding temperature (20°C) as well as new and corroded rail conditions (see example in the Appendix 4, pp. 227). Meanwhile, limit of pressure on ballast is defined using Heukelom & Klomp method for number of load cycles of 2.10^5.

The results of FEA static simulations are shown in the Figure 65, Figure 66 and Figure 67.

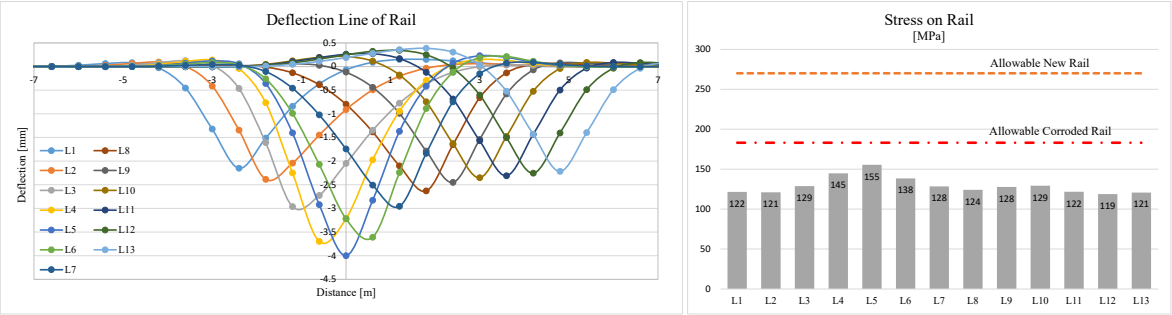

Figure 65. Impact of uneven support of ballasted track with hanging sleepers of Scenario 2 due to moving point load

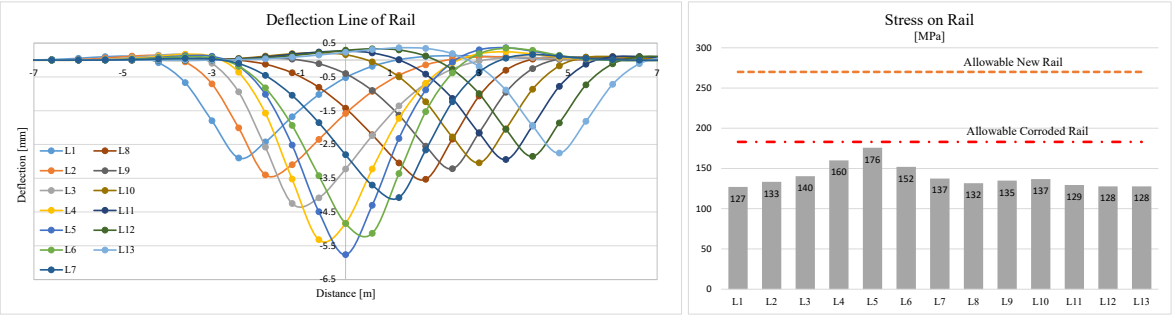

Figure 66. Impact of uneven support of ballasted track with hanging sleepers of Scenario 4 due to moving point load

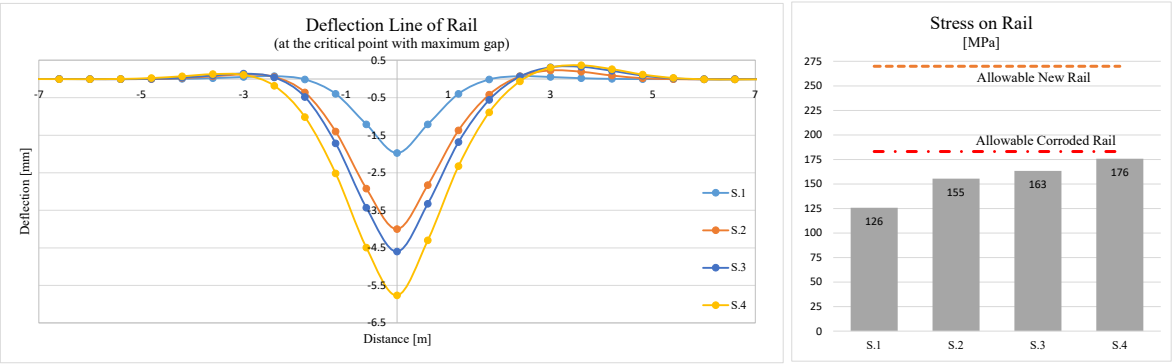

Figure 67. Impact of uneven support of ballasted track with hanging sleepers of different soil bearing capacity levels and due to point load at the critical location of gap

From the Figure 65 and Figure 66, it reveals that uneven support due hanging sleepers leads to a discontinuity of the displacement of rail. The impact can be also obviously seen from the level of flexural stress on the rail. In a poor condition of track (Scenario S.4), the level of flexural stress on rail is fairly high (176 MPa). This is very close to the allowable flexural strength of rail (183 MPa) considering corroded rail condition. The hanging sleepers cause an increase of the level of stress on rail. This can be unsecure for rail against rail crack. At the location of the maximum gap of hanging sleeper (Figure 67), the higher the gap distance, the more level of discontinuity as well as the displacement and flexural stress magnitudes of rail.

The critical location is found in between the beginning of the gap up to the location where the maximum gap takes a place. In this point, there is a high level of discontinuity shown by a sharp difference of flexural stress levels. When the gap distance is higher beyond the maximum displacement of the hanging sleepers, due to load traffic the sleeper on the area of the hanging sleepers has no support and there is no contact between the bottom surface of sleepers and the top of ballast layer. Opposite with that condition, when the gap distance is lower than the maximum displacement of hanging sleeper, due to traffic load the sleeper is displaced down and touched the top of ballast layer. However, there is already initial displacement, thus the support level of ballast is reduced and the absolute displacement of rail will be higher. In the actual condition, the impact even becomes worse.due to cyclic loading of running trains. Then the gap distance gets also higher within a longer time of cyclic loading. Later, it can reach a state of sleepers without support from ballast. This can cause an ill track geometry condition.

The investigation of uneven support is proceeded with dynamic FEA simulation in frequency domain and different train speeds to observe the impact of hanging sleepers due to dynamic loading. The FEA model is extended for dynamic simulation. The masses and damping of track elements and soil are included. Fastening system is modelled nonlinear, which is identical to the models used in the simulations of the previous subchapters. The dynamic load is according to the load model of four-wheel loading with different excitation frequencies (see Figure 42, pp. 85), which is located at the location of maximum gap. The results are shown in the Figure 68, Figure 69 and Figure 70.

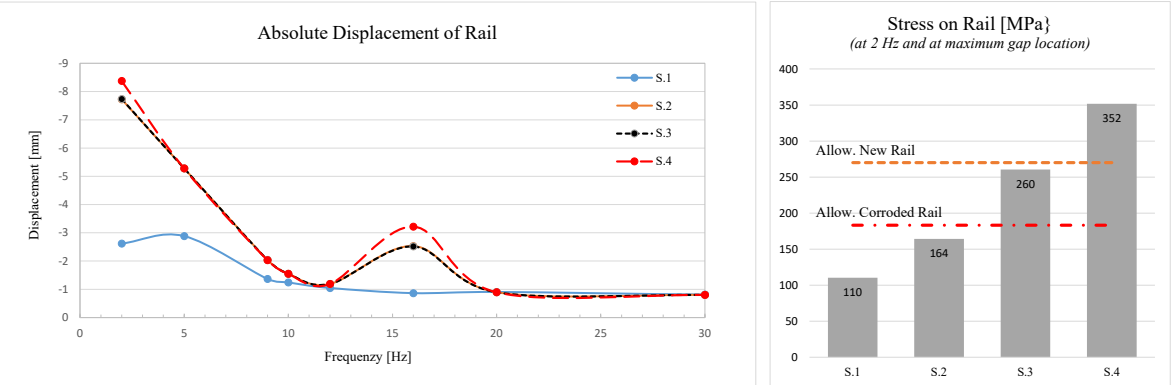

Figure 68. Dynamic impact of uneven support of ballasted track with hanging sleepers to the maximum levels of displacement and flexural stress of rail

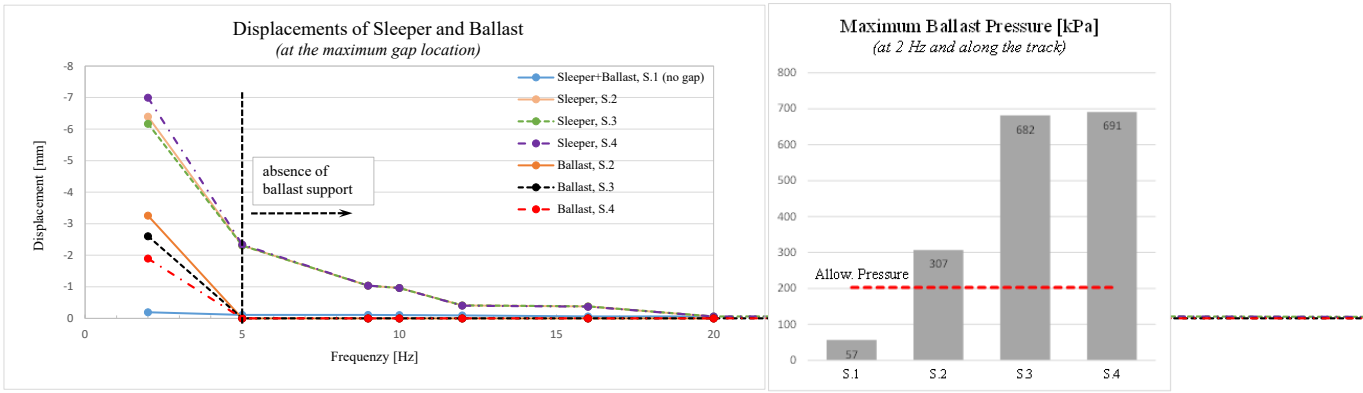

Figure 69. Dynamic impact of uneven support of ballasted track with hanging sleepers to the maximum levels of displacement and pressure of ballast

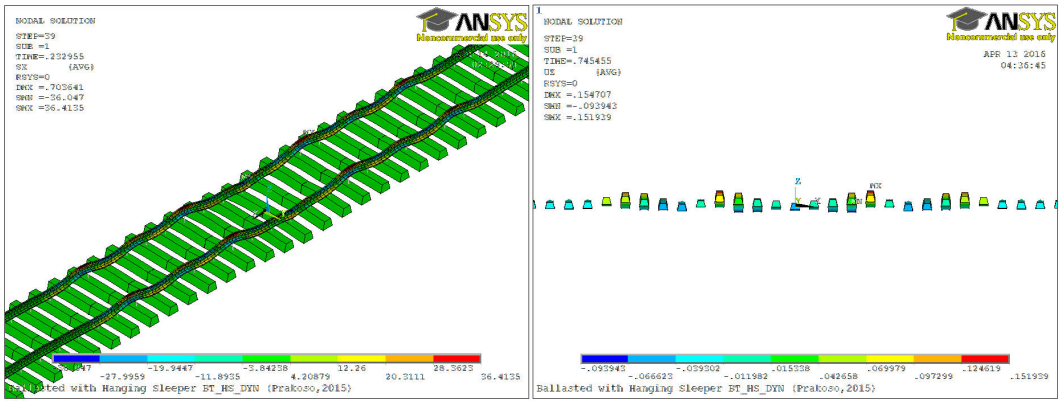

(a) *(b)*

Figure 70. (a) Long term cyclic loading on ballasted track with hanging sleeper can cause poor condition of track geometry. (b) Sleeper bouncing due to hanging sleepers

It can be observed from the Figure 68 that of the Scenario S.1 (new track) and S.2 (moderate quality track), the levels of rail flexural stress are still below the allowable ones. However, of the Scenario S.2 the level of stress is close to the allowable one considering corroded rail condition. Even a worse state is revealed from the Scenario S.3 and S.4 (poor and bad quality tracks). Although considering a new rail condition, the level of flexural stress of S.3 is closed to the permissible one. The stress magnitude of S.4 exhibits a very high level more than the permissible ones. This implies that there is a decay of a continuous support from the ballast layer, due to voids below the sleepers. Because the rails and sleepers are majorly laid only on two points of support of S.3 and S.3, therefore the levels of stress of rails are very high. In this condition, the analysis is almost close to conventional three-point-bending of a beam.

Figure 69 demonstrates that due to the existence of hanging sleepers, the ballast pressure is increased. Of the Scenario S.3 and S.4 the ballast pressure levels are almost similar and far beyond the permissible limit due to cyclic loading. The impact of hanging sleepers due to

dynamic loading is worse than that of a steady state loading. It can lead to a decrease of the quality of track geometry as can be seen in the Figure 70(a). Furthermore, there will be a higher level of ballast pressure, which is caused by sleeper bouncing as shown in the Figure 70(b). This dynamic loading impact is like a “hammered on” effect to the top surface of ballast.

The investigation is continued to running train simulation with artificial train model ICE-1 (according to Figure 44). The train speeds are varied from 60 to 300 km/hours. The impact of uneven support due to differential settlements and existence of hanging sleepers is observed. The results of FEA are presented as correlations of speed and displacement, speed and flexural stress of rail and ballast pressure (Figure 71), as well as in a specific time of dynamic response along the ballasted tracks with train speed of 60 km/hours (Figure 72).

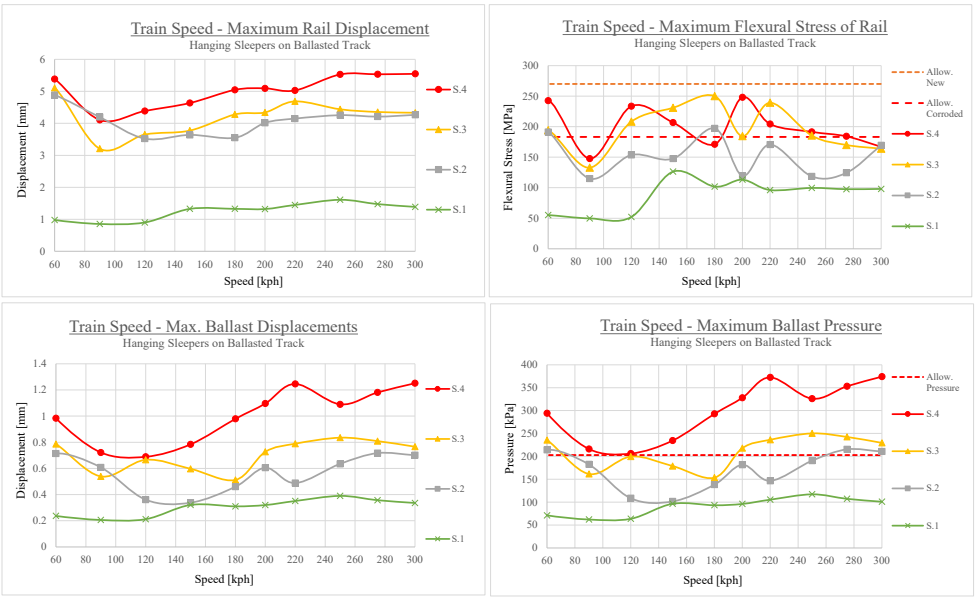

Figure 71. The impact of hanging sleepers to the dynamic response of the rail and ballast in various train speeds

It is shown from Figure 71 that at different train speed levels, uneven support causes higher levels of displacement and flexural stress of rail and ballast pressure. Of Scenario S.2, the magnitudes of rail flexural stress and ballast pressure in some train speeds are reached the maximum allowable levels of corroded rail and of pressure on ballast. And of Scenario S.3 and S.4 (bad quality tracks), most of the flexural stress levels of rail exceed the permissible one of corroded rail, especially in high speeds of a running train. The maximum ballast pressures of a very poor track condition (S.4) are all above the permissible level.

In the Figure 72, it can be observed clearer the comparison of deflection lines between a good and poor quality of tracks. When a train passes the location of hanging sleepers, a

maximum level of rail deflection occurs, which is concentrated in this area and beyond the desired level. This also leads to a differential flexural stress levels of the rail, which can be unsecure for rail against the risk of rail crack. When the displacement of the sleeper is below the gap distance, then the ballast pressures are concentrated on two points where the sleepers still touch the ballast surface. In this area, the highest level of pressure is found. Within longer time and more traffic and when the pressure levels are beyond the allowable one, this can cause degradation and abrasion of the ballast stones as well as reduction of ballast support to sleepers.

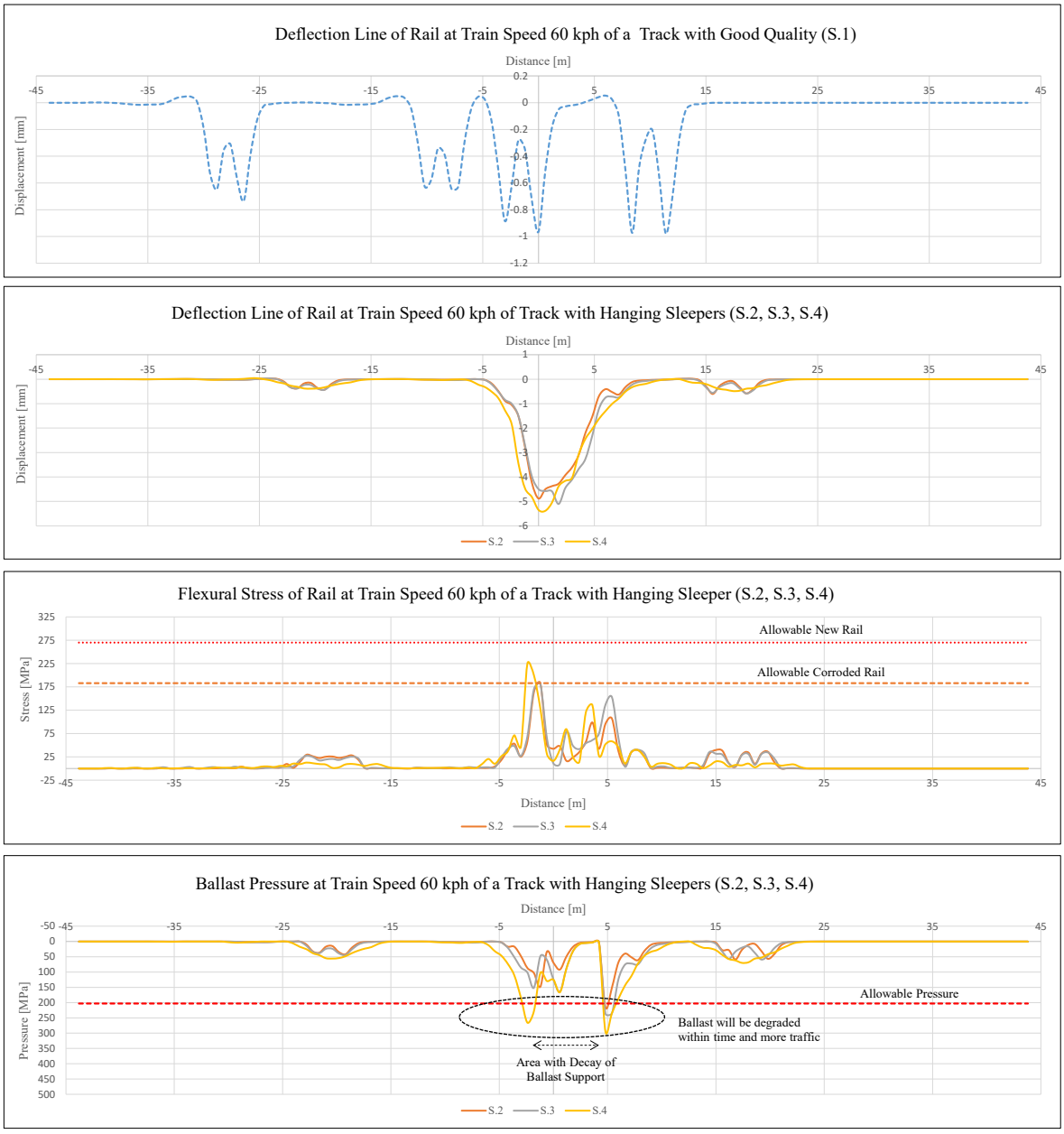

Figure 72. Dynamic response of ballasted track with a continuous support (good quality track) and with uneven support (bad quality track) due to hanging sleepers

This occurrence is often found in the reality and is called “white spots” as depicted in the Figure 73 (a). The white spots indicate the presence of dusts due to ballast abrasion under cyclic loadings and the voids between bottom surface of sleeper and top layer of ballast. It also takes a place due to settlements resulted from high explicit loads and short-pitch rail corrugation[107][56]. This condition becomes worse when water exists in the gaps of hanging sleepers, which can be called as “mud holes” shown in the Figure 73 (b). Muds are formatted from the dusts of degraded ballast stones and water. On soft soils with a high-water table, this impact can be even worse. Maintenance of the white spots existence is by doing overlaying and re-tamping of the ballast. Trackbed layer should be also designed greater than the highest flood water level to avoid the appearance of mud holes.

(a) White spots *(b) Mud holes from ballast breakdown*

Note: pictures are courtesy of (a) Lechner (2011)[69]and (b) ATSB (2013)[7]

Figure 73. Occurrence of “white spots” and “mud holes” of a ballasted track system due to hanging sleepers in good (dry) track and poor drainage (wet) conditions

The nature of soft soil is that differential settlements are likely to occur. In addition, soft soils are often found surrounded with high amount of water. Differential settlements of subsoils can induce a severe problem to the superstructure. High level of stress on rails can cause rail cracks. And without proper and regular inspection and maintenance, when this condition becomes worse, it can increase the risk of train derailment. What is more, a track is subjected with dynamic loading. The impact of dynamic loading in longer time are accumulated. Degradation of ballast can rapidly take a place and the negative impact will affect more and more to the overlaying superstructure.

As it is shown from the FEA analysis performed in this chapter, the level of stress on rail is more maintained below the allowable one of a slab track system than that of a ballasted track, in particular on soft soils. The reason is that concrete slab has certain higher capability against discontinuity of the subgrade. This is the major benefit of slab track in comparison

to ballasted track regarding soft soils. However, a thin concrete slab will be more suffered when the level of discontinuity support on the trackbed is higher. Meanwhile, in ballasted track system, rail is subjected more and has to bear higher capacity when uneven support takes a place. Therefore, advanced foundation, such as piled raft foundation is required when the level of differential settlements and discontinuity on soft soil is already in unsecure level for the superstructure. This is taken to provide quasi continuous support to the overlaying track structure.

7. Railway Track on Soft Soil

From the soil model of track-soil interaction, there is a dimensionless frequency factor of conventional concrete foundation, a_o (see Eq. 46 and Eq. 47, pp. 77). It is shown in these equations that a_o is strongly influenced by the excitation frequency and shear wave velocity of soil. Since the width of the foundation slab B is limited, this value is increased when soil is subjected to a high frequency and/or low shear wave velocity. This means that a high frequency loading is subjected to a soft soil. Using the approach of Dobry & Gazetas (1986)[30], when a_o value is high, the stiffness and damping coefficients become negative.

Bowles (1996)[12] suggested maximum value of dimensionless frequency factor of dynamic foundation $a_o = 1.5$ for applications of a simple concrete slab foundation and when a_o more than 1.5 then soil stabilization or installing piles should be done. This can be used as a preliminary consideration to define soil ranges for railway track applications on soft soil. Two important factors are the ranges of excitation frequencies induced from running train and soil bearing capacity. Indeed, it is hard to define specific excitation frequencies from a running train on a railway track. And therefore, it is also difficult to characterize the actual response of a track in a specific frequency. The reason is that these excitation frequencies have a wide spectrum and their responses depend on many factors. They come from several known and unknown parameters such as: (a) *vehicle*: train speed, bogies and axles configuration, and axle load; (b) *superstructure*: track quality, damping property of elastic-pad, sleeper spacing, inertia, mass and stiffness of rail and concrete slab; (c) *vehicle-track interaction*: level of geometry's misalignment, wheel-rail interaction, track irregularity (d) *substructure*: soil's stiffness and damping characteristics. Dynamic characteristic is combination of those all factors and changes in one element influence to the overall behaviour of track. However, instead of defining a specific excitation frequency, some ranges of dominant frequencies, which affect significantly can be approximated. This is more convenient to investigate track-soil interaction with consideration of a need of soil improvements.

As quoted by Dahlberg (2003)[27] from Oscarsson (1999), a resonance from 20 to 40 Hz in a track which is built on a soft ground may happen. This resonance occurs when the track and multilayer soil subgrade vibrate on. In this situation, Dahlberg (2003)[27] mentioned that the track superstructure contributes a minor role for this resonance, meanwhile the major part of the resonance comes from the layered subgrade. The effect is that the vibrations can

be felt several distance away from the track. Dahlberg (2003)[27] also noted that some resonances were found on a ballasted track. Firstly, a track resonance usually occurs in a range of 50 to 300 Hz, when the rails and sleepers vibrate on the ballast layer. Secondly, another frequency from 200 to 600 Hz can often take a place as the rail bouncing on the elastic-pads, due to function of elastic-pads which acts as a spring between rail and sleeper. Thirdly, a so-called pinned-pinned resonance may also be found. This resonance has the highest frequency up to 1000 Hz and a narrow distance between two peaks. Dahlberg (2003)[27] mentioned that this occurs when the wavelength of the bending waves of the rail is twice than the sleeper spacing. Most of these ranges of dynamic frequency response of a track exhibit a good agreement with the FEA simulations done before.

In addition, based on the results from the previous Chapter 5 of trackbed design and Chapter 6 of track-soil interaction, it is shown that static design procedure has limitation, especially for applications in soft soil condition. Conventional static design concept is more applicable in the range of an ideal condition of bearing capacity of soil from moderate to good. For instance, in a ballastless track system, it is shown that increasing the thickness of slab track is not always the most appropriate solution when soil is too soft. Static design (Zimmermann and Westergaard) implies a transformation from classical three-point bending theory to a beam/slab on continuous elastic foundation. Nevertheless, it indicates that this can be fairly accepted when soil bearing capacity is within a sufficient level. When bearing capacity is low, deflection on the beam model is much higher. In fact, when soil is too soft, due to primary consolidation and plastic deformation, certain level of settlements may already occur in the first stage before traffic is introduced to the track. This is due to high self-weigh of the slab concrete and construction works. Then it becomes worse after traffic due to existence of gaps and un-uniform settlements of soil. The appearance of gaps loses the existence of continuous support. Therefore, static design assumption of continuous support is not fully appropriate anymore in soft soil condition. In the case of very weak soil, track structure can be assumed laying on semi continuous foundation or even back to quasi-discrete-point-bending analysis with some modifications. This also means that a track structure needs at least two points of support. This supports the idea of installing group of piles.

Therefore, in can be summarized that when soil has very low bearing capacity, track needs pile reinforcement. Three important factors should be identified to assess this:

1. Dimensionless frequency factor of $a_o \geq 1.5$, which represents soil characteristics and its interaction with piles due to excitation frequency.
2. Longitudinal distance between pile groups to give two point supports of a track as well as an effective pile spacing.
3. Required length of piles to give sufficient bearing capacity to the track.

7.1. Classical Approach of Modelling and Design of Pile Foundation

7.1.1. Ultimate Bearing Capacity of a Pile

A total pile ultimate carrying capacity of an axial static load can be generally defined as follows:

[12] $$Q_u = Q_b + Q_s = q_b A_p + \sum f_s A_s \qquad Eq.\ 56$$

and the allowable bearing capacity considering a safety factor is:

[12] $$Q_a = \frac{Q_b}{SF_b} + \frac{Q_s}{SF_s} \qquad Eq.\ 57$$

where: Q_u is ultimate pile capacity, Q_a is allowable pile capacity, Q_b is bearing capacity at pile tip (base), Q_s is sum of shaft/skin friction resistance[N]. q_b is unit pile tip resistance [kPa], A_b is pile tip area [mm^2], f_s is unit skin friction [kPa] and A_s is pile skin surface area [mm^2]. SF_b is safety factor for pile tip capacity (typically 3) and SF_s is respectively safety factor for shaft friction capacity (typically 1.5).

a) Indirect Methods

Indirect approaches employ theoretical, semi-empirical analysis and in-situ tests to estimate ultimate base and skin resistances of pile. This group of methods comprises Vesic (1977)[142], Coyle & Castello (1981)[24], S_u-method (Bowles, 1996)[12], α-method (Tomlinson, 1971)[137], β-method (Burland, 1973)[14] and λ-method (Vijayvergiya & Focht, 1972)[143], as quoted from Salgado & Lee (FHWA, 1999)[121]. These methods are not discussed further in detail because the soil-pile modelling applied in this study will be majorly built based on direct methods and load-transfer methods.

b) Direct Methods

In-situ Standard Penetration Test (SPT) and Cone Penetration Test (CPT) are frequently conducted to approximate the bearing capacity soil for a deep foundation design. SPT method express the load capacity in the term of number of blows (N-SPT). Summary of the

approximations from different approaches of base and shaft resistances estimated from N-SPT are shown in the Appendix 11, Table 83, pp. 274 as well as from CPT in the Table 84, pp. 276, as summarized from Salgado & Lee (FHWA, 1999)[121], Pando, et. al (FHWA, 2006)[102] and Lai (2012)[66].

7.1.2. Load Transfer Method of a Pile-Soil Model

The load transfer method is widely use in the analysis of pile-soil interaction. This method correlates soil and pile into a relation of unit resistance-displacement. Pile-soil can be then idealized as beam on nonlinear Winkler's foundation (BNWF). This can be solved using finite element or finite difference methods. Failure limit and yield point can be defined in load transfer model so that nonlinear elasto-plastic from perfectly plastic, hardening, to softening plasticity behaviors of soil is able to be idealized. There are generally three types of resistance-displacement curves: *p-y* curve for lateral soil resistance, *t-z* curve (or *f-z* curve) for axial resistance, and *q-z* curve for base resistance of soil beneath pile's base. The curves respectively present the relations of lateral force resistance per unit length of pile *p* and lateral displacement *y*, shaft friction resistance per unit area of pile's skin surface *t* and vertical displacement *z*, and base/tip resistance per unit cross section area of pile *q* and vertical displacement *z*. Different approaches are available from the literature, which have different ranges from bilinear to hyperbolic to describe linear elastic, elasto-plastic and cyclic behaviours of different soils. This method can be combined with numerical method (FEA) as well as with field measurements and/or laboratory tests. So that a more realistic prediction of pile-soil behaviours can be obtained. Load transfer model of a pile-soil is illustrated in this following figure:

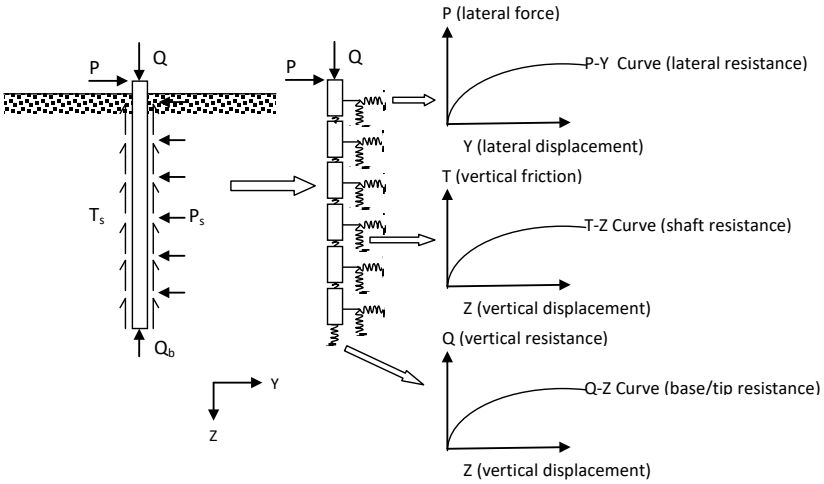

Figure 74. Sketch of load transfer method of pile-soil interaction

Load transfer model describes soil as discrete (or semi-continuous) elements idealized as set of springs. In comparison with continuum model (using solid elements) one disadvantage of load transfer model is the ignorance of the transfer of shear forces between layers of soil. However, above simplification taken in load transfer model gives an advantage that a nonlinear dynamic analysis using this model can be more convenient to be performed in FEA software. The reason is that using continuum model for complex nonlinear dynamic analysis includes different inputs of contact elements. The recent development of implicit dynamic FEA in ANSYS allows only simple nonlinearity of contact as simple point-to-point contact, which covers only for simple modelling purpose. For complex dynamic analyses conducted in this research, dynamic simulations using continuum model lead to a greater number of nonlinearities and higher risk of mismatching degree of freedoms as well as a huge number of iterations of stiffness matrix inversion. This is inefficient in terms of calculation time and is extremely hard to achieve a convergence solution. Second major advantage of load transfer model is that it can be easily linked with different theoretical-empirical approaches and field measurement data.

Different approaches of load transfer method which are commonly used are summarized in this following Table 20 (adopted from Mosher & Dawkins, 2000[87], Reese, et.al, 2006[115], Pando, 2013[103]).

Table 20. Summary of example of different load transfer methods available from literature

Method	Type of soil	Author
t-z & q-z	clay	Coyle & Reese (1966)[23], Aschenbrener & Olson (1984)[6]
t-z	clay	Heydinger & O'Neill (1986)[54]
t-z& q-z	sand	Coyle & Castello (1981)[22], Mosher (1984)[88], Briaud & Tucker (1984)[13]
t-z& q-z	sand and clay	Kraft, Ray & Kagawa (1981)[65]
t-z& q-z	sand, silt and clay	Vijayvergiya (1977)[144]
t-z	sand	Coyle & Sulaiman (1967)[21]
p-y	soft clay below water table	Matlock (1970)[81]
p-y	stiff clay below water table	Reese, Cox & Koop (1975)[117]
p-y	stiff clay above water table	Reese & Welch (1975)[113]
p-y	clay	O'Neill & Gazioglu (1984)[101]
p-y	sand	Reese, Cox & Koop (1974)[116], API RP2A (1991)[4]
p-y	unified soil	Reese & Sullivan (1980)[114], Murchison & O'Neill (1984)[89]
p-y	soil with cohesion & friction	Evan & Duncan (1982) (cited from [115][103])
p-y	weak rocks	Reese (1997) (cited from [115][103])
p-y	strong rocks	Nyman (1982) (cited from [115][103])

The works of Matlock (1970)[81], O'Neill & Gazioglu (1984)[101] of p-y curve for pile in clays are frequently referred in many studies. As well as the ones by Reese, Cox & Koop (1974)[116], API RP2A (1991)[4] are often referred for p-y load transfer model of pile in

sands. Vijayvergiya (1977)[144] is often employed for t-z and q-z pile-soil models in sand and Kraft, Ray & Kagawa (1981)[65] is for t-z model of pile in sands and clays.

Concerning this study, generally there are two types of soil: clays (soft clay and unified clay) and sands, two soil data source namely theoretical-empirical data and field data (SPT and CPT based on Dutch method). The load transfer models, which are assigned to investigate pile-soil interaction are summarized in the diagram on the Figure 75.

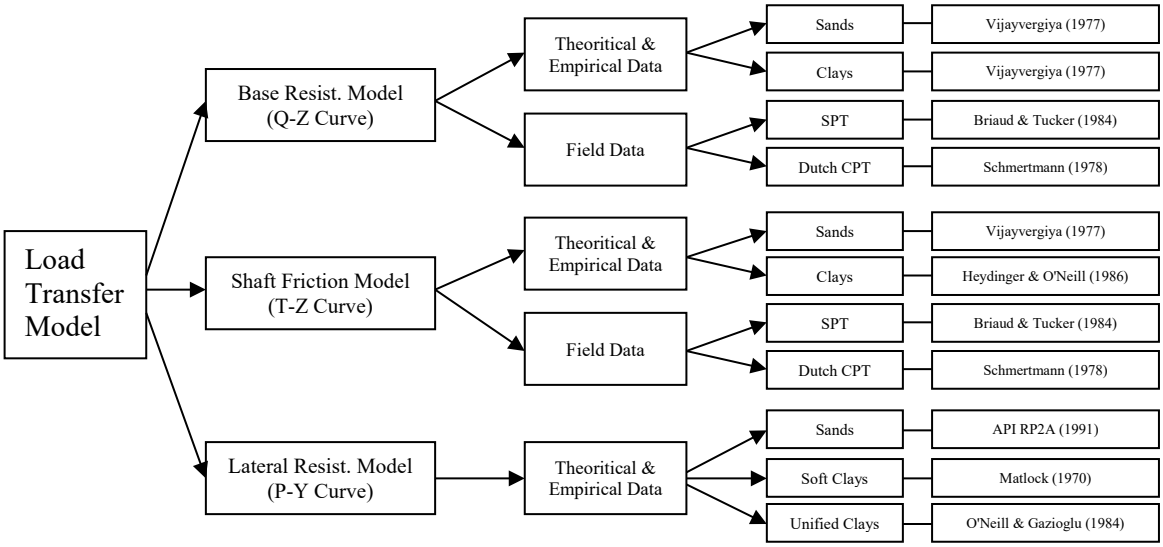

Figure 75. Different load transfer models chosen for the study

7.2. Modelling of Dynamic Pile-Soil Interaction

Dynamic pile-soil interaction models have been proposed by several authors. Several works from Novak (1974)[99], Novak & Aboul-Ella (1978)[95] presented impedance functions of frequency-dependent dynamic stiffness and damping of a pile in homogenous and layered media. Nogami & Konagai (1986)[94] developed further the impedance functions and transform them to the time domain.

7.2.1. Frequency-Dependent Dynamic Stiffness and Damping of Pile

Initial formulations from Novak (1974)[99] utilizes Winkler model which is able to deal with dynamic analysis problem. For impedance function of a pile in horizontal vibrations (S_u) as function of dimensionless frequency factor a_o and μ is shown below:

[99] $$S_u(a_o,\mu) = G_s[S_{u1}(a_o,\mu) + iS_{u2}(a_o,\mu)] \qquad \textit{Eq. 58}$$

[99] $$S_u(a_o,\mu) = 2\pi G_s a_o \left[\frac{\frac{1}{\sqrt{q}}H_2{}^{(2)}(a_o)H_1{}^{(2)}(x_o) + H_1{}^{(2)}(x_o)H_1{}^{(2)}(a_o)}{H_0{}^{(2)}(a_o)H_2{}^{(2)}(x_o) + H_0{}^{(2)}(x_o)H_2{}^{(2)}(a_o)}\right] \qquad \textit{Eq. 59}$$

where $q = \frac{(1-2\mu)}{2(1-\mu)}$ *and* $a_o = \frac{r_o \omega}{V_s} = r_o \omega \sqrt{\frac{\rho_s}{G_s}}$ *and* $x_o = a_o \sqrt{2}$ *Eq. 60*

and for vertical vibrations (S_w):

[99] $$S_u(a_o) = G_s[S_{w1}(a_o) + iS_{w2}(a_o)] \quad \textit{Eq. 61}$$

[99] $$S_{w1}(a_o) = 2\pi a_o \left[\frac{J_1(a_o)J_0(a_o) + Y_1(a_o)Y_0(a_o)}{{J_0}^2(a_o) + {Y_0}^2(a_o)}\right] \quad \textit{Eq. 62}$$

[99] $$S_{w2}(a_o) = \frac{4}{{J_0}^2(a_o) + {Y_0}^2(a_o)} \quad \textit{Eq. 63}$$

$H_n^{(2)}$ is Hankel function of the second kind of order *n*. Novak (1974)[99] mentioned that the Eq. 59 was proposed by Baranov in 1967[9]. For vertical vibration mode, Eq. 62 (Baranov, 1967[9]; Novak & Beredugo, 1972[97], as quoted from Novak (1974)[99]) utilizes J_n function, which J_0 and J_1 are Bessel functions of the first kind of order zero and one and correspondently Y_0 and Y_1 are Bessel function of the second kind of order zero and one.

The real part of this formulation is the stiffness of soil reaction and the imaginary part is the damping of soil per unit length of a pile. Novak (1974)[99] showed further calculations of these expressions to estimate stiffness and damping of pile in vertical, horizontal, rocking and torsion directions.

Novak also proposed other formulations of soil reactions due to horizontal and vertical vibration modes. Soil is modelled as plain strain technique per unit length of pile. Then the formulation takes into account soil damping factor *D*. This damping factor is frequency independent and hysteretic type of damping (Novak & Sheta, 1982)[96].

[96] $$D = \frac{G_s'}{G_s} = tan\delta = 2\beta \quad \textit{Eq. 64}$$

where: δ is the loss angle, β is material damping ratio and G_s' is the imaginary part of the complex shear modulus $G_s^* = G(1+iD)$.

Soil impedance reaction in horizontal direction is[95]:

[95] $$k_u = G_s[S_{u1}(a_o, \mu, D) + iS_{u2}(a_o, \mu, D)] \quad \textit{Eq. 65}$$

then $$S_u(a_o, \mu) = \pi G_s {a_o}^2 \left[\frac{4K_1(b_o^*)K_1(a_o^*) + a_o^* K_1(b_o^*)K_0(a_o^*) + b_o^* K_0(b_o^*)K_1(a_o^*)}{b_o^* K_0(b_o^*)K_1(a_o^*) + a_o^* K_1(b_o^*)K_0(a_o^*) + a_o^* b_o^* K_0(b_o^*)K_0(a_o^*)}\right] \quad \textit{Eq. 66}$$

$$a_o = \frac{r_o \omega}{V_s} = r_o \omega \sqrt{\frac{\rho_s}{G_s}} \quad and \quad a_o^* = \frac{a_o . i}{\sqrt{1+iD}} \quad \textit{Eq. 67}$$

$$b_o^* = \frac{a_o^*}{\eta} \quad and \quad \eta = \sqrt{\frac{2(1-\mu)}{1-2\mu}} \quad \textit{Eq. 68}$$

For vertical vibration, Novak et.al (1978)[100] formulated the impedance function as follows:

$$S_w(a_o) = 2\pi G_s \frac{a_o^* K_1(a_o^*)}{K_0(a_o^*)} \text{ and } a_o^* = i a_o \quad \textit{Eq. 69}$$ *[100]*

7.2.2. Soil Impedance Function in Time Domain

The Novak's formulation in 1978[95] showed in the Eq. 66 for lateral direction considers a limit a Poisson's ratio of 0.5. Nogami & Konagai (1986)[94] modified the Novak's formulation of Eq. 69[100] to lateral direction by consider the inertia effect of mass equal to the volume of cylinder of plain strain model. Therefore, for lateral/horizontal vibrations, this formulation for Poisson's ratio of 0.5 can be expressed as:

$$S_x = 2S_z - m_s\omega^2 \quad \textit{Eq. 70}$$ *[100]*

$$a_o^* = i\frac{r_o\omega}{V_s} = i r_o \omega \sqrt{\frac{\rho_s}{G_s}} \;,\; m_s = \rho_s \pi {r_o}^2 \text{ and } S_z = 2\pi G_s \frac{a_o^* K_1(a_o^*)}{K_0(a_o^*)} \quad \textit{Eq. 71}$$ *[100]*

where: ρ_s is mass per unit volume of soil. S_z expresses the same formulation for vertical vibration from Novak et.al (1978)[100].

Comparison both approach by Novak & Aboul.Ella (1978)[95] and Nogami & Konagai (1986)[94] shows that those two models are identical although they are expressed in different ways, as it can be seen in this figure, which are solved using computer:

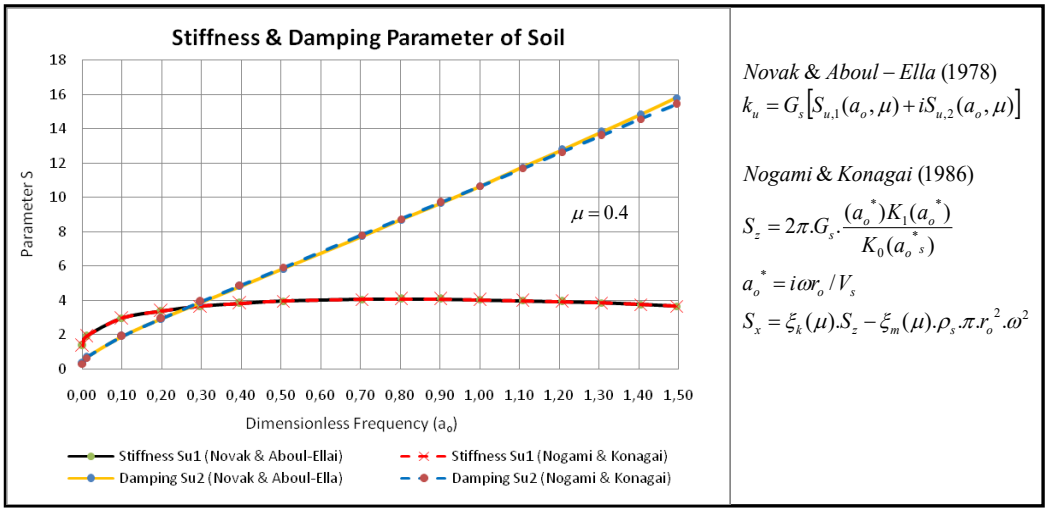

Figure 76. Stiffness and damping parameters of soil according to Novak & Aboul-Ella (1978) and Nogami & Konagai (1986)[94]

Nogami & Konagai (1986)[94] also figured out that the formulation above can be approximately derived in the same form for other values of Poisson's ratio by using Poisson's ratio factors for complex stiffness and for mass as follows:

$$S_x = \xi_k(\mu) S_z - \xi_m(\mu)\rho_s \pi {r_o}^2 \omega^2 \quad \textit{Eq. 72}$$ *[94]*

Nogami & Konagai (1986)[94] gave the values of Poisson's ratio factors in this following table and figure:

μ	ξk	ξm
0.50	2.000	1.0000
0.49	1.940	0.7828
0.48	1.883	0.6420
0.47	1.831	0.5336
0.46	1.784	0.4464
0.45	1.741	0.3740
0.43	1.667	0.2628
0.40	1.580	0.1428
0.35	1.476	0.0352
0.25	1.351	0.0000
0.20	1.311	0.0000
0.10	1.252	0.0000
0.00	1.213	0.0000

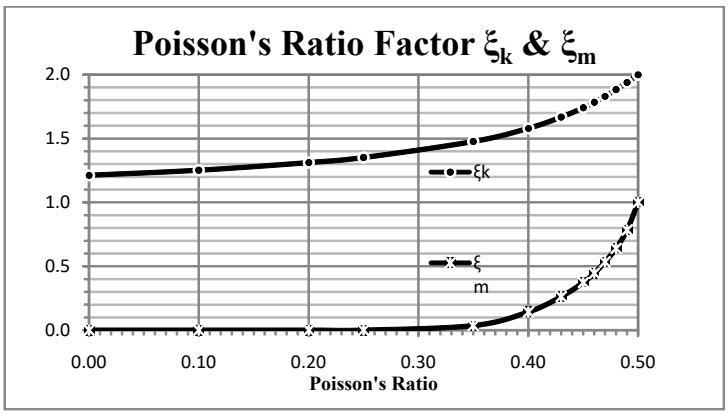

Figure 77. Poisson's ratio factors of complex stiffness and mass (after Nogami & Konagai, 1986)

Nogami & Konagai (1986)[94] employed three-Voigt-spring model in series. This converts the frequency-dependent dynamic stiffness and damping into frequency-independent Voigt model which consist of springs, dashpots and masses as shown in this following figure:

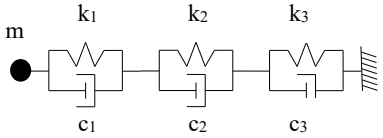

Figure 78. Three-Voigt-Spring model of pile-soil in lateral direction

The spring stiffness, mass and damping can be defined as follows (Kogami & Konagai, 1986)[94]:

[94] $$m_s = \xi_m(\mu)\rho_s \pi {r_o}^2 \qquad \textit{Eq. 73}$$

[94] $$k_n = \xi_k(\mu) G_s \begin{cases} 3.518, & n = 1 \\ 3.581, & n = 2 \\ 5.529, & n = 3 \end{cases} \qquad \textit{Eq. 74}$$

[94] $$c_n = \xi_k(\mu) \frac{G_s r_o}{V_s} \begin{cases} 113.097, & n = 1 \\ 25.133, & n = 2 \\ 9.362, & n = 3 \end{cases} \qquad \textit{Eq. 75}$$

For vertical vibration response, the expressions above can be used by taking Poisson's ratio factor of $\xi_k(\mu) = 1$ for stiffness k_n and damping c_n.[94].

This model is frequency-independent and can deal with dynamic problem with wide range of frequency. Cofer & Modak (1997)[20] mentioned that Kogami & Konagai (1986)[94] model works well for the range of frequency of $0.002 < a_o < 2.0$. Notwithstanding, the point of interest of dynamic response of a track due to soft soil is in the range of low frequencies

below 20 Hz as it has been shown in the previous results (subchapter 6.3.3). Therefore, this approach can be accepted.

This is the major advantage of using this frequency-independent model for modelling pile-soil interaction using FEA software. The programming procedure can be then reduced and the model is able to be subjected with the desired range of dynamic excitation frequencies.

7.3. Pile Supported Railway Track on Soft Soil

In areas with soft subsoil the embankments are often supported by piles due to the settlement problems. For sufficient load transfer into piles different construction methods are possible. For instance, as reported by Raithel, Kirchner & Kempfert (2008)[109], in the construction of the 115-km-railway project for high-speed train between Beijing and Tianjin there was the use of pile-supported embankments. The variations of this construction are (summarized from the report by Raithel et al, (2008)[109]:

7.3.1. Pile Foundation with Reinforced Concrete Slab and Cantilever Retaining Wall

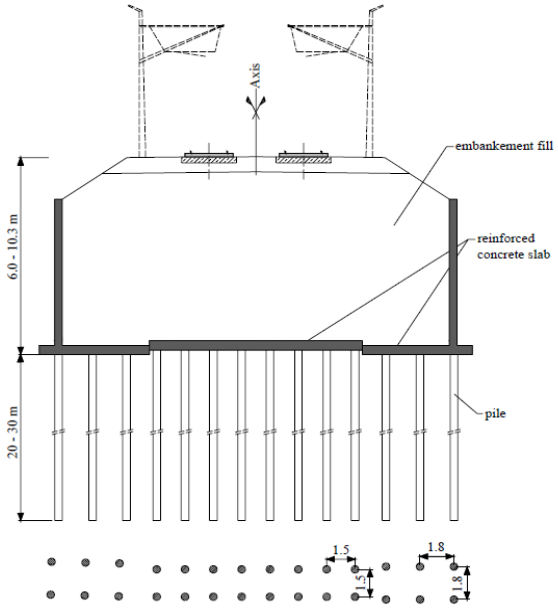

Note: picture courtesy of Raithel et al, (2008)

Figure 79. Pile supported embankment with concrete slab on the piles

Normally a reinforced concrete slab with a thickness of about 50 cm is constructed on top of the piles for a safe load transfer, distribution and concentration. Cantilever retaining wall was constructed on both sides. A schematic view of the pile supported embankment with reinforced concrete slab and cantilever retaining wall is shown in the Figure 79.

7.3.2. Pile Foundation with Horizontal Geogrid Reinforcement

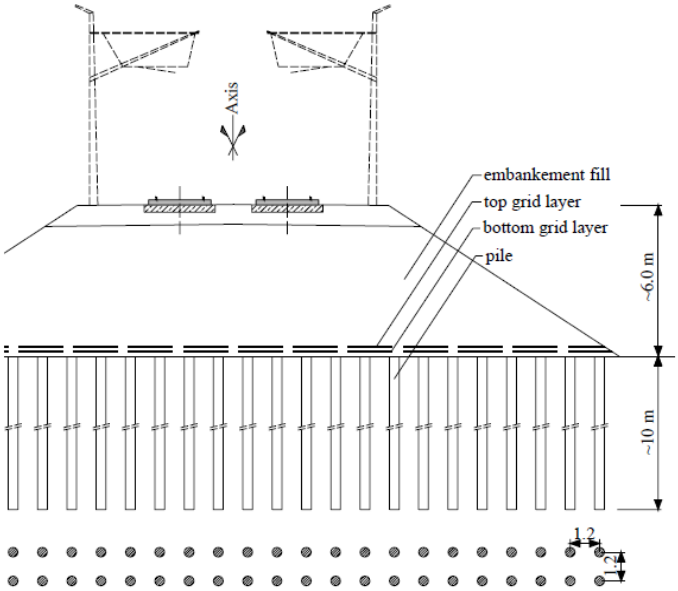

Note: picture courtesy of Raithel et al, (2008)

Figure 80. Geosynthetic-reinforced and pile-supported embankment in Beijing

A new type of foundation "geosynthetic-reinforced and pile-supported embankment" (GPE) was developed in the recent years. This reinforcement of one or more layers of geosynthetics (mostly geogrids) is placed above the pile heads (Raithel et al, 2008)[109].

An example of this type of construction is the construction of the railway line from Beijing to Tianjin. A scheme of the pile supported embankment with the geogrid reinforcement is shown in the Figure 80.

7.3.3. Pile Foundation with Cement Stabilization of the Embankment Material

According to Raithel et. al. (2008)[109], in the construction's sections, where a very low embankment is allowed, instead of the geosynthetic reinforcement, a cement stabilization of the embankment material is more reasonable to be used. In this construction, the cost of expensive reinforcement can be reduced, because the cement stabilized embankment can act similar to a slab over the pile heads. A scheme of the pile supported embankment with the cement stabilization is shown in the Figure 81.

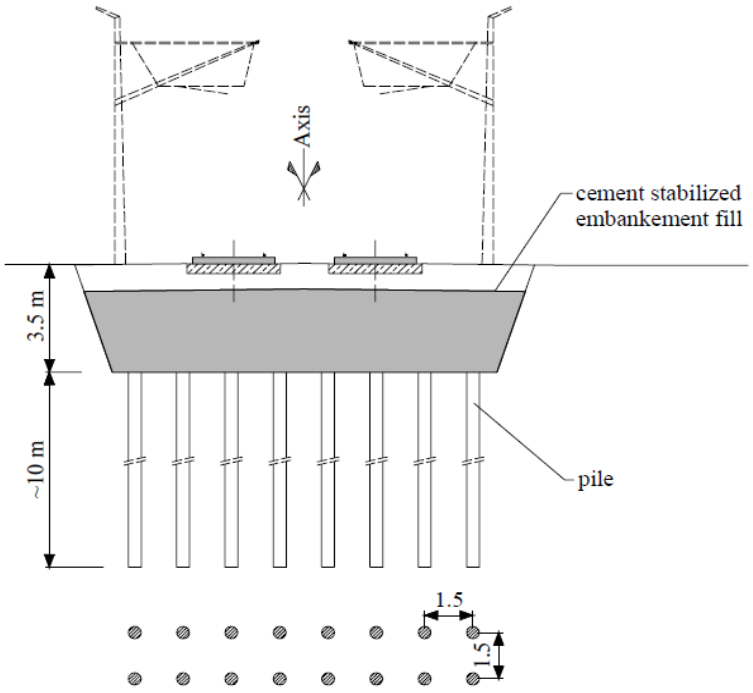

Note: picture courtesy of Raithel et al, (2008)

Figure 81. Cement stabilization of the embankment material and pile-supported embankment in Beijing

7.4. *Cakar Ayam* Foundation

7.4.1. Overview

Cakar Ayam foundation or chicken claw foundation or chicken-foot foundation was invented and patented by Professor Sedijatmo from Indonesia in 1961. Initial design of *Cakar Ayam* system consists of a concrete slab with thickness 10-20 cm which is supported by concrete pipes with diameter 1.2 m, length 2 m, thickness 8 cm and spacing between pipes 2.5 m as it is shown in the Figure 82[105].

These pipes work as support and stiffeners of the slab. Both slab and pipe components are made monolithic and reinforced. The mechanism of this foundation mainly lies on the use of passive soil's pressure, which in the most of other traditional foundations may not be fully considered and they work only by using the active soil's pressure, side frictions and the end-bearing capacity of piles. Due to loading, the deflection of the slab is transferred as moment rotations to the pipes and then these pipes tend to rotate to outward direction. This rotation is hold by lateral passive soil's pressure from the sides of pipes, which have direction against this moment rotation. Therefore, in a short-term loading, this passive pressure will reduce the deflection and settlement on the slab[105].

However, if this system is subjected with a long term static loading, the bearing capacity of this foundation against deflections is reduced. The reason is that the pipes tend to rotate permanently, which leads to primary consolidation and secondary consolidation (creep) of the soil during the long term of loading. As Hardiyatmo (2010a)[49] quoted from Hadmodjo (1994), this system works more appropriate in the condition of soil with compressive strength of 15-35 kPa.

This system has been widely applied for construction of highway (e.g. toll roads mainly in northern Jakarta), airfield runway and apron (e.g. Surabaya and Jakarta International Airports), electricity tower, power plant, and also building[105]. Tandjiria (1999)[132] noted that there have been many arguments on the performance of this foundation due to lack of research and investigation regarding this system, although the fact that the chicken-foot foundation has been successfully implemented in many projects (summarized from Likaytanjua, 2010[77]; Hardiyatmo, 2010a[49]; Istiawan, 2008[59]; Daud et. al., 2009[28]; Tandjiria, 1999[132]).

The initial *Cakar Ayam* system is then further developed by Suhendro, Hardiyatmo, and Darmokumoro in 2007 by substituting the concrete pipe with steel pipe which is lighter than concrete pipe. The steel pipe has diameter 0.6-0.8 m, thickness 1.4 mm and length 1.0-1.2 m as it is depicted in the Figure 83. The modified system is then named *CakMod* or modified *Cakar Ayam* (from Hardiyatmo, 2010a)[49][8].

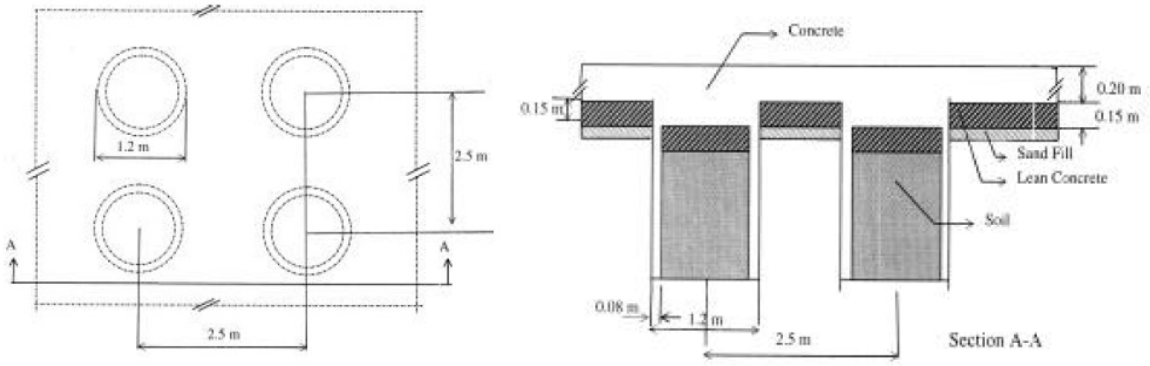

Note: picture courtesy of Tandjiria (1999)

Figure 82. Schematic view of initial design of „Cakar Ayam" foundation

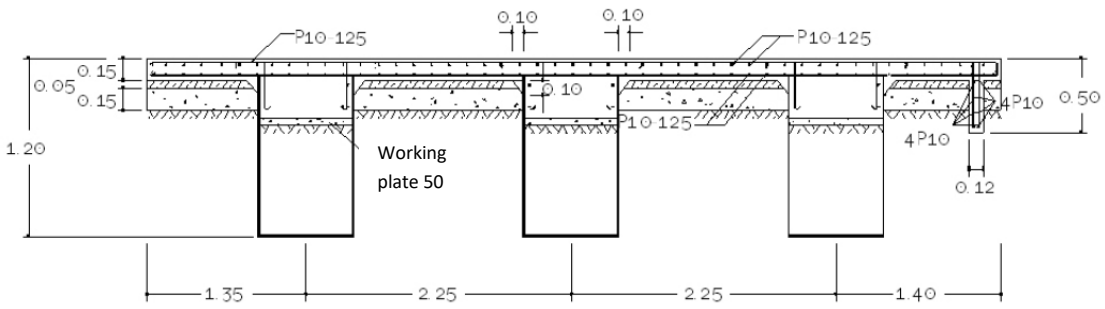

Note: picture courtesy of Balitbang PU (2011)

Figure 83. Schematic view of modified „Cakar Ayam" foundation supporting concrete slab

7.4.2. Static Design of *Cakar Ayam* for Roadway Application

The mechanism concept of *Cakar Ayam* foundation has been investigated analytically for instance by Ismail (2006)[58] and numerically using FEA for instance by Suhendro (1992[129], 2006[130]), Hardiyatmo, et.al. (2000)[51], Nawangalam (2008)[91], Romadhoni (2008)[110] and Firdiansyah (2009)[41] (from Hardiyatmo, 2010b)[50].

Ismail (2006)[58] studied a simple analytical approach based on theory of stability of moment equilibrium assumption proposed by Sedijatmo (1961). The lateral soil's reaction is simply assumed to follow Rankine's theory. Rankine's passive soil pressure coefficient is:

[58] $$K_p = tan^2\left(45^0 + \frac{\emptyset}{2}\right)$$ *Eq. 76*

[58] $$P_p = \frac{1}{2}.{L_p}^2.\gamma_s.K_p.d_p + c\sqrt{K_p.d_p}$$ *Eq. 77*

Ismail (2006)[58] mentioned that the founder of this foundation, Sedijatmo (1961) seems to neglect the cohesion of soil. Thus, the moment reaction of passive soil pressure is for *n* numbers of piles:

[58] $$M_p = n.\frac{2}{3}.P_p.L_p = \frac{1}{3}.n.{L_p}^3.\gamma_s.K_p.d_p$$ *Eq. 78*

where: K_p is Rankine's soil passive resistance [-], ϕ is angle of internal friction of soil [°], P is a unit passive soil pressure on a pile [N], L_p is length of pile [m], γ_s is soil density [N/m^3], d_p is diameter of pile [m], c is soil cohesion [N/m^2], M_p is moment reaction of passive soil pressure [N.m] and n is the number of piles [-].

A basic analytical design of *Cakar Ayam* foundation suggested by Ismail (2006)[58] considers quasi-2D of a plane strain. Therefore, the calculation treats 3D structure as 2D and the analysis is performed in the cross-sectional direction of the structure. Illustration of the analytical approach for roadway application is depicted in the Figure 84.

Ismail (2006)[58] also noted that the pressure on the soil should be less or equal than the ultimate compressive strength of soil (q_u). The design criterion is a stable slab where there is almost no deflection due to equilibrium moments. As quoted from Ismail, Sedijatmo (1961) assumed that when equilibrium moments occur, then the soil reaction under a stable state of a flat slab can be idealized as a trapezium. This is different from conventional foundation slab with higher bending which has a parabolic shape. Sedijatmo (1961) assumed that when the slab is stable, then the pressure is spread wider and evenly to the soil[58].

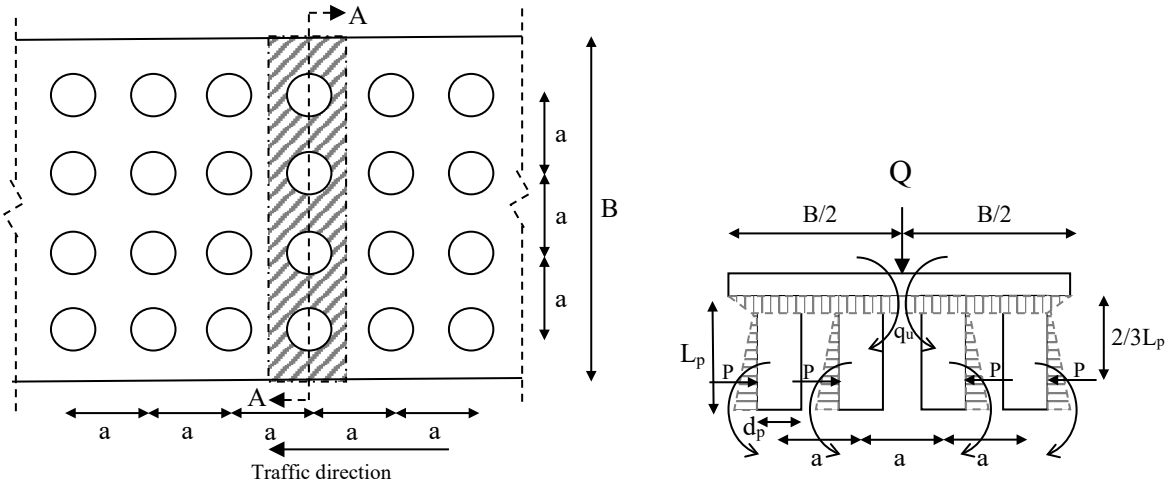

(a) Top view *(b) Cross section A-A*

Note: picture is reproduced from Ismail (2006)[58] with some modifications

Figure 84. Sketch of Cakar Ayam static design for roadway

Because the pile spacing is equal in transversal and longitudinal directions, the total maximum vertical load (P_Q), which can be beard by soil in a transverse section of a pile, which has width of distance between pile's center line (a_p) and length of B is then:

[58] $$P_Q = q_u . a_p . B$$ *Eq. 79*

The maximum moment in the transverse direction occurs when the point load is located in the edge of the foundation slab with eccentricity of *B/2*. In a stable slab with almost no deflection (flat slab), therefore this maximum moment of a point load (M_Q) is:

[58] $$M_Q = P_Q . \frac{1}{2} B = \frac{1}{2} q_u . a_p . B^2$$ *Eq. 80*

The goal is to have a stable foundation slab with a very small deflection (very small bending) due to rotation resistances contributed from the piles. Therefore, these maximum rotation moment (M_Q) should be lower than the total passive reaction moment capacity of all piles and soil (M_p) and by introducing safety factor (SF), it can be written as follows:

[58] $$M_Q \leq \frac{M_p}{SF}, \text{ with } SF \geq 1$$ *Eq. 81*

Ismail (2006)[58] argued that the safety factor is assigned to cover uncertainties factor in the estimations of soil's passive resistance due to variability of soil's parameters with its actual condition. The minimum required length of the pile can be defined by combining all those formulas:

[58]

$$L_{p,min} = \sqrt[3]{\frac{1.5SF.q_u.a_p.B^2}{n.\gamma_s.K_p.d_p}} \qquad \textit{Eq. 82}$$

In a semi-infinite slab (longitudinal direction), Ismail (2006)[58] explained Sedijatmo's assumption that under a stable state (stability theory) of a flat slab, the length of the trapezium area (s) of soil's bearing capacity (q_u) is proportional to the load and the pressure subjected to the soil is assumed almost remaining constant.

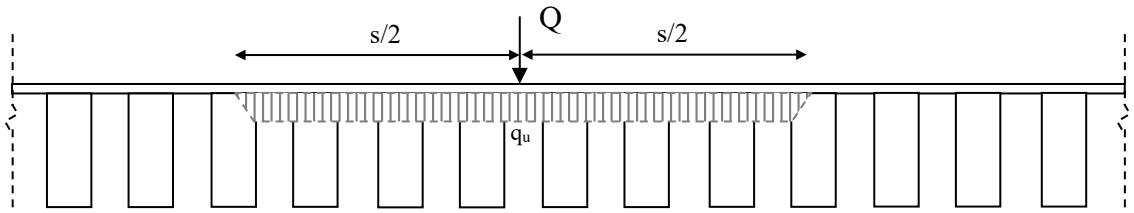

Figure 85. Illustration of Cakar Ayam analysis of semi-infinite slab

The length of the trapezium area of soil's resistance (s) is:

[58]

$$Q = q_u.a_p.s \quad \rightarrow \quad s = \frac{Q}{q_u.a_p} \qquad \textit{Eq. 83}$$

Seeing from above expressions analyzed by Ismail (2006)[58], it is clearly seen that the stiffness and thickness of concrete slab are not directly included in the formulation. *Cakar Ayam* pile design formulation requires precondition from the concrete slab (foundation plate/slab) that the slab should be firstly designed with a sufficient strength so that the pressure subjected to soil is less than its ultimate bearing capacity (q_u). Critical state is defined when the load pressure is equal to q_u (see Eq. 80) and a very small deflection due to bending of the slab occurs (assumption of a flat slab). The minimum pile's length is estimated according to this critical state. Thus, this indicates that the piles have a function to contribute supplementary resistances (as stiffeners) to the concrete slab against rotations to acquire a stable slab state.

Ismail (2006)[58] also noted that this system will work like a conventional foundation if:

- the external load is a uniform load, which is distributed equally on the top surface of a finite (narrow) foundation plate,

- a point load is subjected to a very thick foundation slab, in which a thick slab has very small bending.

In this case the rotation moments do not fully take a place and the piles do not trigger optimum soil's passive moment resistances.

For a simple design, it is not really necessary to consider bending moment in the initial estimation of the length of *Cakar Ayam's* pile. The reason is that under an assumption of a flat slab, the bending moment is smaller than the rotation moment capacity. Therefore, it is more conservative to estimate the minimum length of the pile based on the maximum value of moment rotation capacity showed in the Eq. 80.

A design of *Cakar Ayam* will have a good performance when passive soil resistance contributes optimally to the stability of foundation slab by:

- combining a thin slab and/or a semi-infinite slab
- designing a sufficient length of pile
- having a good estimation of soil's passive reactions and its failure limit.
- maintaining the soil's pressure within its elastic range (below the ultimate limit).
- considering the combination of loading (in particular concentrated point loading) and overlaying structure, which is still able to trigger passive moment resistances of piles.

The suggested range of soil bearing capacity from 15 to 35 kPa[49] for applications of *Cakar Ayam* is a proximally comparable with resilient modulus around 10-15 MPa (using correlation of Thompson and Robnett, 1979[135], see Eq. 32). This range is not recommended for conventional trackbed applications designed using the proposed methods before.

7.4.3. Development of Static Design of *Cakar Ayam* for Railway Applications

a) Design Concept

A previous study done by the author (2011)[105] showed a design concept of *Cakar Ayam* foundation for railway application as it shown in the Figure 86 and Figure 87. It presents an idea of implementing *Cakar Ayam* foundation for slab track and ballasted track systems. In the previous study, this design concept had not been further analyzed. In this research, it will be proceeded with a proposal of analytical method of static design of *Cakar Ayam* for railway application.

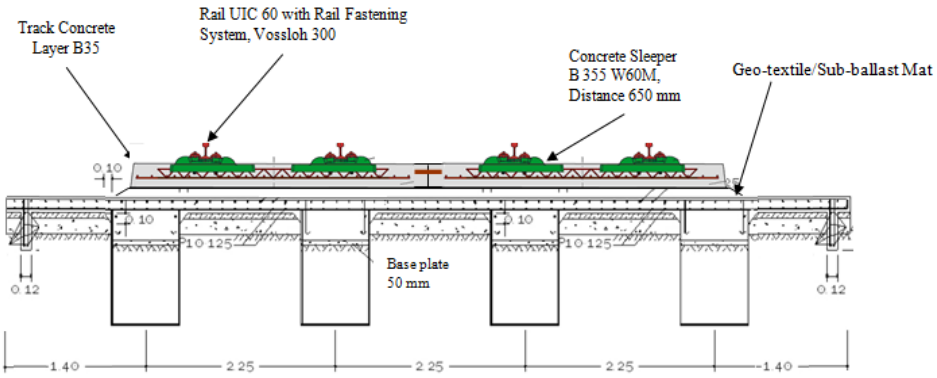

Figure 86. Design concept of slab track supported with Cakar Ayam foundation

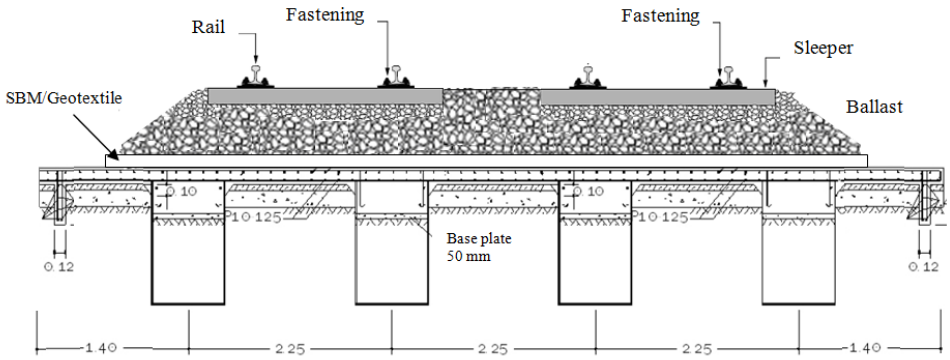

Figure 87. Design concept of ballasted track supported with Cakar Ayam foundation

b) Basic Theory of Analytical Method

The concept of *Beam on Elastic Foundatio*n (BOEF) can be utilized to simplify the analysis of railway track on elastic soil. Three conditions of BOEF, which are frequently found in the traffic infrastructure applications are (as cited from [19] and Hetenyi, 1975[53]):

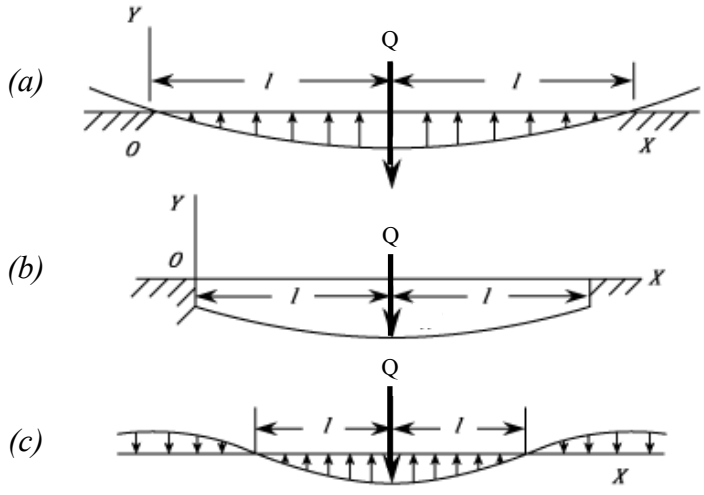

Note: picture courtesy of Codecogs (2015)

Figure 88.Three conditions of beam on elastic foundation theory

The basic formulations of beam on elastic foundation consider characteristic length of a beam structure $L = 1/\alpha$. Characteristic length constant α is:

[19]

$$\alpha = \sqrt[4]{\frac{k}{4EI}} \qquad \textit{Eq. 84}$$

and correlation between deflection (y) and bending moment (M) in the distance of x of a beam is:

[19]

$$\frac{M}{EI} = \frac{d^2y}{dx^2} \qquad \textit{Eq. 85}$$

A railway track can be assumed as a (semi) infinite beam in the longitudinal direction, therefore, condition (c) presents a simple idealization of a track on elastic foundation.

In condition (c), an infinite beam bears a point load. The maximum deflection and bending moment in the distance of $l = L/2$ are:

[19]

$$y_{max} = \frac{Q\alpha}{2k} \qquad \textit{Eq. 86}$$

[19]

$$M_{max} = \frac{Q}{4\alpha} \qquad \textit{Eq. 87}$$

The length of the beam in the downward deflection is:

[19]

$$L_{m(c)} = 2l = \frac{3\pi}{2\alpha} = \frac{3}{2}\pi\sqrt[4]{\frac{4EI}{k}} \qquad \textit{Eq. 88}$$

In the beam on elastic foundation theory, parameter k presents continuous support of elastic soil [N/mm]. To apply the theory of beam on elastic foundation for a slab problem, this formulation should be modified to make k' proportional to the modulus of subgrade reaction of soil (k_s) [N/mm^3] of a plate theory. Different correlations are available in the literature. One example of them is the approach by Vesic (1963)[141], which is widely used as shown in this following equation:

[141]

$$k' = 0.65\frac{E_s}{1-\mu^2}\sqrt[12]{\frac{E_s B^4}{EI}} = 0.65\frac{E_s}{1-\mu^2}\sqrt[12]{\frac{12.E_s B^3}{E.h^3}} \qquad \textit{Eq. 89}$$

where: E_s [MPa] is soil's modulus of elasticity of soil, μ is Poisson's ratio of soil, B [mm] is the slab width, E [MPa] is modulus elasticity of slab, I [mm^4] is moment of inertia of slab and h [mm] is thickness of the slab.

c) Analytical Method of Static Design of Cakar Ayam for Railway Application

Analytical method of *Cakar Ayam* design can be derived from combination of analytical formulations of superstructure and the method analyzed by Ismail (2006)[58]. The connection between these methods is based on the correlation between ultimate limit criteria of soil's bearing capacity and analytical method of trackbed.

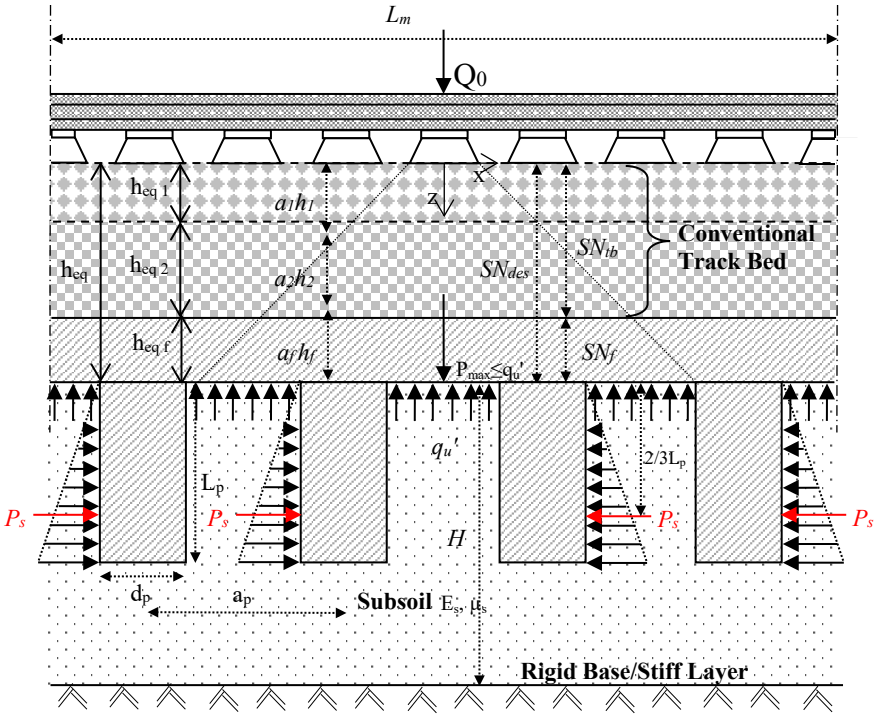

Figure 89. Illustration of analytical approach of Cakar Ayam static design based on ultimate limit of soil's bearing capacity

The illustration of this approach is described in the Figure 89. In this approach, the foundation slab is considered as a part of trackbed in the design calculation. The reason for this is that foundation slab of *Cakar Ayam* also contributes bearing capacity to the overlaying layers (trackbed layer). As a part of supporting layers above the subsoil, trackbed and foundation slab have to be designed according to the ultimate bearing capacity of soil. So that the actual required thickness of trackbed can be reduced.

To contemplate dynamic impact and cyclic loading to soil, dynamic compressive strength of soil (q_u') can be used as major design criteria. The dynamic compressive strength can be derived from deviator stress limit, which can be approximated from static compressive strength (q_u) using Li and Selig (1998)[74][75] method. The actual structural number of trackbed is reduced, hence the required thickness of trackbed is also reduced. Since

foundation slab provides certain number of stiffness, which can be presented as structural number of foundation (SN_f), then the required structural number of trackbed (SN_{tb}) is:

$$SN_{tb} = SN_{des} - SN_f = SN_{des} - a_f h_f \qquad Eq.\ 90$$

where a_f is coefficient of relative strength of foundation slab (see subchapter 5.3 and Table 8) and h_f is the actual thickness of foundation slab.

SN_{des} is firstly estimated from the design charts of the proposed approach of trackbed thickness design. Then the design of trackbed thickness follows the steps as given before in the examples of trackbed design (subchapter 5.4.2 and 5.4.3).

The next step is to define the required length of the pile. This is derived from moment equilibrium between piles resistances coming from passive soil pressures and the maximum rotation moment capacity based on the dynamic compressive strength of soil.

Since track system can be assumed as a semi-infinite structure, the calculation can be performed concerning the longitudinal direction of the track. The maximum rotation moment occurs when the load position is in the half of the length of moment (L_m). Track can be idealized either as a beam (BOEF) concerning for slab application or a Westergaard's theory of slab, and both are resting on elastic foundation. When it is considered as a BOEF concerning for slab application, the length of the beam within the downward deflection ($L_{m(c)}$) shows in the Eq. 88 in combination with Vesic's (1963)[141] approach described in the Eq. 89 can be assigned to define L_m. Meanwhile, when a track is assumed following a slab theory, Westergaard's line influence of moment can be used to approximate L_m. From the Westergaard's line influence moment diagram, it is shown that in the distance of $x/L_w \geq 4$ from the point load location, the moment is close to zero. Then L_m can be assumed as $8L_w$. Where L_w is Westergaard's influence length of moment (or radius of relative stiffness). The maximum bending moment can be estimated to take a place in the distance of $L_m/2$ or $4L_w$. Based on the limit of dynamic compressive strength of soil (q_u') and by using Eq. 80 introduced by Ismail (2006)[58], the minimum length of pile is therefore:

$$L_{p,min} = \sqrt[3]{\frac{1.5SF.q_u'.a_p.{L_m}^2}{n.\gamma_s.K_p.d_p}} \qquad Eq.\ 91$$

where

$$L_{m,BOEF} = \frac{3}{2}\pi\sqrt[4]{\frac{4.E_{eq}.B.{h_{eq}}^3}{12.k'}} \qquad Eq.\ 92$$

or

$$L_{m,slab} = 8.\sqrt[4]{\frac{E_{eq}.{h_{eq}}^3}{12.k_s(1-\mu^2)}} \qquad \textit{Eq. 93}$$

The greatest value of L_m between the two idealizations as a BOEF or slab is taken as the decisive one. Because it will result the longest pile requirement (see Eq. 91). This assumption is taken to locate the design in a safer side.

Example F

A design example following this approach is given as follows:

(1) Soil's design parameters: soil's type CH (clays of high plasticity & compacted) with angle of internal friction ϕ = 19°. Li & Selig's cyclic parameters of soil: a = 1.2, b = 0.18 and m = 2.4. Resilient modulus E_s = 15 MPa, density γ_s =17 kN/m^3 and Poisson's ratio μ = 0.4.

(a) Approximation of static compressive strength is using correlation of Thompson and Robnett (1979)[135], see Eq. 32, then:

$$q_u \; or \; \sigma_s = \frac{M_r - 5.93}{0.31} = \frac{15 - 5.93}{0.31} = 29.26 \approx 30 \; kPa$$

(b) Estimation of modulus of subgrade reaction using AASHTO (1993)[1] formula Eq. 31, then $k_s = 2.029x10^{-3}M_r$ = 2.029x10^{-3}(15) = 0.03 N/mm^3.

(c) Criteria of maximum plastic deformation limit is 1 cm. Number of load cycles N = 2x10^6 and the depth until rigid base H is assumed 5 m. Then the dynamic soil's compressive strength q_u' or allowable deviator stress σ_d = 4.78 kPa.

(2) Computation of structural number based on Li & Selig's method:

(a) σ_d/E_s= 4.78/15 = 0.31 (lower than 0.5 which means not in the range of conventional trackbed design chart).

(b) Using additional chart specialized for trackbed supported with *Cakar Ayam*, (see Figure 149 in the Appendix 5), with σ_d/E_s= 0.31 then SN_{reff} = 112 cm.

(c) A critical state without safety factor is considered for this example. A trackbed design considering dynamic amplification factor f_d = 1.6, slab track system (using 60E2 rails and 22.5 kN/mm elastic-pads, then f_{Lr} = 1) and straight line track ($f_{c,d}$ = 1) needs design factor DF = 1.6. Then SN_{des} = 1.6(112) = 180 cm.

(d) Foundation plate of *Cakar Ayam* is built using concrete C40/50, then its coefficient of relative strength a_f = 3.34

(e) Thickness of foundation plate h_f = 30 cm, then the actual structural number of trackbed $SN_{tb} = SN_{des} - a_f.h_f$ = 180 - 3.34(30) = 80 cm.

(3) A single layer concrete C40/50 with thickness of 24 cm gives $SN \approx 80$ cm.

(4) Computation of the required length of pile:

(a) Both concrete slabs have the same type C40/50 (the same property of stiffness and Poisson's ratio) and full bond contact is assumed between slab track and foundation plate, then $h_{eq} = h_{tb} + h_f = 24 + 30 = 54$ cm.

(b) Rankine's soil passive resistance coefficient:

$$K_p = tan^2\left(45^0 + \frac{\emptyset}{2}\right) = tan^2\left(45^0 + \frac{19^0}{2}\right) = 1.97$$

(c) A single-track design, hence the width of foundation slab is $W_f = 3.6$ m. In the transverse direction, two piles ($n_{trans} = 2$) are installed, in which each pile has diameter $d_p = 90$ cm, then the distance between piles centerlines:

$$a_p = \frac{W_f}{n_{trans}} = \frac{360}{2} = 180cm$$

(d) Length of moment rotation is derived from:

Using Vesic (1963)[141] approach of BOEF theory modified for slab application, hence k' is:

$$k' = 0.65\frac{\mathrm{E_s}}{1-\mu^2}\sqrt[12]{\frac{12.\mathrm{E_sB^4}}{\mathrm{E.h^3}}} = (0.65)\frac{15}{1-(0.4)^2}\sqrt[12]{\frac{12(15)(3600)^4}{36000(540)^3}} = 23.73\ \mathrm{N/mm}$$

$$L_{m,BOEF} = \frac{3}{2}\pi\sqrt[4]{\frac{4.\mathrm{E_{eq}.B.h_{eq}^3}}{12.\mathrm{k'}}} = \frac{3}{2}\pi\sqrt[4]{\frac{4(36000)(3600)(540)^3}{12(23.73)}} = 19.39\ \mathrm{m}$$

Using Westergaard's approach of slab theory:

$$L_{m,slab} = 8.\sqrt[4]{\frac{E_{eq}.h_{eq}^3}{12.k_s(1-\mu^2)}} = 8.\sqrt[4]{\frac{36000.(540)^3}{12(0.03)(1-0.2^2)}} = 16.1\,m$$

Then BOEF theory is more decisive, $L_m = 19.39$ m is taken.

(e) Piles have the same spacing in longitudinal and transverse directions. The number of piles in the longitudinal direction along the L_m:

$$n_{long} = \frac{L_m}{a_p} = \frac{1939}{180} = 10.77 \approx 11$$

(f) Minimum length of pile, with $SF_{pile} = 1.5$:

$$L_{p,min} = \sqrt[3]{\frac{1.5SF.q_u'.a_p.L_m^2}{n.\gamma_s.K_p.d_p}} = \sqrt[3]{\frac{1.5(1.5)(4.78x10^{-3})(1800)(19390)^2}{11(17x10^{-6})(1.97)(900)}} = 2800mm \approx 2.8m$$

Therefore, in a proximally every 20 m longitudinal section of a single track, it needs 11 piles, with diameter of 90 cm, distance between piles of 180 cm and minimum length of 2.8m.

7.5. Finite Element Analysis of *Cakar Ayam* Foundation

Two major groups of finite element analysis are performed. First analysis is a static analysis to verify the proposed method of *Cakar Ayam* foundation for railway application. The second one is to present advanced model for dynamic analysis using advanced pile-soil interaction model.

7.5.1. Static Finite Element Analysis of *Cakar Ayam* Foundation

a) Simple Static Linear-elastic Modelling and Simulation of Cakar Ayam Foundation

Cakar Ayam foundation is modelled according to the proposed analytical method. An idealization of Rankine soil's passive resistances is done by using spring elements as Winkler model. Initially, a correct spring constant should be defined to mimic the Rankine's passive soil model. This can be done by doing a simple beam model of a pile, which is laterally supported by set of spring elements. Spring stiffness is distributed per unit length of pile according to Rankine model, namely as triangle form. A load of P, which follows Rankine model (see Eq. 77) is located in the 2/3 of the beam length. A small rotation at the beam end of 0.5 mm is required to define the equivalent stiffness of the spring. It is obtained that with $n = 20$, the value of $k_1 = 11.18$ kN/mm is equivalent with the given parameters in the example static design of *Cakar Ayam* above. Spring stiffness of k_2 to k_n is distributed according to triangle shape along the pile's length. The idealization and its result are presented in this following figure:

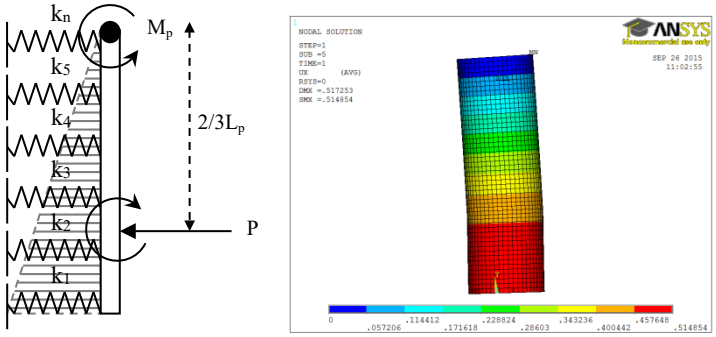

Figure 90: Idealization of Rankine's soil passive resistance in FEA

Secondly, the soil's vertical resistance is also verified using FEA to obtain equivalent modulus of subgrade reaction k_{FEA} of FEA model. This is done by performing static analysis of three models of simple concrete slab laid on soil using (1) full solid elements (SOLID186) for both slab and soil, (2) solid element (SOLID186) for concrete slab and surf element (SURF154) for soil with elastic foundation stiffness properties (*EFS* or k_{FEA}) and (3) shell

element (SHELL281) for concrete slab and spring element (COMBIN14) for soil. The third model is later employed for modelling slab track supported with *Cakar Ayam*. All of the parameters follows the given example before. It is obtained that the equivalent (dummy) modulus of subgrade reaction of FEA model for the soil with elastic modulus of 15 MPa with a finite depth of 5 m located on a fixed base is k_{FEA} = 0.004 N/mm^3. This dummy k_{FEA} of model (2) and model (3) gives a proportional result of deflection of 1.51 mm as it is obtained in model (1). Soil is idealized in model (1) as solid with E_s = 15 MPa and depth of 0.5 m as shown in this following figure:

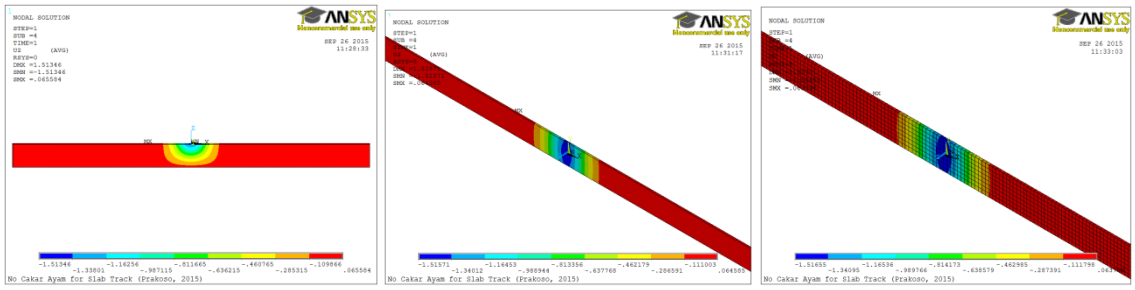

(1) *(2)* *(3)*

Figure 91. Verification of soil's modulus of subgrade reaction in FEA

In the main model, multilayer trackbed, which contains slab track and *Cakar Ayam*'s foundation slab is modelled in ANSYS as composite structure using SHELL281 elements. The piles of *Cakar Ayam* and rails are modelled as a beam using BEAM188 elements. Other viscous-elastic elements (elastic-pad, soil vertical and passive resistances) are modelled as springs using COMBIN14 elements.

Two conditions of soil are examined: first one is a soil which is considered to have moderate bearing capacity (Es = 15 MPa and depth of 5 m but lays on a rigid base) based on the given example analytical calculation and the second one is a soft soil. A model of conventional concrete slab without and with *Cakar Ayam* thickness of 30 cm and width of 3.5 m and 7.2 m is subjected with a single point load of 45 kN (to mimic a rail-seat load of 22.5 kN/mm elastic-pad's stiffness and 2 mm rail deflection) in the middle of the slab. The results are shown on the Figure 92, Figure 93, Figure 94 and Table 21.

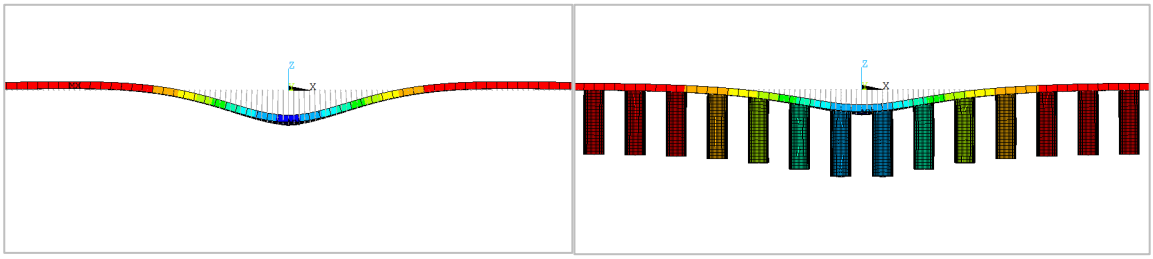

Figure 92. Comparison of conventional concrete slab without and with Cakar Ayam

Table 21. FEA result of conventional concrete slab without and with Cakar Ayam placed on soil with moderate bearing capacity

Result FEA	Without *Cakar Ayam*		With *Cakar Ayam*	
Slab Width	3.6 m	7.2 m	3.6 m	7.2 m
Max. deflection of slab [mm]	0.55	0.36	0.40	0.28
Max. bending stress of slab [N/mm^2]	1.23	1.12	1.02	0.99
Pressure on soil [kPa]	2.18	1.42	1.60	1.11

It can be seen that utilizing this simple model, adding *Cakar Ayam* piles to conventional concrete slab system on a moderate stiff soil generally improves the performance of the slab. The bending tensile stress of the slab is slightly decreased. Deflection of slab and pressure on soil are considerably reduced. In addition, widening the slab causes very small change in bending tensile stress and fairly reduction of slab deflection and pressure on soil.

The second variation is by placing the foundation slab on soft soil. A reduction of 10 times of k_{FEA} from the previous model is taken to idealize a very soft soil. The results can be seen on the Table 22, Figure 95 and Figure 96 below.

Table 22. Result FEA of conventional concrete slab without and with Cakar Ayam placed on soft soil

Result FEA	Without *Cakar Ayam*		With *Cakar Ayam*	
Slab Width	3.6 m	7.2 m	3.6 m	7.2 m
Max. deflection of slab [mm]	2.94	1.55	1.52	0.84
Max. bending stress of slab [N/mm^2]	1.71	1.36	1.42	1.03
Pressure on soil [kPa]	1.18	0.62	0.61	0.34

On a soft soil (Table 22) it can be seen that the slab deflections are much higher than the ones of the previous results in

Table 21. It can also be observed that although the slab deflections are much higher, but the soil pressures are lower. What is more, on soft soil, the reductions of deflection, bending tensile stress and soil pressure by installing *Cakar Ayam* piles are quite significant in comparison to a conventional concrete slab. It is also found that on soft soil *Cakar Ayam* system works more optimal in a wider slab as it is shown in the Table 22 that widening twice of the slab width reduces almost twice the deflections of slab and pressure on soil. The major disadvantage is that although it is widely spread, the slab deflection is still considerably higher when *Cakar Ayam* is constructed on soft soil.

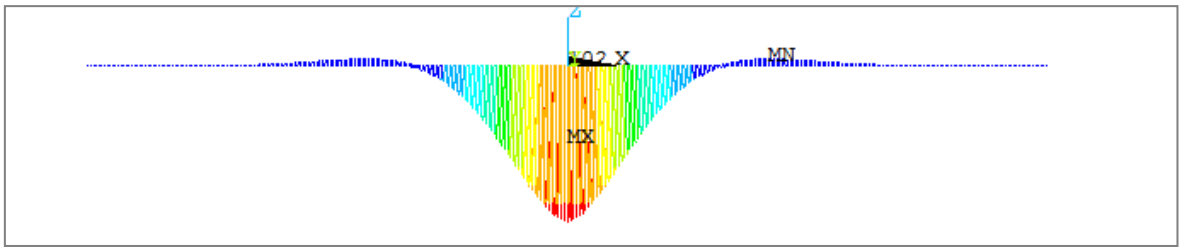

Figure 93. Contour obtained from ANSYS of soil pressure of conventional concrete slab placed on soil with moderate bearing capacity

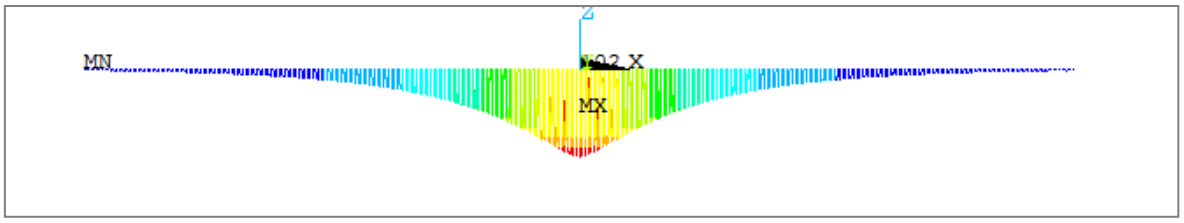

Figure 94. Contour obtained from ANSYS of soil pressure of Cakar Ayam foundation placed on soil with moderate bearing capacity

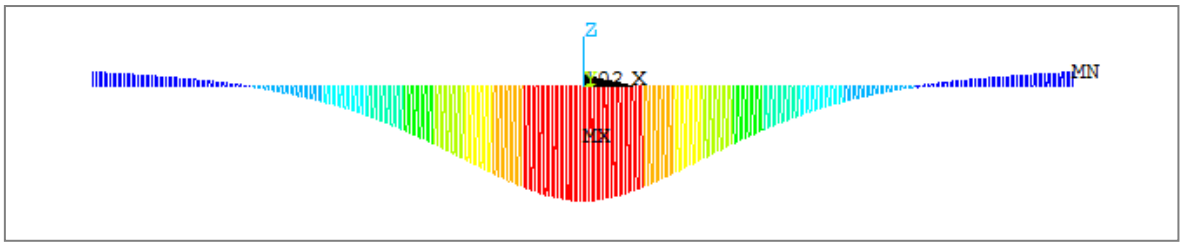

Figure 95. Contour obtained from ANSYS of soil pressure of conventional concrete slab placed on soft soil

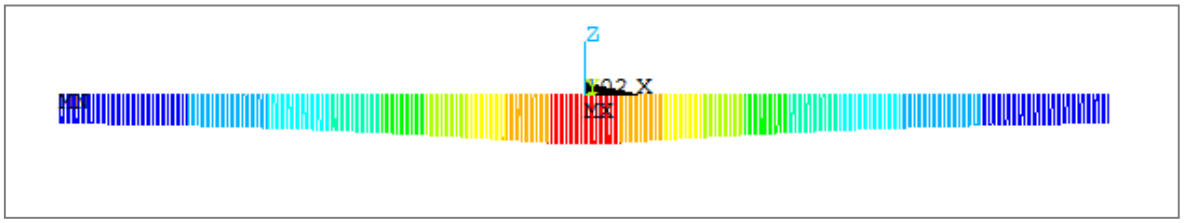

Figure 96. Contour obtained from ANSYS of soil pressure of Cakar Ayam foundation placed on soft soil

Pressure on soil is distributed wider by installing *Cakar Ayam* piles in comparison to conventional foundation as it is shown from the Figure 93 to Figure 96. One interesting thing is that on soft soil, the soil pressures are distributed almost evenly and the shape of the pressure contour is nearly close to trapezium as the simplification was assumed by Soedijatmo (1961).

The next FEA modelling is an application of *Cakar Ayam* for slab track system. Figure 97 depicts a comparison of single-line slab track models constructed without and with *Cakar*

Ayam piles. The design parameters of *Cakar Ayam* follow the given example static design above.

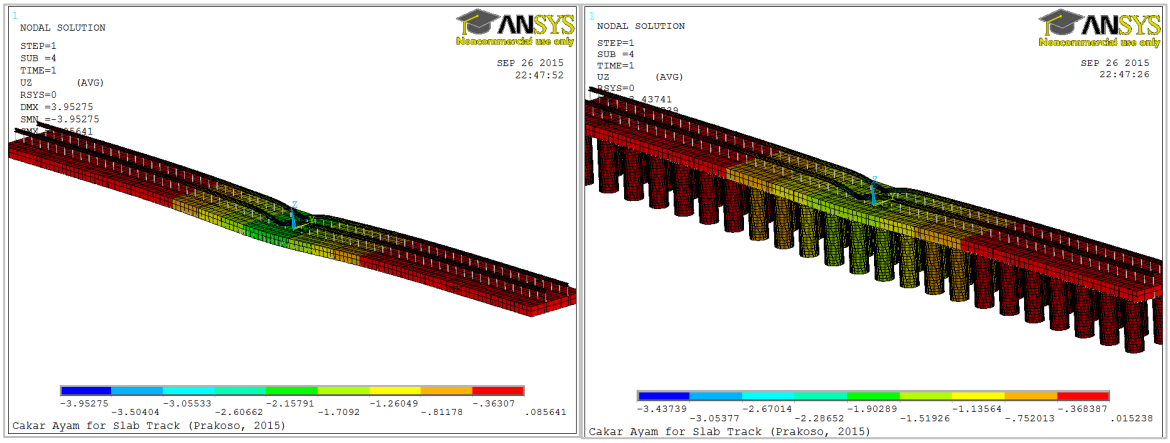

Figure 97. Comparison of single-line slab track without and with Cakar Ayam

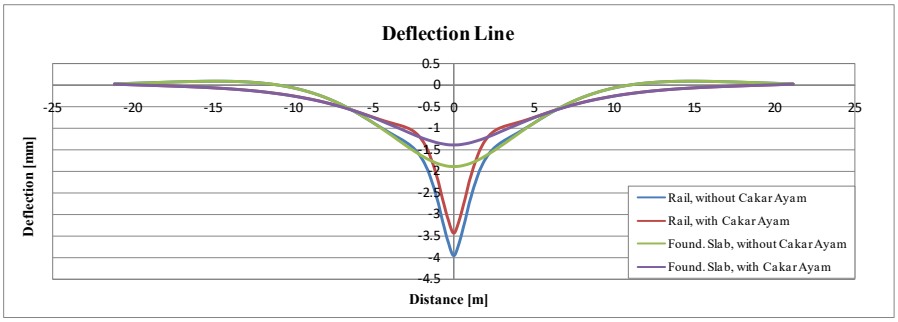

Figure 98. Deflection lines of rail and foundation slab of the slab track systems with and without Cakar Ayam

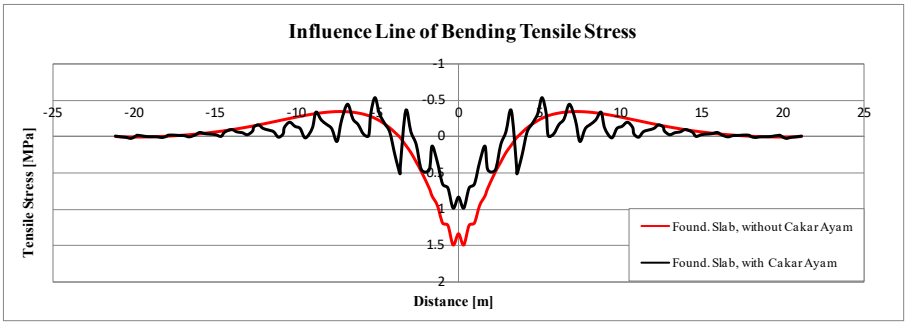

Figure 99. Influence line of bending tensile stress of foundation slab of the slab track systems with and without Cakar Ayam

From the Figure 98 and Figure 99, it is exhibited that the estimation of span length of 19.39 m for moment calculation in the proposed analytical method (subchapter 7.4.3. c) has nearly similar with the result of FEA of foundation slab's deflection line of the track system without *Cakar Ayam* (around 21.89 m). However, the span of bending tensile stress resulted from FEA is slightly higher. For initial design of *Cakar Ayam* design, therefore, the assumed span length in the analytical calculation can be used to estimate the required pile length.

Foundation slab with *Cakar Ayam* actually demonstrates lower values of maximum deflection and bending tensile stress than the system without *Cakar Ayam*. In addition, by installing the piles, it gives wider dispersion of stress, which causes greater span of influence line of bending tensile stress and lower stress level. In the Figure 99, the bending tensile stress does not show a smooth curve but a saw tooth shape. This takes a place due to the influence of discrete supporting points of the piles. Thus, the bending stresses are reduced into several segments. These segments are the locations where piles contribute supplementary bearing capacity (distance between piles).

The summary of result comparison of deflections and stresses gained from static FEA considering axle load of 250 kN and elastic-pad stiffness of 22.5 kN/mm is shown in this following table:

Table 23. Result FEA of slab track without and with Cakar Ayam

Result FEA	Without *Cakar Ayam*	With *Cakar Ayam*
Max. deflection of rail [mm]	3.95	3.44
Max. deflection of foundation slab [mm]	1.90	1.38
Max. bending stress of foundation slab [N/mm^2]	1.49	0.99
Pressure on soil [kPa]	7.61	5.51

It is found that installing *Cakar Ayam* only lightly improves the performance of slab track on a soft soil with resilient modulus of 15 MPa and depth of 5 m laid on a firm base (considered as moderate stiff). Moreover, the reduction of pressure on soil is also not really significant by installing *Cakar Ayam* piles. In addition, the resulted pressure on soil of 5.51 kPa is slightly greater than the defined design parameter of dynamic compressive strength limitation of $q_u' = 4.78$ kPa in the given example. It indicates that constructing *Cakar Ayam* with very thick overlaying concrete slab (24 cm CRCP and 30 cm foundation slab) on a moderate stiff soil does not optimally activate the soil's passive lateral resistance.

Above results are obtained with uniform pile spacing of 1.8 m and the width of the foundation plate is 3.6 m and the slab track has the same width. The distance between rails centerlines is 1.5m. Wheel loads are located in this distance. Greater transverse moment, which should be beard by piles will be greater if transverse distance between piles are greater than 1.5 m. However, greater transverse distance between piles demands wider slab. This will give two advantages. Firstly, the slab area, which is assigned to distribute the load will

be greater. This will reduce the loading pressure to soil. Secondly, this will trigger more utilization of the passive soil resistances.

A static FEA simulation of changing the transverse distance of piles is conducted. The number of piles in the transverse direction is two. The transverse distances are varied from 1.5 m to 3 m and the longitudinal pile distance is set to be constant of 1.8 m. Pile's length is also varied from 1.5 to 3.5 m. Spring constants, which are idealized Rankine's passive soil resistances are also differentiated according to pile lengths. The results are shown in the charts in the Figure 100.

Figure 100 demonstrates that firstly, setting the transverse distance between pile greater than 1.5 m (distance between rails) and lower than 2.75 m reduces the pressure on soil. The minimum pressure on soil as well as rail and slab displacements are reached when transverse pile spacing is 2.75 m. The longitudinal bending tensile stress is optimized when the transverse distance between piles is 2.25 m. Yet, the bending tensile stress of foundation slab in transverse direction is increased. However, the transverse bending tensile stress is lower than the longitudinal one. Thus, the longitudinal bending tensile stress is then more decisive for the foundation slab. Passive soil force is slowly reduced when the transverse pile distance is extended until 2.75 m. But then it is reduced faster when transverse pile distance is more than 2.75 m. It reveals a condition that to optimize the reactions from passive soil, then the piles should be located outside of the locations of the wheel loads. When a transverse distance of pile of 2.5 m or 2.75 m is taken, then the foundation slab should be greater than slab track (2.8 m), namely for a single-line track around 4 m or 4.25 m respectively.

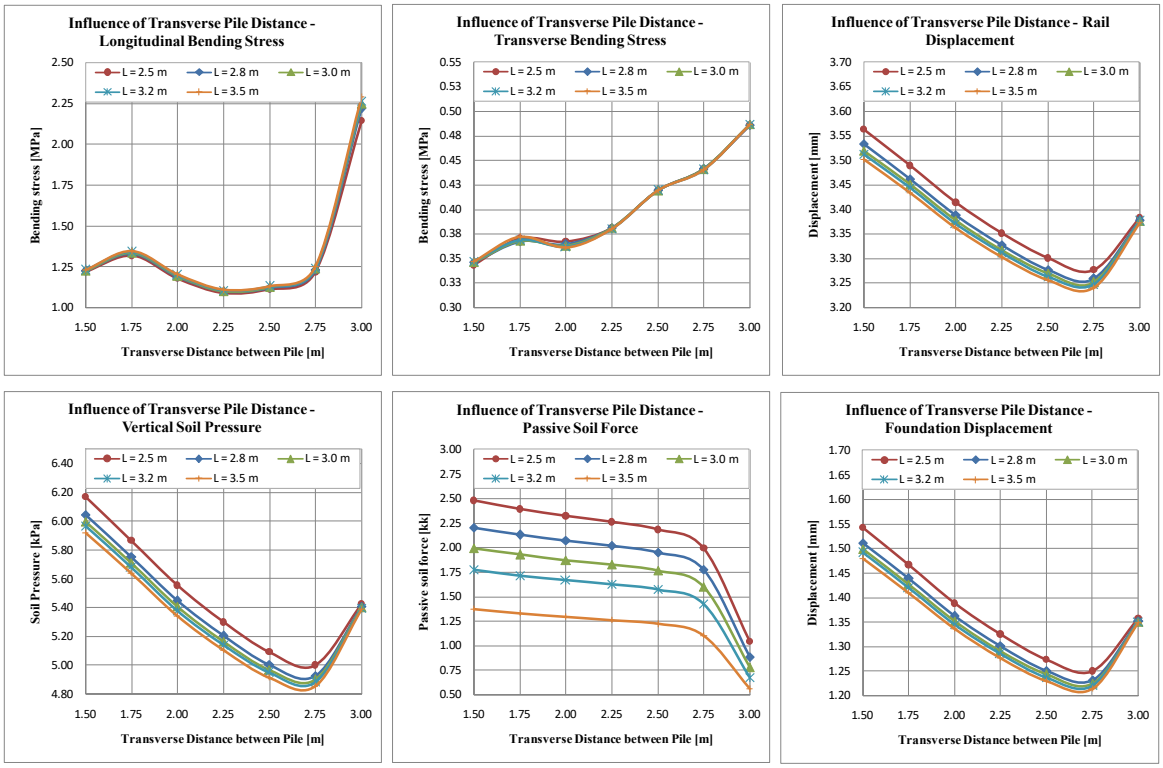

Figure 100. Influence of transverse distance between piles and pile's length to the static behaviour of slab track provided with Cakar Ayam foundation

Secondly, the changes of pile length do not make a significant change to the bending tensile stresses in both directions. They change more obvious in the levels of soil pressure and displacements of rail and slab foundation as well as the magnitudes of the transferred horizontal forces against soil's passive resistance. These changes to soil pressure, displacements of rail and slab are less significant when the length of the pile is more than 2.8 m. The length of 2.8 m is the approximated pile length from calculation before.

Second variation of simulations is when the transverse pile distance is set 2.5 m and the longitudinal one is differentiated from 1.5 to 3 m. The results of simulations are described in the Figure 101 below.

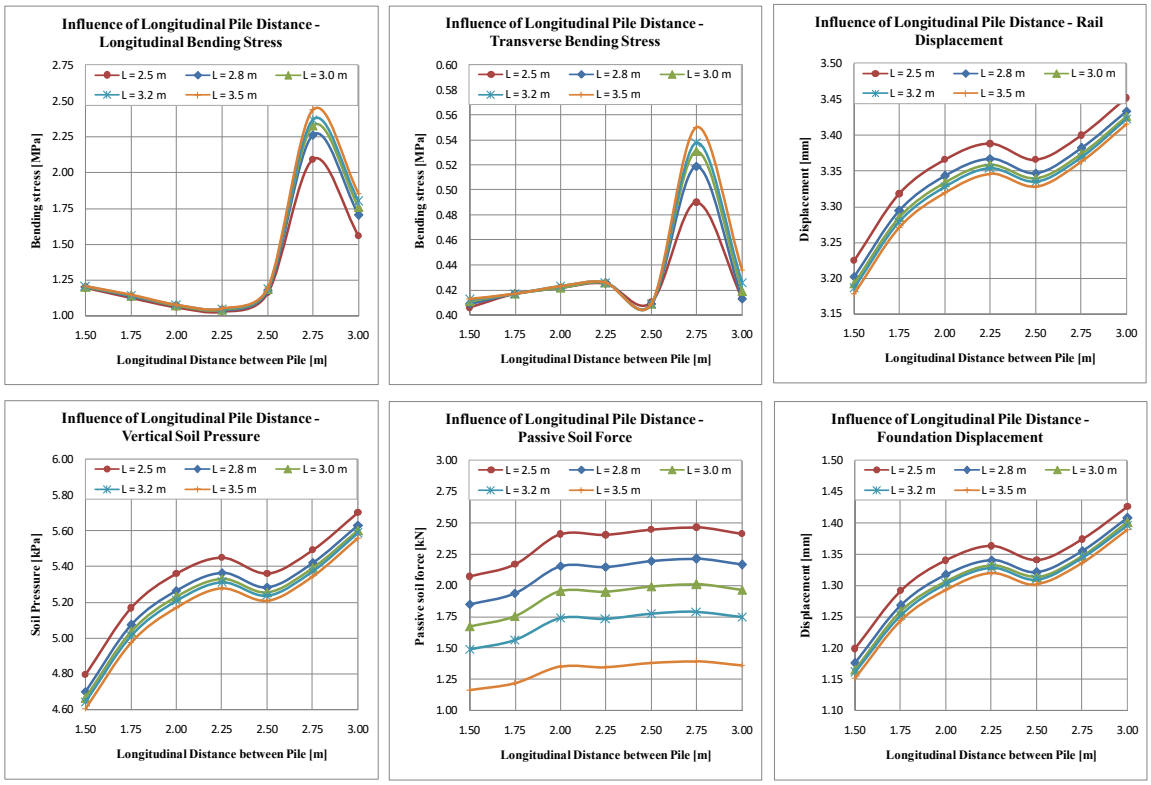

Figure 101. Influence of longitudinal distance between piles and pile's length to the static behaviour of slab track provided with Cakar Ayam foundation

From the Figure 101, it can be seen that optimal reduction of longitudinal bending stress is reached when the longitudinal pile spacing is 2.25 m. When longitudinal pile spacing is more than 2.5 m and up to 2.75 m, the longitudinal bending stress becomes higher. And then when it is more than 2.75 m the longitudinal bending stress is again reduced. However, if the pile longitudinal spacing is set greater than 2.5 m then the pressure on soil and displacement of rail and foundation slab turn higher. In the transverse direction, bending tensile stress begins to be minimum of the pile spacing of 2.5 m. Pile spacing of 2.5 m delivers also a small reduction of the pressure on soil and displacements of rail and foundation slab.

Alterations of longitudinal pile length show almost similar behaviour as the transverse ones. In this evaluation, the pile length of 2.8 m brings an effective solution. Therefore, transverse and longitudinal pile spacing of 2.5 m and pile length of 2.8 m deliver the optimum performance of the track supported with *Cakar Ayam* foundation according to this simple analysis. Nevertheless, the given dimensions deliver soil pressure of 5.29 kPa, which is slightly higher than the target limit of 4.78 kPa of dynamic compression strength of the given example.

It is demonstrated from simple analytical and numerical investigations that in this example for slab track application, increasing the length of the pile does not obviously increase the performance of *Cakar Ayam* foundation seeing from the lateral passive soil resistance of pile. The reason is that *Cakar Ayam* foundation basic analysis does not take into account the skin/shaft friction resistance contributed from the piles. It only considers the passive soil resistance. Vertical bearing capacity in both analyses done before are majorly delivered from foundation slab resting on elastic soil. Above analysis of slab track reveals that interaction between passive soil resistances and piles only contributes minor supplementary bearing capacity to the foundation slab. Actually, pile skin frictions are increased when the length of the pile is also increased. This will improve more the actual bearing capacity of a piled foundation system.

In addition, the fact is that the load distribution mechanism of train wheel load on a railway track is different than a single point wheel load of a road vehicle subjected on a wide and thin concrete slab in a roadway. A slab track has multilayered components and consists combination of continuous (rail and slab track) and discrete (rail pad and/or sleeper) points. The load on the top of foundation slab of *Cakar Ayam* in a slab track application will be already transformed as distributed load (as pressure). Hence, this is far different from single point (concentrated) load assumed in a roadway application. As preliminary hypothesis, this is the reason why *Cakar Ayam* foundation is not really appropriate for railway application. It also indicates that *Cakar Ayam* pile works like a conventional pile. Thus, it needs longer pile.

Therefore, next investigations of *Cakar Ayam* foundation supporting slab track with consideration of longer pile and the contribution of pile skin frictions will be investigated.

b) Modelling and Simulation of Cakar Ayam Foundation using Nonlinear Load Transfer Model

Load transfer models of base resistance q-z curve, shaft friction resistance t-z curve and lateral resistance p-y curve are now assigned to idealize a nonlinear pile-soil interaction of *Cakar Ayam* foundation. Theoretical-empirical data of fat clay (CH, clays of high plasticity & compacted) which is defined based on the example before (subchapter 7.4.3. c, pp. 129) is used as inputs to define these curves.

The q-z curve for idealization of vertical soil reaction beneath the foundation plate also follows the approach by Vijayvergiya (1977)[144] by setting the $q_{max} = 9S_u$ (S_u = undrained

shear strength of soil) for a static simulation (as suggested by Skempton, 1951[124]) and close to q_u' (ultimate dynamic compression strength of soil) defined in the example design (subchapter 7.4.3. c, pp. 129) for a cyclic simulation. The static unit vertical resistance of pile tip is higher than the one beneath the foundation slab. This will give reasonable idealization in the FEA models that the unit spring stiffness value will be turned around due to the fact that the surface area of foundation slab is much higher than the cross section of the piles. *Alpha method* (Tomlinson, 1971)[137] is chosen to estimate t-z shaft resistance with value of reduction factor $\alpha = 0.7$ (bored pile).

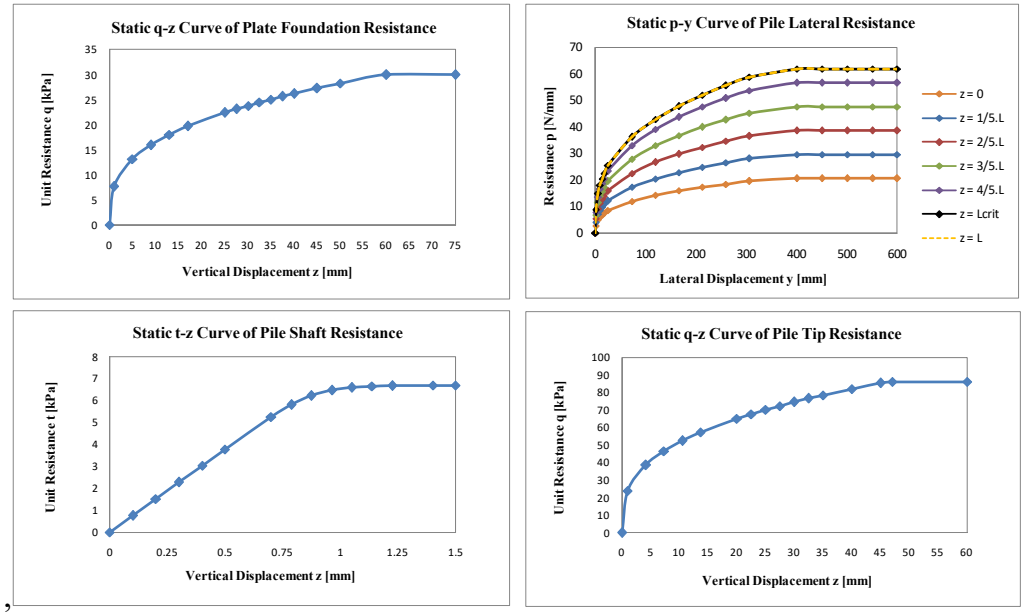

Figure 102. Load transfer curves for static modelling of pile-soil interaction of Cakar Ayam

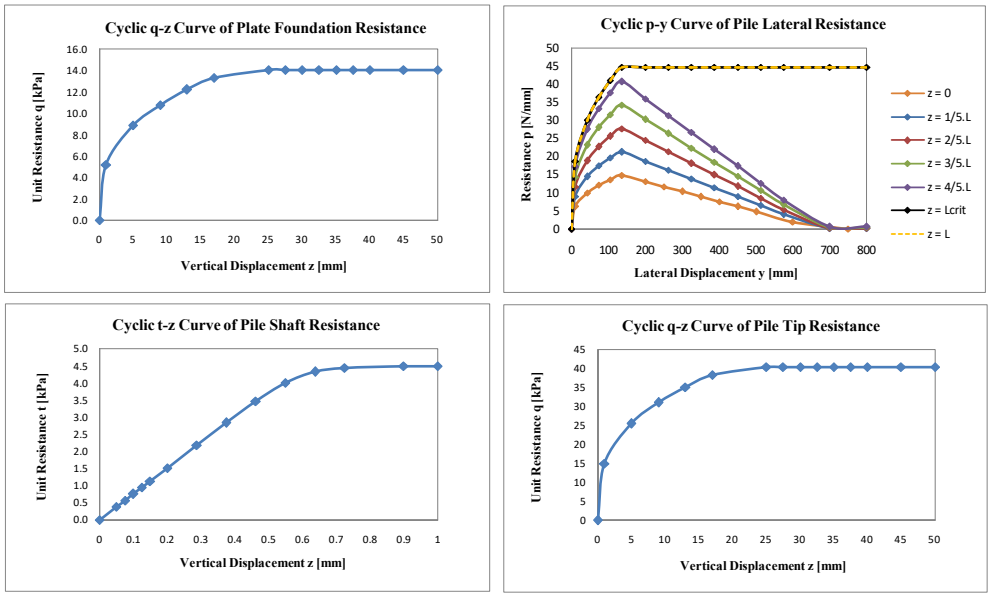

Figure 103. Load transfer curves for cyclic modelling of pile-soil interaction of Cakar Ayam

Pile group effect in the lateral direction is taken into account by assuming a reduction factor (p-y multiplier) of 0.8 (due to pile spacing of 2.5 m and pile diameter of 0.9 m, or 2.7D). As reference, Curras, et. al. (2001)[26] assigned p-y multiplier 0.7 for pile group effect, in which the pile spacing is four time pile diameter (4D). Reduction factor is also applied to q-w (soil beneath the plate and pile tip) and t-z to idealize degradation factor of soil bearing capacity due to cyclic loading.

Static and cyclic p-y models follow Matlock (1970)[81] method. Critical depth of pile 2.6 m is obtained using this method. Matlock (1970)[81] as many other researchers argue that pile length more than the critical depth does not influence the lateral displacement behaviours of pile head. This demonstrates a correlation with the previous FEA static analysis that only considering lateral resistance, pile length of more than 2.5 m does not deliver a significant influence to the displacements of foundation plate as well of the rails.

First of all, four different track systems are compared to analyze the mechanism of *Cakar Ayam* foundation, namely:

- ***No CA*** model, which is. a conventional slab track without *Cakar Ayam*.
- ***CA Full*** model, which is a slab track provided with *Cakar Ayam* by considering all resistances delivered from a pile, namely base/tip, shaft and lateral resistances
- ***CA+L+S*** model, which is similar to the second model but it only considers lateral and shaft and resistances.
- ***CA+L*** model, which is similar to the third model but it takes into account only the pile lateral resistance.

All of the track models are subjected with a static axle load of 250 kN and considering dynamic amplification factor of 1.6 (total static axle load of 400 kN or a proximally 40 tons). Rail profile 60E2 and elastic-pad with static stiffness of 22.5 kN/mm are idealized in the track models. Degradation factors of soil bearing capacity are assumed 53% and 84% of the initial soil stiffness. Degradation factor is a reduction factor, which is assumed to describe a state of soil bearing capacity after it is subjected to certain number of repeated (cyclic) loadings. The selections of 53% and 84% degradation factors are based on some trials of static simulations with various ranges of degradation factors from 5 to 95%. But only those two factors are showed here as the most relevant results of static simulations to the actual cyclic simulations discussed hereafter.

Table 24. Result of nonlinear FEA model of slab track without and with Cakar Ayam

Result FEA	Static				Cyclic (53% degradation factor)				Cyclic (84% degradation factor)			
	CA Full	CA+ L+S	CA+ L	No CA	CA Full	CA+ L+S	CA+ L	No CA	CA Full	CA+ L+S	CA+ L	No CA
Max. absolute deflection of rail [mm]	4.19	4.20	***6.77***	***7.08***	4.97	4.99	***12.45***	***12.84***	12.88	13.28	***24.96***	***28.27***
Max. absolute deflection of trackbed [mm]	0.95	0.96	***3.54***	***3.87***	1.74	1.77	***9.27***	***9.67***	9.73	10.13	***21.83***	***25.18***
Max. bending stress of trackbed [N/mm^2]	1.60	1.61	***2.29***	***2.57***	2.17	2.19	***3.38***	***3.56***	3.83	3.89	***4.55***	***5.18***
Max. Pressure on soil [kPa]	2.49	2.23	***8.86***	***9.65***	1.25	1.27	***7.06***	***7.36***	2.51	2.61	***4.63***	***4.69***
Max. Pile Tip Axial Displacement [mm]	0.88	0.89	**3.46**	-	1.67	1.69	**9.14**	-	9.56	9.96	**21.63**	-
Max. Pile Shaft Sliding [mm]	0.82	0.84	**3.46**	-	1.57	1.59	**9.14**	-	9.36	9.75	**21.63**	-
Max. Pile Lateral Displacement [mm]	0.41	0.42	**1.06**	-	0.89	0.90	**2.40**	-	2.88	2.98	**4.31**	-

Note: *No CA* = *system without Cakar Ayam*
CA Full = *system with Cakar Ayam considering lateral, shaft and base resistances*
CA+L+S = *system with Cakar Ayam considering lateral and shaft resistances*
CA+L = *system with Cakar Ayam considering only lateral resistance*

From the Table 24 it can be seen that a significant improvement of bearing capacity is delivered from ***CA Full*** model in comparison of a conventional track system without CA (***No CA***). From the third model (***CA+L+S***) it can be observed that the contribution of base resistance is relatively small to the overall bearing capacity. The reason is that *Cakar Ayam* is constructed using a pipe pile. Hence the cross-section area of the pile base/tip is small. Moreover, this system is categorized as floating pile system. In a design and analysis of a floating pile system, normally the base resistance is neglected. The reason is that the pile base does not lay on a rigid/firm layer. A conservative design usually employs the approach shown in the third model.

One interesting point can be found in the last model. When the pile mechanism takes into account only the lateral resistance (***CA+L)***, this system contributes a small improvement in comparison with a conventional slab track system without *Cakar Ayam* pile. The results of all track and foundation components show fairly lower improvements. This is clear that for slab track application, the shaft resistance of a piled foundation plays very important role. *Cakar Ayam* foundation in this case works like a conventional floating piled foundation system, in which shows come characteristics:

- the shaft resistances supply the main vertical bearing capacity. Since the major loading is in vertical direction, thus the fundamental bearing capacity is conveyed from the shaft resistance.
- the rotation of pile is also small, as it is shown form lateral displacements in the Table 14. Therefore, mobilization of the lateral resistance is also small.
- for a slab track application, there is greater total thickness of concrete slab track and foundation, thus the bending of the concrete slab track and foundation is small. This does not trigger the utilization of soil's lateral passive resistances contributed from the piles.

The failure of this system is mainly caused by permanent lateral deformation of the pile due to secondary consolidation (creep) induced by traffic (cyclic loadings)[49]. This indicates that when there is a lateral gap due to permanent lateral deformation, the pile loses not only some of its lateral resistance but also the shaft resistance. This is a possible cause of the major failure of the system. As it is shown from the analysis that ignorance of shaft resistance makes the pile has a small vertical bearing capacity function. This also implies that to reduce the impact of losing the shaft resistance, the pile should be designed with a sufficient length, which should be greater than its critical length. So that the pile is rigid enough. Hence, although some lateral gaps occur after some period of time but longer pile will still have residual shaft resistances.

Secondly, it is also shown from the simulation that the estimated cumulative plastic deformations of the slab foundation of 9.73 and 10.13 mm due to cyclic loading of ***CA Full*** model and ***CA+L+S*** model respectively are close to the assumed initial design parameter of 10 mm. This is obtained if the degradation factor achieves level of 84%.

Thirdly, it is found from nonlinear ***CA Full*** model that a critical depth of pile is around 2.2 m. This is lower than the previous estimation of 2.5 m gained from FEA linear model as well as of 2.6 m obtained from Matlock (1970)[81] approach.

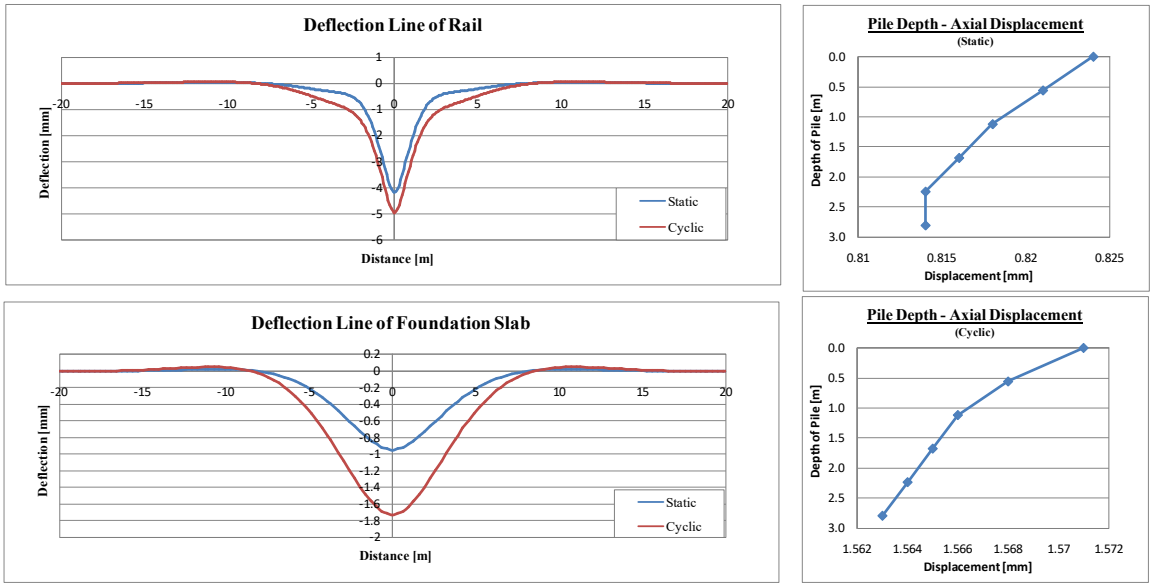

Figure 104. Deflection lines of rail and foundation slab and axial pile deflection profiles obtained from static and cyclic (53% degradation factor) of CA Full model

Considering degradation factor of 84% in the nonlinear soil and slab track model without *Cakar Ayam* foundation (***No CA*** model) exhibit a very high displacement (28.27 mm) and extremely high level of bending stress of foundation slab as well as pressure on soil due to cyclic loading at the end of service (see Table 24). In this condition, excessive settlements may take a place. The substructure's bearing capacity is too low if a conventional slab track system constructed. Although the slab concrete is supported with foundation slab and the total thickness is 54 cm, but when the soil has very low bearing capacity, it can lead a failure of the structure. This supports the arguments before that there is a limitation of bearing capacity of soil where a construction of a conventional slab track is not sufficient even though a very thick slab is installed.

Cakar Ayam foundation systems of the ***CA Full*** and ***CA+L+S*** nonlinear models present an obvious improvement of the bearing capacity of a slab track. In the initial state (static loading), the installation of *Cakar Ayam* foundation demonstrates a significant impact of increasing bearing capacity and providing better stability to the overlaying structure. Yet, a cumulative settlement of around 10 mm predicted in the design may occur within the service period after cyclic loadings. Therefore, track rehabilitation is lately needed.

Nevertheless, the model has shown a good prediction of *Cakar Ayam* foundation in comparison with a linear model. A result of analysis from a linear model may bring underestimation of the real behaviours, which is unsecure for design applications.

c) Prediction Model of Cakar Ayam Behaviours due to Cyclic Loading

Instead of employing degradation factors and p-y model by Matlock (1970) to estimate cyclic load transfer curves (Figure 103) and then to predict the cyclic behaviour of a slab track supported by *Cakar Ayam* foundation, a non-conservative simulation can be done in ANSYS. Non-conservative FEA means that a material behaviour after unloading keeps a certain level of deformation resulted from the previous loading. Therefore, the material plasticity behaviour can be included in the analysis. Furthermore, a hysteretic behaviour of a material can be taken into account in the non-conservative simulation.

The static nonlinear load transfer curves (Figure 102) can be used as input of nonlinear material model in ANSYS. A simple cyclic behaviour of soil can be described by using these material models. Static-cyclic loadings are then subjected to the models. Unloading path of the curve is parallel to the initial slope of stiffness of the previous loading in the elastic region. The initial slope stiffness of the material models described in the Figure 102 are then utilized as the backbones for the cyclic stiffness of the next load cycles. This can be explained in the following Figure 105:

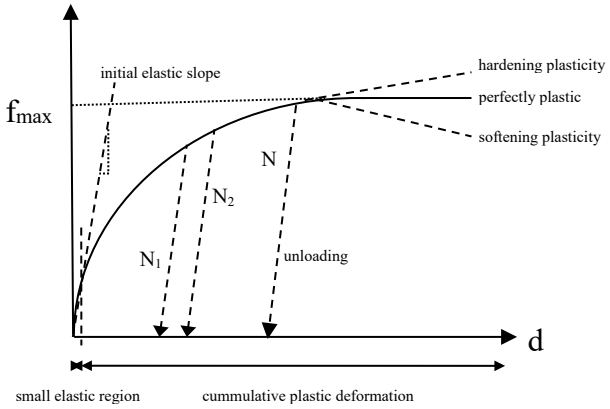

Figure 105. Non-conservative material model

Actually, soils exhibit plasticity behaviour after the subjected loads exceed soil's ultimate strength (yield point). Region of plasticity can be modelled as softening, perfectly plastic or hardening. Assigning COMBIN39 nonlinear element for non-conservative analysis unfortunately is not able to idealize softening behaviour. Restriction in ANSYS for COMBIN39 element is that the slope at the end should be positive. This means that it is only able to model either perfectly plastic (slope = 0) or hardening plasticity (positive slope) behaviours. However, a small trick can be done to idealize a softening behaviour in the plastic region is by making parallel the COMBIN39 nonlinear spring element with COMBIN40 linear spring in series with a slider element. Maximum limit of the slider is

defined as the ultimate limit displacement at the yield point. After the displacement limit is reached, the slider reaches its maximum sliding and then the second spring (COMBIN40) is deactivated. Thus, in this state, the total stiffness is reduced (softening). Nevertheless, after some trial simulations, it is found that the levels of resulted stresses or forces are under the ultimate limits of the given example soil model. Therefore, a nonlinear elastic with perfectly plastic idealization is sufficient for this particular analysis.

The cyclic FEA simulation of ***CA Full*** model in ANSYS demands a very high computation time. The simulation was done for 5000 load cycles, which took time a proximally 2 day-continuously simulation in a computer with 4 cores of i5 processor and 16 GB of memory. Therefore, a power regression model is assigned to make a prediction of the cyclic behaviour of rail and foundation slab deflections and level of soil pressure for the number of loading more than 5000 as it is shown in the Figure 106.

From the Figure 106, the predicted deflection of the rail after 2 million load cycles is 5.05 mm. This is identical with the result from the static model of cyclic load transfer with degradation factor of 53% shown before in the Table 24. Nevertheless, this is half than the initial assumption of cumulative plastic deformation of 10 mm taken in the proposed analytical method, which similar with the static model with cyclic load transfer and degradation factor of 84%. The difference is reasonable since safety factor as reduction of allowable dynamic soil pressure is applied in the analytical method. Hence, it can be said that the proposed analytical method places the design in a safer side. The assumption is then able to contemplate the nonlinearities and variety of soil properties in the actual condition.

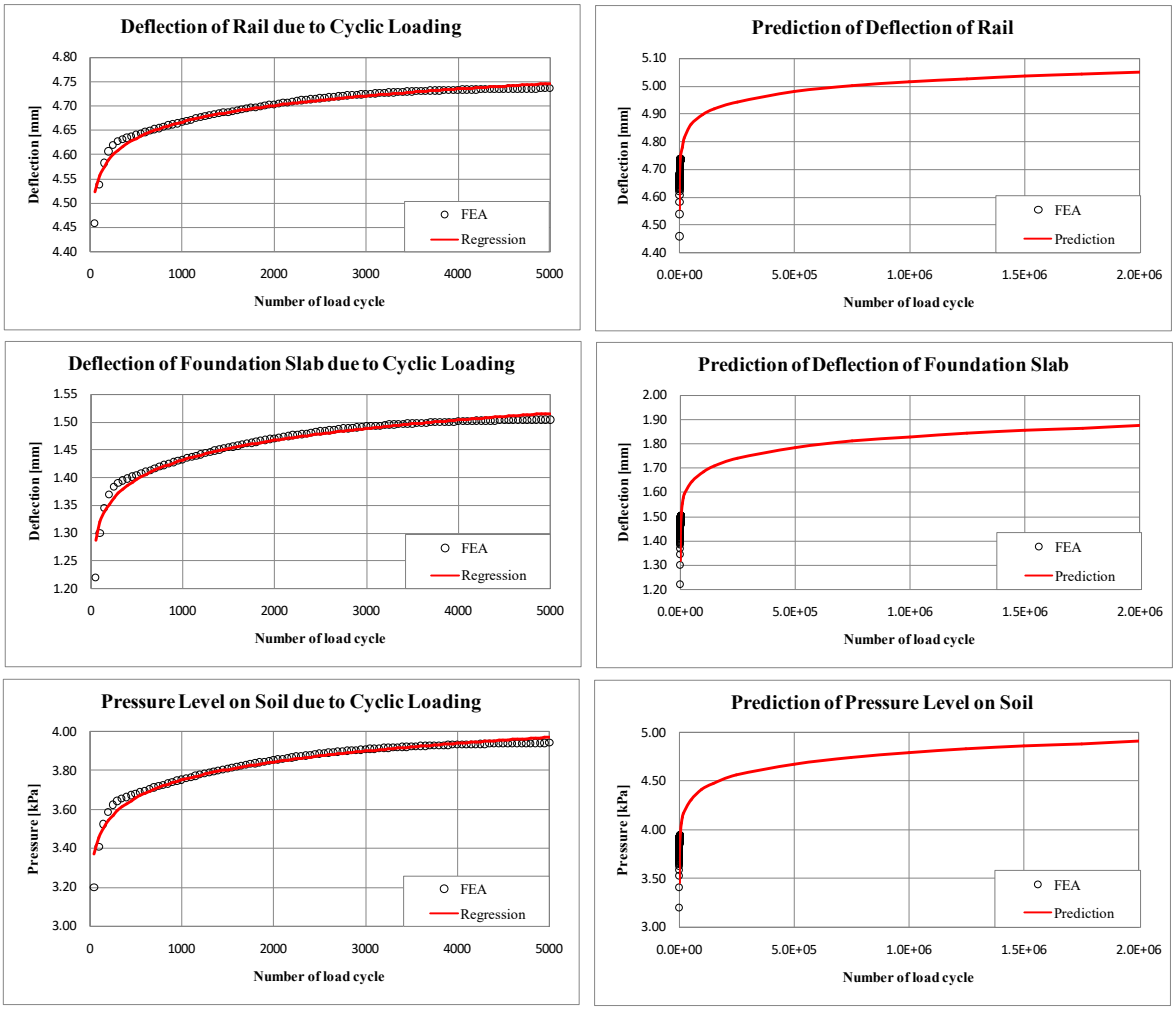

Figure 106. FEA results, regression models and prediction models of rail and slab deflections as well as pressure level on soil due to cyclic loading

Therefore, the cyclic load transfer model with a correct degradation factor can be used as well to predict the cyclic behaviour of slab track provided with *Cakar Ayam*. Using this approach is quicker than full FEA cyclic analysis. Indeed, appropriate degradation factor should be firstly defined. This can be done by utilizing empirical factor or field test to obtain load transfer's degradation factor.

Going from all of the results of static FEA performed for a slab track provided with *Cakar Ayam*, it can be concluded that:

- Installing *Cakar Ayam* foundation basically improves the performance of conventional concrete slab on soft soil in terms of reduction of the maximum displacement, bending tensile stress of foundation slab as well as pressure on soil. *Cakar Ayam* piles distributes the load wider to soil, thus the pressure on soil is reduced. However, the level of displacement by considering only soil's passive lateral resistance is still in a high level when this system is constructed on very soft soils.

- For a slab track application, the mechanisms of *Cakar Ayam* foundation exhibits that lateral resistance gives minor contribution to the vertical bearing capacity. The fundamental vertical bearing capacity is supplied by shaft resistance. In this case, *Cakar Ayam* works like a normal piled foundation.
- It has been shown that there is a critical length of pile where the lateral response of the pile-soil does not influence significantly to the lateral and axial displacements of overlaying structure. Pile with longer length contributes more bearing capacity delivered from shaft friction resistances. Furthermore, *Cakar Ayam* utilizes pipe piles, therefore, tip bearing capacity contributes minor resistance to the overlaying structure, which can be neglected in the design.
- To avoid excessive reduction of vertical bearing capacity of *Cakar Ayam* foundation, the length of the pile should be more than its critical length and has sufficient rigidity to contribute residual resistances after some period of service.
- Distance between *Cakar Ayam* piles has a significant role to the total bearing capacity of foundation. It has been investigated that for a single track, it is suggested that the piles should be located outer of the wheel load locations in transverse direction. Addition of one pile in between this distance surely contributes more stability. However, this option should consider the costs of construction when the number of pile is increased.
- The proposed analytical method can be employed for initial design of required thickness of trackbed, minimum critical length of floating pile and quick assessment of *Cakar Ayam* foundation for railway track, when the contribution of soils under the foundation slab to the bearing capacity of the overlaying structure can still be considered (in the range of soft to moderate soils, but not very soft soils).
- Nonlinear model of pile-soil interaction of *Cakar Ayam* foundation describes better the behaviour of this system due to static and cyclic loading. A FEA model to predict the cyclic behaviours of this system has been shown and exhibits a good connection with theoretical approaches. This model can be extended by using field test data to obtain more real behaviour of pile-soil interaction.

7.5.2. Dynamic Analysis of *Cakar Ayam* Foundation

a) Detailed FEA Model for Dynamic Analysis of Pile-Soil Interaction

Dynamic FEA is performed to study the dynamic response of slab track system supported with *Cakar Ayam* foundation. The analysis is conducted in frequency domain as it has been done in the previous subchapter 6.3.3. Slab track model parameters follow the previous dynamic simulation in subchapter 7.5.1 b and c. Theoretical-empirical data of fat clay (CH, clays of high plasticity & compacted) which is defined based on the example before (subchapter 7.4.3. c) is again used as input for the soil model. The major difference is that the soil is idealized as more complex nonlinear model. Soil regions are distinguished into two parts: near field and far field. This idealization has been widely used in pile-soil interaction as well as seismic engineering studies. The pile-soil model of a single pile embedded in soil is illustrated in this following figure:

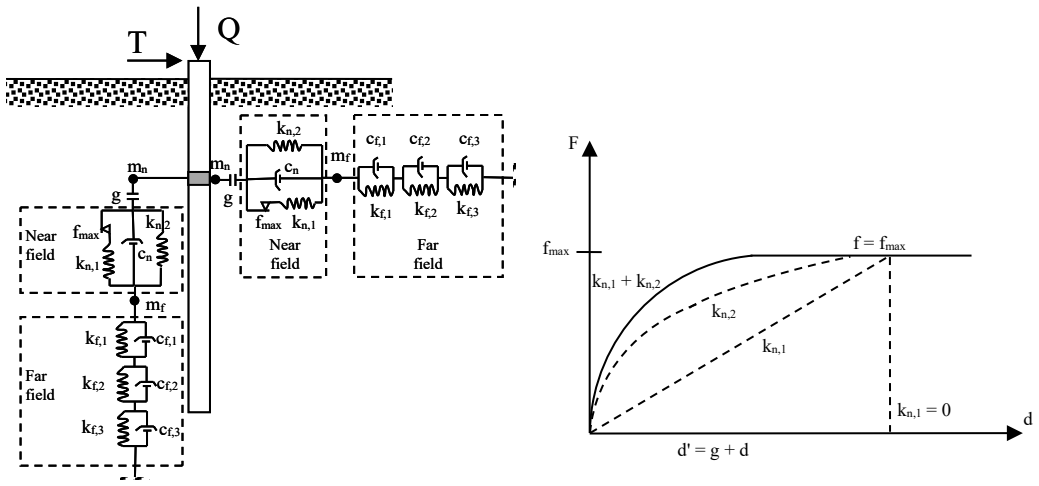

(a) pile-soil model with near and far fields *(b) soil model of near field elements*

Figure 107. Pile-soil model for dynamic analysis of Cakar Ayam

The soil model in the near field element consists two springs with frequency-dependent viscous damping. First spring is linear spring and the second spring is nonlinear spring based on load transfer model. The total stiffness of these parallel springs works before the maximum limit of force is reached. The sum of displacement contains components of gap and displacement resulted from the forces acted on the springs. The mechanism of this model is that when the limit of force is reached, the linear spring stiffness drops to zero, then only nonlinear spring gives contribution to the total stiffness of soil. This idealizes softening plasticity behaviour after sliding takes a place.

In the near field, damping parameter of soil is idealized as simple fraction frequency-dependent damping as it was also utilized by Cofer & Modak (1997)[20] in their study. The damping constant of soil is defined using this correlation:

[20]
$$C = \frac{2\xi K}{\omega_{exc}} = \frac{\xi K}{\pi f_{exc}} \qquad \textit{Eq. 94}$$

where: K is the initial stiffness of soil [N/mm], ξ is material damping ratio, ω_{exc} is angular excitation frequency [rad/s] or as f_{exc} [Hz]. The material damping ratio is assumed 0.05, since soil has hysteresis damping in the range from 0.01 to 0.1 as suggested by Whitman & Richart (1967)[145], from Bowles, 1996 [12].

Lumped mass of near field elements is approximated using the formulation of mass matrix as suggested by Cofer & Modak (1997)[20] as follows:

- *Lateral direction:*

  [20]
  $$m_{n,l} = \pi . \rho_s . {r_o}^2 . s \left\{ \frac{(m-1)\{m+(2n+1)\}}{2(n+1)(m+1)} + \frac{\rho_p}{\rho_s} \right\} \qquad \textit{Eq. 95}$$

- *Vertical direction:*

  $$m_{n,v} = \pi . \rho_s . {r_o}^2 . t(m^2-1) f'_{11}(m) \qquad \textit{Eq. 96}$$

where:

[20]
$$m = r_1 / r_o \qquad \textit{Eq. 97}$$

[20]
$$f_{11}(m) = 0.25 - \left\{ 1 + 2(ln\, m) + \frac{2(ln\, m)^2}{m^2} \right\} \qquad \textit{Eq. 98}$$

[20]
$$f_{22}(m) = f_{11}(m) + 0.5 \left(1 - \frac{1}{m^2}\right)\left(1 - \frac{3}{ln\, m}\right) \qquad \textit{Eq. 99}$$

[20]
$${f_{11}}'(m) = \frac{f_{11}(m)}{f_{11}(m) + f_{22}(m)} \qquad \textit{Eq. 100}$$

and r_1 is radius of near field zone, r_o is radius of pile, ρ_s is soil density, ρ_p is pile density, s is spacing of the node in the vertical direction and n is power in the shape function. As reference, Nogami took n = 1 arbitrarily in his study (from Cofer & Modak, 1997)[20].

In the far field, the soil is modelled according to Nogami & Konagai (1986)[94], namely as series of three frequency-independent Voigt springs. Radius of far field elements are assumed as four times pile diameter (4D). Far field's lumped mass is assumed as mass point at auxiliary node following the approach by Cofer & Modak (1997)[20]:

- *Lateral direction:*

  [20]
  $$m_{a,l} = m_{11} + m_f \qquad \textit{Eq. 101}$$

- *Vertical direction:*

  [20]
  $$m_{a,v} = \pi . \rho_s . {r_o}^2 . t(m^2-1) f'_{22}(m) \qquad \textit{Eq. 102}$$

where:

$$m_{11} = m(2n + 1) + 1 \qquad \textit{Eq. 103}$$ *[20]*

$$f_{22}'(m) = \frac{f_{22}(m)}{f_{11}(m) + f_{22}(m)} \qquad \textit{Eq. 104}$$ *[20]*

and m_f is lateral soil mass contributed from far field following the approach (see Eq. 73) of Nogami & Konagai (1986)[94].

The soil beneath the foundation slab is modelled similarly using near and far fields in vertical and lateral directions. In the near field, of soil's vertical reaction under foundation slab, q-w method is utilized. And for lateral direction, p-y method by taking depth of z = 0 is taken. Far fields are modelled the same for axial and lateral soils, but by arbitrarily taking the far field radius is twice of the width of foundation slab (2B). Lumped mass of soil below the foundation is approximated using formulation of lumped mass by Nogami & Konagai (1986)[94].

Two main states regarding gaps are defined, namely: initial state where the gap does not exist and the second state when the gap occurs after some period of time. Maximum gap values are taken from the prediction model of cyclic loading presented before in subchapter 7.5.1 c. The vertical gaps beneath foundation slab are modelled as controlled random gaps, which are generated from a random distribution function. These vertical gaps are arbitrarily distributed surrounding the area of point of interest (in the middle of the track model) and within a radius of 2.5 m. The gaps of lateral foundation are also included to idealize a small zero stiffness zone before lateral frictions between the bottom surface of foundation and soil are activated. Vertical gap below pile tip is assigned uniformly under the cross section area of pile tip. The lateral gaps of shaft friction and soil's lateral resistance are ramped along the pile by considering the pile length and two assumptions namely:

1) Flexible pile, which has length less or equal than its critical length. The maximum lateral gaps of shaft friction and lateral resistance are located on the pile tip and the minimum ones are placed on the pile head to idealize the soil's lateral degradation impact due to rotation of the piles.
2) Rigid pile, which has length greater than its critical length. The lateral gaps are distributed along the pile from the pile head to the critical length, where the maximum gaps of shaft friction and lateral resistance are located on the pile head.

b) Transient Dynamic Analysis in Frequency Domain of Slab Track with Cakar Ayam

The detailed FEA models presented above are simulated. The rails are subjected with a wheel load of 125 kN and considering dynamic factor 1.6 (total wheel load of 200 kN). Elastic-pad with static stiffness of 60 kN/mm and frequency-dependent dynamic stiffness is assigned in the model. Soft soil formatted by fat clays (CH type, clays of high plasticity & compacted) which is defined based on the example before (subchapter 7.4.3. c) and has permissible dynamic soil's compressive strength of 4.78 kPa is selected for this example of FEA.

The results of dynamic FEA in different excitation frequencies of slab track system constructed without and with *Cakar Ayam* and by considering conditions without and with gap are shown in these following charts.

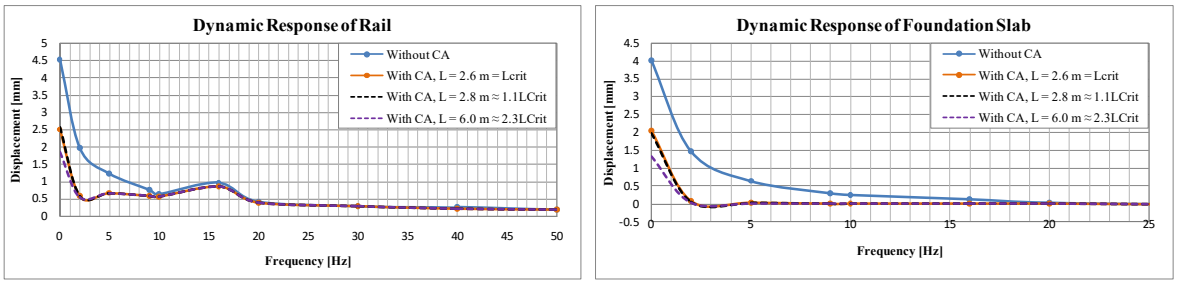

Figure 108. Dynamic response of rail and foundation slab of the track systems constructed without and with Cakar Ayam under conditions without gaps

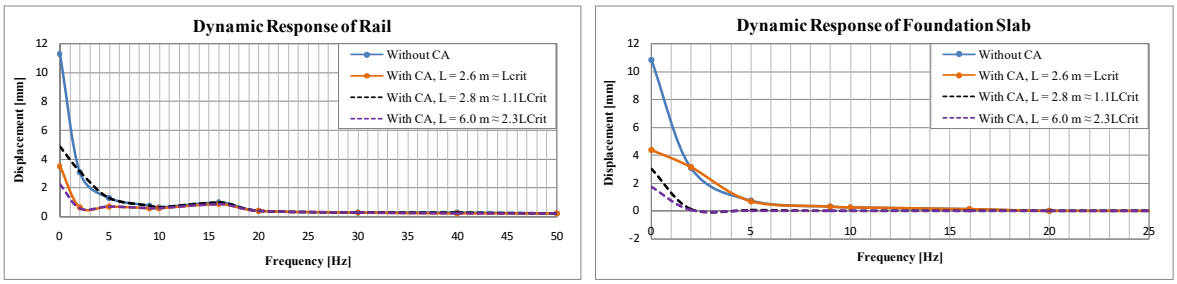

Figure 109. Dynamic response of rail and foundation slab of the track systems constructed without and with Cakar Ayam under conditions with gaps

Firstly, it can be generally seen that the influence of different constructions without and with *Cakar Ayam* piles and conditions of without and without gap are within the low frequency range up to 20 Hz. This range takes a place in both rail and slab foundation, which indicates that this is influenced by soil stiffness parameter. Once again this supports the previous results of track-soil interaction that soil treatments have more impact in a low frequency range up to 20 Hz. In the mid and high excitation ranges, the rail and slab have a more stable dynamic response and are almost constant. This happens due to sufficient thickness of slab track (24 cm) in combination with thick foundation slab (30 cm).

Secondly, from the Figure 108, it is figured out that conventional concrete foundation system without piles constructed on soft soil does not fulfill the requirement of desired rail and foundation slab displacement although the slab is very thick and gaps do not exist yet. In the initial condition without gaps, the different between piles with lengths of 2.6 m and 2.8 m is not significant.

Last but not least, from the results with gaps (Figure 110), a conventional foundation without pile delivers a very high displacement of rail and slab almost 12 mm. This shows that there is a high level of settlements due to the existence of gaps. When pile length is greater than its critical length, it is found that there still remains certain level of residual resistances although some gaps already present due to cyclic loading. Only track system, which is constructed with piles far longer than its critical length (6 m or $2.3L_{Crit}$) still delivers the desired level of displacement of rail (2 mm) and sufficient residual bearing capacity after the existence of gaps.

c) Transient Dynamic Analysis with Different Train Speeds of Slab Track with Cakar Ayam

The next FEA dynamic simulations are conducted to study slab the dynamic response of track systems provided with *Cakar Ayam* piles under condition of running train loading with different speeds. Two conditions of without and with gap are simulated.

Figure 110 presents the results of different slab tracks under condition of without gap. Conventional track system without piles on soft soil results very high levels of absolute displacement of rail and foundation slab. All other systems provided with piles generally exhibit great improvements.

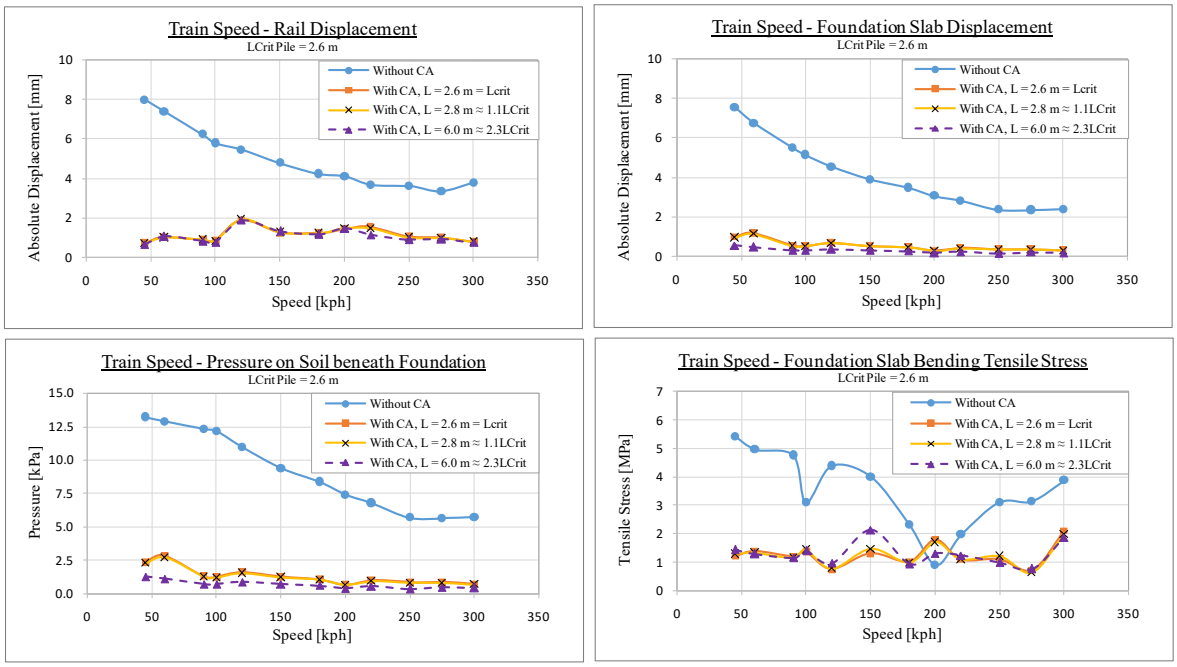

Figure 110. Correlations of train speed, rail displacement and pressure on soil of a slab track constructed without and with Cakar Ayam foundation considering initial condition without gap and different pile lengths

Some important points are found:

- the impact of pile length under condition without gap is not significant to the rail displacement.
- displacement and bending tensile stress of foundation slab as well as pressure on soil exhibit a magnificent reduction when pile with length far longer than its critical length is installed.
- the shorter piles of 2.6 m ($L = L_{Crit}$) and 2.8 m ($L = 1.1L_{Crit}$) present similar level of foundation slab's displacement and bending tensile stress as well as pressure on soil in almost all simulated train speeds.
- only pile with far longer length of 6 m (($L = 2.3L_{Crit}$) achieves the target of limiting the dynamic soil's compressive strength below 4.78 kPa. Meanwhile the other two shorter piles generate higher levels of pressure on soil at the train speed of 60 kph.
- the bending tensile peak levels of foundation slab at train speeds of 200 and 300 km/hour are already quite high although the far longer pile is used and this is estimated within the condition of without gap.

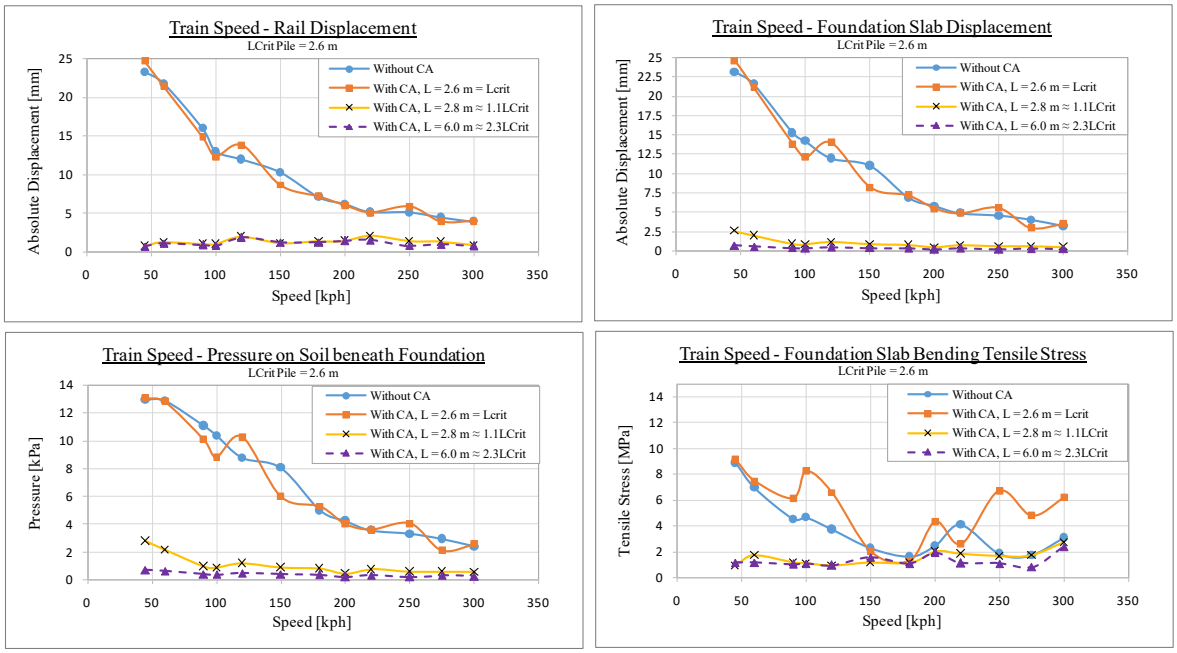

Figure 111. Correlations of train speed, rail displacement and pressure on soil of a slab track constructed without and with Cakar Ayam foundation considering condition with gap and different pile lengths

Under the condition of presence of gaps, some essential findings are:

- pile with length equal to its critical length does not perform an improvement in comparison to the conventional foundation system without pile when gaps exist. The resulted displacements of rail and of foundation slab as well as pressure on soil are similar between this pile foundation system with $L = L_{Crit}$ and conventional foundation. Furthermore, within the condition of with gaps, the installation of shorter pile with $L = L_{Crit}$ even shows some peaks of foundation slab's bending tensile stress higher than conventional foundation due to natural frequencies contributed by addition of shorter pile length.
- pile with length of 2.8 m ($L = 1.1L_{Crit}$) presents a good performance seeing from the level of displacements of rail and of foundation slab as well as pressure on soil. However, bending tensile stress are still in a high level when gaps occur. This system with pile length of 2.8 m is according to the proposed analytical method of *Cakar Ayam* design. It indicates that the estimated length is insufficient when gaps exist.
- only the system with pile length far greater than its critical length (6 m or $L = 2.3L_{Crit}$) presents a good performance even though gaps exist. This indicates that longer pile is more recommended.

As summary from all simulations and analyses have been performed, the mechanism of *Cakar Ayam* foundation is not fully appropriate for railway track application. Some points regarding this are:

- Firstly, the passive soil resistances are not mobilized optimally. This is because the load on the top of foundation slab is already distributed as pressure by the overlaying multilayered track elements. Thus, there is only small bending and small rotation of piles and then soil passive pressure are not triggered. This mechanism is different with the application of roadway using *Cakar Ayam* on soft soil.
- Secondly, railway track requires a strict level of displacement regarding safety, riding comfort, maintenance and long term performance of the track. Therefore, sufficient bearing capacity of soil is a "must" requirement. The estimated length of the pile designed using the concept of moment rotation is insufficient for railway application. It is show that the length of pile should be far greater than its critical length. A sufficient length until it reaches a rigid base is more preferable and recommended. This is to guarantee a good performance of railway track on soft soil within a long term of service.
- Thirdly, failure of *Cakar Ayam* system has been found to take a place due to permanent deformations of soil surrounding the piles. Thus, a detailed analysis concerning possibility of gap existence should be carefully taken into account. For railway application, dynamic and transient analysis plays very important role in the predication of track systems within a long period of time.
- Finally, *Cakar Ayam* can be optionally considered as an alternative solution for railway track application. However, this system will work like a conventional piled foundation system. Hence, its capacity should be estimated majorly from pile shaft friction resistance and not the lateral resistance. This indicates that *Cakar Ayam* requires improvement by having much longer pile for railway application. When the soft soil depth until a firm layer is considerably small, this lightweight drilled *Cakar Ayam* pile system can be implemented. Nevertheless, when the soft soil layer depth is much greater, a conventional deep foundation using driven pile are more appropriate solution. For slab track application, this system is not recommended for a deep layer of very soft soils which have resilient modulus lower than 15 MPa.

7.6. Design Consideration and Optimization of Railway Track Supported with Pile Foundation on Soft Soil

7.6.1. Parameter for preliminary assessment

As suggested by Bowles (1996)[12], for a conventional foundation the value of dimensionless frequency factor a_o greater than 1.5 demands advanced geotechnical treatments. High value of a_o means that a high frequency loading is subjected to a soft soil (see introduction of Chapter 7). Nevertheless, it is proven that the dynamic impact, which is majorly influenced from substructure and soil is within the range of excitation frequencies only up to 20 Hz. At the frequencies lower than 5 Hz (quasi-static state), the impact of soil stiffness changes is more obvious to the superstructure's response shown from the previous analysis (subchapter 6.3.3 and 7.5.2.c).

Taking a_o= 1.5 and excitation frequency of 5 Hz as the reference values and assumptions of standard values of soil's properties of density 17 kN/m^3, Poisson's ratio of 0.4 and considering per meter width of foundation plate give shear wave velocity of soil of a proximally 20.9 m/s, shear modulus of soil 7.5 MPa and elastic modulus of 18.4 MPa. Very roughly, it can be said that soil's resilient modulus less than 18 MPa demands geotechnical treatments. This affirms the suggested range of bearing capacity in this study that soil' resilient modulus above 18 MPa is the range of recommended trackbed applications and less than 15 MPa requires advanced geotechnical solutions. The suggested range of application of *Cakar Ayam* foundation is within the soil bearing capacity 10 - 15 MPa with a careful consideration of the condition of soft soil regarding its depth and bearing capacity.

7.6.2. Selection of Pile Diameter, Pile Spacing and Minimum Required Length of Pile

Piled foundation systems which are discussed in this study can be categorized into two groups: bored piles (*Cakar Ayam*) and driven deep-pile foundation. Since *Cakar Ayam* utilizes a large diameter of pipe pile, the installation of this piles are either bored in a natural soil or embedded in an embankment filled soil material. Therefore, a longer pile of *Cakar Ayam* is more difficult to be constructed on soil concerning installation and compaction of soils surrounding the piles skin. This pipe pile system is more effective when the depth of natural soft soil or of an embankment until a firm layer is low. Deeper piled foundation is installed by driven the piles to soil. Then driven pile can have smaller diameter but longer length than *Cakar Ayam* pipe pile.

Since the diameter of *Cakar Ayam* pipe piles are between 90 and 120 cm, then the pile spacing is also limited in the transverse direction due to construction efficiency. It has been shown that the optimal spacing of *Cakar Ayam* pile with diameter of 90 cm is 2.5 m for a single-track system. Adding a pile in between this spacing is possible, but it requires greater foundation slab width. Some example of conventional piles system constructed in China as reported by Raithel et al, 2008)[109] showed in subchapter 7.3, the pile spacing of slender driven pile is 1.5 m. Hence, it needs greater number of piles but it can have smaller diameter and longer length.

Minimum required length of *Cakar Ayam* pile should be greater than its critical length. Critical length can be estimated using the approach of Matlock (1970), other authors or the proposed method based on moment equilibrium concept. This is taken to define flexible or rigid behaviour of pile. Pile far longer than its critical length (*2 0r 3*L_{Crit}) or even far greater until it reaches a firm base layer is more recommended. Analysis of *Cakar Ayam* to define the required pile length should be performed by the total pile capacity, which is majorly contributed by skin friction (for floating pile) and/or tip resistance (for end-bearing pile) for a railway application and considering a possibility of existence of gaps due to cyclic loading to guarantee a long term stable performance.

7.6.3. Softer Elastic-pad with Higher Damping for Ballastless Track

The ballastless track system has been analyzed is slab track provided with piled foundation, especially *Cakar Ayam* foundation. Two concrete slabs of superstructure slab track and foundation slab are assumed bonded. Piles are also assumed have a rigid connection to the foundation slab due to condition that they are constructed reinforced, monolith and embedded into the concrete foundation slab. Hence, a very rigid system is built. Dynamic response of a very rigid track structure should be balanced with some portions of elastic elements which provide elasticity and high damping capability. In the construction mentioned above of slab track, besides soil, the major track components, which are responsible for giving contribution of elastic-damping behaviours are the elastic-pads.

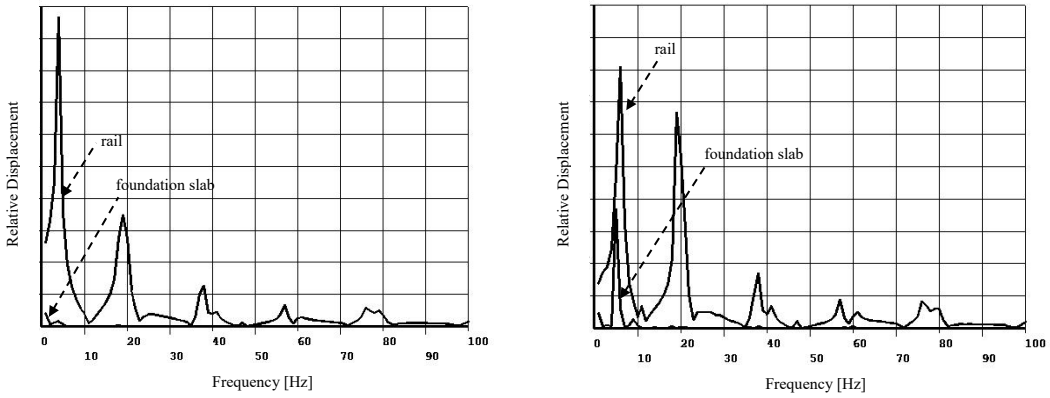

(a) elastic-pad with k_{dyn}= 27.2 kN/mm (b) elastic-pad with k_{dyn} = 72.5 kN/mm

Figure 112. Comparison of the use softer and harder elastic-pad to the harmonic vibration response of a slab track provided with 6-m piles analyzed using harmonic simulation

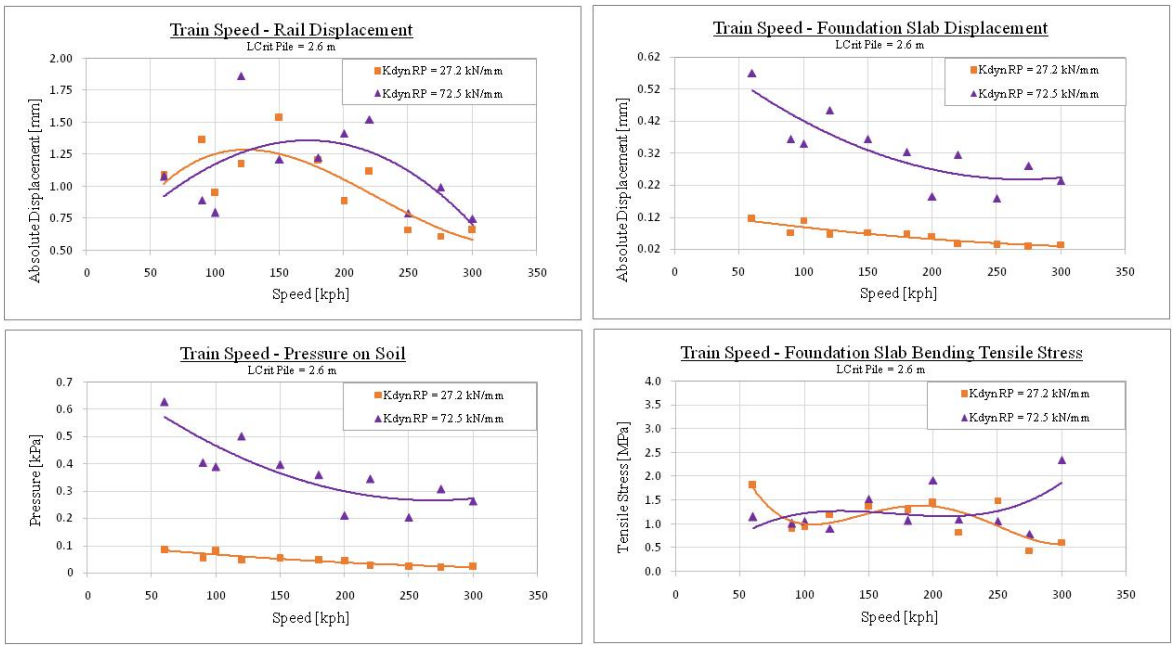

Figure 113. Comparison of the use softer and harder elastic-pad to the dynamic vibration response of a slab track provided with 6-m piles analyzed using running train simulation

Then the optimization of slab track with piled foundation can be followed by selecting softer elastic-pads with high damping capability. This will enhance the overall performance and vibration response of the track structure due to dynamic loading induced from a running train. It has been shown from the dynamic analysis of track-soil interaction (TSI) before (Figure 50), as well as the example data from measurement (Figure 51) that high resilient elastic-pad with high damping capability improves the dynamic response of track due to vibrations generated from running train. The comparison of the use of softer and harder elastic-pad analyzed again using harmonic simulation and dynamic train FEA simulations

on slab track provided with 6 m length of pile and considering of gap existence is presented in the Figure 114 and Figure 113 respectively.

7.6.4. Natural Frequency of Track System

Adding a piled foundation to a conventional track also has an influence regarding the natural frequency of the overall track system. Comparison of harmonic analysis in ANSYS of three different track systems with: a conventional foundation without pile, piled foundation with $L = L_{Crit}$ and longer pile $L = 2.3L_{Crit}$and elastic-pad with dynamic stiffness of 27.2 kN/mm within initial condition without gap is shown below:

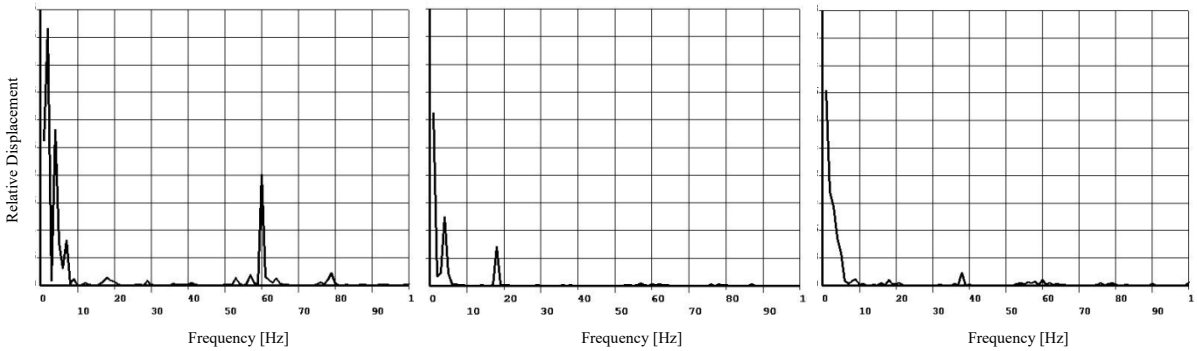

(a) without pile *(b) with pile $L = L_{Crit}$* *(c) with pile $L = 2.3L_{Crit}$*

Figure 114. Frequency-relative displacement amplitude of foundation slab of a track system without pile and with different lengths of pile

Comparing those systems considering initial condition without gap, obvious changes are seen on the dynamic response of concrete foundation when piles are installed. Adding piles generally stabilizes the track system constructed on soft soil, as the number of and level of the peaks of foundation displacement are reduced in comparison to a conventional foundation system without pile. What is more, the longer the pile, the smoother and more stable the performance of the concrete foundation to bear the overlaying track superstructure within the range of low and high frequencies. This show that constructing piled foundation for slab track constructed on soft soil enhances the track performance on low frequency excitations in line with greater substructure bearing capacity as well as it reduces the vibration impact in high frequency excitations.

7.6.5. Multilayer Ballasted Track System

Conventional ballasted track system can be also an option of a track system provided with piled foundation slab on soft soil. Some advantages (+) and disadvantages (-) of ballasted and slab tracks regarding construction on soft soil are:

1. Slab track is considerably higher in initial costs in comparison of conventional ballasted track (-). Concerning application on soft soil, a slab track has to be carefully designed in a long-term service period due to fact that this system is more rigid, permanent and fixed. Rehabilitation of a local failure of a continuously reinforced concrete (CRCP) of slab track (e.g. excessive cracks) due to settlements of soil demands more difficult method and possibly higher costs (-). An option to anticipate this is by implementing unit slab built of precast concrete or jointed concrete slab.
2. Settlements of a track on soft soil is highly possible to occur. When a local settlement takes a place, maintenance of re-leveling the rail (vertical track irregularity) is relatively more practically doable of a ballasted track by overlaying some ballast stones and doing re-tamping under the hanging sleepers (+). In a slab track, certain re-leveling due to settlement of soil can be done by inserting a steel plate under the elastic-pad. According to commercial fastening systems available in the market and German Railway *Deutsche Bahn*, the maximum height of re-leveling by inserting steel plate under elastic-pad is 76 mm. However, this also has a consequence that the track quality is decreased as well as higher vibration in high frequency concerning generated pin to pin natural frequency (-).
3. The use of granular material (ballast) and multilayer trackbed provides higher flexibility and damping. This gives better dynamic response of the overall track systems due to dynamic loading and vibrations (+).

Regarding performance of ballasted track systems provided with piled foundation, a sensitivity analysis is conducted to obtain an optimum solution. Three main groups of variation are taken. The differences are generally varied from (1) multilayer using trackbed when the stiffness of the top-down layers is increased, as well as (2) decreased from the top to the bottom layer, and (3) the use of asphalt pavement in between ballast and concrete foundation.

There are three variations of ballasted tracks are compared with one slab track system. The variations of these systems are shown in the Table 25.

Table 25. Variations of ballasted track system in comparison of slab track

Layer/ System	CA-BT-1	CA-BT-2	CA-BT-3	CA-ST
Top	Ballast E = 250 MPa, H = 60 cm	Ballast E = 250 MPa, H = 45 cm	Ballast E = 250 MPa, H = 30 cm	Reinf. Concrete E = 36 GPa, H = 24 cm
Base	Ballast E = 300 MPa, H = 60 cm	Ballast E = 300 MPa, H = 45 cm	Granular E = 150 MPa, H = 60 cm	-
Sub Base	Ballast Mat (in practice, but not considered in FEA)	Asphalt E = 5 GPa, H = 12 cm	Embankment E = 80 MPa, H = 70 cm	-
Foundation	Reinf. Concrete E = 36 GPa, H = 30 cm			
Total H	150 cm	132 cm	190 cm	54 cm
Total SN	180.6 cm	181.6 cm	181.8 cm	180.2 cm
Pile	L = 6 m, L_{Crit} = 2.6 m, D = 90 cm, Spacing = 2.5 m			

The results of dynamic FEA of running train simulation with different speeds of CA-BT-1, CA-BT-2, CA-BT-3 and CA-ST models are presented in the Figure 115.

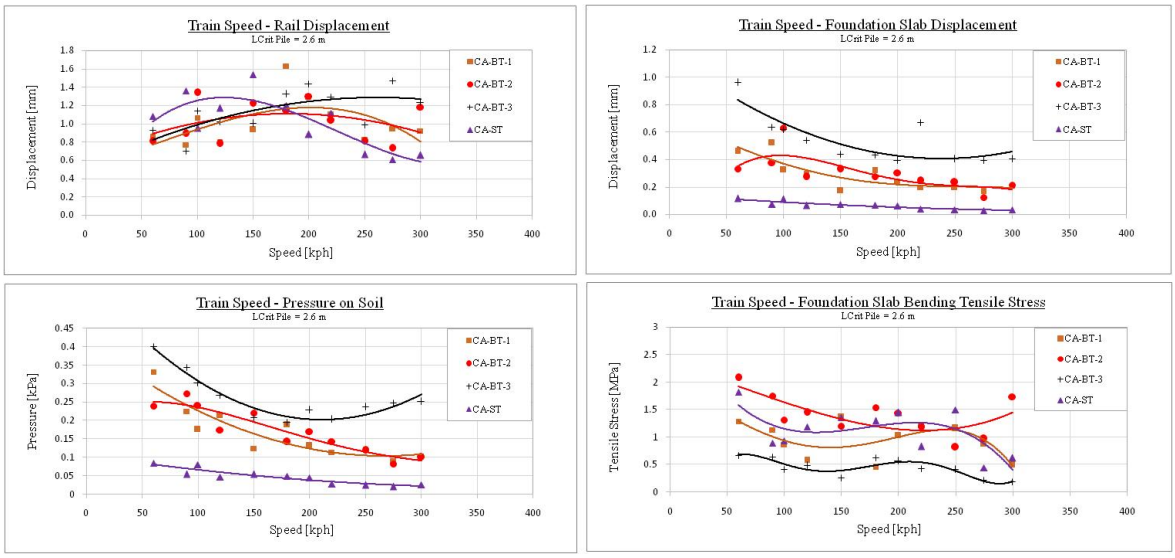

Figure 115. Comparison of dynamic response of ballasted track systems and slab track under running train simulation and considering gap existence

Generally, the changes of rail dynamic displacement of all models are within the range of 0.6 - 1.7 mm. These changes are within the desirable maximum level of 2 mm. Displacement levels of concrete foundation of the ballasted track systems are slightly higher than the ones of slab track. The highest level of displacement of foundation slab is given by the CA-BT-3. This is caused by higher mass contributed from the overlaying layers above the foundation slabs because the base and sub base layers are very thick. Greater mass of those layers considered in dynamic analysis influences the vibrations of the foundation slab.

Pressure on soil under foundation slab of all models shows very small pressure magnitudes far under the maximum limit of soft soil. This happens due to sufficient length of piles and bearing capacity delivered from the piles even though under the condition of with gaps.

Some remarkable points can be found from the level of bending tensile stress of foundation slab. CA-BT-1 is formatted of 2-layer ballasted trackbed and CA-BT-2 and CA-BT-3 are constructed as 3-layer trackbed. CA-BT-1 shows maximum levels of foundation's bending tensile stress close to the ones of slab track system (CA-ST). The highest magnitude of bending tensile stress of foundation slab is generated from CA-BT-2 model. Only system of CA-BT-3 performs a significant reduction of bending tensile stress lower than CA-ST. The stiffness of the layers above the foundation slab of CA-BT-1 and CA-BT-2 models are increased from the top to the bottom layers. Nevertheless, a better reduction of bending tensile stress is presented by CA-BT-3, which its stiffness is reduced from the top to the bottom layers. This is similar to a conventional trackbed design concept. It indicates that the use of multilayered system, in which the stiffness is gradually reduced from the top to the bottom layers delivers better reduction of bending tensile stress of concrete foundation.

It is demonstrated that the value of SN ≈ 180 cm of CA-BT-1 and CA-BT-3 (ballasted) and CA-ST (slab track) delivers a good approximation of the required bearing capacity as well as thickness to reduce the bending tensile stress of foundation within its safe level. This affirms that the estimated thickness using the proposed trackbed thickness design can be applied for track system provided with piled foundation on soft soil. It should be noted that this approach considers a certain level of bearing capacity from the soil below the foundation slab. If the soils are very soft with almost neglectable bearing capacity and the fundamental bearing capacity is delivered from the deep pile foundation, the foundation slab thickness should be designed following the approach close to analysis of a discrete point supports, such as quasi three-point-bending analysis. Hence, the major design criteria of the trackbed should be according to the limit of bending tensile stress of the concrete foundation against flexural tensile failure.

Finally, it can be summarized that a multilayer trackbed of a ballasted track system resting on a piled foundation slab on soft soil should be designed by providing a sufficient thickness and by gradually decreasing the stiffness of the layers. This is done to deliver optimum solution as well as more stable dynamic response of the overall structure.

7.6.6. Design Procedure, Construction Process and Field Test

Analytical design of piled foundation supported railway track can be combined with field tests. The actual bearing capacity of contributed by the piles can be evaluated by doing pile load test. This can be assessment of the analytical method of whether the estimated bearing capacity of pile is within the safe range or not. Since construction of railway track on soft soils is more complicated than other traffic infrastructures, the evaluation and assessment within the design and construction process is fundamentally important. Another field test which can be performed during the construction process is foundation slab load test. Then the estimated thickness of trackbed using analytical method can be assessed based on the results of slab load test.

Second important consideration is primary consolidation of soft soils. All of the analytical and numerical approaches have been discussed above do not consider initial settlements due to primary consolidation state. This initial settlement is possible to occur within the construction process. Therefore, additional settlements which are beyond the estimated level should be avoided.

7.6.7. Soil Bearing Capacity Range

As summary of all analyses and evaluations have performed, the range of bearing capacity of soil related to the alternative solutions are presented in this matrix:

Table 26. Matrix of soil bearing capacity range for railway application

<table>
<tr><td colspan="5">Soil Bearing Capacity (BC) Range</td></tr>
<tr><td>Very Soft</td><td>Soft</td><td>Moderate</td><td>Moderate Firm</td><td>Firm/Rigid</td></tr>
<tr><td>E_s < 5 MPa</td><td>5 - 10 MPa</td><td>18 - 45 MPa</td><td>45 - 120 MPa</td><td>E_s > 120 MPa</td></tr>
<tr><td>k_s < 0.05 N/mm^3</td><td>0.05 - 0.08 N/mm^3</td><td>0.1 - 0.15 N/mm^3</td><td>0.18 - 0.2 N/mm^3</td><td>k_s > 0.2 N/mm^3</td></tr>
<tr><td></td><td></td><td colspan="3">Trackbed</td></tr>
<tr><td></td><td></td><td>Major function of BC</td><td colspan="2">Additional function of supplementary BC + special functions (against excessive cracks, frost, drainage etc.)</td></tr>
<tr><td></td><td colspan="2">Cakar Ayam Floating pile*</td><td></td><td></td></tr>
<tr><td></td><td colspan="2">Cakar Ayam End-Bearing Pile**</td><td></td><td></td></tr>
<tr><td colspan="2">Conventional End-Bearing Pile**</td><td></td><td></td><td></td></tr>
</table>

Note: Between E_s and k_s shown in the same column does not mean a direct conversion of both values
** with careful considerations of pile dimensions & configurations, BC and the depth of the soft soil*
*** more recommended*

8. Implementation of Jointed Concrete Pavement for Slab Track Application

Due to high level of thermal stresses induced from extreme temperature changes/ differences between the top and the bottom surfaces of a concrete slab, excessive random cracks can take a place, particularly of a long concrete slab. Random cracks decrease the performance of a concrete slab. The level of thermal stress majorly depends on the dimension of the slab (especially its length) and critical temperature. When there is an extreme temperature difference, especially due to heating, cracks due to thermal stresses in an infinite concrete slab can cause a severe performance problem.

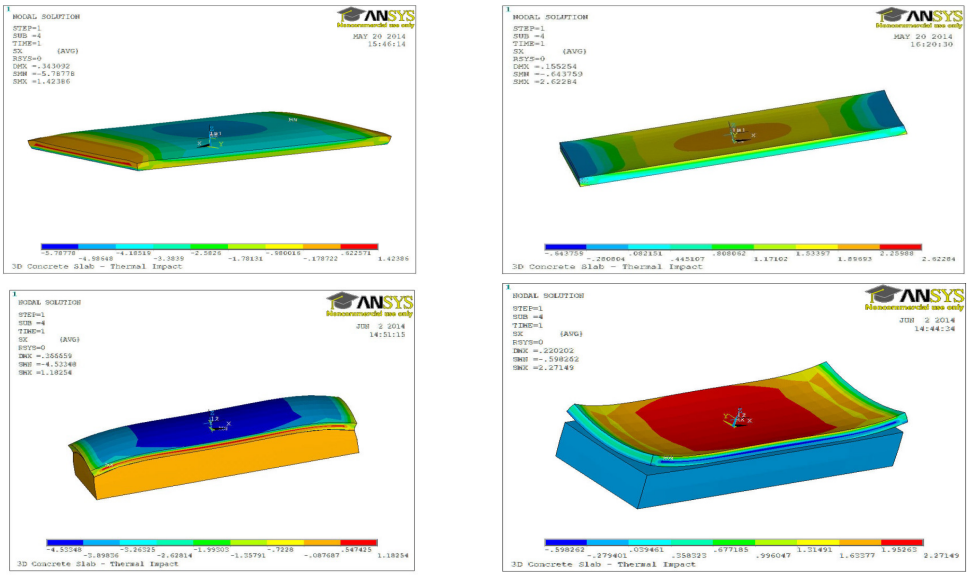

(a) heating *(b) cooling*

Figure 116. Thermal impact causes slab warping due to heating and curling due to cooling

This is the reason that on a Rheda-2000 system, it utilizes *Continuously Reinforced Concrete Pavement* (CRCP). So that even if some random cracks exist, the function of continuous reinforcement bars (rebars) is to provide load transfer continuity. The design of CRCP for Rheda-2000 generally follows the *German Highway Construction Regulation for Concrete Pavement* (ZTV Beton-StB 07/2013), and requires a minimum diameter of the rebar of 20 mm and the total amount of the rebar area is 0.8 - 0.9% of the cross section area of the slab[70][68][80]. The rebars are positioned near to the middle of cross section of the slab. In the design, the crack width is limited up to maximum 0.5 mm.

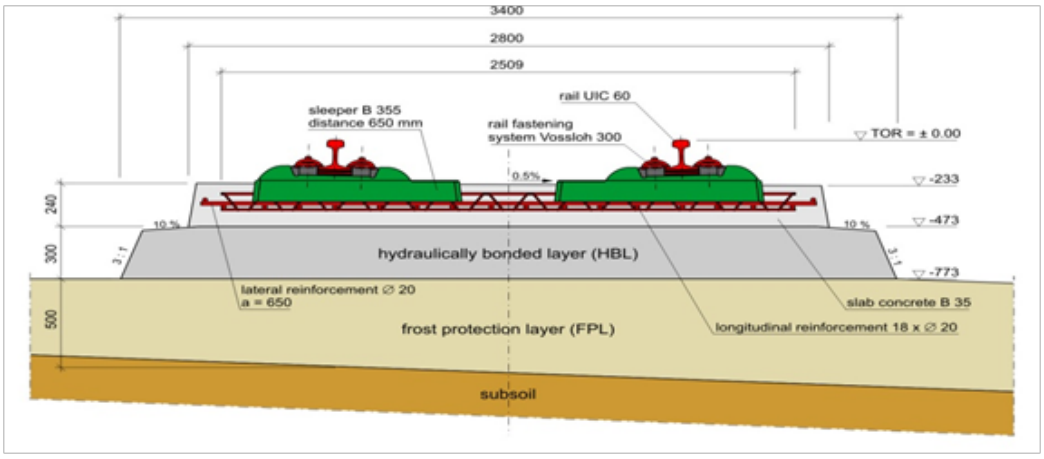

Note: picture courtesy of Rail One

Figure 117. The cross section of Rheda-2000 on embankment

8.1. Jointed Reinforced Concrete Slab for Slab Track Application

Other construction types of concrete slab are jointed concrete slabs, such as *Jointed Plain Concrete Pavement* (JPCP) or *Jointed Reinforcement Concrete Pavement* (JRCP). The joint spacing of an infinite slab can be defined empirically where the major cracks are expected to form and/or analytically regarding the critical length of the concrete slab. The method of providing joints to reduce the risk of excessive cracks due to temperature stress and traffic on an infinite concrete slab can be called as *active control crack* (ACC). There is a challenge to implement jointed concrete slabs for slab track applications. CRCP is considerably more expensive in term of the amount of reinforcements in comparison to JRCP and even more to JPCP.

Rheda-2000 slab track system is investigated through FEA in ANSYS. The Rheda-2000's cross section is illustrated in the Figure 117. Detailed idealization of this system in FEA is depicted in the Figure 118. The model is able to idealize CRCP, JPCP and JRCP construction types, CTB (in original Rheda-2000) or other base materials and soil layers. This model is also able to simulate the impacts of thermal stress through physics thermal analysis and different bonding and debonding conditions through the setting of the contact element behaviours.

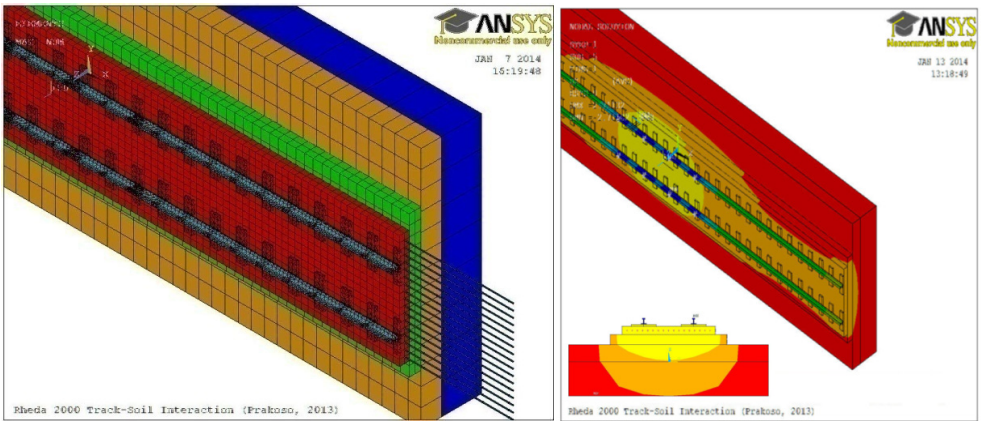

Figure 118. Discretization and displacement contour of 3D FEA-model in ANSYS

Static simulations of Rheda-2000 system are performed by varying the joint spacing and modulus of elasticity of soil. The slab model of JRCP is selected to investigate the range of the optimal joint spacing when CRCP (in standard design of Rheda-2000) is substituted by JRCP or JPCP. Load model of UIC71, which is commonly used to model train load on a railway bridge is applied to the model. Self-weight of the structure and thermal load due to positive temperature gradient are also included in the simulations. The resulted bending tensile stresses and the allowable stresses considering thermal impact and dimension of the concrete slab are compared. The thermal stress levels are estimated using two different approaches, namely employing (1) Eisenmann approach and (2) the result of FEA thermal analysis. The allowable flexural stresses due to traffic and both resulted thermal stresses (Eisenmann and FEA approaches) are estimated using Smith method (see Eq. 129 - Eq. 135 in the Appendix 1 Section A.1.2, pp. 221 about Eisenmann and Smith approaches).

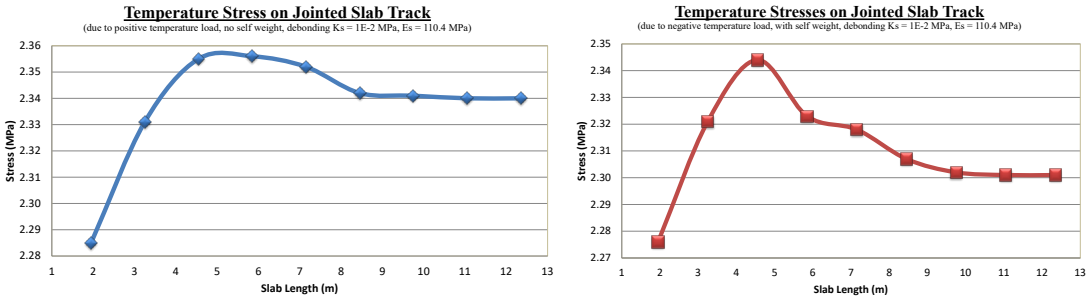

(a) without self-weight *(b) with self-weight*

Figure 119. Thermal stress on concrete slab obtained from FEM physic solution

From the results of simulations, it is found that shorter joints of a JRCP reduce the resulted bending tensile stress due to thermal and traffic. This can be achieved when the bonding condition is partly bonding as it is shown in the Figure 120.

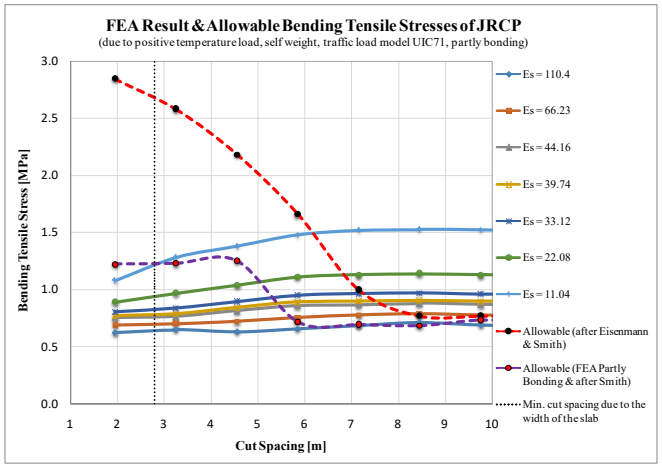

Figure 120. Correlation of joint spacing and bending tensile stresses of the JRCP with consideration of partly (soft) bonding condition

Similar behaviours are shown in the study done by Lechner (2008)[68]. He investigated ballastless track located on unbound base course layers and the possibility of implementing jointed slabs. In his study, FEA result of a ballastless track with discrete rail-seats on concrete slabs with doweled dummy joints located on unbound base layers (crushed stones) is depicted in the Figure 121.

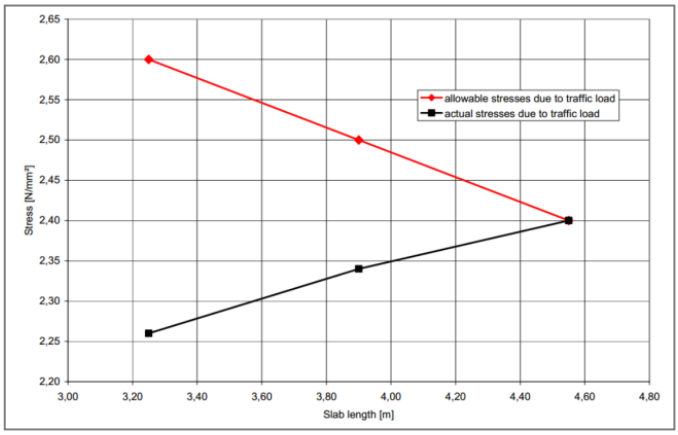

Note: picture courtesy of Lechner (2008) [68]

Figure 121. Impact of slab length on allowable and actual stresses of a ballastless track built using jointed concrete slabs on unbound base layers after Lechner (2008)

The result of analysis shown in the Figure 121 also demonstrates a reduction of bending tensile stress of concrete slab when the joint spacings are shorter, which is similar with the one presented in the Figure 120.

This is in line with the suggestion by Lechner (2008)[68][67] that to modify the standard Rheda-2000 system using jointed slab, instead of constructing CTB as base layer below the jointed slab, it can be also an option to construct the jointed concrete slab resting on a stiff unbound granular material, such as crushed stones ballast layer.

From the results presented in the Figure 120, the minimum longitudinal joint spacing is 2.8 m due to consideration of the width of the slab. The maximum joint spacing of JRCP is around 6 m considering thermal stress analyzed with FEM and Smith allowable flexural tensile stress limit as well as moderate stiff of the underlying layer (E_s = 110 MPa). Lower bearing capacity of the layer below the JRCP demands shorter maximum joint spacing. Indeed, having shorter joint spacing gives advantage of a lower thermal stress, but it also means more efforts and costs in the initial construction in terms of more number of cuttings and joints. Hence, the range of joint spacing between 4.5 and 6 m of the jointed slab can be considered. Another reason is that in this study regarding soft soil, the jointed slab will be designed resting on moderate to stiff base layers and/or foundation slab.

Another important consideration to improve the performance of slab track built using jointed slab is the bonding condition between the jointed concrete slab and foundation slab. Partly (soft) bonding condition can be introduced by filling an intermediate layer of a thin and soft elastic mat or unbound ballast layer in between jointed concrete slab and foundation slab. This will give advantages that:

1. Partly (soft) bonding condition between jointed concrete slab and foundation slab is provided by the intermediate layer, so that providing joints will work optimally to reduce the impact of thermal stress and the risk of excessive random cracks on jointed concrete slab.
2. Above mentioned materials of intermediate layers have certain level of flexibility and damping higher than concrete. Provided this layer in between the jointed slab and foundation slab enhances the overall performance of the track response regarding dynamic vibrations.
3. Ballast (crushed stones) has range of elastic modulus from 80 to 300 MPa. Meanwhile reinforced concrete slab has elastic modulus around 34 - 40 GPa. Hence, in line with the previous optimization that using multilayer trackbed by gradually decreasing the stiffness of overlaying layers above the foundation slab will improve the performance of the slab track in terms of more stable dynamic response and reduction of bending tensile stress level of foundation slab.
4. Providing an intermediate layer also has function to reduce of the risk of induced (mirror) cracks from the jointed slab to the foundation slab.
5. The difficulty of rehabilitation of a slab track when a failure in a local settlement area occurs can be overcome. Because when a local failure takes a place on a jointed slab,

the rehabilitation of the unit slabs within this area can be done relatively more achievable by replacing the slabs only in that area. This is also in line with the suggestion of providing intermediate layer with soft bonding condition in between the jointed slab and foundation slab. Hence, the replacement of unit slabs in a failure area can be relatively doable in comparison when a hard-bonding condition presence in interface between jointed slab and foundation slab.

8.2. Jointed Plain Concrete Slab Resting on a Piled Raft Foundation

Due to the consideration of the relatively higher cost of CRCP (and also JRCP), implementing JPCP can be an option of building slab track provided with piled foundation on soft soil as alternative replacement of conventional CRCP. The study reports done by Lechner (2008)[68][67] had earlier discussed as well regarding JPCP implementation.

To investigate the impact of applying jointed plain concrete in comparison to CRCP, bonding conditions and different base layers, FEA static thermal and structural analyses are performed in this research. In FEA thermal analysis, a high level of positive temperature different between the top and the bottom surfaces of concrete slab is assigned. The temperature gradient (Δt) is influenced by the thickness of a slab. According to Eid (2012) [31], based on experimental tests in Germany, the thickness-dependent temperature gradient can be estimated based on this empirical approach:

Positive temperature gradient: [31] $$\Delta t = \frac{0.191}{e^{0.0028h}}$$ *Eq. 105*

Negative temperature gradient: [31] $$\Delta t = \frac{-0.370}{e^{0.022h}} - 0.035$$ *Eq. 106*

where: h is the thickness of the concrete [mm].

Two variations of the base layer; using bounded material of asphalt pavement with elastic modulus of 5 GPa and thickness of 8 cm and unbound granular material with elastic modulus of 250 MPa and 45 cm of thickness. Bonding conditions at the interface between the bottom of concrete slab track and the top of base layer are distinguished as hard and soft bonds (partly bonding). Instead utilizing contact elements, very thin bonding interfaces are modelled as dense-discrete soil springs acting majorly in compression using nonlinear COMBIN39 elements in ANSYS. This is taken to model partly bonding conditions, so that there is no full transfer of bending stresses between concrete slab track and foundation slab. The amount of tension stiffness is adjusted to idealize soft and hard-bonding conditions. Soil

has resilient modulus of 15 MPa based on the same example data used before and idealized using load transfer model. The foundation slabs have thickness of 30 and 40 cm and supported by piles with length of 6 m. Static analysis is performed by considering single point wheel load 125 kN (250 kN axle load) on the rails. Concrete C40/50 parameters are assigned for both slabs. The allowable stress limits are estimated using Smith approach, which can be seen in the Table 82 of Appendix 8, pp. 262.

To compare the systems of conventional CRCP and JPCP with and without dowel bars, three scenarios are defined regarding the presence of cracks in FEA, namely:

1. Conventional CRCP with neglectable number of cracks. The amount of the rebars is 0.8% and the rebars are installed continuously along a very long (semi-infinite) slab track. This describes a good condition of CRCP.
2. JPCP with dowel bars, which has joint spacing variations from 1.95 to 7.15 m.
3. Similar to (2) but this JPCP has no dowel bars, in which connection between slabs is only provided by interlocks among aggregates in the cutting location. Thus, load transfer efficiency within the joints is lower.

There are also two thickness variations, namely 24 cm and 30 cm. The results of the FEA analysis are presented in these following figures:

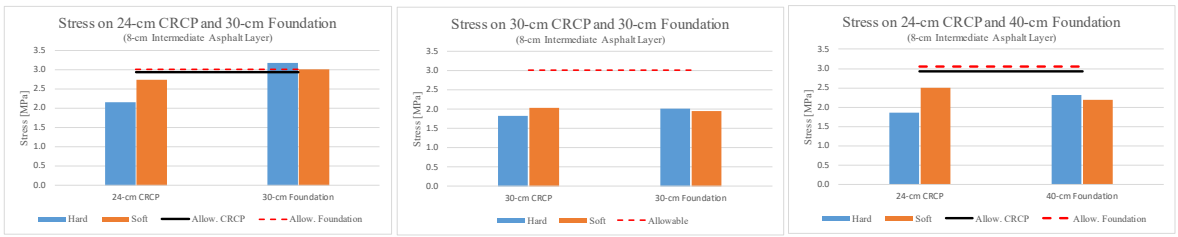

Figure 122. Impact of bonding condition to the stress level of CRCP

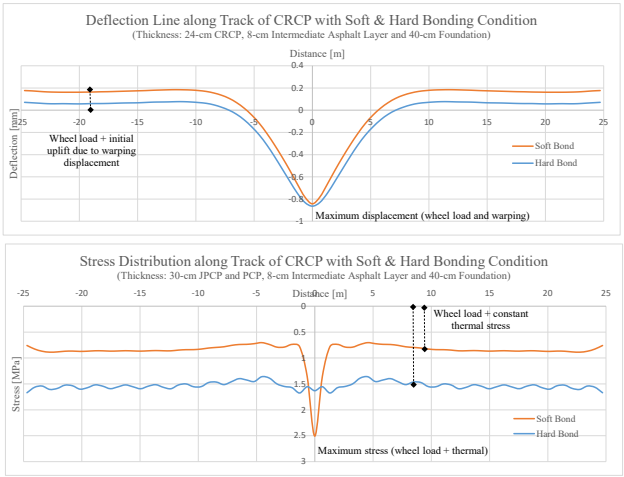

Figure 123. Comparison of deflection line and stress distribution along the track between hard and soft bonding condition of CRCP

Hard bonding interface gives a positive effect to the CRCP slab, in which the level of stress is decreased in comparison to the one with soft bonding condition. However, there is a negative impact to the foundation slab that the magnitude of stress on foundation slab is higher when hard bond interface exists. An almost balance condition of stress levels is found when the CRCP and foundation slabs have the same thickness of 30 cm. In this variation, the influence of bonding condition is relatively small. The stress levels of both slabs are safer under the permissible one when both slabs thickness are 30 cm or 24-cm CRCP and 40-cm foundation slab are constructed. Hence, hard bond gives more advantages to a thin CRCP resting on piled-raft foundation in terms of reduction of stress of CRCP. Yet, this combination should be followed by the use a thicker foundation slab.

Of a JPCP system, the impact of slab length (joint spacing) and slab thickness variations on the levels of stress on JPCP and foundation as well as their permissible stresses are shown in these following figures:

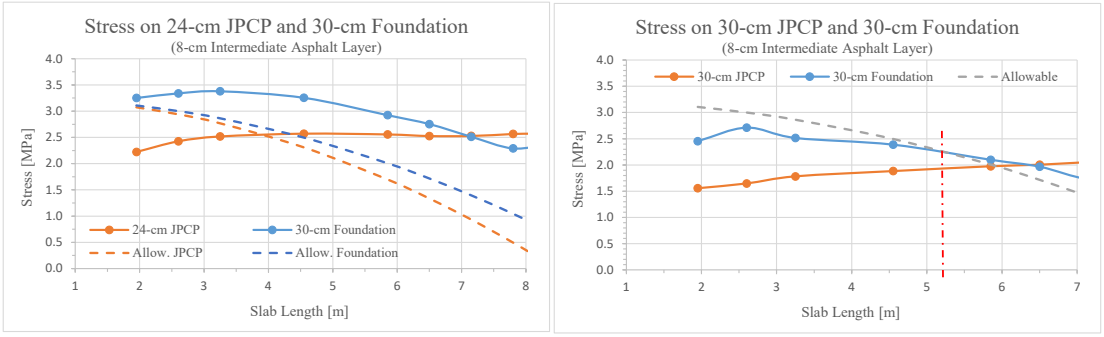

Figure 124. Impact of JPCP slab length variations to the levels of stress on 24-cm and 30-cm JPCP as well as 30-cm foundation slab considering thermal impact and soft bond

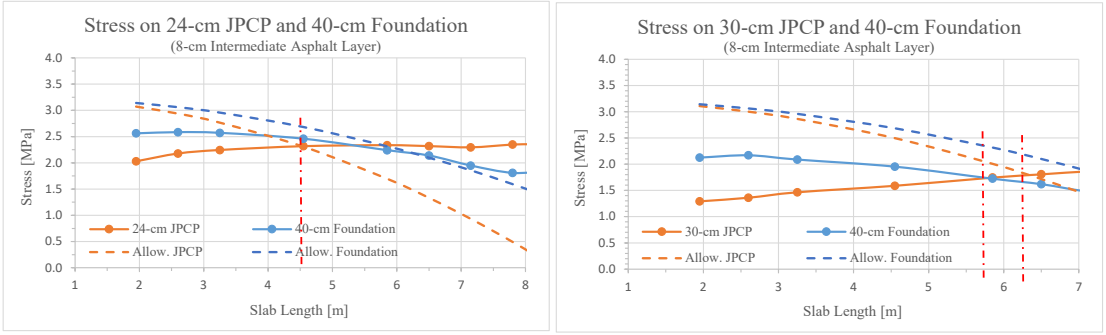

Figure 125. Impact of JPCP slab length variations to the levels of stress on 24-cm and 30-cm JPCP as well as 40-cm foundation slab considering thermal impact and soft bond

If JPCP is constructed as an alternative to CRCP, similar performance of JPCP in comparison to CRCP is demonstrated when the thickness of JPCP is increased to 30 cm. Thin JPCP slab of 24 cm resting on 30-cm foundation slab does not fulfill the permissible levels of stress of both slabs. Thin JPCP slab can meet the criteria of stress limitations when the thickness of

foundation slab is increased to 40 cm and followed by 4.55 m of joint spacing. Efficient combination is found when both slabs have thickness of 30 cm and JPCP has joint spacing of 4.55 m. This gives more secure state to JPCP, in which its stress level is far below the allowable one. Meanwhile, although foundation slab stress level is close to the permissible one, the foundation slab is already reinforced to avoid excessive crack formation.

Figure 126 presents the other alternative of constructing JPCP without dowel bars resting on piled-raft foundation slab.

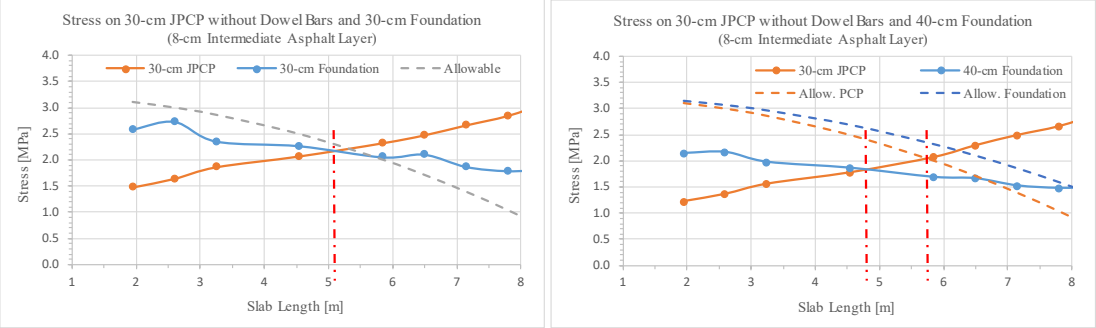

Figure 126. Impact of JPCP slab length variations to the levels of stress on 30-cm JPCP without dowel bars as well as 30-cm and 40-cm foundation slab considering thermal impact and soft bond

A balance of stress levels far below the allowable ones is exhibited from the 30-cm JPCP without dowel bars resting on 40-cm foundation slab and JPCP slab length of 4.55 m.

JPCP without dowel bars has almost similar level of displacement to JPCP with dowel bars as depicted in the Figure 127. Meanwhile, a different static behaviour of JPCP with and without dowel bars is shown from the stress distribution along the track.

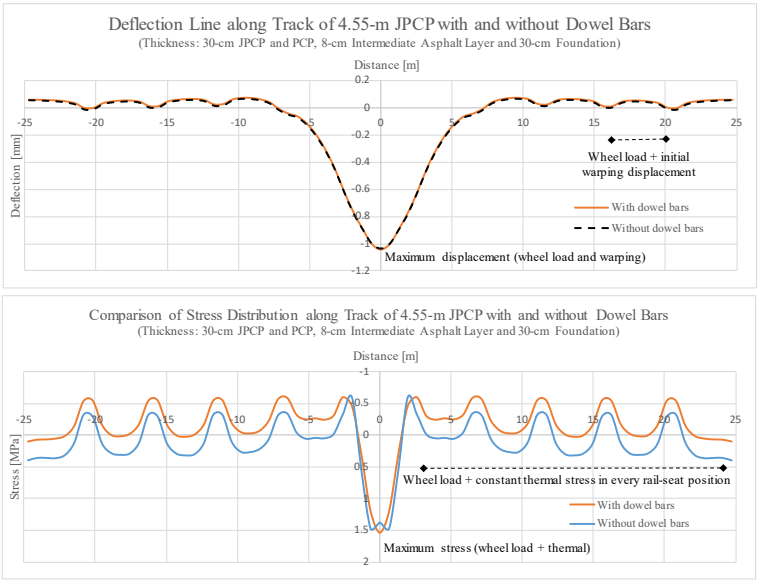

Figure 127. Comparison of deflection line and stress distribution along the track between 4.55 m - JPCP with and without dowel bars

One of the unbeneficial impact is that the constant stress induced by thermal change in a JPCP without dowel bars is higher than that in JPCP with dowel bars. However, if this constant stress level is maintained far below the permissible one, namely by selecting proper thickness and length, JPCP without dowel bars can deliver performance as good as JPCP with dowel bars. It is shown that to mitigate the impact of thermal stress, the slab length of 4.55 m can be selected for implementation of JPCP without dowel bars.

The use of thick ballast as intermediate layer with sufficient thickness also demonstrates similar performance to the use of thin asphalt layer shown before. Ballast layer can be also an option to be constructed as intermediate layer and to provide soft bonding condition between JPCP and foundation slab. According to *Deutsche Bahn* a ballast layer resting on concrete slab should have minimum thickness of 45 cm. JPCP without dowel bars and with low joint efficiency constructed on ballast stones as intermediate layer is not suggested. The reason is that it provides a very small lateral resistance to the rails against lateral buckling, since the absence of rigid joints in between two slabs. The results of using ballast layer as intermediate layer for a track constructed with JPCP with dowel bars is shown in this following figure:

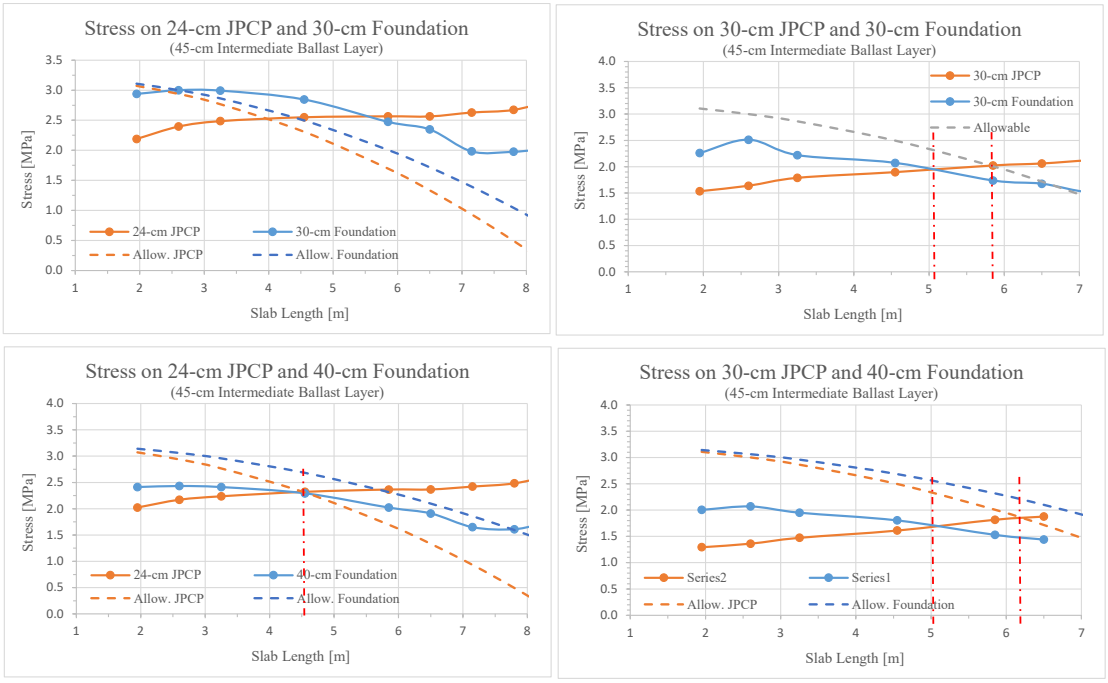

Figure 128. The use of ballast as intermediate layer and the impact of slab length variations to the levels of stress of JPCP with dowel bars as well of foundation slab

Therefore, as summary of the implementation of continuous and jointed slab for railway construction of soft soil:

- Conventional CRCP has better performance as a composite structure with stiff bounded base layers and together with hard bonding interface, such as with CTB or asphalt layers. However, the existence of hard bond will increase the stress level on the foundation slab. To overcome this problem, a thin CRCP can be combined with a thicker concrete base layer.
- Jointed concrete slabs are more advantageous when they are constructed with soft bonding interface.
- JRCP and JPCP can be an alternative of superstructure construction on soft soil regarding the future maintenance efforts of replacing local slab when unpredicted settlements take a place.
- CRCP of 24 cm can be replaced by 30 cm JPCP with joint spacing of 4.55 m. A thin JPCP can be still constructed but should be followed by thicker foundation slab.
- JPCP without dowel bars can be also an option. Curb or locking system should be provided to have sufficient lateral resistance and to avoid change in geometry of slab track as well as track buckling. JPCP without dowel bars and with low joint efficiency resting on ballast is not recommended due to absence of adequate level of lateral resistance.

9. Case Study

9.1. Location and Field Test Data

Some samples of field test data of Standard Penetration Test (SPT) and Cone Penetration Test (CPT- Dutch method, commonly called as "Sondir Test" in Indonesia) are collected from *CV. Geo Inti Perkasa Geotest Consulting, Banjarbaru* and *Soil Mechanics Laboratory of Civil Engineering Department, Faculty of Engineering, Lambung Mangkurat University Banjarmasin, South Kalimantan, Indonesia*. The locations were near to the watershed of Barito River in Central Kalimantan. Three examples are taken for the case study, namely:

9.1.1. Data of Example Case I

Project Package: Bridge of Coal Hauling Road, Coal Washing Plant and River Port Paring Lahung.

Location: Kecamatan (Sub District) Pujon, Kabupaten (District) of Kapuas, Province of Central Kalimantan, Indonesia.

One of example data for this project was taken for the project of building coal washing plant and river port. The data was obtained from SPT, CPT and undisturbed soil (UDS) tests. The UDS sample test results are showed in the Table 27. The results of SPT test is described in the Figure 129 and CPT is presented in the Table 28 and Figure 130.

Table 27. Laboratory test data of soil properties from drilling cores of Example Case I

Sample No	Depth	*Gs*	W_n	γ_m	*WL*	*WP*	*PI*	S_r	*e*	% Finer #200	q_u	S_t	*C*	ϕ
	[m]	[-]	[%]	[g/cm^3]	[%]	[%]	[%]	[%]	[-]	[%]	[kg/cm^2]	[-]	[kg/cm^2]	[°]
B.I.1	1.5 - 2.0	2.61	21.97	1.80	41.50	27.06	14.44	74.61	0.77	93.04	0.723	1.18	0.15	17
B.I.2	4.0 - 4.5	2.62	20.35	1.89	39.00	26.09	12.91	79.77	0.67	79.96	0.735	2.16	0.28	15

Note: G_s is unit density based on specific gravity and not shear modulus of soil

The top soil layer contains organics silt and silty clay soils, which has a total depth about 2 m. This subsoil surface is considered soft. The SPT and UDS test were first conducted in the depth of 2 m. The N-SPT value of 5 as well as q_u of 0.723 kg/cm^2 or around 70 kPa were obtained at this depth. From the depth of 2 - 4 m, soil is formatted by clays mixed with fine grained sands. At the depth around 4 m, second UDS sample was also taken and the soil at this depth has slightly greater q_u of 0.735 kg/cm^2 or around 72 kPa. Below this layer up to the depth around 8 m the soils are formatted by clay stones and have higher bearing capacity from moderate stiff to stiff. From the depth of 8 m and deeper, the soil layers have greater N-SPT values about 50 and these layers can be categorized as stiff to very stiff layers.

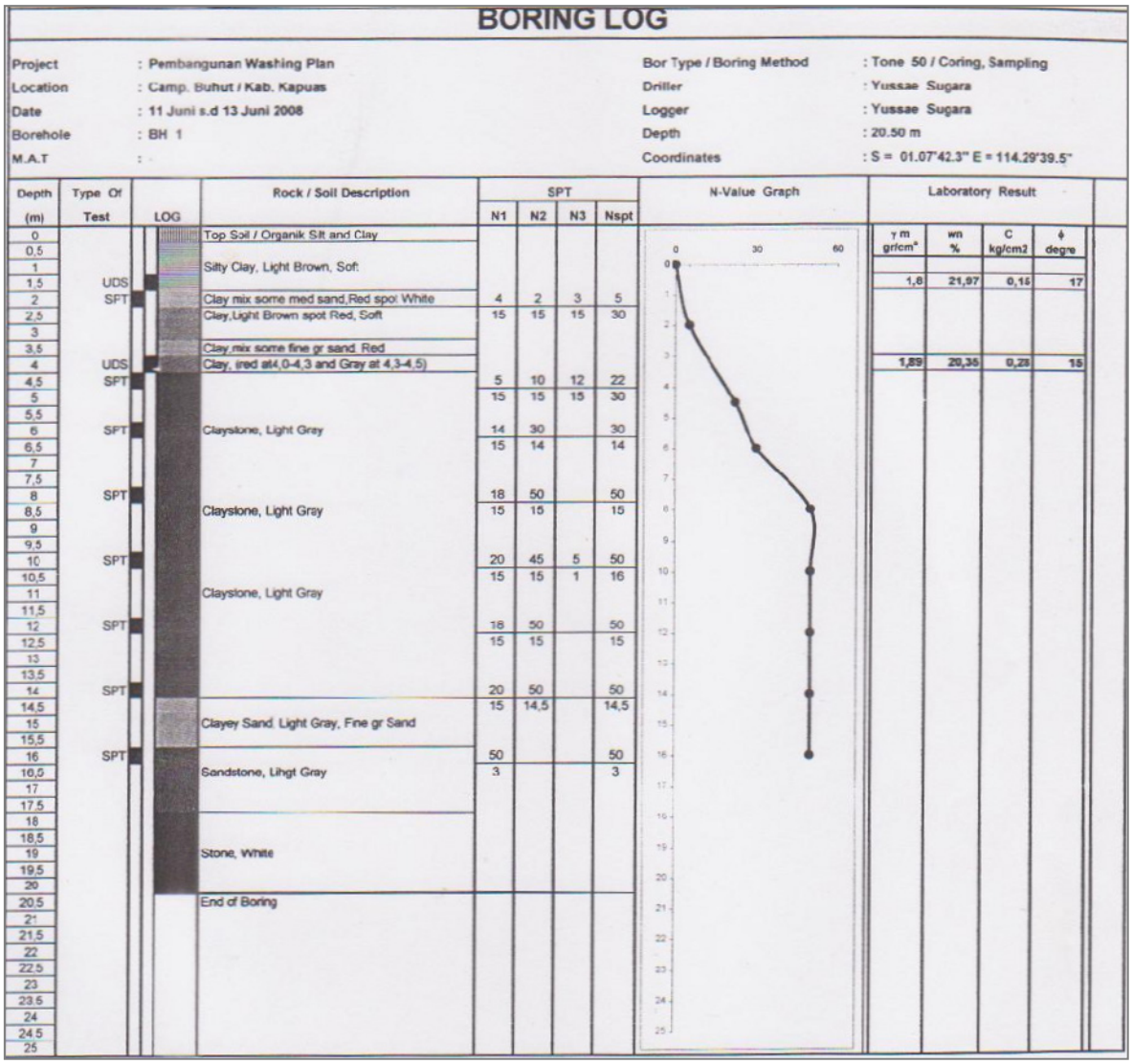

BORING LOG

Project	: Pembangunan Washing Plan	Bor Type / Boring Method	: Tone 50 / Coring, Sampling
Location	: Camp. Buhut / Kab. Kapuas	Driller	: Yussae Sugara
Date	: 11 Juni s.d 13 Juni 2008	Logger	: Yussae Sugara
Borehole	: BH 1	Depth	: 20.50 m
M.A.T	:	Coordinates	: S = 01.07'42.3" E = 114.29'39.5"

Depth (m)	Type Of Test	Rock / Soil Description	SPT N1	SPT N2	SPT N3	SPT Nspt
0		Top Soil / Organik Silt and Clay				
0,5		Silty Clay, Light Brown, Sof:				
1						
1,5	UDS					
2	SPT	Clay mix some med sand,Red spot White	4	2	3	5
2,5		Clay,Light Brown spot Red, Soft	15	15	15	30
3						
3,5		Clay,mix some fine gr sand, Red				
4	UDS	Clay, ired at4,0-4,3 and Gray at 4,3-4,5)				
4,5	SPT		5	10	12	22
5			15	15	15	30
5,5						
6	SPT	Claystone, Light Gray	14	30		30
6,5			15	14		14
7						
7,5						
8	SPT		18	50		50
8,5		Claystone, Light Gray	15	15		15
9						
9,5						
10	SPT		20	45	5	50
10,5			15	15	1	16
11		Claystone, Light Gray				
11,5						
12	SPT		18	50		50
12,5			15	15		15
13						
13,5						
14	SPT		20	50		50
14,5			15	14,5		14,5
15		Clayey Sand, Light Gray, Fine gr Sand				
15,5						
16	SPT		50			50
16,5		Sandstone, Lihgt Gray	3			3
17						
17,5						
18						
18,5						
19		Stone, White				
19,5						
20						
20,5		End of Boring				
21						
21,5						
22						
22,5						
23						
23,5						
24						
24,5						
25						

N-Value Graph: 0 | 30 | 60

Laboratory Result	γ m gr/cm³	wn %	C kg/cm2	ϕ degre
	1,8	21,97	0,16	17
	1,89	20,36	0,28	15

Figure 129. SPT data of Example Case I

Roughly seeing from the SPT data, it looks that in this condition, the implementation of *Cakar Ayam* with longer pile and considering the shaft resistance of the piles can be an option of solution for this case. However, the depth of the rigid layer is only around 8 m, in which application of end-bearing pile by using longer pile until the rigid base and with smaller diameter seems more appropriate. Therefore, the options of solution using floating pile of *Cakar Ayam* as well as end-bearing conventional pile will be evaluated for this example case.

Table 28. CPT test data of Example Case I

Project : Pembangunan Washing Plan
Date : 14 Juni 2008

Point No : S. A
Location : Camp Buhut Kab. Kapuas
: Kalimantan Tengah
Tested by : Team

Coordinates : S = 01.07'42.9"
: E = 114.29' 37,8"

Depth m	C kg/cm²	C + F kg/cm²	F kg/cm	F.Total kg/cm	*F* kg/cm²	Fr %	Depth m	C kg/cm²	C + F kg/cm²	F kg/cm	F.Total kg/cm	*F* kg/cm²	Fr %
0,00	0,00	0,00	0,00	0,00	0,00	0,00	7,20						
0,20	3,00	5,00	4,00	4,00	0,18	6,09	7,40						
0,40	3,00	5,00	4,00	8,00	0,18	6,09	7,60						
0,60	5,00	10,00	10,00	18,00	0,46	9,14	7,80						
0,80	10,00	20,00	20,00	38,00	0,91	9,14	8,00						
1,00	15,00	25,00	20,00	58,00	0,91	6,09	8,20						
1,20	35,00	40,00	10,00	68,00	0,46	1,31	8,40						
1,40	35,00	50,00	30,00	98,00	1,37	3,92	8,60						
1,60	55,00	65,00	20,00	118,00	0,91	1,66	8,80						
1,80	50,00	65,00	30,00	148,00	1,37	2,74	9,00						
2,00	60,00	80,00	40,00	188,00	1,83	3,05	9,20						
2,20	65,00	75,00	20,00	208,00	0,91	1,41	9,40						
2,40	65,00	80,00	30,00	238,00	1,37	2,11	9,60						
2,60	55,00	75,00	40,00	278,00	1,83	3,32	9,80						
2,80	45,00	65,00	40,00	318,00	1,83	4,06	10,00						
3,00	30,00	40,00	20,00	338,00	0,91	3,05	10,20						
3,20	50,00	65,00	30,00	368,00	1,37	2,74	10,40						
3,40	50,00	60,00	20,00	388,00	0,91	1,83	10,60						
3,60	100,00	115,00	30,00	418,00	1,37	1,37	10,80						
3,80	125,00	150,00	50,00	468,00	2,28	1,83	11,00						
4,00	115,00	150,00	70,00	538,00	3,20	2,78	11,20						
4,20	40,00	50,00	20,00	558,00	0,91	2,28	11,40						
4,40	90,00	105,00	30,00	588,00	1,37	1,52	11,60						
4,60	105,00	115,00	20,00	608,00	0,91	0,87	11,80						
4,80	55,00	65,00	20,00	628,00	0,91	1,66	12,00						
5,00	50,00	60,00	20,00	648,00	0,91	1,83	12,20						
5,20	135,00	160,00	50,00	698,00	2,28	1,69	12,40						
5,40	145,00	175,00	60,00	758,00	2,74	1,89	12,60						
5,60	110,00	140,00	60,00	818,00	2,74	2,49	12,80						
5,80	135,00	155,00	40,00	858,00	1,83	1,35	13,00						
6,00	125,00	140,00	30,00	888,00	1,37	1,10	13,20						
6,20	115,00	135,00	40,00	928,00	1,83	1,59	13,40						
6,40	145,00	175,00	60,00	988,00	2,74	1,89	13,60						
6,60	100,00	125,00	50,00	1038,00	2,28	2,28	13,80						
6,80	>200						14,00						
7,00							14,20						

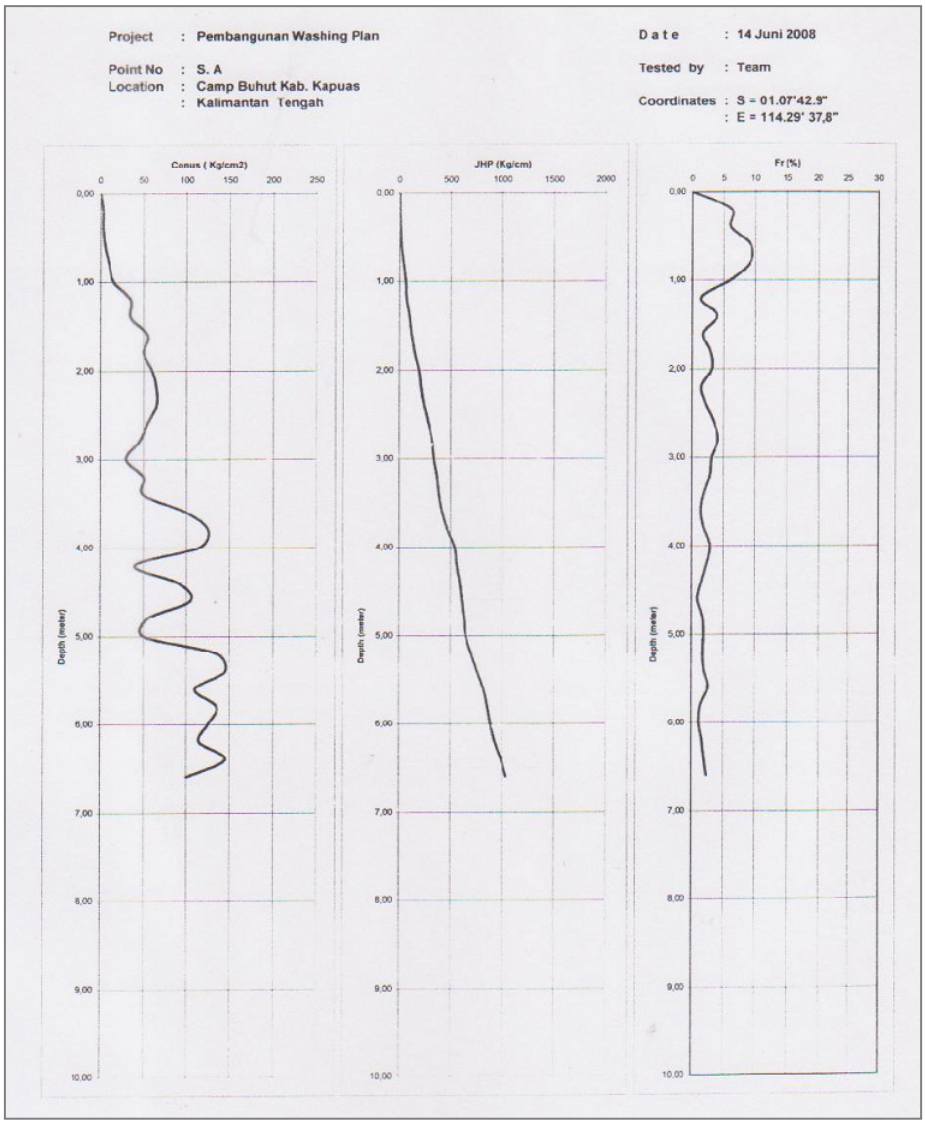

Figure 130. CPT profile data of Example Case I

9.1.2. Data of Example Case II

Project Package: Conveyor Belt and River Port Muara Lahung for transporting coals. Kab. Murung Raya, Central Kalimantan.

Location: Kecamatan (Sub District) Pujon, Paring Lahung and Teluk Timbau, Kabupaten (District) of Kapuas, Province of Central Kalimantan, Indonesia.

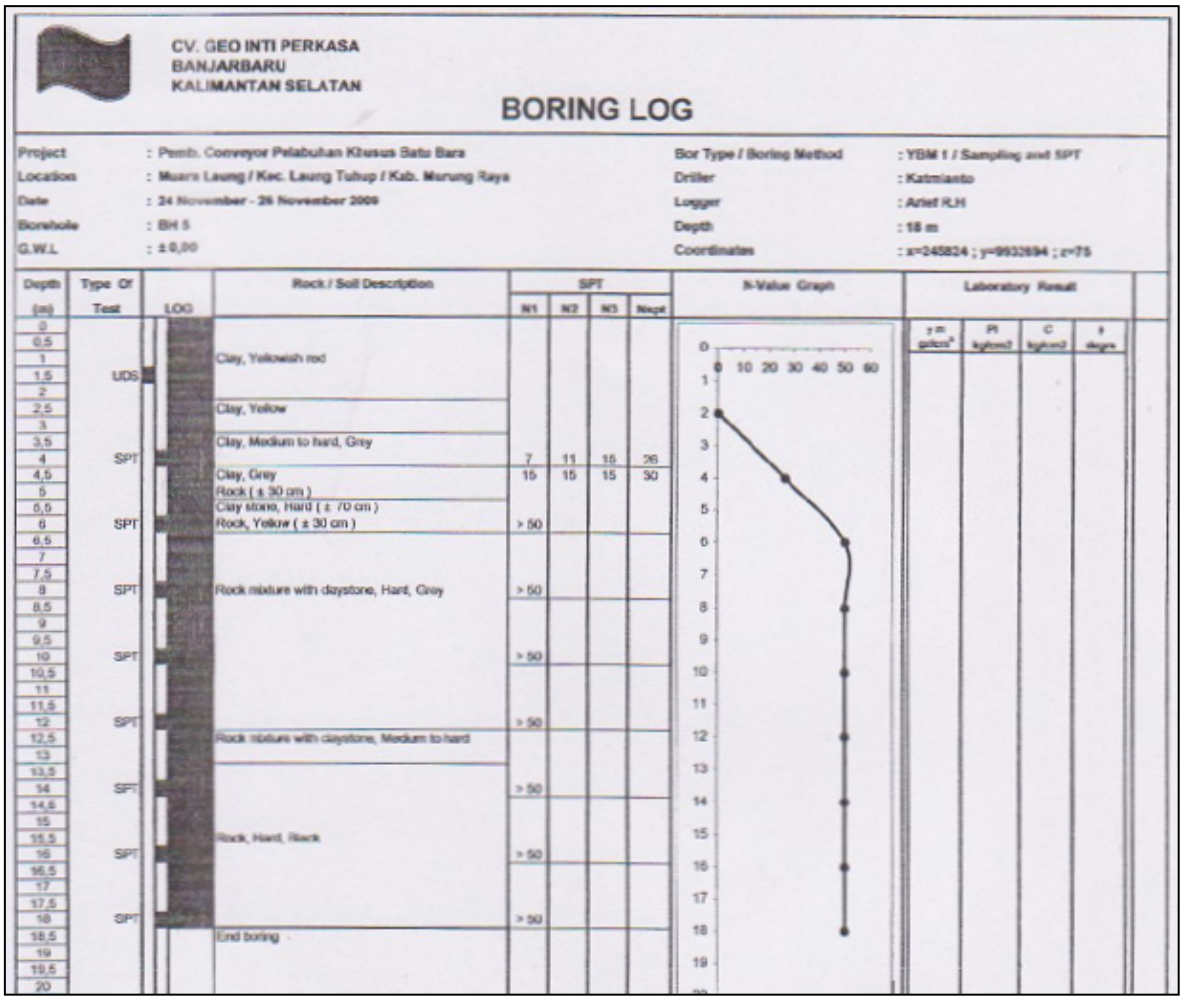

Figure 131. SPT Data-1 of Example Case II

From Figure 131, SPT Data-1 describes that the top surface layer of the soils is formatted by soft clays. It is also shown that until the depth of 2 m, the soil surface layer is extremely soft with almost no bearing capacity. This area is close to the river and a swamp area. It is frequently found in Kalimantan that swamp areas with a high-water table level have very low bearing capacity. A moderate stiff soil is found in the second SPT test at the depth of 4 m. Firm soil layer is found from the depth of 6 m and below.

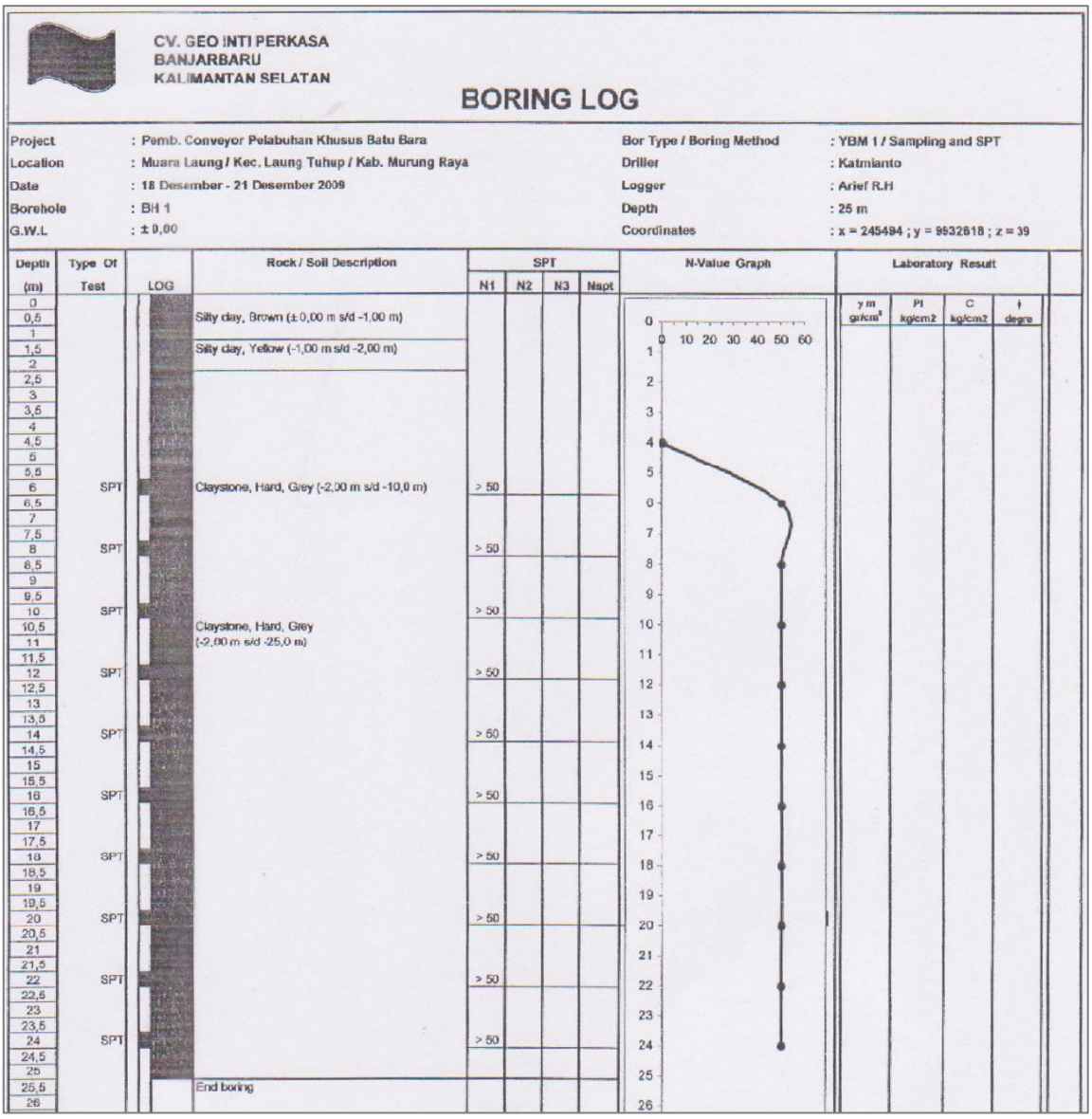

Figure 132. SPT Data-2 of Example Case II

In the Figure 132, the depth of very soft soil is up to 4 m and the firm soil layer is found in the depth of 6 m. Observing those two example of SPT tests, end-bearing pile foundation is more appropriate for this case. Removing the top subsoil layer is also not an economically effective solution due to consideration of the depth of this layer. When an end-bearing pile with foundation plate system is constructed, then the soils beneath the foundation plate do not contribute a bearing capacity. Hence, end-bearing piles are the fundamental foundation element, which provide the bearing capacity to the overlaying track structure. Floating pile foundation is not sufficient to give bearing capacity to the track structure, due to the soil layer profile as well as the absence of the bearing capacity delivered from the soils below the raft foundation plate.

What is more, in this case, the foundation plate is then supported by discrete points of piles. Thus, the analysis is close to with a quasi-bridge structure, where the pile spacing is the location of the points of support. In this case the conventional and analytical methods of trackbed to define the thickness of the multilayer track structure are not applicable.

9.1.3. Data of Example Case III

Project Package: Planning of Betanjung River Port in Central Kalimantan.

Location: Desa Betanjung, Kabupaten (District) of Kapuas, Province of Central Kalimantan, Indonesia.

The SPT data logs are presented in the Figure 133. From this soil test data, it can be seen that the soft soil layers are extremely deep until 50 m. This extreme condition is not something strange and can be often found in Kalimantan. If a railway track should be forcedly constructed in this area, a very deep end-bearing pile foundation should be constructed with very careful consideration in the design.

The soil bearing capacity, which is described from the compressive strength data shows a very soft soil formatted by clays. From the UDS test the soil's compressive strength is 0.191 kg/cm^2 (18.73 kPa) at depth of 5 m and 0.21 kg/cm^2 (20.59 kPa) at the depth of 15 m, which has very low bearing capacity for construction of railway track. In the depth of 35 m, drilled UDS sample shows the level of soil's compressive strength of 0.62 kg/cm^2 (60.8 kPa), which still indicates soft soil layer. Roughly can be approximated that the fundamental carrying capacity of piles will be delivered from the pile tip. Significant shaft friction resistances are given only within around half of the pile length (after the depth of 30 m). It reveals that a construction of railway track in this area is not economically and almost practically not feasible.

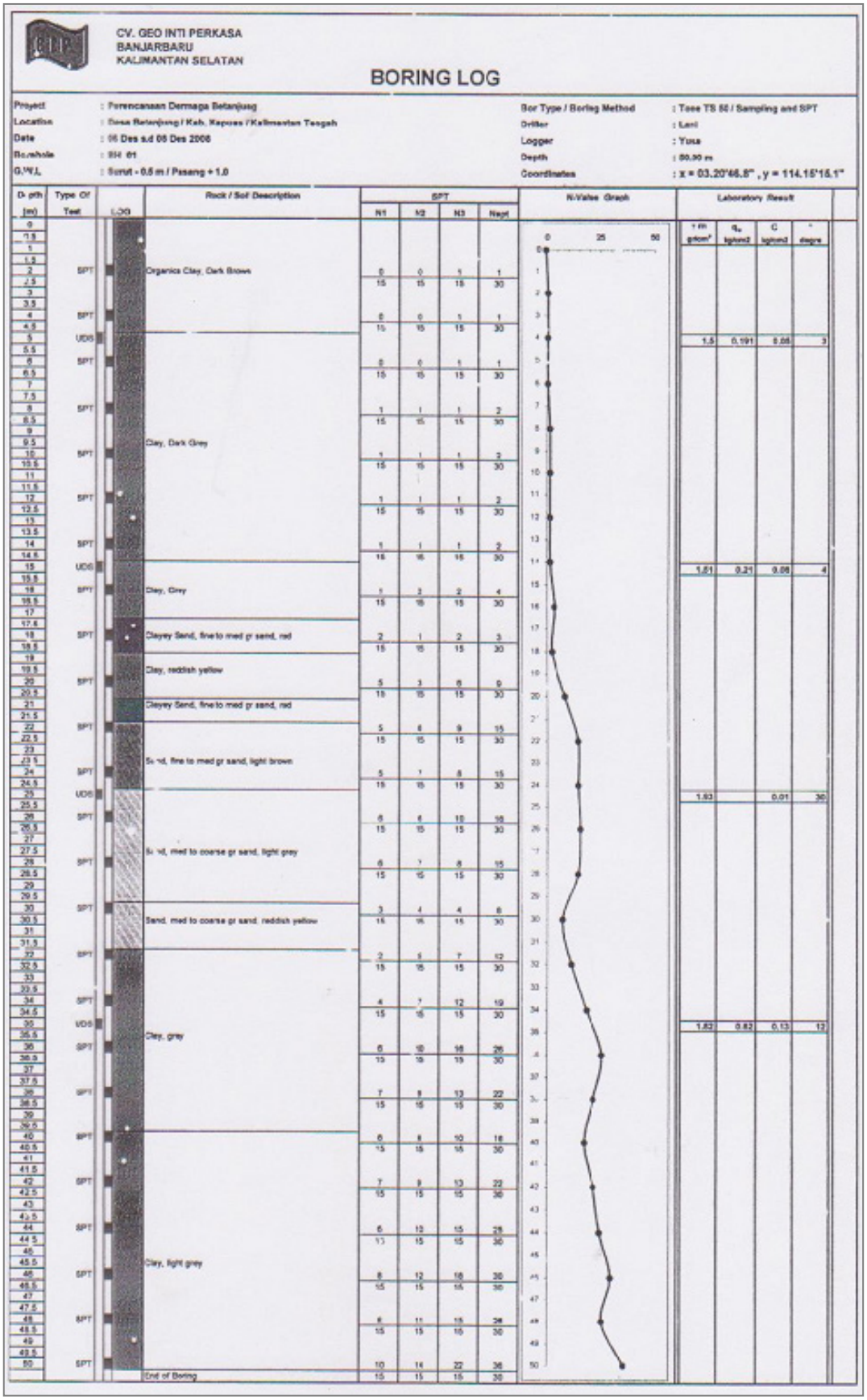

CV. GEO INTI PERKASA
BANJARBARU
KALIMANTAN SELATAN

BORING LOG

Project : Perencanaan Dermaga Betanjung
Location : Desa Betanjung / Kab. Kapuas / Kalimantan Tengah
Date : 05 Des s.d 05 Des 2006
Borehole : BH 01
G.W.L : Surut - 0.5 m / Pasang + 1.0

Bor Type / Boring Method : Tone TS 50 / Sampling and SPT
Driller : Lani
Logger : Yusa
Depth : 50.00 m
Coordinates : x = 03.20'46.8" , y = 114.15'15.1"

Depth (m)	Type Of Test	LOG	Rock / Soil Description	SPT N1	SPT N2	SPT N3	SPT Nspt	N-Value Graph	Laboratory Result: γ dry gr/cm³	Laboratory Result: q_u kg/cm2	Laboratory Result: C kg/cm2	Laboratory Result: φ degre
0								0 25 50				
1			Organics Clay, Dark Brown	0	0	1	1					
2	SPT			15	15	15	30					
3				0	0	1	1					
4	SPT			15	15	15	30					
5	UDS		Clay, Dark Grey						1.5	0.191	0.08	3
6	SPT			0	0	1	1					
7				15	15	15	30					
8	SPT			1	1	1	2					
9				15	15	15	30					
10	SPT			1	1	1	2					
11				15	15	15	30					
12	SPT			1	1	1	2					
13				15	15	15	30					
14	SPT			1	1	1	2					
15	UDS		Clay, Grey						1.61	0.31	0.08	4
16	SPT			1	3	2	4					
17				15	15	15	30					
18	SPT		Clayey Sand, fine to med gr sand, red	2	1	2	3					
19				15	15	15	30					
20	SPT		Clay, reddish yellow	5	3	6	9					
21				15	15	15	30					
22	SPT		Clayey Sand, fine to med gr sand, red	5	6	9	15					
23				15	15	15	30					
24	SPT		Sand, red, fine to med gr sand, light brown	5	7	8	15					
25	UDS			15	15	15	30		1.83		0.01	30
26	SPT			6	6	10	16					
27				15	15	15	30					
28	SPT		Sand, red, med to coarse gr sand, light grey	6	7	8	15					
29				15	15	15	30					
30	SPT		Sand, med to coarse gr sand, reddish yellow	3	4	4	8					
31				15	15	15	30					
32	SPT		Clay, grey	2	5	7	12					
33				15	15	15	30					
34	SPT			4	7	12	19					
35	UDS			15	15	15	30		1.82	0.82	0.13	13
36	SPT			6	10	16	26					
37				15	15	15	30					
38	SPT			7	9	13	22					
39				15	15	15	30					
40	SPT		Clay, light grey	6	8	10	18					
41				15	15	15	30					
42	SPT			7	9	13	22					
43				15	15	15	30					
44	SPT			6	13	15	28					
45				15	15	15	30					
46	SPT			8	12	18	30					
47				15	15	15	30					
48	SPT			6	11	15	26					
49				15	15	15	30					
50	SPT		End of Boring	10	14	22	36					
				15	15	15	30					

Figure 133. SPT Data of Example Case III

From the sample data shown before, the data of Example Case I is selected as example design case to be analyzed and evaluated further for a potential of building railway track on soft soil.

9.2. Design of Railway Track for the Example Case I

9.2.1. Trackbed Design and Pile Foundation Design of Example Case I

Two options of track superstructure can be applied for this example case, namely slab track and ballasted track. The initial thickness design for these track types follow the proposed method of *Cakar Ayam* pile design. Since the method employs moment equilibrium and slab theory to estimate the minimum required length of a floating pile, then a slab track design calculation should be firstly done. Ballasted trackbed thickness design can be derived from the slab track design by using equivalent *Structural Number* (*SN*). Two types of pile foundation will be evaluated, namely using floating foundation of *Cakar Ayam* pipe piles and using end-bearing using conventional piles.

The design procedure and calculation based on the soil sample data is explained as follows:

(1) ***Soil design parameters***:

(a) From the soil description of SPT boring log, the soil can be classified as MH type (organic elastic silts and clays).

(b) Soil's design parameters obtained from UDS test with sample No B.I.1 at the depth of 2 m below the subsoil surfaces (see Table 27):

- Static compressive strength q_u = 0.723 kg/cm^2 = 70.90 kPa
- Undrained shear strength S_u or C_u= 0.15 kg/cm^2 = 14.71 kPa
- Angle of internal friction: ϕ = 17°
- Density γ_s =1.80 g/cm^3 = 17.66 kN/m^3

(c) The information about soil's bearing capacity at the subsoil surface is only available through CPT test data. A design of conventional shallow foundation without pile normally considers the depth up to *1.5B* of CPT data, where *B* is the width of the foundation. Due to the existence of floating piles, the considered depth to approximate bearing capacity of soil beneath the foundation slab is assumed only up to 40 cm. The average cone resistances within these depths is 3 kg/cm^2 (see Table 28). Ultimate bearing capacity of soil can be roughly estimated from the a very simple approximation suggested by Meyerhof (1965)[83] concerning a conservative design, assumption of maximum

settlement 25 mm and without taking into account foundation width factor, then $q_u = q_c/20 = 3/20 = 0.15$ kg/cm^2 = 14.72 kPa.

(2) ***Defining soil plastic deformation limit criteria (floating pile design)***:

(a) Li & Selig's cyclic parameters of soil with MH type: $a = 0.84$, $b = 0.13$ and $m = 2.0$. Value of Poisson's ratio is assumed $\mu_s = 0.33$.

(b) Estimation of modulus of elasticity of soil using approach from Bowless (1996)[12], then $E_s = 600S_u = 600(14.71) = 8.83$ MPa.

(c) Estimation of modulus of subgrade reaction using AASHTO (1993)[1] formula Eq. 31, then $k = 2.029x10^{-3}M_r = 2.029\text{x}10^{-3}(8.83) = 0.018$ N/mm^3.

(d) Criteria of maximum plastic deformation of soil under foundation slab is limited up to 25 mm (equal to the assumption of Meyerhof (1965)[83] approach taken in the step 1(c) above). Number of load cycles within the design period is selected $N = 2\text{x}10^6$ and the depth until rigid base H from soil profile of SPT test is 8 m. Then the allowable soil's dynamic compressive strength q_u' or allowable deviator stress σ_d:

$$q_u' = \sigma_d = \sigma_s \sqrt[m]{\frac{100.\rho}{a.N^b.H}} = (14.72)\sqrt{\frac{100(25)}{0.84(2x10^6)^{0.13}(8000)}} \approx 3.5 \text{ kPa}$$

(3) ***Computation of structural number (floating pile design)***:

(a) Using plastic deformation criteria based on Li & Selig's method $\sigma_d/E_s = 3.5/8.83 \approx 0.4$

(b) Using additional chart specialized for trackbed supported with piled foundation (see Figure 149 in the Appendix 5), with $\sigma_d/E_s = 0.4$ and $E_s = 8.83$ MPa then $SN_{reff} \approx 109$ cm.

(c) Design of trackbed using 60E2 rails and 22.5 kN/mm elastic-pads ($f_{Lr} = 1$), considering dynamic amplification factor $f_d = 1.6$ and a straight line ($f_{c,d} = 1$) requires $DF = 1.6$. $SF_{tb} = 1.5$ is taken into account, then $SN_{des} = SF_{tb} * DF * SN_{reff} = 1.5(1.6)(109) \approx$ **262 cm**.

(d) Foundation plate of *Cakar Ayam* is built using reinforced concrete C40/50, then its coefficient of relative strength $a_f = 3.34$

(e) Thickness of foundation plate $h_f = 30$ cm, then the actual structural number of trackbed $SN_{tb} = SN_{des} - a_f.h_f = 262 - 3.34(30) \approx 162$ cm.

(4) ***Trackbed thickness design (floating pile)***:

(a) Slab track type is constructed using conventional CRCP and JRCP and underneath of the slabs are provided with asphalt and ballast layer respectively.

(b) Design of multilayer trackbed system including foundation slab:

Table 29. Trackbed thickness design of slab track for Example Case I (floating pile)

Layer	Example Case I.1 (Slab Track)				Example Case I.2 (Slab Track)			
	Material	***a***	***h* [cm]**	***SN***	**Material**	***a***	***h* [cm]**	***SN***
Soil	$E_s \approx 8.83$ *MPa,* $SN_{des} \approx 262$ *cm*				$E_s \approx 8.83$ *MPa,* $SN_{des} \approx 262$ *cm*			
Top Course	CRCP, E = 36 GPa	3.34	**24**	80.16	JRCP, E = 36 GPa	3.34	**30**	100.2
Base Course	Asphalt concrete, E = 5 GPa	1.76	**18**	31.68	Crushed stones, E = 300 Mpa, provided with sub ballast mat	0.69	**90**	62.1
Foundation	Reinf. C40/50, E = 36 GPa	3.34	**45**	150.3	Reinf. C40/50, E = 36 GPa	3.34	**30**	100.2
	Total Thickness/*SN*		**87**	**262.14**	**Total Thickness/*SN***		**150**	**262.5**

For this example case, (1) asphalt concrete is selected as base layer when CRCP is constructed as top layer and the pile foundation is designed as end-bearing pile and (2) ballast base layer is chosen when JRCP is built as top layer and floating pile using *Cakar Ayam* is used. This considers economical aspect of the costs of the construction, width of foundation, possible track rehabilitations and maintenances within the service period, optimization which has been discussed in the subchapter 8 as well as safety design aspect.

The other reasons of selection combination (1) are:

- end-bearing pile has considerably better performance than floating pile, thus it has lower risk of having unpredicted level of cumulative settlements during the service period. CRCP has better performance when it is built as composite structure with bounded asphalt layer and hard bonding interface. Due to the fact that this combination is constructed permanently and more rigid, it is expected that it will deliver a less (or even relatively no) major maintenances.
- this combination is considered more expensive, therefore, it should be compensated with higher level of safety of carrying capacity of the end-bearing piles. Hence, future maintenance costs can be reduced.
- asphalt layer contributes hard bonding condition between two concrete layer and delivers better thermal distribution of continuously reinforced slab as well as provides frost and drainage protection to the foundation slab.

And the arguments for second configuration (2) are:

- improvement of performance of a floating pile can be done by widening the foundation slab. But it has a consequence of higher construction costs. Thus

providing crushed stones as intermediate layer, which is relatively less expensive than asphalt or concrete base layer is able to compensate this.

- ballast layer also needs wider cross section regarding slope stability of its height and properties of unbound granular material. Then this in line with the improvement way of widening the slab of floating pile foundation.
- floating pile system has considerably higher risk of excessive settlements than end-bearing pile, therefore constructing ballast layer provides relatively more affordable future maintenance ways.

(5) ***Alternative design for the trackbed layer using ballasted track system (floating pile)***:

Using the same designed structural number for slab track design above, the trackbed thickness design of ballasted track can be also estimated as follows:

Table 30. Trackbed thickness design of ballasted track for Example Case I

Layer	**Example Case I.3 (Ballasted Track)**			
	Material	***a***	***h* [cm]**	***SN***
Soil	$E_s \approx 8.83$ *MPa,* $SN_{tb} \approx 162$ *cm,* $SN_{des} \approx 262$ *cm*			
Top Course	Ballast E = 250 MPa	0.65	**60**	39
Base Course	Crushed Stones E = 150 MPa	0.55	**100**	55
Subbase Course	Good quality embankment E = 80 MPa	0.45	**150**	67.5
Foundation	Reinf. C40/50, E = 36 GPa	3.34	**30**	100.2
	Total Thickness/*SN*		**340**	**261.7**

(6) ***Cross section design***:

Cross section should be defined first before estimating the required length of pile. This is done to estimate the required width of the slab foundation as well as the reasonable pile spacing and diameter pile according to the designed width.

It is shown from the Figure 134 that there are three options of the construction of railway track on soft soil for Example Case I. Based on the trackbed estimation, the Design I.3 of ballasted track system requires a high thickness of trackbed. Then it has to be followed with sufficient width of the base of trackbed layers to guarantee sufficient slope stability of the trackbed. This also has a consequence of higher mass contribution to the foundation slab. It will lead to higher displacement of the foundation slab and vibration as it has been evaluated in the subchapter 7.6.5. Then it should be followed with installation of end-bearing piles.

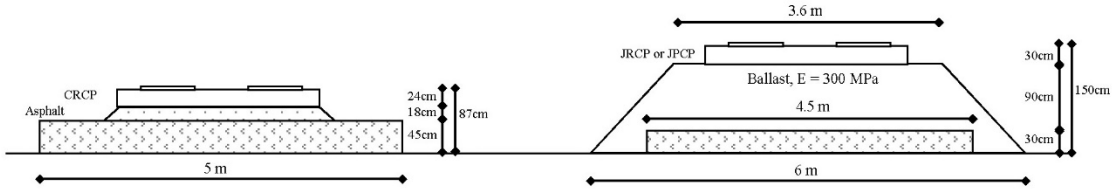

(a) Design I.1. Slab Track – Asphalt Base *(b) Design I.2. Slab Track – Ballast Base*

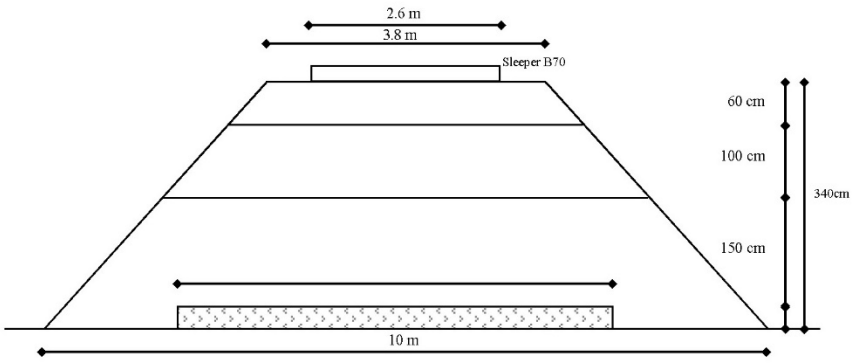

(c) Design I.3. Ballasted Track - High Embankment

Figure 134. Cross section design of trackbed layer of slab track and ballasted track for Example Case I

To obtain more efficient construction, the foundation slab can be embedded in the embankment layer. The reasons are that 1) the critical area of foundation to provide vertical bearing capacity to the overlaying layers does not need much wider area as the embankment needs it to avoid sliding and 2) the mass from the overlaying layers subjected to foundation slab can be reduced.

Indeed, a high level of thickness of embankment still demands slope stabilization against sliding. Therefore, installation of micro piles, anchors, retaining wall or steel sheet piles on the sides of slab foundation can be an option to stabilize the embankment. Another alternative is by constructing geogrid layer below the embankment.

(7) ***Selection of foundation width and pile type, diameter and spacing***

A single-track design, the designed widths of foundation slab based on the cross-section design on Figure 134 are:

(1) Design I.1, W_f = 5 m, number of end-bearing pile n_{trans} = 3, diameter d_p = 45 cm and the distance between piles centerlines a_p = 1.8 m.

(2) Design I.2, W_f = 4.5 m, floating pile n_{trans} = 2, d_p = 90 cm and a_p = 2.5 m (*Cakar Ayam*).

(3) Design I.3, W_f = 6 m, end-bearing pile n_{trans} = 3, d_p = 45 cm and a_p = 2 m.

(8) ***Computation of the critical length of floating pile based on equilibrium moment rotation***:

(a) Example of equivalent thickness of all trackbed layers and foundation slab of Design I.2 (floating pile):

Table 31. Equivalent thickness of trackbed for Example Case I

Layer	**Example Case I.2 (Slab Track)**				
	Material	***E* [Mpa]**	***μ***	***h* [cm]**	***H_{eq}* [cm]**
Top Course	JRCP, E = 36 GPa	36000	0.15	30	30
Base Course	Crushed stones, E = 300 Mpa	300	0.30	90	18.69
Foundation	Reinf. C40/50, E = 36 GPa	36000	0.15	30	30
	Total Thickness			150	**78.69**

(b) Rankine's soil passive resistance coefficient:

$$K_p = tan^2\left(45^0 + \frac{\emptyset}{2}\right) = tan^2\left(45^0 + \frac{17^0}{2}\right) = 1.83$$

(c) Example calculation of length of moment influence of Design I.2 (floating):

Using Vesic (1963)[141] approach of BOEF theory modified for slab application, k' is:

$$k' = 0.65\frac{E_s}{1-\mu^2}\sqrt[12]{\frac{12.E_s B^4}{E.h^3}} = (0.65)\frac{8.83}{1-(0.33)^2}\sqrt[12]{\frac{12(8.83)(4500)^4}{36000(786.9)^3}} = 12.35\ \text{N/mm}$$

$$L_{m,BOEF} = \frac{3}{2}\pi\sqrt[4]{\frac{4.E_{eq}.B.h_{eq}^{\ 3}}{12.k'}} = \frac{3}{2}\pi\sqrt[4]{\frac{4(36000)(4500)(786.9)^3}{12(12.35)}} = 32{,}015\ \text{mm} \approx 32.02\ \text{m}$$

Using Westergaard's approach of slab theory:

$$L_{m,slab} = 8.\sqrt[4]{\frac{E_{eq}.h_{eq}^{\ 3}}{12.k_s(1-\mu_c^{\ 2})}} = 8.\sqrt[4]{\frac{36000.(786.9)^3}{12(0.018)(1-0.15^2)}} = 24{,}152\ mm \approx 24.15m$$

BOEF theory is more decisive, L_m = 32.02 m is taken.

(d) Piles have the same spacing in longitudinal and transverse directions. The number of piles in the longitudinal direction along the L_m of Design I.2:

$$n_{long} = \frac{L_m}{a_p} = \frac{32.02}{2.5} = 12.81 \approx 13$$

(e) Minimum length of pile, with SF_{pile} = 1.5:

$$L_{p,min} = \sqrt[3]{\frac{1.5SF.q_u'.a_p.L_m^{\ 2}}{n.\gamma_s.K_p.d_p}} = \sqrt[3]{\frac{1.5(1.5)(3.5x10^{-3})(2500)(32020)^2}{13(17.66x10^{-6})(1.83)(900)}} = 3765\ mm \approx 3.8\ m$$

(9) Check the critical length of pile:

Based on lateral resistance using Matlock (1970)[81] method, for pile in clays, J = 0.5, then for Design I.2 of floating pile:

$$L_{crit} = \frac{6S_u D_p}{\gamma'_s D_p + JS_u} = \frac{6(14.71x10^{-3})(900)}{17.66x10^{-6}(900) + 0.5(14.71x10^{-3})} = 3417\ mm \approx 3.5\ m$$

and 2.6 m respectively for end-bearing pile of Design I.1 and I.3.

(10) ***Pile length selection and design***:

The design of pile length should be far more than its critical length. Pile length of 6 m ($1.6L_{Crit}$) can be actually taken for a floating pile design. However, looking from the soil layer profile obtained from SPT boring log, the depth until a firm layer with N-SPT of 50 blows is 8 m. To evaluate the three design variations, therefore, two options of pile design can be taken, namely:

(a) Floating pile: using *Cakar Ayam* pipe piles with diameter of 90 cm, pile spacing of 2.5 m and pile length of 6 m.

(b) End-bearing piles: using solid steel/concrete piles with diameter of 45 cm, pile spacing of 1.8 and 2 m ($a_p \geq 4D$ = 1.8 m) and pile length of 9 m.

The design variations and sketches are summarized in following Table 32, Table 33 and Figure 135.

Table 32. Pile length design variations for Example Case I

Variation	Diameter	Spacing	L_{min}	L_{crit}	L_{design}	Type
Design I.1	45 cm	1.8 m	3.8 m	2.6 m	9 m	End-Bearing
Design I.2	90 cm	2.5 m	3.8 m	3.5 m	6 m	Floating
Design I.3	45 cm	2.0 m	3.8 m	2.6 m	9 m	End-Bearing

Table 33. Summary of track elements for evaluations of Example Case I

Component	Type/Variation	Details	Dimensions/Properties
Rail	60E2	-	Follow the standard from manufacturer
Elastic-pad	K_{stat} = 22.5 kN/mm	Spacing: 60 cm (ballasted), 65 cm (slab track)	K_{dyn} = 27.2 kN/mm C_{dyn} = 213 kN.s/m
Sleeper (Ballasted)	B70	C40/50, Reinforced	E = 40 GPa
Embedded sleeper (Slab Track)	B.355.4 U65-20M	C40/50, Reinforced	E = 40 GPa
Top Layer (Slab Track)	- Conventional CRCP (I.1)	Hard bond with asphalt base layer	H = 24 cm, W = 2.8 m E = 36 GPa
		Cont. rebars	0.8%, ϕ = 20 mm
	- JRCP (I.2) or JPCP	Soft bond with unbound ballast base layer	H = 30 cm, W = 2.8 m E = 36 GPa
		Joint spacing	4.55 m
		Rebars	0.25% in trans. & long. direction (JRCP)
		Doweled bars	0.5%, ϕ = 20 mm, L = 30 cm (JRCP/JPCP)
Top Layer (Ballasted)	- Ballast (I.3)	Crushed stones	H = 60 cm, W = 3.8 - 4 m E = 250 MPa
Base/ Intermediate Layer	- Asphalt concrete (I.1)	-	H = 18 cm, W = 2.8 m E = 5 GPa
	- Ballast (I.2) with sub ballast mat	Crushed stones	H = 90 cm, W = 3.6 - 4 m E = 300 MPa
	- Ballast (I.3)	Crushed stones	H = 100 cm, W = 4 - 6 m E = 150 MPa
Sub Base	Embankment (I.3)	Good quality embankment	H = 150 cm, W = 6 - 12 m E = 80 MPa
Foundation	Concrete Slab	C40/50, Reinforced	H = 45 cm (I.1), 30 cm (I.2, I.3) W = 5 m (I.1), 4.5 m (I.2) and 6 m (I.3) E = 36 GPa, Rebars 0.25% in trans. & long. directions
Pile	- Floating (I.2)	Pipe concrete, reinforced	ϕ = 90 cm, thickness = 8 cm, L = 6 m, spacing = 2.5 m, E = 36 GPa
	- End-bearing (I.1, I.3)	Solid concrete pile, reinforced	ϕ = 45 cm, L = 9 m, spacing = 1.8 m (I.1) and 2 m (I.3) E = 36 GPa
Thermal impact	Heating	Only for slab track (I.1 and I.2)	ΔT = 16.8°C
FEA	Dynamic simulation	Running train test ICE-1	DAF = 1.6 Speed: 45 - 300 kph
Gaps			Pile-soil gaps & settlement beneath foundation slab

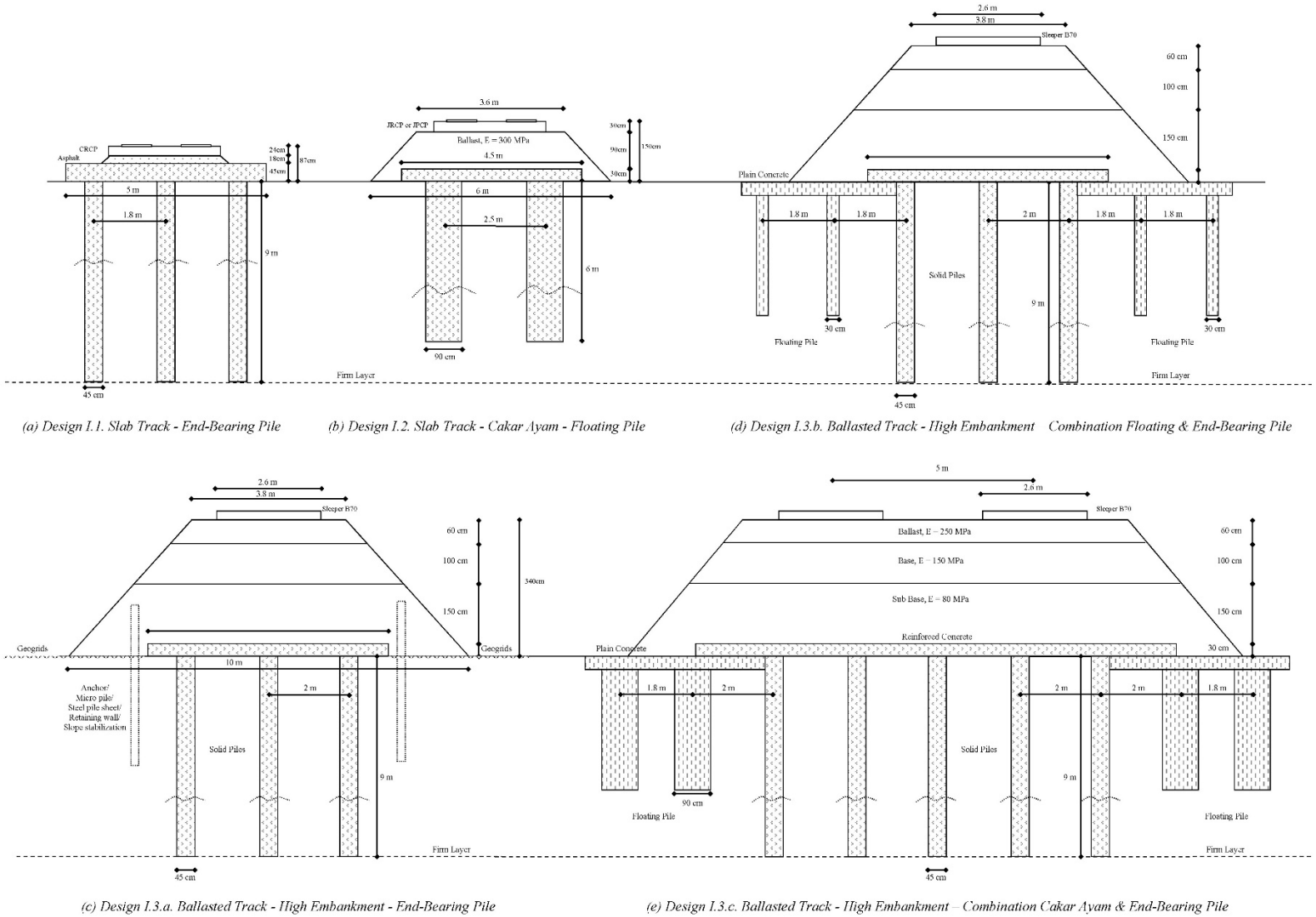

(a) Design I.1. Slab Track - End-Bearing Pile

(b) Design I.2. Slab Track - Cakar Ayam - Floating Pile

(d) Design I.3.b. Ballasted Track - High Embankment Combination Floating & End-Bearing Pile

(c) Design I.3.a. Ballasted Track - High Embankment - End-Bearing Pile

(e) Design I.3.c. Ballasted Track - High Embankment – Combination Cakar Ayam & End-Bearing Pile

Figure 135. Cross sections of different alternative solutions for Example Case I

In the case of building track on soft soil, implementing slab track has an advantage that the total height of the trackbed is lower than that of ballasted track. On a ballasted track system laying on a thick embankment on soft soil, the need of thicker trackbed layer also means greater width of the trackbed. Certain level of slope inclination of the trackbed layer is required to have stability of the unbound materials against sliding. Widening of the foundation slab is also not an effective solution. The reason is that this means high construction costs of reinforced concrete slab and also addition of end-bearing piles. The solution using concrete cantilever walls above the piles as it was constructed in China (see again Figure 79) reported by Raithel et al, 2008)[109], has advantages of limitation of embankment width as well as greater stability against sliding of the embankment. However, this demands higher construction costs.

Instead of constructing anchors, sheet piles or retaining wall, on the side parts of the bottom trackbed layer can be supplemented with floating pile foundation. Since the side areas of trackbed have to bear lower axial pressure than that in the middle areas, then floating foundation can be an option to stabilize these side areas against sliding, as it can be seen in the Figure 135 (d). Hence, the length of the floating piles within these areas can be lower. The floating piles can be embedded in a raft foundation constructed using plain concrete without reinforcements. This gives more cost-effective and optimal solution.

Similar alternative is by implementing *Cakar Ayam* foundation in combination with end-bearing pile foundation as it is in the Figure 135 (e). Considering the features of *Cakar Ayam* that it employs greater diameter of hollow pipe piles filled by soil, thus this combination is more advantageous in an application of double track of ballasted system. Furthermore, since the function of the *Cakar Ayam* is to provide supplementary bearing capacity to avoid potential sliding rotation of the trackbed, thus the mechanism of *Cakar Ayam* pipe piles to utilize soil's passive lateral resistances will be more optimized. This will trigger higher mobilization of lateral resistances as the major feature of *Cakar Ayam* foundation.

9.2.2. Load Transfer Model of Example Case I

Based on the tests data of Example Case I, the soil layers are modelled using direct methods of SPT and CPT tests as well indirect methods based on laboratory soil data of UDS test to obtain a safe design. The load transfer curves contain q-z curve for soil's vertical resistance beneath the foundation plate, p-y curve for pile-soil lateral resistance along the pile embedment depth as well as on the soil surface for lateral soil-foundation resistance, t-z curve for pile shaft resistance and q-z curve for pile tip resistance for end-bearing pile, which are shown in the Figure 136 and Figure 137 below for static loading as well as for cyclic loading in the Figure 168 and Figure 169 in the Appendix 11.

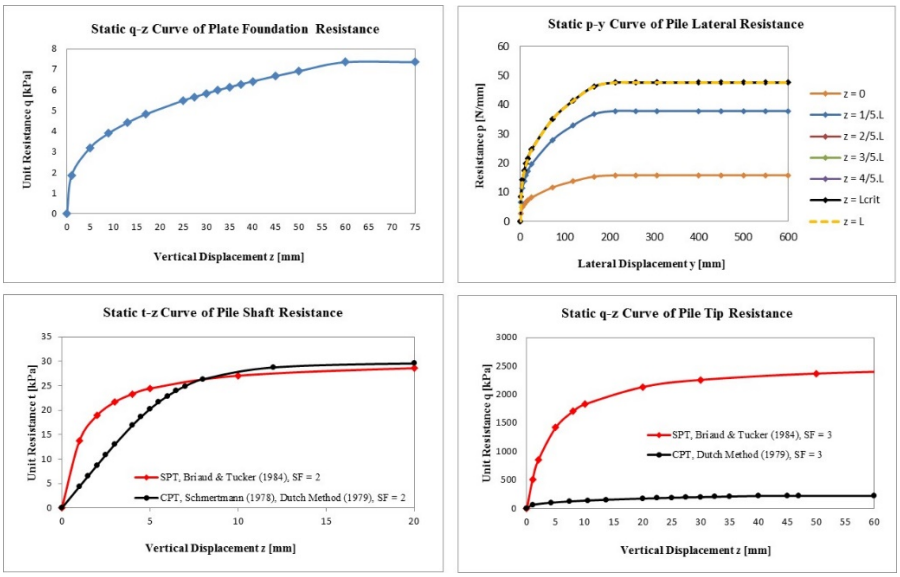

Figure 136. Static load transfer models for the Example Case I - Design I.1 and Design I.3

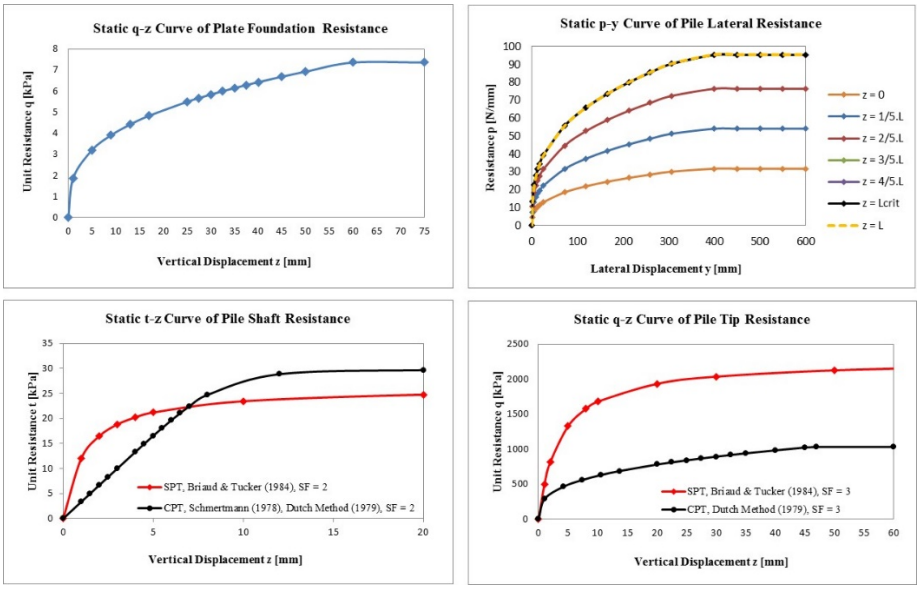

Figure 137. Static load transfer models for the Example Case I - Design I.2

For end-bearing pile design of Design I.1 and I.3 showed in the Figure 136, pile shaft resistances which are estimated using SPT and CPT field test data show similar levels of maximum shaft resistance (t_{max}) before sliding occurs. Yet the level of sliding of CPT after t_{max} is reached is higher than SPT. The t-z curve based on SPT is taken for the design since the data of SPT represents more appropriate idealization for the evaluation of end-bearing piles designs than that of CPT.

Meanwhile pile tip resistance model for Design I.1 and I.3 estimated from CPT is lower than the one from SPT. Observing the data of CPT, the data was not recorded after the depth of 6.6 m. This indicates that the soil bearing resistance is already higher than the capacity of CPT measurement device, so that the test was stopped. SPT test recorded the data until a depth of 16 m. From SPT log profile, it can be seen that the firm soil layer is located in the depth of 8 m. Since the length of the pile for Design I.1 and I.3 is 9 m, the resistance of pile tip should be in a sufficient level, as depicted by SPT number of blows of 50. Therefore, SPT data is used to model the tip resistance of end-bearing pile.

For floating pile design of Design I.2, shaft resistance model from SPT data has t_{max} lower than the one from CPT. The t-z curve based on SPT data is taken in the design and evaluation for the example case. This is taken by taking into account some factors that: 1) certain uncertainties in soil parameters, 2) some linearizations which are taken in the designs of trackbed and pile, and 3) reduction factor of shaft resistance since the *Cakar Ayam* pipe piles are drilled. Furthermore, since pipe piles of Cakar Ayam have a hollow cylinder cross section, thus the pile tip resistance is really small. Therefore, for Design I.2, the q-z curve gained from CPT, which is much smaller than the one from SPT is considered.

9.2.3. Finite Element Analysis and Evaluation of the Design for the Example Case I

FEA models based on the data of Example Case I and their design shown in the Figure 135 above are built in ANSYS. The models are more detailed. In the slab track models, CRCP is modelled including the continuous steel reinforcements in the neutral axis of the slab. JRCP of concrete slab is modelled including the steel reinforcements in the depth of 2/3 from the top concrete surface as well as the doweled bars in the middle of the concrete and within the area of the joints. Foundation slab is also idealized including the steel reinforcements in transverse and longitudinal directions in the depth of around 2/3 from the top surface.

The results of dynamic analysis of a running train on the designed railway track of Design I.1, I.2 and I.3 by considering dynamic amplification factor, thermal impacts (Design I.1 and I.2), self-weight (Design I.3), gaps under the foundation slab and in the interfaces between piles and soils are presented in this following figure:

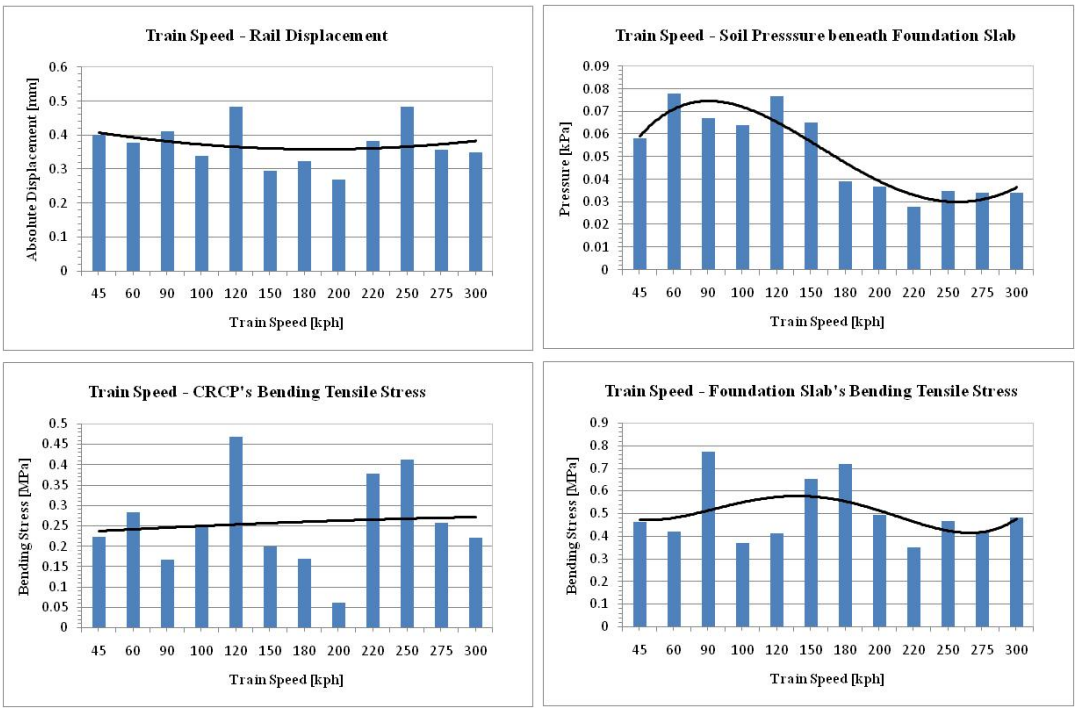

Figure 138. The FEA result of Design I.1 of slab track utilizing conventional CRCP and asphalt base on end-bearing pile foundation by considering DAF, thermal impact and gaps

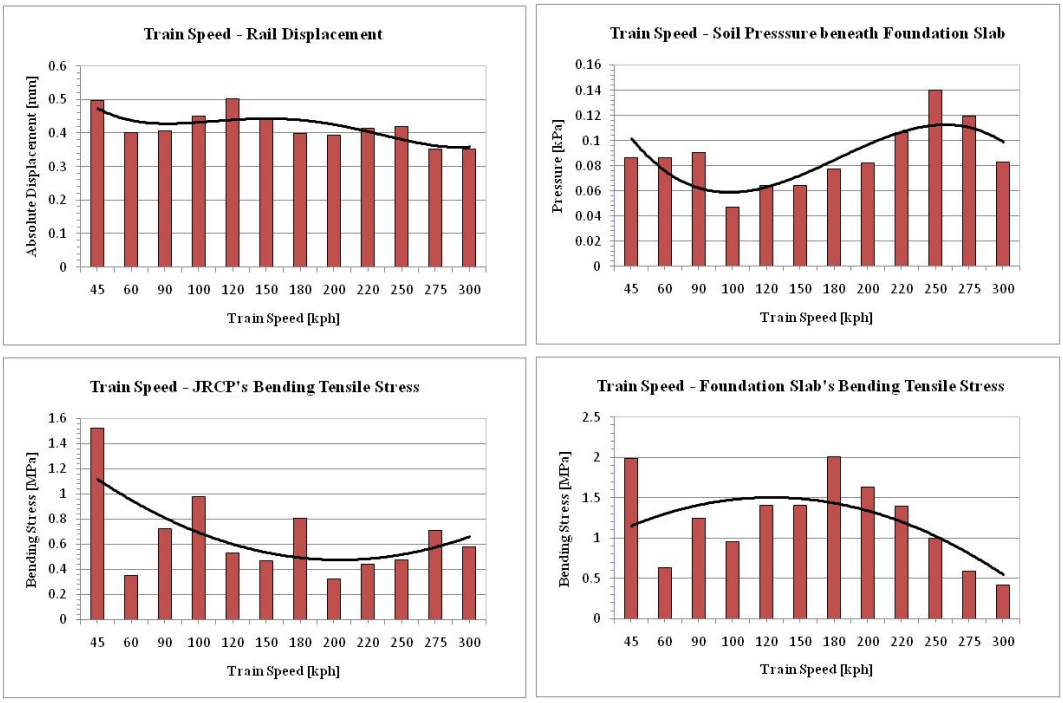

Figure 139. The FEA result of Design I.2 of slab track utilizing JRCP and unbound granular base on floating pile foundation by considering DAF, thermal impact and gaps

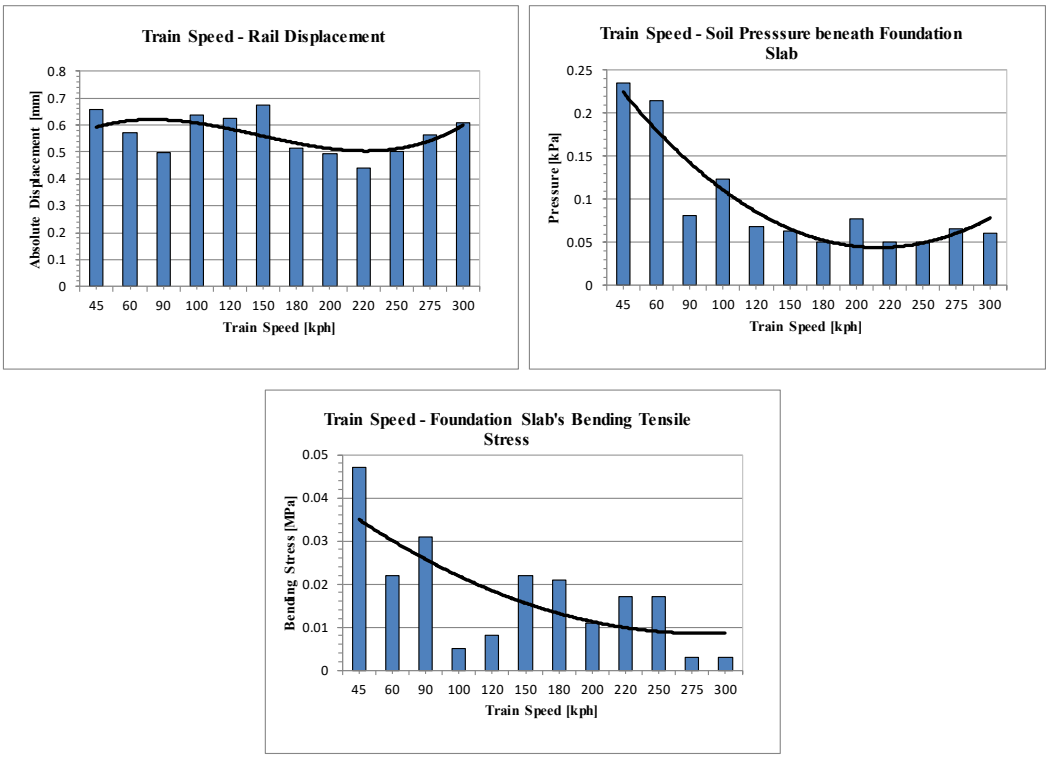

Figure 140. The FEA result of Design I.3 of ballasted track on end-bearing pile foundation by considering DAF and gaps existence

Observing the results of FEA dynamic simulation of running train of ICE-1 artificial loading scheme, it is shown that all of the rail displacements are within the desired level of below 2 mm. Actual bending tensile stress of the CRCP of Design I.1 (0.47 MPa) is below the allowable one (0.94 MPa). The allowable limits of flexural stress of semi-infinite and finite concrete slabs due to thermal and traffic are estimated using Smith's approach (see Table 82, in Appendix 8, pp. 262). The same performances are presented by the foundation slabs of Design 1.1 and 1.3 with end-bearing piles, which have actual bending tensile stresses (0.77 MPa and 0.05 MPa) diminished under the allowable ones (2.02 MPa and 1.4 MPa respectively). The pressures of soil beneath the foundation slab of Design I.1 and I.3 are in a very low level due to installation of end-bearing piles. The residual bearing capacity of end-bearing piles is still sufficient to bear the superstructure within the service period although gaps appear.

After some number of traffics during the service period, in which gaps are predicted to occur, of Design I.2 with floating piles, the actual bending tensile stress of JRCP with 4.55 m joint spacing (1.52 MPa) is still under to the allowable one (2.5 MPa). However, the foundation slab, which is designed as infinite reinforced concrete slab, the actual bending tensile stress (2 MPa) is greater than the allowable one (1.4 MPa) by considering the existence of gaps.

Therefore, end-bearing pile delivers better performance and long term stability, which is more recommended. The installation of floating-piles may need some track rehabilitations after some numbers of traffics and occurrence of gaps. The implementation of JRCP and unbound ballast base layer with soft bonding interface is then more suitable for the design using floating piles, which have advantage regarding possible future maintenance ways, such as replacements of unit slabs only within the area where excessive settlements take a place.

10. Conclusion and Recommendation

The study is conducted to present analysis and evaluation of railway track design on soft soil. Different perspectives of analyses as well as wide range of assessments are performed to understand the characteristics and interactions of track-soil under a condition of low bearing capacity of soft soils. It has been figured out that the conventional methods have limitations regarding soft soil and that they are more appropriate within the range of ideal bearing capacity of soil.

Mathematical formulations based on combination of classical beam and slab models are constructed and programmed in computer. Sensitivity analysis is performed by synchronizing the mathematical models with fatigue criteria of soils and concrete slab to investigate the critical thickness of concrete slab track under various soil bearing capacities. It reveals that soil's reaction modulus of 0.25 N/mm^3 can be considered as the threshold of minimum bearing capacity on the top of a base layer of a thin concrete slab track to secure the concrete slab against excessive cracks. It is also found that to assess performance of a slab track, soil fatigue criterion becomes more dominant than criterion of flexural strength of concrete when the reaction modulus is below 0.25 N/mm^3.

A static analytical design method of trackbed in combination with three different limit criteria of soil's fatigue strength, shear failure and plastic deformation has been proposed to estimate the minimum required thickness of trackbed. The core of the method is by introducing *Structural Number* (*SN*) to represent the overall strength of trackbed and *Coefficient of Relative Strength* (*a*) to describe the strength of individual layer of trackbed. This method is simplified and presented as design charts. It demonstrates a good initial estimation of the required thickness of a trackbed and has been compared with other approaches available from literature. The method also includes the impact of trackbed width as simple correction factor. The major advantages of this method are: (1) simple due to the utilization of design charts, (2) it allows variations of changing rail profiles, elastic-pad stiffness, wheel loads, dynamic amplification factor (train speed, track quality), wheel load distribution (straight line or in a curve), (3) the flexibility of assigning correction factors, and (4) multilayered trackbed design is possible. The fundamental limitations are: (1) it only deals with single axle load of a train, (2) it considers linear, homogenous and isotropic material of track components and soil, and (3) it strongly depends on the failure criteria and the set boundaries, thus, correct and clear definitions of these criteria are very essential.

In real design applications, the use of the method should contemplate not only soil bearing capacity, but also (1) proper selection of trackbed stiffness (stiffness ratio between layers) and thickness (height limitation, self -weight), (2) material characteristics and behaviours, (3) top-down gradual reduction of the layers stiffness, (4) special function of trackbed layers, (5) geographic and climate conditions (topography, frost action, rain intensity, water table level, drainage system), (6) subsoil conditions, and (7) construction procedure. Future improvements are: (1) to correlate the method with laboratory tests (2) to develop measurement test of trackbed material to obtain good approximation of coefficient relative strength of trackbed materials and (3) to include other parameters beside stiffness and Poisson's ratio, such as cyclic and fatigue strength as well as empirical factors of drainage.

FEA track-soil interaction exhibits that (1) soil stabilization and elastic-pad stiffness adjustment majorly influence the track performance in low excitation frequencies, (2) superstructure strength improvements by stiffness and thickness modifications affect more significantly to the stability of the track in high excitation frequencies and (3) fastening stiffness and damping alterations can be taken into action to mitigate the vibration impact of high excitation frequencies. Furthermore, it has been found that the traditional assumption of only increasing the thickness and stiffness of track structure is not always the most effective solution when the soil is below the limit of ideal bearing capacity.

Cakar Ayam foundation mechanism works optimally for quasi single point load subjected on a thin and semi-infinite foundation slab. For railway application this mechanism does not perform optimally due to (1) multilayer structure of a track already distributes the wheel loads as vertical pressure under the trackbed, hence soil’s lateral resistances are not optimally activated, (2) there is greater total thickness of trackbed and foundation, then the bending of foundation slab is small and the utilization of soil's lateral passive resistances from the piles is also small, (3) *Cakar Ayam* works like a normal piled raft foundation, in which the shaft resistances should supply the main vertical bearing capacity. Thus, longer pile is required.

A static analytical method is also proposed to approximate the required thickness of trackbed as well as length of the pile. The method is developed based on combination between equilibrium rotation moment concept and the proposed method of trackbed design. This method can be implemented when the soils beneath the foundation slab are still considered to provide supplementary bearing capacity to the one delivered from the floating piles. The length of a floating pile should be far greater than its critical length ($> 2L_{crit}$). In a condition

of extremely soft soils, this method to estimate pile length is not fully appropriate as well as the approximation of trackbed thickness is not valid. In this case end-bearing pile and advanced geotechnical analysis are more recommended. Combination of end-bearing pile and *Cakar Ayam* floating pile can be an option for construction of double track ballasted track system. This combination is suggested for future studies to be further analyzed concerning not only static but also dynamic interactions of two trains as well as deeper geotechnical analysis regarding assessment of slope stability of a high embankment.

Some improvements related to problems of building railway track on soft soil to enhance the performance of the track are: (1) the use of softer rail -pad with high damping capability, (2) identification and adjustment of the natural frequency of the overall track system, and (3) the implementation of multilayer trackbed layer (4) the use of jointed slabs.

Implementation of jointed slabs built using JRCP or JPCP can be an alternative of superstructure constructions on soft soil particularly regarding the future maintenance efforts. It is found that jointed slabs are more advantageous when they are constructed with soft bonding interface. Meanwhile, a thin CRCP delivers better performance as a composite structure with stiff and thick bounded base layers and together with a hard-bonding interface. The use of JRCP and JPCP can be an option as replacement of CRCP. It can be more cost-effective by selecting proper joint spacing in combination with the use of thicker slab. A thin JPCP can be still constructed but should be followed by thicker rigid base layer.

Finally, the treatments of substructure concerning soil bearing capacity of soil can generally categorized based on soil's resilient modulus (E_s and k_s): (1) trackbed applications are suggested for $E_s > 18$ MPa or $k_s > 0.1$ N/mm^3 in the range of moderate to firm soils, (2) *Cakar Ayam* with longer floating pile can be an option for $10 < E_s < 15$ MPa or $0.05 < k_s < 0.1$ N/mm^3 in the range of soft soils and (3) end-bearing piles of *Cakar Ayam* or of conventional piled foundation are more recommended for $E_s < 15$ MPa or $k_s < 0.08$ N/mm^3 of soft and very soft soils with careful consideration of the geotechnical aspects.

11. Bibliography

[1] AASHTO (1993). *AASHTO Guide for Design of Pavement Structures*. American Association of State Highway and Transportation Officials

[2] ACI Committee 360 (2006). *Design of Slabs-on-Ground.* American Concrete Institute

[3] AFTES (2013), *Rail Tracks and Track Beds in Tunnels*. 2013. [Online]. Available: http://www.aftes.asso.fr/contenus/upload/File/Publications/Recommandations/GT40R2A1.pdf. [Accessed 21 July 2014].

[4] American Petroleum Institute (API), (1991), *Recommendations for Planning, Designing and Constructing Fixed Offshore Platforms, API Recommended Practice 2A (RP 2A)*, Nineteenth Edition of American Petroleum Institute.

[5] Aoki, N. & Velloso, D. A. (1975), *An Approximate Method to Estimate the Bearing Capacity of Piles*, Proceedings of 12th International Conference on Soil Mechanics and Foundation Engineering, Balkema, Rotterdam, Vol. 1, pp. 165-170.

[6] Aschenbrenner, T. B. & R. E. Olson (1984), *Prediction of Settlement of Single Piles in Clay*, Analysis and Design of Pile Foundations. ASCE, J. R. Meyer, ed.

[7] ATSB (2013), *Safety of Rail Operations on the Interstate Rail Line between Melbourne and Sydney*, Asutralian Transport Safety Bureau (ATSB) Report, Rail Safety Issue Investigation RI-2011-015. August 2013, pp. 14.

[8] Balitbang PU (2011), *CakMod: Cakar Ayam Modifikasi* (Modification of Chicken Claw Foundation).

[9] Baranov, V. A. (1967), *On the Calculation of Excited Vibrations of an Embedded Foundation (in Russian)*, Voprosy Dynamiki Prochnocti, No. 14, Polytech. Inst. Riga, pp.195-209.

[10] Barkan, D. D. (1962), *Dynamics of Bases and Foundations*. McGraw-Hill, New York, pp. 434.

[11] Bond, A.J. (1989), *Behaviour of displacement piles in over-consolidated clays*, PhD Thesis, University of London, London, UK.

[12] Bowles J.E. (1996). *Foundation Analysis and Design*. 5th Edition, McGraw-Hill, New York

[13] Briaud, J. L. & Tucker, L. (1984), *Piles in Sand: A Method Including Residual Stresses*, Journal of Geotechnical Engineering, ASCE, 110 (11), pp. 1666-1680.

[14] Burland, J. B. (1973), *Shaft Friction of Piles in Clay - A Simple Fundamental Approach*, Ground Engineering, 6 (3), pp. 30-42.

[15] Burrow, M.P.N., S.G. Ghataora, H. Evdorides (2011), *Railway Foundation Design Principles*, Journal of Civil Engineering and Architecture, Vol. 5, No. 3 (Serial No. 40), pp. 224-232, David Publishing, USA.

[16] Bustamante, M., & L. Gianeselli (1982), *Pile Bearing Capacity Prediction by Means of Static Penetrometer CPT*, Proceedings of 2nd European Symposium on Penetration Testing*,* Amsterdam, The Netherlands, II,1982, pp. 493-500.

[17] Chair & Institute for Road, Railway and Airfield Construction, TU München (2013). *Lecture Note Rail and Road Design*. Master Program in Transportation Systems, TU München

[18] Chow, F.C. (1996), *Investigations into the behaviour of displacement piles for offshore foundations*, PhD thesis, Imperial College of Science, Technology, and Medicine, University of London, London, UK.

[19] Codecogs (2015), *Elastic Foundation. Beam on Elastic Foundation.* http://www.codecogs.com/library/engineering/materials/beams/elastic-foundations.php

[20] Cofer, W. F. & S. Modak (1997), *Determination of Rheological Parameters of Pile Foundations for Bridges for Earthquake Analysis*, Summary Report for Research Project T9234-07: Modelling Pile Foundations for Seismic Analysis, Washington State Transportation Center (TRAC) - FHWA - Washington State University.

[21] Coyle, H. M. & I. H. Sulaiman (1967), *Skin Friction for Steel Piles in Sand*, Journal Soil Mechanics and Foundations Division, Proceedings Paper 5590, ASCE, Vol 93 (SM6).

[22] Coyle, H. M. & R. R. Castello (1981), *New Design Correlations for Piles in Sand*, Journal of the Geotechnical Engineering Division, Proceedings Paper 16379, ASCE, Vol 107 (GT7).

[23] Coyle, H. M. & Reese, L. C. (1966), *Load Transfer for Axially Loaded Piles in Clay*, Journal Soil Mechanics and Foundations Division, Proceedings Paper 4702, ASCE, Vol 93 (SM6).

[24] Coyle, N. M. & Castello, R. R. (1981), *New Design Correlations for Piles in Sand*, Journal of the Geotechnical Engineering Division, ASCE, 107 (GT7), pp. 965-986.

[25] Cunny, R. W. and Z. B. Fry (1973), *Vibratory in Situ and Laboratory Soil Moduli Compared*. JSMFD, ASCE, Vol. 99, SM 12, Dec, pp. 1055-1076.

[26] Curas, C. J., R. W. Boulanger, B. L. Kutter & D. W. Wilson (2001), *Dynamic Experiments and Analyses of a Pile-Group-Supported Structure*, Journal of Geotechnical and Geo-environmental Engineering, ASCE, Vol. 127, No. 7, July, 2001.

[27] Dahlberg, T. (2003), *Railway Track Dynamics- A Survey*, Linkoping University, Sweden.

[28] Daud, S. et. al. (2009), *Kajian dan Monitoring Hasil Uji Coba Skala Penuh Teknologi Cakar Ayam Modifikasi* (Study and Investigation of Full Scale Tests on Modified Cakar Ayam Technology), Puslitbang Jalan dan Jembatan, Indonesia, http://www.pusjatan.pu.go.id/upload/kolokium/2009/KKBGTJ200902.pdf, last accessed: 08.03.2011

[29] DeRuiter, J. & Beringen, F. L. (1979), *Pile Foundations for Large North Sea Structures*, Marine Geotechnology, 3 (3), pp. 267-314.

[30] Dobry, R. & G. Gazetas (1986), *Dynamic Response of Arbitrary Shaped Foundations*. JGED, ASCE, Vol. 112, No. 2, Feb, pp. 109-135.

[31] Eid, J. (2012), *Theoritische und Experimentelle Untersuchungen dünner Betondecken auf Asphalt (Whitetopping)*. Dissertation. Chair & Institute for Road, Railway and Airfield Construction, TU München.

[32] Eisenmann J., & Rump R., (1997). *Ein Schotteroberbau für hohe Geschwindigkeiten*. ETR 46, H.3, März, p.99-108.

[33] Eisenmann J., (2004). *Die Schiene als Tragbalken*. Eisenbahningenieur (55), 5/2004, p. 22-25.

[34] Eisenmann, J. & G. Leykauf (1990). *Simplified Calculation Method of Slab Curling Caused by Surface Shrinkage*. Proceedings, 2nd International Workshop on Theoretical Design of Concrete Pavements: 185-197. Madrid, Spain.

[35] Eisenmann, J. (1979). *Concrete Pavements – Design and Construction* (in German). Wilhelm Ernst &Sohn: Berlin/Munich/Dusseldorf

[36] Eisenmann, J., &Leykauf, G. (2000). *Feste Fahrbahn für Schienenbahnen*. In Beton Kalender 2000. Berlin: Ernst &SohnVerlag.

[37] Eisenmann, J., &Leykauf, G. (2003). *Betonfahrbahnen*. 2. Aufl. Berlin, Ernst (Handbuch für Beton-, Stahlbeton- und Spannbetonbau).

[38] EN1992-1-1 (2004)). *Eurocode 2: Design of concrete structures - Part 1-1: General rules and rules for buildings*. European Comitte for Standardization, Brussel.

[39] Esveld, C. (2001), *Modern Railway Track*. Second Edition, MRT Production, Delf University of Technology, Netherland.

[40] FHWA (2012). *Estimation of Key PCC, Base, Subbase, and Pavement Engineering Properties from Routine Tests and Physical Characteristics*. 1st and 2nd Edition, John Wiley and Sons

[41] Firdiansyah, A. (2000), *Evaluasi Dimensi Sistem Cakar Ayam Akibat Pengaruh Variasi Letak Beban dan Kondisi Tanah* (Evaluation of Cakar Ayam Dimension due to Variations of Load Position and Soil Condition). Master Thesis, Magister Pengelolaan Sarana Prasarana (MPSP), Program Pasca Sarjana, Universitas Gadjah Mada, Yogyakarta.

[42] Freudenstein, S. (2004), *Ballasted Track Systems for High Speed Traffic*. European Railway Review, Issue 4, 2004, pp. 79-85.

[43] Freudenstein, S., K. Geisler, T. Mölter, M. Mißler, C. Stolz (2015), *Beton Kalender 2015, Sonderdruck, X Feste Fahrbahnen in Betonbauweise*. Ernst & Sohn.

[44] Fwa, T. F. (2006), *The Handbook of Highway Engineering*, Taylor & Francis Group, New York

[45] Garcia, Gabriel S (2007). *Concepts for Mechanistic-empirical Design Procedure for Extended Life Hot Mix Asphalt Pavements with a Multi-layered Structure*, ProQuest Publisher.

[46] Giannakos, K. (2014), *Secondary Stiffness of Fastening's Clip: Influence on the Behaviour of the Railway Track Panel*. Transport Research Arena 2014, Paris.

[47] Hardin, B. O. & V. P. Drnevich (1972), *Shear Modulus and Damping in Soils: Design Equations and Curves*. JSMFD, ASCE, Vol. 98, SM 7, July, pp. 667-692.

[48] Hardin, B. O. & W. L. Black (1968), *Vibration Modulus of Normally Consolidated Clay*. JSMFD, ASCE, Vol. 94, SM 2, March, pp. 27-42.

[49] Hardiyatmo, H. C. (2010), *Mengenal Seluk Beluk Cakar Ayam Bersama Pakarnya*. An interview by Dito Anurogo with Hary Christady Hardiyatmo", http://netsains.com/2010/02/mengenal-seluk-beluk-pondasi-cakar-ayam-bersama-pakarnya/

[50] Hardiyatmo, H. C. (2010), *Method of Calculations for the Deflections, Moments and Shears on Cakar Ayam System to Design Concrete Road Pavements*. Dinamika Teknik Sipil, Vol. 10, January 2010. pp. 27-33.

[51] Hardiyatmo, H. C., B. Suhendro, A. D. Adi (2000), *Perilaku Fondasi Cakar Ayam pada Model di Laboratorium - Kontribusi untuk Perancangan* (Behaviours of Cakar Ayam Foundation from a Laboratory Model - Contribution for Design). Lembaga Penelitian, Universitas Gadjah Mada, Yogyakarta.

[52] Heath, D.L., M.J. Shenton, R.W. Sparrow and J.M. Waters (1972), *Design of Conventional Rail Track Foundations*, Proceeding Institute of Civil Engineering 51 pp. 251-267.

[53] Hetenyi, M. (1974), *Beam on Elastic Foundation,* The University of Michigan, USA.

[54] Heydinger, G. H. & M. W. O' Neill (1986), *Analysis of Axial Pile-Soil Interaction in Clay*, International Journal for Numerical and Analytical Methods in Geomechanics, 10 (4), pp. 367-381.

[55] Huang Y.H., C. Lin & J. G. Rose (1984), *Asphalt Pavement Design: Highway versus Railroad*, March 1984. Journal of Transportation Engineering, Vol. 110, No. 2, Paper No. 18611, ASCE.

[56] Ignasiak-Szulc, A. & Kosiedowski, W. (2009), *Between Europe and Russia. Problems of Development and Transborder Co-operation in North-Eastern Borderland of the European Union*. Scientific Publishing House of Nicolaus Copernicus University, Torun, pp. 206-207.

[57] Ioannides, A.M. et.al (1985), *Westergaard Solutions Reconsidered*, Transportation Research Record, Issue No. 1043, Transportation Research Board

[58] Ismail, S. (2006), *Pondasi Cakar Ayam - Menjabarkan Teori Prof. Sedijatmo*. PT. Perca. Jakarta

[59] Istiawan, S. (2008), The *Cakar Ayam - Indonesian Chicken Claw Structural Floating Foundation*, http://uwong.blogspot.com/2008/10/cakar-ayam-structure-foundation-by.html, last accessed: 08.03.2011

[60] Jardine, R.J (1985), *Investigations of pile-soil behaviour with special reference to the foundations of offshore structures*, PhD dissertation, Imperial College of Science, Technology and Medicine, University of London, London, UK.

[61] Kaewunruen, S. & Remennikov, A. (2008), *An Alternative Rail Pad Tester for Measuring Dynamic Properties of Rail Pads under Large Preloads*. Experimental Mechanics 48, Research Online, University of Wollongong, Faculty of Engineering-Paper (Archive).

[62] Kim, T. C. & M. Novak (1981), *Dynamic Properties of Some Cohesive Soils in Ontario*. CGJ, Vol. 18, No. 3, Aug, pp. 371-389.

[63] Knothe, K, M. Yu, H. I lias (2003), *Measurement and Modelling of Resilient Rubber Rail-Pads*, in "System Dynamics and Long-Term Behaviour of Railway Vehicles, Track and Subgrade". Eds. Popp and Schiehlen, Springer Verlag, Berlin, pp. 265-274.

[64] Koroma, S.G, M.F.M. Hussein & J.S. Owen (2013), *The Effects of Preload and Nonlinearity on the Vibration of Railway Tracks under Harmonic Load*. 11th International Conference on Vibration Problems, 9-12 September 2013, Lisbon, Portugal.

[65] Kraft, L. M., R. P. Ray & T. Kagawa (1981), *Theoretical t-z Curves*, Journal Geotechnical Engineering Division, Proceedings Paper 16653, ASCE, Vol 107 (GT11).

[66] Lai, P. W. (2012), *An Introduction to the Design Methodology of FB-Deep*, PowerPoint Presentation, Design Training Expo 2012, FDOT Structure Design Office, State Geotechnical Engineering Section.

[67] Lechner, B. (2008). *Concrete Pavements for Railway Track*. Proceeding of 9th International Conference on Concrete Pavements, International Society for Concrete Pavements; Federal Highway Administration; American Concrete Pavement Association. pp 964-975

[68] Lechner, B. (2008). *Design and Layout of Ballastless Track Systems using Unbound Base Course Layers*. Retrieved January 14, 2014, from International Union of Railways: http://www.uic.org/cdrom/2008/11_wcrr2008/pdf/I.1.4.1.2.pdf

[69] Lechner, B. (2011). *Railway Concrete Pavement*. PowerPoint presentation. 2nd International Conference on Best Practices for Concrete Pavements, Florianopolis, November 2011.

[70] Lechner, B., &Leykauf, G. (2005). *Dimensionierung und konstruktive Durchbildung von FF-Systemen mit ungebundenen Tragschichten*. Munich: Lehrstuhl und Prüfamt für Bau von Landverkehrswegen TU München.

[71] Lehane, B.M. (1992), *Experimental investigations of pile behavior using instrumented field piles*, PhD Thesis, University of London, London, UK.

[72] Leykauf, G., B. Lechner, and W. Stahl (2006), *Trends in the use of slab track/ballastless tracks*. RTR Special State of the Art. Slab Track, Track System Development. Issue September 2006.

[73] Li, D. & E.T. Selig (1996). *Cumulative Plastic Deformation for Fine-grained Subgrade Soils*, Journal of Geotechnical Engineering, ASCE, 122 (12), pp. 1006-1013.

[74] Li, D. & E.T. Selig (1998). *Method for Railroad Track Foundation Design. I: Development*, April 1998. Journal of Geotechnical &Geoenvironmental Engineering, Vol. 124, No. 4, Paper No. 15812, ASCE.

[75] Li, D. & E.T. Selig (1998). *Method for Railroad Track Foundation Design. II: Applications*, April 1998. Journal of Geotechnical &Geoenvironmental Engineering, Vol. 124, No. 4, Paper No. 15811, ASCE.

[76] Li, D. (1994). *Railway Track Granular Layer Thickness Design based on Subgrade Performance under Repeated Loading*, PhD Dissertation, Dept. of Civil Engineering, University of Massachusetts, Amherst, Mass.

[77] Likaytanjua, E. (2010), *Sedijatmo - Penemu Konstruksi Fondasi Cakar Ayam* (Sedijatmo: The Inventor of Construction Foundation "Chicken Claw"), http://elanglikaytanjua.blogspot.com/2010/03/sedijatmo-penemu-konstruksi-fondasi.html, last accessed: 08.03.2011

[78] López Pita, A. (2002), *The Importance of Vertical Stiffness of the Track on High–Speed Lines*, Transportation Research Board 81st Annual Meeting, Washington DC, 13-17 January 2002.

[79] Lunne, T., P.K. Robertson, and J.J.M. Powell (1997), Cone penetration testing in geotechnical practice, Blackie Academic and Professional, New York.

[80] Mathur, R., &Negi, S. (2005). *Innovative Track Systems under Development on Foreign Railways*, Indian Railway Institute of Civil Engineering. Retrieved January 14, 2014, from http://wiki.iricen.gov.in/doku/lib/exe/fetch.php?media=525:4innovative.pdf

[81] Matlock, H. (1970), *Correlations for Design of Laterally Loaded Piles in Soft Clay*, Preprints, Second Annual Offshore Technology Conference, Paper No. 1204, Vol 1, pp. 577-588.

[82] Mattner, L. (1986), *Analyse von Versuchen mit Eisenbahnschotter und Simulationsberechnung der Gleislageverschlechterung unter einem oftmals überrollenden Rad*, Prüfamt Verkehrswegebau, Technische Universität München, Germany.

[83] Meyerhof, G.G. (1965). *Shallow foundations*. ASCE J. Soil Mech. and Foundations Div., 91, No. SM2, pp. 21–31.

[84] Meyerhof, G.G. (1976), *Bearing Capacity and Settlement of Pile Foundations*, Journal of Geotechnical Engineering, ASCE, 102 (3), pp. 197-228.

[85] Meyerhof, G.G. (1983), *Scale Effect of Ultimate Pile Capacity*, Journal of Geotechnical Engineering, ASCE, 109 (6), pp. 797-806.

[86] Molenaar, A.A.A. (2009), *Structural Design of Pavements. Part III. Design of Flexible Pavement*, Handbook of Lecture, Faculty of Civil Engineering and Geosciences, TU Delft, Netherlands.

[87] Mosher, R. L. & W. P. Dawkins (2000), *Theoretical manual for Pile Foundations, Computer-Aided Structural Engineering Project*, ERDC/ITL TR-00-5, US Army Corps of Engineers.

[88] Mosher, R. L. (1984), *Load Transfer Criteria for Numerical Analysis of Axially Loaded Piles in Sand; Part 1: Load Transfer Criteria*, Technical Report K-84-1, U.S. Army Engineer Waterways Experiment Station, Vicksburg, MS.

[89] Murchison, J. M. & M. W. O'Neill (1984), *Evaluation of p-y Relationships in Cohesionless Soils*, Analysis and Design of Pile Foundations, ASCE, J. R. Meyer, ed., pp. 174-191.

[90] NAVFAC Design Manual 7.02 (1986)

[91] Nawangalam (2008), *Permodelan Elemen Hingga Sistem Cakar Ayam dengan Analisis Tanah-dasar-Non-Linear* (Finite Element Modelling of Cakar Ayam System with Non-linear Analysis of Subgrade). Master Thesis, Program Pasca Sarjana, Universitas Gadjah Mada, Yogyakarta.

[92] Nelder, L.M., et.al. (2008), *A comparison of trackbed design methodologies: a case study from a heavy haul freight railway*. Advances in Transportation Geotechnics: Proceedings of the International Conference, August 2008, Nottingham, UK, pp. 135-142.

[93] Network Rail (2005), *Company Code of Practice, Formation Treatments NR/SB/TRK/9039*, Network Rail, December 2005, London.

[94] Nogami, T. & Konagai, K. (1988), *Time Domain Flexural Response of Dynamically Loaded Single Piles*, Journal of Engineering Mechanics, Vol. 114, No. 9, September, 1988. ASCE Specialty Conference, Pasadena, California, June 19-21, 1978, pp. 704-719.

[95] Novak, M & Aboul-Ella, F. (1978), *Stiffness and Damping of Piles in Layered Media*, Proceeding of Earthquake Engineering and Soil Dynamics, ASCE Specialty Conference, Pasadena, California, June 19-21, 1978, pp. 704-719.

[96] Novak, M. & Sheta (1982), *Dynamic Response of Piles and Pile Groups*, 2nd International Conference of Numerical Methods Offshore Piling. Austin, Texas.

[97] Novak, M. & Y. O. Beredugo (1972), *Vertical Vibration of Embedded Footings*, Journal of Soil Mechanic and Foundation Division, ASCE, 12, pp. 1291-1310.

[98] Novak, M. & Y. O. Beredugo (1972), *Vertical Vibration of Embedded Footings*. JSMFD, ASCE, Vol. 98, SM 12, Dec, pp. 1291-1310.

[99] Novak, M. (1974), *Dynamic Stiffness and Damping of Piles*, Canadian Geotechnical Journal, 1974, 11, No. 4. pp. 574-598.

[100] Novak, M., Nogami, T. & Aboul-Ella, F. (1978), *Dynamic Soil Reactions for Plain Strain Case*, Journal Engineering Mechanics Division, ASCE, 104 (EM4), pp.953-959.

[101] O'Neill, M. W. & S. M. Gazioglu (1984), *An Evaluation of p-y Relationships in Clays*, American Petroleum Institute, University of Houston.

[102] Pando, M. A, C. D. Ealy, G. M. Filz, J. J. Lesko & E. J. Hoppe (2006), *A Laboratory and Field Study of Composite Piles for Bridge Substructures*, FHWA-HRT-04-043 Report, Virginia Transportation Research Council, FHWA.

[103] Pando, M. A. (2013), *Analyses of Lateral Loaded Piles with P-Y Curves - Observations on the Effect of Pile Flexural Stiffness and Cyclic Loading*, PowerPoint Presentation, NCDOT 7th Geo^3 T^2, Raleigh, NC, April 2013.

[104] Popp, K & W. Schiehlen (2003), *System Dynamics and Long-Term Behaviour of Railway Vehicles, Track and Subgrade*. Springer Verlag, Berlin, pp. 265-274.

[105] Prakoso, P. B. (2011). Master's thesis: *Analysis and Evaluation of Railway Track Systems on Soft Soil Using Finite Element Method, Case Study Kalimantan, Indonesia*. Munich: MSc. Program in Transportation Systems, TU München.

[106] Puzavac, L., Z. Popovic, L. Lazatevic (2012). *Influence of Track Stiffness on Track Behaviour under Vertical Load*. PROMET-Traffic & Transportation, Scientific Journal on Traffic and Transportation Research. Vol. 24, No 5 (2012), pp. 405-412.

[107] Quirchmair, M. & Loy, H. (2015). *Railway Gazette International*. August 2015. www.railwaygazette.com.

[108] Rail Safety & Standards Board (2005). *Review of the Effects of Track Stiffness on Track Performance.* United Kingdom.

[109] Raithel, M, A. Kirchner & H.-G. Kempfert (2008), *Pile-supported embankments on soft ground for a high speed railway – Load Transfer, Distribution and Concentration by different construction methods*. Kempfert + Partner Geotechnik. http://www.kup-geotechnik.de/kup/Veroeffentlichungen/2008/2008_Raithel_Nottingham.pdf

[110] Ramadhoni, J. (2008), *Perilaku Perkerasan Sistem Cakar Ayam dengan Metode Elemen Hingga* (Behaviours of Cakar Ayam Reinforcement using Finite Element Method). Bachelor Thesis, Jurusan Teknik Sipil dan Lingkungan, Universitas Gadjah Mada, Yogyakarta.

[111] Rao, S. &Roesler, J. (2005). *Characterization of Effective Built-in Curling and Concrete Pavement Cracking on the Palmdale Test Sections*. Retrieved March 2014, from University of California Berkeley, Institute of Transportation Studies, Pavement Research Center: http://www.ucprc.ucdavis.edu/PDF/Eff%20Built-In%20Curling%20DRAFT.pdf

[112] Reese, L. C. & O'Neill, M. W. (1989), *New Design Method for Drilled Shaft from Common Soil and Rock Test*, Proceedings of Congress Foundation Engineering: Current Principles and Practices, ASCE, Vol. 2, pp. 1026-1039.

[113] Reese, L. C. & R. C. Welch (1975), *Lateral Loading of Deep Foundations in Stiff Clay*, Journal Geotechnical Engineering Division, ASCE, Vol 101 (GT7), pp. 633-649.

[114] Reese, L. C. & W. R. Sullivan (1980), *Documentation of Computer Program COM624; Parts I and II, Analysis of Stresses and Deflections for Laterally-Loaded Piles Including Generation of p-y Curves*, Geotechnical Engineering Software SG80-1, Geotechnical Engineering Center, Bureau of Engineering Research, University of Texas at Austin.

[115] Reese, L. C., W. M. Isenhower & S. T. Wang (2006), *Analysis and Design of Shallow and Deep Foundations*, John Wiley and Sons, Hoboken, NJ.

[116] Reese, L. C., W. R. Cox & F. D. Koop (1974), *Analysis of Laterally Loaded Piles in Sand*, Proceedings, Fifth Annual Offshore Technology Conference, Paper No. OTC 2080, Houston, Texas.

[117] Reese, L. C., W. R. Cox & F. D. Koop (1975), *Field Testing and Analysis of Laterally Loaded Piles in Stiff Clay*, Proceedings, Seventh Annual Offshore Technology Conference, Paper No. OTFC 2312, Houston, Texas.

[118] Richard, F. E., Jr, et.al. (1970), *Vibrations of Soils and Foundations*. Prentice-Hall Inc. Englewood Cliffs, NJ, pp. 414.

[119] Romero, M.J.G., Edwards, J.R., Barkan, C.P.L, Wilson, B., Mediavilla, J. (2010), *Advancements in Fastening System Design for North American Concrete Crossties in Heavy-Haul Service*. AREMA 210 Annual Conference & Exposition.

[120] Rump, R. (1997), *Warum Feste Fahrbahn*. Edition ETR – Feste Fahrbahn, pp. 8-11.

[121] Salgado, R. and J. Lee (1999), *Pile Design Based on Cone Penetration Test Results*, Final Report, Joint Transportation Research Program (JTRP), FHWA/IN/JTRP-99/8, Indiana Dept. of Transportation and Purdue University.

[122] Sall, O.A, M. Fall, Y. Berthaud and M. Ba (2013), *Influence of the Elastic Modulus of the Soil and Concrete Foundation on the Displacements of a Mat Foundation.* Open Journal of Civil Engineering, 2013, 3, 228-233. December 2013. http://dx.doi.org/10.4236/ojce.2013.34027

[123] Schmertmann, J. H. (1978), *Guidelines for Cone Penetration Test, Performance and Design*, U.S. Department of Transportation, FHWA-TS-78-209, 3 (3), pp. 267-314.

[124] Skempton, A.W. (1951), The Bearing Capacity of Clays. Building Research Congress, 1, pp. 897-905

[125] Söderqvist, J., (2006). *Design of Concrete Pavements - Design Criteria for Plain and Lean Concrete*. Licentiate Thesis, TRITA-BKN. Bulletin 87, 2006. Royal Institute of technology (KTH). Retrieved March 2014, from DIVA Academic Archive On-line: http://www.diva-portal.org/smash/get/diva2:11234/FULLTEXT01.pdf

[126] Steenbergen, M.J.M.M., A.V. Metrikine and C. Esveld (2006), *Stiffness Requirements for Slab Track Railways: Soil Improvement versus Slab Reinforcement, and Effects on the Dynamic Response*. The 13th International Congress on Sound and Vibration (ICSV13) Vienna, July 2-6, 2006, Vienna, Austria.

[127] Steenbergen, M.J.M.M., C. Esveld (2006) and A.V. Metrikine, *Stiffness Requirements for Slab Track Railway Systems from a Dynamic Viewpoint*. 6th International PhD Symposium in Civil Engineering Institute of Structural Engineering ETH Zurich, 23 -26 August 2006, Zurich

[128] Steidl, M (2007), *Standards and Test of Fastening Systems*. Conference and Proceeding 2007. Arema.org.

[129] Suhendro, B. (1992), *Laporan kemajuan ke III, Studi Optimalisasi Formula Cakar Ayam* (3rd Progress Report: Study of Optimization the Formulation of Cakar Ayam). Jurusan Teknik Sipil Universitas Gadjah Mada, Yogyakarta.

[130] Suhendro, B. (2006), *Sistem Cakar Ayam Modifikasi sebagai Alternatif Solusi Konstruksi Jalan di atas Tanah Lunak* (Modified Cakar Ayam System as an Alternative Solution for Roadway Construction on Soft Soil). Saduran dari buku 60 tahun RI, Jakarta.

[131] Sussmann, T. R., Ebersohn, W., Selig, E. T (2001), *Fundamental Non-Linear Track Load-Deflection Behavior for Condition Evaluation*. Transportation Research Record, Volume 1742, 2001, pp. 61-67.

[132] Tandjiria, V. (1999), *Numerical Modelling of Chicken-Foot Foundation*. Civil Engineering Department, Petra Christian University, Indonesia. http://puslit2.petra.ac.id/ejournal/index.php/civ/article/viewFile/15502/15494

[133] Terzaghi, K. & Peck, R.B. (1948 & 1967). *Soil Mechanics in Engineering Practice*. 1st and 2nd Edition, John Wiley and Sons.

[134] Thompson, D.J., W.J. van Vliet & J.W. Verheij (1998). *Development of an indirect method for measuring the high frequency dynamic stiffness of resilient elements*. Journal of Sound and Vibration, 213(1), 1998, pp. 169–188.

[135] Thompson, M.R. and Q.L. Robnett (1979). *Resilient Properties of Subgrade Soils*. Transportation Engineering Journal, Vol. 105, No. TE1, 1979, pp. 71-89.

[136] Timoshenko, S., and Goodier, J.N. (1951). *Theory of Elasticity*. Mc Graw-Hill, Book Company Inc, New York

[137] Tomlinson, M. J. (1971), *Some Effects of Pile Driving on Skin Friction*, Proceedings of Conference on Behaviour of Piles, ICE, London, pp. 107-114.

[138] Tompai, Z. (2008). *Conversion between static and dynamic load bearing capacity moduli and introduction of dynamic target values*. Periodica Polytechnica 2008. www.pp.bme.hu/ci

[139] Transportation Research Board (2008). *Estimating Stiffness of Subgrade and Unbound Materials for Pavement Design, A Synthesis of Highway Practice*. NCHRP Synthesis 382. National Cooperative Highway Research Program, Transportation Research Board of the National Academies, Washington.

[140] UIC (1994), *Earthworks and Track-bed Layers for Railway Lines. UIC Code 719R*, International Union of Railways, Paris.

[141] Vesic A.B. (1963), *Beams on Elastic Subgrade and the Winkler's Hypothesis.* Proceeding of 5th International Conference of Soil Mechanics, 00. 845-850

[142] Vesic, A. S. (1977), *Design of Pile Foundations*, NCHRP Synthesis of Practice No. 42, Transportation Research Board, Washington, D.C., pp. 68.

[143] Vijayvergiya, V. N. & J. A. Focht (1972), *A New Way to Predict Capacity of Piles in Clay*, OTC Paper 1718, 4th Offshore Technology Conference, Houston, Texas.

[144] Vijayvergiya, V. N. (1977), *Load-movement Characteristics of Piles*, Proceedings, Port 77, ASCE, Vol II, pp. 269-286.

[145] Whitman, R. V. & F. E. Richart, Jr. (1967), *Design Procedures for Dynamically Loaded Foundations*. JSMFD, ASCE, Vol. 93, SM 6, Nov, pp. 169-193.

[146] Wikipedia (2016), *Hooke's Law*. Last revision: 14:03, 27 February 2016, Accessed: 22 March 2016. https://en.wikipedia.org/wiki/Hooke%27s_law

[147] Wikipedia (2016), *Newton's Method*. Last revision: 11:28, 16 March 2016, Accessed: 22 March 2016. https://en.wikipedia.org/wiki/Newton%27s_method

[148] Woods, R. D. (1986), *In Situ Tests for Foundation Vibrations*. 14th PSC, ASCE, pp. 336-375.

12. Appendixes

Appendix 1. Review of Analytical, Numerical and Empirical Methods of Railway Track Design

A.1.1. Classical Theories of Deflection and Stress Analysis of Railway Track

Zimmermann Model

Zimmermann in 1888 developed beam on elastic foundation (BOEF) method based on Winkler's model by transforming the discrete bearing areas of the elastic-pad and sleeper into continuously supported beam. This model utilizes *radius of relative stiffness* or often referred as well as *characteristic length* or *elastic length*, thus there is continuity of deflection and force relationship between the loaded and unloaded areas.

This method for ballasted track is illustrated in this figure:

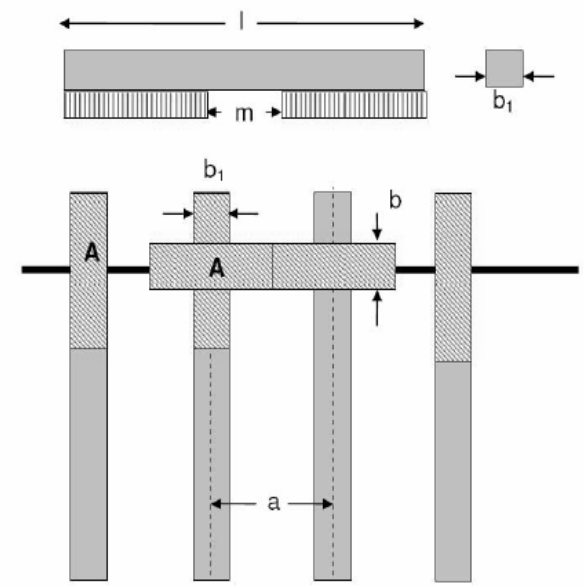

where:

l = length of sleeper

m= length of area without support

b_1= width of sleeper

An equivalent continuously supported area $F = (l-m)*b_1/2$ is transformed from connecting the support areas of adjacent sleepers. Then it comes to a theoretical continuously supported rail. The length of this transformed area is the sleeper spacing a, thus the width of this transformed area is $b = F/a$. [17]

Note: picture courtesy of Steidl (2007)[128]

Figure 141. The concept of Zimmermann theory

Zimmermann calculation method is described as follows[17]:

- for ballasted track system: *[17]* $$L = \sqrt[4]{\frac{4.E.I}{b.C}}$$ *Eq. 107*
- for ballastless track system: *[17]* $$L = \sqrt[4]{\frac{4.E.I.a}{k}}$$ *Eq. 108*

where: L is the radius of relative stiffness, E is the modulus elasticity [N/mm^2] and I is the area moments of inertia of rail beam [mm^4]. For ballasted track application: b is the width of transformed area of the sleeper [mm] and C is the total stiffness combination of elastic-pads, ballast, intermediate layers (if applied, e.g. frost protection layer, sub-ballast-mat) and soil subgrade reaction [N/mm^3]. For concrete slab track application, a is the support spacing or elastic-pads spacing [mm] and k is the stiffness of elastic-pad [N/mm].

Zimmermann calculation employs line of influence to distribute a single load act on the top of rail into reaction forces (rail-seat loads) at the elastic-pads by using influence factor of deflection (η) and influence factor of bending moment (μ):

[17] $$\eta = \frac{\sin\xi + \cos\xi}{e^{\xi}} \qquad \textit{Eq. 109}$$

[17] $$\mu = \frac{-\sin\xi + \cos\xi}{e^{\xi}} \quad where \quad \xi = \frac{x}{L} \qquad \textit{Eq. 110}$$

and x is the distance between point of interest and the location of the applied load, while L is the characteristic length.

The rail deflection y activates the contact pressure between rail and sleeper. This contact pressure gives a rail-seat load. The deflection line and rail-seat load can be defined by:

- for ballasted track system:

[17] $$y = \frac{Q}{2.b.C.L}.\eta \qquad \textit{Eq. 111}$$

[17] $$S = b.a.C.y \qquad \textit{Eq. 112}$$

- for ballastless track system:

[17] $$y = \frac{Q.a}{2.k.L}.\eta \qquad \textit{Eq. 113}$$

$$S = k.y \qquad \textit{Eq. 114}$$

and bending moment and the bending tensile stress in the middle of the rail is:

[17] $$M = \frac{Q.L}{4}\mu \qquad \textit{Eq. 115}$$

[17] $$\sigma = \frac{M}{Wx} \qquad \textit{Eq. 116}$$

where: Q is the load applied on the top of the rail [N] and W_x is the section modulus (static moment) of the rail [mm^3].

The maximum deflection is located under the applied load, where η value is equal to 1. Therefore, if the deflection is limited in certain value, the minimum track stiffness (ballasted) or elastic-pad stiffness can be defined as follow:

- for ballasted track system:

$$C_{min} = \frac{1}{4b} \cdot \sqrt[3]{\frac{\left(\frac{Q}{y_{max}}\right)^4}{E.I}} \qquad \textit{Eq. 117}$$

- for ballastless track system:

$$k_{min} = \frac{1}{4} . a . \sqrt[3]{\frac{\left(\frac{Q}{y_{max}}\right)^4}{E.I}} \qquad \textit{Eq. 118}$$

What is shown from the Zimmermann formulation is that the softer the elastic-pads stiffness, the wider load is distributed but the more deflection on the rail.

The main advantage of this model is the continuous relationship between force and deflection. In addition, due to the application of radius relative stiffness in this method, it makes possible to obtain reaction force and deflection at any point, especially at every elastic-pad/sleeper position, which is more interesting for railway engineers for further analysis. Furthermore, it can take into account the influence of longitudinal neighboring loads as well.

The main deficiencies of Zimmermann model are:

- The linear elastic, homogenous and isotropic idealization of soil
- Although can be analyzed separately, normally it uses a total stiffness value for overall elastic supports (elastic-pads, ballast, and soil)
- Model fits for one dimensional problem, therefore this approach is not able to analyze the real impact coming from the transverse neighboring rail beam.

Westergaard Method

Westergaard (1926, 1938) developed fracture tensile analysis for concrete slab. Similar to Boussinesq, this solution based on assumption of a homogenous, isotropic, and elastic slab resting on an ideal subgrade. Yet, Westergaard uses an assumption of infinite slab. Westergaard solutions have been extensively applied as basic model for many designs, especially for concrete pavement[2].

However, this solution has some limitations:

- It assumes that the elastic media are rigid in the lateral direction, and allows only vertical pressure for enforced stress[2].

- Only available for particular loading acting on slab: at the center, corner and edge.
- Based on infinite slab assumption which is not realistic for practical solution. According to Fwa et al. (1996) when the slab length is four time greater than its radius of relative stiffness, then this approach is not appropriate[44].

Westergaard (1926) solution utilizes formulation of radius of relative stiffness *L* as follow:

[17]
$$L = \sqrt[4]{\frac{E.h^3}{12.k(1-\mu^2)}} \qquad \textit{Eq. 119}$$

where: *E* is modulus of elasticity [MPa], *h* is the thickness [mm], and μ is Poisson's ratio of concrete; *k* is modulus reaction of subgrade [N/mm^3].

According to Westergaard, the maximum bending tensile stress due to circular load on the center of the slab is defined by[17]:

[17]
$$\sigma_c = \frac{0.275.Q}{h^2}(1-\mu)\left[log\left(\frac{E.h^3}{k.{b_r}^4}\right) - 0.436\right] \qquad \textit{Eq. 120}$$

And the maximum deflection due to circular load area on the top of the slab[57]:

[57]
$$y = \frac{Q}{8k.L^2}\left\{1 + 0.159\left(\frac{r}{L}\right)^2\left[ln\left(\frac{r}{2L}\right) - 0.673\right]\right\} \qquad \textit{Eq. 121}$$

Westergaard's stress pot distribution due to thickness of the concrete slab:

[17]
$$\begin{gathered} if\ r < 1.724h\ then\ b_r = \sqrt{1.6r^2 + h^2} - 0.675h \\ if\ r > 1.724h\ then\ b_r = r \end{gathered} \qquad \textit{Eq. 122}$$

where: *Q* is the applied circular load [N] with radius of *r* [mm]; *E* is modulus of elasticity [MPa], μ is Poisson's ratio, and *h* is thickness [mm] of concrete slab; b_r is the radius of load distribution in the bottom of the concrete slab [mm], see Eq. 122; and *k* is modulus of subgrade reaction [N/mm^3].

Westergaard solution also gives charts of line of influence of moment (λ) and deflection (γ), which can be seen in the Appendix 2. Then moments and deflections out of the load location can be computed using these formulas [17]:

$$M_i = \lambda_i Q \qquad \textit{Eq. 123}$$

$$y_i = \gamma_i \frac{Q}{k.L^2} \qquad \textit{Eq. 124}$$

Odemark Method

Boussinesq and Westergaard developed method of stress calculation for a single homogenous layer. For a multi-layer system, Odemark introduced a method, also known as the *Method of Equivalent Stiffness* (MET), to transfer multi-layer system into single layer semi-half-space. Thus single value of stiffness and equivalent thickness are designated, which is based on the ratio of the thickness, stiffness and Poisson's ratio values of the top layers relative to the bottom layer[45]. Therefore, using Odemark's MET, the Boussinesq and Westergaard methods can be extended to solve stress distribution on a multilayer system. The formulation of Odemark of equivalent thickness function is:

[45]

$$\frac{{h_i}^3.E_i}{1-{\mu_i}^2} = \frac{{h_e}^3.E_1}{1-{\mu_1}^2} \; or \; h_e = h_i.\sqrt[3]{\frac{E_i.(1-{\mu_1}^2)}{E_1.(1-{\mu_i}^2)}} \qquad Eq.\ 125$$

where: h_e is equivalent thickness [mm], h_i is thickness [mm], E_i is modulus of elasticity [MPa], μ_i is Poisson's ratio of layer *i*; and $E_1$is modulus elasticity [MPa], μ_1 is Poisson's ratio of layer 1 (bottom).

A.1.2. Ultimate Limit State Design Criteria

Ultimate limit state method in structural engineering takes into account a condition of a structure until it closely reaches the boundaries of the design criteria (e.g. limit of fracture, fatigue, crack). This method may include the combination of analytical, empirical methods as well as design correction and safety factors, which may come from the personal judgment of the engineers based on their experience.

In the railway track design, the structural limit state design criteria are mainly pointed to the limit criteria of:

- strength of prefabricated elements against fatigue, fracture, crack or buckling (e.g. rail profile, fastening system, precast concrete),
- strength of bounded trackbed (track pavement) materials against crack, flexural and fatigue damages (e.g. concrete or asphalt pavement); and
- maximum allowable pressure stress, shear stress or deflection against excessive settlement and plastic deformation of unbound materials (e.g. granular materials: ballast stones, or fine materials: embankment, subsoil layers).

Flexural Fatigue Strength Limit Criteria of Rail

The limit criteria of the rail might be defined by using *Flexural Tensile Fatigue Model* of Wöhler. It considers the maximum allowable oscillating stress due to impact of residual stress, temperature difference as well as corrosion on the rail. A residual stress is generated during the differential cooling of rail head, web and foot and rail straightening procedures during the production. Usually, to consider this, a constant stress value of 80 MPa is used and the stresses caused by temperature difference are also taken into account. Thus, the constant minimum stress σ_u by temperature change can be determined by this [17]:

[17]

$$\sigma_u = \sigma_T + 80 = E.\alpha.\Delta T + 80 \ [MPa], \quad \text{for steel rail: } \sigma_u = 2.52\Delta T + 80 \qquad \textit{Eq. 126}$$

where: ΔT is the temperature changes. The allowable oscillating stress σ_d on the rail is determined by using this chart on Figure 142 or a proximally using linear regression Eq. 127 and Eq. 128:

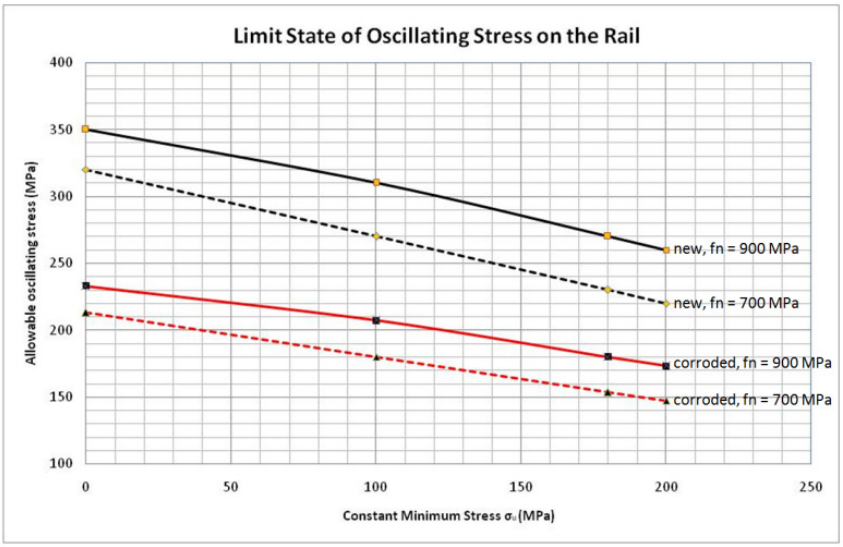

Figure 142. Limit state criteria of oscillating stress on the rail (after [17])

Allowable oscillating stress on the rail:

for a new rail:

$$\sigma_d = -0.48\sigma_u + 0.19f_n + 185.85 \qquad \textit{Eq. 127}$$

and for a corroded rail:

$$\sigma_d = -0.32\sigma_u + 0.13f_n + 123.98 \qquad \textit{Eq. 128}$$

where: f_n is the nominal strength of the steel rail (MPa).

Flexural Fatigue Strength Limit Criteria of Concrete Elements

For concrete track components, such as CRCP and CTB layer of ballastless track system, the limit state criterion of stress can be estimated by using the Smith's fatigue model. This approach superposes the loading cases as a combination of traffic and temperature loads by taking into account the bending strength of concrete under cyclic loading as it is formulated in this equation (Eisenmann & Leykauf, 2003)[37], quoted from [31]:

[31] [37]

$$\sigma_{max} = f'_t \left[(log(N) - 2) \left(\frac{0.0875\sigma_w}{f'_t} - 0.07 \right) + 0.8 \right] - \sigma_w \qquad \textit{Eq. 129}$$

where: f'_t (also often referred as β_{BZ} in German standard) is the bending tensile strength of the concrete [MPa], σ_w is the minimum constant stresses [MPa] due to temperature change and N is the number of load cycles $\leq 2\text{x}10^6$ based on laboratory fatigue test. In the design and field application in Germany and Central Europe, N can be taken as 5% of the total traffic during the service life of the track [17]. However, in other cases or countries, this might be different, which depends on different nature and climate conditions as well as different constraints.

The strength parameters of concrete for structural analysis are normally modulus elasticity, Poisson's ratio, compressive strength and flexural tensile strength. Many design standards categorize concrete group based on its compressive strength. The best way to get accurate strength parameters is by doing laboratory tests. However, some researchers and design standards had made empirical prediction models of those parameters. FHWA (2012)[40] summarized the works from some researchers and design standards as described in the Table 34 and Table 35 in the Appendix 3.

The calculation of the curling stresses generated due to temperature changes of full restraint concrete slab may follow the approach suggested e.g. by Westergaard-Bradbury (1938) and Einsenmann (1979), as it is shown in this formula [17][125]:

[17][125] $$\sigma_w = \frac{1}{1-\mu}.\frac{\alpha.E.\Delta t}{2}.h$$ *Eq. 130*

Eisenmann (1979)[35]studied the warping stresses at the bottom of a simply supported beam due to positive temperature gradient of thermal load and showed a critical length (L_{crit}). The longer the slab the higher warping stress up to this L_{crit}, but this stress then remains almost the same above this L_{crit} as formulated below[17][125][111]. Due to dimension/shape factor of the slab, the criterion for critical length may be reduced into $0.9L_{crit}$ for a quadratic slab, where $0.8 \leq Length/Width \leq 1.2$ and *slab's length (or width respectively)* $< 0.9L_{crit}$[17].

[17] $$L_{crit} = h.\sqrt{\frac{4.\alpha.E.\Delta t}{5.(1-\mu).\gamma}}$$ *for a positive temperature gradient* *Eq. 131*

[17] $$\sigma_w' = (1.2)\sigma_w \qquad if\ L > 0.9L_{crit}$$ *Eq. 132*

[17] $$\sigma_w'' = \sigma_w\left[\frac{L}{L_{cr}}\right]^2 \qquad if\ L \leq 0.9L_{crit}$$ *Eq. 133*

where: Δt is the temperature gradient [K/mm], α is the thermal expansion coefficient [K^{-1}], μ is the Poisson's ratio [-], E is the Young's modulus [MPa], h is the thickness [mm] and γ is the dead load per unit length of concrete [N/mm].

Eisenmann and Leykauf (1990) investigated further the effect of thickness, joint spacing and support condition[34]. Regarding the positive temperature gradient, an uplift deflection occurs. This uplift leads to a contact loss between the slab and the subgrade. Hence, slab is only supported by its ends through a support length of[125]:

[125] $$L' = L - 3\sqrt{\frac{h}{k.\Delta t'}}$$ *Eq. 134*

where: k is the modulus subgrade reaction [N/mm^3].

The negative temperature gradient is the source of concave curling on concrete slab. The calculation of this stress follows the Eq. 130 above. The critical length for negative temperature gradient is given by this formula[17]:

[17] $$L_{crit(-)} = h.\sqrt{\frac{2.\alpha.E.\Delta t}{3.(1-\mu).\gamma}}$$ *for a negative temperature gradient* *Eq. 135*

Fatigue Limit Criteria for Granular Material, Subgrade and Subsoil

The distributed stresses from the traffic load and superstructure part should be reduced to the subgrade layer under the limit of its bearing capacity. The criteria in the static design is mainly taken at the maximum stress or strain at the soil's surface to guarantee certain safe limit against disproportionate plastic deformation and settlement after cyclic loading during the service.

A conventional approach, e.g. fatigue model after Heukelom and Klomp (1962), is still frequently used to approximate the mechanistic failure of granular materials of trackbed (ballast, subgrade or protection layer), asphalt and soil layers under a cyclic loading. This method was initially developed to analyze the fatigue due to cyclic loading on an asphalt pavement. Although this mechanistic failure model is simple, but it is quite useful to make general consideration in the practical application in railway track design. This approach gives suggestion of the allowable pressure limit (P_{allow}) of the substructure layer by only considering the property of dynamic modulus of the material (E_{dyn}) and the number of load cycles (N), as can be seen here[70]:

[17] $$P_{allow} = \frac{0.006E_{dyn}}{1 + 0.7log(N)}$$ *Eq. 136*

Appendix 2. Westergaard's Influence Lines of Moments and Deflection

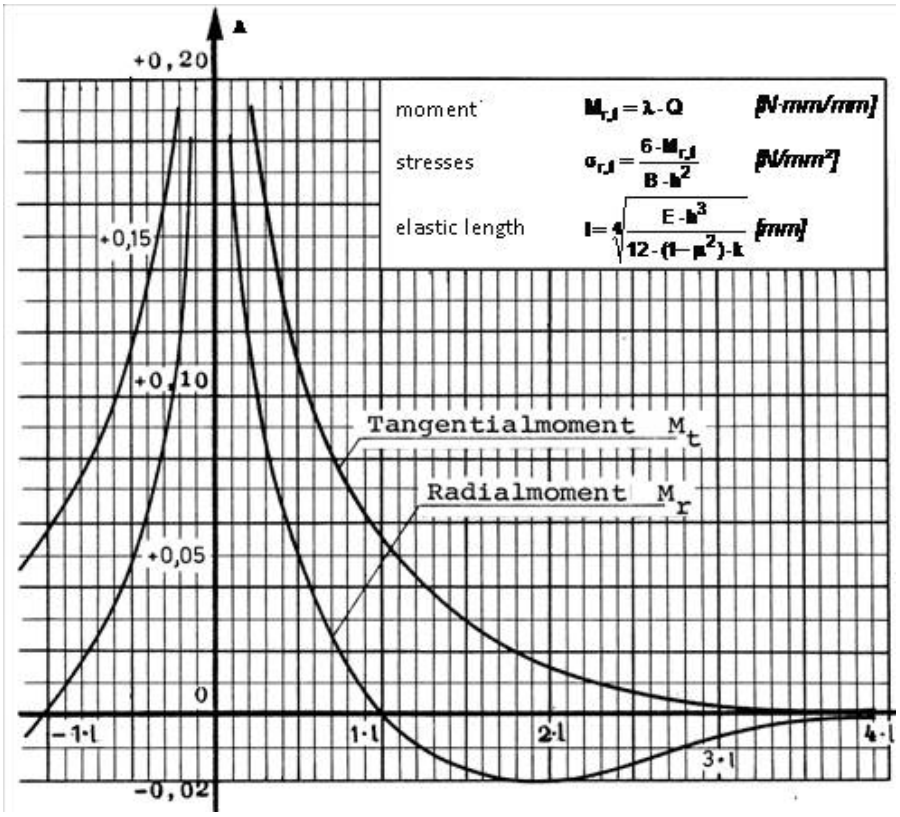

Figure 143. Westergaard's influence line of moments

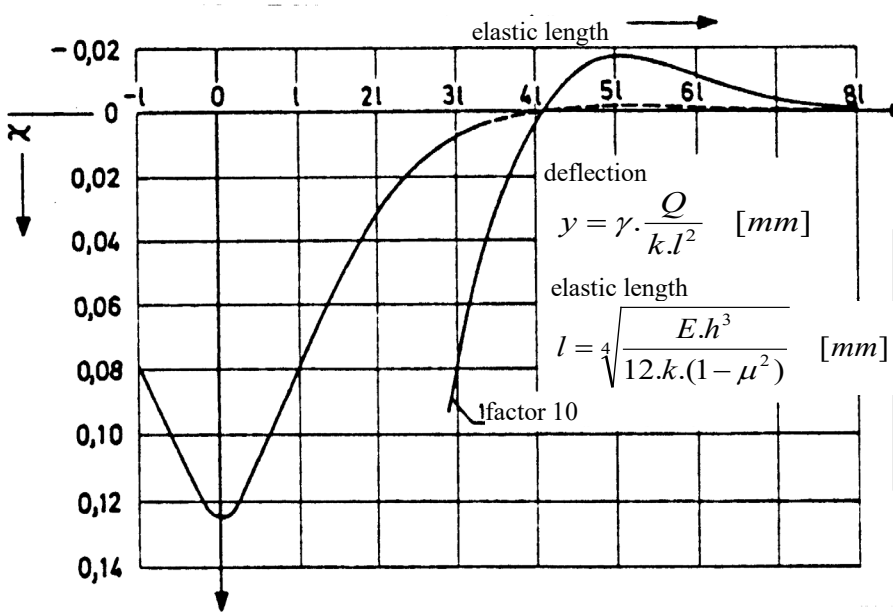

Figure 144. Westergaard's influence line of deflection

Appendix 3. Prediction Models of Flexural Strength, Tensile Strength and Modulus of Elasticity of Concrete

Table 34. Prediction models of flexural strength/modulus of rupture (MR) and tensile strength (f'_t) of concrete (all unit in MPa)

Equation	Parameter	Author
$MR = a * (f'_c)^b$	a = 0.747; b = 0.5	Wood, S.L. (1992)
	a = 0.623; b = 0.5	Namyong, J., et.al (2004)
	a = 0.689, b = 0.5	Teychenne, D.C. (1954)
	a = 0.797, b = 0.5	The Concrete Society (2003)
	a = 0.972, b = 0.5 for high-strength mixes	Carrasquillo, R.L., et.al. (1981)
	a = 0.855, b = 0.4543	Wang, K. et.al. (2008)
	a = 0.055, b = 0.66	CEB-FIP (1993)
	a = 0.484, b = 0.66	Lageron, F. & Paultre, P. (2000)
$f'_t = a * (f'_c)^b$	a = 0.462, b = 0.55	Mindess, S. & Young, J.F. (1981)
	a = 0.530, b = 0.7	Neville, A.M. (1996)
	a = 0.590, b = 0.5 for high-strength mixes	Iravani, S. (1996)
	a = 0.258, b = 0.7068	Wang, K., Zhi, G.E. (2008)
	a = 0.56, b = 0.67	CEB-FIP (1993)
	a = 0.30, b = 0.67 for mean tensile strength $f'_{t,m}$, lower value $0.7f'_{t,m}$, upper value $1.3f'_{t,m}$	EN1992-1-1

Note: Summarized from FHWA (2012)[40] and EN1992-1-1[38]

Table 35. Prediction models of modulus of elasticity of concrete (all unit in MPa) (summarized from FHWA (2012) *and EN1992-1-1)*

Equation	Parameter	Author
$E_c = a * (f'_c)^b$	a = 4732.98; b = 0.5	Namyong, J., et.al (2004)
	a = 9817.24; b = 0.33	CEB-FIP (1993))
	a = 5251.29, b = 0.46	Kim, J-K., et.al. (2002)
	a = 5662.70, b = 0.4659	Wang, K., Zhi, G.E. (2008)
$E_c = 0.043\ \rho^{1.5}(f'_c)^{0.5}$	ρ = unit weight [kg/m^3]	ACI 318
$E_c = 9500(f'_c + 8)^{0.33}$		EN1992-1-1

Note: Summarized from FHWA (2012) [40] and EN1992-1-1[38]

Appendix 4. Example Calculation of CZW Methods

1) Dynamic Amplification Factor:

Example G

Table 36. Track quality factor δ

Track quality	Acc. to Eisenmann	Acc. to Deutsche Bahn AG	
	δ	Track condition	δ
Very good	0.1	New main lines, rehabilitated main lines	0.1
Good/moderate	0.2	Trunk lines, commuter lines	0.15
Bad/poor condition	0.3	Other main lines	0.2
Very bad		Other tracks	0.25

Note: source [17]

The values η are the factor regarding the speed V [km/hour], which are suggested as follow:

- η = 1, for train speeds up to 60 km/hour
- $\eta = 1 + \frac{V - 60}{140}$, for train speeds from 60 up to 200 km/hour

Other recommended values η: [17]

- $\eta = 1 + \frac{V - 60}{380}$, for passenger train, but only for speed which results φ ≥ 1 or speed ≥ 60 km/hour
- $\eta = 1 + \frac{V - 60}{160}$, for freight train.

Meanwhile t is the values, which depends on the upper confident limit (UCL), which is suggested in the following table:

Table 37. Coefficient of variation t

UCL (%)	Acc. to Eisenmann	From measurement on high speed line Mannheim-Stuttgart*
50.0	0	
68.3		1
84.1	1	
90.0		1.65
95.0		1.96
97.7	2	
99.7		3
99.9	3	

Note: source [17]

Then the maximum deflection (y) or stress (σ) or rail-seat load (S) can be defined by:

$$\sigma_{\max} = \sigma_{mean}.\varphi = \sigma_{mean}(1 + \delta.n.t)$$

Track in the good condition, δ = 0.2

Speed up to 250 km/hour: $\eta = 1 + \frac{V - 60}{380} = 1 + \frac{250 - 60}{380} = 1.5$

UCL = 95%, then t = 1.96

$$\varphi = 1 + \delta.\eta.t = 1 + 0.2 * 1.5 * 1.96 = 1.59 \approx 1.6$$

2) Flexural Fatigue Strength Limit Criteria of Rail (Wöhler)

Example H

ΔT = 40 K, maximum rail heating against neutral temperature of 20°

ΔT = 40 K, maximum rail cooling against neutral temperature, hence:

$$\sigma_u = 2.52\Delta T + 80 = 2.52(50) + 80 = 180.8 \ N/mm^2$$

New rail with a nominal strength of 900 MPa:

$\sigma_{d,allow} = -0.48\sigma_u + 0.19f_n + 185.85 = -0.48(180.8) + 0.19(900) + 185.85 = 270.07\ MPa$

Corroded rail with a nominal strength of 900 MPa:

$\sigma_{d,allow} = -0.32\sigma_u + 0.13f_n + 123.98 = -0.32(180.8) + 0.13(900) + 123.98 = 183.12\ MPa$

3) Flexural Fatigue Strength Limit Criteria of Concrete Slab

Example I

The thickness-dependent temperature gradients are estimated according to Eid (2012) [31]:

Positive temperature gradient: [31]

$$\Delta t = \frac{0.191}{e^{0.0028h}} \qquad \textit{Eq. 137}$$

Negative temperature gradient: [31]

$$\Delta t = \frac{-0.370}{e^{0.022h}} - 0.035 \qquad \textit{Eq. 138}$$

where: h is the thickness of the concrete [mm].

For this example, 24-cm concrete, the temperature gradients are Δt = 0.098 (summer) and 0.037 (winter) and respectively Δt = 0.082 (summer) and 0.036 (winter) for 30-cm concrete slab.

Thermal expansion coefficient $\alpha = 1.2\text{x}10^{-5}$. Poisson's ratio of concrete: 0.15

For example, concrete C35/45 is taken. According to EN1992-1-1[38]: $f'_c = 35$ MPa. Modulus of elasticity of the concrete is 34 GPa. Taking into account EN1992-1-1[38] empirical approach, the mean flexural strength of concrete is then:

$$f'_t = 0.3 * \left(f'_c\right)^{0.67} = 0.3 * (35)^{0.67} = 3.2\ MPa$$

Maximum constant thermal stress on and critical length of a semi-infinite slab (see Eq. 130, Eq. 131 and Eq. 135, pp. 223-224):

Table 38. Maximum constant thermal stress and critical length of concrete slab

Thickness	h = 24 cm		h = 30 cm	
Season	Summer	Winter	Summer	Winter
σ_w [MPa]	5.7	2.2	6.1	2.6
L_{crit} [m]	9.7	5.4	11.1	6.7

The mean crack spacing of a CRCP can be predicted using the empirical approach from AASHTO (1993)[1]:

$$\bar{x} = \frac{1.32\left(1 + \frac{f_t}{1000}\right)^{6.70}\left(1 + \frac{\alpha_s}{2\alpha_c}\right)^{1.15}(1 + \emptyset)^{2.19}}{\left(1 + \frac{\sigma_w}{1000}\right)^{5.20}(1 + P)^{4.60}(1 + 1000Z)^{1.79}} \qquad \textit{Eq. 139}$$

where: f_t is concrete tensile stress at 28 days [psi], α_s/α_c is ratio of the steel thermal coefficient to concrete thermal coefficient [-], ϕ is steel bar diameter [in], σ_w is wheel load stress [psi], P is cross sectional amount of steel as percentage of cross sectional slab area [%] and Z is concrete shrinkage coefficient [-].

For the given data of f_t = 3.2 MPa, α_s/α_c = 1.04, ϕ = 20 mm, σ_w = 3 MPa, P = 0.8% and Z = 0.00035 then the maximum crack spacing is predicted 2.6 m.

Correction of thermal stress due to finite slab length of 2.6 m (see Eq. 132 and Eq. 133, pp. 223) and the allowable stress of concrete due to thermal and traffic loadings (Eq. 129, pp. 222) are:

Table 39. Correction of thermal stress and allowable stress of concrete

Thickness	h = 24 cm		h = 30 cm	
Season	Summer	Winter	Summer	Winter
σw" [MPa]	0.41	0.50	0.33	0.40
σ_{allow} [MPa]	**1.61**	**1.55**	**1.67**	**1.62**

For other values for different slab thickness are calculated in the programmed spreadsheet.

Appendix 5. Design Charts of Trackbed Thickness Design

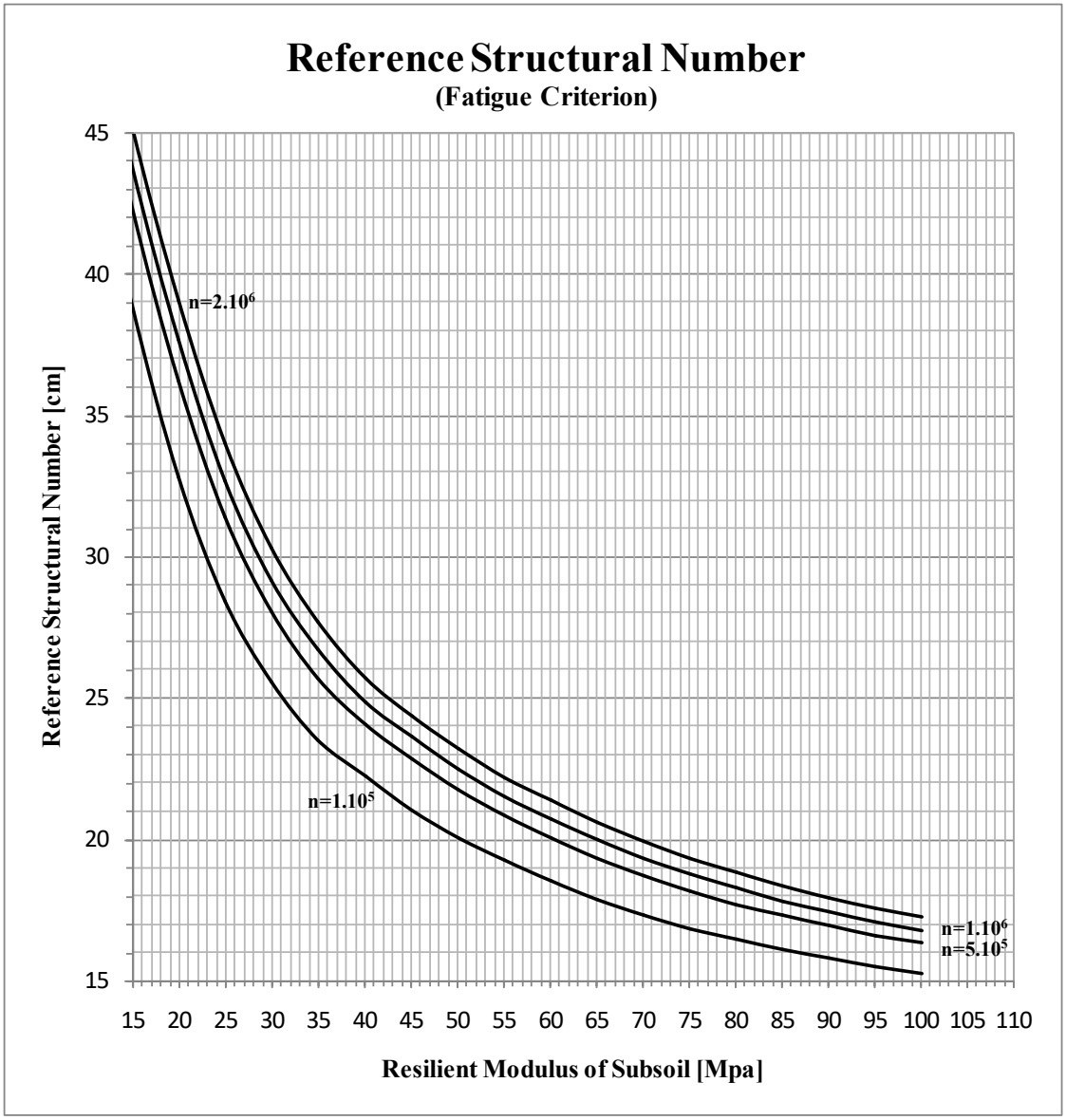

Figure 145. Reference structural number of trackbed thickness design using soil fatigue criterion up to 2 million load cycles

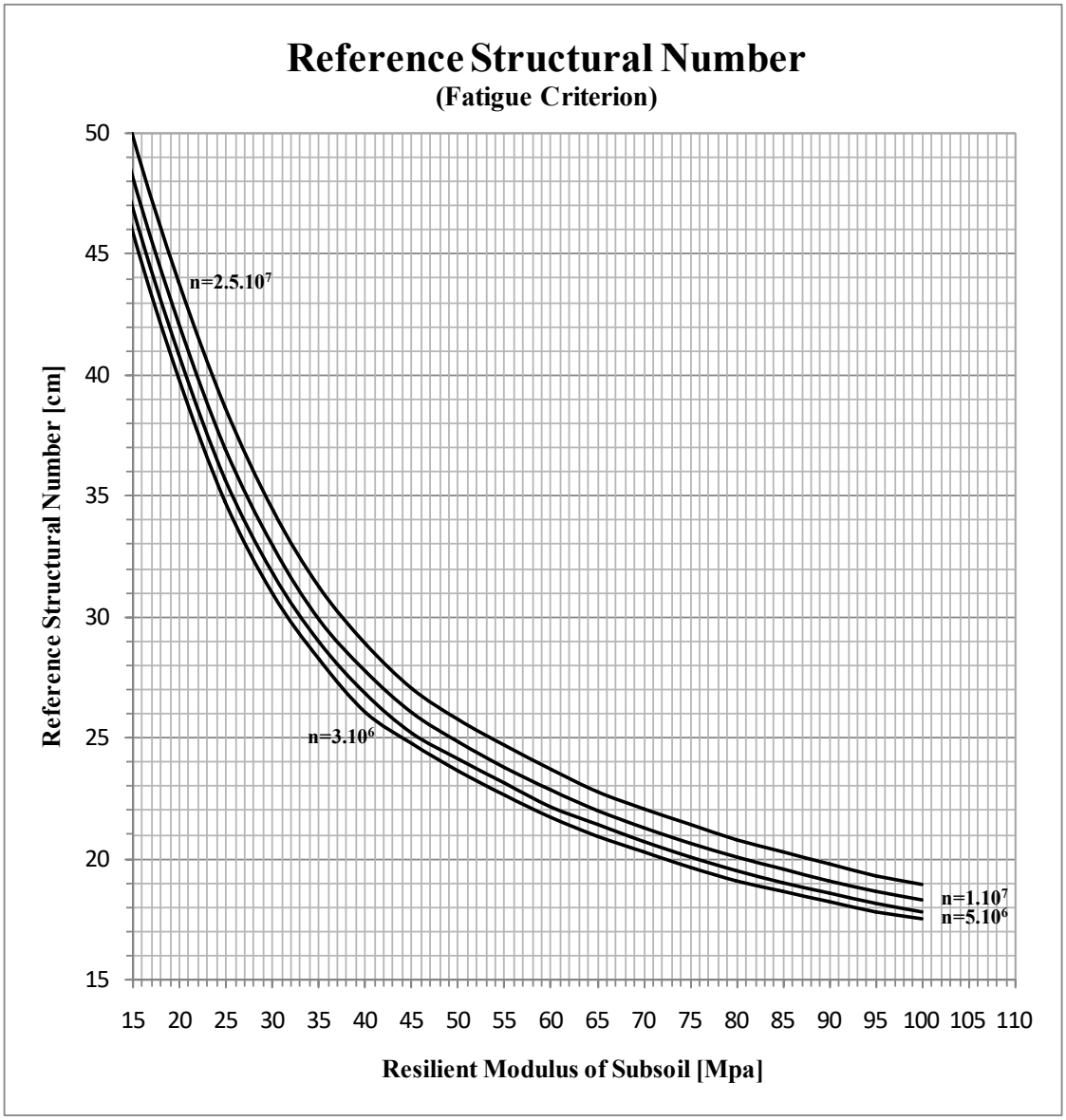

Figure 146. Reference structural number of trackbed thickness design using soil fatigue criterion from 3 million to 25 million load cycles

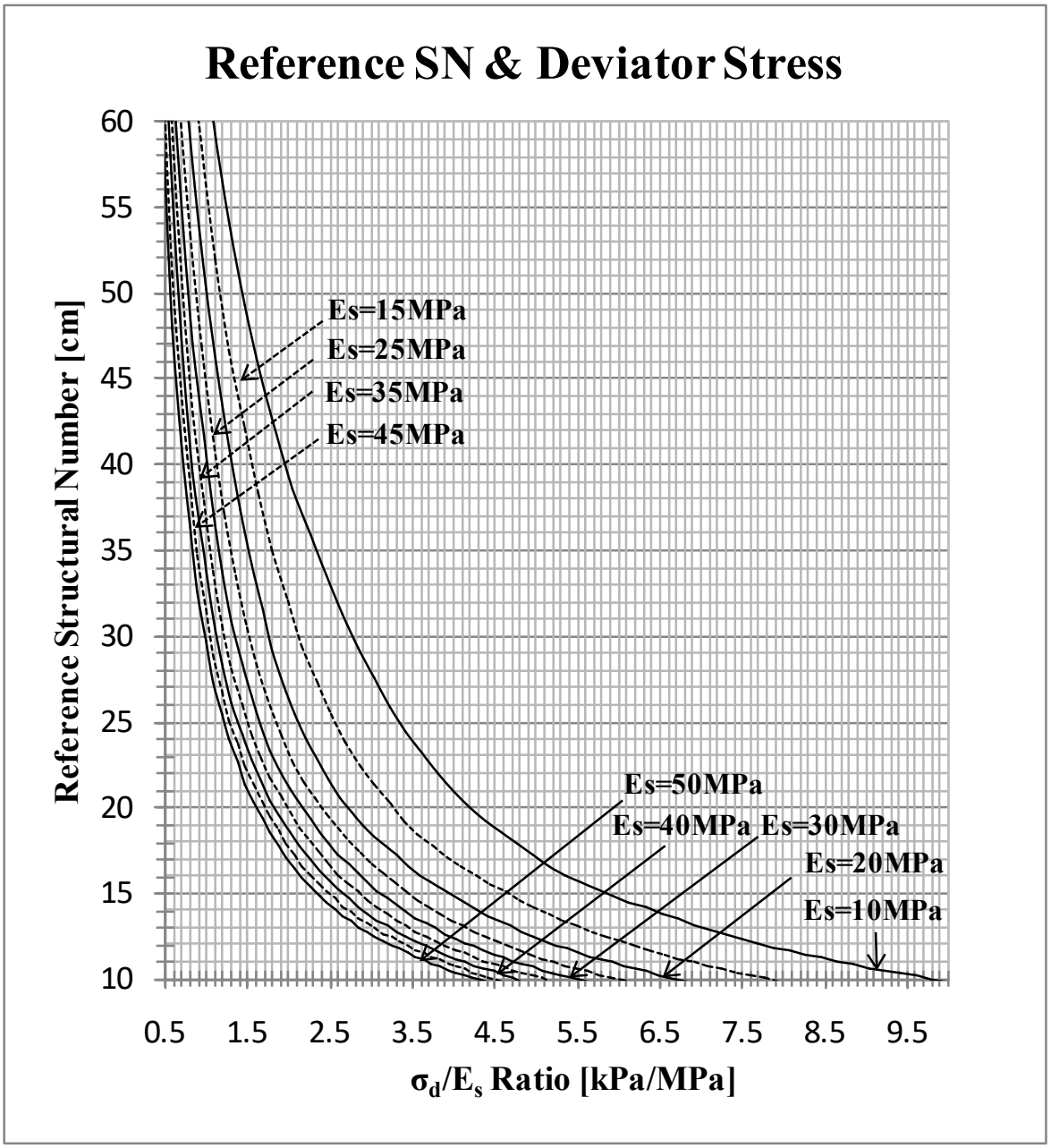

Figure 147. Reference structural number of trackbed thickness design and deviator stress level of soft to moderate soils

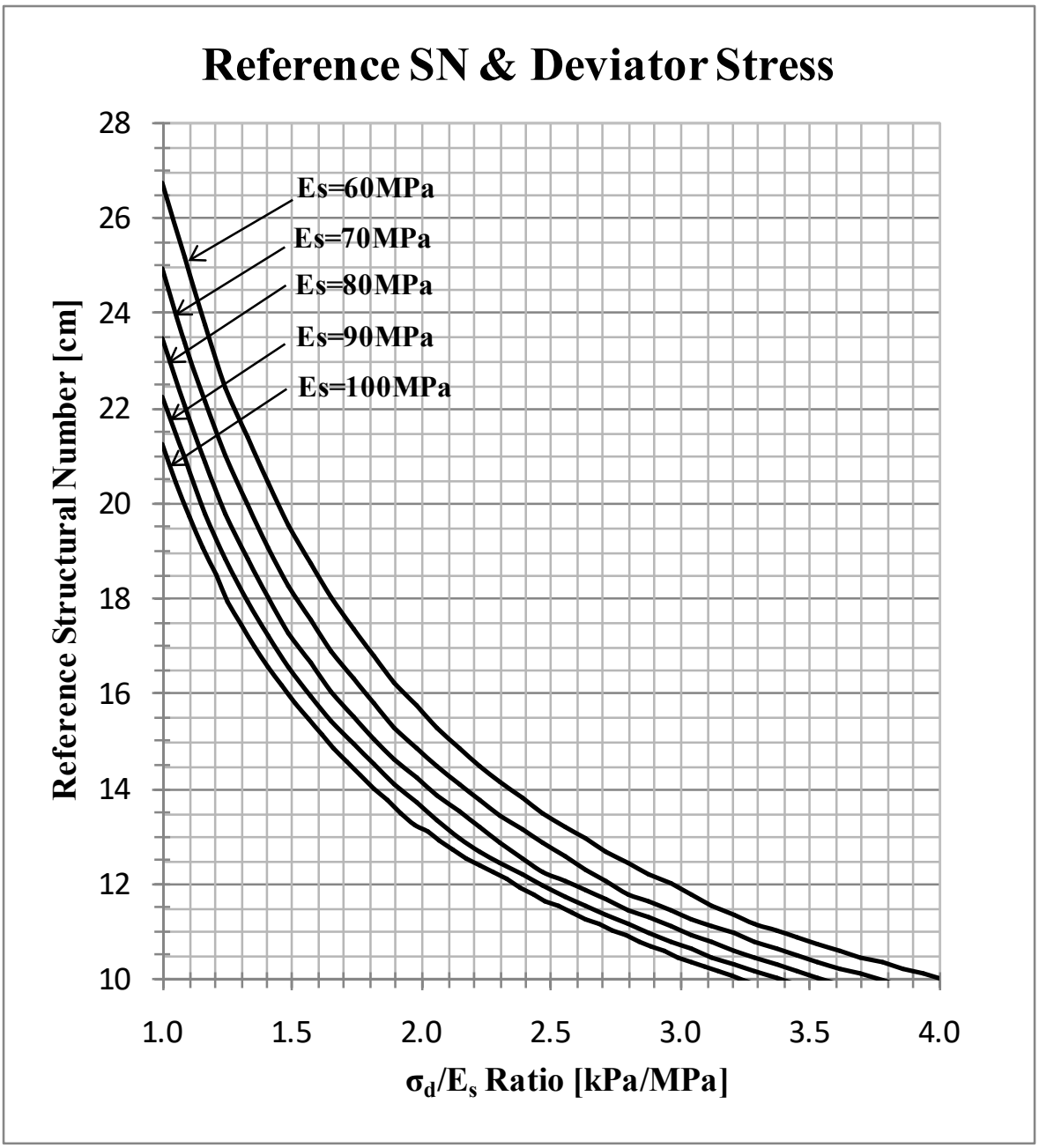

Figure 148. Reference structural number of trackbed thickness design and deviator stress level of moderate stiff soils

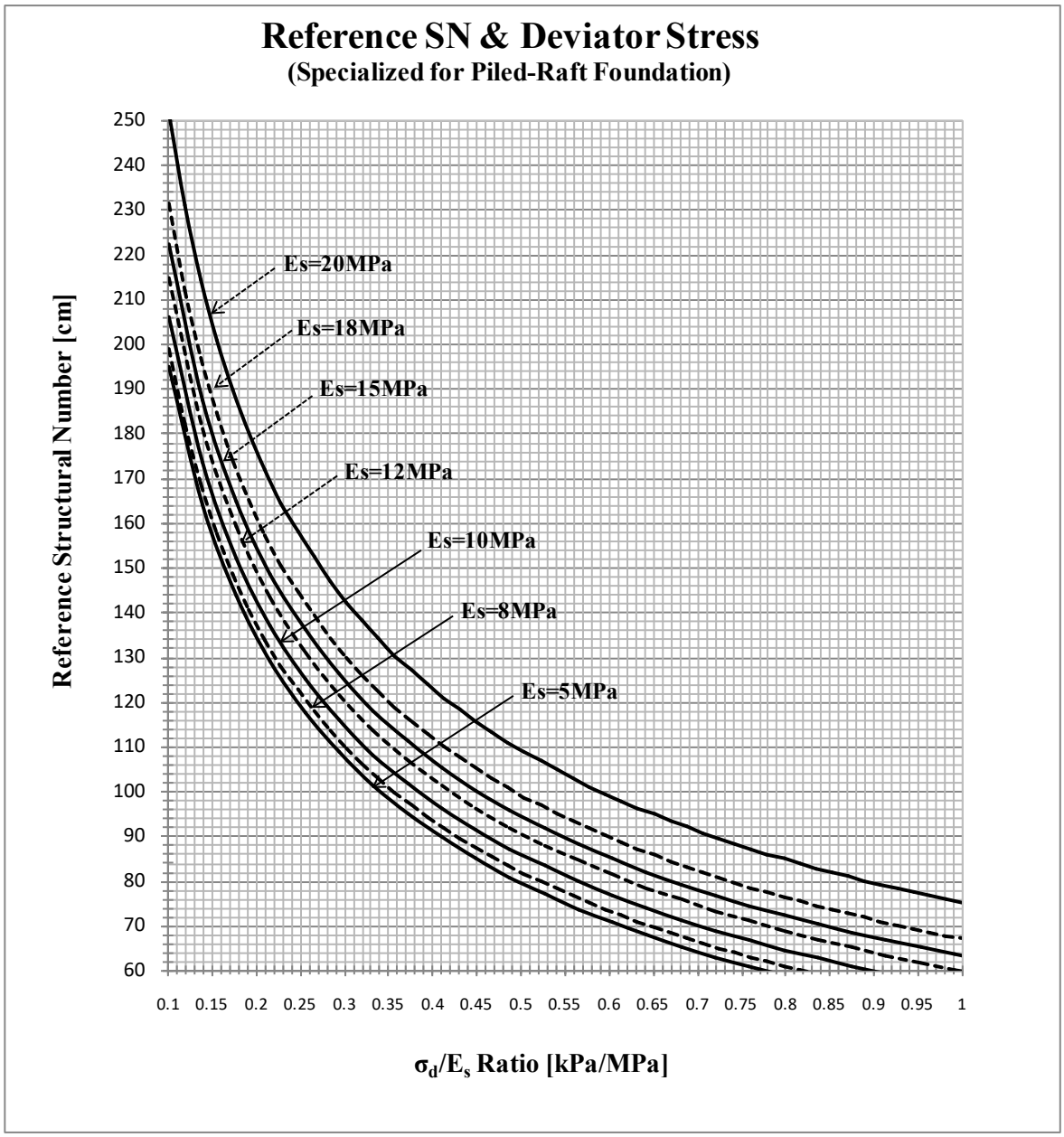

Figure 149. Reference structural number of trackbed thickness design and deviator stress specialized for piled-raft foundation

Appendix 6. Examples of Trackbed Thickness Calculation

A.6.1. Calculation of Design Factors of Trackbed for Static Analysis

Example J

- Train's design speed 250 km/hour, gives dynamic amplification factor (DAF) of f_d = **1.6** (see Appendix 4 for more detail)
- Wheel load distribution factors of inner and outer rail: $f_{c,i}$= 1.2 and $f_{c,j}$= 0.8 give ratio of $f_c\ Ratio = \frac{f_{c,i}}{f_{c,j}} = \frac{1.2}{0.8} = 1.5$
- Design factor of deflection, from Figure 24 with f_c Ratio = 1.5, then it is obtained $f_{c,d}$ = **1.2**
- Wheel load of 125kN gives f_Q = **1.0**
- Ballastless track system:
  - × Rail profile 60E2 (E = 2.1x10^5 and I = 30.55x10^{6}mm^4), elastic-pad spacing of 65 cm and elastic-pad stiffness of 40 kN/mm give:

    $$L_r = \sqrt[4]{\frac{4.E.I.a}{k_{rp}}} = \sqrt[4]{\frac{4*2.1x10^5*30.55x10^6*650}{40x10^3}} = 803.6mm$$

  - × $f_{Lr}\ Ratio = \frac{L_r}{928} = \frac{803.6}{928} = 0.87$ and from Figure 25, gives f_{Lr}= **1.12**
  - × $DF = f_Q * f_d * f_{c,d} * f_{Lr} = 1 * 1.6 * 1.2 * 1.12 = \mathbf{2.15}$
- Ballasted track system:
  - × Rail profile 60E2 (E = 2.1x10^5 and I = 30.55x10^{6}mm^4), elastic-pad spacing of 60 cm and elastic-pad stiffness of 22.5 kN/mm (the same as reference values) give f_{Lr}= **1.0**
  - × $DF = f_Q * f_d * f_{c,d} * f_{Lr} = 1 * 1.6 * 1.2 * 1.0 = \mathbf{1.92}$

To compare this method with FEA simulation results, an adjustment factor is added to the structural number design. An example of adjustment factor (AF) = 2, then structural number design:

$$SN_{des\ (ballastless)} = AF * DF * SN_{ref(chart)} = 2 * 2.15 * SN_{ref(chart)} = 4.3 * SN_{ref(chart)}$$

$$SN_{des\ (ballasted)} = AF * DF * SN_{ref(chart)} = 2 * 1.92 * SN_{ref(chart)} = 3.8 * SN_{ref(chart)}$$

Examples of structural number calculation using AF = 2.0; 1.5; 1.2; 1.0 and above multiplication factors are shown in the next section of this appendix.

A.6.2. Structural Number Calculation

Example K

Calculation of reference structural number using Heukelom & Klomp fatigue criterion

- Design traffic is for 2 million load cycles (heavy traffic line) with wheel load 125 kN (a proximally 25 tons of axle load). When a train assumed has 2 cars and 4 axles in a car then the traffic tonnage is a proximally 400 MGT during the service time.
- Reference structural numbers of different subsoil bearing capacity levels:

Table 40. Examples of reference Structural Number considering Heukelom & Klomp criterion

SN / Es	15 MPa	20 MPa	35 MPa	45 MPa	50 MPa	60 MPa	80 MPa
SN_{reff} [cm]	44.7	39	27.7	24.3	23.2	21.4	18.8

- Design values of structural number due to different subsoil bearing capacity levels, design factors and adjustment factors are defined as follows:

Table 41. Examples of design values of Structural Number considering Heukelom & Klomp criterion

Design Factor		Type / Es	Design value of Structural Number [cm]						
DF	AF		15 MPa	20 MPa	35 MPa	45 MPa	50 MPa	60 MPa	80 MPa
2.15	2.0	Ballastless	192.2	167.7	119.1	104.5	99.8	92.0	80.8
1.92	2.0	Ballasted	171.6	149.8	106.4	93.3	89.1	82.2	72.2
2.15	1.5	Ballastless	144.2	125.8	89.3	78.4	74.8	69.0	60.6
1.92	1.5	Ballasted	128.7	112.3	79.8	70.0	66.8	61.6	54.1
2.15	1.2	Ballastless	115.3	100.6	71.5	62.7	**59.9***	**55.2***	**48.5***
1.92	1.2	Ballasted	103.0	89.9	63.8	56.0	53.5	49.3	43.3
2.15	1.0	Ballastless	96.1	83.9	**59.6***	**52.2***	**49.9***	**46.0***	**40.4***
1.92	1.0	Ballasted	85.8	74.9	53.2	46.7	44.5	41.1	36.1

Note: **Design values do not meet the requirement of minimum SN for a slab track, which is 60 cm. In this condition, a slab track should be designed by considering SN ≥ 60 cm. This will lead a requirement to increase AF, which will place the design in a safer side. In the practice, this should also accommodate other design considerations of a trackbed such a need of special function (protection layer) as well as cost-effective track design criteria.*

Example L

Calculation of structural number reference using Li & Selig criteria

- Design traffic is for 2 million load cycles
- Soil types: CH (fat clay), CL (lean clay), MH (elastic silt) and ML (silt) with example data of modulus elasticity of 15, 20, 45 and 60 MPa respectively.
- Soil compressive strengths (σ_s) and Li & Selig's soil cyclic parameters can be seen in the Table 42.
- Criterion for limit shear failure is set $\varepsilon_p = 2\%$
- Criterion for limit plastic deformation is defined ρ_p = 2 cm and for this example assuming the height of soil until rigid base is 200 cm.

Table 42. Examples of reference Structural Number considering Li & Selig criteria

Soil Type	E_s [MPa]	σ_s [kPa]	Soil Cyclic Parameter			Shear Limit Criterion			Plastic Deform. Criterion		
			a	b	m	σ_d [kPa]	σ_d/E_s [kPa/MPa]	**SN_{ref}**	σ_d [kPa]	σ_d/E_s [kPa/MPa]	**SN_{ref}**
CH	15	75	1.20	0.18	2.4	31.3	2.1	**29.6**	23.4	1.6	**39.0**
CL	20	100	1.10	0.16	2.0	42.2	2.1	**25.2**	29.9	1.5	**34.5**
MH	45	150	0.84	0.13	2.0	90.1	2.0	**17.5**	63.7	1.4	**23.9**
ML	60	200	0.64	0.10	1.7	174.8	2.9	**12.2**	116.3	1.9	**16.2**

- Design values of structural number due to different subsoil bearing capacity levels, design factors and adjustment factors are defined as follows:

Table 43. Examples of design values of Structural Number considering Li & Selig criteria

Design Factor		Type Es	SN Design-Shear Limit Criterion [cm]				SN Design-Plastic Deform. Criterion [cm]			
DF	AF		15 MPa	20 MPa	45 MPa	60 MPa	15 MPa	20 MPa	45 MPa	60 MPa
2.15	2	Ballastless	127.3	108.4	75.3	52.5	167.7	148.4	102.8	69.7
1.92	2	Ballasted	113.7	96.8	67.2	46.8	149.8	132.5	91.8	62.2
2.15	1.5	Ballastless	95.5	81.3	**56.4***	**39.3***	125.8	111.3	77.1	**52.2***
1.92	1.5	Ballasted	85.2	72.6	50.4	35.1	112.3	99.4	68.8	46.7
2.15	1.2	Ballastless	76.4	65.0	**45.2***	**31.5***	100.6	89.0	61.7	**41.8***
1.92	1.2	Ballasted	68.2	58.1	40.3	28.1	89.9	79.5	55.1	37.3
2.15	1	Ballastless	63.6	**54.2***	**37.6***	**26.2***	83.9	74.2	**51.4***	**34.8***
1.92	1	Ballasted	56.8	48.4	33.6	23.4	74.9	66.2	45.9	31.1

Note: **Design values do not meet the requirement of minimum SN for a slab track, which is 60 cm. In this condition, a slab track should be designed by considering SN ≥ 60 cm. This will lead a requirement to increase multiplication factor (MF), which will place the design in a safer side. In the practice, this should also accommodate other design considerations of a trackbed such a need of special function (protection layer) as well as cost-effective track design criteria.*

Values in the Table 43 show that in these examples of input design parameters, criterion of limiting of plastic deformation is more decisive than the one of limiting shear failures.

Table 44. Summary of examples of design values of Structural Number

Es [MPa]	Example No	Type	Criteria	FEA Model Code	Variant			
					2.0	1.5	1.2	1.0
					A	B	C	D
15	EX-1	Ballastless	H&K	-	192	144	115	96
	EX-2	Ballasted	H&K	-	172	129	103	86
	EX-3	Ballastless	L&S (Shear)	-	127	95	76	64
	EX-4	Ballasted	L&S (Shear)	-	114	85	68	57
	EX-5	***Ballastless***	***L&S (Plastic)***	***E15-ST-LSP***	***168***	***126***	***101***	***84***
	EX-6	***Ballasted***	***L&S (Plastic)***	***E15-BT-LSP***	***150***	***112***	***90***	***75***
20	EX-7	Ballastless	H&K	-	168	126	101	84
	EX-8	Ballasted	H&K	-	150	112	90	75
	EX-9	Ballastless	L&S (Shear)	-	108	81	65	54
	EX-10	Ballasted	L&S (Shear)	-	97	73	58	48
	EX-11	***Ballastless***	***L&S (Plastic)***	***E20-ST-LSP***	***148***	***111***	***89***	***74***
	EX-12	***Ballasted***	***L&S (Plastic)***	***E20-BT-LSP***	***132***	***99***	***79***	***66***
35	***EX-13***	***Ballastless***	***H&K***	***E35-ST-HK***	***119***	***89***	***71***	***60***
	EX-14	***Ballasted***	***H&K***	***E35-BT-HK***	***106***	***80***	***64***	***53***
45	EX-15	Ballastless	H&K	-	104	78	63	52
	EX-16	Ballasted	H&K	-	93	70	56	47
	EX-17	Ballastless	L&S (Shear)	-	75	56	45	38
	EX-18	Ballasted	L&S (Shear)	-	67	50	40	34
	EX-19	***Ballastless***	***L&S (Plastic)***	***E45-ST-LSP***	***103***	***77***	***62***	**51**
	EX-20	***Ballasted***	***L&S (Plastic)***	***E45-BT-LSP***	***92***	***69***	***55***	***46***
50	EX-21	Ballastless	H&K	-	100	75	60	50
	EX-22	Ballasted	H&K	-	89	67	53	45
60	***EX-23***	***Ballastless***	***H&K***	***-***	***92***	***69***	**55**	**46**
	EX-24	***Ballasted***	***H&K***	***-***	***82***	***62***	***49***	***41***
	EX-25	Ballastless	L&S (Shear)	E60-ST-LSS	52	39	31	26
	EX-26	Ballasted	L&S (Shear)	E60-BT-LSS	47	35	28	23
	EX-27	Ballastless	L&S (Plastic)	-	70	52	42	35
	EX-28	Ballasted	L&S (Plastic)	-	62	47	37	31
80	***EX-29***	***Ballastless***	***H&K***	***E80-ST-HK***	***81***	***61***	**49**	**40**
	EX-30	***Ballasted***	***H&K***	***E80-BT-HK***	***72***	***54***	***43***	***36***

The shaded rows in Table 44 are chosen as samples for trackbed thickness design in the following Appendix A.6.3. These samples will be modelled for static FEA simulations in ANSYS. This will be used for doing comparative analysis between proposed analytical method and FEA.

A.6.3. Examples of Trackbed Design for Static Analysis

Trackbed Thickness Design of *E15-ST-LSP&E15-BT-LSP*

Table 45. Trackbed thickness Example 5&6 with adjustment factor, AF = 2.0

Layer	Example 5-A (Slab Track) / E15-ST-LSP				Example 6-A (Ballasted Track) / E15-BT-LSP			
	Material	**a**	**h [cm]**	**SN**	**Material**	**a**	**h [cm]**	**SN**
Soil	*$E_s \approx 15$ MPa, $SN_{ref} \approx 39$ cm*				*$E_s \approx 15$ MPa, $SN_{ref} \approx 39$ cm*			
Top Course	Concrete C40/50	3.34	**24**	80.2	Ballast E = 250 MPa	0.65	**60**	39.0
Base Course	CTB 10 GPa	2.17	**30**	65.1	Coarse Grained 150 MPa	0.55	**90**	49.5
Subbase Course	Fine Grained 45 MPa	0.37	**60**	22.2	Fine Grained 60 MPa	0.41	**150**	61.5
	Total Thickness/SN		**114**	**167.5**	**Total Thickness/SN**		**300**	**150.0**

Table 46. Trackbed thickness Example 5&6 with adjustment factor, AF = 1.5

Layer	Example 5-B (Slab Track) / E15-ST-LSP				Example 6-B (Ballasted Track) / E15-BT-LSP			
	Material	**a**	**h [cm]**	**SN**	**Material**	**a**	**h [cm]**	**SN**
Soil	*$E_s \approx 15$ MPa, $SN_{ref} \approx 39$ cm*				*$E_s \approx 15$ MPa, $SN_{ref} \approx 39$ cm*			
Top Course	Concrete C40/50	3.34	**24**	80.2	Ballast E = 250 MPa	0.65	**45**	29.3
Base Course	Coarse Grained 150 MPa	0.55	**30**	16.5	Coarse Grained 100 MPa	0.47	**60**	28.2
Subbase Course	Fine Grained 60 MPa	0.41	**70**	28.7	Fine Grained 60 MPa	0.41	**135**	55.4
	Total Thickness/SN		**124**	**125.4**	**Total Thickness/SN**		**240**	**112.8**

Table 47. Trackbed thickness Example 5&6 with adjustment factor, AF = 1.2

Layer	Example 5-C (Slab Track) / E15-ST-LSP				Example 6-C (Ballasted Track) / E15-BT-LSP			
	Material	**a**	**h [cm]**	**SN**	**Material**	**a**	**h [cm]**	**SN**
Soil	*$E_s \approx 15$ MPa, $SN_{ref} \approx 39$ cm*				*$E_s \approx 15$ MPa, $SN_{ref} \approx 39$ cm*			
Top Course	Concrete C40/50	3.34	**24**	80.2	Ballast E = 250 MPa	0.65	**45**	29.3
Base Course	Coarse Grained 120 MPa	0.51	**40**	20.4	Coarse Grained 80 MPa	0.45	**60**	27.0
Subbase Course					Coarse Grained 45 MPa	0.37	**90**	33.3
	Total Thickness/SN		**64**	**100.6**	**Total Thickness/SN**		**195**	**89.6**

Table 48. Trackbed thickness Example 5&6 with adjustment factor, AF = 1.0

Layer	Example 5-D (Slab Track) / E15-ST-LSP				Example 6-D (Ballasted Track) / E15-BT-LSP			
	Material	**a**	**h [cm]**	**SN**	**Material**	**a**	**h [cm]**	**SN**
Soil	*$E_s \approx 15$ MPa, $SN_{ref} \approx 39$ cm*				*$E_s \approx 15$ MPa, $SN_{ref} \approx 39$ cm*			
Top Course	Concrete C35/45	3.26	**20**	65.2	Ballast E = 250 MPa	0.65	**45**	29.3
Base Course	Coarse Grained 120 MPa	0.51	**35**	17.9	Coarse Grained 100 MPa	0.47	**45**	21.2
Subbase Course	-	-	**-**	-	Coarse Grained 45 MPa	0.37	**65**	24.1
	Total Thickness/SN		**55**	**83.1**	**Total Thickness/SN**		**155**	**74.5**

Trackbed Thickness Design of *E20-ST-LSP&E20-BT-LSP*

Table 49. Trackbed thickness Example 11&12 with adjustment factor, AF = 2.0

Layer	Example 11-A (Slab Track) / E20-ST-LSP				Example 12-A (Ballasted Track) / E20-BT-LSP			
	Material	**a**	**h [cm]**	**SN**	**Material**	**a**	**h [cm]**	**SN**
Soil	*$E_s \approx 20$ MPa, $SN_{ref} \approx 34.5$ cm*				*$E_s \approx 20$ MPa, $SN_{ref} \approx 34.5$ cm*			
Top Course	Concrete C40/50	3.34	**24**	80.2	Ballast E = 250 MPa	0.65	**60**	39.0
Base Course	CTB 5 GPa	1.72	**30**	51.6	Coarse Grained 120 MPa	0.51	**60**	30.6
Subbase Course	Fine Grained 45 MPa	0.37	**45**	16.7	Coarse Grained 80 MPa	0.45	**140**	63.0
	Total Thickness/SN		**99**	**148.4**	**Total Thickness/SN**		**260**	**132.6**

Table 50. Trackbed thickness Example 11&12 with adjustment factor, AF = 1.5

Layer	Example 11-B (Slab Track) / E20-ST-LSP				Example 12-B (Ballasted Track) / E20-BT-LSP			
	Material	**a**	**h [cm]**	**SN**	**Material**	**a**	**h [cm]**	**SN**
Soil	*$E_s \approx 20$ MPa, $SN_{ref} \approx 34.5$ cm*				*$E_s \approx 20$ MPa, $SN_{ref} \approx 34.5$ cm*			
Top Course	Concrete C40/50	3.34	**24**	80.2	Ballast E = 250 MPa	0.65	**45**	29.3
Base Course	Coarse Grained 150 MPa	0.55	**30**	16.5	Coarse Grained 150 MPa	0.55	**60**	33.0
Subbase Course	Fine Grained 60 MPa	0.41	**35**	14.4	Fine Grained 60 MPa	0.41	**90**	36.9
	Total Thickness/SN		**89**	**111.0**	**Total Thickness/SN**		**195**	**99.2**

Table 51. Trackbed thickness Example 11&12 with adjustment factor, AF = 1.2

Layer	Example 11-C (Slab Track) / E20-ST-LSP				Example 12-C (Ballasted Track) / E20-BT-LSP			
	Material	**a**	**h [cm]**	**SN**	**Material**	**a**	**h [cm]**	**SN**
Soil	*$E_s \approx 20$ MPa, $SN_{ref} \approx 34.5$ cm*				*$E_s \approx 20$ MPa, $SN_{ref} \approx 34.5$ cm*			
Top Course	Concrete C35/45	3.26	**20**	65.2	Ballast E = 250 MPa	0.65	**45**	29.3
Base Course	Coarse Grained 120 MPa	0.51	**25**	12.8	Coarse Grained 120 MPa	0.51	**45**	23.0
Subbase Course	Coarse Grained 45 MPa	0.37	**30**	11.1	Coarse Grained 80 MPa	0.45	**60**	27.0
	Total Thickness/SN		**75**	**89.1**	**Total Thickness/SN**		**150**	**79.2**

Table 52. Trackbed thickness Example 11&12 with adjustment factor, AF = 1.0

Layer	Example 11-D (Slab Track) / E20-ST-LSP				Example 12-D (Ballasted Track) / E20-BT-LSP			
	Material	**a**	**h [cm]**	**SN**	**Material**	**a**	**h [cm]**	**SN**
Soil	*$E_s \approx 20$ MPa, $SN_{ref} \approx 34.5$ cm*				*$E_s \approx 20$ MPa, $SN_{ref} \approx 34.5$ cm*			
Top Course	Concrete C35/45	3.26	**20**	65.2	Ballast E = 250 MPa	0.65	**30**	19.5
Base Course	Coarse Grained 80 MPa	0.45	**20**	9.0	Coarse Grained 150 MPa	0.55	**45**	24.8
Subbase Course	-	-	**-**	-	Fine Grained 60 MPa	0.41	**55**	22.6
	Total Thickness/SN		**40**	**74.2**	**Total Thickness/SN**		**130**	**66.8**

Trackbed Thickness Design of *E35-ST-HK&E35-BT-HK*

Table 53. Trackbed thickness Example 13&14 with adjustment factor, AF = 2.0

Layer	Example 13-A (Slab Track) / E35-ST-HK				Example 14-A (Ballasted Track) / E35-BT-HK			
	Material	**a**	**h [cm]**	**SN**	**Material**	**a**	**h [cm]**	**SN**
Soil	$E_s \approx 35$ *MPa*, $SN_{ref} \approx 27.7$ *cm*				$E_s \approx 35$ *MPa*, $SN_{ref} \approx 27.7$ *cm*			
Top Course	Concrete C35/45	3.26	**24**	78.2	Ballast E = 250 MPa	0.65	**60**	39.0
Base Course	Coarse Grained 150 MPa	0.55	**30**	16.5	Coarse Grained 120 MPa	0.51	**60**	30.6
Subbase Course	Fine Grained 60 MPa	0.41	**60**	24.6	Fine Grained 60 MPa	0.41	**90**	36.9
	Total Thickness/SN		**114**	**119.3**	**Total Thickness/SN**		**210**	**106.5**

Table 54. Trackbed thickness Example 13&14 with adjustment factor, AF = 1.5

Layer	Example 13-B (Slab Track) / E35-ST-HK				Example 14-B (Ballasted Track) / E35-BT-HK			
	Material	**a**	**h [cm]**	**SN**	**Material**	**a**	**h [cm]**	**SN**
Soil	$E_s \approx 35$ *MPa*, $SN_{ref} \approx 27.7$ *cm*				$E_s \approx 35$ *MPa*, $SN_{ref} \approx 27.7$ *cm*			
Top Course	Concrete C35/45	3.26	**20**	65.2	Ballast E = 250 MPa	0.65	**30**	19.5
Base Course	Coarse Grained 100 MPa	0.47	**25**	11.8	Coarse Grained 120 MPa	0.51	**60**	30.6
Subbase Course	Fine Grained 60 MPa	0.41	**30**	12.3	Coarse Grained 80 MPa	0.45	**65**	29.3
	Total Thickness/SN		**75**	**89.3**	**Total Thickness/SN**		**155**	**79.4**

Table 55. Trackbed thickness Example 13&14 with adjustment factor, AF = 1.2

Layer	Example 13-C (Slab Track) / E35-ST-HK				Example 14-C (Ballasted Track) / E35-BT-HK			
	Material	**a**	**h [cm]**	**SN**	**Material**	**a**	**h [cm]**	**SN**
Soil	$E_s \approx 35$ *MPa*, $SN_{ref} \approx 27.7$ *cm*				$E_s \approx 35$ *MPa*, $SN_{ref} \approx 27.7$ *cm*			
Top Course	Concrete C35/45	3.26	**20**	65.2	Ballast E = 250 MPa	0.65	**30**	19.5
Base Course	Fine Grained 60 MPa	0.41	**15**	6.2	Coarse Grained 120 MPa	0.51	**30**	15.3
Subbase Course	-	-	**-**	-	Fine Grained 60 MPa	0.41	**70**	28.7
	Total Thickness/SN		**35**	**71.4**	**Total Thickness/SN**		**130**	**63.5**

Table 56. Trackbed thickness Example 14 with adjustment factor, AF = 1.0

Layer	Example 14-D (Ballasted Track) / E35-BT-HK			
	Material	**a**	**h [cm]**	**SN**
Soil	$E_s \approx 35$ *MPa*, $SN_{ref} \approx 27.7$ *cm*			
Top Course	Ballast E = 250 MPa	0.65	**45**	29.3
Base Course	Fine Grained 60 MPa	0.41	**60**	24.6
Subbase Course	-	-	**-**	-
	Total Thickness/SN		**105**	**53.9**

Trackbed Thickness Design of *E45-ST-LSP&E45-BT-LSP*

Table 57. Trackbed thickness Example 19&20 with adjustment factor, AF = 2.0

Layer	Example 19-A (Slab Track) / E45-ST-LSP				Example 20-A (Ballasted Track) / E45-BT-LSP			
	Material	**a**	**h [cm]**	**SN**	**Material**	**a**	**h [cm]**	**SN**
Soil	*$E_s \approx 45$ MPa, $SN_{ref} \approx 23.9$ cm*				*$E_s \approx 45$ MPa, $SN_{ref} \approx 23.9$ cm*			
Top Course	Concrete C35/45	3.26	**24**	78.2	Ballast E = 250 MPa	0.65	**45**	29.3
Base Course	Coarse Grained 100 MPa	0.47	**28**	13.2	Coarse Grained 150 MPa	0.55	**60**	33.0
Subbase Course	Fine Grained 60 MPa	0.41	**28**	11.5	Coarse Grained 80 MPa	0.45	**65**	29.3
	Total Thickness/SN		**80**	**102.9**	**Total Thickness/SN**		**170**	**91.5**

Table 58. Trackbed thickness Example 19&20 with adjustment factor, AF = 1.5

Layer	Example 19-B (Slab Track) / E45-ST-LSP				Example 20-B (Ballasted Track) / E45-BT-LSP			
	Material	**a**	**h [cm]**	**SN**	**Material**	**a**	**h [cm]**	**SN**
Soil	*$E_s \approx 45$ MPa, $SN_{ref} \approx 23.9$ cm*				*$E_s \approx 45$ MPa, $SN_{ref} \approx 23.9$ cm*			
Top Course	Concrete C35/45	3.26	**20**	65.2	Ballast E = 200 MPa	0.60	**30**	18.0
Base Course	Fine Grained 100 MPa	0.47	**25**	11.8	Coarse Grained 100 MPa	0.47	**45**	21.2
Subbase Course	-	-	**-**	-	Coarse Grained 80 MPa	0.45	**65**	29.3
	Total Thickness/SN		**45**	**77.0**	**Total Thickness/SN**		**140**	**68.4**

Table 59. Trackbed thickness Example 19&20 with adjustment factor, AF = 1.2

Layer	Example 19-C (Slab Track) / E45-ST-LSP				Example 20-C (Ballasted Track) / E45-BT-LSP			
	Material	**a**	**h [cm]**	**SN**	**Material**	**a**	**h [cm]**	**SN**
Soil	*$E_s \approx 45$ MPa, $SN_{ref} \approx 23.9$ cm*				*$E_s \approx 45$ MPa, $SN_{ref} \approx 23.9$ cm*			
Top Course	Concrete C40/50	3.34	**18**	60.1	Ballast E = 250 MPa	0.65	**30**	19.5
Base Course	-	-	**-**	-	Coarse Grained 80 MPa	0.45	**80**	36.0
Subbase Course	-	-	**-**	-	-	-	**-**	-
	Total Thickness/SN		**18**	**60.1**	**Total Thickness/SN**		**110**	**55.5**

Table 60. Trackbed thickness Example 20 with adjustment factor, AF = 1.0

Layer	Example 20-D (Ballasted Track) / E45-BT-LSP			
	Material	**a**	**h [cm]**	**SN**
Soil	*$E_s \approx 45$ MPa, $SN_{ref} \approx 23.9$ cm*			
Top Course	Ballast E = 250 MPa	0.65	**30**	19.5
Base Course	Fine Grained 60 MPa	0.41	**65**	26.7
Subbase Course	-	-	**-**	-
	Total Thickness/SN		**95**	**46.2**

Trackbed Thickness Design of *E60-ST-HK&E60-BT-HK*

Table 61. Trackbed thickness Example 23&24 with adjustment factor, AF = 2.0

Layer	Example 23-A (Slab Track) / E60-ST-HK				Example 24-A (Ballasted Track) / E60-BT-HK			
	Material	a	h [cm]	SN	Material	a	h [cm]	SN
Soil	$E_s \approx 60$ MPa, $SN_{ref} \approx 12.2$ cm				$E_s \approx 60$ MPa, $SN_{ref} \approx 12.2$ cm			
Top Course	Concrete C35/45	3.26	**20**	65.2	Ballast E = 200 MPa	0.60	**30**	18.0
Base Course	Coarse Grained 100 MPa	0.47	**30**	14.1	Coarse Grained 100 MPa	0.47	**60**	28.2
Subbase Course	Fine Grained 80 MPa	0.45	**30**	13.5	Fine Grained 80 MPa	0.45	**80**	36.0
	Total Thickness/SN		**80**	**92.8**	**Total Thickness/SN**		**170**	**82.2**

Table 62. Trackbed thickness Example 23&24 with adjustment factor, AF = 1.5

Layer	Example 23-B (Slab Track) / E60-ST-HK				Example 24-B (Ballasted Track) / E60-BT-HK			
	Material	a	h [cm]	SN	Material	a	h [cm]	SN
Soil	$E_s \approx 60$ MPa, $SN_{ref} \approx 12.2$ cm				$E_s \approx 60$ MPa, $SN_{ref} \approx 12.2$ cm			
Top Course	Concrete C40/50	3.34	**21**	70.1	Ballast E = 250 MPa	0.65	**40**	26.0
Base Course	-	-	**-**	-	Coarse Grained 100 MPa	0.47	**75**	35.3
Subbase Course	-	-	**-**	-	-	-	**-**	-
	Total Thickness/SN		**21**	**70.1**	**Total Thickness/SN**		**115**	**61.3**

Table 63. Trackbed thickness Example 24 with adjustment factor, AF = 1.2

Layer	Example 24-C (Ballasted Track) / E60-BT-HK			
	Material	a	h [cm]	SN
Soil	$E_s \approx 60$ MPa, $SN_{ref} \approx 12.2$ cm			
Top Course	Ballast E = 250 MPa	0.65	**30**	19.5
Base Course	Fine Grained 100 MPa	0.47	**65**	30.6
Subbase Course	-	-	**-**	-
	Total Thickness/SN		**95**	**50.1**

Table 64. Trackbed thickness Example 24 with adjustment factor, AF = 1.0

Layer	Example 24-D (Ballasted Track) / E60-BT-HK			
	Material	a	h [cm]	SN
Soil	$E_s \approx 60$ MPa, $SN_{ref} \approx 12.2$ cm			
Top Course	Ballast E = 300 MPa	0.69	**30**	20.7
Base Course	Coarse Grained 100 MPa	0.47	**45**	21.2
Subbase Course	-	-	**-**	-
	Total Thickness/SN		**75**	**41.9**

Trackbed Thickness Design of *E80-ST-HK&E80-BT-HK*

Table 65. Trackbed thickness Example 29&30 with adjustment factor, AF = 2.0

Layer	Example 29-A (Slab Track) / E80-ST-HK				Example 30-A (Ballasted Track) / E80-BT-HK			
	Material	a	h [cm]	SN	Material	a	h [cm]	SN
Soil	$E_s \approx 80$ MPa, $SN_{ref} \approx 18.8$ cm				$E_s \approx 80$ MPa, $SN_{ref} \approx 18.8$ cm			
Top Course	Concrete C40/50	3.34	**20**	66.8	Ballast E = 250 MPa	0.65	**60**	39.0
Base Course	Coarse Grained 100 MPa	0.47	**30**	14.1	Coarse Grained 120 MPa	0.51	**65**	33.2
Subbase Course	-	-	**-**	-	-	-	**-**	-
	Total Thickness/SN		**50**	**80.9**	**Total Thickness/SN**		**125**	**72.2**

Table 66. Trackbed thickness Example 29&30 with adjustment factor, AF = 1.5

Layer	Example 29-B (Slab Track) / E80-ST-HK				Example 30-B (Ballasted Track) / E80-BT-HK			
	Material	a	h [cm]	SN	Material	a	h [cm]	SN
Soil	$E_s \approx 80$ MPa, $SN_{ref} \approx 18.8$ cm				$E_s \approx 80$ MPa, $SN_{ref} \approx 18.8$ cm			
Top Course	Concrete C40/50	3.34	**18**	60.1	Ballast E = 200 MPa	0.60	**30**	18.0
Base Course	-	-	**-**	-	Coarse Grained 120 MPa	0.51	**70**	35.7
Subbase Course	-	-	**-**	-	-	-	**-**	0.0
	Total Thickness/SN		**18**	**60.1**	**Total Thickness/SN**		**100**	**53.7**

Table 67. Trackbed thickness Example 30 with adjustment factor, AF = 1.2

Layer	Example 30-C (Ballasted Track) / E80-BT-HK			
	Material	a	h [cm]	SN
Soil	$E_s \approx 80$ MPa, $SN_{ref} \approx 18.8$ cm			
Top Course	Ballast E = 250 MPa	0.65	**30**	19.5
Base Course	Fine Grained 100 MPa	0.47	**50**	23.5
Subbase Course	-	-	**-**	-
	Total Thickness/SN		**80**	**43.0**

Table 68. Trackbed thickness Example 30 with adjustment factor, AF = 1.0

Layer	Example 30-D (Ballasted Track) / E80-BT-HK			
	Material	a	h [cm]	SN
Soil	$E_s \approx 80$ MPa, $SN_{ref} \approx 18.8$ cm			
Top Course	Ballast E = 300 MPa	0.69	**30**	20.7
Base Course	Coarse Grained 120 MPa	0.51	**30**	15.3
Subbase Course	-	-	**-**	-
	Total Thickness/SN		**60**	**36.0**

Table 69. Example calculation of the total heights of trackbed

Subsoil		FEA Model			Design Criteria	Total Height of Trackbed			
Es [MPa]	Condition	Type	Model Code	Group No.		AF = 2.0	AF = 1.5	AF = 1.2	AF = 1.0
						[cm]	[cm]	[cm]	[cm]
						A	B	C	D
15	Very Soft	Slab Track	E15-ST-LSP	EX-5	L&S (Plastic)	114	124	64	55
15	Very Soft	Ballasted	E15-BT-LSP	EX-6	L&S (Plastic)	300	240	195	155
20	Soft	Slab Track	E20-ST-LSP	EX-11	L&S (Plastic)	99	260	75	40
20	Soft	Ballasted	E20-BT-LSP	EX-12	L&S (Plastic)	260	89	150	130
35	Soft	Slab Track	E35-ST-HK	EX-13	H&K	114	75	35	-
35	Soft	Ballasted	E35-BT-HK	EX-14	H&K	210	155	130	105
45	Moderate	Slab Track	E45-ST-LSP	EX-19	L&S (Plastic)	80	45	18	-
45	Moderate	Ballasted	E45-BT-LSP	EX-20	L&S (Plastic)	170	140	110	95
60	Moderate	Slab Track	E60-ST-HK	EX-23	H&K	80	21	-	-
60	Moderate	Ballasted	E60-BT-HK	EX-24	H&K	170	115	95	75
80	Moderate	Slab Track	E80-ST-HK	EX-29	H&K	50	18	-	-
80	Moderate	Ballasted	E80-BT-HK	EX-30	H&K	125	100	80	60

Table 70. Example of FEA results of displacements of rail with different trackbed layers

Subsoil		FEA Model			Design Criteria	Displacement of Rail			
Es [MPa]	Condition	Type	Model Code	Group No.		AF = 2.0	AF = 1.5	AF = 1.2	AF = 1.0
						[cm]	[cm]	[cm]	[cm]
						A	B	C	D
15	Very Soft	Slab Track	E15-ST-LSP	EX-5	L&S (Plastic)	6.8	7.03	7.3	7.6
15	Very Soft	Ballasted	E15-BT-LSP	EX-6	L&S (Plastic)	5.5	6.0	6.5	6.5
20	Soft	Slab Track	E20-ST-LSP	EX-11	L&S (Plastic)	6.3	6.4	6.8	6.9
20	Soft	Ballasted	E20-BT-LSP	EX-12	L&S (Plastic)	4.9	5.2	5.3	5.5
35	Soft	Slab Track	E35-ST-HK	EX-13	H&K	5.4	5.5	5.5	-
35	Soft	Ballasted	E35-BT-HK	EX-14	H&K	4.3	4.4	4.7	4.6
45	Moderate	Slab Track	E45-ST-LSP	EX-19	L&S (Plastic)	5.1	5.1	5.0	-
45	Moderate	Ballasted	E45-BT-LSP	EX-20	L&S (Plastic)	3.8	4.3	4.1	4.3
60	Moderate	Slab Track	E60-ST-HK	EX-23	H&K	4.8	4.6	-	-
60	Moderate	Ballasted	E60-BT-HK	EX-24	H&K	4.0	3.6	3.6	3.6
80	Moderate	Slab Track	E80-ST-HK	EX-29	H&K	4.4	4.3	-	-
80	Moderate	Ballasted	E80-BT-HK	EX-30	H&K	3.1	3.3	3.4	3.1

Note. These values are the maximum displacements, which are located under the critical rail and are resulted from FEA by considering design factor of load distribution in a curve with factor of 1.2 and additionally DAF of 1.6. Therefore, the displacements are quite high, which consider a prediction of the most critical state within the design period.

A.6.4. Calculation of Design Factors and Structural Numbers of Trackbed for Dynamic Analysis

Example M

- Dynamic amplification factor is not necessary to be taken into account, then DAF = 1, which gives f_d = 1.0
- Wheel load distribution factors of inner and outer rail: $f_{c,i}$= 1.0 and $f_{c,j}$= 1.0 (straight line) give $f_{c,d}$ = *1.0*
- Wheel load of 125kN gives f_Q = 1.0
- Soil data: E_s = 20 MPa, type CL.
- Soil critical limit criteria: number of load cycles = $2x10^6$
  - × Heukelom and Klomp's fatigue limit criteria gives reference structural number (SN_{reff}) = 39 cm.
  - × Li & Selig's limit of shear failure ε_p = 2%, deviator stress limit σ_d = 42.2 kPa, σ_d/E_s= 42.2/20 = 2.1, gives SN_{reff} = 25.2 cm.
  - × Li & Selig's limit of plastic deformation failure ρ_p = 2 cm, and depth of soil 2 m give deviator stress limit σ_d = 29.9 kPa, σ_d/E_s= 29.9/20 = 1.5, gives SN_{reff} = 34.5 cm.

  In these examples, Heukelom & Klomp's fatigue limit criteria is considered for trackbed design of ballasted track system and Li & Selig's plastic deformation criteria is taken into account for trackbed design of slab track system.
- ***Slab track system I:***
  - × Rail profile 60E2 (E = $2.1x10^5$ and I = $30.55x10^6$mm4), elastic-pad spacing of 65 cm and elastic-pad stiffness of **22.5 kN/mm** (the same as reference value) gives f_{Lr}= 1.0
  - × $DF = f_Q * f_d * f_{c,d} * f_{Lr} = 1 * 1 * 1 * 1 = 1.0$
  - × Safety factor = 2
  - × Structural number design (Li & Selig's plastic failure criteria):
    $SN_{des} = SF * DF * SN_{reff} = 2 * 1 * 34.5 = \mathbf{69\ cm}$
- ***Slab track system II:***
  - × Rail profile 60E2 (E = $2.1x10^5$ and I = $30.55x10^6$mm4), elastic-pad spacing of 65 cm and elastic-pad stiffness of **60 kN/mm**, gives:

$$L_r = \sqrt[4]{\frac{4.E.I.a}{k_{rp}}} = \sqrt[4]{\frac{4*2.1x10^5*30.55x10^6*650}{60x10^3}} = 726.13mm$$

- × $f_{Lr}\ Ratio = \frac{L_r}{928} = \frac{726.13}{928} = 0.78$ and from Figure 25, gives f_{Lr}= 1.24
- × $DF = f_Q * f_d * f_{c,d} * f_{Lr} = 1 * 1 * 1 * 1.24 = 1.24$
- × Safety factor = 2
- × Structural number design (Li & Selig's plastic failure criteria):
  $SN_{des} = SF * DF * SN_{reff} = 2 * 1.24 * 34.5 = \mathbf{85.6\ cm}$

- ***Ballasted track system I:***
  - × Rail profile 60E2 (E = 2.1x10^5 and I = 30.55x10^{6}mm4), elastic-pad spacing of 60 cm and elastic-pad stiffness of **22.5 kN/mm** (the same as reference value) gives f_{Lr}= 1.0
  - × $DF = f_Q * f_d * f_{c,d} * f_{Lr} = 1 * 1 * 1 * 1 = 1$
  - × Safety factor = 2
  - × Structural number design (Heukelom & Klomp's fatigue limit criteria):
    $SN_{des} = SF * DF * SN_{reff} = 2 * 1 * 39 = \mathbf{78\ cm}$
- ***Ballasted track system II:***
  - × Rail profile 60E2 (E = 2.1x10^5 and I = 30.55x10^{6}mm4), elastic-pad spacing of 60 cm and elastic-pad stiffness of **40 kN/mm**, gives:
    $$L_r = \sqrt[4]{\frac{4.E.I.a}{k_{rp}}} = \sqrt[4]{\frac{4*2.1x10^5*30.55x10^6*600}{40x10^3}} = 787.67mm$$
  - × $f_{Lr}\ Ratio = \frac{L_r}{910} = \frac{787.67}{910} = 0.87$ and from Figure 25, gives f_{Lr}= 1.12
  - × $DF = f_Q * f_d * f_{c,d} * f_{Lr} = 1 * 1 * 1 * 1.12 = 1.12$
  - × Safety factor = 2
  - × Structural number design (Heukelom & Klomp's fatigue limit criteria):
    $SN_{des} = SF * DF * SN_{reff} = 2 * 1.12 * 39 = \mathbf{87.4\ cm}$

Example N

- Train's design speed 250 km/hour, gives dynamic amplification factor (DAF) of f_d = 1.6 (see Appendix 4 for more detail)
- Wheel load distribution factors of inner and outer rail: $f_{c,i}$= 1.0 and $f_{c,j}$= 1.0(straight line) give $f_{c,d} = 1.0$
- Wheel load of 125kN gives f_Q = 1.0
- Soil data: E_s = 20 MPa, type CL.
- Soil critical limit criteria: number of load cycles = $2x10^6$
    - × Heukelom and Klomp's fatigue limit criteria gives reference structural number (SN_{reff}) = 39 cm.
    - × Li & Selig's limit of shear failure ε_p = 2%, deviator stress limit σ_d = 42.2 kPa, σ_d/E_s= 42.2/20 = 2.1, gives SN_{reff} = 25.2 cm.
    - × Li & Selig's limit of plastic deformation failure ρ_p = 2 cm, and depth of soil 2 m give deviator stress limit σ_d = 29.9 kPa, σ_d/E_s= 29.9/20 = 1.5, gives SN_{reff} = 34.5 cm.

  In these examples, Heukelom & Klomp's fatigue limit criteria is considered for trackbed design of ballasted track system and Li & Selig's plastic deformation criteria is taken into account for trackbed design of slab track system.
- ***Slab track system I:***
    - × Rail profile 60E2 (E = $2.1x10^5$ and I = $30.55x10^6$mm4), elastic-pad spacing of 65 cm and elastic-pad stiffness of **22.5 kN/mm** (the same as reference value) gives f_{Lr}= 1.0
    - × $DF = f_Q * f_d * f_{c,d} * f_{Lr} = 1 * 1.6 * 1 * 1 = 1.6$
    - × Safety factor = 2
    - × Structural number design (Li & Selig's plastic failure criteria):
      $SN_{des} = SF * DF * SN_{reff} = 2 * 1.6 * 34.5 = \mathbf{110.4\ cm}$
- ***Slab track system II:***
    - × Rail profile 60E2 (E = $2.1x10^5$ and I = $30.55x10^6$mm4), elastic-pad spacing of 65 cm and elastic-pad stiffness of **60 kN/mm**, gives:

      $$L_r = \sqrt[4]{\frac{4.E.I.a}{k_{rp}}} = \sqrt[4]{\frac{4*2.1x10^5*30.55x10^6*650}{60x10^3}} = 726.13mm$$
    - × $f_{Lr}\ Ratio = \frac{L_r}{928} = \frac{726.13}{928} = 0.78$ and from Figure 25, gives f_{Lr}= 1.24
    - × $DF = f_Q * f_d * f_{c,d} * f_{Lr} = 1 * 1.6 * 1 * 1.24 = 1.98$

- × Safety factor = 2
- × Structural number design (Li & Selig's plastic failure criteria):

  $SN_{des} = SF * DF * SN_{reff} = 2 * 1.98 * 34.5 = \mathbf{136.6\ cm}$

- ***Ballasted track system I:***
  - × Rail profile 60E2 (E = 2.1x10^5 and I = 30.55x10^{6}mm4), elastic-pad spacing of 60 cm and elastic-pad stiffness of **22.5 kN/mm** (the same as reference value) gives f_{Lr}= 1.0
  - × $DF = f_Q * f_d * f_{c,d} * f_{Lr} = 1 * 1.6 * 1 * 1 = 1.6$
  - × Safety factor = 2
  - × Structural number design (Heukelom & Klomp's fatigue limit criteria):

    $SN_{des} = SF * DF * SN_{reff} = 2 * 1.6 * 39 = \mathbf{124.8\ cm}$

- ***Ballasted track system II:***
  - × Rail profile 60E2 (E = 2.1x10^5 and I = 30.55x10^{6}mm4), elastic-pad spacing of 60 cm and elastic-pad stiffness of **40 kN/mm**, gives:

    $$L_r = \sqrt[4]{\frac{4.E.I.a}{k_{rp}}} = \sqrt[4]{\frac{4*2.1x10^5*30.55x10^6*600}{40x10^3}} = 787.67mm$$

  - × $f_{Lr}\ Ratio = \frac{L_r}{910} = \frac{787.67}{910} = 0.87$ and from Figure 25, gives f_{Lr}= 1.12
  - × $DF = f_Q * f_d * f_{c,d} * f_{Lr} = 1 * 1.6 * 1 * 1.12 = 1.79$
  - × Safety factor = 2
  - × Structural number design (Heukelom & Klomp's fatigue limit criteria):

    $SN_{des} = SF * DF * SN_{reff} = 2 * 1.79 * 39 = \mathbf{139.8\ cm}$

A.6.5. Examples of Trackbed Design for Dynamic Analysis

EXAMPLE 31 and 32. Slab Track System with Multilayer Trackbed

Table 71. Multilayer trackbed thickness design of slab track with elastic-pad stiffness of 22.5 kN/mm (Example 31) and 60 kN/mm (Example 32) and safety factor of 2.0

Layer	Example 31 (Slab Track), Li & Selig, SF = 2				Example 32 (Slab Track), Li & Selig, SF = 2			
	Material	**a**	**h [cm]**	**SN**	**Material**	**a**	**h [cm]**	**SN**
Soil	*$E_s \approx 20$ MPa, $SN_{ref} \approx 34.5$ cm*				*$E_s \approx 20$ MPa, $SN_{ref} \approx 34.5$ cm*			
Top Course	Concrete C35/45	3.26	**20**	65.2	Concrete C35/45	3.26	**20**	65.2
Base Course	Fine Grained 60 MPa	0.41	**12**	4.9	Fine Grained 60 MPa	0.41	**20**	8.2
Subbase Course					Fine Grained 45 MPa	0.37	**35**	13.0
	Total Thickness/SN		**32**	**70.1**	**Total Thickness/SN**		**75**	**86.4**

EXAMPLE 33 and 34. Ballasted Track System with Multilayer Trackbed

Table 72. Multilayer trackbed thickness design of ballasted track with elastic-pad stiffness of 22.5 kN/mm (Example 33) and 40 kN/mm (Example 34) and safety factor of 2.0

Layer	Example 33 (Ballasted), H & K, SF = 2				Example 34 (Ballasted), H & K, SF = 2			
	Material	**a**	**h [cm]**	**SN**	**Material**	**a**	**h [cm]**	**SN**
Soil	*Es ≈ 20 MPa, SNref ≈ 39 cm*				*Es ≈ 20 MPa, SNref ≈ 39 cm*			
Top Course	Ballast E = 250 MPa	0.65	**45**	29.3	Ballast E = 250 MPa	0.65	**45**	29.3
Base Course	Coarse Grained 120 MPa	0.51	**45**	23.0	Coarse Grained 80 MPa	0.45	**60**	27.0
Subbase Course	Coarse Grained 80 MPa	0.45	**60**	27.0	Coarse Grained 45 MPa	0.37	**85**	31.5
	Total Thickness/SN		**150**	**79.2**	**Total Thickness/SN**		**190**	**87.7**

EXAMPLE 35 and 36. Ballasted Track System with Single Layer Trackbed

Table 73. Single layer trackbed thickness design of ballasted track with elastic-pad stiffness of 22.5 kN/mm (Example 35) and 40 kN/mm (Example 36) and safety factor of 2.0

Layer	Example 35 (Ballasted), H & K, SF = 2				Example 36 (Ballasted), H & K, SF = 2			
	Material	**a**	**h [cm]**	**SN**	**Material**	**a**	**h [cm]**	**SN**
Soil	*Es ≈ 20 MPa, SNref ≈ 39 cm*				*Es ≈ 20 MPa, SNref ≈ 39 cm*			
Top Course	Ballast E = 250 MPa	0.65	**120**	78.0	Ballast E = 250 MPa	0.65	**135**	87.8
Base Course								
Subbase Course								
	Total Thickness/SN		**120**	**78.0**	**Total Thickness/SN**		**135**	**87.8**

Appendix 7. MATHCAD Listing Program of Calculation of Soil's Static and Dynamic Stiffness and Damping

Load Data

$f := 120Hz$

$\omega := 2 \cdot \pi \cdot f = 753.982 \cdot rad \cdot s^{-1}$ $\quad g = 9.807 \cdot m \cdot s^{-2}$

Foundation Data

$Bf := 0.5m$ half width of foundation

$Lf := 0.5m$ half length of foundation

$Hf := 0.3m$ height of foundation

Soil Data

$\gamma s := 22 \cdot kN \cdot m^{-3}$

$\rho s := \frac{\gamma s}{g} = 2.243 \times 10^{3} \cdot kg \cdot m^{-3}$

$Es := 100 \cdot MPa$ modulus elasticity of soil

$\mu := 0.3$

$Gs := \frac{Es}{2 \cdot (1 + \mu)} = 38.462 \cdot MPa$ shear modulus of soil

$Vs := \sqrt{\frac{Gs}{\rho s}} = 130.937 \cdot m \cdot s^{-1}$ shear wave velocity of soil

SOIL MODELLING

$\gamma c := 24 \cdot kN \cdot m^{-3}$

$Volf := Lf \cdot Bf \cdot Hf = 0.075 \cdot m^{3}$ $\quad \rho c := \frac{\gamma c}{g} = 2.447 \times 10^{3} \cdot kg \cdot m^{-3}$

$mf := Volf \cdot \rho c = 183.549\ kg$

$I\theta x := \frac{mf}{12} \cdot Bf^{2} \cdot \left(1 \cdot kg^{-1} \cdot m^{2}\right) = 3.824 \cdot m^{4}$

$I\theta y := \frac{mf}{12} \cdot Lf^{2} \cdot \left(1 \cdot kg^{-1} \cdot m^{2}\right) = 3.824 \cdot m^{4}$

$Jm := \frac{Lf \cdot Bf^{3}}{12} + \frac{Bf \cdot Lf^{3}}{12} = 0.021 m^{4}$

$Af := 4 \cdot Lf \cdot Bf = 1 m^{2}$

$Ja := \frac{Af}{4 \cdot Lf^{2}} = 1$

Si Factor for Stiffness ----------

$Sz := \begin{cases} 0.8 \text{ if } Ja \le 0.02 & = 2.27 \quad \text{vertical} \\ 0.73 + 1.54 \cdot Ja^{0.75} \text{ otherwise} \end{cases}$

$Sy := \begin{cases} 2.24 \text{ if } Ja \le 0.16 & = 4.5 \quad \text{horizontal} \\ 4.5 \cdot Ja^{0.38} \text{ otherwise} \end{cases}$

$S\theta x := \begin{cases} 2.54 \text{ if } \frac{Bf}{Lf} < 0.4 & = 3.2 \quad \text{rotation} \\ 3.2 \cdot \sqrt[4]{\frac{Bf}{Lf}} \text{ otherwise} \end{cases}$

$S\theta y := 3.2$ rotation

$St := 3.8 + 10.7 \cdot \left(1 - \frac{Bf}{Lf}\right)^{10} = 3.8$ torsion

---

$Rf := \frac{Lf}{Bf} = 1$

$ao := \omega \cdot \frac{Bf}{Vs} = 2.879$

$VLA := \frac{3.4Vs}{\pi \cdot (1 - \mu)} = 202.439 \frac{m}{s}$

$f\lambda(ao, R, X1, X2, X3, X4) := X1 + ao \cdot R \cdot X2 + (ao \cdot R)^{2} \cdot X3 + X4 \cdot e^{(-ao \cdot R)}$

$Rz := \begin{pmatrix} 1 \\ 2 \\ 4 \\ 6 \\ 10 \end{pmatrix}$ $\lambda zX1 := \begin{pmatrix} 0.9716 \\ 1.2080 \\ 1.0900 \\ 1.2285 \\ 1.3112 \end{pmatrix}$ $\lambda zX2 := \begin{pmatrix} -0.0500 \\ -0.1640 \\ -0.0025 \\ -0.0359 \\ 0.0285 \end{pmatrix}$ $\lambda zX3 := \begin{pmatrix} 0.0520 \\ 0.0385 \\ 0.0012 \\ 0.0024 \\ 0.0011 \end{pmatrix}$ $\lambda zX4 := \begin{pmatrix} -0.0660 \\ -0.2515 \\ 0.0000 \\ 0.1515 \\ 0.4388 \end{pmatrix}$

$f\lambda z1(z) := interp(pspline(Rz, \lambda zX1), Rz, \lambda zX1, z)$ $\quad f\lambda z1(Rf) = 0.972$

$f\lambda z2(z) := interp(pspline(Rz, \lambda zX2), Rz, \lambda zX2, z)$ $\quad f\lambda z2(Rf) = -0.05$

$f\lambda z3(z) := interp(pspline(Rz, \lambda zX3), Rz, \lambda zX3, z)$ $\quad f\lambda z3(Rf) = 0.052$

$f\lambda z4(z) := interp(pspline(Rz, \lambda zX4), Rz, \lambda zX4, z)$ $\quad f\lambda z4(Rf) = -0.066$

$\lambda z10 := f\lambda(ao, 10, f\lambda z1(10), f\lambda z2(10), f\lambda z3(10), f\lambda z4(10)) = 1.402$

$\lambda zmore10 := \lambda z10 \cdot (1 + 0.001 \cdot Rf) = 1.404$

$\lambda z := \begin{cases} f\lambda(ao, Rf, f\lambda z1(Rf), f\lambda z2(Rf), f\lambda z3(Rf), f\lambda z4(Rf)) \text{ if } Rf \le 10 & = 1.255 \\ \lambda zmore10 \text{ otherwise} \end{cases}$

$Ry := \begin{pmatrix} 1 \\ 2 \\ 4 \\ 10 \end{pmatrix}$ $\lambda yX1 := \begin{pmatrix} 1.5720 \\ 1.0200 \\ 1.7350 \\ 1.8040 \end{pmatrix}$ $\lambda yX2 := \begin{pmatrix} -0.6140 \\ 0.0000 \\ -0.2915 \\ -0.1273 \end{pmatrix}$ $\lambda yX3 := \begin{pmatrix} 0.2118 \\ 0.0000 \\ 0.0288 \\ 0.0051 \end{pmatrix}$ $\lambda yX4 := \begin{pmatrix} -0.7062 \\ 0.0000 \\ -0.4950 \\ 0.7960 \end{pmatrix}$

$fy1(y) := interp(pspline(Ry, \lambda yX1), Ry, \lambda yX1, y)$ $\quad fy1(Rf) = 1.572$

$fy2(y) := interp(pspline(Ry, \lambda yX2), Ry, \lambda yX2, y)$ $\quad fy2(Rf) = -0.614$

$fy3(y) := interp(pspline(Ry, \lambda yX3), Ry, \lambda yX3, y)$ $\quad fy3(Rf) = 0.212$

$fy4(y) := interp(pspline(Ry, \lambda yX4), Ry, \lambda yX4, y)$ $\quad fy4(Rf) = -0.706$

$\lambda y10 := f\lambda(ao, 10, fy1(10), fy2(10), fy3(10), fy4(10)) = 2.367$

$\lambda ymore10 := \lambda y10 \cdot (1 + 0.0025 \cdot Rf) = 2.372$

$\lambda y1 := f\lambda(ao, 1, fXy1(1), fXy2(1), fXy3(1), fXy4(1)) = 1.52$

$\lambda y := \begin{cases} f\lambda(ao, Rf, fXy1(Rf), fXy2(Rf), fXy3(Rf), fXy4(Rf)) & \text{if } Rf \le 10 \\ \lambda ymore10 & \text{otherwise} \end{cases} = 1.52$

$fXr(ao, X1, X2, X3, X4) := ao \cdot X1 + ao^2 \cdot X2 + ao^3 \cdot X3 + ao^4 \cdot X4$

$Rrx := \begin{pmatrix} 1 \\ 2 \\ 5 \\ 10 \end{pmatrix} \quad \lambda rxX1 := \begin{pmatrix} 0.0337 \\ 0.0337 \\ 1.0757 \\ 1.6465 \end{pmatrix} \quad \lambda rxX2 := \begin{pmatrix} 1.1477 \\ 1.1477 \\ -0.4492 \\ -1.5247 \end{pmatrix} \quad \lambda rxX3 := \begin{pmatrix} -1.0369 \\ -1.0369 \\ -0.1621 \\ 0.8516 \end{pmatrix} \quad \lambda rxX4 := \begin{pmatrix} 0.2849 \\ 0.2849 \\ 0.1550 \\ -0.2046 \end{pmatrix}$

$fXrx1(rx) := interp(pspline(Rrx, \lambda rxX1), Rrx, \lambda rxX1, rx) \qquad fXrx1(Rf) = 0.034$

$fXrx2(rx) := interp(pspline(Rrx, \lambda rxX2), Rrx, \lambda rxX2, rx) \qquad fXrx2(Rf) = 1.148$

$fXrx3(rx) := interp(pspline(Rrx, \lambda rxX3), Rrx, \lambda rxX3, rx) \qquad fXrx3(Rf) = -1.037$

$fXrx4(rx) := interp(pspline(Rrx, \lambda rxX4), Rrx, \lambda rxX4, rx) \qquad fXrx4(Rf) = 0.285$

$\lambda rx := \begin{cases} f\lambda r(ao, fXrx1(Rf), fXrx2(Rf), fXrx3(Rf), fXrx4(Rf)) & \text{if } Rf < 10 \\ f\lambda r(ao, fXrx1(10), fXrx2(10), fXrx3(10), fXrx4(10)) & \text{otherwise} \end{cases} = 4.441$

$Rry := \begin{pmatrix} 1 \\ 2 \\ 3 \\ 4 \\ 5 \end{pmatrix} \quad \lambda ryX1 := \begin{pmatrix} 0.0337 \\ 0.2383 \\ 0.6768 \\ 1.4238 \\ 1.4238 \end{pmatrix} \quad \lambda ryX2 := \begin{pmatrix} 1.1477 \\ 1.6257 \\ 1.5620 \\ 0.5046 \\ 0.5046 \end{pmatrix} \quad \lambda ryX3 := \begin{pmatrix} -1.0369 \\ -1.6804 \\ -2.0227 \\ -1.5762 \\ -1.5762 \end{pmatrix} \quad \lambda ryX4 := \begin{pmatrix} 0.2849 \\ 0.4895 \\ 0.6382 \\ 0.6052 \\ 0.6052 \end{pmatrix}$

$fXry1(ry) := interp(pspline(Rry, \lambda ryX1), Rry, \lambda ryX1, ry) \qquad fXry1(Rf) = 0.034$

$fXry2(ry) := interp(pspline(Rry, \lambda ryX2), Rry, \lambda ryX2, ry) \qquad fXry2(Rf) = 1.148$

$fXry3(ry) := interp(pspline(Rry, \lambda ryX3), Rry, \lambda ryX3, ry) \qquad fXry3(Rf) = -1.037$

$fXry4(ry) := interp(pspline(Rry, \lambda ryX4), Rry, \lambda ryX4, ry) \qquad fXry4(Rf) = 0.285$

$\lambda ry := \begin{cases} f\lambda r(ao, fXry1(Rf), fXry2(Rf), fXry3(Rf), fXry4(Rf)) & \text{if } Rf < 100 \\ 1 & \text{otherwise} \end{cases} = 4.441$

$f\lambda t(ao, R, X1, X2, X3, X4) := ao \cdot X1 + ao^2 \cdot X2 + ao^3 \cdot X3 + \frac{X4}{\tan\left(\frac{R}{ao}\right)}$

$Rt := \begin{pmatrix} 1 \\ 2 \\ 3 \\ 4 \end{pmatrix} \quad \lambda tX1 := \begin{pmatrix} -0.0452 \\ 0.8945 \\ 1.6330 \\ 2.6028 \end{pmatrix} \quad \lambda tX2 := \begin{pmatrix} 0.5277 \\ -0.2226 \\ -0.8238 \\ -2.0521 \end{pmatrix} \quad \lambda tX3 := \begin{pmatrix} -0.1843 \\ -0.0042 \\ 0.1156 \\ 0.5312 \end{pmatrix} \quad \lambda tX4 := \begin{pmatrix} 0.0214 \\ -0.0612 \\ -0.0962 \\ -0.1070 \end{pmatrix}$

$fXt1(t) := interp(pspline(Rt, \lambda tX1), Rt, \lambda tX1, t) \qquad fXt1(Rf) = -0.045$

$fXt2(t) := interp(pspline(Rt, \lambda tX2), Rt, \lambda tX2, t) \qquad fXt2(Rf) = 0.528$

$fXt3(t) := interp(pspline(Rt, \lambda tX3), Rt, \lambda tX3, t) \qquad fXt3(Rf) = -0.184$

$fXt4(t) := interp(pspline(Rt, \lambda tX4), Rt, \lambda tX4, t) \qquad fXt4(Rf) = 0.021$

$\lambda t := \begin{cases} f\lambda t(ao, Rf, fXt1(Rf), fXt2(Rf), fXt3(Rf), fXt4(Rf)) & \text{if } Rf \le 100 \\ 1 & \text{otherwise} \end{cases} = -0.095$

Static Stifness and Damping

$Kz := Sz \cdot \frac{2Lf \cdot Gs}{1 - \mu} = 124.725 \cdot kN \cdot mm^{-1}$

$Ky := Sy \cdot \frac{2Lf \cdot Gs}{2 - \mu} = 101.81 \cdot kN \cdot mm^{-1}$

$Kx := Ky - \frac{0.21 \cdot Lf \cdot Gs}{0.75 - \mu}\left(1 - \frac{Bf}{Lf}\right) = 101.81 \cdot kN \cdot mm^{-1}$

$K\theta x := S\theta x \cdot \frac{Gs \cdot If\theta x^{0.75} \cdot 1m^{-2}}{(1 - \mu) \cdot \sqrt[4]{\frac{Bf}{Lf}}} = 480.797 \cdot kN \cdot mm^{-1}$

$K\theta y := S\theta y \cdot Gs \cdot \frac{If\theta y^{0.75} \cdot 1m^{-2}}{1 - \mu} = 480.797 \cdot kN \cdot mm^{-1}$

$Kt := St \cdot Gs \cdot Jm^{0.75} \cdot 1m^{-2} = 4.765 \cdot kN \cdot mm^{-1}$

$Cz := \rho s \cdot Vs \cdot Af - 0.454 \cdot kN \cdot s \cdot mm^{-1}$

$Cy := \rho s \cdot Vs \cdot Af = 0.294 \cdot kN \cdot s \cdot mm^{-1}$

$Cx := \rho s \cdot Vs \cdot Af = 0.294 \cdot kN \cdot s \cdot mm^{-1}$

$C\theta x := \rho s \cdot VLA \cdot If\theta x \cdot 1m^{-2} = 1.737 \cdot kN \cdot s \cdot mm^{-1}$

$C\theta y := \rho s \cdot VLA \cdot If\theta y \cdot 1m^{-2} = 1.737 \cdot kN \cdot s \cdot mm^{-1}$

$Ct := \rho s \cdot Vs \cdot Jm \cdot 1m^{-2} = 3.06 \times 10^{-3} \cdot kN \cdot s \cdot mm^{-1}$

Dynamic Stifness and Damping

$$\eta z_{0.5} := \begin{pmatrix} \text{"ao/Rf"} & 1 & 2 & 3 & 4 & 5 & 6 & 10 \\ 0.00 & 1.000 & 1.000 & 1.000 & 1.000 & 1.000 & 1.000 & 1.000 \\ 0.10 & 0.995 & 0.995 & 0.995 & 0.995 & 0.995 & 0.995 & 0.995 \\ 0.20 & 0.980 & 0.989 & 0.998 & 1.007 & 1.016 & 1.025 & 1.225 \\ 0.30 & 0.975 & 0.990 & 1.005 & 1.020 & 1.035 & 1.050 & 1.250 \\ 0.40 & 0.970 & 0.988 & 1.006 & 1.024 & 1.042 & 1.060 & 1.240 \\ 0.50 & 0.950 & 0.970 & 0.990 & 1.010 & 1.030 & 1.050 & 1.220 \\ 0.60 & 0.925 & 0.945 & 0.965 & 0.985 & 1.005 & 1.025 & 1.180 \\ 0.70 & 0.910 & 0.924 & 0.938 & 0.952 & 0.966 & 0.980 & 1.075 \\ 0.80 & 0.890 & 0.892 & 0.894 & 0.896 & 0.898 & 0.900 & 1.000 \\ 0.90 & 0.850 & 0.850 & 0.850 & 0.850 & 0.850 & 0.850 & 0.900 \\ 1.00 & 0.820 & 0.806 & 0.792 & 0.778 & 0.764 & 0.750 & 0.760 \\ 1.10 & 0.786 & 0.752 & 0.717 & 0.683 & 0.648 & 0.614 & 0.536 \\ 1.20 & 0.752 & 0.697 & 0.642 & 0.588 & 0.533 & 0.478 & 0.312 \\ 1.30 & 0.718 & 0.643 & 0.568 & 0.492 & 0.417 & 0.342 & 0.088 \\ 1.40 & 0.684 & 0.588 & 0.493 & 0.397 & 0.302 & 0.206 & -0.136 \\ 1.50 & 0.650 & 0.534 & 0.418 & 0.302 & 0.186 & 0.070 & -0.360 \end{pmatrix}$$

$$Rf\eta z_{0.5} := \text{submatrix}\left(\eta z_{0.5}, \text{ORIGIN}, \text{ORIGIN}, \text{ORIGIN}-1, \text{ORIGIN}+\text{cols}\left(\eta z_{0.5}\right)-1\right)^{T}$$

$$aoi := \text{submatrix}\left(\eta z_{0.5}, \text{ORIGIN}+1, \text{rows}\left(\eta z_{0.5}\right)-1, \text{ORIGIN}, \text{ORIGIN}\right)$$

$$Vah\eta z_{0.5} := \text{submatrix}\left(\eta z_{0.5}, \text{ORIGIN}+1, \text{rows}\left(\eta z_{0.5}\right)-1, \text{ORIGIN}+1, \text{cols}\left(\eta z_{0.5}\right)-1\right)$$

$$Find\eta z_{0.5}(aon, Rfn) := \begin{| O \leftarrow \text{ORIGIN} \\ \text{for } col \in O..\text{cols}\left(Vah\eta z_{0.5}\right)-1 \\ \quad T_{col} \leftarrow \text{interp}\left(\text{cspline}\left(aoi, Vah\eta z_{0.5}^{\langle col\rangle}\right), aoi, Vah\eta z_{0.5}^{\langle col\rangle}, aon\right) \\ \text{return } \text{interp}\left(\text{cspline}\left(Rf\eta z_{0.5}, T\right), Rf\eta z_{0.5}, T, Rfn\right)|$$

$$myn\eta z_{0.5} := \begin{| Find\eta z_{0.5}(ao, Rf) \text{ if } Rf < 10 \quad = 0.049 \\ Find\eta z_{0.5}(ao, 10) \text{ otherwise}|$$

$$a_{oi} := \text{submatrix}\left(\eta z_{0.5}, \text{ORIGIN}+1, \text{rows}\left(\eta z_{0.5}\right)-1, \text{ORIGIN}, \text{ORIGIN}\right)$$

$$\eta z_{0.5\_1} := \text{submatrix}\left(\eta z_{0.5}, \text{ORIGIN}+1, \text{rows}\left(\eta z_{0.5}\right)-1, \text{ORIGIN}+1, \text{ORIGIN}+1\right)$$

$$\eta z_{0.5\_2} := \text{submatrix}\left(\eta z_{0.5}, \text{ORIGIN}+1, \text{rows}\left(\eta z_{0.5}\right)-1, \text{ORIGIN}+2, \text{ORIGIN}+2\right)$$

$$\eta z_{0.5\_3} := \text{submatrix}\left(\eta z_{0.5}, \text{ORIGIN}+1, \text{rows}\left(\eta z_{0.5}\right)-1, \text{ORIGIN}+3, \text{ORIGIN}+3\right)$$

$$\eta z_{0.5\_4} := \text{submatrix}\left(\eta z_{0.5}, \text{ORIGIN}+1, \text{rows}\left(\eta z_{0.5}\right)-1, \text{ORIGIN}+4, \text{ORIGIN}+4\right)$$

$$\eta z_{0.5\_5} := \text{submatrix}\left(\eta z_{0.5}, \text{ORIGIN}+1, \text{rows}\left(\eta z_{0.5}\right)-1, \text{ORIGIN}+5, \text{ORIGIN}+5\right)$$

$$\eta z_{0.5\_6} := \text{submatrix}\left(\eta z_{0.5}, \text{ORIGIN}+1, \text{rows}\left(\eta z_{0.5}\right)-1, \text{ORIGIN}+6, \text{ORIGIN}+6\right)$$

$$\eta z_{0.5\_10} := \text{submatrix}\left(\eta z_{0.5}, \text{ORIGIN}+1, \text{rows}\left(\eta z_{0.5}\right)-1, \text{ORIGIN}+7, \text{ORIGIN}+7\right)$$

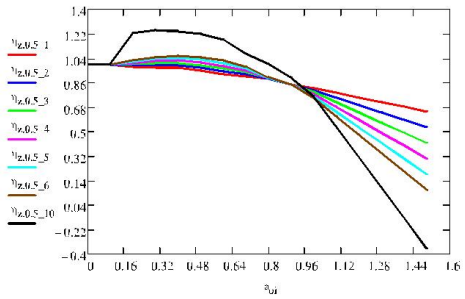

$$\eta z_{0.33} := \begin{pmatrix} \text{"ao/Rf"} & 1 & 2 & 3 & 4 & 5 & 6 & 10 \\ 0.00 & 1.000 & 1.000 & 1.000 & 1.000 & 1.000 & 1.000 & 1.000 \\ 0.10 & 0.995 & 1.000 & 1.005 & 0.995 & 1.000 & 1.001 & 0.995 \\ 0.20 & 0.980 & 1.000 & 1.020 & 1.050 & 1.070 & 1.093 & 1.225 \\ 0.30 & 0.975 & 1.000 & 1.025 & 1.075 & 1.100 & 1.133 & 1.300 \\ 0.40 & 0.970 & 1.000 & 1.030 & 1.140 & 1.170 & 1.224 & 1.325 \\ 0.50 & 0.950 & 1.010 & 1.070 & 1.180 & 1.240 & 1.315 & 1.350 \\ 0.60 & 0.940 & 1.025 & 1.110 & 1.190 & 1.275 & 1.359 & 1.370 \\ 0.70 & 0.920 & 1.025 & 1.130 & 1.195 & 1.300 & 1.393 & 1.360 \\ 0.80 & 0.900 & 1.010 & 1.120 & 1.200 & 1.310 & 1.411 & 1.330 \\ 0.90 & 0.880 & 1.005 & 1.130 & 1.190 & 1.315 & 1.421 & 1.310 \\ 1.00 & 0.850 & 1.000 & 1.150 & 1.196 & 1.346 & 1.467 & 1.300 \\ 1.10 & 0.840 & 0.980 & 1.120 & 1.178 & 1.318 & 1.433 & 1.258 \\ 1.20 & 0.830 & 0.960 & 1.090 & 1.159 & 1.289 & 1.400 & 1.216 \\ 1.30 & 0.820 & 0.940 & 1.060 & 1.139 & 1.259 & 1.367 & 1.174 \\ 1.40 & 0.810 & 0.920 & 1.030 & 1.120 & 1.230 & 1.333 & 1.132 \\ 1.50 & 0.800 & 0.900 & 1.000 & 1.100 & 1.200 & 1.300 & 1.090 \end{pmatrix}$$

$$Rf\eta z_{0.33} := \text{submatrix}\left(\eta z_{0.33}, \text{ORIGIN}, \text{ORIGIN}, \text{ORIGIN}+1, \text{ORIGIN}+\text{cols}\left(\eta z_{0.33}\right)-1\right)^{T}$$

$$Vah\eta z_{0.33} := \text{submatrix}\left(\eta z_{0.33}, \text{ORIGIN}+1, \text{rows}\left(\eta z_{0.33}\right)-1, \text{ORIGIN}+1, \text{cols}\left(\eta z_{0.33}\right)-1\right)$$

$$Find\eta z_{0.33}(aon, Rfn) := \begin{| O \leftarrow \text{ORIGIN} \\ \text{for } col \in O..\text{cols}\left(Vah\eta z_{0.33}\right)-1 \\ \quad T_{col} \leftarrow \text{interp}\left(\text{cspline}\left(aoi, Vah\eta z_{0.33}^{\langle col\rangle}\right), aoi, Vah\eta z_{0.33}^{\langle col\rangle}, aon\right) \\ \text{return } \text{interp}\left(\text{cspline}\left(Rf\eta z_{0.33}, T\right), Rf\eta z_{0.33}, T, Rfn\right)|$$

$$myn\eta z_{0.33} := \begin{| Find\eta z_{0.33}(ao, Rf) \text{ if } Rf < 10 \quad = 1.038 \\ Find\eta z_{0.33}(ao, 10) \text{ otherwise}|$$

$$\mu i := \begin{pmatrix} 0 \\ 0.33 \\ 0.5 \end{pmatrix} \qquad \eta zi := \begin{pmatrix} 0 \\ myn\eta z_{0.33} \\ myn\eta z_{0.5} \end{pmatrix}$$

$$\eta z(\nu) := \text{interp}\left(\text{pspline}\left(\mu i, \eta zi\right), \mu i, \eta zi, \nu\right) \qquad \eta z(\mu) = 1.105$$

$$\eta z_{0.33\_1} := \text{submatrix}\left(\eta z_{0.33}, \text{ORIGIN}+1, \text{rows}\left(\eta z_{0.33}\right)-1, \text{ORIGIN}+1, \text{ORIGIN}+1\right)$$

$$\eta z_{0.33\_2} := \text{submatrix}\left(\eta z_{0.33}, \text{ORIGIN}+1, \text{rows}\left(\eta z_{0.33}\right)-1, \text{ORIGIN}+2, \text{ORIGIN}+2\right)$$

$$\eta z_{0.33\_3} := \text{submatrix}\left(\eta z_{0.33}, \text{ORIGIN}+1, \text{rows}\left(\eta z_{0.33}\right)-1, \text{ORIGIN}+3, \text{ORIGIN}+3\right)$$

$$\text{Findhy}_{0.33}(aon, Rfn) := \begin{| 0 \leftarrow \text{ORIGIN} \\ \text{for } col \in 0..cols(Vahy_{0.33}) - 1 \\ \quad T_{col} \leftarrow interp\left(cspline\left(aoi, Vahy_{0.33}^{\langle col \rangle}\right), aoi, Vahy_{0.33}^{\langle col \rangle}, aon\right) \\ \text{return } interp\left(cspline\left(Rfhy_{0.33}, T\right), Rfhy_{0.33}, T, Rfn\right)}$$

$$myhy_{0.33} := \begin{| \text{Findhy}_{0.33}(ao, Rf) \quad \text{if } Rf < 10 \quad = 0.909 \\ \text{Findhy}_{0.33}(ao, 10) \quad \text{otherwise}}$$

$$\mu i := \begin{pmatrix} 0 \\ 0.33 \\ 0.5 \end{pmatrix} \qquad \eta yi := \begin{pmatrix} 0 \\ myhy_{0.33} \\ myhy_{0.5} \end{pmatrix}$$

$\eta y(\nu) := interp(pspline(\mu i, \eta yi), \mu i, \eta yi, \nu)$ $\qquad \eta y(\mu) = 0.875$

$\eta x(\mu) := 1$

$\eta_{y.0.33\_1} := submatrix\left(\eta y_{0.33}, ORIGIN + 1, rows\left(\eta y_{0.33}\right) - 1, ORIGIN + 1, ORIGIN + 1\right)$
$\eta_{y.0.33\_2} := submatrix\left(\eta y_{0.33}, ORIGIN + 1, rows\left(\eta y_{0.33}\right) - 1, ORIGIN + 2, ORIGIN + 2\right)$
$\eta_{y.0.33\_3} := submatrix\left(\eta y_{0.33}, ORIGIN + 1, rows\left(\eta y_{0.33}\right) - 1, ORIGIN + 3, ORIGIN + 3\right)$
$\eta_{y.0.33\_4} := submatrix\left(\eta y_{0.33}, ORIGIN + 1, rows\left(\eta y_{0.33}\right) - 1, ORIGIN + 4, ORIGIN + 4\right)$
$\eta_{y.0.33\_5} := submatrix\left(\eta y_{0.33}, ORIGIN + 1, rows\left(\eta y_{0.33}\right) - 1, ORIGIN + 5, ORIGIN + 5\right)$
$\eta_{y.0.33\_6} := submatrix\left(\eta y_{0.33}, ORIGIN + 1, rows\left(\eta y_{0.33}\right) - 1, ORIGIN + 6, ORIGIN + 6\right)$
$\eta_{y.0.33\_10} := submatrix\left(\eta y_{0.33}, ORIGIN + 1, rows\left(\eta y_{0.33}\right) - 1, ORIGIN + 7, ORIGIN + 7\right)$

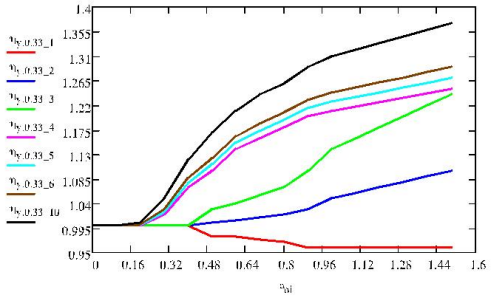

$$\eta rx := \begin{pmatrix} \text{"ao"} & \text{"ηr.x"} \\ 0.0000 & 1.0000 \\ 0.1000 & 1.0000 \\ 0.2000 & 0.9900 \\ 0.3000 & 0.9750 \\ 0.4000 & 0.9570 \\ 0.5000 & 0.9375 \\ 0.6000 & 0.9200 \\ 0.7000 & 0.8975 \\ 0.8000 & 0.8775 \\ 0.9000 & 0.8525 \\ 1.0000 & 0.8275 \\ 1.1000 & 0.8050 \\ 1.2000 & 0.7800 \\ 1.3000 & 0.7550 \\ 1.4000 & 0.7275 \\ 1.5000 & 0.7000 \end{pmatrix}$$

$Vahr_x := submatrix\left(\eta r_x, ORIGIN + 1, rows\left(\eta r_x\right) - 1, ORIGIN + 1, 1\right)$
$\eta\theta x(aon) := interp\left(pspline\left(aoi, Vahr_x\right), aoi, Vahr_x, aon\right)$
$\eta\theta x(ao) = 0.415$

$\eta_{r.x} := submatrix\left(\eta r_x, ORIGIN + 1, rows\left(\eta r_x\right) - 1, ORIGIN + 1, 1\right)$

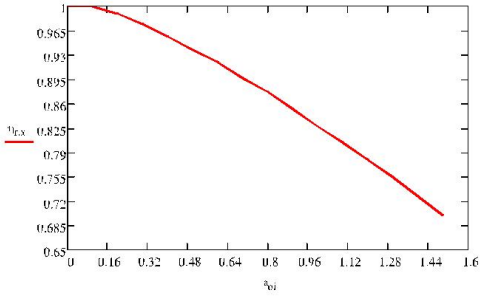

$\eta r_y :=$

"ao/Rf"	"L/B = 1"	"2 <= L/B <= 5"
0.0000	1.0000	1.0000
0.1000	1.0000	0.9500
0.2000	0.9650	0.9100
0.3000	0.9650	0.8800
0.4000	0.9450	0.8500
0.5000	0.9250	0.8225
0.6000	0.9050	0.8000
0.7000	0.8825	0.7720
0.8000	0.8600	0.7500
0.9000	0.8350	0.7300
1.0000	0.8100	0.7100
1.1000	0.7875	0.6900
1.2000	0.7650	0.6750
1.3000	0.7425	0.6560
1.4000	0.7200	0.6375
1.5000	0.7000	0.6200

$Vah\eta r_{y\_1} := submatrix\left(\eta r_y, ORIGIN + 1, rows\left(\eta r_y\right) - 1, ORIGIN + 1, 1\right)$

$Vah\eta r_{y\_2to5} := submatrix\left(\eta r_y, ORIGIN + 1, rows\left(\eta r_y\right) - 1, 2, 2\right)$

$\eta r y(aon, Rfn) := \begin{cases} interp\left(pspline\left(aoi, Vah\eta r_{y\_1}\right), aoi, Vah\eta r_{y\_1}, aon\right) & \text{if } Rfn = 1 \\ interp\left(pspline\left(aoi, Vah\eta r_{y\_2to5}\right), aoi, Vah\eta r_{y\_2to5}, aon\right) & \text{otherwise} \end{cases}$

$\eta r y(ao, Rf) = 0.749$

$\eta_{r\_y} := submatrix\left(\eta r_y, ORIGIN + 1, rows\left(\eta r_y\right) - 1, ORIGIN + 1, 1\right)$

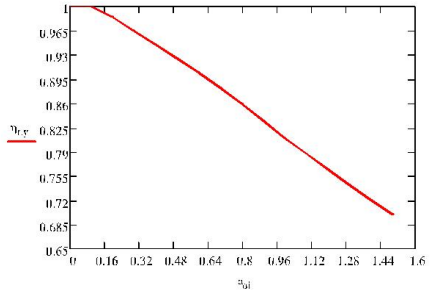

$\eta t :=$

"ao/Rf"	1	2	3	4
0.00	1.0000	1.0000	1.0000	1.0000
0.10	1.0000	0.9900	0.9800	0.9700
0.20	0.9950	0.9750	0.9550	0.9350
0.30	0.9850	0.9567	0.9283	0.9000
0.40	0.9700	0.9367	0.9033	0.8700
0.50	0.9550	0.9158	0.8767	0.8375
0.60	0.9350	0.8950	0.8550	0.8150
0.70	0.9150	0.8783	0.8417	0.8050
0.80	0.8950	0.8653	0.8357	0.8060
0.90	0.8750	0.8540	0.8330	0.8120
1.00	0.8575	0.8467	0.8358	0.8250
1.10	0.8375	0.8383	0.8392	0.8460
1.20	0.8225	0.8342	0.8458	0.8575
1.30	0.8025	0.8233	0.8442	0.8650
1.40	0.7875	0.8125	0.8375	0.8625
1.50	0.7750	0.8033	0.8317	0.8600

$Rf\eta_t := submatrix(\eta t, ORIGIN, ORIGIN, ORIGIN + 1, ORIGIN + cols(\eta t) - 1)^T$

$Vah\eta_t := submatrix(\eta t, ORIGIN + 1, rows(\eta t) - 1, ORIGIN + 1, cols(\eta t) - 1)$

$\eta_t(aon, Rfn) := \begin{array}{l} O \leftarrow ORIGIN \\ \text{for } col \in O .. cols\left(Vah\eta_t\right) - 1 \\ \quad T_{col} \leftarrow interp\left(cspline\left(aoi, Vah\eta_t^{\langle col \rangle}\right), aoi, Vah\eta_t^{\langle col \rangle}, aon\right) \\ \text{return } interp\left(cspline\left(Rf\eta_t, T\right), Rf\eta_t, T, Rfn\right) \end{array}$

$\eta_t(ao, Rf) = -3.275$

$\eta_{t\_1} := submatrix\left(\eta y_{0.33}, ORIGIN + 1, rows\left(\eta y_{0.33}\right) - 1, ORIGIN + 1, ORIGIN + 1\right)$

$\eta_{t\_2} := submatrix\left(\eta y_{0.33}, ORIGIN + 1, rows\left(\eta y_{0.33}\right) - 1, ORIGIN + 2, ORIGIN + 2\right)$

$\eta_{t\_3} := submatrix\left(\eta y_{0.33}, ORIGIN + 1, rows\left(\eta y_{0.33}\right) - 1, ORIGIN + 3, ORIGIN + 3\right)$

$\eta_{t\_4} := submatrix\left(\eta y_{0.33}, ORIGIN + 1, rows\left(\eta y_{0.33}\right) - 1, ORIGIN + 4, ORIGIN + 4\right)$

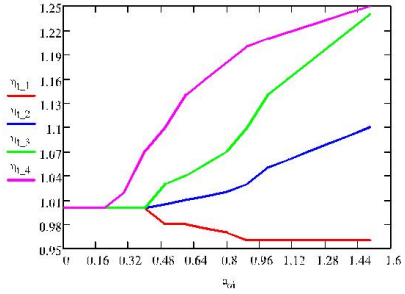

$Kiz := \eta z(\mu) \cdot Kz = 137.759 \cdot kN \cdot mm^{-1}$

$Kiy := \eta y(\mu) \cdot Ky = 89.134 \cdot kN \cdot mm^{-1}$

$Ciz := \begin{cases} \lambda z \cdot ps \cdot VLA \cdot Af & \text{if } 0 \le ao \le 1.5 \\ ps \cdot VLA \cdot Af & \text{otherwise} \end{cases} = 0.454 \cdot kN \cdot s \cdot mm^{-1}$

$Kix := \eta x(\mu) \cdot Kx = 101.81 \cdot kN \cdot mm^{-1}$

$Kiy := \eta y(\mu) \cdot Ky = 199.511 \cdot kN \cdot mm^{-1}$

$K\theta ix := \eta \theta x(ao) \cdot K\theta x = 360.135 \cdot kN \cdot mm^{-1}$

$K\theta iy := \eta \theta y(ao, Rf) \cdot K\theta y = 360.135 \cdot kN \cdot mm^{-1}$

$Kit := \eta_t(ao, Rf) \cdot Kt = -15.609 \cdot kN \cdot mm^{-1}$

$$Ciy := \begin{cases} \lambda y \cdot \rho s \cdot Vs \cdot Af & \text{if } 0 \le ao \le 1.5 \\ \rho s \cdot Vs \cdot Af & \text{otherwise} \end{cases} = 0.294 \cdot kN \cdot s \cdot mm^{-1}$$

$$Cix := \begin{cases} \lambda y1 \cdot \rho s \cdot Vs \cdot Af & \text{if } 0 \le Rf \le 3 \\ \rho s \cdot Vs \cdot Af & \text{otherwise} \end{cases} = 0.447 \cdot kN \cdot s \cdot mm^{-1}$$

$C\theta ix := \lambda rx \cdot \rho s \cdot VLA \cdot If\theta x \cdot 1m^{-2} = 7.712 \cdot kN \cdot s \cdot mm^{-1}$

$C\theta iy := \lambda ry \cdot \rho s \cdot VLA \cdot If\theta y \cdot 1m^{-2} = 7.712 \cdot kN \cdot s \cdot mm^{-1}$

$Cit := \lambda t \cdot \rho s \cdot Vs \cdot Jm \cdot 1m^{-2} = -2.917 \times 10^{-4} \cdot kN \cdot s \cdot mm^{-1}$

$\beta d := 0.01$ 0.01 - 0.1 (Whitman & Richard); 0.02 - 0.05 (Barkan)

SUMMARY

$Kz_{dyn} := Kiz - \omega \cdot Ciz \cdot \beta d = 134.335 \cdot kN \cdot mm^{-1}$

$Ky_{dyn} := Kiy - \omega \cdot Ciy \cdot \beta d = 86.919 \cdot kN \cdot mm^{-1}$

$Kx_{dyn} := Kix - \omega \cdot Cix \cdot \beta d = 98.443 \cdot kN \cdot mm^{-1}$

$K\theta x_{dyn} := Ki\theta x - \omega \cdot Ci\theta x \cdot \beta d = 141.363 \cdot kN \cdot mm^{-1}$

$K\theta y_{dyn} := Ki\theta y - \omega \cdot Ci\theta y \cdot \beta d = 301.987 \cdot kN \cdot mm^{-1}$

$Kt_{dyn} := Kit - \omega \cdot Cit \cdot \beta d = -15.607 \cdot kN \cdot mm^{-1}$

$Cz_{dyn} := Ciz + 2 \cdot \frac{Kiz \cdot \beta d}{\omega} = 0.458 \cdot kN \cdot s \cdot mm^{-1}$

$Cy_{dyn} := Ciy + 2 \cdot \frac{Kiy \cdot \beta d}{\omega} = 0.296 \cdot kN \cdot s \cdot mm^{-1}$

$Cx_{dyn} := Cix + 2 \cdot \frac{Kix \cdot \beta d}{\omega} = 0.449 \cdot kN \cdot s \cdot mm^{-1}$

$C\theta x_{dyn} := Ci\theta x + 2 \cdot \frac{Ki\theta x \cdot \beta d}{\omega} = 7.717 \cdot kN \cdot s \cdot mm^{-1}$

$C\theta y_{dyn} := Ci\theta y + 2 \cdot \frac{Ki\theta y \cdot \beta d}{\omega} = 7.722 \cdot kN \cdot s \cdot mm^{-1}$

$Ct_{dyn} := Cit + 2 \cdot \frac{Kit \cdot \beta d}{\omega} = -7.057 \times 10^{-4} \cdot kN \cdot s \cdot mm^{-1}$

$Ki := \left[Kz_{dyn} \cdot \left(1 kN^{-1} \cdot mm\right) \quad Ky_{dyn} \cdot \left(1 kN^{-1} \cdot mm\right) \quad Kx_{dyn} \cdot \left(1 kN^{-1} \cdot mm\right) \right]$

$Ci := \left[Cz_{dyn} \cdot \left(1 kN^{-1} \cdot s^{-1} \cdot mm\right) \quad Cy_{dyn} \cdot \left(1 kN^{-1} \cdot s^{-1} \cdot mm\right) \quad Cx_{dyn} \cdot \left(1 kN^{-1} \cdot s^{-1} \cdot mm\right) \right]$

$Ki = (134.335 \quad 86.919 \quad 98.443)$

$Ci = (0.458 \quad 0.296 \quad 0.449)$

Table 74. Data of dynamic damping and stiffness of soil model

F	E_s	μ	Υ_s	Stiffness/m² [kN/mm]			Damping/m² [kN.s/mm]			F	E_s	μ	Υ_s	Stiffness/m² [kN/mm]			Damping/m² [kN.s/mm]		
[Hz]	[MPa]	-	[kN/m³]	Vert.	Long.	Trans.	Vert.	Long.	Trans.	[Hz]	[MPa]	-	[kN/m³]	Vert.	Long.	Trans.	Vert.	Long.	Trans.
0	10	0.4	17	13.51	10.05	10.05	0.14	0.08	0.08	0	80	0.3	20	99.78	81.45	81.45	0.39	0.25	0.25
2	10	0.4	17	13.91	10.46	10.04	0.15	0.09	0.09	2	80	0.3	20	96.14	78.44	81.42	0.50	0.34	0.35
5	10	0.4	17	13.68	10.47	10.02	0.14	0.08	0.08	5	80	0.3	20	95.15	78.43	81.38	0.41	0.27	0.27
9	10	0.4	17	13.05	10.22	10.01	0.14	0.07	0.07	9	80	0.3	20	93.77	78.33	81.32	0.39	0.25	0.25
10	10	0.4	17	12.85	10.17	10.00	0.14	0.07	0.07	10	80	0.3	20	93.62	78.30	81.31	0.38	0.25	0.25
16	10	0.4	17	11.44	9.98	9.97	0.14	0.07	0.07	16	80	0.3	20	92.77	78.16	81.23	0.37	0.24	0.24
20	10	0.4	17	10.71	9.96	9.95	0.14	0.08	0.08	20	80	0.3	20	90.76	76.55	81.17	0.37	0.24	0.24
30	10	0.4	17	9.19	9.85	9.88	0.14	0.08	0.09	30	80	0.3	20	86.51	75.87	81.02	0.37	0.23	0.23
40	10	0.4	17	9.49	9.43	9.76	0.14	0.08	0.12	40	80	0.3	20	80.77	74.79	80.87	0.38	0.23	0.24
50	10	0.4	17	13.51	8.34	9.56	0.14	0.08	0.16	50	80	0.3	20	78.88	74.61	80.71	0.38	0.24	0.24
60	10	0.4	17	23.08	6.27	9.25	0.14	0.08	0.21	60	80	0.3	20	76.82	74.40	80.53	0.39	0.26	0.25
63	10	0.4	17	27.32	5.41	9.14	0.14	0.08	0.23	63	80	0.3	20	76.28	74.35	80.47	0.39	0.25	0.25
70	10	0.4	17	40.09	2.87	8.81	0.14	0.08	0.28	70	80	0.3	20	75.46	74.18	80.31	0.39	0.25	0.26
80	10	0.4	17	66.41	-2.18	8.20	0.15	0.08	0.37	80	80	0.3	20	76.08	73.76	80.05	0.39	0.25	0.28
90	10	0.4	17	103.91	-9.26	7.39	0.15	0.08	0.47	90	80	0.3	20	79.97	73.02	79.73	0.39	0.25	0.31
92	10	0.4	17	112.92	-10.90	7.20	0.15	0.08	0.49	92	80	0.3	20	81.25	72.83	79.66	0.39	0.25	0.31
100	10	0.4	17	154.46	-18.59	6.35	0.15	0.08	0.59	100	80	0.3	20	88.41	71.84	79.35	0.39	0.25	0.34
120	10	0.4	17	302.18	-45.62	3.47	0.15	0.08	0.87	120	80	0.3	20	124.12	67.65	78.33	0.39	0.25	0.42
0	20	0.4	17	27.02	20.09	20.09	0.20	0.11	0.11	0	100	0.3	22	124.73	101.81	101.81	0.45	0.29	0.29
2	20	0.4	17	28.02	20.93	20.08	0.23	0.13	0.13	2	100	0.3	22	120.20	98.06	101.78	0.60	0.41	0.42
5	20	0.4	17	27.45	20.90	20.06	0.20	0.11	0.11	5	100	0.3	22	119.09	98.04	101.73	0.49	0.32	0.32
9	20	0.4	17	27.02	20.72	20.03	0.19	0.11	0.11	9	100	0.3	22	117.36	97.94	101.66	0.46	0.29	0.30
10	20	0.4	17	26.70	20.49	20.03	0.19	0.11	0.11	10	100	0.3	22	117.13	97.90	101.65	0.45	0.29	0.29
16	20	0.4	17	25.18	20.24	19.99	0.19	0.10	0.10	16	100	0.3	22	116.41	98.00	101.55	0.44	0.28	0.28
20	20	0.4	17	23.59	19.97	19.96	0.19	0.10	0.10	20	100	0.3	22	114.08	96.13	101.48	0.44	0.28	0.28
30	20	0.4	17	20.98	19.90	19.89	0.20	0.11	0.11	30	100	0.3	22	109.37	95.07	101.31	0.43	0.27	0.27
40	20	0.4	17	18.75	19.77	19.79	0.20	0.11	0.12	40	100	0.3	22	102.80	93.44	101.14	0.44	0.27	0.28
50	20	0.4	17	18.02	19.37	19.64	0.20	0.11	0.14	50	100	0.3	22	99.41	93.33	100.95	0.45	0.28	0.28
60	20	0.4	17	20.12	18.48	19.44	0.20	0.11	0.17	60	100	0.3	22	96.96	93.12	100.75	0.46	0.29	0.29
63	20	0.4	17	21.50	18.07	19.36	0.20	0.11	0.19	63	100	0.3	22	96.24	93.02	100.68	0.46	0.30	0.29
70	20	0.4	17	26.37	16.84	19.14	0.20	0.11	0.22	70	100	0.3	22	94.85	92.86	100.51	0.46	0.30	0.30
80	20	0.4	17	38.10	14.23	18.75	0.20	0.11	0.27	80	100	0.3	22	94.31	92.50	100.23	0.46	0.30	0.32
90	20	0.4	17	56.62	10.41	18.22	0.20	0.11	0.33	90	100	0.3	22	96.65	91.85	99.90	0.46	0.30	0.34
92	20	0.4	17	61.26	9.48	18.10	0.20	0.11	0.35	92	100	0.3	22	97.59	91.67	99.82	0.46	0.30	0.35
100	20	0.4	17	83.27	5.14	17.46	0.20	0.11	0.41	100	100	0.3	22	103.22	90.79	99.50	0.46	0.30	0.37
120	20	0.4	17	166.20	-10.66	15.67	0.21	0.11	0.59	120	100	0.3	22	134.34	86.92	98.44	0.46	0.30	0.45
0	40	0.45	18	56.93	40.04	40.04	0.31	0.16	0.16	0	150	0.3	22	187.09	152.72	152.72	0.56	0.36	0.36
2	40	0.45	18	58.88	41.48	40.03	0.38	0.21	0.20	2	150	0.3	22	180.39	147.09	152.68	0.79	0.55	0.56
5	40	0.45	18	57.87	41.46	40.00	0.32	0.17	0.17	5	150	0.3	22	179.28	147.06	152.62	0.62	0.41	0.41
9	40	0.45	18	57.34	41.47	39.97	0.31	0.16	0.16	9	150	0.3	22	176.94	147.01	152.54	0.57	0.37	0.37
10	40	0.45	18	57.25	41.50	39.96	0.31	0.15	0.15	10	150	0.3	22	176.45	146.97	152.52	0.56	0.36	0.37
16	40	0.45	18	54.84	40.51	39.90	0.30	0.15	0.15	16	150	0.3	22	175.25	146.92	152.40	0.54	0.35	0.35
20	40	0.45	18	53.30	40.24	39.87	0.30	0.15	0.15	20	150	0.3	22	174.44	146.90	152.31	0.54	0.34	0.34
30	40	0.45	18	47.22	39.57	39.77	0.31	0.15	0.15	30	150	0.3	22	169.03	143.58	152.11	0.53	0.34	0.34
40	40	0.45	18	41.73	39.46	39.66	0.31	0.16	0.16	40	150	0.3	22	161.64	142.11	151.90	0.53	0.34	0.34
50	40	0.45	18	36.32	39.30	39.53	0.32	0.16	0.17	50	150	0.3	22	153.08	140.19	151.69	0.54	0.34	0.34
60	40	0.45	18	31.30	38.94	39.35	0.32	0.16	0.19	60	150	0.3	22	149.54	140.02	151.46	0.54	0.34	0.34
63	40	0.45	18	29.92	38.76	39.29	0.32	0.16	0.19	63	150	0.3	22	148.56	139.95	151.39	0.55	0.34	0.34
70	40	0.45	18	26.99	38.17	39.12	0.31	0.16	0.21	70	150	0.3	22	146.51	139.77	151.21	0.55	0.35	0.35
80	40	0.45	18	23.74	38.82	38.82	0.31	0.16	0.25	80	150	0.3	22	143.58	139.46	150.94	0.56	0.37	0.36
90	40	0.45	18	21.88	34.68	38.43	0.31	0.16	0.29	90	150	0.3	22	141.63	139.14	150.63	0.56	0.37	0.38
92	40	0.45	18	21.71	34.14	38.34	0.31	0.16	0.30	92	150	0.3	22	141.45	139.05	150.56	0.56	0.37	0.38
100	40	0.45	18	21.75	31.56	37.94	0.31	0.16	0.34	100	150	0.3	22	141.69	138.62	150.27	0.56	0.36	0.39
120	40	0.45	18	28.00	21.66	36.57	0.31	0.16	0.46	120	150	0.3	22	152.23	136.56	149.37	0.56	0.36	0.45

F	E_s	μ	Υ_s	Stiffness/m² [kN/mm]			Damping/m² [kN.s/mm]			F	E_s	μ	Υ_s	Stiffness/m² [kN/mm]			Damping/m² [kN.s/mm]		
[Hz]	[MPa]	-	[kN/m³]	Vert.	Long.	Trans.	Vert.	Long.	Trans.	[Hz]	[MPa]	-	[kN/m³]	Vert.	Long.	Trans.	Vert.	Long.	Trans.
0	50	0.45	18	71.16	50.06	50.06	0.35	0.18	0.18	0	200	0.3	22	249.45	203.62	203.62	0.64	0.42	0.42
2	50	0.45	18	73.66	51.85	50.04	0.44	0.24	0.24	2	200	0.3	22	240.56	196.13	203.58	0.97	0.67	0.69
5	50	0.45	18	75.55	51.84	50.01	0.36	0.19	0.19	5	200	0.3	22	239.49	196.09	203.51	0.74	0.49	0.49
9	50	0.45	18	71.73	51.77	49.97	0.35	0.18	0.18	9	200	0.3	22	236.84	196.05	203.41	0.67	0.43	0.44
10	50	0.45	18	71.68	51.83	49.96	0.34	0.17	0.17	10	200	0.3	22	236.17	196.02	203.39	0.66	0.43	0.43
16	50	0.45	18	69.45	50.60	49.90	0.34	0.17	0.17	16	200	0.3	22	233.90	195.74	203.25	0.63	0.41	0.41
20	50	0.45	18	67.63	50.55	49.86	0.34	0.17	0.17	20	200	0.3	22	233.52	196.09	203.16	0.62	0.40	0.40
30	50	0.45	18	61.27	49.47	49.75	0.34	0.17	0.17	30	200	0.3	22	226.96	191.42	202.92	0.62	0.39	0.39
40	50	0.45	18	56.07	49.38	49.64	0.35	0.17	0.17	40	200	0.3	22	221.13	190.64	202.69	0.61	0.39	0.39
50	50	0.45	18	48.93	49.24	49.50	0.35	0.18	0.18	50	200	0.3	22	212.97	188.15	202.44	0.62	0.39	0.39
60	50	0.45	18	43.02	49.00	49.33	0.35	0.18	0.19	60	200	0.3	22	202.10	186.98	202.19	0.62	0.39	0.39
63	50	0.45	18	41.33	48.88	49.27	0.35	0.18	0.20	63	200	0.3	22	201.14	186.89	202.12	0.62	0.39	0.39
70	50	0.45	18	37.61	48.48	49.12	0.35	0.18	0.22	70	200	0.3	22	199.10	186.67	201.93	0.63	0.39	0.39
80	50	0.45	18	33.01	47.51	48.85	0.35	0.18	0.24	80	200	0.3	22	195.63	186.39	201.64	0.64	0.40	0.40
90	50	0.45	18	29.52	45.91	48.50	0.35	0.18	0.28	90	200	0.3	22	192.18	186.02	201.33	0.65	0.42	0.41
92	50	0.45	18	28.98	45.50	48.42	0.35	0.18	0.28	92	200	0.3	22	191.56	185.96	201.26	0.65	0.42	0.42
100	50	0.45	18	27.43	43.52	48.07	0.35	0.18	0.32	100	200	0.3	22	189.50	185.68	200.98	0.65	0.42	0.43
120	50	0.45	18	28.67	35.69	46.87	0.35	0.18	0.42	120	200	0.3	22	190.01	184.45	200.15	0.65	0.42	0.47
0	60	0.3	18	74.84	61.09	61.09	0.32	0.21	0.21	0	250	0.3	22	311.81	254.53	254.53	0.72	0.46	0.46
2	60	0.3	18	72.08	58.83	61.06	0.40	0.27	0.28	2	250	0.3	22	300.73	245.18	254.47	1.13	0.79	0.81
5	60	0.3	18	71.21	58.82	61.03	0.34	0.22	0.22	5	250	0.3	22	299.71	245.12	254.40	0.84	0.56	0.57
9	60	0.3	18	70.23	58.73	60.98	0.32	0.20	0.20	9	250	0.3	22	296.88	245.08	254.30	0.76	0.49	0.50
10	60	0.3	18	70.15	58.72	60.97	0.31	0.20	0.20	10	250	0.3	22	296.10	245.06	254.27	0.75	0.49	0.49
16	60	0.3	18	68.96	58.11	60.90	0.31	0.19	0.20	16	250	0.3	22	292.78	244.74	254.11	0.71	0.46	0.46
20	60	0.3	18	67.77	57.39	60.86	0.30	0.19	0.19	20	250	0.3	22	292.13	244.79	254.01	0.70	0.45	0.45
30	60	0.3	18	63.98	56.50	60.74	0.31	0.19	0.19	30	250	0.3	22	286.84	241.71	253.75	0.69	0.44	0.44
40	60	0.3	18	60.16	56.03	60.61	0.31	0.19	0.19	40	250	0.3	22	281.00	239.32	253.48	0.69	0.43	0.44
50	60	0.3	18	58.42	55.89	60.47	0.32	0.20	0.20	50	250	0.3	22	270.85	237.21	253.22	0.69	0.43	0.43
60	60	0.3	18	56.91	55.72	60.31	0.32	0.21	0.21	60	250	0.3	22	261.96	233.75	252.94	0.69	0.43	0.43
63	60	0.3	18	56.65	55.65	60.25	0.32	0.21	0.22	63	250	0.3	22	257.38	233.59	252.86	0.69	0.43	0.43
70	60	0.3	18	56.68	55.44	60.11	0.32	0.21	0.23	70	250	0.3	22	251.50	233.64	252.66	0.70	0.44	0.44
80	60	0.3	18	59.01	54.92	59.86	0.32	0.21	0.25	80	250	0.3	22	248.14	233.29	252.36	0.71	0.44	0.44
90	60	0.3	18	65.17	54.03	59.56	0.32	0.21	0.27	90	250	0.3	22	244.32	232.97	252.03	0.72	0.45	0.45
92	60	0.3	18	66.97	53.80	59.49	0.32	0.21	0.28	92	250	0.3	22	243.54	232.90	251.97	0.72	0.45	0.45
100	60	0.3	18	76.42	52.64	59.18	0.32	0.21	0.31	100	250	0.3	22	240.45	232.54	251.69	0.73	0.47	0.46
120	60	0.3	18	119.33	47.87	58.17	0.32	0.21	0.39	120	250	0.3	22	235.65	231.68	250.88	0.72	0.47	0.49

Appendix 8. Fatigue Limit Criteria of Jointed Concrete Pavement

Table 75. Strength characteristics of different concrete classes

Concrete Class	f'_c [MPa]	$f'_{c,mean}$ [MPa]	E_c (EN1992-1) [MPa]	$f't$ [MPa]
C30/37	30	38	33607	3.8
C35/45	35	43	34771	4.2*
C40/50	40	48	35861	4.6
C45/55	45	53	36888	5.0
C50/60	50	58	37859	5.4
C60/75	60	68	39664	6.1

*) Comparison to laboratory data in *Chair and Institute of Road, Railway and Airfield Construction* of a concrete with E = 34 GPa: 5.5 MPa (for modelling CRCP) [68], 5.25 MPa of whitetopping concrete[31].

Table 76. Temperature gradients of concrete slab with various thicknesses

Slab Thickness h [mm]	Temperature Gradient	
	Summer	Winter
	$\Delta t+$	$\Delta t-$
200	0.1091	0.0395
240	0.0975	0.0369
300	0.0825	0.0355
400	0.0623	0.0351
450	0.0542	0.0350
600	0.0356	0.0350

Table 77. Maximum thermal stress in a semi-infinite concrete slab

Concrete Class	σ_w [MPa]											
	h = 20 cm		h = 24 cm		h = 30 cm		h = 40 cm		h =45 cm		h = 60 cm	
	Summer	Winter	Summer	Winter	Summer	Winter	Summer	Winter	Summer	Winter	Summer	Winter
C30/37	5.2	1.9	5.6	2.1	5.9	2.5	5.9	3.3	5.8	3.7	5.1	5.0
C35/45	5.4	1.9	5.7	2.2	6.1	2.6	6.1	3.4	6.0	3.9	5.2	5.2
C40/50	5.5	2.0	5.9	2.2	6.3	2.7	6.3	3.5	6.2	4.0	5.4	5.3
C45/55	5.7	2.1	6.1	2.3	6.4	2.8	6.5	3.7	6.3	4.1	5.6	5.5
C50/60	5.8	2.1	6.3	2.4	6.6	2.8	6.7	3.7	6.5	4.2	5.7	5.6
C60/75	6.1	2.2	6.6	2.5	6.9	3.0	7.0	3.9	6.8	4.4	6.0	5.9

Table 78. Critical length of concrete slab with different concrete classes and thicknesses

Concrete Class	L_{crit} [m]											
	h = 20 cm		h = 24 cm		h = 30 cm		h = 40 cm		h =45 cm		h = 60 cm	
	Summer	Winter	Summer	Winter	Summer	Winter	Summer	Winter	Summer	Winter	Summer	Winter
C30/37	8.4	4.6	9.5	5.3	10.9	6.6	12.7	8.7	13.3	9.8	14.4	13.0
C35/45	8.5	4.7	9.7	5.4	11.1	6.7	12.9	8.8	13.5	9.9	14.6	13.2
C40/50	8.7	4.8	9.8	5.5	11.3	6.8	13.1	9.0	13.7	10.1	14.8	13.4
C45/55	8.8	4.8	10.0	5.6	11.5	6.9	13.3	9.1	13.9	10.2	15.1	13.6
C50/60	8.9	4.9	10.1	5.7	11.6	7.0	13.5	9.2	14.1	10.4	15.3	13.8
C60/75	9.1	5.0	10.3	5.8	11.9	7.1	13.8	9.4	14.4	10.6	15.6	14.1

Table 79. Impact of concrete slab length to the thermal stress of concrete class C35/45

Slab Length [m]	σ_w" [MPa]											
	h = 20 cm		*h* = 24 cm		*h* = 30 cm		*h* = 40 cm		*h* =45 cm		*h* = 60 cm	
	Summer	Winter	Summer	Winter	Summer	Winter	Summer	Winter	Summer	Winter	Summer	Winter
1.95	0.28	0.34	0.23	0.28	0.19	0.22	0.14	0.17	0.12	0.15	0.09	0.11
2.6	0.50	0.60	0.41	0.50	0.33	0.40	0.25	0.30	0.22	0.27	0.17	0.20
3.25	0.78	0.93	0.65	0.78	0.52	0.62	0.39	0.47	0.35	0.41	0.26	0.31
4.55	1.52	2.33	1.27	1.52	1.02	1.22	0.76	0.91	0.68	0.81	0.51	0.61
5.85	2.52	2.33	2.10	2.61	1.68	2.01	1.26	1.51	1.12	1.34	0.84	1.01
6.5	3.11	2.33	2.59	2.61	2.07	3.14	1.55	1.87	1.38	1.66	1.04	1.24
7.15	3.76	2.33	3.13	2.61	2.51	3.14	1.88	2.26	1.67	2.01	1.25	1.50
7.8	6.43	2.33	3.73	2.61	2.98	3.14	2.24	2.69	1.99	2.39	1.49	1.79
8.45	6.43	2.33	4.38	2.61	3.50	3.14	2.63	4.13	2.33	2.80	1.75	2.10
9.1	6.43	2.33	6.89	2.61	4.06	3.14	3.05	4.13	2.71	4.64	2.03	2.44

Table 80. Allowable tensile stress levels of concrete class C35/45 with different lengths

Slab Length [m]	σ_{allow} [MPa]											
	h = 20 cm		*h* = 24 cm		*h* = 30 cm		*h* = 40 cm		*h* =45 cm		*h* = 60 cm	
	Summer	Winter	Summer	Winter	Summer	Winter	Summer	Winter	Summer	Winter	Summer	Winter
1.95	2.77	2.72	2.80	2.77	2.83	2.81	2.87	2.85	2.88	2.86	2.90	2.89
2.6	2.61	2.53	2.67	2.61	2.73	2.68	2.79	2.75	2.81	2.78	2.85	2.83
3.25	2.40	2.28	2.49	2.40	2.59	2.51	2.69	2.63	2.72	2.67	2.78	2.74
4.55	1.85	1.25	2.04	1.85	2.22	2.07	2.41	2.30	2.47	2.37	2.60	2.52
5.85	1.12	1.25	1.42	1.05	1.73	1.49	2.04	1.86	2.15	1.98	2.35	2.23
6.5	0.68	1.25	1.06	1.05	1.44	0.66	1.83	1.60	1.95	1.75	2.21	2.06
7.15	0.20	1.25	0.66	1.05	1.12	0.66	1.59	1.31	1.74	1.49	2.05	1.86

Table 81. Impact of concrete slab length to the thermal stress of concrete class C40/50

Slab Length [m]	σ_w" [MPa]											
	h = 20 cm		*h* = 24 cm		*h* = 30 cm		*h* = 40 cm		*h* =45 cm		*h* = 60 cm	
	Summer	Winter	Summer	Winter	Summer	Winter	Summer	Winter	Summer	Winter	Summer	Winter
1.95	0.28	0.34	0.23	0.28	0.19	0.22	0.14	0.17	0.12	0.15	0.09	0.11
2.6	0.50	0.60	0.41	0.50	0.33	0.40	0.25	0.30	0.22	0.27	0.17	0.20
3.25	0.78	0.93	0.65	0.78	0.52	0.62	0.39	0.47	0.35	0.41	0.26	0.31
4.55	1.52	2.40	1.27	1.52	1.02	1.22	0.76	0.91	0.68	0.81	0.51	0.61
5.85	2.52	2.40	2.10	2.69	1.68	2.01	1.26	1.51	1.12	1.34	0.84	1.01
6.5	3.11	2.40	2.59	2.69	2.07	3.24	1.55	1.87	1.38	1.66	1.04	1.24
7.15	3.76	2.40	3.13	2.69	2.51	3.24	1.88	2.26	1.67	2.01	1.25	1.50
7.8	6.63	2.40	3.73	2.69	2.98	3.24	2.24	2.69	1.99	2.39	1.49	1.79
8.45	6.63	2.40	4.38	2.69	3.50	3.24	2.63	4.26	2.33	2.80	1.75	2.10
9.1	6.63	2.40	7.11	2.69	4.06	3.24	3.05	4.26	2.71	4.79	2.03	2.44

Table 82. Allowable tensile stress levels of concrete class C40/50 with different lengths

Slab Length [m]	σ_{allow} [MPa]											
	h = 20 cm		*h* = 24 cm		*h* = 30 cm		*h* = 40 cm		*h* =45 cm		*h* = 60 cm	
	Summer	Winter	Summer	Winter	Summer	Winter	Summer	Winter	Summer	Winter	Summer	Winter
1.95	3.04	3.00	3.08	3.04	3.11	3.09	3.15	3.13	3.16	3.14	3.18	3.17
2.6	2.88	2.81	2.94	2.88	3.01	2.96	3.07	3.03	3.09	3.05	3.13	3.10
3.25	2.68	2.56	2.77	2.68	2.87	2.79	2.96	2.91	3.00	2.94	3.06	3.02
4.55	2.13	1.48	2.31	2.13	2.50	2.35	2.69	2.58	2.75	2.65	2.88	2.80
5.85	1.39	1.48	1.70	1.27	2.01	1.76	2.32	2.14	2.43	2.26	2.63	2.51
6.5	0.96	1.48	1.34	1.27	1.72	0.86	2.10	1.87	2.23	2.03	2.49	2.33
7.15	0.48	1.48	0.94	1.27	1.40	0.86	1.86	1.59	2.02	1.77	2.33	2.14

Appendix 9. Calibration of FEA Model for Dynamic Analysis

A.9.1. Linear and Nonlinear Fastening Models

Firstly, LIN-FAST linear and NL-FAST nonlinear models are both used to model linear behaviour of a fastening system. Nonlinear model of NL-FAST is utilized for linear behaviour of fastening system means that stiffness in tension and compression directions are set equally (60 kN/mm) and preloading force is neglected. This comparison is done as verification to observe if both models work linearly similar before nonlinearity of fastening system is introduced to the complex model. A small constant damping of 2.N.s/mm is firstly assigned to the elastic-pad to idealize quasi-undamped system. Lumped mass of soil are not taken into account. The dynamic response resulted from 200 kN wheel load exhibits that both models using LIN-FAST and NL-FAST are almost identical to idealize linear viscous-damping elastic behaviour of fastening system as presented in Figure 150:

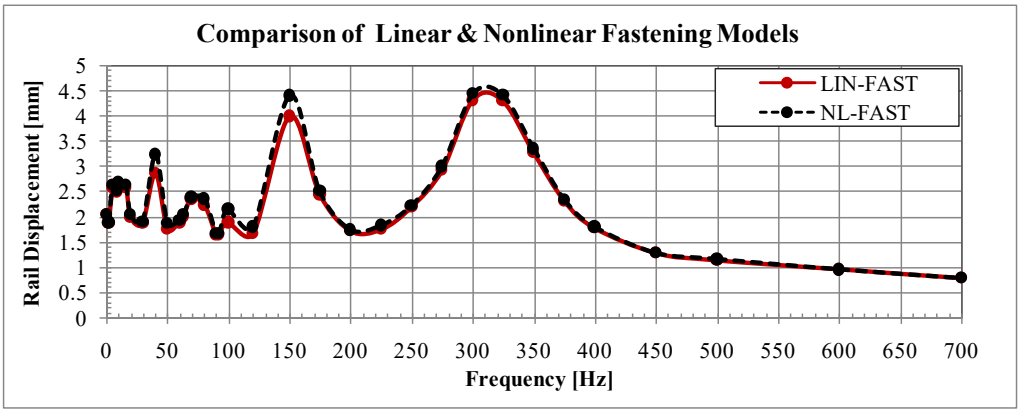

Figure 150. Comparison and verification of linear elastic viscous-damping behaviour of fastening system using two different models

Secondly, a comparison is done to compare the differences between LIN-FAST and NL-FAST models to idealize linear and nonlinear behaviours of fastening systems. To model nonlinear behaviour of fastening system, NL-FAST model considers: 1) static compression stiffness of 60 kN/mm, 2) preloaded compression force of 20 kN, 3) a high value of a dummy tension stiffness a proximally 5 times of the compression stiffness. In FEA, spring elements can have free body motion, which the level is limited by the spring stiffness.

The preloading forces of point (2) are varies in different types of fastening, manufacturers, maximum wheel load capacities, standards, and countries. The common values of preloading forces are in between 18 and 25 kN[119][46][61]. The artificial tension stiffness of point (3)

has to be set higher in COMBIN39 of the NL-FAST model to idealize the actual condition of fastening system that the maximum uplift displacement of rail is limited because a fastening is attached to a sleeper or concrete slab. This assumption of point (3) is gained through some trials of simulation in FEA especially for single point loading. For the second comparison, a small damping of 2 N.s/m is assigned to both models. Mass of the soil is initially neglected. The comparison of those different fastening models is depicted in the Figure 151.

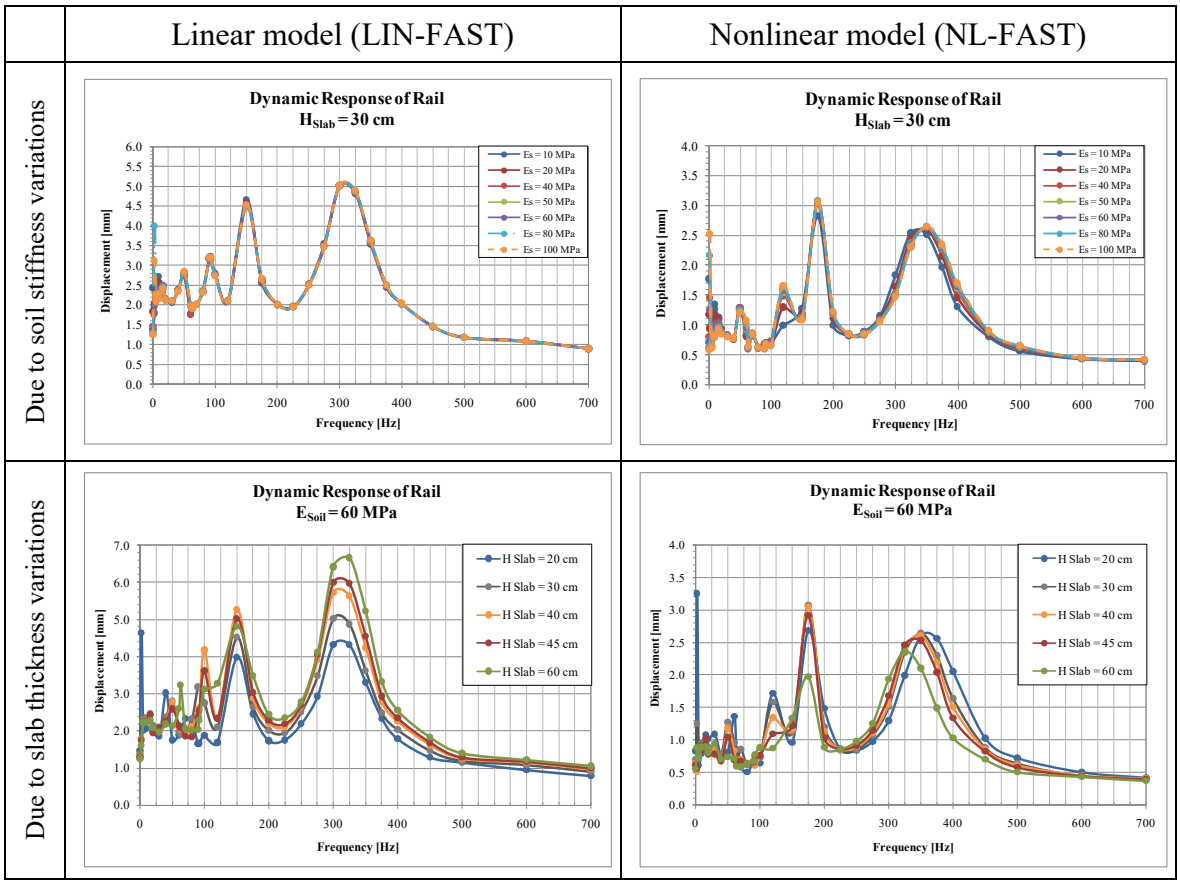

Figure 151. Matrix comparison of dynamic response of rail obtained from linear and nonlinear models of fastening systems

From top charts of Figure 151 it can be seen that both models generate similar shape of curves but have different levels of displacement. In the static as well as quasi-static and low frequency ranges, linear and nonlinear models demonstrate significant changes in the dynamic response of rail due to different soil's bearing capacity. However, in the high frequency ranges, linear model does not show remarkable changes, while nonlinear model demonstrates slight changes due to soil stiffness variations.

Harmonic analysis conducted before (subchapter 6.3.1) has demonstrated that within the range of high excitation frequency (200 and 300 Hz), the vibration characteristic is

influenced by the properties of fastening system. The results in Figure 151 also exhibit that the different behaviours between linear and nonlinear models come from impact of the different ways of modelling of fastening system.

The bottom charts of Figure 151 exhibit dynamic response of rail due to variations of slab's thickness. Linear and nonlinear models deliver contrasting behaviours. From the linear model it can be observed that at the same natural frequency around 325 Hz, the thicker the concrete slab is, the more absolute displacement on the rail occurs. Meanwhile from the nonlinear model show the opposite: the thicker the concrete slab is, the lower the absolute displacement generates on the rail. In addition, in the nonlinear model, thicker concrete slabs shift the natural frequency to lower values. This phenomenon can be explained as follows:

- In the linear model, the tension stiffness against uplift is the same with compression stiffness (60 kN/mm). Hence, linear model has a higher uplift and then rail bending curve has a form of a deeper cliff, which also shows a higher displacement amplitude. Therefore, when a thicker concrete slab is used, deflection of the concrete slab will be lower. But then due to higher uplift occurs in a linear model, elastic-pads deflect down more as shown in bottom left chart of the Figure 151. In this case, linear model does not represent the real situation for a dynamic analysis considering single point load applied on the rail.
- In the nonlinear model, the high value of dummy tension stiffness and preloading force of fastening system reduces the level of downward displacement of rail. This has advantages to mimic real behaviour of fastening and to have more realistic results concerning the impact of variations in slab thickness. The greater the thickness of the concrete slab, the higher its mass, hence the vibration impact in high frequency should be reduced as depicted in right bottom chart of the Figure 151.

Linear model of fastening system, which is used commonly used in many studies shows a good performance for static analysis. For dynamic analysis, the use of linear model depends on the applications, type of loading and point of interest of investigation. Linear model can be applied for harmonic and modal analysis, which is able to deliver a good estimation of the natural frequencies and track dynamic response.

However, for the investigations in this study, nonlinear model presents better estimation of the impact of variations in soil stiffness and slab thickness of a slab track system due to a single point dynamic loading. For a train load model or load model of a railway bridge (e.g.

load model UIC71), a linear model of fastening may already fulfill the requirement. The reason is that the train load or load model UIC71 are distributed to more points of loadings along the rail, thus the uplifts of rail in a linear model is already limited by these loads.

A.9.2. Soil's Mass Effect

This calibration is performed to observe the impact soil's mass to the dynamic behaviours of a slab rack. Fastening is modelled nonlinearly using NL-FAST model with 60 kN/mm elastic-pad stiffness and 20 N.s/m damping. Lumped mass model of soil is added as described in the sketch of FEA model depicted in the Figure 40. The results of the simulations are presented in the Figure 152.

As it can be seen from the Figure 152, adding soil's mass in the model changes the dynamic response of the rail. This implies an impact of soil mass which makes the substructure has more rigidity against vibration. The difference can be obviously seen in the high frequency range as well as thicker slab. It demonstrates that the higher the frequency and the thicker the slab are, the lower the rail displacement amplitude takes a place.

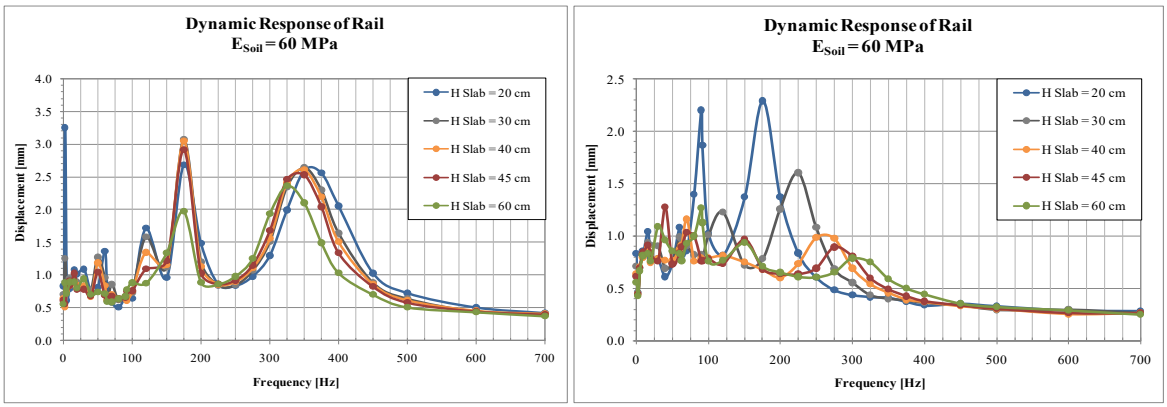

(a) without soil's mass *(b) with soil's mass*

Figure 152. *Comparison of dynamic response of FEA models with and without considering soil's mass*

In a track structure, from the top to the bottom components, the lower the location of the elements, the more rigidity, mass and damping exist as a sum of all upper components. Actually, soil can be assumed as a solid structure with high mass and damping capabilities. Therefore, modelling soil as semi-continuous elements (dense springs in parallel) in FEA has to be followed with consideration of its lumped mass. This is done to idealize solidity and mass effect of soil.

A.9.3. Comparison of the Impact of Fastening's Damping Changes of a Linear Fastening Model

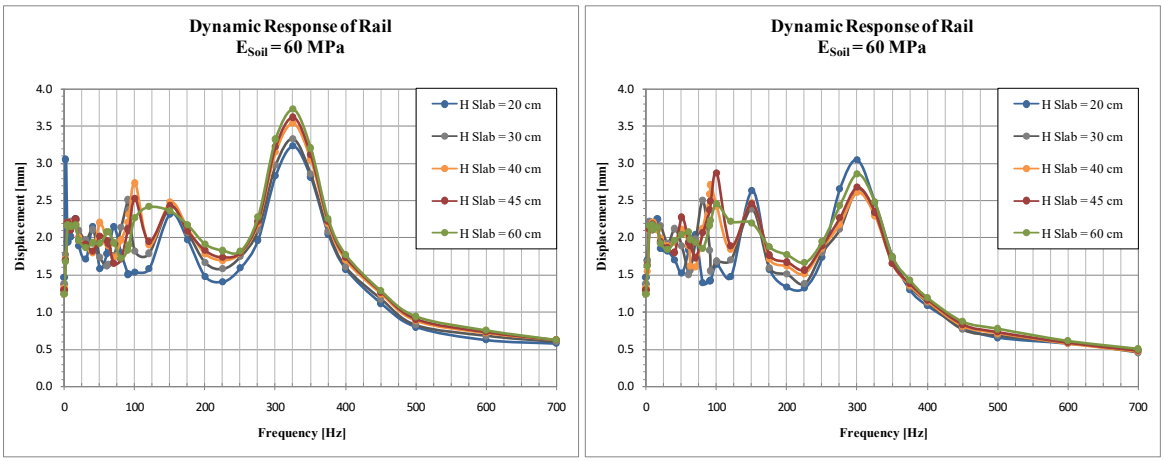

(a) Dependent-damping *(b) Dependent-damping 10x increased*

Figure 153. Comparison of the changes in damping of linear fastening model without consideration of lumped mass

A.9.4. Comparison of the Linear and Nonlinear of Undamped Track Model with a Small Soil's Effect

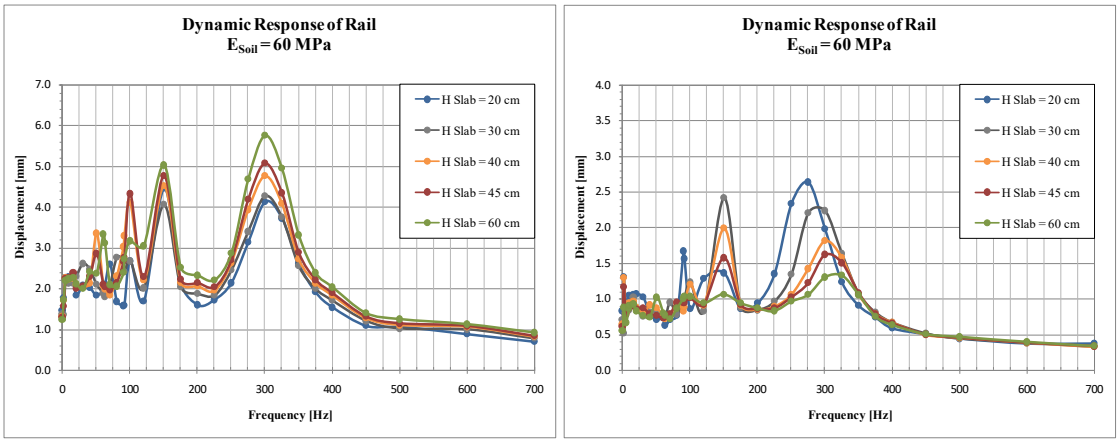

(a) Linear model of fastening *(b) Nonlinear model of fastening*

Figure 154. Comparison of nonlinearity modelling of fastening of undamped track model with 20% consideration of lumped mass

A.9.5. Comparison of the Soil's Mass Effect of Undamped Track Model with Nonlinear Fastening System

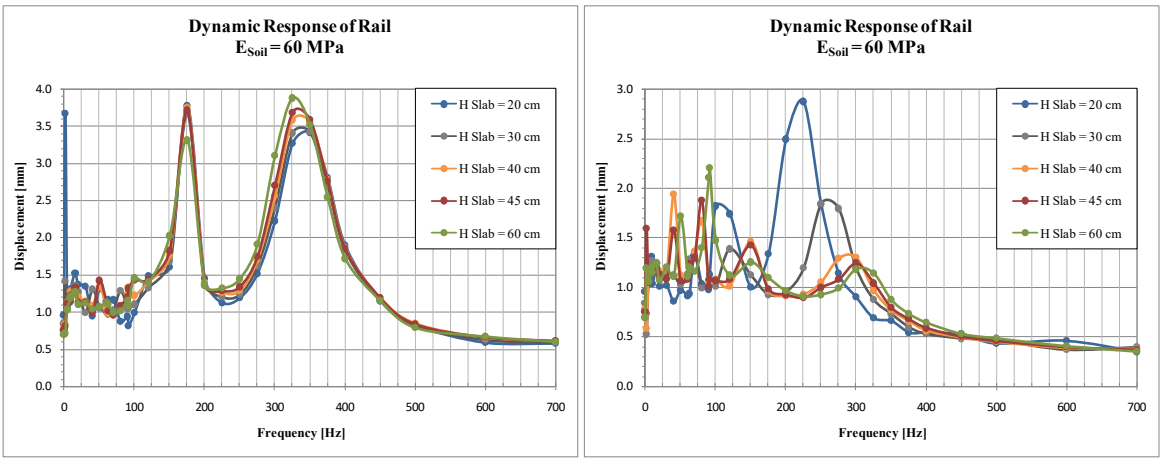

(a) Soil's mass neglected *(b) Soil's mass 100% included*

Figure 155. Comparison of soil's mass effect of undamped track model with 180 kN/mm of the tension stiffness of elastic-pad

A.9.6. Comparison of the Soil's Mass Effect and Impact Tension Stiffness Changes of Nonlinear Fastening of Undamped Track Model

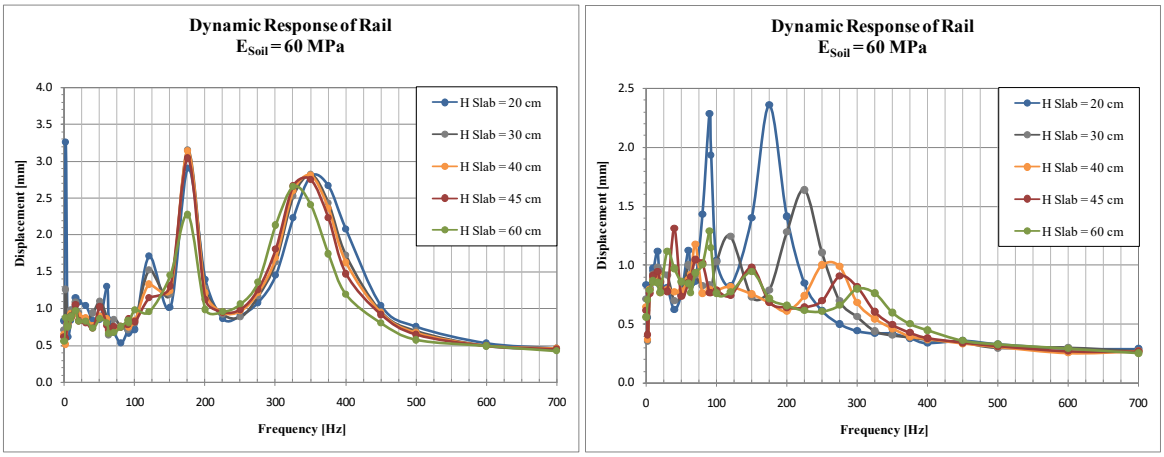

(a) Soil's mass neglected *(b) Soil's mass 100% included*

Figure 156. Comparison of soil's mass effect of undamped track model with a change to 300 kN/mm of the tension stiffness of elastic-pad

Appendix 10. FEA Simulations of Dynamic Track Interaction

A.10.1. Result of Transient Dynamic in Frequency Domain for FEA model with elastic-pad fastening resilient of 60 kN/mm

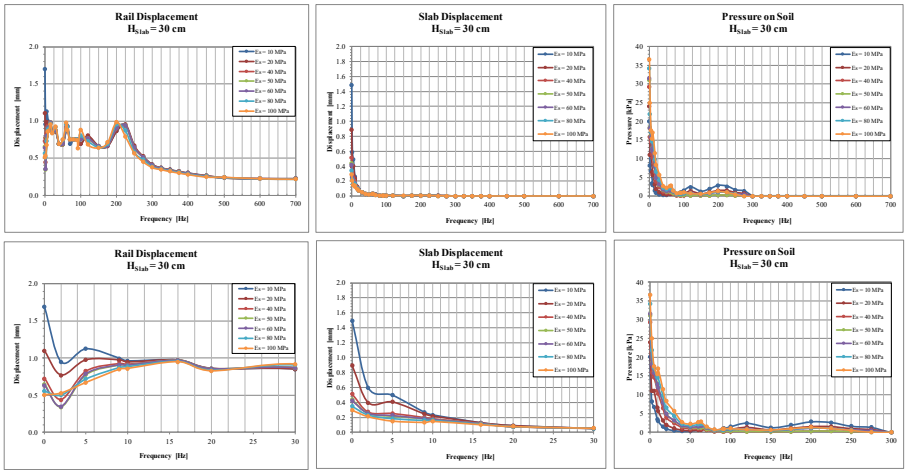

Figure 157. Dynamic response of rail, concrete slab and soil of a single-layer slab with thickness of 30 cm and elastic-pad resilient of 60 kN/mm

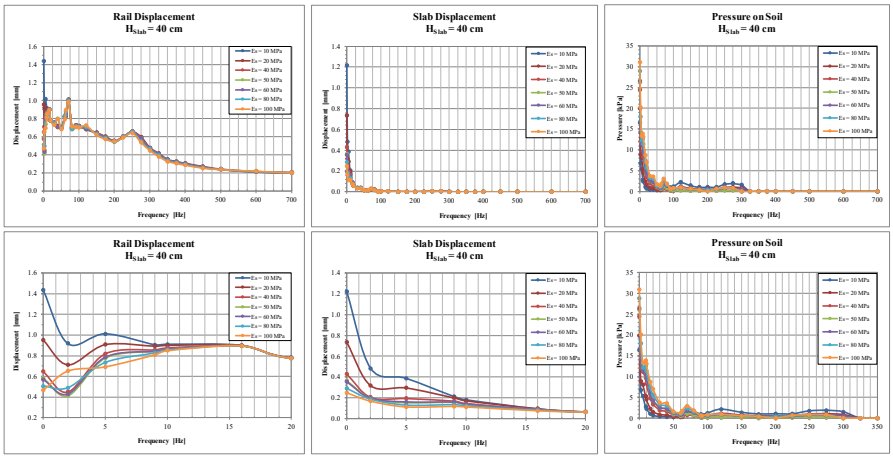

Figure 158. Dynamic response of rail, concrete slab and soil of a single-layer slab with thickness of 40 cm and elastic-pad resilient of 60 kN/mm

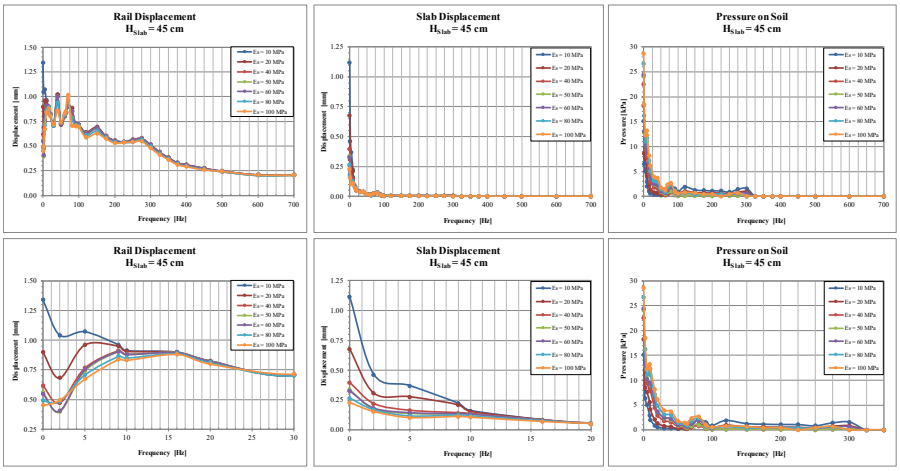

Figure 159. Dynamic response of rail, concrete slab and soil of a single-layer slab with thickness of 45 cm and elastic-pad resilient of 60 kN/mm

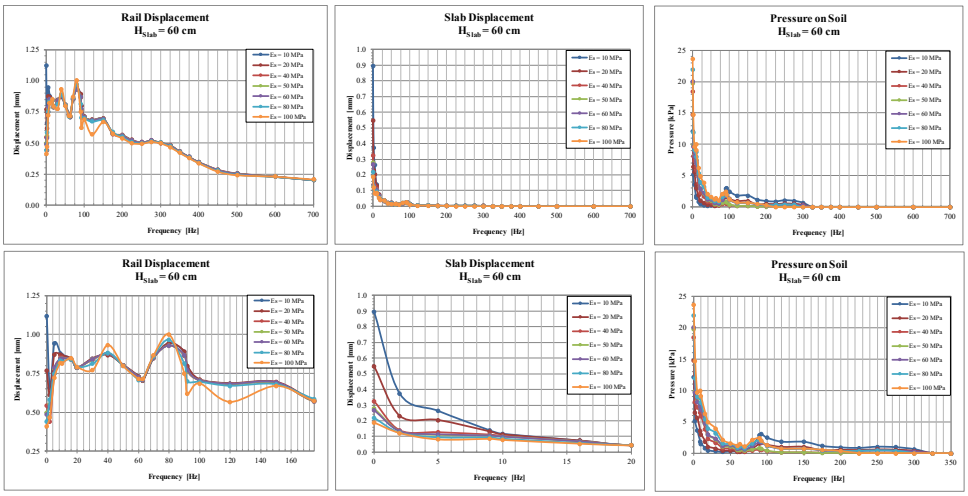

Figure 160. Dynamic response of rail, concrete slab and soil of a single-layer slab with thickness of 60 cm and elastic-pad resilient of 60 kN/mm

A.10.2.Result of Transient Dynamic in Frequency Domain for FEA model with elastic-pad fastening resilient of 22.5 kN/mm

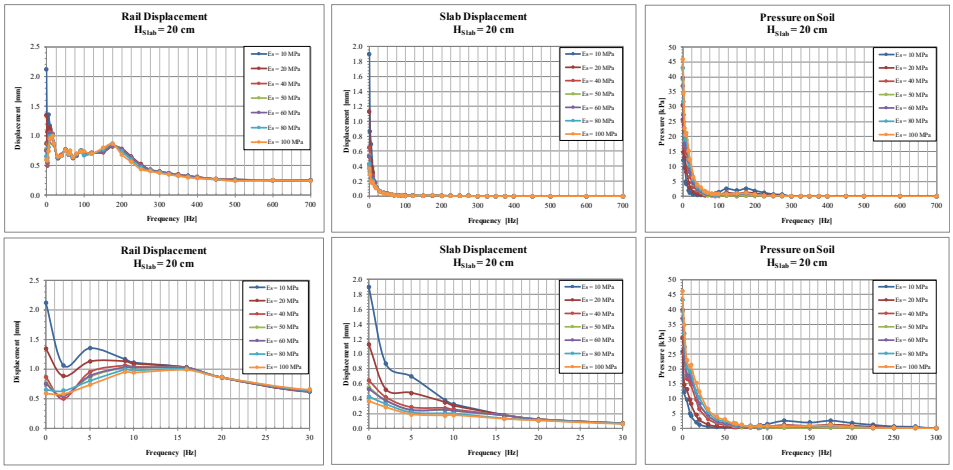

Figure 161. Dynamic response of rail, concrete slab and soil of a single-layer slab with thickness of 20 cm and elastic-pad resilient of 22.5 kN/mm

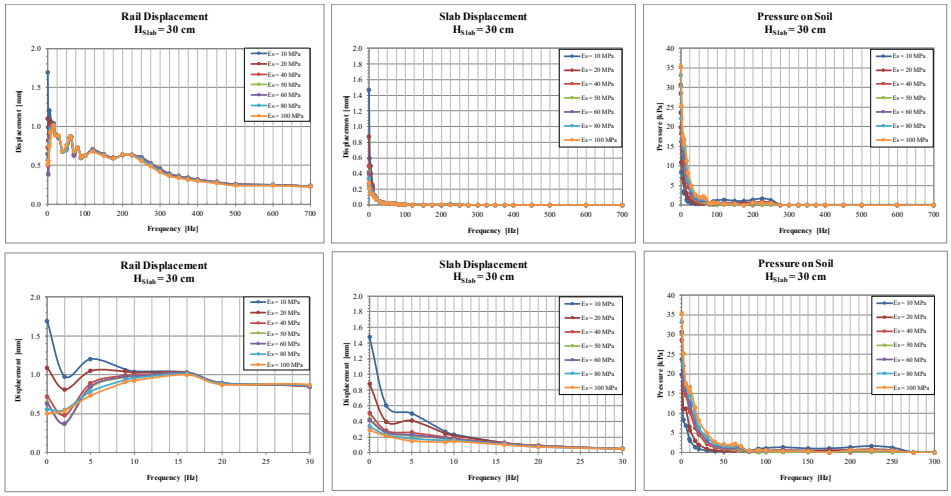

Figure 162. Dynamic response of rail, concrete slab and soil of a single-layer slab with thickness of 30 cm and elastic-pad resilient of 22.5 kN/mm

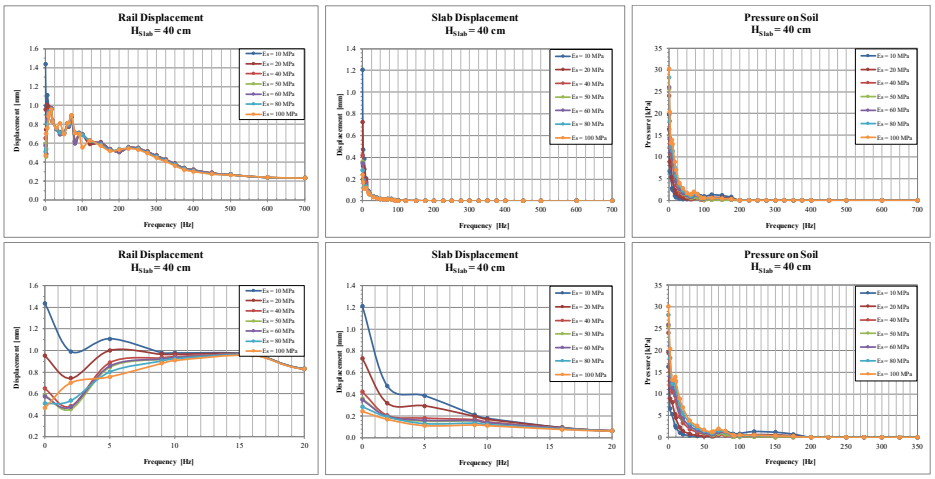

Figure 163. Dynamic response of rail, concrete slab and soil of a single-layer slab with thickness of 40 cm and elastic-pad resilient of 22.5 kN/mm

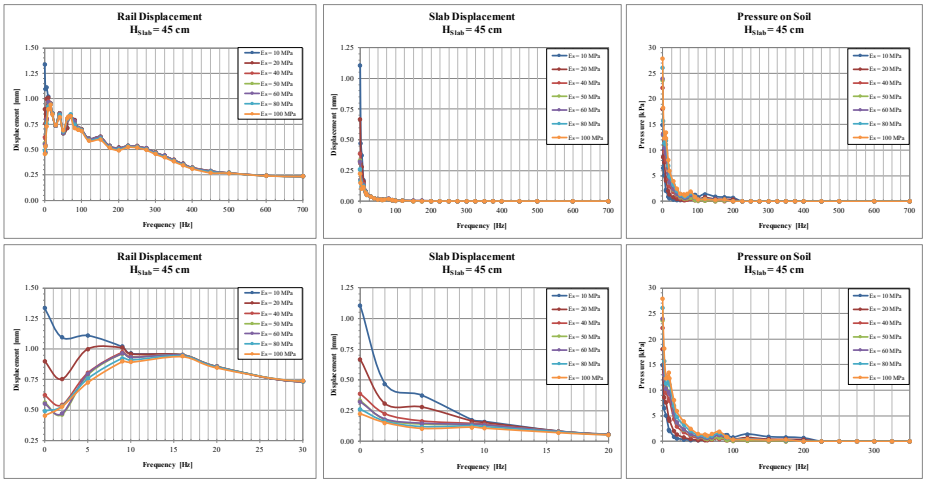

Figure 164. Dynamic response of rail, concrete slab and soil of a single-layer slab with thickness of 45 cm and elastic-pad resilient of 22.5 kN/mm

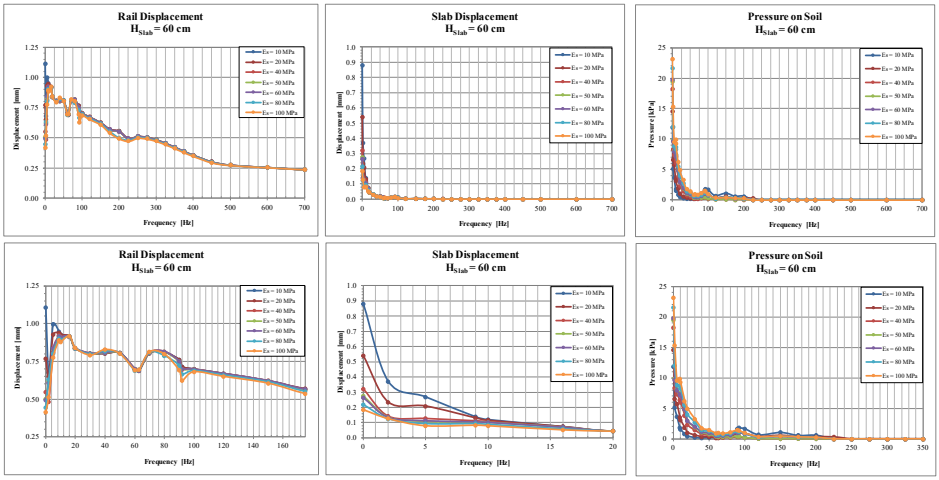

Figure 165. Dynamic response of rail, concrete slab and soil of a single-layer slab with thickness of 60 cm and elastic-pad resilient of 22.5 kN/mm

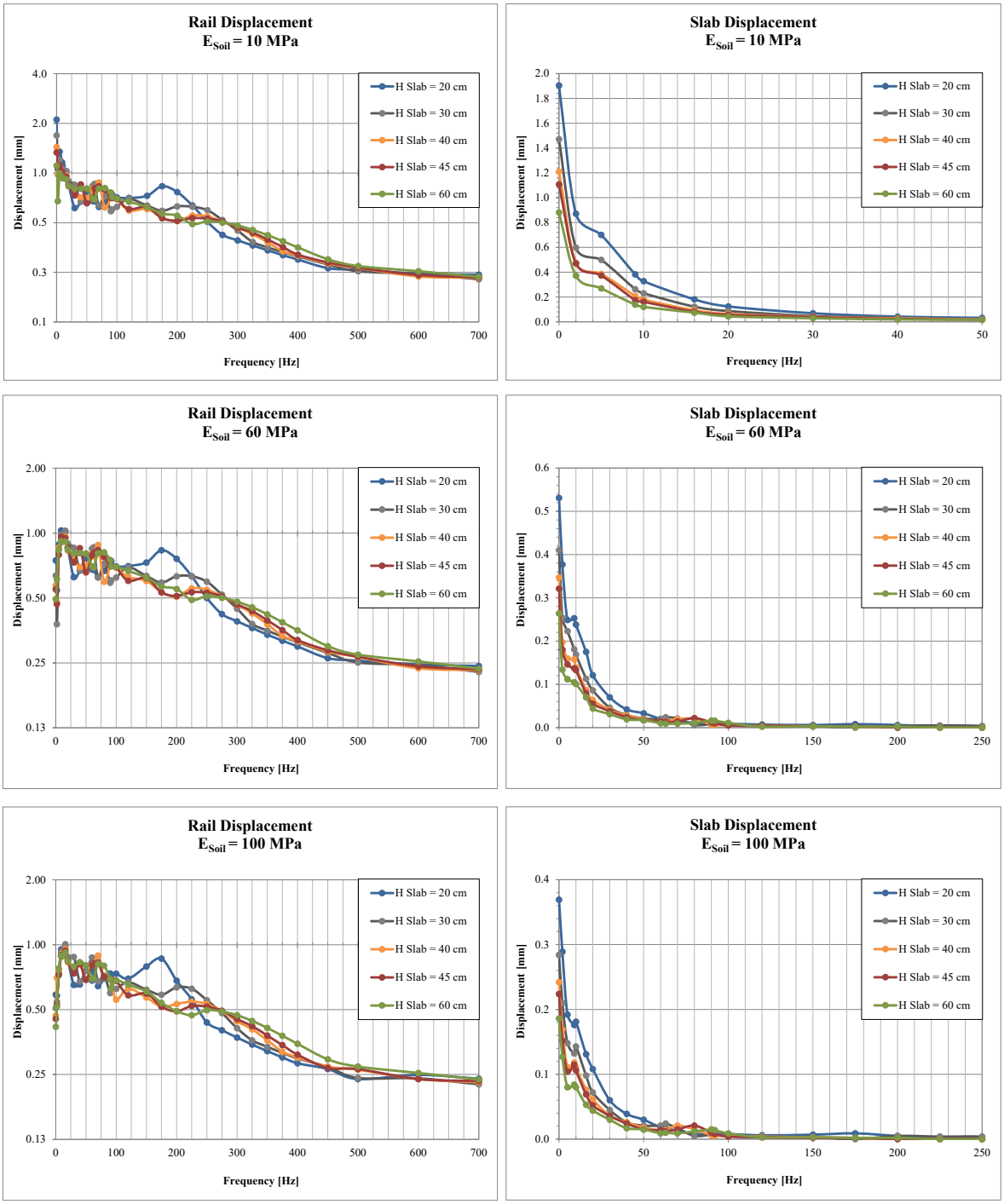

Figure 166. Dynamic response of rail and concrete slab track with different thicknesses, soil's stiffness of 10, 60 and 100 MPa, elastic-pad resilient of 22.5 kN/mm and in different excitation frequencies

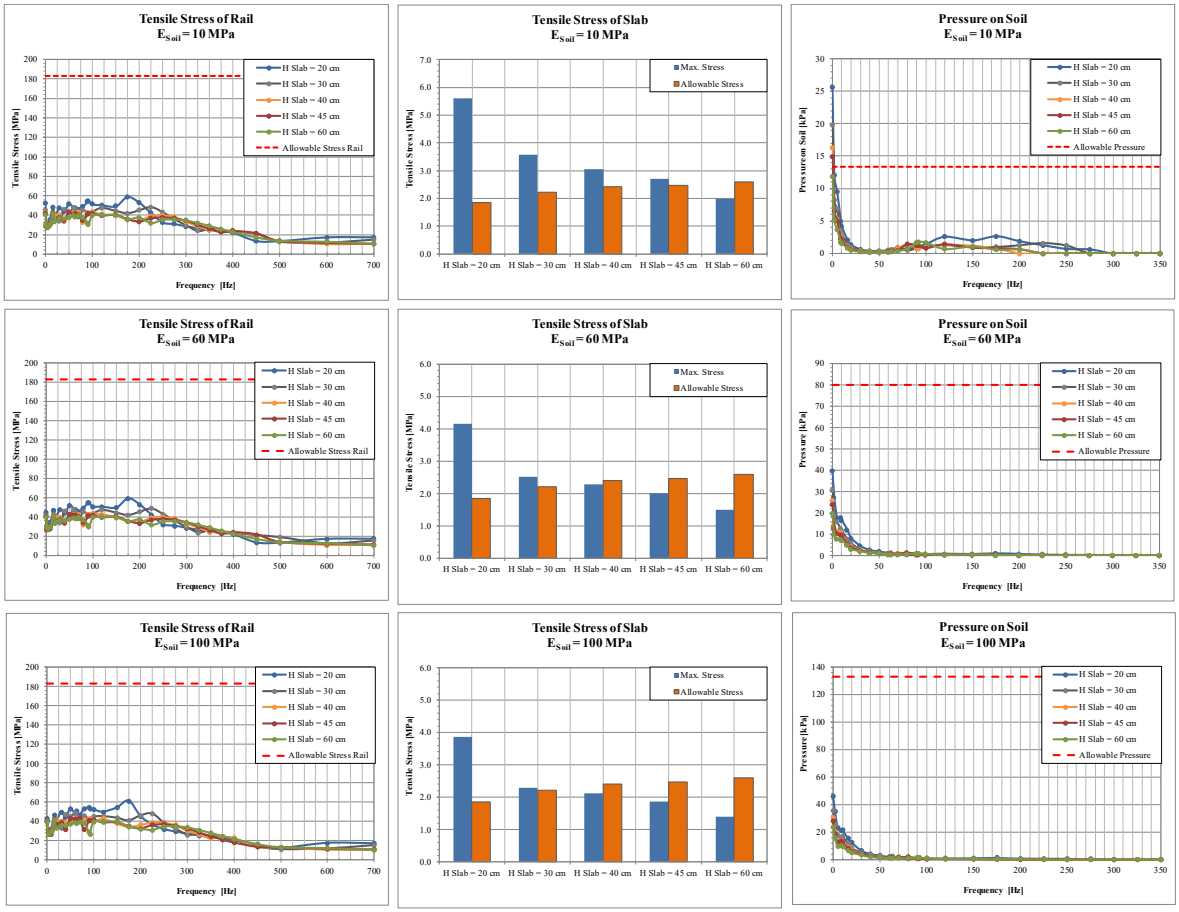

Figure 167. Actual and allowable tensile stresses of the slab and pressure on soil of a slab track with elastic-pad resilient of 22.5 kN/mm

Appendix 11. Estimation of Base and Shaft Resistances from SPT and CPT

Table 83. Summary of different estimations of pile base and shaft resistances from SPT

Method	Formulation		Note
Meyerhof (1976[84], 1983[85])	$q_b = n_b\, N_b \frac{L}{B} \leq m\, N_b\ [kPa]$ $f_s = n_s\, N_s\ [kPa]$	*Eq. 140*	– N_b= average of N between 8B above and 3B below pile tip – Sands and gravel n_b = 40, m = 40 – Non-plastic silts n_b = 40, m = 30 – Drilled piles n_b = 1.2, m = 12, n_s = 1 – Driven piles n_b = 4, m = 40, n_s = 2 – Small-displacement piles in cohesionless soil n_s = 1 – Large-displacement piles in cohesionless soil n_s = 1
Aoki & Velloso (1975)[5]	$q_b = 100 \frac{K}{F_1} N_b\ [kPa]$ $f_s = 100 \frac{\alpha K}{F_2} N_s\ [kPa]$	*Eq. 141*	– N_b= average of three values of N close to the pile tip – N_s = average of N along embedment depth of pile, excluding those to estimate N_b – K= empirical factor as function of soil type – $F_1$and F_2= empirical factor as function of pile type – α = shaft resistance factor, which depends on soil type – Bored piles n_b = 1.2, m = 12, n_s = 1
Reese and O'Neil (1989)[112]	$q_b = 60N\ \leq 4500\ [kPa]$ $q_{b,r} = 1.25 \frac{B_R}{B_b}.q_b\ [kPa]$, for $B_b \geq 1.25\ B_R$	*Eq. 142*	– For drilled piles embedded in sands – Not recommended for drilled piles with L< 4.6 m or B< 60 cm – $q_{b,r}$= reduced base resistance to reduce settlement of large diameter piles – They suggested to use β method to approximate f_s
Briaud & Tucker (1984)[13]	$q_b = \frac{s}{\frac{1}{K_p} + \frac{s}{q_{max} - q_{res}}} + q_{res}$ $f_s = \frac{s}{\frac{1}{K_\tau} + \frac{s}{q_{s,max} - q_{s,res}}} - q_{s,res}$ $K_p = 100 * 18684 (N_b)^{0.0065}$ $q_{max} = 1975 (N_b)^{0.36}, q_{res} = 557 L \sqrt{\frac{K_\tau B}{A E_p}}$ $K_\tau = 2 * 10^4 * (N_s)^{0.27}$ $q_{s,max} = 22.4 (N_s)^{0.29}, q_{s,res} = q_{res} \frac{A_p}{A_s} < q_{s,max}$	*Eq. 143*	– q_b and f_s as hyperbolic function of pile settlement (s) – N_b = average N within 4B above and 4B below pile tip – N_s= average of N around embedment depth of pile – L = length [m] of, B = diameter [m] of, E_p = modulus of elasticity [N/m^2] of, A = cross section area [m^2] of-pile. A_p= pile base area [m^2], A_s = pile shaft area [m^2].

Method	Formulation		Note
FB-Deep, SPT97[66]	$q_b = n_b\, N_b$[kPa]	*Eq. 144*	– N_b= average of N between 8B above and 3.5B below pile tip – Concrete piles square, round and cylinder with B ≤ 0.9 m: (a) plastic clay: n_b = 22.34;(b) clay, silty sand: n_b = 51.07; (c) clean sand: n_b= 102.14; (d) limestone, very shelly sand: n_b = 114.91 – Concrete piles cylinder with B > 0.9 m: (a) plastic clay: n_b = 7.11; (b) clay, silty sand: n_b = 13.09; (c) clean sand: n_b = 18.12; (d) limestone, very shelly sand: n_b = 114.91 – Steel pipe piles with B ≤ 0.9 m: (a) plastic clay: n_b = 22.34; (b) clay, silty sand: n_b = 51.07; (c) clean sand with N ≤ 30:n_b = 102.14 – Steel pipe piles with B > 0.9 m: (a) plastic clay: n_b = 21.32; (b) clay, silty sand: n_b = 39.27; (c) clean sand: n_b = 54.35;(d) limestone, very shelly sand: n_b = 91.93
	$q_b = (\, n_b N_b - m)$ [kPa]	*Eq. 145*	– Steel pipe piles with B ≤ 0.9 m: (c) clean sand with N > 30: m = 280.58, n_b = 12.74; (d) limestone, very shelly sand: m = 555.41, n_b = 22.34
	$f_s = (xN_s - yN_s{}^2)$ [kPa]	*Eq. 146*	– Concrete piles square, round and cylinder with B ≤ 0.9 m: (a) plastic clay: x = 5.27, y = 0.048;(b) clay, silty sand: x = 4.59, y = 0.042
	$f_s = n_s N_s$[kPa]	*Eq. 147*	– Concrete piles square, round and cylinder with B ≤ 0.9 m: (c) clean sand: n_s = 1.82; (d) limestone, very shelly sand: n_s = 0.96 – Steel pipe piles with B ≤ 0.9 m; limestone, very shelly sand: n_s = 0.96 – Steel pipe piles with B > 0.9 m; limestone, very shelly sand: n_s = 0.766
	$f_s = a + bN_s + c(N_s)^2 + d(N_s)^3$	*Eq. 148*	– Steel pipe piles with B ≤ 0.9 m: (a) plastic clay: a = -0.077, b = 5.554, c = -0.115, d = 8.413*10^{-4} (b) clay, silty sand: a = 2.777, b = 4.309, c = -0.086, d = 6.101*10^{-4} (c) clean sand: a = -2.489, b = 2.203, c = -0.014, d = 6.25*10^{-5}
	$f_s = a \ln(N_s) - b$	*Eq. 149*	– Steel pipe piles with B > 0.9 m: (a) plastic clay: a = 4.956, b = 51.749 (b) clay, silty sand: a = 38.4, b = 44.34 (c) clean sand: a = 19.42, b = 25.338

Table 84. Summary of different estimations of pile base and shaft resistances from Dutch Method and CPT

Method	Formulation		Note
Dutch Method, DeRuiter & Beringen (1979)[29]	$q_b = \frac{w(q_{c,1} - q_{c,2})}{2} \leq 15\ MPa$	*Eq. 150*	– $q_{c,1}$= average cone resistance for the layer in the depth between pile base and 4B below pile base – $q_{c,2}$= average cone resistance for the layer in the depth between pile base and 8B above pile base – w = correlation factor: w = 1.0 for sand with OCR = 1, w = 0.67 for very gravelly coarse sand and sand with OCR = 2 to 4; w = 0.50 for fine gravel and sand with OCR = 6 to 10
Schmertmann (1978)[123]	$q_b = \frac{w(q_{c,1} - q_{c,2})}{2} \leq 15\ MPa$ $f_s = c_{s,i} f_{s,i}\ [kPa]$	*Eq. 151*	– $q_{c,1}$= average cone resistance for the layer in the depth between 0.7B below pile base and 4B below pile base – $q_{c,2}$= average cone resistance for the layer in the depth between pile base and 8B above pile base – $c_{s,i}$ = empirical constant to convert cone sleeve friction to shaft resistance – Sands: c_s = 0.008 for open-end steel tube piles, c_s = 0.012 for precast concrete and steel displacement piles, c_s = 0.018 for vibro and cast-in-place displacement piles with steel driving tube removed as well as timber piles – Cohesive soils, c_s values are given by Schmertmann (1978) – $f_{s,i}$= cone sleeve friction of layer i
Aoki & Velloso (1975)[5]	$q_b = \frac{q_c}{F_1}$ $f_s = \frac{\alpha q_c}{F_2}$	*Eq. 152*	– α, F_1, $F_2$are the same empirical factors as SPT correlation given by Aoki & Velloso (1975)
French's Method LCPC (1984)[16][79]	$q_b = k_c q_{ca}$ $f_s = \frac{q_c}{k_s}$	*Eq. 153*	– k_c base resistance factor according to LCPC – q_{ca} = equivalent cone resistance at pile base level – k_s = shaft resistance factor – q_c = representative cone resistance for the respective layer.
Imperial College London Method (1985)[60][11][71][18]	$q_b = \bar{q_c}\left[1 - 0.5log\left(\frac{B}{D_{CPT}}\right)\right] \geq 0.13\bar{q_c}$ $f_s = \sigma'_{rf} tan(\delta_f)$	*Eq. 154*	– $\bar{q_c}$ = average CPT tip resistance within 1.5B above and below pile base – D_{CPT} = diameter of CPT cone = 0.036 m – σ'_{rf} = the local radial effective stress at failure – δ_f = failure or constant volume interface friction angle

Appendix 12. Cyclic Load Transfer Model of Case Study I

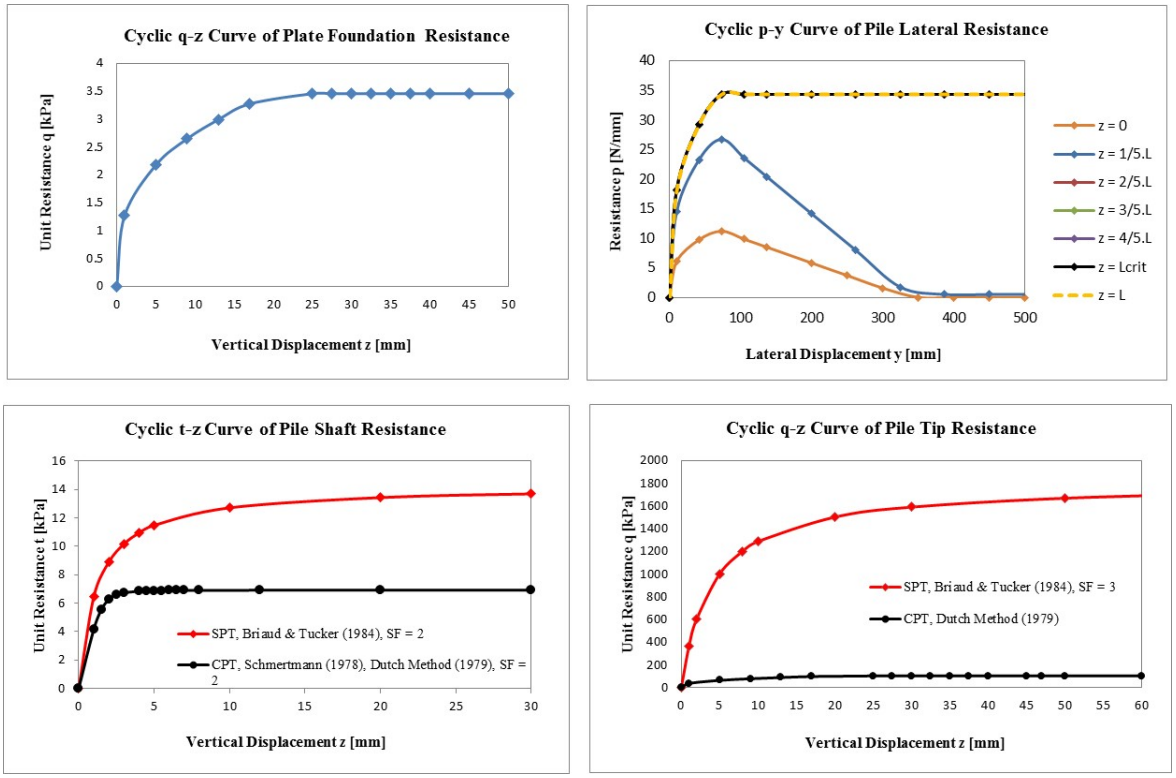

Figure 168. Cyclic load transfer models for the Example Case I - Design I.1 & Design I.3

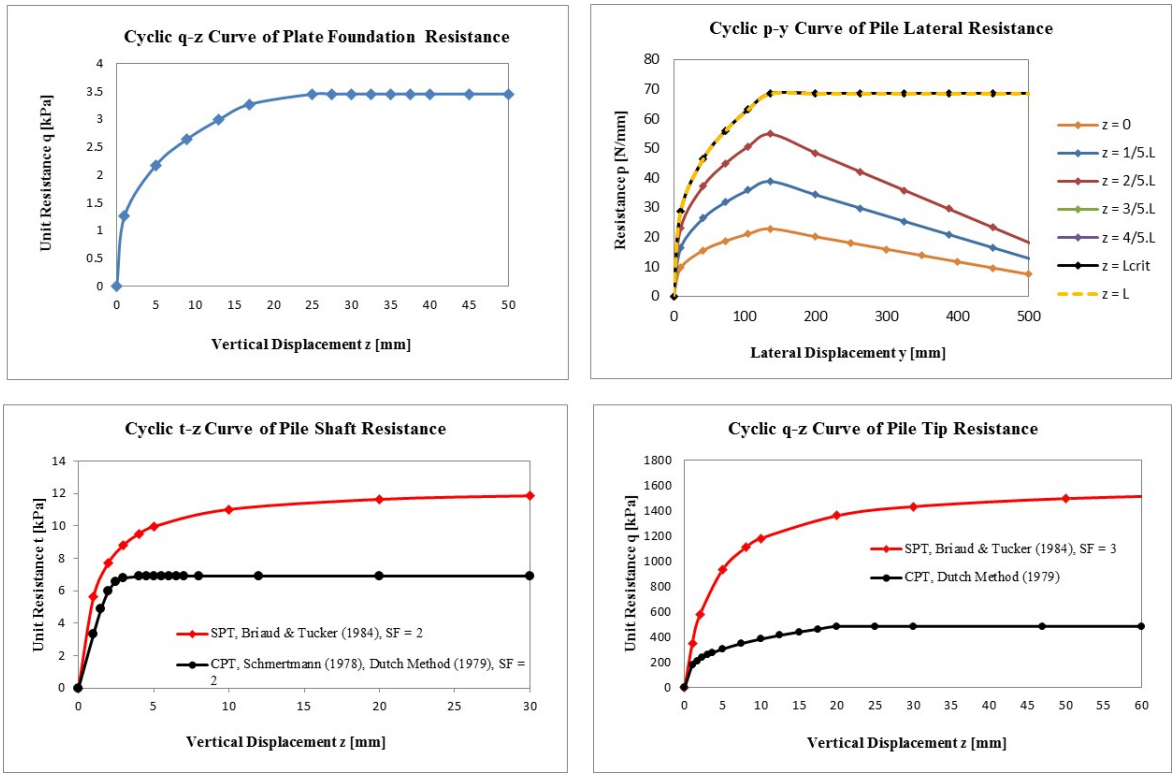

Figure 169. Cyclic load transfer models for the Example Case I - Design I.2

Appendix 13. List of Figures

Appendix 14. List of Tables